FEBRUARY 1, 1990

Analytical CHEMISTRY

Pittsburgh Conference

New York, NY

THE
pH AND
CONDUCTIVITY
HANDBOOK

Portable pH/ORP Meters From $175

Resistivity Controller From $695

Rugged Chemical Metering Pumps From $270

Litmustik High Performance Tester From $44

Microprocessor Based Chemical Metering Pumps From $512

Handheld Conductivity Meter From $323

OMEGA Laboratory Electrodes From $49

pH, Conductivity/ Temperature Tester From $357

Conductivity Calibration Standards From $10/qt

Benchtop/Portable pH Meter From $395

Ion Selective Electrodes

Industrial Pump

In-line, Self Cleaning Industrial Electrodes From $95

4-20 mA Chemical Metering Pumps From $302

Conductivity Controllers From $695

pH Transmitters

pH Controller With Pulse Output From $445

Buffer Solutions

Labora M

NEW FREE NOW! HARDBOUND!

The 1990/91 OMEGA Complete pH and Conductivity Measurement Handbook and Encyclopedia®

Over 300 Full Color Pages

Loaded with Technical Data

Ask For Your FREE Handbook Qualification Form!

Dial **(203) 359-RUSH**
(203) 359-7874

OMEGA
An OMEGA Technologies Company

One Omega Drive, Box 4047, Stamford, CT 06907
Telex 996404 Cable OMEGA FAX (203) 359-7700

For Orders and Technical Information Call

1-800-82 66342
1-800-TC OMEGA

IN CT. (203) 359-1660

©COPYRIGHT 1990, OMEGA ENGINEERING INC., ALL RIGHTS RESERVED

CIRCLE 130 ON READER SERVICE CARD

Finally, a real GC/MS for under $50,000!

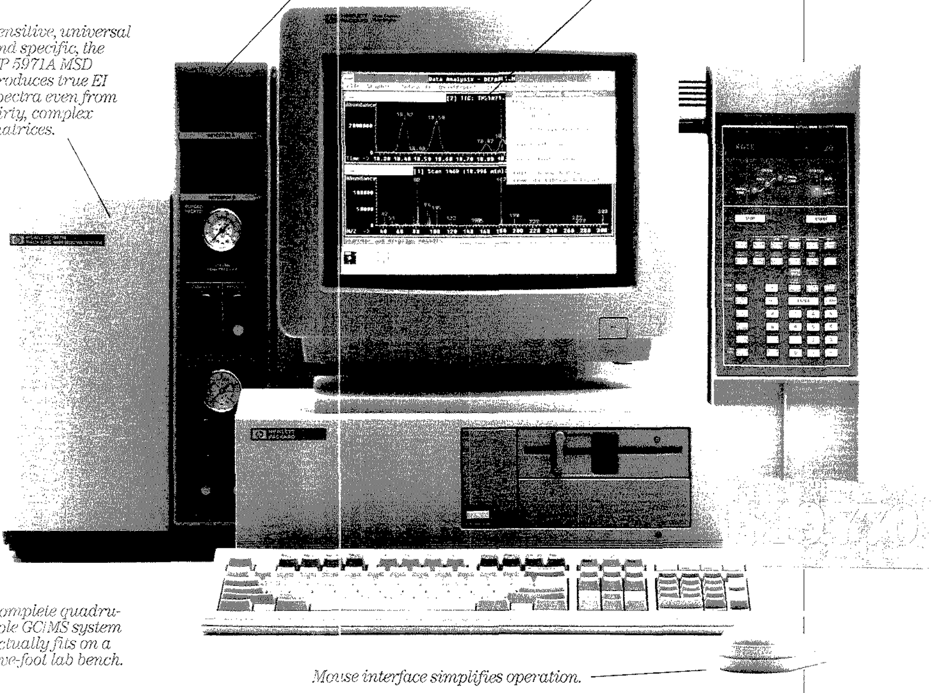

HP 5890 Series II GC sets new industry standards with high temperature operation, cool-on-column injection and pressure programming.

MS ChemStation (DOS series) is 386-based to provide speed and multitasking for highest lab productivity.

Sensitive, universal and specific, the HP 5971A MSD produces true EI spectra even from dirty, complex matrices.

Complete quadrupole GC/MS system actually fits on a five-foot lab bench.

Mouse interface simplifies operation.

Now any lab can afford a GC/MS with an HP mass selective detector (MSD). Our new PC-controlled system costs only $49,770,* yet gives you high performance.

There's multitasking for acquiring and analyzing data simultaneously. There's true, classical EI spectra that stand up to challenge. There's Microsoft® Windows software for ease of use. Plus access to PC word processing, spreadsheets and desktop publishing. And for total automation, you can add an optional autosampler and bar-code reader.

Put the system to work in *any* size laboratory. Even network it to other vendors' data systems. Then enjoy the highest uptime in the industry because HP is consistently rated number 1 for reliability, service and support. For more, call **1 800 556-1234, Ext. 10218.** In CA, **1 800 441-2345, Ext. 10218.**

*U.S. list price

Microsoft® is a U.S. registered trademark of Microsoft Corporation

HEWLETT PACKARD

© 1989 The Hewlett-Packard Company
AG-04910

CIRCLE 73 ON READER SERVICE CARD

Mattson Instruments
Is Getting Stronger In
FTIR Spectroscopy!

TGA-FTIR

GC-FTIR

FT-RAMAN

FTIR-MICROSCOPY

The Galaxy™ Series
FTIR Spectrometers

Call us at (608) 831-5515
Visit Mattson Instruments at PITTCON-1990
Booth #6018-6118

Mattson Instruments, Inc. 1001 Fourier Drive, Madison, WI 53717 U.S.A. Tel. (608) 831-5515 Fax: (608) 831-2093

CIRCLE 114 ON READER SERVICE CARD

FEBRUARY 1, 1990
VOLUME 62
NUMBER 3

The Audit Bureau
ANCHAM
62(3) 107A–252A/225–320 (1990)
ISSN 0003-2700

Registered in U.S. Patent and Trademark Office; Copyright 1990 by the American Chemical Society

Analytical Chemistry (ISSN 0003-2700) is published semimonthly by the American Chemical Society at 1155 16th St., N.W., Washington, DC 20036. Editorial offices are located at the same ACS address (202-872-4570; FAX 202-872-6325; TDD 202-872-8733). Second-class postage paid at Washington, DC, and additional mailing offices. Postmaster: Send address changes to Analytical Chemistry Member & Subscriber Services, P.O. Box 3337, Columbus, OH 43210.

Claims for missing numbers will not be allowed if loss was due to failure of notice of change of address to be received in the time specified; if claim is dated (a) North America: more than 90 days beyond issue date, (b) all other foreign: more than one year beyond issue date, or if the reason given is "missing from files."

Copyright Permission: An individual may make a single reprographic copy of an article in this publication for personal use. Reprographic copying beyond that permitted by Section 107 or 108 of the U.S. Copyright Law is allowed, provided that the appropriate per-copy fee is paid through the Copyright Clearance Center, Inc., 27 Congress St., Salem, MA 01970. For reprint permission, write Copyright Administrator, Publications Division, ACS, 1155 16th St., N.W., Washington, DC 20036.

Registered names and trademarks, etc., used in this publication, even without specific indication thereof, are not to be considered unprotected by law.

Advertising Management: Centcom, Ltd., 500 Post Rd. East, Westport, CT 06880 (203-226-7131)

1990 subscription rates include air delivery outside the U.S., Canada, and Mexico

	1 yr	2 yr
Members		
Domestic	$ 29	$ 49
Canada and Mexico	64	119
Europe	96	183
All Other Countries	118	227
Nonmembers		
Domestic	59	100
Canada and Mexico	94	170
Europe	186	336
All Other Countries	208	380

Three-year and other rates contact: Member & Subscriber Services, ACS, P.O. Box 3337, Columbus, OH 43210 (614-447-3776 or 800-333-9511).

Subscription orders by phone may be charged to VISA, MasterCard, Barclay card, Access, or American Express. Call toll free 800-ACS-5558 in the continental United States; in the Washington, DC, metropolitan area and outside the continental United States, call 202-872-8065. Mail orders for new and renewal subscriptions should be sent with payment to the Business Management Division, ACS, P.O. Box 28597, Central Station, Washington, DC 20005.

Subscription service inquiries and changes of address (Include both old and new addresses with ZIP code and *recent mailing label*) should be directed to the ACS Columbus address noted above. Please allow six weeks for changes to become effective.

ACS membership information: Lorraine Bowlin (202-872-4567)

Single issues, current year, $8.00 except review issue, $14.00, and LabGuide, $49.00; **back issues and volumes and microform editions** available by single volume or back issue collection. For information or to order, call the number listed for subscription orders by phone; or write the Microform & Back Issues Office at the Washington address.

Nonmembers rates in Japan: Rates above do not apply to nonmember subscribers in Japan, who must enter subscription orders with Maruzen Company Ltd., 3–10 Nihonbashi 2-chome, Chuo-ku, Tokyo 103, Japan. Tel: (03) 272-7211.

Analytical Chemistry

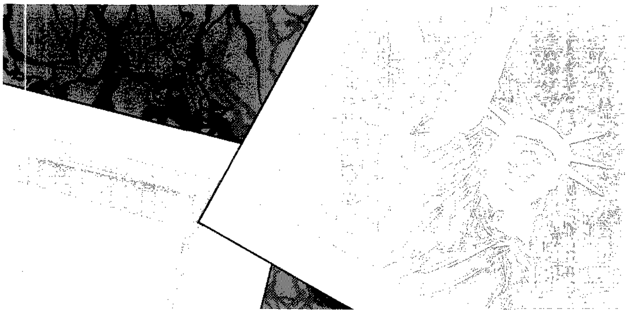

PITTSBURGH CONFERENCE 123 A

On the cover. **The 1990 Pittsburgh Conference and Exposition on Analytical Chemistry** will be held at the Jacob Javits Convention Center in New York City, March 5–9. The technical program will feature 31 symposia and more than 1200 contributed papers and poster presentations. The Exposition of Modern Laboratory Equipment will feature 800 exhibitors in more than 2500 booths and seminar rooms showing state-of-the-art analytical instrumentation, chemicals, equipment, supplies, and services

BRIEFS 112 A

EDITORIAL 121 A

Journals online. The chemistry community that uses Cornell University's Mann Library will participate in the Chemistry Online Retrieval Experiment (CORE)

NEW PRODUCTS & MANUFACTURERS' LITERATURE 242 A

AUTHOR INDEX 225

GILSON

LIQUID CHROMATOGRAPHY

GILSON

The Master Pump

HPLC Pump and System Controller

Operating across a wide range of pressures and flowrates, the 305 Master Pump directly controls all other modules in a Gilson HPLC system.

Circle no. 221

Minipuls 3

Versatile Peristaltic Pump

Equipped with interchangeable heads, this peristaltic pump operates at high pressures while producing a remarkably smooth flow.

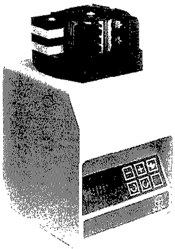

Circle no. 224

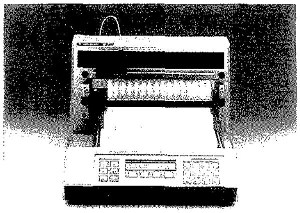

FC 203 Fraction Collector

Special Low Pressure LC

The FC 203 is a multi-mode unit for 128 fractions. A built-in keyboard allows easy parameter selection, and a special HELP key provides on-line instruction.

Circle no. 220

231-401 Auto-Sampling Injector

Flexible Automation

The 231-401 automates HPLC sampling and injection procedures. Fully programmable, the unit accepts up to 128 vials with or without caps.

Circle no. 222

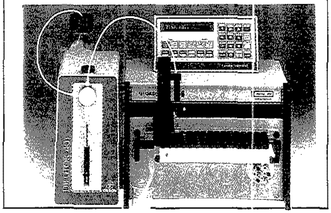

232-401 Sample Processor and Injector

High Capacity

The 232-401 completely automates preparation and injection of up to 560 samples for unattended HPLC. Options include thermostatted racks and a column switching valve. **Circle no. 225**

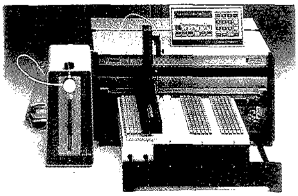

SAMPLE PROCESSORS

GILSON

221 and 222 Auto Samplers

Automate Sample Preparation and Sample Transfer

Adaptable to a wide variety of applications, these samplers dispense, pipette, dilute and mix liquids, and then transfer the prepared samples to an analytical instrument.

Circle no. 223

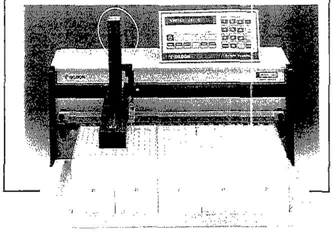

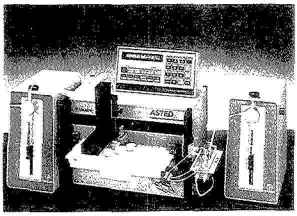

ASTED Sample Preparation

Increases HPLC Throughput

This patented system uses dialysis and trace enrichment to isolate low molecular weight analytes from samples prior to HPLC analysis.

Circle no. 226

GILSON

GILSON

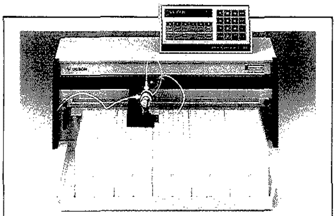

202 Fraction Collector

With 15 Operating Modes

The 202 offers 540-tube collection in a versatile five-rack configuration.
15 operating modes permit complex fractionation schemes including double column collection.

Circle no. 227

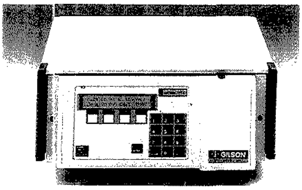

116 UV Detector

Programmable for Variable Wavelengths

The 116 UV detects in a range of 190-380 nm. Choose the single wavelength, dual wavelength or scan operating mode. Sensitivity (0.001-200 AUFS) depends on the flow cell used.

Circle no. 230

PIPETTES AND TIPS

GILSON

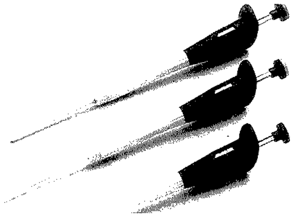

Microman ™

Pipette for Problem Liquids

Microman measures viscous, volatile, or high-density samples. Capillaries and pistons can be ejected safely without hand contact, for hazardous samples.

Circle no. 228

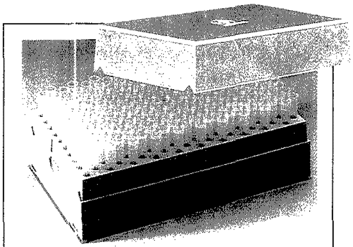

Pipetman Tips

Guaranteed Performance

Manufactured by Gilson for Pipetman, these tips are your assurance of performance according to specifications.

Circle no. 231

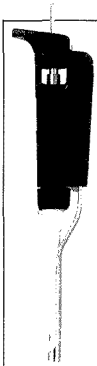

Pipetman ™

Continuously Adjustable Digital Pipette

Pipetman is the instrument you know you can depend on for critical research applications. Pipetman is the world's standard for microliter pipetting.

Circle no. 233

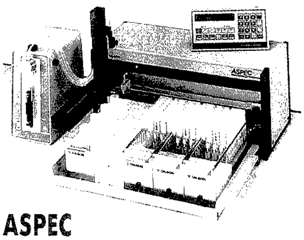

ASPEC

Automatic Solid Phase Extraction

For clean-up or trace enrichment, ASPEC automates all liquid handling in solid phase extraction. ASPEC accepts standard extraction columns.

Circle no. 229

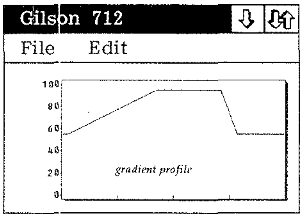

HPLC Software

System Control and Data Analysis

Gilson 712 and 714 HPLC system controllers offer ternary or quaternary gradient control and single or multiple channel data analysis.

Circle no. 232

For the name of your nearest Gilson representative please contact us directly.

GILSON

Gilson Medical Electronics
(France) S.A. BP 45,
95400 Villiers-le-Bel,
France
Tel.: 33 (1) 34.29.50.00
Telex: 606 682
Fax: 33 (1) 34.29.50.80

GILSON

BRIEFS

Articles

Automated Selection of Library Subsets for Infrared Spectral Searching 226

Principal components analysis is used to select an appropriate subset of an FT-IR spectral library for subsequent Euclidean distance searching. Based on the relationships between library spectra and the computed principal components of the library, a series of ordered lists are created that help to pinpoint similar spectra.

Joanne M. Bjerga and Gary W. Small*, Department of Chemistry, The University of Iowa, Iowa City, IA 52242

Accuracy of Peak Deconvolution Algorithms within Chromatographic Integrators 234

Significant chromatographic peak deconvolution parameters (minimizing inaccuracies for the tangent skim and perpendicular drop deconvolution methods) are compared with the parameters used by commercial integrators.

Andrew N. Papas*, U.S. Food & Drug Administration, Winchester Engineering and Analytical Center, Winchester, MA 01890 and **Terrence P. Tougas**, Chemistry Department, University of Lowell, University Avenue, Lowell, MA 01854

Measurement of Vanadium Impurity in Oxygen-Implanted Silicon by Isotope Dilution and Resonance Ionization Mass Spectrometry 240

Trace analysis is performed on surface layers that are chemically removed from a semiconductor material and weigh < 1 mg. Picogram levels of vanadium are detected.

Santos Mayo, Semiconductor Electronics Division, National Institute of Standards and Technology, Gaithersburg, MD 20899 and **John D. Fassett*, Howard M. Kingston, and Richard J. Walker**, Inorganic Analytical Research Division, National Institute of Standards and Technology, Gaithersburg, MD 20899

Application of Countercurrent Chromatography/Thermospray Mass Spectrometry for the Identification of Bioactive Lignans from Plant Natural Products 244

The capability of thermospray CCC/MS is demonstrated in identifying and validating the bioactive and structurally known lignans from a crude extract of *Schisandra rubriflora* Rhed et Wils, a traditional Chinese herbal medicine for the treatment of hepatitis.

Yue Wei Lee*, Robert D. Voyksner, Terry W. Pack, and C. Edgar Cook, Research Triangle Institute, P.O. Box 12194, Research Triangle Park, NC 27709, **Q. C. Fang**, Institute of Materia Medica, Chinese Academy of Medical Sciences, Beijing, China, and **Yoichiro Ito**, Laboratory of Technical Development, National Heart, Lung, and Blood Institute, Bethesda, MD 20892

Adaptation of a Thermospray Liquid Chromatography/Mass Spectrometry Interface for Use with Alkaline Anion Exchange Liquid Chromatography of Carbohydrates 248

An interface is described for coupling alkaline anion exchange HPLC with thermospray MS. Sugars are used as model compounds to evaluate system performance in both the isocratic and gradient elution modes. Mass spectra obtained on line are compared with those obtained by the direct injection method.

Richard C. Simpson* and Catherine C. Fenselau, Department of Chemistry and Biochemistry, University of Maryland, Baltimore County, Baltimore, MD 21228, **Mark R. Hardy, R. Reid Townsend, and Yuan C. Lee**, Department of Biology, Johns Hopkins University, Baltimore, MD 21218, and **Robert J. Cotter**, Department of Pharmacology, Johns Hopkins University, Baltimore, MD 21205

Determination of Regulatory Organic Compounds in Radioactive Waste Samples. Semivolatile Organics in Aqueous Liquids 253

Regulatory semivolatile organic compounds are readily extracted from small volumes of aqueous, highly radioactive liquids and quantitated in a conventional GC/MS laboratory.

Bruce A. Tomkins*, John E. Caton, Jr., G. Scott Fleming, Manuel E. Garcia, Sara H. Harmon, Robert L. Schenley, Cheryl A. Treese, and Wayne H. Griest, Organic Chemistry Section, Analytical Chemistry Division, Oak Ridge National Laboratory, Oak Ridge, TN 37831-6120

Cross-Linked Redox Gels Containing Glucose Oxidase for Amperometric Biosensor Applications 258

Two materials, based on a cross-linkable poly(vinylpyridine) complex of $[\mathrm{Os(bpy)_2Cl}]^{+/2+}$ that communicates electrically with flavin adenine dinucleotide redox centers of enzymes such as glucose oxidase, are described for use in amperometric biosensors. The glucose response time of the resulting electrode is < 10 s.

Brian A. Gregg and Adam Heller*, Department of Chemical Engineering, University of Texas at Austin, Austin, TX 78712

Flow System for Starch Determination Based on Consecutive Enzyme Steps and Amperometric Detection at a Chemically Modified Electrode 263

Starch is totally hydrolyzed to glucose by using immobilized α-amylase and amyloglucosidase. Coimmobilized mutarotase and glucose oxidase oxidize glucose to hydrogen peroxide, which is amperometrically detected. Calibration curves are linear between 10 μM and 0.6 mM. Sample throughput is 15 h^{-1}.

J. Emnéus and L. Gorton*, Department of Analytical Chemistry, University of Lund, P.O. Box 124, S-221 00 Lund, Sweden

* Corresponding author

The only integrated solution for radio-chromatography.

System Gold,™ the Personal™ Chromatograph, brings control of complex HPLC to a single, simple point.

For radiochromatography, that point is the integration of our Model 171 Radioisotope Detector and new on-line Model 507 Autosampler into System Gold for Radiochromatography.

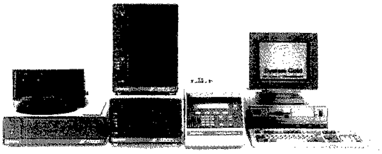

Now, your analysis of radiolabeled compounds is simpler, easier, more automated than ever. Just point and click. Fully automated System Gold for Radiochromatography does the rest. Quickly. Automatically. Error-free.

And it's *all* from Beckman, a recognized world leader in both HPLC and Liquid Scintillation. Which makes your service and support as swift and sure as your system.

For the only integrated radiochromatograph, contact your local Beckman representative. Offices in major cities worldwide.

Call 800/742-2345 in the US.
Or write Beckman Instruments, Inc.,
Altex Division, 2350 Camino Ramon,
P.O. Box 5101, San Ramon, CA 94583.

BECKMAN

Australia, Sydney **Austria,** Vienna **Canada,** Toronto **Denmark,** Birkerød **France,** Gagny **Germany,** Munich **Hong Kong,** Aberdeen **Italy,** Milano **Japan,** Tokyo **Mexico,** Mexico City **Netherlands,** Mijdrecht **Norway,** Oslo **Puerto Rico,** Carolina **Singapore. South Africa,** Johannesburg **Spain,** Madrid **Sweden,** Bromma **Switzerland,** Nyon **Taiwan,** Taipei **United Kingdom,** High Wycombe © 1989 Beckman Instruments, Inc. AX88-1046A

PittCon NYC, March 5–8, Booth 5005

Circle 25 for Representative & Literature
Circle 26 for Literature only

MAXIMIZE YOUR SENSITIVITY...
for Volatile Organic Compounds by Dynamic Headspace Concentration

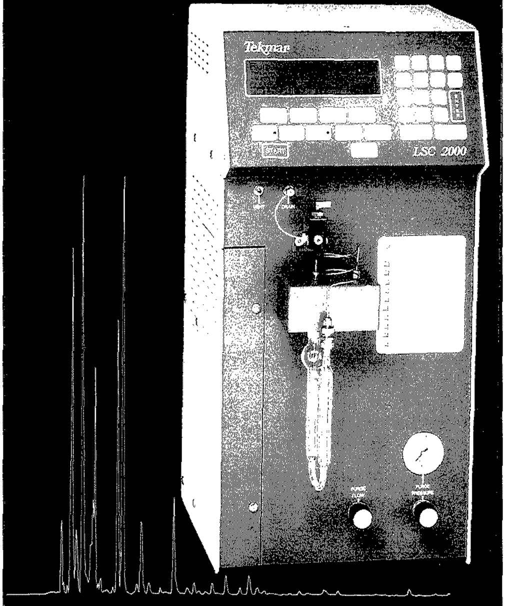

5 ml **Coffee** on Tekmar's LSC 2000 and Capillary Interface

Flavor/Fragrance
Competitive Analysis
Off Flavor/Odor Analysis
Packaging Materials
Pharmaceuticals/Residual Solvents
Building Products/Outgassing Studies
Polymers
Residual Monomers/Solvents

Ask for our FREE bibliography of reprints on a wide range of applications

P.O. Box 371856 • Cincinnati, OH 45222-1856
(800) 543-4461 Sales • (800) 874-2004 Service
Fax (513) 761-5183 • Telex 21-4221

See Us At PittCon—Booth #'s 1735/1736
CIRCLE 178 ON READER SERVICE CARD

BRIEFS

Simulation of Two-Electron Homogeneous Electrocatalysis for Steady-State Voltammetry at Hemispherical Microelectrodes 268

Simulations of two-electron homogeneous electrocatalysis for hemispherical microelectrodes show that as electrode radii decrease, larger catalytic rates are needed for significant current amplification.

Chang Ling Miaw, James F. Rusling*, and Azita Owlia, Department of Chemistry (U-60), University of Connecticut, Storrs, CT 06269-3060

Determination of Copper at Electrodes Modified with Ligands of Varying Coordination Strength: A Preamble to Speciation Studies 274

To ascertain the use of chemically modified electrodes in speciation studies, electrodes modified with seven different ligands whose formation constants for copper vary over a broad range are used to determine copper in solution.

Seong K. Cha and Héctor D. Abruña*, Department of Chemistry, Baker Laboratory, Cornell University, Ithaca, NY 14853-1301

Determination of Linkage Position and Identification of the Reducing End in Linear Oligosaccharides by Negative Ion Fast Atom Bombardment Mass Spectrometry 279

The reducing end and monosaccharide sequences are identified, and the 1–4, 1–6, 1–3, and 1–2 linkage positions are discriminated by analysis of the negative metastable ions produced in FAB-MS linked scans.

Domenico Garozzo, Mario Giuffrida, and Giuseppe Impallomeni, Istituto per la Chimica e la Tecnologia dei Materiali Polimerici, Consiglio Nazionale delle Ricerche, Viale A. Doria 6, 95125 Catania, Italy and **Alberto Ballistreri and Giorgio Montaudo***, Dipartimento di Scienze Chimiche, Università di Catania, Viale A. Doria 6, 95125 Catania, Italy

Nitric Oxide Chemical Ionization Mass Spectrometry of Long-Chain Unsaturated Alcohols, Acetates, and Aldehydes 287

CI-NO$^+$-MS is used to determine double bond location in long-chain monounsaturated alcohols, acetates, and aldehydes, mostly through the formation of an acylium diagnostic ion. An extension of the method for assigning the external double bond in di- or tri-ethylenic compounds is described.

Christian Malosse and Jacques Einhorn*, INRA-CNRS, Laboratoire des Médiateurs Chimiques, Magny-les-Hameaux, 78470 St-Rémy-les-Chevreuse, France

Amperometric Monitoring of Ozone in Gaseous Media by Gold Electrodes Supported on Ion Exchange Membranes (Solid Polymer Electrolyes) 293

An in situ amperometric sensor is described that permits a limit of detection of 10^{-8} M (0.5 μg L^{-1}, 2.24 × 10^{-7} atm) with a response time of 0.5 s.

Gilberto Schiavon* and Gianni Zotti, CNR-IPELP, corso Stati Uniti 4, I-35100 Padova, Italy, **Gino Bontempelli***, Institute of Chemistry, University of Udine, viale Ungheria 43, I-33100 Udine, Italy, and **Giuseppe Farnia and Giancarlo Sandonà**, Department of Physical Chemistry, University of Padova, via Loredan 2, I-35131 Padova, Italy

SIEMENS

Ask for performance - ask for the new D 5000 x-ray diffractometer

Detector configurations include:
- PSD (Position Sensitive Detector).
- Solid-state detector for improved detector efficiency.
- Std. scintillation counter.

Complete set of attachments for specific applications:
- Eulerian cradle for texture.
- Open Eulerian cradle for texture/ stress.
- Automatic sample changer.
- High and low temperature stages.
- Programmable sample rotation.

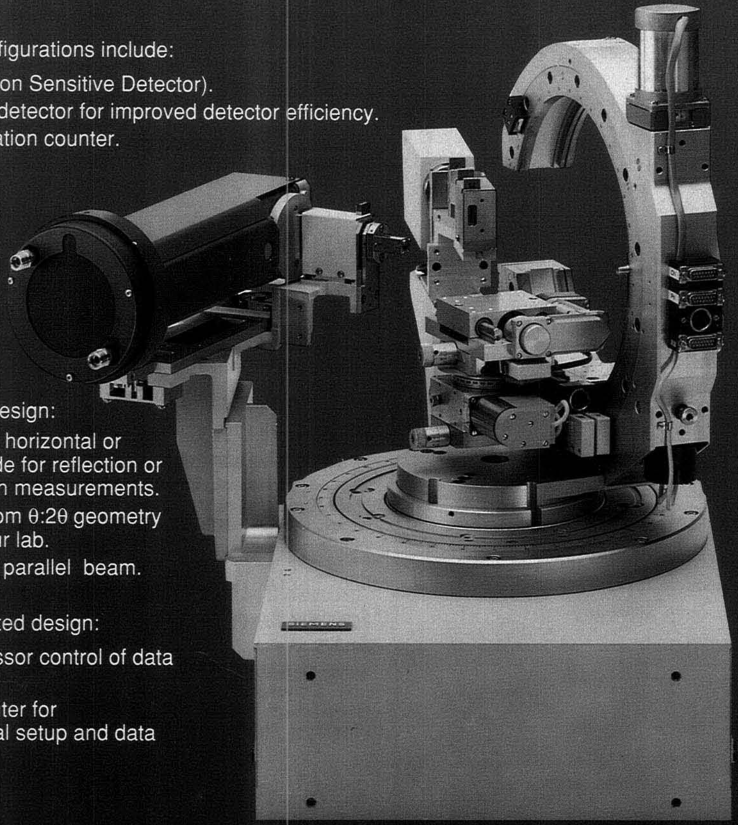

Versatile goniometer design:
- Operates in horizontal or vertical mode for reflection or transmission measurements.
- Converts from θ:2θ geometry to θ:θ in your lab.
- Converts to parallel beam.

Fully automated design:
- Microprocessor control of data collection.
- Host computer for experimental setup and data analysis.

Available with computer controlled variable aperture slits in incident and diffracted beam paths to control divergence and reduce background.

For maximum performance in your lab, Siemens has engineered a new generation of x-ray diffractometer designed to meet your requirements. The D 5000 features a new goniometer design manufactured to the strictest tolerances. Complete with application specific attachments and advanced software routines, the D 5000 has the precision and flexibility to outperform other systems in every x-ray application.

Your Solution is Siemens

In USA & Canada contact Siemens Analytical X-Ray Instruments, Inc., a joint venture of Siemens & Nicolet.
6300 Enterprise Lane • Madison, WI 53719-1173 • Tel. (608) 276-3000 • FAX (608) 276-3015
Worldwide Contact: Siemens AG, Analytical Systems E 689 • D 7500 Karlsruhe 21 • P.O. Box 21 1262 • Federal Republic of Germany • Tel. (0721) 595-4295

CIRCLE 160 ON READER SERVICE CARD

RENT
Analytical Instruments
lease or rent-to-own

- ✓ Free instrument delivery & setup in selected areas.
- ✓ GC•MSD•FTIR•AA•ICP•LC•IR
- ✓ Choose from many major manufacturers
- ✓ Hewlett-Packard GC•MSD Systems in stock
- ✓ New Catalog of Chromatography Supplies.

1-800-7-ON-SITE

On-Site Instruments®
ENVIRORENTAL®
689 North James Road Columbus, Ohio 43219-1837
(614) 237-3022
USA—CANADA

CIRCLE 125 ON READER SERVICE CARD

THE UNIVERSITY OF DAYTON RESEARCH INSTITUTE
ENVIRONMENTAL SCIENCES

- TOXIC WASTE INCINERATION
  - INCINERABILITY TESTING
  - BY-PRODUCT IDENTIFICATION
  - TRIAL BURN SUPPORT
- THERMAL STABILITY
  - FIRE SAFETY
  - EVOLVED GAS ANALYSIS
  - LAB-SCALE PROCESS SIMULATION
- ANALYTICAL SERVICES
  - GC-FID/MS/FTIR
  - CUSTOM ANALYSIS
  - TGA

The University of Dayton
ENVIRONMENTAL SCIENCES GROUP
RESEARCH INSTITUTE
300 College Park
Dayton, Ohio 45469-0001
(513) 229-2846

CIRCLE 44 ON READER SERVICE CARD

BRIEFS

Comparison of Photoacoustic Spectroscopy, Conventional Absorption Spectroscopy, and Potentiometry as Probes of Lanthanide Speciation 298

Photoacoustic spectroscopy provides the same information about the number and strength of metal–ligand complexes as conventional absorption spectroscopy or potentiometry at metal concentrations where the latter techniques are insensitive.

Richard A. Torres*, Cynthia E. A. Palmer, Patricia A. Baisden, Richard E. Russo, and Robert J. Silva, Lawrence Livermore National Laboratory, P.O. Box 808, L-234, Livermore, CA 94551

Kinetics of the Reaction between Aromatic Aldehydes and *o*-Dianisidine 304

Kinetic studies of the Schiff base formation reaction between aromatic aldehydes and *o*-dianisidine provide evidence of a three-path mechanism. Two paths are catalyzed by acetic acid and the other by stannic chloride. Analytical implications of the kinetic studies are discussed.

Mayda Lopez-Nieves, Peter D. Wentzell, and S. R. Crouch*, Department of Chemistry, Michigan State University, East Lansing, MI 48824

Correspondence

Comparison of Diffuse Reflectance and Diffuse Transmittance Spectrometry for Infrared Microsampling 308

David J. J. Fraser, Kelly L. Norton, and Peter R. Griffiths, Department of Chemistry, University of California, Riverside, CA 92521-0403

Differentiation of Leucine and Isoleucine Residues in Peptides by Consecutive Reaction Mass Spectrometry 311

Takemichi Nakamura*, Hidemi Nagaki, Yasuko Ohki, and Takeshi Kinoshita, Analytical and Metabolic Research Laboratories, Sankyo Co., Ltd., 2-58, Hiromachi 1-Chome, Shinagawa-ku, Tokyo 140, Japan

Continuous On-Line Monitoring of Biomolecules Based on Automated Homogeneous Enzyme-Linked Competitive Binding Assays 314

Sylvia Daunert and Leonidas G. Bachas*, Department of Chemistry, University of Kentucky, Lexington, KY 40506-0055 and **Genevieve S. Ashcom and Mark E. Meyerhoff,** Department of Chemistry, The University of Michigan, Ann Arbor, MI 48109-1055

Technical Notes

Polishable and Robust Biological Electrode Surfaces 318

Joseph Wang* and Kurian Varughese, Department of Chemistry, New Mexico State University, Las Cruces, NM 88003

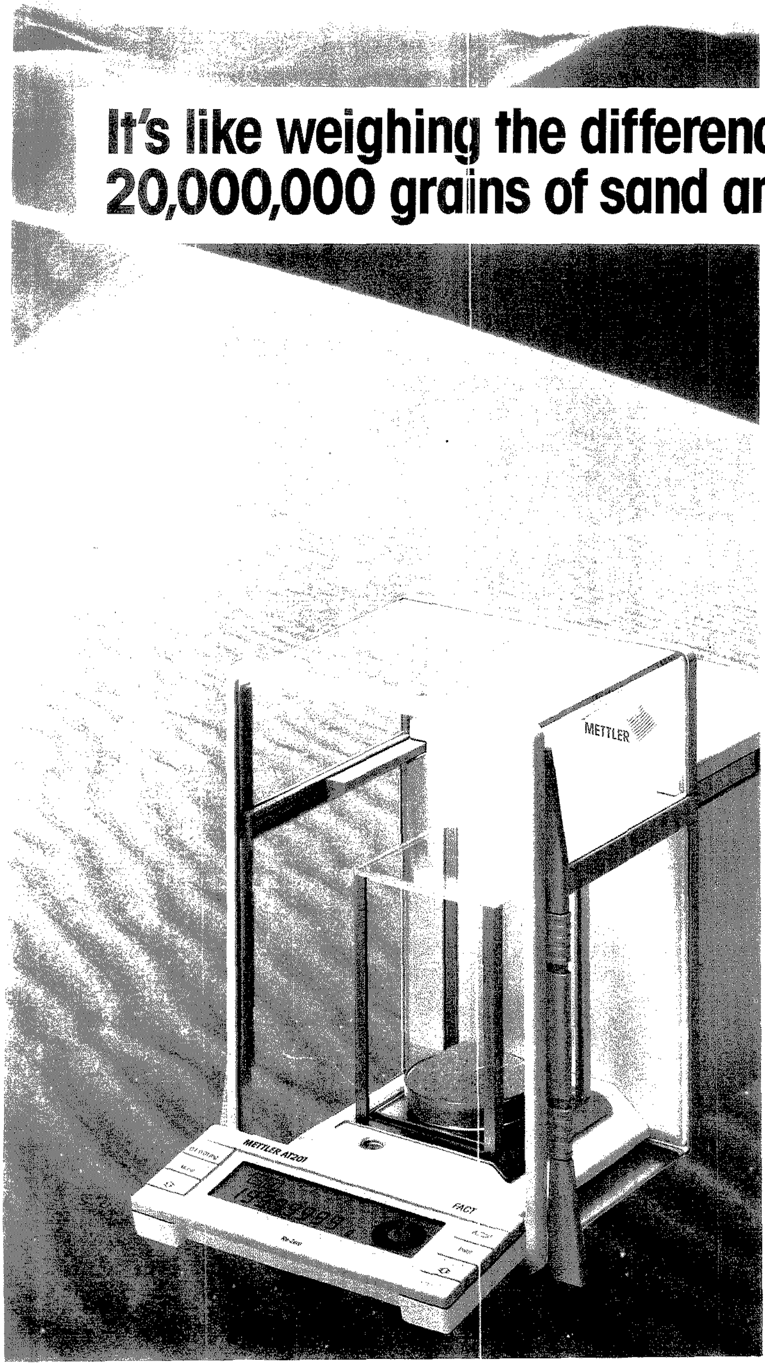

It's like weighing the difference between 20,000,000 grains of sand and 19,999,999.

As infinitesimal as that difference may be, it marks a huge milestone in weighing capabilities: the new METTLER AT201 analytical balance.

It takes you to the peak of technology, with a weighing range of 205 g, readable to one hundred thousandth of a gram.

METTLER not only breaks new ground in bringing you the ultimate in precision, but keeps it intact with FACT—our Fully Automatic Calibration Technology.

All that, plus our exclusive DeltaTrac® automatic weighing chamber doors and the best ergodynamic design. For DeltaRange®, too, ask for our new AT261, with a weighing range of 205 g readable to 0.1 milligram and a DeltaRange of 62 g to .01 milligrams.

When you get down to the nitty-gritty, it's like having 20 million reasons to move up to METTLER.

METTLER balances are available only from Fisher Scientific or VWR Scientific. All products are backed by METTLER Service Plus®

Mettler Instrument Corporation
Box 71
Hightstown, NJ 08520
1-800-METTLER
(NJ 1-609-448-3000)

Come see us at
the Pittsburgh Conference
Booth 4672

CIRCLE 111

METTLER

We understand.
Precisely.

For state-of-the-art research and technology

Journal of Chemical Information and Computer Sciences

An American Chemical Society Publication

George W.A. Milne, **Editor,**
National Institutes of Health

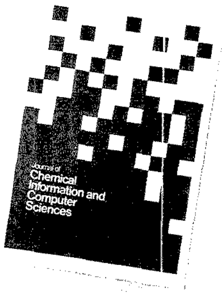

Edited for chemists, chemical engineers, and computer scientists, this international quarterly journal provides highly topical coverage of:

- data acquisition and analysis
- pattern recognition and artificial intelligence
- new algorithms and applications of existing algorithms
- interfacing techniques
- computer systems and components
- graphics, simulation, and modeling
- operations research
- econometric and management systems
- indexing classification and notation systems
- data correlation, information systems, nomenclature, and linguistics and communication
- information sources and services
- design and applications of computerized information and data systems.

The **Journal of Chemical Information and Computer Sciences** includes peer-reviewed research studies, programming innovations, software reviews, invited papers, and book reviews.

Submit your original work!

Under new editorship, the **Journal of Chemical Information and Computer Sciences** is designed to attract the exact audience of experts whom you want to reach. For manuscript guidelines please contact: George W.A. Milne, Building 37, Room 5C28, National Institutes of Health, Bethesda, MD 20892, 301/496-3597.

Associate Editors

W.A. Warr, *ICI, UK*
R. Luckenbach, *Beilstein Institute, Germany*

Software Editor

S. R. Heller, *U.S.D.A.*

Advisory Board

B.A. Hohne, *Rohm & Hass*
C.P. Jochum, *Beilstein Inst., Germany*
G. Kramer, *Purdue Univ.*
C.H. Lochmuller, *Duke Univ.*
S.R. Lowry, *Nicolet Analytical Instruments*
M. Munk, *Arizona State Univ.*
F.A. Settle, Jr., *Virginia Military Inst.*
W.G. Town, *Hampden Data Services Limited, England*
T. Yamamoto, *Univ. of Library Information Science, Japan*

1990 Subscription Information

	U.S	Canada and Mexico	Europe**	All Other Countries**
ACS Members*				
One year	$ 18	$ 22	$ 24	$ 26
Two years	$ 32	$ 40	$ 44	$ 48
Nonmembers	$108	$112	$114	$116

*Member rates are for personal use only.
**Air service included.

For more information or to subscribe, write:

American Chemical Society
Marketing Communications Department
1155 Sixteenth Street, NW
Washington, DC 20036
1-800-227-5558 or (202) 872-4363
TLX 440159
FAX 202/872-4615

For nonmember rates in Japan contact Maruzen Co., Ltd.
This publication is available on microfiche, microfilm, and online on CJO on STN International.

VCH

PITTCON ATTENDEES...

New Titles

METALS AND THEIR COMPOUNDS IN THE ENVIRONMENT
Occurrence , Analysis, & Biological Relevence
Ediitor:Ernest Merian
1990 c.1000pp Cloth 73562-8 $250.00

COME SEE US

THINLAYER CHROMATOGRAPHY
Reagents And Detection Methods, Vol.1a: Physical And Chemical Detection Methods Fundamentals, Reagents
Editors: Hellmut Jork, Werner Funk, Walter Tischer & Hans Wimmer
1990 368pp. Cloth 73876-7 $89.00

AT BOOTH #1314

Two-Dimensional NMR Methods for Establishing Molecular Connectivity
A Random Walk Through Fractal Dimensions
Merck FT-IR Atlas

Journals

ELECTROANALYSIS
Editor:Joseph Wang
Published 8 Times Yearly
ISSN 1040-0397
Institution Rate: $250.00
Individual Rate: $95.00

ELECTROPHORESIS
Editor:B.J.Radola
Published monthly
ISSN 01-73083-5
Institution Rate: $355.00
Individual Rate: $135.00

✱

Order Information
Customer Service Inquiries:
VCH 303 NW12th Avenue
Deerfield Beach,FL 33442
(800)422-8824 ✆ (305)428-5566
For Orders Outside of North America, Please Contact:
VCH , PO Box 101161, D-6940
Weinheim (FRG)
VCH ,(UK)Ltd. 8 Wellington
Court, Wellington Street,
Cambridge CB11HW, England
VCH ,Hardstrasse 10, CH-402
Basel, Switzerland

THERMOCHEMICAL DATA OF PURE SUBSTANCES
Ihasan Barin
KHD Humboldt Wedag Company
Collection of thermodynamic data for 2,450 pure substances stresses chemicals of practical interest to the metallurgist and includes 100 organic compounds.
1989 816pp. Cloth 73866-X $395.00

RAMAN/IR ATLAS OF ORGANIC COMPOUNDS
Second Edition
B.Schrader, University of Essen
Only collection available of Raman and IR spectra plotted on the same wavenumber scale for a large number of carefully selected substances.
1989 1118pp. Cloth 73854-6 $445.00

A RANDOM WALK THROUGH FRACTAL DIMENSIONS
Brian H.Kaye, Laurentian University
Lavishly and beautifully illustrated introduction to the fascinating world of fractal geometry is intended as a "first reader" for those who want to apply fractal systems to their work. Contains numerous graphic examples and suggestions for experiments.
1989 421pp. Cloth 73496-6 $85.00
Paper 73888-0 $39.50

Highlights

TWO-DIMENSIONAL NMR METHODS FOR ESTABLISHING MOLECULAR CONNECTIVITY
A Chemist's Guide to Experiment Selection,Performance, & Interpretation
Gary E. Martin &Andrew S.Zektzer
University of Houston
1988 508pp. Cloth 73703-5 $59.00

MERCK IR ATLAS
A Collection of FT-IR Spectra Part 1
Ediitor:Klaus Pachler Merck
Collection of 3000 frequently used standard spectra .
1988 1174pp. Cloth 73488-5 $550.00

STEREOCHEMICAL APPLICATIONS OF GAS- PHASE ELECTRON DIFFRACTION
Part A The Electron DiffractionTechnique
Part B Structural Information for Selected Classes of Compounds
Editors: Istvan & Magdolna Hargittai
Part A: 1988 563pp. Cloth 73337-4 $100.00
Part B: 1988 511pp. Cloth 73292-0 $100.00
Part A&B 73719-1 $180.00

CIRCLE 193 ON READER SERVICE CARD

TASK MASTER.

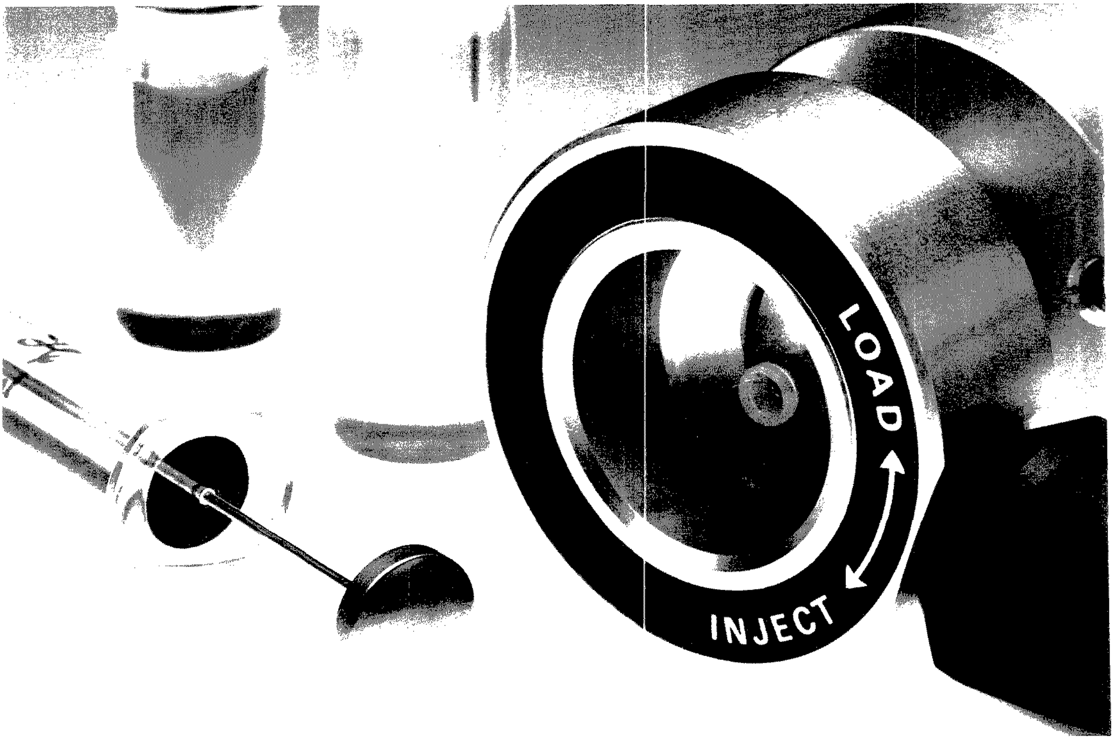

The Rheodyne 7125 LC sample injector is equipped with two operating modes to master every injection task.

In the "partial-fill" mode, the sample from a syringe fills a sample loop only partially. No sample is lost. The amount injected is the exact volume dispensed from the syringe.

You use this mode when you need to conserve sample or change sample volume frequently. You can inject from 1 μL to 2.5 mL with a precision of 1%.

In the "complete-fill" mode, sample from a syringe fills the loop completely–using excess sample. The amount injected is the exact volume of the loop.

You use this mode when you need the maximum volumetric precision of 0.1%, or you wish to load sample without having to read syringe calibrations carefully. You can inject from 5 μL to 5 mL using one of ten interchangeable sample loops.

Variations of the Model 7125 perform yet other tasks. Model 8125 minimizes sample dispersion with micro columns. And Model 9125 uses inert plastic flow passages to prevent the mobile phase from contacting metal.

For more information about these versatile injectors, phone your Rheodyne dealer. Or contact Rheodyne, Inc., P.O. Box 996, Cotati, California, 94931, U.S.A. Phone (707) 664-9050.

CIRCLE 152 ON READER SERVICE CARD

RHEODYNE
THE LC CONNECTION COMPANY

EDITORIAL

Journals Online

Starting this year there will be an ongoing experiment at Cornell University that has the potential to affect every research chemist in the world. It does not involve cold fusion or superconductivity but rather the way in which information about these and many other topics is disseminated and digested. The Chemistry Online Retrieval Experiment (CORE) is exploring the vast potential of electronic search and storage technology and attempting to optimize its use in scientific research.

The hardware required for online literature searching and document storage and display exists, but the CORE project seeks to answer key questions regarding the ideal use of such technology. The human factor is critical to this experiment, and chemists are being provided with the opportunity to directly influence its outcome. The CORE project involves the cooperation of Cornell University's Mann Library, Bellcore, the American Chemical Society, Chemical Abstracts, and the Online Computer Library Center in providing the technical personnel and equipment as well as the documents required for this undertaking. Chemists at Cornell have the honor of serving as subjects in this experiment; they will provide crucial data that should lead to the optimization of this system.

Online searching has been a part of the chemist's literature toolbox for some time. The CORE project seeks to extend this power to full-text search and display. Journals and reports will be fully accessible from the library workstation. What are the questions and problems the experiment will seek to answer? Full-text storage and display adds new dimensions to searching. In addition to key word and subject searches, the user may browse among articles, tables of contents, indices, and so on.

One purpose of this experiment is to determine the optimal searching and browsing features from both the user's perspective and that of an efficient system. The display and storage formats are also critical. Should text be stored as text, with figures added, or will full-page digital reproductions be required? The economics underlying such a project encompass the concerns of publishers, libraries, and users. The overall usefulness of such a system is tied to all of these factors.

The CORE project will seek to answer questions and identify key areas of concern by providing a prototype system at Cornell. Seven years' worth of 20 ACS-published journals will represent a "critical mass" of literature. Workstations will be made accessible so that researchers may use the system. User preferences, comments, and complaints will be used to redesign and reconfigure the system for optimal utility.

The chemistry community is being provided with a rare opportunity to help shape its own future. The success of this experiment will help determine the way in which chemists seek and retrieve information in the next century. Many of us will be closely watching the CORE project with great excitement and anticipation.

Readers who want to learn more about CORE should contact Jan Olsen, Director, Mann Library, Cornell University, Ithaca, NY 14853.

G. H. Morrison

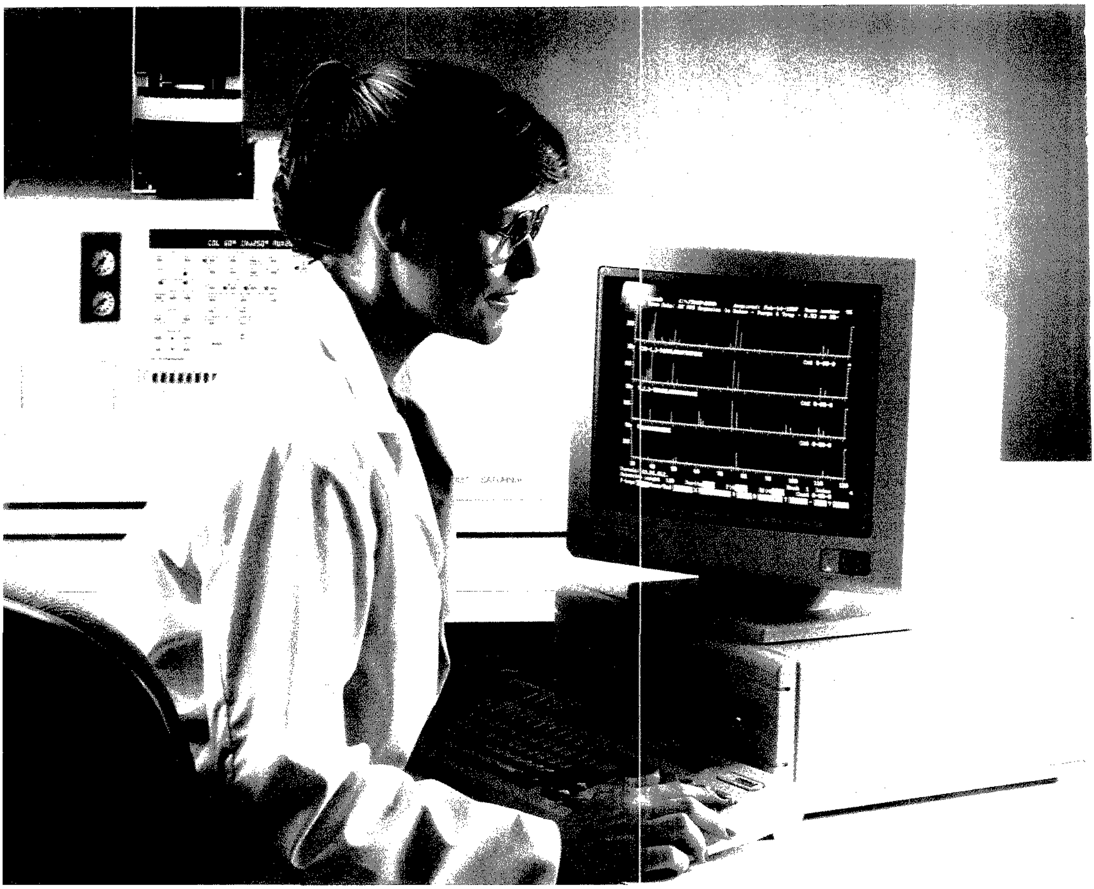

THE FUTURE OF GC/MS IS WITH VARIAN.

The best GC/MS, now and in the future, starts with chromatographic excellence. After all, if you don't start with expert chromatographic techniques, how can you trust the final results? Look to the company known for its expertise — from sample handling to the most sensitive detection — Varian.

The combination of our proven 3400 Gas Chromatograph with second generation ion trap technology brings the most sensitive and reliable benchtop GC/MS to the market.

The new Varian Saturn GC/MS System gives picture perfect spectra even at picogram levels, a significant advantage over conventional benchtop quadrupoles. It's important to know that you can count on the Saturn GC/MS to give you the whole picture when you're confirming compounds, because you're doing scientific analyses that affect our environment, our health, the products we use, and must meet regulatory protocols.

Chromatographic excellence and the most sensitive mass spec detector, coupled with Varian's renowned service and support throughout the world, make this the GC/MS with a future.

Let us show you why you should invest your GC/MS future with Varian. For more information, call **800-231-8134**.
In Canada, call **416-457-4130**.

VIG-5159/259 9/89

See you at Pittsburgh Conference, Booth 4736-4934 & 5042.
CIRCLE 204 ON READER SERVICE CARD

GC WITH A FUTURE

41st Pittsburgh Conference and Exposition

Jacob K. Javits Convention Center
New York City, March 5–9, 1990

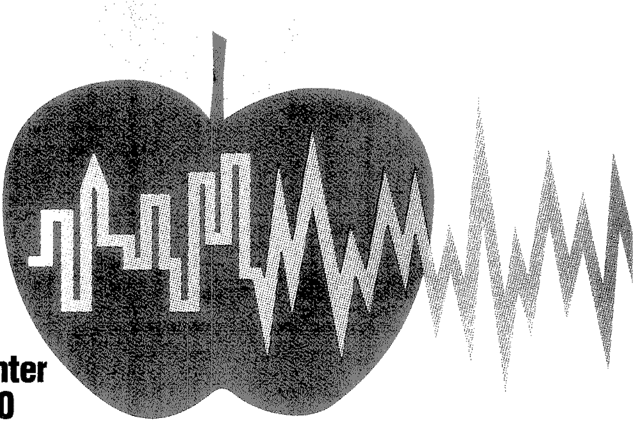

The 41st Pittsburgh Conference and Exposition on Analytical Chemistry and Applied Spectroscopy will be held March 5–9 in New York City. This year's technical program will include 31 symposia and more than 1200 contributed papers and poster presentations. The Exposition of Modern Laboratory Equipment, to be held Monday through Thursday, will feature 800 exhibitors in more than 2500 booths showing state-of-the-art analytical instrumentation, chemicals, equipment, supplies, and services. The exposition and all technical sessions will be housed in a single facility, the Jacob K. Javits Convention Center.

Eight scientists who have contributed extensively to analytical chemistry and applied spectroscopy will receive awards during conference symposia.

The 1990 Pittsburgh Analytical Chemistry Award, sponsored by the Society for Analytical Chemistry of Pittsburgh, will be presented to George H. Morrison of Cornell University at an award symposium on Tuesday, March 6. Morrison, Editor of ANALYTICAL CHEMISTRY, has made significant contributions in the fields of trace element chemistry and materials characterization and has been a leader in the development of a number of analytical methods, including ion microscopy, neutron activation analysis, and atomic spectroscopy.

The 1990 Pittsburgh Spectroscopy Award will be given to Charles B. Harris of the University of California, Berkeley, in recognition of his contributions to the field of spectroscopy. Harris' research is in the areas of optically detected magnetic resonance, energy transfer in solids, vibrational relaxation, picosecond spectroscopy, and chemical dynamics in liquids. Sponsored by the Spectroscopy Society of Pittsburgh, the award will be presented on Wednesday, March 7.

The Dal Nogare Award will be presented by the Chromatography Forum of the Delaware Valley to Robert L. Grob of Villanova University. Grob is being recognized for his achievements in the field of chromatography, particularly for his work on theory, instrumentation, and applications of GC and LC to environmental analysis. The award presentation will be made at a symposium on Monday, March 5.

The Charles N. Reilley Award will be presented to Jean-Michel Saveant of the Université de Paris VII at a symposium on Tuesday, March 6. Saveant's research has focused on the rates and mechanisms of chemical reactions that are triggered by electron transfer at electrodes. The award is sponsored by Bioanalytical Systems and the Reilley Endowment Fund of the Society for Electroanalytical Chemistry (SEAC) and is administered by SEAC.

The 1990 Williams–Wright Award, sponsored by the Coblentz Society, will be given to John F. Rabolt of IBM Almaden Research Laboratory for his contributions to the field of vibrational spectroscopy. Rabolt, whose current research involves the characterization of polymer structure, morphology, and orientation in the solid state using FT-IR and Raman spectroscopy, will be presented with the award on Tuesday, March 6.

The Keene P. Dimick Award will be presented to Milos Novotny of Indiana University on Monday, March 5. The award, sponsored by Keene P. Dimick and administered by the Society for Analytical Chemists of Pittsburgh, recognizes Novotny for his achievements in the field of chromatography.

The Bomem–Michelson Award will be presented by the Coblentz Society to William Klemperer of Harvard University. Klemperer's research interests are in the areas of molecular structure, energy transfer, and intermolecular forces. Klemperer will receive the award on Thursday, March 8.

The Tomas Hirschfeld Award will be given to Charles E. Miller of the University of Washington on Tuesday, March 6. Sponsored by Bran+Luebbe Analyzing Technologies, the award recognizes Miller's contributions to the field of near-IR spectroscopy.

The 1989 Pittsburgh Conference Memorial National College Grants, sponsored by the Pittsburgh Conference on Analytical Chemistry and Applied Spectroscopy, the Spectroscopy Society of Pittsburgh, and the Society for Analytical Chemists of Pittsburgh, have been awarded to these colleges: Allen University, Columbia, SC; Ashland College, Ashland, OH; College of St. Mary, Omaha, NE; Earlham College, Richmond, IN; Gordon College, Wenham, MA; Hope College, Holland, MI; Lake City Community College, Lake City, FL; Messiah College, Grantham, PA; Mount Holyoke College, South Hadley, MD; Northland Community College, Thief River Falls, MN; and St. Mary's College, Winona, MN.

Summary of Technical Sessions

March 5

Monday Morning

SYMPOSIUM: Keene P. Dimick Award
SYMPOSIUM: Frontiers in Analytical Toxicology and Substance Abuse Testing
SYMPOSIUM: Multidimensional Analysis Systems
Applications on Surface-Enhanced Raman Spectroscopy
Advances in CCD/Raman Spectroscopy
Electrochemistry—Spectroelectrochemistry and Mechanisms
Environmental MS
GC/FT-IR/MS-PAS-ATR Methods
Microwave Digestion
GC—Food and Pharmaceutical Separations
GC—High-Purity Gases
HPLC—Food Analysis
ICP-AES—Analytical Procedures I
Infrared I—Quantitative Analyses
Instrumentation in Biochemistry
New Developments in Well-Known Biochemical Techniques
LIMS Implementation Topics
Polymer Separations
SFC
Tandem MS
POSTER SESSIONS

Monday Afternoon

SYMPOSIUM: Biosensors et al.—Analysis Outside the Laboratory
SYMPOSIUM: Characterization of High-Temperature Superconducting Oxides
SYMPOSIUM: Dal Nogare Award
SYMPOSIUM: Role of Array Detectors in Spectrochemical Analysis
Clinical Analyses
Countercurrent Chromatography
Electrochemistry—Microelectrodes and Modified Electrodes
GC—New Instruments and Techniques
HPLC—Ion Chromatography
HPLC—Stationary-Phase Chemistry
ICP/MS and Glow Discharge MS
ICP-AES—Analytical Procedures II
Infrared II—Microspectroscopy
Quality Assurance through Automation and Information
Separations of Pharmaceutical Interest
Spectral Absorption: Fluorescence—Environmental Applications
POSTER SESSIONS

March 6

Tuesday Morning

SYMPOSIUM: Advances in Raman Spectroscopy
SYMPOSIUM: Data Tools for Solving Analytical Chemistry Problems
SYMPOSIUM: Laboratory Management—An International Perspective on Excellence
SYMPOSIUM: Pittsburgh Analytical Chemistry Award—Biomedical Analytical Chemistry
SYMPOSIUM: Quality and Productivity with Chromatographic Methods I
Electrochemistry—Microelectrodes and Modified Electrodes
AA—Analytical Procedures I
Environmental—Air and Soil Analysis
GC—Petroleum
GC—Theoretical Aspects
HPLC—Stationary Phases I
HPLC—Novel Detection
ICP-AES—Nebulizers and Sample Introduction
Infrared III—Apparatus and Techniques A
Near-IR (Tomas Hirschfeld Award in Near-IR Analysis)
Separations of Pharmaceutical Interest
SFE
POSTER SESSIONS

Tuesday Afternoon

SYMPOSIUM: Recent Advances in High Molecular Weight MS
SYMPOSIUM: Laboratory Accreditation and Standardization: Perspectives on Europe in 1992 (EC '92)
SYMPOSIUM: Quality and Productivity with Chromatographic Methods II
SYMPOSIUM: Charles N. Reilley Award
SYMPOSIUM: Williams-Wright Award
Atomic Spectroscopy—Insights and Analysis
Environmental Water Analysis I
Food Analysis
Hadamard Spectrometry
GC—Techniques
HPLC—Stationary Phases II
HPLC—In the Life Sciences
Near-IR Processes
Flow Analysis
Planar Chromatography
Raman Spectroscopy
Spectral Absorption: Fluorescence—Chemical Applications
SFE—Chromatography
POSTER SESSIONS

In 1990 at least 10 colleges will be selected to receive grants, which are to be used for the purchase of equipment, audiovisual and other teaching aids, and library materials for undergraduate-level science instruction. Information about eligibility and the submission of proposals appears in the Nov. 15, 1989, issue (p. 1255 A).

For the first time at the Pittsburgh Conference, a symposium will be held to recognize groups of people who have collaborated on the invention, development, and implementation of analytical instrumentation of exceptional importance. This year's James L. Waters Symposium Recognizing Pioneers in the Development of Analytical Instrumentation, to be held on Wednesday, March 7, will be devoted to the field of gas chromatography.

Registration fees are $40 for advance and $70 for on-site registration; $10 for advance or on-site registration of students; $35 for advance and $50 for on-site registration of spouses; and $20 for advance or on-site registration for the exposition only. Registration forms are available in the preliminary program or can be obtained from Mary Louise Theodore, Pittsburgh Conference, 300 Penn Center Blvd., Suite 332, Pittsburgh, PA 15235.

Conferees can arrange hotel and airline reservations at special rates by contacting Travel Planners, Inc., 114 East 25th St., New York, NY 10010 (1-800-221-3531; fax 212-995-5644). Additional information about housing and transportation appears in the preliminary program.

A continuing education program will again be offered. Registration and fee information is available in the preliminary program. Course offerings include the following: LIMS for Laboratory Managers—Strategic Issues, A Basic Introduction to Chirality and Its Impact on Industrial Analytical Separations, Write Way to Success, Practical MS/MS Analysis, Professional Analytical Chemists in Industry, Overview of Near-Infrared Spectroscopy, Basic Statistics for the Analytical Chemist, Introduction to Quality Assurance, Integrating Computer Spreadsheets into the Analytical Chemistry Course, LC and GC for Technicians, On-line Analysis, Principles and Practices of Capillary Zone Electrophoresis, Safety in Science Laboratories, Searching and Using Chemical Information, Applications of Supercritical Fluid Extraction to Environmental Analysis, Atmospheric Pressure Ionization MS Detection for the Separation Sciences, Environmental Laboratory Services—Communicating Your Needs, Introduction to SFC, Laboratory PC Applications—

March 7

Wednesday Morning

SYMPOSIUM: Catastrophic Environmental Problems
SYMPOSIUM: Chromatography and MS in Studies on Human Diseases
SYMPOSIUM: International Regulatory Issues on Chiral Drugs
SYMPOSIUM: Pittsburgh Spectroscopy Award
Capillary Electrophoresis
Electrochemistry—Detectors
GC—Environmental I
HPLC—Chiral Separations
HPLC—Pharmaceutical Applications
HPLC—Stationary Phases III
ICP-AES—Instrumental Concepts
Infrared IV—Apparatus and Techniques B: Applications
Near-IR—Applications and Data Processing
Personal Computer Networking Solutions for Laboratory Data Management
Postanalysis Data Processing
Remote Chemical Vapor Sensing
Spectral Fluorescence and Absorption
POSTER SESSIONS

Wednesday Afternoon

SYMPOSIUM: ASTM E-42: Recent Advances in Surface Analysis
SYMPOSIUM: Characterization and Analysis of Chiral Compounds
SYMPOSIUM: Selectivity in Capillary Electrophoresis
SYMPOSIUM: James L. Waters First Annual Symposium Recognizing Pioneers in the Development of Analytical Instrumentation: GC
Advanced Topics in Chemical Computing
AA—Analytical Procedures II
Electrochemistry—Detectors and Sensors
GC—Environmental II
HPLC—In the Life Sciences II
LC; GC/MS
Laser MS; FT-MS
Microseparations
New Atomic Spectroscopy Instrumentation; X-ray Fluorescence
Pattern Recognition and Signal-Processing Techniques for Organic Spectroscopic Analysis
Preparative LC
Thermal Analysis for Process Monitoring
POSTER SESSIONS

March 8

Thursday Morning

SYMPOSIUM: Bomem-Michelson Award
SYMPOSIUM: Information Technology: Integrating the Laboratory into the Corporation
SYMPOSIUM: Women in Science: A Blueprint for Progress
Analysis of Fuels
Capillary Electrophoresis
Characterization of Polymers and Coatings Using Thermal Analysis
Electrochemistry—Voltammetry
Environmental Water Analysis II
GC—Instrumentation I
HPLC—Environmental and Solubility
HPLC—Multiwavelength Detectors
MS Ion Sources
New Spectrometer Designs
Optical Methods—Biomedical Applications
Powder Characterization
Particle Size Analysis
Sampling—Sample Preparation: General
Biological Sequences and Profiles
POSTER SESSIONS

Thursday Afternoon

SYMPOSIUM: Applications of Microdialysis in Biological Systems
SYMPOSIUM: Polymer Characterization in Food Packaging Applications
SYMPOSIUM: Selective Detectors for GC—Practical Aspects
AA—Instrumentation
Clinical Fluorescence
Surface Characterization of Materials
Electrochemistry
Environmental; Pesticide Analysis Methods
GC—Instrumentation II
HPLC—Instrumentation
HPLC—Systems and Validation
Infrared V—Hyphenated Techniques and IR-Raman
MS General/Data Systems
New Instrumentation for Chromatography
New Instrumentation—General
Novel Separation, Extraction, and Detection Techniques
On Line; In-Line; Quality Control; Process Analysis
Spectrometric Instrumentation and Techniques
POSTER SESSIONS

Combining the Power of Spreadsheet and Data Management Programs, Precontrol as an Effective Method of Statistical Process Control, Preparation and Presentation of Posters, Presentation Strategies for Scientists, Principles and Practices of Spectroscopic Calibration, and Understanding and Meeting Quality Standards.

The American Chemical Society is also sponsoring 40 short courses in conjunction with the conference. For additional information, see the Jan. 15, 1989, issue of ANALYTICAL CHEMISTRY (pp. 76 A–78 A) or contact the Department of Continuing Education, American Chemical Society, 1155 16th St., N.W., Washington, DC 20036 (202-872-4508).

User–Manufacturer Information Exchanges on chromatography data systems, ICP-AES, LC/MS, and near-IR spectroscopy will be held on Friday, March 9. Preregistration information is available in the preliminary program.

An employment bureau will be available to regular conferees and students during the conference. Preregistration information for prospective employers and candidates is available in the preliminary program or can be obtained from H. Schultz, Pittsburgh Conference, 300 Penn Center Blvd., Suite 332, Pittsburgh, PA 15235.

The Spouses Committee has planned a variety of activities, including a tour of lower Manhattan, a quilting workshop, breakfast and shopping at Bloomingdale's, a trip to the Cloisters, and a traditional Japanese tea party. The Spouses Hospitality Suite, in the Rhinelander Ballroom of the Hilton Hotel, will be open daily for use by registered spouses. For further information, contact Patrick Byrne at the Pittsburgh Conference address given below.

Social activities planned for the conference include a registration mixer on Sunday evening and a conference mixer on Tuesday evening, tours of New York and the Statue of Liberty, and the Broadway show, "Phantom of the Opera." Additional details are available in the preliminary program or at the activities booth in the North Concourse of the Javits Center.

For additional information about any aspect of the conference or exposition, contact the Pittsburgh Conference, 300 Penn Center Blvd., Suite 332, Pittsburgh, PA 15235 (1-800-825-3221).

The complete technical program begins on p. 129 A. The NEW PRODUCTS section (p. 242 A) features instruments and other products that will be introduced at the conference.

1990 Board of Directors

President: Ann E. Cibulas
Vice-President: Ernest F. Tretow
Immediate Former President: Paul E. Bauer
Chairman, Society for Analytical Chemists of Pittsburgh: Mary Louise Theodore
Chairman-Elect, Society for Analytical Chemists of Pittsburgh: Gary W. Christian
Chairman, Spectroscopy Society of Pittsburgh: John W. Novak
Chairman-Elect, Spectroscopy Society of Pittsburgh: Herald L. Barnett
Treasurer: W. Richard Howe
Assistant Treasurer: Joanne H. Smith
Secretary: Andrew G. Sharkey

Ann E. Cibulas
President

Ernest F. Tretow
Vice-President

Gerst A. Gibbon
Program Chairman

Gary W. Christian
Exposition Chairman

Mary Louise Theodore
Registration Chairman

Conference Committees

Activities
Chairman: Charles W. Gardner
Chairman-Elect: Mildred B. Perry

Audiovisual
Chairman: Samuel S. Oliverio
Chairman-Elect: Arthur J. Olszewski

Committee Arrangements
Chairman: John P. Auses
Chairman-Elect: Betty J. Sparr

Computer Utilization
Chairman: Dennis R. Balya
Chairman-Elect: Keith K. Trischan

Employment
Chairman: Hyman Schultz
Chairman-Elect: Lan K. Wong

Exposition
Chairman: Gary W. Christian
Chairman-Elect: Victor C. Zadnik

Security
New York Liaison: John W. Enyart
Chairman-Elect: Herald A. Barnett

Finance
Chairman: Joanne H. Smith

Housing
Chairman: Debbie C. Hreha
Chairman-Elect: Edward A. Naylor

Label Service
Assistant Treasurer: Joanne H. Smith

Meetings Coordinator
Chairman: Sarah L. Shockey
Chairman-Elect: David F. Pensenstadler

Negotiations
John E. Graham

Philatelic
Chairman: John A. Queiser
Chairman-Elect: Roy Backer

Policy
Chairman: John E. Graham

Printing and Mailing
Chairman: Kathy J. Rygle
Chairman-Elect: Jonell Kerkoff

Program
Chairman: Gerst A. Gibbon
Chairman-Elect: David R. Weill, III

Property, Insurance, and Equipment
Chairman: Denton M. Albright
Chairman-Elect: Neal Dando

Publicity/Public Relations
Chairman: John D. Sember
Chairman-Elect: John W. Novak

Registration
Chairman: Mary Louise Theodore
Chairman-Elect: Michael N. Carmosino

Relocation Advance
Chairman: Ernest F. Tretow
Chairman-Elect: John P. Auses

Site Selection
Chairman: Richard S. Danchik

Special Projects
Chairman: Paul E. Bauer

Spouses Program
Chairman: Patrick J. Byrne
Chairman-Elect: Mariene L. Bauer

Transportation
Chairman: Jon N. Peace
Chairman-Elect: Thomas J. Conti

More choices.
The ITD™ works with the column of your choice. And you can add CI capabilities now or later.

Easier to use.
You don't need a lot of experience to be up and running fast on the ITD. Just ask an ITD user.

Simple maintenance.
The ITD is designed so that you spend less time cleaning the ion source and more time running samples and producing results.

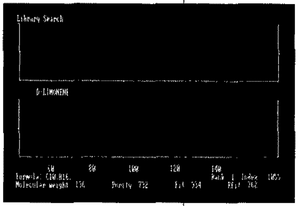

More information.
Get library-searchable, full-scan mass spectra for positive identification throughout the entire concentration range.

To profit from the performance that only the ITD can deliver, contact your Finnigan MAT representative today.

The ITD just gained one more advantage over the MSD.

More value.
A *complete* GC/MS/DS for $49,500. Place your order for the ITD 804A GC/MS with COMPAQ® PC by March 15, 1990, and receive a 23% discount off the U.S. list price.*

Finnigan MAT

U.S. DISTRICT OFFICES
Southwest, Placentia CA · (714) 961-0727
Northwest, San Jose, CA · (408) 433-4800
Atlanta, Marietta, GA · (404) 424-7880
Midwest, Schaumburg, IL · (708) 310-0140
Washington, D.C., Frederick, MD · (301) 698-9750
Boston, Andover, MA · (508) 975-5339
New Jersey, Livingston, NJ · (201) 740-9177
Central, Cincinnati, OH · (513) 891-1255
Houston, Houston, TX · (713) 449-0253

*For orders placed and delivered within the United States only.

ITD is a trademark of Finnigan Corporation. COMPAQ is a registered trademark of Compaq Computer Corporation.

CIRCLE 60 ON READER SERVICE CARD

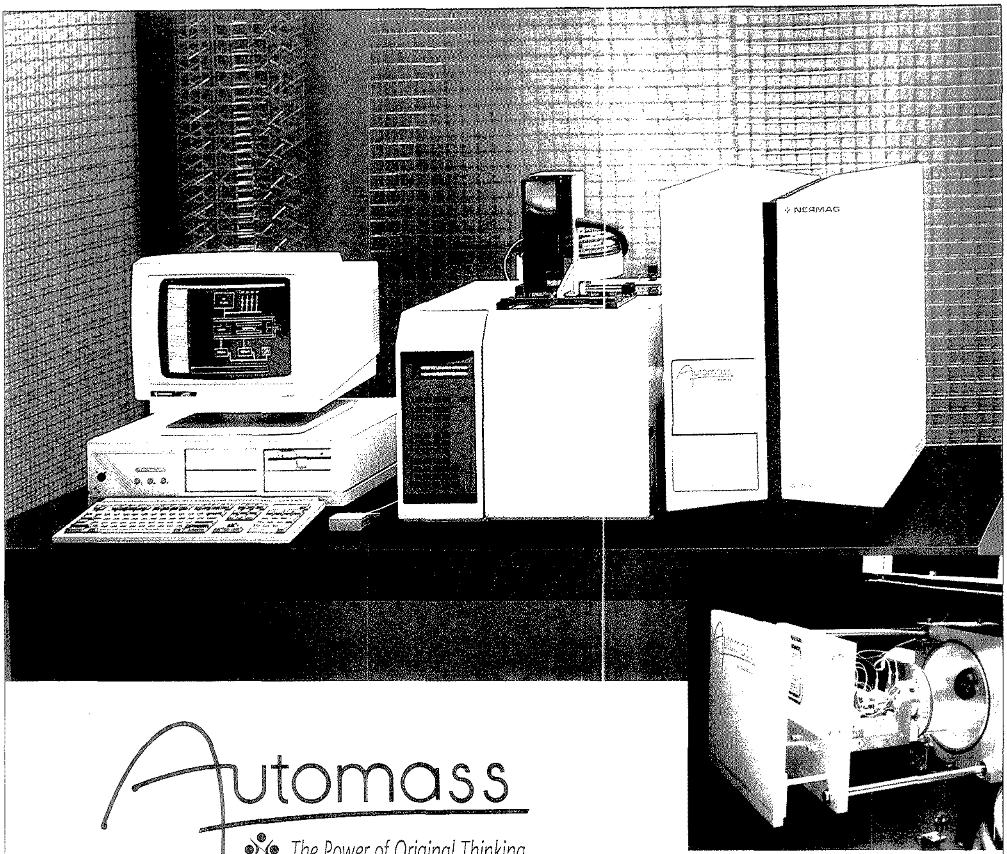

Automass

The Power of Original Thinking

When Nermag set out to develop the premier Automated Benchtop GC/MS Workstation, we were aware there was a need - *your need*, for more analytical power. Power that is simple to use, yet flexible enough to tackle the toughest problems. A true research-grade mass spectrometer was required, not a compromised mass analyzer camouflaged by glitzy game-show software.

Introducing Automass, the benchtop mass spectrometer that only Nermag could build, and the only one of its kind in the world today. The basis of Automass is a state of the art quadrupole with plug-in prefilters and an optimized Ionization Source for EI, CI, and negative ions. Our original Off Axis Ion - Photon Conversion Detector and patented Resolver electronics are enhanced by a differentially pumped vacuum system for real CI spectra.

Automass is controlled by our exclusive LUCY™ software. LUCY does window after window of instrument configuration setting, auto or manual tuning, calibration, mass spectra, chromatographic trace, and data reduction; while simultaneously examining the complete library and quantifying results. You'll Love LUCY.

Automass can flawlessly perform routine analysis all day virtually unattended, or help you tackle the most difficult analytical problem.

Automass advances Mass Spectrometry into the 90's.

Powerfully.

DELSI
NERMAG
INSTRUMENTS

France: Delsi-Nermag Instruments, 98terBlvd. Heloise, Argenteuil 9500, Tel: (1) 39.47.66.22, Fax: (1) 39.47.85.66
USA: Delsi Inc., 15701 West Hardy Rd. Houston, TX 77060, Tel: (713) 847-0811, Fax (713) 591-2132
Netherlands: Delsi Instruments BV, Gebouw aetsvelt, van Houten Ind Pk 11, 1381 Weesp, Tel: (0)2940-19611
U.K.: Delsi Instruments Ltd, 38 Thrapston Rd., Brampton, Huntington, Cambs PE 18 8TE, Tel: 0480 431 609
West Germany: Delsi Instruments Gmbh, Otzbachstr 1 D4020 Mettmann, Tel: 02104/25086-87-88
Belgium: Intersmatt, 103, Av. des Volontaires, 1160 Bruxelles, Tel: 2 733.16.32

CIRCLE 38 ON READER SERVICE CARD

1990 Technical Program

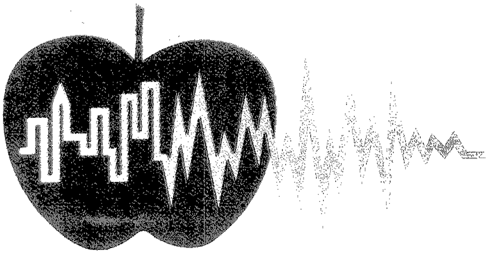

Monday, March 5, 1990

SYMPOSIUM

Keene P. Dimick Award - arranged by M.V. Novotny of Indiana University

Monday Morning, Room 1A06

8:30 (001) **New Selective Stationary Phases for Microcolumn Chromatography**—M.L. LEE, Brigham Young University

9:05 (002) **Combined Techniques in Microcolumn Chromatography**—K.D. BARTLE, The University of Leeds

9:40 (003) **When Other Separation Techniques Can't Do the Job, Can SFC?**—S.V. OLESIK, The Ohio State University

10:15 RECESS

10:30 (004) **Resolution in Chemical Analysis**—J.W. JORGENSON, University of North Carolina, Chapel Hill

11:05

Keene P. Dimick Award
Presented by
Keene P. Dimick
to
Milos V. Novotny
Indiana University

11:15 (005) **Award Address: Development of Bioanalytical Methods Based on Capillary Chromatography and Electrophoresis**—M.V. NOVOTNY, Indiana University

SYMPOSIUM

Frontiers in Analytical Toxicology and Substance Abuse Testing - arranged by S.H.Y. Wong of University of Connecticut

Monday Morning, Room 1A23
S.H.Y. Wong, Presiding
University of Connecticut

8:30 (006) **Keynote Address: Challenges and Opportunities of Analytical Toxicology in the '90s**—I. SUNSHINE, Case Western University

9:05 (007) **Olympic Drug Testing: Advances in Analytical Considerations of Doping Control of Banned Substances and Anabolic Steroids**—B. SAMPLE, Indiana University Medical Center

9:40 (008) **GC/MS Analysis of High Potency Drugs of Abuse - Fentanyl, LSD, and Triazolam**—R.L. FOLTZ, University of Utah

10:15 RECESS

10:30 (009) **LC/MS, SFC/MS and Capillary Electrophoresis/MS for Pharmaceutical Analysis**—J. VAN DER GREEF, Leiden University

11:05 (010) **Supercritical Fluid and Microbore Liquid Chromatography for Clinical Analysis**—S.H.Y. WONG, University of Connecticut

SYMPOSIUM

Multidimensional Analysis Systems - arranged by J.F.K. Huber of University of Vienna

Monday Morning, Room 1D01
J.F.K. Huber, Presiding
University of Vienna

8:30 **Introductory Remarks**—J.F.K. HUBER

8:35 (011) **Multidimensional Chromatography**—J.F.K. HUBER, University of Vienna

9:10 (012) **Multidimensional Systems Involving Mass Spectrometry**—F.W. McLAFFERTY, Cornell University

9:45 (013) **Multidimensional Systems Involving Molecular Spectroscopy**—P.R. GRIFFITHS, University of Idaho

10:20 RECESS

10:35 (014) **Multidimensional Systems Involving Atomic Spectroscopy**—G.M. HIEFTJE, Indiana University

11:10 (015) **Analysis of Data in the Multidimensional Space**—B.R. KOWALSKI, University of Washington

Applications on Surface Enhanced Raman Spectroscopy

Monday Morning, Room 1E06
A. Ahern, Presiding
Aluminum Company of America

8:30 (016) **Surface-Enhanced Raman Spectroscopy of Oligopeptides**—T.M. HERNE, University of Pittsburgh, R.L. Garrell

8:50 (017) **Surface-Enhanced Hyper-Raman and FT-Raman Scatterings Excited in the Near-IR Region**—S. NIE, Georgia Institute of Technology, N.T. Yu

9:10 (018) **Investigating Subsurface and Surface of Graphite-Like Carbons and Silicon Carbide Ceramics by Raman/Surface-Enhanced Raman Spectroscopy**—M.A. TADAYYONI, Long Island University, N.R. Dando

9:30 (019) **Surface-Enhanced Raman Spectroscopy of Phenylthiol, Benzylthiol and *p*-Cyanobenzylthiol Adsorbed on Gold Electrodes**—W. TANNER, University of Pittsburgh, R.L. Garrell

9:50 (020) **High Temperature Micro-Surface Enhanced Raman Measurements of Organic Chlorine Derivatives in the Adsorbed State**—E. KOGLIN, Institute of Applied Phys. Chem., C.G.B. Frischkorn

Advances in CCD/Raman Spectroscopy

Monday Morning, Room 1E06
A. Ahern, Presiding
Aluminum Company of America

10:25 (021) **Evaluation of a Diode Laser/CCD Raman Spectrometer for Near-Infrared Raman Spectroscopy**—Y. WANG, The Ohio State University, R.L. McCreery

10:45 (022) **Development and Application of a Rugged, Portable Raman/CCD Spectrometer for Fiber Optic Spectroscopy**—A. LEUGERS, Dow Chemical Company, R. McLachlan, L. Wright

11:05 (023) **Raman Spectroscopic Applications with a Near-IR Laser and CCD Detector**—F.J. PURCELL, SPEX Industries, Inc., J. Bello

11:25 (024) **Two-Dimensional Encoding of Raman Scattering for Detection with a Charge Coupled Device**—M.J. PELLETIER, The Procter & Gamble Company

11:45 (025) **Recent Advances in CCD Detection Raman Spectroscopy**—J.S. BABIS, Photometrics Ltd.

Electrochemistry: Spectroelectrochemistry and Mechanisms

Monday Morning, Room 1E12
J.G. Osteryoung, Presiding
State University of New York at Buffalo

8:30 (026) **Diffusion Layer Imaging and the Related Electrochemistry Studied by Spatially Resolved Spectroelectrochemical Technique**—H.P. WU, The Ohio State University, R.L. McCreery

8:50 (027) **Fluorescence Spectroelectrochemistry of Pyrene on Silver Electrodes**—J.F. RUSLING, University of Connecticut, M.F. Ahmadi

9:10 (028) **Spectroelectrochemical Characteristics of the Reticulated Vitreous Carbon Electrode**—J.W. SORRELS, Ohio University, H.D. Dewald

9:30 (029) **Electrochemical and Thermodynamic Behavior of N_2O_5 in Aprotic and Protic Media: Nitrating Characteristics**—A. BOUGHRIET, University of Lille, E.H. Jackson, M. Wartel

9:50 (030) **Influence of Iron on the Oxidation State of Manganese in Seawater: Electrochemical and ESR Spectroscopic Studies**—A. BOUGHRIET, University of Lille, P. Guegueniat, M. Wartel

10:10 RECESS

10:25 (031) **Hydrogen Reduction at Pd in 0.1 M LiOH: Electrochemical Impedance Spectroscopy**—R.S. RODGERS, EG&G Princeton Applied Research

10:45 (032) **Problems of Data Analysis in Cyclic Voltammetry**—D.K. GOSSER, The City College of CUNY

11:05 (033) **Spectroelectrochemistry: Construction of a Gold Minigrid Optically Transparent Thin Layer Electrode by Vaporizing and Etching**—J. DENG, Fudan University, X. Wu, Z. Deng, H. Chen, Z. Fang, Q. Yan

Environmental Mass Spectrometry

Monday Morning, Room 1E08
R.A. Hites, Presiding
Indiana University

8:30 (034) **Networking in a Major Environmental GC/MS Laboratory Enhances Productivity and QA/QC**—J.M. SOROKA, US Environmental Protection Agency, J. Griffiths, J. Rubin, D. Lillian

8:50 (035) **A Graphics-Driven Totally Automated System for Environmental Analyses**—S. KENNERLEY, Kratos Analytical, D. Milton, P.A. Ryan, R. J. Greathead

9:10 (036) **The Design and Performance of a New Mass Spectrometer for Fully Automated Analysis**—A.D. HOFFMAN, Kratos Analytical, M. Kearns, P.A. Ryan, R.J. Greathead

9:30 (037) **Use of a Temperature-Programmable Injector for Improved Performance in Environmental GC/MS Analyses**—K.L. JOHNSON, Finnigan MAT, M.M. Booth, C.S. Campbell

9:50 (038) **Ultratrace Analysis of Dioxin Using Bench Top GC/MS in Full Scan Mode**—W. HOLMES, Varian Instrument Group, N. Kirshen

10:10 RECESS

10:25 (039) **Analysis of Semi-Volatile Organics in Drinking Water by EPA Method 525 Using Solid Phase Extraction and the Ion Trap System**—J.L. STEPHENSON, JR., Finnigan MAT, D.C. Bradford, C.H. Hameister, W. Holmes

10:45 (040) **Performance Assessment of a Mass Selective Detector for the Determination of Extractable Trace Organics in Water**—L.C. DOHERTY, Hewlett-Packard Company, D.E. McIntyre, P.D. Perkins

11:05 (041) **Validation Studies with a Particle Beam LC/MS Method for Selected Environmental Compounds**—T. MARECIC, Extrel Corporation, R.C. Willoughby, M. Dilts

11:25 (042) **The Environmental Monitoring of Corrosive Gases by Mass Spectrometry**—T.M. DAVIDSON, The Perkin-Elmer Corporation, P. Peacock, W. Niu

11:45 (043) **Advances in EPA Method 524,2 Purge and Trap Analysis**—B.B. BERNARD, O. I. Analytical

GC/FTIR-MS-PAS-ATR Methods

Monday Morning, Room 1E15
C.W. Brown, Presiding
University of Rhode Island

8:30 (044) **Identification of Decomposition Products of Polyphenylethers by GC/FTIR-MS**—E.W. PITZER, Wright Research & Develop. Center

8:50 (045) **Studies of the Cross-Linking of Cotton Cellulose by FTIR Photoacoustic Spectroscopy**—C.Q. YANG, Marshall University

9:10 (046) **Studies of the Oxidation of Cotton Fabrics by FTIR Photoacoustic Spectroscopy**—C.Q. YANG, Marshall University, J.M. Freeman

9:30 (047) **Comparison of Transmission and Reflection Fourier Transform-Infrared (FTIR) Methods for the Analysis of Cement Blends**—T.V. REBAGAY, Westinghouse Hanford Company, D.A. Dodd, J.P. Sloughter

9:50 (048) **Infrared and Mass Spectrometric Studies of Plasticizer Decomposition During Ceramic Sintering**—A. NAIR, University of Oklahoma, R.L. White

10:10 RECESS

Microwave Digestion

Monday Morning, Room 1E15
C.W. Brown, Presiding
University of Rhode Island

10:25 (049) **And They Said It Couldn't Be Done by Microwave Digestion**—D. MATHE, Questron Corp., Prolabo, F. Barbier, A. Grillo

10:45 (050) **A New Robotics System for Microwave Digestion**—R. RUBIN, Questron Corporation, R. Reilly, C. Balas, D. Bell

11:05 (051) **Microwave Digestion - Pressure Control and Monitoring, a Meaningful Step Towards True Reproducibility**—T. FLOYD, Floyd Associates, A. Grillo

11:25 (052) **Use of Microwave Digestion as a Method of Sample Preparation for the Compositional Analysis of Electrically-Active Ceramics**—E.C. GAPASIN, Raychem Corporation, C.A. Austin

11:45 (053) **An Evaluation of Microwave Technology for the Hydrolysis of Proteins**—C. WOODWARD, Hewlett-Packard Company, L.B Gilman

Gas Chromatography—Food and Pharmaceutical Separations

Monday Morning, Room 1E10
K.J. Erwin, Presiding
McNeil CPC

8:30 (054) **Specially Tested Capillary Column for Reproducible Equivalent Chain Length Analysis of Fatty Acid Methyl Esters**—L.S. SIDISKY, Supelco, Inc., H.J. Sullivan, K.H. Kiefer

8:50 (055) **GC/Tracer Analysis of Flavors and Fragrances**—J.R. POWELL, Bio-Rad, Digilab Division

9:10 (056) **Quantitative Analysis of Alcohols by GC/FTIR**—M.R. YAZDI, Mississippi State University, V.F. Kalasinsky

9:30 (057) **Rapid Analysis of Amphetamine and Methamphetamine, Coupled with Confidence in Their Full Scan GC/MS Identification**—M.D. UHRICH, Finnigan MAT, J.L. Stephenson, Jr.

9:50 (058) **High Resolution Gas Chromatography with Fourier Transform Infrared, Mass Spectroscopy and Atomic Emission Detection, as an Aid in the Structure Elucidation of Unknowns**—D. WULFF

10:10 RECESS

10:25 (059) **Comparison of Performance Characteristics in Chromatography: Pharmaceuticals vs. Pesticide Formulations**—M. MARGOSIS, US Food and Drug Administration, R. Alber, W. Horwitz

10:45 (060) **Comparison of Internal and External Standard Approach in Quantitation of Volatiles from Particulate Food Material**—R. PANDYA, Rutgers University, Cook Campus, T.G. Hartman, H. Daun

11:05 (061) **Determination of Residual Acetic Acid in Cellulose Acetate by Headspace Gas Chromatography**—K.Y. AL-TIMIMI, Eastman Kodak Company, J.L. Hensley

11:25 (062) **GC Determination of Volatile Nitrosamines in Trifluralin by Direct Injection into a 0.53 mm Fused Silica Column**—Z. PENTON, Varian Instrument Group

11:45 (063) **A Novel Approach to the Determination of Volatile Organics in Pharmaceuticals, Polymers, and Food Stuffs, etc.**—E. WOOLFENDEN, Perkin-Elmer Ltd.

Gas Chromatography—High-Purity Gases

Monday Morning, Room 1E18
E. Guthrie, Presiding
J&W Scientific

8:30 (064) **Measurement of CO and CO_2 in H_2 and N_2 at the sub-ppm Level**—R.F. KRUPPA, Hewlett-Packard Company, W.J. Sanders

8:50 (065) **Generation of Low ppm Atmospheric Gas Reference Standards**—R.C. GEIB, Scott Specialty Gases, K. Maguire, G. Bean

9:10 (066) **Analyses of Soil Gas Samples by Evacuated, Stainless Steel Canisters and Gas Chromatography**—M.J. LACY, University of Connecticut, J.D. Stuart, G.A. Robbins, B.G. Deyo

9:30 (067) **The Use of Summa Canisters for Whole Air Sampling on an Automatic Thermal Desorber**—A.K. SENSEL, Tekmar Company, J.E. Griffiths

9:50 (068) **Ultra-High Purity Helium for Electronic Application**—J. SHAPIRO, Scott Specialty Gases, Inc., G. Pines, R. Postiff

10:10 RECESS

10:25 (069) **Analysis of Trace Impurities in High Purity Oxygen Using an Oxygen Remover Device and Gas Chromatograph with Helium Ionization Detection**—B. PARMELEE, Liquid Air Corporation, A. Shah

10:45 (070) **Quantitative Analysis of High-Purity Gases Using a Gas Chromatograph with a Helium Ionization Detector**—P.J. MAROULIS, Air Products and Chemicals, Inc., A.R. Homyak

11:05 (071) **Comparison of the SCD and FPD for HRGC Determination of Atmospheric Sulfur Gases**—S.O. FARWELL, University of Idaho, K. Gaines, W.H. Chatham

11:25 (072) **Comparison of Chromatographic Detectors for Trace Level Analysis in Semiconductor Process Gases**—R.T. TALASEK, Texas Instruments

11:45 (073) **Discharge Ionization Detector Applications of Electronic Gases and Base Gas Purity**—R.J. MATHIEU, GOW-MAC Instrument Company, R. Strusz, J.B. Lawson

Acrodisc: The Difference is Clear.

Clearly the Widest Selection.

Gelman Sciences Acrodiscs® are available in a wide variety of membrane types, with 0.2µm or 0.45µm pore sizes and 13mm or 25mm diameters.

Clearly Identified.

Acrodiscs are printed with identifying information, and are color-coded to the product packaging. Convenient tube containers allow you to see their contents at a glance.

Clearly the Best Performance.

Gelman Sciences is so certain you'll be satisfied with the performance of its Acrodisc syringe filters, every package is covered by a free-replacement guarantee. So order Gelman Sciences Acrodiscs today through your local laboratory products distributor.

CIRCLE 63 ON READER SERVICE CARD

GelmanSciences

600 S. Wagner Rd. • Ann Arbor, MI 48106-1448 • 313-665-065

ACRODISC LC PVDF 0.45
Acrodisc
GelmanSciences
Acrodisc

HPLC—Food Analysis

Monday Morning, Room 1E13
W. Hinze, Presiding
Wake Forest University

8:30 (074) **The Use of Inverse Liquid Chromatography to Study Food and Packaging Interactions**—B.H. ALLEN, National Food Processors Assoc., H.B. Chin

8:50 (075) **Vitamin D. Separation, Quantitation and Detection by HPLC in Complex Food Matrices**—D. RHODES, Syracuse Research Corporation, L. Gooden

9:10 (076) **Applications in the Food Industry Using an Automated Laboratory Workstation for HPLC Sample Preparation**—W.J. HURST, Hershey Foods Technical Center, R.A. Martin, B.D. Holden, B.G. Lightbody

9:30 (077) **Classification of Orange Juice Concentrates Based on Multicomponent Analysis Using High Performance Liquid Chromatography with Sixteen Channel Electrochemical Detection**—P.H. GAMACHE, ESA, Inc., M.L. Lynch, W.R. Matson

9:50 (078) **Determination of Paraquat in Foods by LC and GC Analysis**—C.W. THORPE, US Food and Drug Administration

10:10 RECESS

10:25 (079) **Niacin Separation, Quantitation and Detection by HPLC in Complex Food Matrices**—D. RHODES, Syracuse Research Corporation

10:45 (080) **HPLC Analysis of Indole in Shrimp**—Y.S. LEE, University of District of Columbia, C. Bertocci, D. Coll, J.B. Thomas, Jr.

11:05 (081) **Silica Based Derivatization Reagents for Off-line and On-line Tagging of Nucleophiles in HPLC**—F.X. ZHOU, Northeastern Univ., H.M. Zhang, C.X. Gao, J. Wahlberg, A.J. Bourque, I.S. Krull

11:25 (082) **Determination of Organic and Inorganic Acids in Food by Ion Chromatography**—Y. ZHU, Test/Tech Inst. of Zhejiang Prov.

ICP/AES—Analytical Procedures I

Monday Morning, Room 1E21
C.J. Belle, Presiding
Lucas Aerospace

8:30 (083) **Simultaneous Determination of As, Sb, and Se in Environmental Soils by Hydride Generation and Inductively Coupled Plasma Optical Emission Spectrometry**—J.D. HWANG, Occidental Chemical Corporation, E.J. Ashford, J.P. Diomiguardi, H.P. Huxley, W.J. Vaughn

8:50 (084) **Determination of Trace Metals in Foods by DCP/AES**—G.J. DEMENNA, Libra Labs, Inc., W.B. Jacobs

9:10 (085) **A New Technique for Automatically Interpreting ICP-MS Spectra**—D. POLK, SCIEX, J. Zarycky, R. Ediger

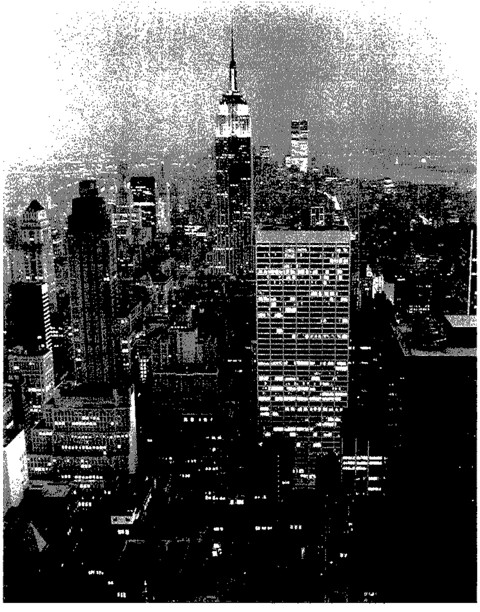

9:30 (086) **Serum Trace Elements and Electrolytes: Rapid Analysis Using a Novel Protein Precipitating Solution and ICP**—G. MOLLER, University of California, Davis, L. Melton, M.L. Tracy

9:50 (087) **Current Status of Direct Solids Analysis of Ceramic, Geological and Related Refractory Materials by Slurry Injection (SI)**—I.B. BRENNER, Geological Survey of Israel, G. Long

10:10 RECESS

10:25 (088) **Rapid Screening Analysis with a Sequential ICAP Plasma Spectrometer**—A.E. GRINDLE, Thermo Jarrell Ash Corporation, J.J. Sotera

10:45 (089) **Determination of Non-Metals by Vacuum Ultraviolet ICP-AES Using CID Detection**—M.J. PILON, University of Arizona, M.B. Denton

11:05 (090) **Automation of the US EPA's Contract Laboratory Program Requirements for the Determination of Elements in Waste Waters by Inductively Coupled Plasma Emission Spectrometry (ICP-ES) and Graphite Furnace Atomic Absorption Spectrometry (GF-AAS)**—D.E. SHRADER, Varian Associates, F. Delles, M. Knowles, A. Marks, B. Allen, T. Nham, F. Finotello

11:25 (091) **Recent Developments in Automated Analysis of Geological and Environmental Materials by ICP-AES, and Chemometric Data Interpretation**—M. BORSIER Bureau Recherches, I.B. Brenner, A. Le Marchand

11:45 (092) **Direct Analysis of Molten Steel in a Converter**—K. CHIBA, Nippon Steel Corporation, A. Ono, M. Saeki, M. Yamauchi, M. Kanamoto, T. Ohno

Infrared I—Quantitative Analysis

Monday Morning, Room 1E19
J.A. de Haseth, Presiding
University of Georgia

8:30 (093) **The On-Line Determination of Trace Moisture in HCl Gas by Fourier Transform Infrared Spectroscopy**—D.E. PIVONKA, Hercules Incorporated

8:50 (094) **Rapid Quantitative Characterization of Copolymers by FTIR Photoacoustic/Factor Analysis**—J.F. McCLELLAND, Iowa State University, R.W. Jones

9:10 (095) **Applications of In Situ FTIR Analysis to Polymer Chemistry**—W.M. DOYLE, Axiom Analytical, Inc.

9:30 (096) **Multivariate Calibration for Quantitative Spectral Analyses: Spectral vs. Fourier Domain**—D.M. HAALAND, Sandia National Laboratories, E.V. Thomas

9:50 (097) **A Comparison of Quantitative Algorithms in the Analysis of Gas Phase FTIR Spectra**—L.A. BURGESS, Nicolet Instrument Corporation, G.L. Ritter

10:10 RECESS

10:25 (098) **Matching Quantitative Methodology to Infrared Applications**—D.T. SPARKS, Nicolet Instrument Corporation, L.A .Burgess

10:45 (099) **Photo/FTIR - A Versatile Technique for Photopolymerization Kinetic Studies**—D.E. PIVONKA, Hercules Incorporated

11:05 (100) **Considerations in Infrared Liquid Autosampling**—J.R. POWELL, Bio-Rad, Digilab Division, K. Krishnan, D. Prasad

11:25 (101) **FTIR Quantitative Analysis for Quality Analysis in the Personal Products Industry**—S.W. STRAND, Spectra Tech Inc., S. Salamanca

11:45 (102) **A Comparison of Three Infrared Methods of Measuring Volatile Organic Chemicals**—S.R. LOWRY, Nicolet Instrument Corporation, R.X. Derler

Instrumentation in Biochemistry

Monday Morning, Room 1E20
K.D. Schlecht, Presiding
SUNY-Brockport

8:30 (103) **Lanthanide-Induced Proton NMR Shift Studies of Bile Salt Aggregates**—S.M. MEYERHOFFER, Duke University, L.B. McGown, T.J. Wenzel

8:50 (104) **Analysis of Total Cholesterol in Egg Yolk by Supercritcal Fluid Chromatography**—W.J. REIGHTLER, Supercritical Processing, Inc., A.D. Scott, Jr.

9:10 (105) **Composition Profile of Wheat Thin Section by FTIR Microspectrometry**—D.L. WETZEL, Kansas State University, J.A. Reffner

9:30 (106) **Determination of Organic Acids, Carbohydrates, Amines and Other Non-Chromophoric Organic Species Using a New Electrochemical Detector with Three Modes of Detection: Conductivity, DC Amperometry, and Integrated Pulsed Amperometry**—R.D. ROCKLIN, Dionex Corp., M.A. Rey, R.W. Slingsby

9:50 (107) **Design and Optimization of a Flow Injection System for Enzymatic Determination of Sugars**—K.S. KURTZ, Michigan State University, S.R. Crouch

Sulfur Specific Chromatograph

Pittcon Booths 3759-3761

MODEL 860

MODEL 825R-D
HYDROGEN SULFIDE GAS ANALYZER
Tracor Atlas
MODEL 856 TOTAL SULFUR HYDROGENATOR
Tracor Atlas
Tracor Atlas, Inc.
CHROMATOGRAPH CONTROL MODULE
Tracor Atlas, Inc.

Our Performance-Proven Sulfur Specific Chromatograph for Gases and Volatile Liquids

The 860 Sulfur Specific Chromatograph is an ideal solution to a wide range of sulfur detection problems. Its state of the art, temperature-programmable chromatograph oven with built-in control module is coupled with the Tracor Atlas 825R-D/856 Total Sulfur Analyzer for reliability and precise analysis of most any gaseous or volatile liquid sample.

Tracor Atlas

Telephone (713) 462-6116 / Telefax (713) 462-1831 / TLX 75-0197 / 9441 Baythorne Dr.
Houston, Texas 77041-7709
Call For Information on our complete line of quality analyzer and sampling systems.

CIRCLE 176 ON READER SERVICE CARD

New Developments in Well-Known Biochemical Techniques

Monday Morning, Room 1E20
K.D. Schlecht, Presiding
SUNY-Brockport

10:25 (108) **Analysis of Pharmaceutical Compounds by Capillary Electrophoresis**—A. WAINRIGHT, Dionex Corporation, J.D. Olechno, J.A. Statler

10:45 (109) **High Performance Isoelectric Focusing**—T. WEHR, Bio-Rad Laboratories, M.D. Zhu, D. Hansen, R. Rodriguez

11:05 (110) **Automated LCEC Determination of Amino Acids in Brain Dialysates**—W.A. JACOBS, Bioanalytical Systems, Inc., P.A. Shea, J. Kehr

11:25 (111) **Latex Particle Infrared Immunoassay (LPIRIA)**—S. BARNETT, McGill University, A.A. Ismail

11:45 (112) **Development of a Data Acquisition and Analysis System for Measuring Protein Binding Constants through Ultracentrifugation**—G.L. FITZGERALD, Smith, Kline & French Labs., W.J. Cassano, K.K. Soneson, F.L. Tobin, P. Hensley

Laboratory Information Management Systems Implementation Topics

Monday Morning, Room 1A08
H.R. Gram, Presiding
Spectrogram Inc.

8:30 (113) **Guidelines for the Selection and Integration of Computer Software and Data Systems into the Small Analytical Laboratory**—J.S. ROTH, National Cancer Institute, NIH, J.A. Kelley

8:50 (114) **Contrasting Logical Information Flow Models of Analytical Services, Quality Assurance, and Research Laboratories**—A.S. NAKAGAWA, Analytical Systems, Inc.

9:10 (115) **Analytical Instrument Data Interchange and Storage Standards**—R. LYSAKOWSKI, Digital Equipment Corporation

9:30 (116) **Computers in the Laboratory: Chemical Information Management**—D. KUEHL, Galactic Industries Corporation, S.C. Simonoff

9:50 (117) **The Blackboard, a Strategy for Laboratory Robotics**—J.R. LEE, Kansas State University, T.L. Isenhour, J.C. Marshall

10:10 RECESS

10:25 (118) **Instrument Interfacing: An Integral Component of Laboratory Information Management**—L. CIABATTONI, Perkin-Elmer Nelson Systems, D. Beggs, J. Fanali

10:45 (119) **Development of a Low-Level LIMS-Instrument Computer Software Interface System**—R. MEGARGLE, Cleveland State University, R. Wilkes

11:05 (120) **A Relational Database LIMS Provides Flexibility for the Future**—J. KUHN, NUS Corporation, J. Bright

11:25 (121) **Document Image Management System Applications in a Laboratory Setting**—R.J. HAAG, Roy F. Weston, Inc., M. Dougherty, J.C. Wallace, J.T. Batten, P.J. Mulligan, E.M. Hansen

11:45 (122) **Computer System Validation by Deterministic Methods**—M. MURPHY, Sema Group System

Polymer Separations

Monday Morning, Room 1E16
K. Sentell, Presiding
University of Vermont

8:30 (123) **Modern HPLC Approaches Coupled to Low Angle Laser Light Scattering Determination for Biopolymer Molecular Weight Determination**—H.H. STUTING, Northeastern University, I.S. Krull, S.L. Wu, W.S. Hancock

8:50 (124) **Quantitative Analysis of Cellulose Esters via GPC/FTIR Using an In-Line Flowcell**—C.W. SAUNDERS, VA Polytechnic Inst. & State Univ., L.T. Taylor

9:10 (125) **Comparative Studies of Three GPC Calibration Methods and Their Suitability to Polymer Analysis**—A.K. WENSKY, Spectra-Physics, Inc., T. Rooney, S. Yarbro

9:30 (126) **Size-Exclusion Chromatography with Supercritical Fluids and Packed Capillary Columns**—W.H. WILSON, VA Polytechnic Inst. & State Univ., V. Sanchez, H.M. McNair

9:50 (127) **An Interferometric Refractometer System for GPC Light Scattering and Liquid Chromatography**—P.J. WYATT, Wyatt Technology Corporation, Y.J. Chang, L. Nilsson

10:10 RECESS

10:25 (128) **A New Integrated Light Scattering Detector for GPC/SEC**—P.J. WYATT, Wyatt Technology Corporation, D.L. Hicks, T.P. Budka

10:45 (129) **Use of an On-Line Viscometer Detector in the GPC Analysis of Polymers**—J.L. EKMANIS, Waters Chrom. Div. Millipore Corp., W.A. Dark

11:05 (130) **High Resolution Separation of Synthetic Polyelectrolytes by Gel Electrophoresis**—D.L. SMISEK, University of Massachusetts, D.A. Hoagland

11:25 (131) **Change of Characteristics of Polyurethane by Gamma-Ray and Autoclave Sterilization**—H. SHINTANI, National Inst. of Hygienic Sci.

Supercritical Fluid Chromatography

Monday Morning, Room 1A07
C. Lunte, Presiding
University of Kansas

8:30 (132) **Evaluation of Nitrous Oxide as a Mobile Phase for SFC**—P. ZIMMERMAN Suprex Corporation, M. Ashraf-Khorassani

8:50 (133) **A New Technique for the Analysis of Hydrocarbon Types in Gasoline by Supercritical Fluid Chromatography with Dual Ultraviolet Absorption and Flame Ionization Detection**—W.W. SCHULZ, Exxon Research & Engineering Co., M.W. Genowitz

9:10 (134) **Evaluation of Different Pore Size Deactivated Stationary Phases for Use in Packed Column Supercritical Fluid Chromatography**—L.J. MULCAHEY, VA Polytechnic Inst. & State Univ., L.T. Taylor, R.A. Henry

9:30 (135) **Tandem Syringe Pump SFC Instrumentation for Packed and Micropacked Capillary Columns Using Pure and Mixed Supercritical Fluids**—A.D. BASHALL, Carlo Erba Instruments/Fisons, G. Mapelli, C. Borra, F. Andreolini

9:50 (136) **Automated Sensitivity Enhancement and Sample Introduction in Supercritical Fluid Chromatography Using Solventless Injection**—K. CROSS, Suprex Corporation, J.M. Levy, A. Rosselli

10:10 RECESS

10:25 (137) **Separation of Very Polar Solutes by Packed Column Supercritical Fluid Chromatography**—T.A. BERGER, Hewlett-Packard Company, J.F. Deye

10:45 (138) **Determination of Aromatic Types of Middle Distillates by Supercritical Fluid Chromatography**—B.J. FUHR, Alberta Research Council, L.L. Klein, C. Reichert, S.W. Lee

11:05 (139) **Pharmaceutical Applications of Supercritical Fluid Chromatography and Microcolumn Liquid Chromatography**—M. ALASANDRO, DuPont Company, A. Baum

11:25 (140) **Determination of Saturates, Aromatics, and Polars in Gas Oils Using Supercritical Fluid Chromatograpny with Backflush Technique**—S. COULOMBE, CANMET

11:45 (141) **Separation of Pyrethroids in Various Phases of Capillary Supercritical Fluid Chromatography**—Y. NISHIKAWA, Sumitomo Chemical Co., Ltd., J. Ohnishi, T. Matsuda

Tandem Mass Spectrometry

Monday Morning, Room 1E11
L.K. Wong, Presiding
University of Pittsburgh

8:30 (142) **Tandem Mass Spectrometry for Bioprocess and Environmental Monitoring**--R.G. COOKS, Purdue University, M. Hayward, T. Kotiaho, A. Lister, G. Austin, R. Narayan, G.T. Tsao

8:50 (143) **A Tandem Quadrupole-Ion Trap Mass Spectrometer**—K.L. MORAND, Purdue University, S.R. Horning, R.G. Cooks

9:10 (144) **Analysis of Glycoproteins by High Sensitivity Tandem Quadrupole Mass Spectrometry**—I. JARDINE, Finnigan MAT, M.E. Hail, S. Lewis, J. Zhou, C. Whitehouse

9:30 (145) **Differentiation of Chlorinated Isomers Using Deuterated Reagents in a Triple Quadrupole Mass Spectrometer**—S. CHAN, Michigan State University, C.G. Enke

9:50 (146) **A New Triple Quadrupole Mass Spectrometer for the Analysis of High Molecular Weight Biomolecules**—S.A. JARVIS, VG MassLab Ltd., M.A. McDowall, D.C. Smith, D. Pudvah

10:10 RECESS

10:25 (147) **Design and Operation of a Cell of Neutralization/Chemical Reionization (NCRMS) on a Four Sector Tandem Mass Spectrometer**—R. ORLANDO, Univ. of Maryland, C. Fenselau, T. Kobayashi, Y.Y. Kammei, R.J. Cotter

10:45 (148) **Determination of the Amino Acid Sequence of S. Aureus V8 Protease by FAB/Tandem Mass Spectrometry**—M. VESTLING, University of Maryland, S. Hua, P. Smith, C. Fenselau

11:05 (149) **A New Automated, High Performance, High Productivity TSQ for High Sensitivity from Low Mass to High Mass and MS to MS/MS**—K.P. MATUSZAK, Finnigan MAT, A.M. Cary, S. Teng, T. Oglesby, E. Petit

11:25 (150) **A Tandem Quadrupole Mass Spectrometer at Atmospheric Pressure Optimized for Intelligent Data Acquisition**—M.A. McDOWALL, VG MassLab Ltd., T.O. Merren, I. Butler

11:45 (151) **Characteristics of RF-Only Multipole Collision Cells**—G.C. STAFFORD, JR., Finnigan MAT, J.E.P. Syka, A.E. Schoen, M.E. Hail, K.P. Matuszak

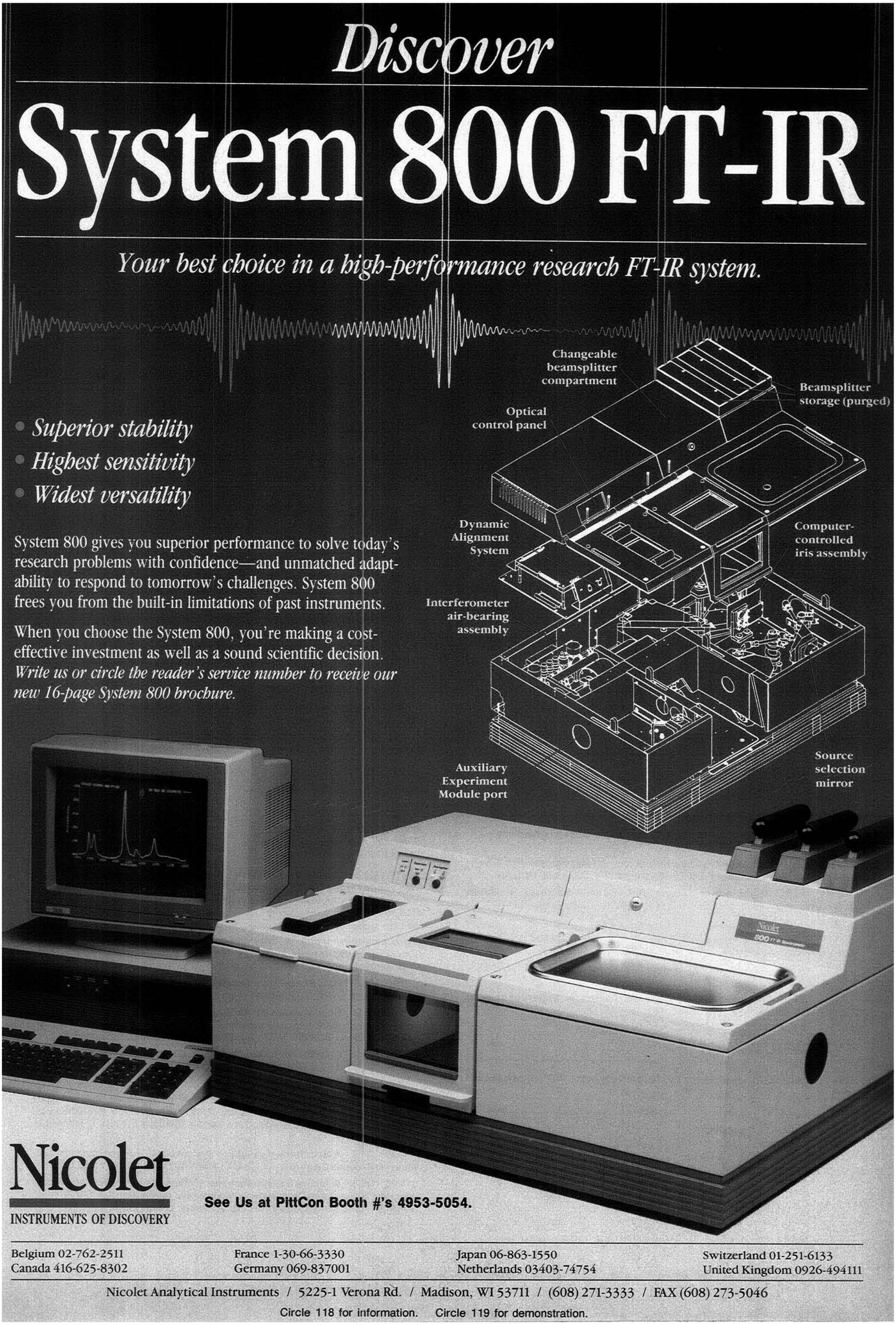
Changeable beamsplitter compartment
Beamsplitter storage (purged)
Optical control panel
Dynamic Alignment System
Computer-controlled iris assembly
Interferometer air-bearing assembly
Auxiliary Experiment Module port
Source selection mirror
Nicolet
800 FT-IR

Discover

System 800 FT-IR

Your best choice in a high-performance research FT-IR system.

- *Superior stability*
- *Highest sensitivity*
- *Widest versatility*

System 800 gives you superior performance to solve today's research problems with confidence—and unmatched adaptability to respond to tomorrow's challenges. System 800 frees you from the built-in limitations of past instruments.

When you choose the System 800, you're making a cost-effective investment as well as a sound scientific decision. *Write us or circle the reader's service number to receive our new 16-page System 800 brochure.*

Nicolet
INSTRUMENTS OF DISCOVERY

See Us at PittCon Booth #'s 4953-5054.

Belgium 02-762-2511	France 1-30-66-3330	Japan 06-863-1550	Switzerland 01-251-6133
Canada 416-625-8302	Germany 069-837001	Netherlands 03403-74754	United Kingdom 0926-494111

Nicolet Analytical Instruments / 5225-1 Verona Rd. / Madison, WI 53711 / (608) 271-3333 / FAX (608) 273-5046

Circle 118 for information. Circle 119 for demonstration.

POSTER PRESENTATIONS

Poster Papers will be on display from 9:30 AM - 4:00 PM Monday and Tuesday. Authors will be available from 2:00 PM - 4:00 PM each day.

Poster Session I

Monday and Tuesday, Room 1A01

Poster Session II

Monday and Tuesday, Room 1B01

SYMPOSIUM

Biosensors et al.—Analysis Outside the Laboratory - **arranged by S.G. Weber of University of Pittsburgh**

Monday Afternoon, Room 1A06
S.G. Weber, Presiding
University of Pittsburgh

1:30 **Introductory Remarks**—S.G. WEBER

1:35 (261) **Operational Characteristics of Competitive Affinity Sensors**—A. WEBER, The Royal Vet. & Agri. Univ.

2:10 (262) **Biosensors: Philosopher's Stone or Fool's Gold**—I.J. HIGGINS, Cranfield Instit. of Technology, M. Alvarez-Icaza, G.F. Hall, R. Wilson, A.P.F. Turner

2:45 (263) **Status and Future of Optical Biosensors**—J.S. SCHULTZ, University of Pittsburgh

3:20 RECESS

3:35 (264) **Problems and Perspectives in Application of Biosensor Technology**—M. THOMPSON, University of Toronto

4:10 (265) **Chemical Control of Timing for Enzyme Spot Tests**—S.G. WEBER, University of Pittsburgh, J.N. Valenta, R.C. Elser

SYMPOSIUM

Characterization of High Temperature Superconducting Oxides - **arranged by A. Pebler of Westinghouse Science & Technology Center**

Monday Afternoon, Room 1A08
A. Pebler, Presiding
Westinghouse STC

1:30 **Introductory Remarks**—A. PEBLER

1:35 (266) **Introduction to High Temperature Superconductivity**—J.R. CLEM, Iowa State University

2:10 (267) **Electron Microscopy of Superconducting Oxides - The Advantage of Spatial Resolution**—R. GRONSKY, University of California, Berkeley

2:45 (268) **Auger Spectroscopy of Fractured Surfaces in Oxide Superconductors**—D.M. KROEGER, Oak Ridge National Labs.

3:20 RECESS

3:35 (269) **Photoelectron and Electron Diffraction Studies of High T_c Superconducting Surfaces**—J. TALVACCHIO, Westinghouse STC

4:10 (270) **FIR Spectroscopy of High T_c Superconductors**—A.T. SIEVERS, Cornell University

4:45 (271) **Thermoanalytical Characterization of Superconducting Oxides**—P.K. GALLAGHER, AT&T Bell Labs.

SYMPOSIUM

Dal Nogare Award - **arranged by M.E. McNally of E. I. du Pont de Nemours & Co., Inc.**

Monday Afternoon, Room 1A23
M.E. McNally, Presiding
E. I. du Pont de Nemours & Co., Inc.

1:30

The 1990 Dal Nogare Award will be presented
to
Dr. Robert L. Grob
Villanova University
by
Dr. W. Vincek, Chairman
Chromatography Forum of the Delaware Valley

1:40 (272) **Award Address: The Impact of Gas Chromatography on the Analysis of Environmental Samples**—R.L. GROB, Villanova University

2:15 (273) **A Better Understanding of Gradient Elution: Some Highlights and Recent Discoveries**—L.R. SNYDER, LC Resources, Inc.

2:50 RECESS

3:05 (274) **The Performance of Polyethylene Glycol Liquid Phases Immobilized by Cobalt-60 Gamma Radiation for Capillary GC**—E.F. BARRY, University of Lowell, W.A. George

3:40 (275) **Recent Developments in Field Flow Fractionation**—J.J. KIRKLAND, E. I. du Pont de Nemours & Co., Inc., W.W. Yau

4:15 (276) **Supercritical Fluids - Applications to Multi-Residue Analysis**—M.E. McNALLY, E. I. du Pont de Nemours & Co., Inc.

SYMPOSIUM

Role of Array Detectors in Spectrochemical Analysis - **arranged by R. Krupa of Baird Corporation and M.B. Denton of University of Arizona**

Monday Afternoon, Room 1D01
M.B. Denton, Presiding
University of Arizona

1:30 **Introductory Remarks**—M.B. DENTON

1:35 (277) **Overview of the Future of Array Detectors from a Manufacturer's Viewpoint**—Y. TALMI, Princeton Instruments, Inc.

2:10 (278) **Detection with Charge Coupled Devices in Atomic Emission and NIR Raman Spectroscopies**—R. BILHORN, Eastman Kodak Company

2:45 (279) **Engineering of, Spectroscopy Performed with, and Frustration Caused by an Echelle Spectrometer Using Charge Coupled Array Detection**—A. SCHEELINE, University of Illinois, Urbana-Champaign, C.A. Bye, S.V. Rynders, D.L. Miller

3:20 RECESS

3:35 (280) **Imaging Spectroscopy with Cooled CCD Array Detectors**—C. MacKAY, Astromed Ltd.

4:10 (281) **Present Applications and Future Trends in High Performance Charge Transfer Device Detectors**—M.B. DENTON, University of Arizona

Clinical Analyses

Monday Afternoon, Room 1E20
G. Meyers, Presiding
Centers for Disease Control

1:30 (282) **The Influence of Chemical Modifiers on the Atomization of Lead from Human Urine by Electrothermal Atomic Absorption Spectrometry**—P.J. PARSONS, New York State Dept. of Health, K.W. Jackson, M. Hughes, S. Chace, S. Jenkins

1:50 (283) **Determination of Menthol-Glucuronide in Human Urine by Gas Chromatography Using an Enzyme-Sensitive Internal Standard and Flame Ionization Detection**—M.J. DOYLE, The Procter & Gamble Company, R.M. Kaffenberger

2:10 (284) **Solid Phase Extraction Sample Preparation of Benzodiazepines from Urine**—A. CARPENTER, Analytichem International, V. Dixit, D.D. Blevins

2:30 (285) **Quantification of Antibodies to Human Growth Hormone in Serum by High Performance Immunoaffinity Chromatography with Fluorescence Detection**—R. SPORTSMAN, Lilly Research Laboratories, A. Riggin, F. Regnier

2:50 (286) **Micellar Microcolumn Liquid Chromatographic Analysis of Oligonucleotides**—J.J. RUSIK, University of Vermont, K.B. Sentell, J.C. Bigelow

3:10 RECESS

3:25 (287) **Examination of the Metabolism of NE-11740, A Novel Anti-Arthritic Drug, in Multiple Species by HPLC with On-Line Radiochemical Detection**—K. WEHMEYER, The Procter & Gamble Company, T. Heise, D. Mitchell, D. Dobrozsi

3:45 (288) **A New Biomedical Image System Using Tongue Image Recognition for Disease Diagnosis**—Y. ZHANG, ADA R&D Group, H. Xie, F. Hu, L. Hua

4:05 (289) **Selective Spectrophotometric Methods for Sodium and Potassium Ions Using Novel Chromogenic Macrocyclic Ionophores**—E. CHAPOTEAU, Technicon Instruments Corp., B.P. Czech, A. Kumar, C.R. Gebauer

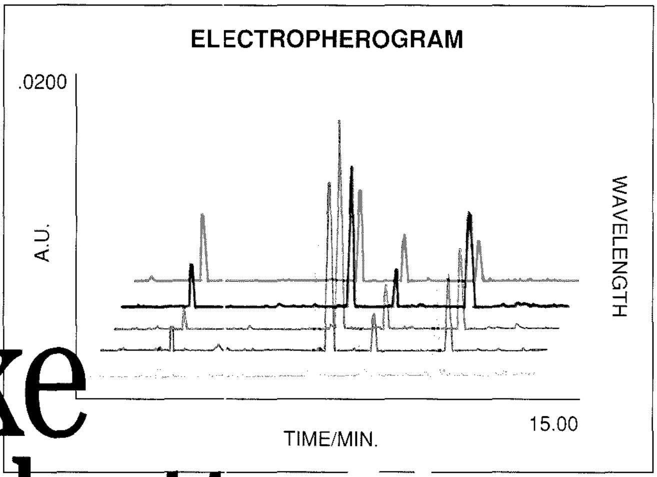

Take a better look at your CE data.

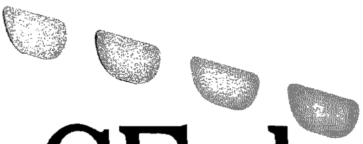

See what's been missing in capillary electrophoresis.

Spectra! The benefits of multi-dimensional detection are yours with the Spectra PHORESIS 1000™ capillary electrophoresis (CE) system now from Spectra-Physics.

Spectra will authenticate your data. Peak purity and spectral scans conform to the latest regulatory requirements. Separation reproducibility is guaranteed by our unique design which cools the entire capillary. Analyze up to 80 samples on our autosampler.

Come see us and our capillary electrophoresis system at the Pittsburgh Conference, booth #3317. Or, call us toll-free at 800-424-7666. Take a better look at your CE data. Now see what you've been missing!

SEE YOU AT PITTCON - BOOTH 3317

Spectra-Physics

Discover the Quality

Circle 154 for Sales Representative. Circle 155 for Information.

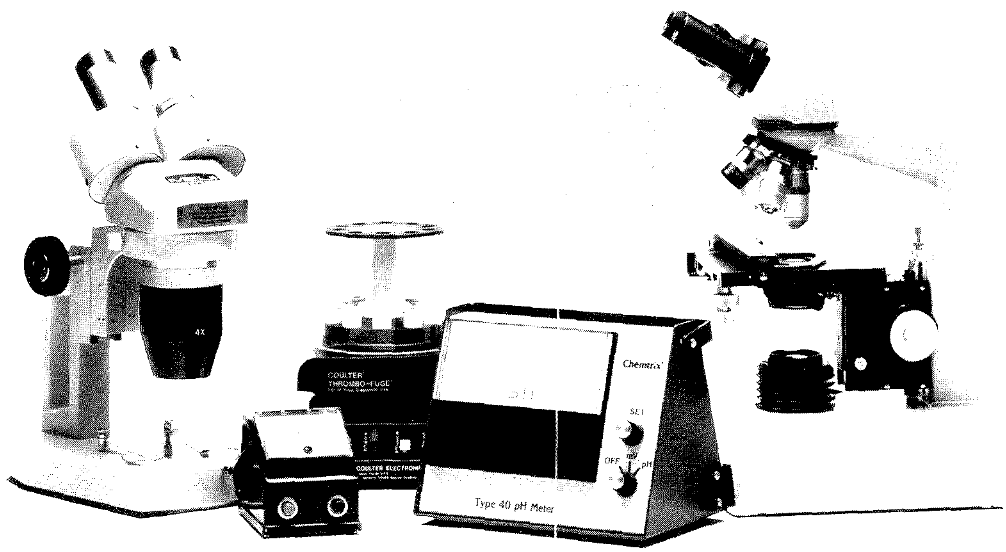
COULTER THROMBO-FUGE
COULTER ELECTRONICS
Chemtrix
SET
OFF
pH
Type 40 pH Meter
4X

MSD Isotopes – research products that work, bringing results to researchers in biology, chemistry, physics, medicine and related fields.

Did you know that we now offer thousands of compounds labeled with deuterium, carbon-13, nitrogen-15 and other stable isotopes too? And did you know that even if you require a compound which is not available from us immediately 'off-the shelf', we have the world's best facilities to custom synthesize it for you?

Just call or write to us for more information on what we have in stock and can make for you.

For technical information call 1-800-361-0460.

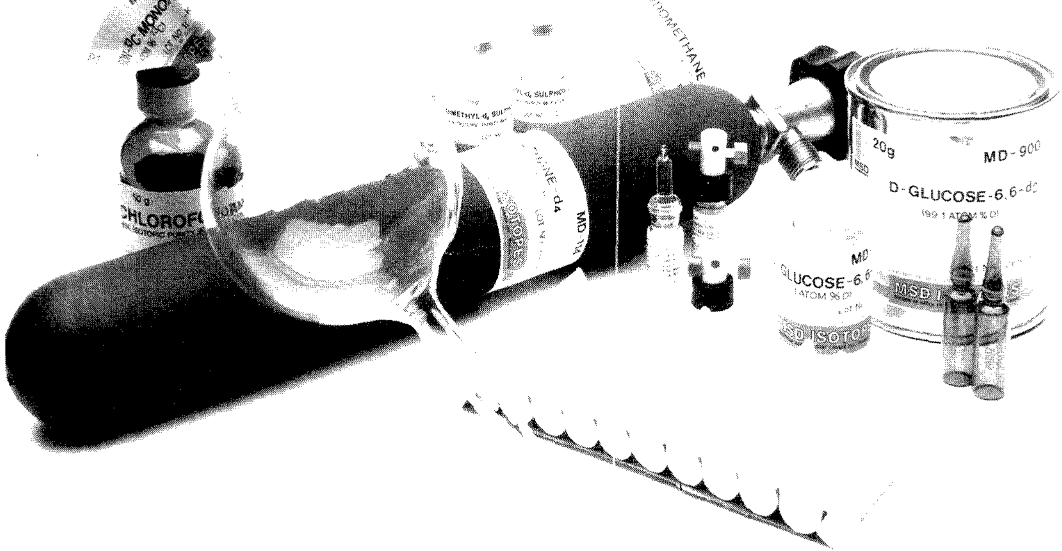
CHLOROFORM
20g
MD-900
D-GLUCOSE-6,6-d2
GLUCOSE-6,6
MSD ISOTOPES
ISOTOPES

WEST COAST
P.O. Box 2951
Terminal Annex
Los Angeles, CA 90051
Los Angeles Area: (213) 723-9521
Outside State of CA: (800) 423-4977
State of CA: (800) 372-6454

EAST COAST & CENTRAL
4545 Oleatha Avenue
St. Louis, MO 63116
Outside state of MO: (800) 325-9034
State of Missouri: (314) 353-7000

CANADA
P.O. Box 899
Pointe Claire/Dorval, Quebec
Canada H9R 4P7
Telephone: (514) 697-2823

CIRCLE 112 ON READER SERVICE CARD

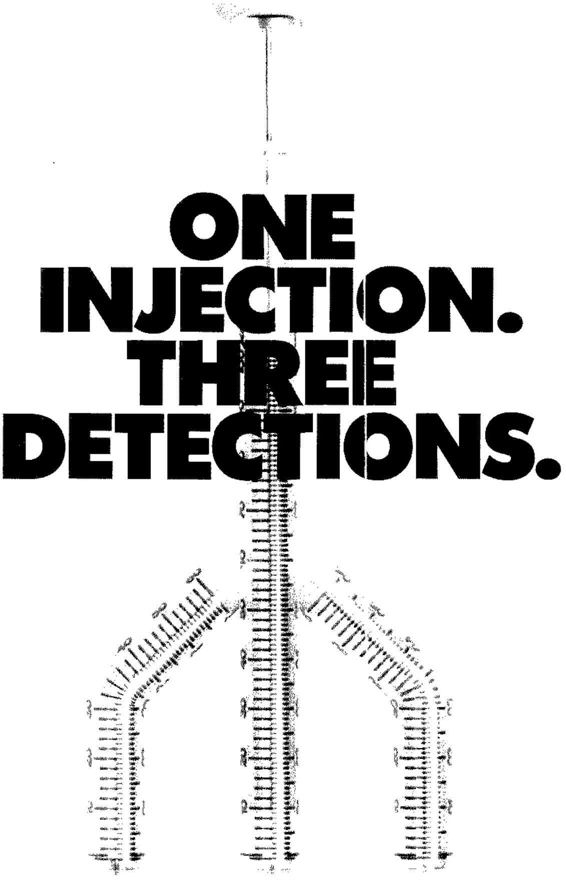

THE 3D HPLC SYSTEM FROM BACHARACH COMBINES THREE DETECTORS IN ONE

Now, you can monitor UV, fluorescence and conductivity separately or simultaneously—with one injection—using a single, compact unit. The 3D HPLC is ideal for laboratory use in quality control, screening and teaching applications.

UV DETECTION
In the UV mode, it is a fixed wavelength detector at 254 nm, where up to 65% of all analytical HPLC applications are performed.

FLUORESCENCE DETECTION
In the fluorescence mode it monitors total emission above 280 nm. The selectivity of fluorescence can confirm the presence of components which may be masked by other UV-absorbing compounds.

CONDUCTIVITY DETECTION
As a conductivity detector, it monitors ionic species—inorganic anions, cations, organic acids and certain vitamins.

The 3D HPLC System comes complete with pump, injector, cartridge column, recorder and trifunctional detector—for under $7000.

For more information, contact:
Bacharach Coleman Instruments,
625 Alpha Drive, Pittsburgh,
PA 15238; (412) 963-2107.

BACHARACH
Coleman® Instruments

CIRCLE 20 ON READER SERVICE CARD

4:25 (290) **Assays of Optimalization of Bicarbonate Reagent with the Use of a Gas-Barrier System**—J. DUTRIEU, Hospital de Warquignies, M. Brognez, K. Gilson

4:45 (291) **A Quantitative Immunoenzymatic Assay for the Human Luteinizing Hormone Employing a Bispecific Monoclonal Antibody**—G. BUGARI, University of Brescia, C. Poiesi, A. Beretta, S. Ghielmi, A. Albertini

Countercurrent Chromatography

Monday Afternoon, Room 1E08
N.B. Mandava, Presiding
SRS International

1:30 (292) **Multi-Coil Countercurrent Chromatograph**—M. KNIGHT, Peptide Technologies Corporation, S. Gluch

1:50 (293) **Evaluation of Analytical Countercurrent Chromatographs: High-Speed Countercurrent Chromatograph-4000 vs. Analytical Toroidal Coil Centrifuge**—H. OKA, Aichi Prefectural Inst. of Public Health, Y. Ikai, N. Kawamura, M. Yamada, K. Harada, M. Suzuki, F.E. Chou, Y.W. Lee, Y. Ito

2:10 (294) **Correlation of Solvent Systems for Countercurrent Chromatography by Means of an Equipollent Index**—W.D. CONWAY, SUNNYAB

2:30 (295) **High Speed Countercurrent Chromatography of Isomeric Mixtures**—Y.W. LEE, Research Triangle Institute, S.F. Yeh, Z. Lee, Y. Ito

2:50 (296) **Rapid Separation of Natural Products by Three Different Models of Analytical Countercurrent Chromatographs**—F.E. CHOU, Pharma-Tech Research Corporation, E. Kitazume, R. Petroski, Y. Ito

3:10 RECESS

3:25 (297) **Analytical High-Speed Countercurrent Chromatography: Applications in Natural Products Chemistry**—D.E. SCHAUFELBERGER, Program Resources, inc., M.P. Koleck, G.M. Muschik

3:45 (298) **Separation of Rare Earth Elements by High-Speed Countercurrent Chromatography**—E. KITAZUME, NHLBI, NIH, M. Bhatnagar, Y. Ito

4:05 (299) **Practice, Theory, and Mechanism of Centrifugal Countercurrent Chromatography**—D.W. ARMSTRONG, University of Missouri-Rolla

4:25 (300) **Resolution Enhancement in Centrifugal Partition Chromatography Through Optimization of Chromatographic Selectivity**—J. CAZES, Sanki Laboratories, Inc., W. Murayama, Y. Kosuge

4:45 (301) **Comparison of Several Aqueous Two Phase Systems for CPC Fractionation of Biopolymers**—A. FOUCAULT, Columbia University, K. Nakanishi

Electrochemistry—Microelectrodes and Modified Electrodes

Monday Afternoon, Room 1E18
W.R. Sharpe, Presiding
Clarion State University

1:30 (302) **Normal and Reverse Pulse Voltammetry at Microcylinder-Electrodes**—M.M. MURPHY, State Univ. of NY at Buffalo, J.G. Osteryoung

1:50 (303) **Pulse Voltammetric Determination of the Stoichiometry of Complex Ions in Ambient Temperature Molten Salts**—R.A. OSTERYOUNG, State University of New York, M. Noel

2:10 (304) **Reverse Pulse Voltammetric Studies of Reproportionation in Ambient Temperature Molten Salts**—R.A. OSTERYOUNG, State University of New York, Z. Karpinski, S.G. Park

2:30 (305) **Ring-Modified Microelectrodes for Multi-Microelectrode Devices**—C.L. WANG, University of Connecticut, B.R. Shaw

2:50 (306) **Steady-State Lateral Charge Transport by a Bilayer Assembly**—C.A. GOSS, University of California, Berkeley, M. Majda

3:10 RECESS

3:25 (307) **Laser Induced Microelectrode Arrays on Carbon Surfaces: Construction and Comparison of Theory to Findings**—K.D. STERNITZKE, The Ohio State University, R.L. McCreery

3:45 (308) **Microstructural Alterations of Glassy Carbon Electrode Surfaces Induced by Laser Irradiation**—R.J. RICE, The Ohio State University, N. Pontikos, R.L. McCreery

4:05 (309) **Solid-State Electrochemical Microcells Based on Zeolite Crystals**—K.E. CREASY, University of Connecticut, B.R. Shaw

4:25 (310) **Surface Renewable Composite Electrodes**—J. PARK, University of Connecticut, B.R. Shaw

4:45 (311) **Metal Based Thin Film Electrodes**—K. HAMDANI, University of Missouri-Kansas City, K.L. Cheng

Gas Chromatography—New Instruments and Techniques

Monday Afternoon, Room 1E21
D. Hassick, Presiding
Calgon Corporation

1:30 (312) **The New Concept in Process Gas Chromatography Double Oven and Dual Detection**—U.K. GOEKELER, ES Industries

1:50 (313) **Process Analysis Using Programmed Temperature Gas Chromatography - A Practical Reality**—T. LECHNER-FISH, Applied Automation, Inc., B. Bade, J. Crandall

2:10 (314) **Constant Flow Operation of Open Tubular Columns via Pressure Programming**—R.J. PHILLIPS, Hewlett-Packard Company, L. Freed, M.Q. Thompson

2:30 (315) **Refinery Gas Analysis Using Automated Gas Chromatography**—J.L. REED, Antek Instruments, Inc., R.A. Salazar, A.J. Britten

2:50 (316) **High Temperature Thermal Desorption Autosampler and Pyrolysis Applications**—D. GRUBBS, Carlo Erba Instruments/ Fisons, A.D. Bashall

3:10 RECESS

3:25 (317) **UV Photolysis of Nitrogenous Pesticides in Ground Water for Fluorescence Detection by HPLC**—B.M. PATEL, University of Florida, H.A. Moye

3:45 (318) **A Novel Polysiloxane Stationary Phase for the Analysis of 2,3,7,8 TCDD and 2,3,7,8 TCDF**—R.M.A. LAUTAMO, J & W Scientific, R.R. Freeman, T.L. Patterson

4:05 (319) **The Analysis of Resin Acids in Rosin by Capillary Gas Chromatography**—M. DINNAUER, J & W Scientific, M. Feeney

4:25 (320) **Determination of Trace Level Hydrogen Chloride Using Packed Column Chromatography with ECD**—P.A. WOJTENA, Liquid Carbonic Industries Corp.

4:45 (321) **Analysis of VLSI Grade Hydrogen Chloride for Trace Metallic Impurities**—.H. YIN, Scott Specialty Gases, Inc.

HPLC—Ion Chromatography

Monday Afternoon, Room 1A07
I.S. Krull, Presiding
Northeastern University

1:30 (322) **Naphthalene Sulfonic Acid Derivatives as Mobile Phases for Indirect Photometric Chromatography of Anions**—S.A. MAKI, Miami University, N.D. Danielson

1:50 (323) **Optimization of Separation and Detection of Anions with Ion-Pairing Reversed Phase HPLC Columns and Indirect Photometric Detection**—B. GLATZ, Hewlett-Packard GmbH, M. Riedmann

2:10 (324) **Suspension Detection Method for Ion Chromatography**—D.T. GJERDE, Sarasep, Inc.

2:30 (325) **New Approach to Gradient Ion Chromatography**—P. JANDIK, Waters Chrom. Div. Millipore Corp., J. Li, W.R. Jones

2:50 (326) **Determination of Lanthanide Metals in Geological Samples Using Chelation Ion Chromatography**—M. HARROLD, Dionex Corporation, J. Riviello, A. Siriraks, H.M. Kingston

3:10 RECESS

3:25 (327) **Speciation of Lead by Ion Chromatography and Post-Column Derivatization**—P.J. PARSONS, New York State Dept. of Health, M. Hughes

3:45 (328) **Determination of Polar and Ionic Components by IC/MS**—R. SLINGSBY, Dionex Corporation, M.A. Brown

4:05 (329) **Inorganic Anion Determination on Cyclodextrin Bonded Phases Using Photochemical Reaction and U.V. Detection**—T.E. BEESLEY, Advanced Separation Tech., Inc.

4:25 (330) **The Use of Membrane Sample Preparation Improves the Performance of Ion Chromatography for Cation Analysis**—P. JACKSON, Waters Chrom. Div. Millipore Corp., P.G. Alden, J. Krol, J. Romano, P. Jandik, W.R. Jones

4:45 (331) **Coelution in Ion Chromatography, New and Old Solutions to an Old Problem**—W.R. JONES, Waters Chrom. Div. Millipore Corp., P. Jandik, J. Li

HPLC—Stationary Phase Chemistry

Monday Afternoon, Room 1E06
R. Henry, Presiding
Keystone Scientific

1:30 (332) **Reduction of Reequilibration Time Following Gradient Elution Reversed-Phase Liquid Chromatography**—L.A. COLE, University of Cincinnati, J.G. Dorsey

1:50 (333) **Further Investigation of Surface Pretreatment Effects in Micro-LC**—W.H. WILSON, VA Polytechnic Inst. & State Univ., H.M. McNair, Y.F. Maa, K.H. Hyver

2:10 (334) **The Role of the Organic Modifier in Micellar Liquid Chromatography**—A.J.I. WARD, Clarkson University, J.H. Han, O. Donoghue, B.K. Lavine

2:30 (335) **Subambient Temperature as a Separation Parameter in Reversed Phase Liquid Chromatography**—K.B. SENTELL, University of Vermont, A.N. Henderson

2:50 (336) **Micro-Structures of HPLC Packing Materials Observed by Scanning Tunneling Microscopy**—H. HATANO, Health Research Foundation, T. Hanai, H. Negishi, T. Fujihara, S. Kurata

DIALOG INTRODUCES ANOTHER TABLE OF BASIC ELEMENTS FOR YOUR LAB.

There's no symbol for *information* in the Periodic Table. Yet nothing could be more crucial to your research than complete, accurate technical and business information.

That's why many chemists consider DIALOG® an essential element in the modern lab.

As the world's largest online knowledgebank, DIALOG gives you access to a whole world of critical information. Right in your own lab.

For starters, you can tap into the crucial scientific data. DIALOG has detailed information on everything from compound identification to chemical safety data, property data, substance and substructure.

Then you can expand your focus by accessing important, related data that will enable you to look at your work in a broader context.

For example, you can investigate patents, competitive projects, new product markets, and worldwide industry trends. In fact, you can investigate any topic, anytime.

And you won't have to sacrifice depth for the sake of breadth. DIALOG is updated continuously, so the data is always comprehensive and current. And many citations can be conveniently retrieved in full text.

Call today for more information and a free Periodic Table Reference Card. Once you've examined them, you'll see how DIALOG can become a basic element of all your research.

Call us toll free at 800-3-DIALOG, (800-334-2564). Or request information by Fax at 415-858-7069.

DIALOG INFORMATION SERVICES, INC.
A Knight-Ridder Company

The world's largest online knowledgebank.

© 1989 Dialog Information Services, Inc., 3460 Hillview Avenue, Palo Alto, California 94304. All rights reserved. DIALOG is a servicemark of Dialog Information Services, Inc. Registered U.S. Patent and Trademark Office.

CIRCLE 40 ON READER SERVICE CARD

Purification of ß-casomorphine from defatted human milk. ß-casomorphines are believed to play a role in postpartum depression. The shaded area shows the ß-casomorphine (1-8) immunoreactivity. Column: Analytical Superpac® Pep-S.

Analysis of synthetic Δ-sleep inducing hormones (9 residues) synthesized on the Biolynx® Plus Peptide Synthesizer. Purity check on PhastSystem®.

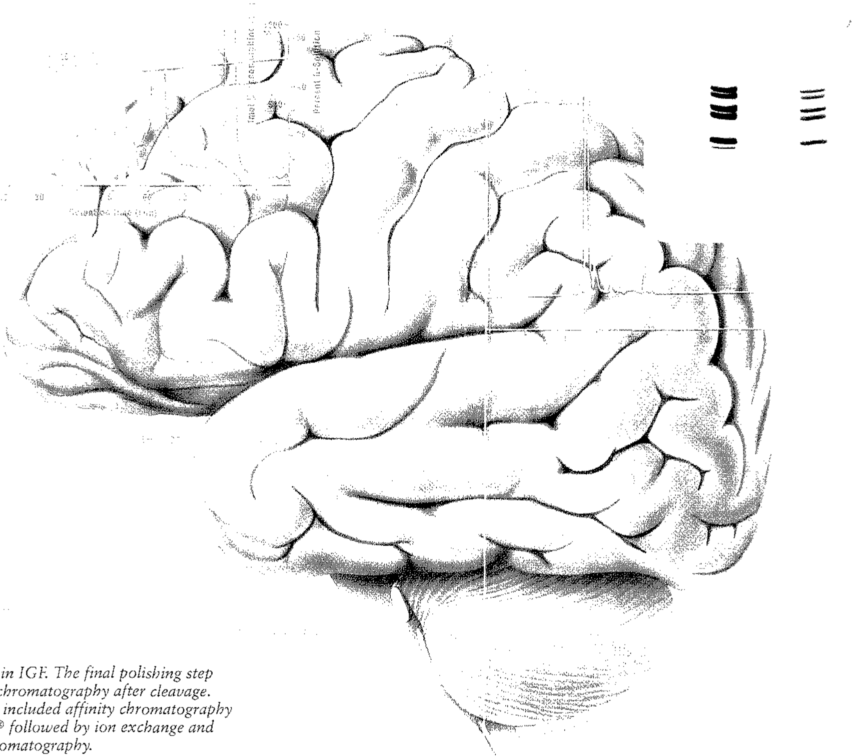

Purification of Brain IGF. The final polishing step with gel filtration chromatography after cleavage. The previous steps included affinity chromatography on IgG-Sepharose® followed by ion exchange and reversed-phase chromatography. Column: Superdex™ 75 prep grade.

What's so special about peptides?

A lot. Peptides wouldn't be peptides otherwise. The fact is that the vast majority are *biologically active* messengers of very special events.

Pharmacia LKB have been isolating and purifying peptides for more than 30 years. Over the years, we've gained unique insights into how to optimize their separation, analysis and synthesis. We maintain updated information on the latest techniques, applications and instrument systems for peptide work. That's one of our specialties. Why not contact us to make it one of yours too?

We help you manage biomolecules

Pharmacia

Pharmacia LKB Biotechnology

Head office Sweden Tel 46 (018) 16 30 00. **Australia** Tel (02) 888 36 22. **Austria** Tel (0222) 68 66 25 0. **Belgium** Tel (02) 242 46 60. **Brazil** Tel 55-11 284 5815/289 8967. **Canada** Tel (514) 457 6661. **Denmark** Tel (02) 26 52 00. **East Europe** Tel 43 (0222) 92 16 07. **Federal Republic of Germany** Tel (0761) 490 30. **Finland** Tel (90) 5021 077. **France** Tel (01) 30 64 34 00. **Great Britain** Tel (0908) 66 11 01. **Holland** Tel (031) 348 077911. **India** Tel (0812) 29634. **Italy** Tel (02) 253 2844/26 700 475. **Japan** Tel (03) 492 91 81. **Norway** Tel (02) 54 90 95. **Soviet Union** Tel 46 (08) 799 80 00. **Spain** Tel (34)-3 675 44 11. **Sweden** Tel 46 (08) 799 80 00. **Switzerland** Tel (01) 821 18 16. **United States** Tel (201) 457 8000. **Far East** Tel 852 (5) 814 8421. **Middle East** Tel 30 (1) 894 7396. **Other countries** Tel 46 (08) 799 80 00 *(8904) 1129*

CIRCLE 136 ON READER SERVICE CARD

WIN A $2,000.00 ROUND-TRIP FOR TWO TO HAWAII AT THE PITTSBURGH CONFERENCE

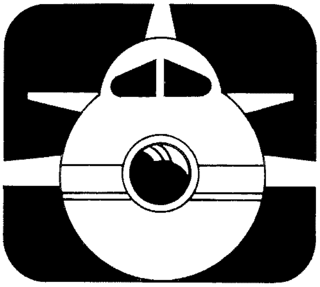

...or, if you elect, $2,000.00 in cash! To participate, simply remove this official entry form and take it to each of the five exhibits shown below. They will each stamp your form. When fully stamped, bring it to the *Analytical Chemistry* booth (#4909) where the winning entry will be drawn by lot immediately after the Pittsburgh Conference closes. The winner will be notified promptly. To qualify, only one entry per participant. Good luck!

EM® EM SCIENCE	BOOTH NUMBERS 3653-3654	*VALIDATION STAMP HERE*
MILLIPORE	BOOTH NUMBERS 5146-5531	*VALIDATION STAMP HERE*
DIONEX	BOOTH NUMBER 5520	*VALIDATION STAMP HERE*
sartorius We take the wait out of weighing— you take the next step towards winning.	BOOTH NUMBER 5373	*VALIDATION STAMP HERE*
Barnstead | Thermolyne	BOOTH NUMBERS 1335-1336	*VALIDATION STAMP HERE*
A&D A&D ENGINEERING, INC.	BOOTH NUMBER 3162	*VALIDATION STAMP HERE*

YOUR NAME: ______________________ TITLE: ______________

ORGANIZATION: ______________________________________

STREET OR BOX #: ______________ CITY: ___________ STATE: _____ ZIP: _______

WORK PHONE: ______________________ HOME PHONE: ______________

3:10 RECESS

3:25 (337) **A General Strategy for Multi-Parameter Optimizations in Micellar Liquid Chromatography**—J.K. STRASTERS, North Carolina State University, M.G. Khaledi

3:45 (338) **Role of Micelles in Selectivity Enhancement in Reversed Phase Liquid Chromatography**—A.S. KORD, North Carolina State University, J.K. Strasters, M.G. Khaledi

4:05 (339) **Influence of Surface Area and Pore Diameter on the Selectivity of Reversed-Phase Separations**—W.B. CALDWELL, ES Industries

4:25 (340) **Reversed-Phase Chromatographic Investigations on Non-Ionic Amphophilic Molecules**—M.E. GANGODA, Kent State University, R.K. Gilpin

4:45 (341) **Solute Dynamics in Chemically Bonded Liquid Chromatographic Phases**—M.J. WIRTH, University of Delaware, J.D. Burbage

ICP-MS and Glow Discharge Mass Spectrometry

Monday Afternoon, Room 1E13
P.M. Castle, Presiding
Westinghouse Idaho Nuclear Corp.

1:30 (342) **Nonspectroscopic Matrix Effects in Laser Ablation Inductively Coupled Plasma-Mass Spectrometry (ICP-MS)**—J.W. HAGER, SCIEX

1:50 (343) **ICP-MS—The Elementary Answer to Troublesome Questions**—C.T. TYE, VG Elemental, R.C. Hutton, P.D. Blair, L. Marshall

2:10 (344) **ICP-Mass Spectrometry, A Total Solution for Analysis of Semiconductor Materials**—E. PRUSZKOWSKI, The Perkin-Elmer Corporation

2:30 (345) **Quantitative Analysis of Metals and Metal Alloys Using Glow Discharge-Quadrupole Mass Spectrometer**—W.S. TAYLOR, Extrel Corporation

2:50 (346) **The Effectiveness of a Low Resolution Analyzer as Applied to Glow Discharge Mass Spectrometry**—J. CLARK, VG Microtrace, P.M. Charalambous, G.A. Ronan, T. Ainscough

3:10 RECESS

3:25 (347) **The Analysis of Semiconductor Materials by the VG 9000 Glow Discharge Mass Spectrometer**—J. CLARK, VG Microtrace, G.A. Ronan, T. Ainscough, D. Wheeler

3:45 (348) **Comparison of XRF and Quadrupole-Based Glow Discharge Mass Spectrometry**—A. AINSCOUGH, VG Microtrace, C.M. Demanet

4:05 (349) **The VG Gloquad - An Analytical Technique for the 1990's**—P.M. CHARALAMBOUS, VG Microtrace, D. Milton, T. Ainscough

4:25 (350) **Trace Transition Element Analysis by High Resolution ICP-MS**—N. BRADSHAW, VG Elemental Ltd., D. Hinds, A. Walsh, N.E. Sanderson

4:45 (351) **ICP-MS Using a 40 MHz ICP**—J. FULFORD, SCIEX, G. Gillson, D. Gallant

ICP/AES—Analytical Procedures II

Monday Afternoon, Room 1E15
C.L. Dobbs, Presiding
Aluminum Company of America

1:30 (352) **An Evaluation of Automated ICP Background Intensity Estimation Approaches**—M.L. SALIT, The Perkin-Elmer Corporation, J.B. Collins

1:50 (353) **Simultaneous Determination of Arsenic, Selenium and Transition Metals by ICAP/AES with On-Line Ion Exchange Sample Pretreatment**—J. RIVIELLO, Dionex Corporation, M. Harrold, R.M. Manabe

2:10 (354) **Line Profiles Studies in an Inductively Coupled Plasma**—T.J. MANNING, University of Florida, J.D. Winefordner, B. Palmer, D. Hof

2:30 (355) **The Role of the Internal Reference in Direct Solids Analysis of Refractory Nonconducting Materials Using Spark Ablation (SA), Slurry Nebulization (SN) and Direct Sample Insertion (DSI) with ICP-AES and Glow Discharge (GD-ES)**—I.B. BRENNER, Geological Survey of Israel, A. LeMarchand, A. Lorber

2:50 (356) **Rapid Preparation of Zeolite Fluid Cracking Catalysts, Silica Gels and Clays for ICP Analyses**—M.E. TATRO, SPECTRA, A. Elabd, P. Kassa

3:10 RECESS

3:25 (357) **Determination of Toxic Elements in Fluid Cracking Catalysts Leachates by ICP-AES Using EPA Recommended TCLP Extraction Procedures**—P.A. GOKHALE, Akzo Chemicals Inc., M.R. Wuensche, D.H. Dodd

3:45 (358) **Remelting of Metals to Prepare Samples for Spectrometric Analysis**—K.D. OHLS, Hoesch Stahl AG, H. Linn

4:05 (359) **A New Attempt to Improve Detection Capabilities of ICP-AES for the Determination of Al in Biological Materials**—D. ARNIAUD, Jobin Yvon (ISA), I.B. Brenner, C.V. Phan, I. Verhaeghe, H. Wald

4:25 (360) **Study of Electrochemical Separation Coupled with ICP Atomic Emission Spectrometry for Simultaneous Multielement Determination of Trace Impurities in High-Purity Metals**—F.H. LI, Trace Analysis Laboratory, F.Guo

4:45 (361) **On-Line Analysis of Molten Steel by Chlorination and Transportation Technique**—K. SUGIMOTO, NKK Corporation - Keihin Works, T. Akiyosi

Infrared II--Microspectroscopy

Monday Afternoon, Room 1E10
V.F. Kalasinsky, Presiding
Mississippi State University

1:30 (362) **Paper Withdrawn**

1:50 (363) **Infrared Microspectroscopic Identification of Binding Media in Paint Cross-Sections: Application to Works of Art**—D.C. STULIK, Getty Conservation Institute, M. Derrick, J.M. Landry, M.R. Bolton

2:10 (364) **Image Reconstruction Improvement Methods for Multidimensional Infrared Microspectroscopy**—K.J. WARD, Sandia National Laboratories

2:30 (365) **Infrared Mapping Microspectroscopy of Furniture Finish Stratigraphy**--J.M. LANDRY, Loyola Marymount University, S.P. Bouffard, M. Derrick, D.C. Stulik

2:50 (366) **Infrared Microimaging of Biological Tissue Samples**—J.R. POWELL, Bio-Rad, Digilab Division, K. Krishnan, D.R. Kodali

3:10 RECESS

3:25 (367) **Analysis of Submicrometer Films on Surfaces by Grazing Angle FTIR Microscopy**—J.A. REFFNER, Spectra-Tech, Inc., W.T. Wihlborg

3:45 (368) **High Temperature Studies Using a Micro FTIR System**—S.L. HILL, Bio-Rad, Digilab Division, K. Krishnan, P.J. Stout

4:05 (369) **Reflectance Spectroscopy with an FTIR Microscope**—D.W. SCHIERING, The Perkin-Elmer Corporation, E.F. Young

4:25 (370) **Improving FTIR Microscopy Detection Limits and Spatial Resolution Through Sample Preparation**—J.A. REFFNER, Spectra-Tech, Inc., W.T. Wihlborg

4:45 (371) **Applications of Recent Development in Differential Scanning Calorimetry/Micro FTIR System**—Y. OKUBO, Japan Spectroscopic Co., Ltd., C. Jin, T.E. Ikeda, H. Okahana, J. Carriker

Quality Assurance Through Automation and Information

Monday Afternoon, Room 1E16
H. Brown, Presiding
PE Nelson Systems

1:30 (372) **Meeting Data Quality Objectives and Managing Information Exchange in Environmental GC/MS Analysis**—C.S. CAMPBELL, Finnigan MAT, M.M. Booth, D.E. Smith

1:50 (373) **Interaction of a Data Base and User-Definable Spreadsheets for Customizable LIMS Data Treatment**—R.D. BEATY, Telecation Associates, P.C. Differding

2:10 (374) **Chromatography Automation in a GLP/GMP Compliant Environment**--S.J. BRUNET, Beckman Instruments, Inc.

2:30 (375) **Software and Hardware Validation in a Fully Automated Sampling System**—R.W. GIUFFRE, Hewlett Packard Company

2:50 (376) **Laboratory Quality Control with a LIMS**—P.J. MULLIGAN, Roy F. Weston, Inc., S. Rowshan, J.C. Wallace, D.S. Therry, E.M. Hansen

3:10 RECESS

3:25 (377) **LIMS and Quality - A Flexible Approach for Meeting Commercial and Regulatory Requirements**—D. RADIN, Radian Corporation

3:45 (378) **Sample Sequence Definition Through Pattern Programming**—C. CHELL, Spectra-Physics, Inc., V. Nau, J. Rupf, B. Handa

4:05 (379) **Practical Application of a Local Area Network to the Management of a Chromatography Laboratory**—M.E. ADASKAVEG, Varian Instrument Group, F.E. Klink, T.L. Sheehan, N. Mostaan, P. Mostaan

4:25 (380) **Techniques for Chromatography Data Systems Validation**—M. CANALES, PE Nelson Systems, H. Brown

4:45 (381) **A Unified Chromatography Instrument Control, Data Handling and Information Management System Providing Unique Operational Modes**—A. BENNETT, ICI Instruments, E. Stone

Separations of Pharmaceutical Interest

Monday Afternoon, Room 1E19
D.F. Pensenstadler, Presiding
Westinghouse Electric Corp.

1:30 (382) **Automated Sample Preparation for the Analysis of Cocaine and Benzoylecgonine by GC/MS**—P. TIMMONEY, MilliLab, P. Beals

1:50 (383) **Analysis of Drugs in Post Mortem Biofluids Using an In-Line Sample Preparation Device (AASP)**—B.K. LOGAN, University of Tennessee, D.T. Stafford

2:10 (384) **Fully Automated Basket Dissolution Testing of Microencapsulated Dosage Forms**—J.A. STEICHEN, Adria Laboratories

SIMPLIFY YOUR LABORATORY WEIGHING WITH THREE SOLID VALUES FROM OHAUS.

These three precise, user-friendly balances from Ohaus can significantly reduce your costs by increasing weighing speed and productivity. 1. The easy-to-use, durable GA Series analytical balances have enhanced stability and rapid response time. Capacities range from 110g to 200g with readabilities from 0.1mg to 0.01mg. Choose this balance when only the highest precision will do. 2. The new MB200 electronic moisture balance is the result of 30 years' experience in this technology. With it you determine solid or moisture content, continuously monitored by a dual display. Multiple temperature settings add to its versatility, and the auto-dry mode gives you a significant time saver. 3. With the versatile GT Series you draw on a broad range of software options. Its capabilities range from batching and mixing to more complex animal weighing and parts counting, and the graphic display lets you access a target filling mode. Let us tell you all about these cost-saving electronic balances. Call or write: Ohaus Corporation, 29 Hanover Rd., Florham Park, NJ 07932. (800) 672-7722.

Weighing solutions from Ohaus...
as easy as 1-2-3:

2
1
3
OHAUS
MB200
GA2000
GT2100
OHAUS

CIRCLE 132 ON READER SERVICE CARD

2:30 (385) **A New Multiple Interaction Sample Preparation Bonded Phase for Pharmaceutical Analysis**—D.D. BLEVINS, Analytichem International, V.M. Dixit, V. Dixit

2:50 (386) **Automated Dissolution Testing for High Performance Liquid Chromatography**—R.W. GIUFFRE, Hewlett Packard Company, S. Titmas, H.J.P. Sievert

3:10 RECESS

3:25 (387) **Ion Mobility Spectrometry/Mass Spectrometry Analysis of Analgesic Drugs and Commercial Pharmaceutical Preparations**—G.A. EICEMAN, New Mexico State University, A.P. Snyder, D.B. Shoff, C.S. Harden, D.A. Blyth

3:45 (388) **Automated Tablet Assays and Content Uniformity Using Modular Robotics**—A.M. PAUL, Zymark Corporation, K. Tucker, G. Johnston

4:05 (389) **Confirmatory Testing for Drugs of Abuse by GC/MS - An Automated Approach to Sample Preparation**—R.K. BROWN, Zymark Corporation, C. Hatfield, J. Tomlinson

4:25 (390) **Enantiomeric Separation by Capillary Gas Chromatography Using Derivatized Cyclodextrin Stationary Phases**—W. LI, University of Missouri-Rolla, D.W. Armstrong

4:45 (391) **Capillary Electrophoresis of Peptides and Small Proteins**—R.I. ROBINSON, Rutgers University, T. Wang, R.A. Hartwick, R. Blain

Spectral Absorption-Fluorescence—Environmental Applications

Monday Afternoon, Room 1E12
J.J. McGovern, Presiding

1:30 (392) **A Novel Field-Portable Microprocessor-Controlled Bichromatic Instrument for Measurement of ppb Levels of Dissolved Oxygen in Water**—N. SPOKES, CHEMetrics, Inc., D.J. Lohr

1:50 (393) **A Field-Portable Chemical Test Kit for Detection of Lead in Drinking Water**—N. SPOKES, CHEMetrics, Inc., H.B. Castaneda, D.J. Lohr, J. Bradley

2:10 (394) **Analysis of Phase-Resolved Fluorescence Spectral Fingerprints of Petroleum-Based Lubricants**—P.M. RITENOUR, Duke University, L.B. McGown

2:30 (395) **Applications of FT-VIS/FL Microscope Spectrometer for Analysis of Contaminant Dust Particles and Forensic Samples**—S. MATSUI, Hitachi Ltd., Y. Maeda, B Variano

2:50 (396) **Paper Withdrawn**

3:10 RECESS

3:25 (397) **A User Friendly Instrument for the Analysis of Atmospheric Pollutants**—N.P. REYNOLDS, Atomic Energy of Canada Limited, P. Harris, A.C. Vikis, R. MacFarlane, P. Driver

3:45 (398) **An Intelligent Detector-Analyzer for Atmospheric Pollutants**—A.C. VIKIS, Atomic Energy of Canada Limited, P. Harris, R. MacFarlane, P. Driver, N.P. Reynolds

4:05 (399) **Temperature Effects on Sample Spectra in UV/VIS Spectroscopy**—T. KLINK, Hewlett-Packard GmbH, G. Hack, F. Koch, T. Owen

4:25 (400) **Applications of Difficult and Large Samples Using a New UV/VIS/NIR Spectrophotometer with an Expanded Sampling Area**—M. RETZIK, Hitachi Instruments, Inc., S. Minakawa

4:45 (401) **Spectrophotometric Determination of Arsenic by Molybdenum Blue Method in Lead-Zinc Concentrates and Related Smelter Products After Chloroform Extraction of Iodide Complex**—V.S. RAO, Hindustan Zinc Limited, B.H.K. Sarma, S.C.S. Rajan

Tuesday, March 6, 1990

SYMPOSIUM

Advances in Raman Spectroscopy - arranged by S.A. Asher of University of Pittsburgh

Tuesday Morning, Room 1A07
S.A. Asher, Presiding
University of Pittsburgh

8:30 **Introductory Remarks**—S.A. ASHER

8:35 (402) **Raman Spectroscopy of Microparticles in Laser Light Traps**—W. KIEFER, Inst. of Physical Chemistry

9:10 (403) **Near Infrared FT Raman Spectroscopy of Photolabile Organocobalt B_{12} Model Compounds**—N.T. YU, Georgia Institute of Technology

9:45 (404) **Time Resolved Resonance Raman Measurements of Cytochrome Oxidase**—D. ROUSSEAU, AT&T Bell Laboratories

10:20 RECESS

10:35 (405) **Novel Measurement Capabilities of Fully Resonant 4 Wave Spectroscopy**—J. WRIGHT, University of Wisconsin

11:10 (406) **UV Resonance Raman Studies of Bacteria**—W.H. NELSON, University of Rhode Island

SYMPOSIUM

Data Tools for Solving Analytical Chemistry Problems - arranged by S.R. Heller of Scitechinform

Tuesday Morning, Room 1A06
S.R. Heller, Presiding
Scitechinform

8:30 **Introductory Remarks**—S.R. HELLER

8:35 (407) **Analytical Chemistry Data in the NIST Standard Reference Data Program**—M. CHASE, NIST, OSRD

9:15 (408) **Analytical Chemistry Data and the Beilstein Online Database**—C. JOCHUM, Beilstein Institute

9:55 (409) **Data Collection and Instrumentation for Atmospheric Chemistry**—V.L. TALROSE, Institute of Chemical Physics

10:35 RECESS

10:50 (410) **Analytical Chemistry Data for the Analysis of Organic Environmental Pollutants**—R. HITES, Indiana University

11:30 **Panel Discussion, Speakers and Session Chairman**

SYMPOSIUM

Laboratory Management—An International Perspective on Excellence - arranged by J.H. Taylor, Jr. of Analytical Technologies, Inc.

Tuesday Morning, Room 1D01
J.H. Taylor Jr., Presiding
Analytical Technologies, Inc.

8:30 **Introductory Remarks**—J.H. TAYLOR, JR.

MS-MS FOR THE MASSES.
VG QUATTRO.

The MS-MS power and accuracy that was once the exclusive province of research labs is available to production laboratories at a truly affordable price. This means that chemists working in areas such as environmental analysis, forensic science, toxicology and biochemistry can now enjoy full MS-MS productivity on a limited budget. VG Quattro, triple quadrupole mass spectrometer offers an easy-to-use LAB-BASE data system linked to transputers with phenomenal processing power. VG Quattro integrates laboratory robotics with mass spectral analysis for fully unattended analysis of both solid and liquid samples. To find out how VG Quattro can make your laboratory more cost-effective, call David Pudvah at (508) 777-8034.

VG INSTRUMENTS

32 Commerce Center
Cherry Hill Drive
Danvers, MA 01923-9896

SEE US AT PITTCON

VG acknowledges the contribution to hexapole gas cell technology of Dr. I. Szabo, University of Lund Chemical Centre.

CIRCLE 191 ON READER SERVICE CARD

8:35 (411) **Developing and Monitoring Performance Indicators**—I. DAINIS, State Chemistry Laboratories

9:05 (412) **Industrial Laboratory Management in Japan**—K. MIURA, Mitsubishi Kasei

9:35 (413) **Comparison of Laboratory Operations in China to the United States**—S. SUN, Eco Tek Laboratory Services, Inc., J. Thean

10:05 RECESS

10:20 (414) **Total Quality Issues in Medical Laboratories of the United Kingdom**—A. McLELLAN, Royal Infirmary

10:50 (415) **A Korean Laboratory's Approach to Excellence**—H.Y. SO, Korea Standards Research Instit.

11:20 (416) **Quality Criteria for all Activities in the Laboratory and an Improvement Process**—R. WOODS, Analytical Technologies, Inc., R.M. Amano, W.F. Bowers, F. Grothkopp, J.H. Taylor, Jr.

1990 Pittsburgh Analytical Chemistry Award—Biomedical Analytical Chemistry - **arranged by G.H. Morrison of Cornell University and R.M. Windisch of Mercy Hospital of Pittsburgh**

Tuesday Morning, Room 1A08
R.M. Windisch, Presiding
Mercy Hospital of Pittsburgh

8:30 (417) **Neutralization Chemical Reionization: Can We Direct Cleavage in Tandem Mass Spectrometry of Middle Molecules**—C. FENSELAU, University of Maryland, R. Orlando, R.J. Cotter

9:10 (418) **The Role of Separation Science in Bioanalytical Chemistry for the 1990's**—B.L. KARGER, Northeastern University

9:50 (419) **Metallobiochemistry: The Resultant of Progress in Instrumental Analysis and Protein Chemistry**—B.L. VALLEE, Harvard Medical School

10:30 RECESS

10:45

Presentation of the
1990 Pittsburgh Analytical Chemistry Award
to
Professor George H. Morrison
Cornell University
by
Mary Louise Theodore, Chairman
Society for Analytical Chemists of Pittsburgh

10:55 (420) **Award Address: Ion Microscopy in Biology and Medicine**—G.H. MORRISON, Cornell University

SYMPOSIUM

Quality and Productivity with Chromatographic Methods (Part I) - **arranged by J.Q. Walker of IBM Corporation**

Tuesday Morning, Room 1A23
J.Q. Walker, Presiding
IBM Corporation

8:30 **Introductory Remarks**—J.Q. WALKER

8:35 (421) **Computer-Assisted LC for Automated Qualitative and Quantitative Analysis of Toxic Drugs**—K. JINNO, Toyohashi Univ. of Technology

9:10 (422) **GC Method Development**—R. VILLALOBOS, The Foxboro Company

9:45 (423) **Column and Stationary Phase Selection in GC**—W. JENNINGS, J & W Scientific

10:20 RECESS

10:35 (424) **Capillary Electrophoresis and Capillary Electrophoresis-Mass Spectrometry**—R.D. SMITH, Battelle Pacific Northwest Labs., H.R. Udseth, C.G. Edmonds

11:10 (425) **Computer-Aided Method Development in LC**—J.W. DOLAN, LC Resources Inc., L.R. Snyder

Electrochemistry—Microelectrodes and Modified Electrodes

Tuesday Morning, Room 1E12
J.F. Coetzee, Presiding
University of Pittsburgh

8:30 (426) **Quantitative PERMS for Electrochemistry**—J. SZPYLKA, The Ohio State University, L.B. Anderson

8:50 (427) **Electrochemical Ultramicrobiosensors for Glucose**—E.R. REYNOLDS, Rutgers, The State Univ. of NJ, A.M. Yacynych

9:10 (428) **Immobilized Enzyme Electrodes Based on Glutamate Oxidase**—D.D. CUNNINGHAM, Universal Sensors, Inc., R.L. Villarta, G.G. Guilbault

9:30 (429) **Biological/Electrochemical Microstructures for Amperometric Sensing**—J. WANG, New Mexico State University, N. Naser, M. Connor, M.S. Lin, L.H. Wu, K. Varughese, J. Sanchez, T. Martinez, M. Smyth

9:50 (430) **Dynamics of Electrocatalytic Oxidation of Cysteine at Nafion Film Coated Electrodes**—P. HE, Fudan University, X. Chen

10:10 RECESS

POSTER PRESENTATIONS

Poster Papers will be on display from 9:30 AM - 4:00 PM
Authors will be available from 10:00 AM - 12:00 Noon and 2:00 - 4:00 PM

GC/Matrix Isolation/FTIR

Tuesday, Room 1C01
M.M. Mossoba, Presiding
Food and Drug Administration

(446) **Picogram Detection Limits for Complex Mixture Analysis Utilizing GC/Matrix Isolation-FTIR-MS**—E.R. BAUMEISTER, University of California, Riverside, C.L. Wilkins

(447) **Characterization of Semivolatile Organic Compounds in Air Sample Extracts by GC/MI-IR**—N.K. WILSON, U.S. Environ. Protection Agency, R.K. Barbour, J.W. Childers

(448) **Matrix Isolation Fourier Transform Infrared Spectra of Natural Products**—W.H. COLEMAN, III, R.J. Reynolds Tobacco Company, B.M. Gordon

(449) **Industrial Applications of Gas Chromatography-Matrix Isolation-Infrared Spectroscopy**—R.R. PAPENFUSS, The Dow Chemical Company, R.A. Nyquist

(450) **Analysis of Semivolatile Pollutants by Gas Chromatography/Matrix Isolation-Infrared Spectrometry/Mass Spectrometry**—L.F. SYTSMA, Trinity Christian College, J.F. Schneider, P.M. Aznavoorian

(451) **Advanced Interface Development for GC/MI/FTIR Analyses**—S.O. VAUGHAN, The Research Triangle Institute

(452) **Increased Dynamic Range by Elevated Matrix Temperature in Matrix Isolation GC-FTIR**—D.E. ROBERTS, Mattson Instruments, Inc.

(453) **Identification of Unknowns in Complex Multi-Component Mixtures Using GC/MS and GC/MI/FTIR**—J.T. CRONIN, E. I. du Pont de Nemours & Co.

(454) **Harnessing the Identification Power of an Injector/Trap - 2D-GC-Mass Spectrometer - Matrix-Isolation FTIR**—P.A. RODRIGUEZ, The Procter & Gamble Company, C.L. Eddy, C. Marcott

(455) **Paper Withdrawn**

(456) **Routine Analysis of Whole Air Samples Using a GC/MI/FTIR Instrument**—H. KIMBALL, U.S. Environ. Protection Agency, J.L. Hudson, B.J. Fairless

(457) **Analysis of Kerogens by Pyrolysis/Gas Chromatography/Matrix Isolation-Infrared Spectrometry/Mass Spectrometry**—A.S. BOPARAI, Argonne National Laboratory, E.L. Delemeester, J.F. Schneider, T.A. Abrajano, Jr.

(458) **Advantages of Functional Group Specific Chromatographic Reconstruction in MI-GC-FTIR**—D.E. ROBERTS, Mattson Instruments, Inc.

(459) **Hydrogenation of Soybean Oil: A Gas Chromatography/Matrix Isolation/Fourier Transform Infrared Study**—M.M. MOSSOBA, Food and Drug Administration, R.E. McDonald, F.S. Fry, Jr., D.J. Armstrong, S.W. Page

Atomic Absorption—Analytical Procedures I

Tuesday Morning, Room 1E12
N.J. Hornung Presiding
Aluminum Company of America

10:25 (431) **The Determination of Au, Pt, and Pd in Acid Digested Ores**—D.F. PFLUGHOEFT-HASSETT, University of North Dakota, D.J. Hassett

10:45 (432) **Optimization of Plasma and Sample Introduction Systems for Spark Ablation Analysis of Metals and Alloys—Comparison of Sequential and Simultaneous Measurement Modes**—A. MANDOKI, Jobin Yvon, Instruments SA, Y. Lang, A. Le Marchand

11:05 (433) **Flow Injection AAS: Precise Automated Determinations at the Trace Level**—Z. GROBENSKI, Bodenseewerk Perkin-Elmer GmbH, T. Guo, G. Schlemmer, W. Schrader

Starting with superior chemistry, we have methodically developed systems that are the logical next step in high pressure liquid chromatography.

HRLC. High resolution liquid chromatography.

Over 15 years in development. Built for the next century.

Find out how the HRLC system can work for your laboratory. Our HRLC technical experts have complete information. Call them at 1-800-4-BIORAD.

Bio-Rad HRLC components are also sold separately. For the sales representative nearest you please call 415/232-7000.

Chemical Division

3300 Regatta Boulevard
Richmond, CA 94804
(415) 232-7000
1-800-4 BIO RAD

Also in Rockville Centre, NY; Hornsby, Australia; Vienna, Austria; Brussels, Belgium; Mississauga, Canada; Hemel Hempstead, England; Paris, France; Munich, Germany; Hong Kong; Milan, Italy; Tokyo, Japan; Veenendaal, The Netherlands; Madrid, Spain; and Glattbrugg, Switzerland.

CIRCLE 30 ON READER SERVICE CARD

11:25 (434) **Common Conditions for the Determination of Trace Elements in Medical Samples Using Graphite Furnace AAS**—G. SCHLEMMER, Bodenseewerk Perkin-Elmer GmbH, W. Schrader, E. Bulska, M. Hasei

11:45 (435) **Preconcentration of Trace Elements for AAS and ICP**—N. PRAKASH, Graz University of Technology, A. Grillo, G. Csanady, M. Michaelis, G. Knapp

Environmental—Air and Soil Analysis

Tuesday Morning, Room 1E10
R. Brna, Presiding
Air Quality Services, Inc.

8:30 (436) **Paper Withdrawn**

8:50 (437) **Evaluation of Isocyanate Monitoring Systems**—K.E. WILLIAMS, U.S. Army Environ. Hyg. Agency, R.J. Moore, G.E. Podalak

9:10 (438) **Analysis of Polynuclear Aromatic Hydrocarbon Mixtures by Laser-Induced Time-Resolved Shpol'skii Fluorescence Spectroscopy**—R.K. FORCE, University of Rhode Island, K.M. Bark

9:30 (439) **Headspace Gas Chromatography Analysis of Petroleum-Derived Contaminants in Soils and Groundwater**—T.C. VOICE, Michigan State University, N.J. Hayden, Y.L. Pan

9:50 (440) **Simultaneous Determination of NO_x and SO_x in Gases Using Ion Chromatography**—K. CRIPPEN, Institute of Gas Technology, S.S. Chao, A. Attari

10:10 RECESS

10:25 (441) **Ultra-Specific and Sensitive Determination of Hexavalent Chromium in Airborne Particulates from Ambient and Stationary Sources**—R.J. JOYCE, Dionex Corporation, M. Doyle, E. Arar

10:45 (442) **Standardization of an Emission Method for Dioxin Measurement**—J.C. PAU, U.S. Environ. Protection Agency, J.E. Knoll, M.R. Midgett

11:05 (443) **Specific Surface Areas and Surface Scaling Behavior of Coal Stack Ash Subfractions**—J.K. SANDERS, University of Tennessee, V.R. Miller, E.L. Wehry, G. Mamantov

11:25 (444) **Applications of Ion Chromatography in Disaster Recovery of Electron Equipment**—M.E. KRZYZANOWSKI, Bellcore

11:45 (445) **A New Fluorescence Detector for Mercury**—P. STOCKWELL, PS Analytical, M. Moses, K.C. Thompson, A. Henson

Gas Chromatography—Petroleum

Tuesday Morning, Room 1E11
R.W. McCoy, Presiding
Amoco Corporation

8:30 (460) **A Thin Film Wide Bore Capillary Column for the Analysis of Petroleum Waxes and Other High Boiling Materials**—P.S. SPOCK, Supelco, Inc., R.E. Long, M.V. Robillard, L.M. Sidisky

8:50 (461) **Residual Simulated Distillation Analysis of Heavy Petroleum Liquids**—C.S. WENTZEL, Arnel Inc.

9:10 (462) **Simultaneous Simulated Distillation and Aromatics Distribution Analysis by Gas Chromatography with Dual Detection**—V. SANCHEZ, VA Polytechnic Inst. & State Univ., H.M. McNair, J.A. Lubkowitz

9:30 (463) **Application of the Helium Ionization Detector (HID) for the Measurement of ppm and ppb Level Contaminations in Light Hydrocarbon and High-Purity Gases**—J.R. CRNKO, Antek Instruments, Inc., O.L. Hollis

9:50 (464) **Characterization of Sulphur in Coal by Pyrolysis - Gas Chromatography**—I. ERICSSON, University of Lund

10:10 RECESS

10:25 (465) **Simultaneous Determination of Nickel and Vanadium Compounds in Petroleum by GC-AED**—B.D. QUIMBY, Hewlett-Packard Company, P.C. Dryden, J.J. Sullivan

10:45 (466) **Determination of Individual Hydrocarbons in Automobile Exhaust from Gasoline-, Methanol-, and Variable-Fueled Vehicles**—F. LIPARI, General Motors Research Labs.

11:05 (467) **Quality Control/Quality Assurance Aspects of Oilfield Emission Grab Sampling at Stationary Sources**—R.S. VISWANATH, Tulsa City-County Health Dept., J.H. VanSandt, W.B. Kuykendal

11:25 (468) **BTU Analysis - A Rapid, Turnkey Approach**—J. STRAUSS, Microsensor Technology, Inc.

11:45 (469) **Continuous Monitoring of Volatile and Non-Volatile Hydrocarbons in Water by an On-Line Water Monitoring System**—J.A. VALADE, GE Silicones

Gas Chromatography—Theoretical Aspects

Tuesday Morning, Room 1E20
M.S. Klee, Presiding
Smith Kline & French Labs.

8:30 (470) **Applications of Chemometrics to Chromatography**—J. DUCKWORTH, Galactic Industries Corporation, D. Kuehl

8:50 (471) **Computer-Aided Optimization of GC Runs**—J.W. DOLAN, LC Resources Inc., D.E. Bautz, L.R. Snyder

9:10 (472) **On-Stream Boiling Point Determination**—F.D. MARTIN, Fluid Data/Amscor

9:30 (473) **Packed vs. Capillary Column Non-Steady State GC for Activity Coefficient Measurement**—D.C. LOCKE, Queens College, CUNY, A. Belfer, I. Landau

9:50 (474) **Optimization of a Chromatographic Method**—P. LU, Dalian Inst. of Chemical Physics

10:10 RECESS

10:25 (475) **Effect of Stationary Phases on Consistency of Kovats Retention Indices in Capillary Gas Chromatography**—N.H. SNOW, VA Polytechnic Inst. & State Univ., H.M. McNair

10:45 (476) **Analysis of Gases by Gas-Solid Chromatography Using PLOT Columns**—M. FEENEY, J & W Scientific, J.J. Harland, J. Knitter

11:05 (477) **Polarity Differences Among Nonpolar 0.53 mm ID Capillary Columns with Differing Film Thicknesses**—N.G. ERVIN, Supelco, Inc., C.L. Woolley, L.M. Sidisky

11:25 (478) **Peak Symmetry and Retention of Polar Compounds: The Effects of Sample Concentration and Stationary Phase Polarity**—J.W. WALSH, Restek Corporation, J.W. Stauffer, C.R. Vargo

11:45 (479) **New Adsorbents on PLOT Columns for Gas Analysis: Separation of N_2, C_2, CO, CO_2, and C1-C3 with Capillary Gas Chromatography**—J. DE ZEEUW, Chrompack International b.v., D. Zwiep

HPLC—Novel Detection

Tuesday Morning, Room 1E16
M.G. Khaled., Presiding
North Carolina State University

8:30 (480) **Analysis of Glycosidic Pharmaceuticals Using Integrated Pulsed Amperometric Detection**—J.A. STATLER, Dionex Corporation, P. Williams

8:50 (481) **Whole Column Detection: Application to High Performance Liquid Chromatography**—K.L. ROWLEN, University of Colorado, K.A. Duell, J.P. Avery, J.W. Birks

9:10 (482) **Responsivity of a Photon Counting System**—T.J. EDKINS, Stevens Institute of Technology, D.C. Shelly

9:30 (483) **An Element-Specific Dual-Beam Flame Infrared Emission (FIRE) Detector for Liquid Chromatography**—M.A. BUSCH, Baylor University, C.K.Y. Lam, D.C. Tilotta, K.W. Busch

9:50 (484) **Direct Measurement of Separation Efficiency in the Inlet Region of a Liquid Chromatographic Column**—C.E. EVANS, Michigan State University, V.L. McGuffin

10:10 RECESS

10:25 (485) **Optimization of Fluorescence Diode Array Detection in Reversed Phase Liquid Chromatographic Separations**—T.L. CECIL, Virginia Commonwealth University, S.C. Rutan

10:45 (486) **Correction of Fluorescence Response Shifts Using a Kalman Filter Shift Determination Method**—T.L. CECIL, Virginia Commonwealth University, S.C. Rutan

11:05 (487) **Selective and Sensitive Determination of Amino Acids by High Performance Liquid Chromatography with Photolysis-Electrochemical Detection (HPLC-$h\nu$-EC)**—L. DOU, Northeastern University, I.S. Krull

11:25 (488) **A New HPLC-MS/CZE-MS Interface for a Triple Quadrupole Mass Spectrometer**—M.A. McDOWALL, VG MassLab Ltd., S.A. Jarvis, D.C. Smith, D. Pudvah

11:45 (489) **Points of Problems and Its Counterplan for Refractive Index Detector**—K. SHIRATO, ERMA CR. Inc., Y. Mori, A. Nagai

HPLC—Stationary Phases I

Tuesday Morning, Room 1E21
J.G. Dorsey Presiding
University of Cincinnati

8:30 (490) **Chromatographic Characterization of New Internal Surface Reversed Phases**—L.J. GLUNZ, Regis Chemical Company, B.J. Invergo, H. Wagner, T.J. Szczerba, J.D. Rateike, J.A. Perry

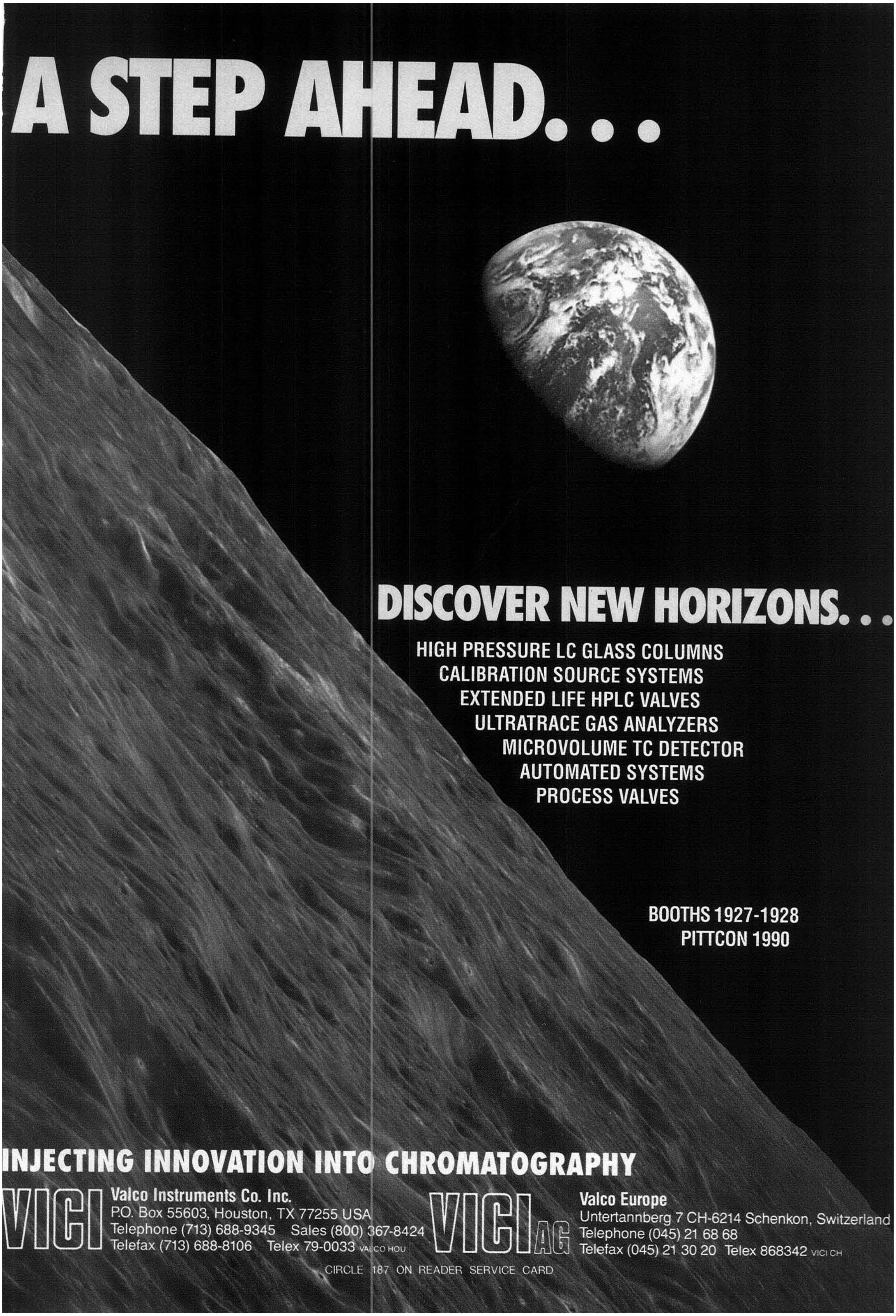

A STEP AHEAD. . .

DISCOVER NEW HORIZONS. . .

HIGH PRESSURE LC GLASS COLUMNS
CALIBRATION SOURCE SYSTEMS
EXTENDED LIFE HPLC VALVES
ULTRATRACE GAS ANALYZERS
MICROVOLUME TC DETECTOR
AUTOMATED SYSTEMS
PROCESS VALVES

BOOTHS 1927-1928
PITTCON 1990

INJECTING INNOVATION INTO CHROMATOGRAPHY

VICI
Valco Instruments Co. Inc.
P.O. Box 55603, Houston, TX 77255 USA
Telephone (713) 688-9345 Sales (800) 367-8424
Telefax (713) 688-8106 Telex 79-0033 VALCO HOU

VICI AG
Valco Europe
Untertannberg 7 CH-6214 Schenkon, Switzerland
Telephone (045) 21 68 68
Telefax (045) 21 30 20 Telex 868342 VICI CH

CIRCLE 187 ON READER SERVICE CARD

8:50 (491) **Retention Behavior and Applications on a Shielded Hydrophobic Phase in the Direct Injection Analyses of Compounds in Biological Fluids by Liquid Chromatography**—C.T. SANTASANIA, Supelco, Inc., T.L. Ascah

9:10 (492) **Novel Bioadsorbents with Selectively Treated External Zones**—D.E. WILLIAMS, Dow Corning Corporation

9:30 (493) **Dual Zone Columns for Bioseparations**—D.E. WILLIAMS, Dow Corning Corporation, P.M. Kabra

9:50 (494) **Clinical Testing of Dual Zone Serum Analysis Columns**—W.H. CAMPBELL, Dow Corning Corporation

10:10 RECESS

10:25 (495) **Simplified Reversed-Phase Separation of Basic Compounds**—G.T. MARSHALL, Interaction Chemicals Inc.

10:45 (496) **Combined On-Column Sample Prep and Separation Using New Latex-Based Multiphase HPLC Columns**—M.A. REY, Dionex Corporation, R. Slingsby

11:05 (497) **Reversed Phase/Ion Exchange: A Powerful Alternative to Conventional Ion Pair Chromatography**—C. POHL, Dionex Corporation

11:25 (498) **Base Deactivated Alkyl Bonded Silica Gels for HPLC and Their Application in Environmental Analysis**—H.J. RITCHIE, Shandon Scientific Ltd., P. Ross, D.R. Woodward

11:45 (499) **An Evaluation of Graphitized Carbon Columns for the Analysis of Environmental Samples**—R.J. DOLPHIN, Shandon Scientific Ltd., B. Monaghan, B. Kaur

ICP/AES—Nebulizers and Sample Introduction

Tuesday Morning, Room 1E13
G. O'Neill, Presiding
Aluminum Company of America

8:30 (500) **Babington Nebulizers, Their Design and Testing**—J. IVALDI, The Perkin-Elmer Corporation, W. Slavin

8:50 (501) **Aerosol Particle Size Effects on ICP-AES Measurements**—J.A. KOROPCHAK, Southern Illinois University, L. Allen

9:10 (502) **The Analysis of Biological Material via Inductively Coupled Plasma/Ultrasonic Nebulization**—S.P. OSBORNE, Applied Research Laboratories, W.J. Kinsey

9:30 (503) **Automated Dilution and ICP Emission Spectrometry**—D.D. NYGAARD, Baird Corporation, T. Alavosus

9:50 (504) **Influence of Sample Introduction Temperature Stabilization in ICP-AES**—M.W. ROUTH, Applied Research Laboratories, P. Cassagne, T.J. Johnson, D. Tasker, R.C. Floyd

10:10 RECESS

10:25 (505) **Comparison of Three Efficient Sample Introduction Techniques for Direct Current Plasma Spectrometry**—M.W. TIKKANEN, Applied Research Laboratories, R. Starek, S. Peters

10:45 (506) **Some Approaches to High Particulate Content Sample Analysis by Inductively Coupled Plasma - Atomic Emission Spectrometry**—S.F. ZHU, Spectro Analytical Instru., Inc., J.E. Goulter, W.J. Angelotti

11:05 (507) **Analysis of Residual Catalyst in the Production of a High Performance Polymer Using ICP and IC**—E.C. GAPASIN, Raychem Corporation, C.S. Austin

11:25 (508) **A New Compact Hydride Generator for As, Se, and Sb Determinations in Environmental Materials by ICP-AES. Influence of Hydrogen, Sheath Gas Flow and Generator Frequency on Analytical Performance**—C.V. PHAN, Jobin Yobin (ISA), A. Le Marchand, I.B. Brenner

11:45 (509) **The Analysis of Major and Minor Elements in Iron Ore and Steel Using Inductively Coupled Plasma Atomic Spectrometry**—P. WEE, Leco Instruments Limited, S. McGeorge, P. Cop

Infrared III—Apparatus and Techniques A

Tuesday Morning, Room 1E18
F.A. Miller, Presiding
University of Pittsburgh

8:30 (510) **FTIR Spectroscopy: Optimized Fiber Optic Probes in Real-World Applications**—R.J. ROSENTHAL, Nicolet Instrument Corporation, M.J. Smith

8:50 (511) **Process Analysis with a Remote Near Infrared Fourier Transform Spectrometer**—R. MACKISON, Perkin-Elmer Limited, D.J. Cutler, H.M. Mould, R.M. Belchamber, S.J. Brinkworth, C. Deeley

9:10 (512) **A New/Old Fiber Optic Material for Infrared Spectroscopy - Potassium Bromide**—R.G. MESSERSCHMIDT, Connecticut Instrument Corp., J.A. Harrington

9:30 (513) **A New Fiber Optic Based IR Chemical Sensor**—R. KELLNER, Technical University of Vienna, C. Weigel

9:50 (514) **Solid State Interferometer "TUNOR" for Gas Analysis**—K.H. ZORNER, Maihak Aktiengesellschaft

10:10 RECESS

10:25 (515) **Field Experience with an Industrialized FTIR Remote Gas Analyzer**—R.L. SANDRIDGE, Proctor Consulting, Inc., R.N. Hunt

10:45 (516) **Realization of the Potential of FTIR PAS by Means of Step-Scan Interferometry**—R.A. PALMER, Duke University, C.J. Manning, R.M. Dittmar, P.J. Thomas, J.L. Chao

11:05 (517) **Recent Developments in Step-Scan Inferometric Spectroscopy**—R. RUBINOVITZ Bruker Instruments, Inc., R. Kenton, A. Simon

11:25 (518) **The Comparison of IIR and FIR Digital Filters for the Detection of Chemical Vapors Using an FTIR Spectrometer**—R.T. KROUTIL, U.S. Army Chemical Research, M.S. DeSha, W.R. Loerop, G.W. Small

11:45 (519) **A Closed Loop FTIR/ATR Liquid Sampling System for Near-Line and On-Line Applications**—W.M. DOYLE, Axiom Analytical, Inc., N.A. Jennings

Near Infrared (Tomas Hirschfeld Award in NIRA)

Tuesday Morning, Room 1E19
E. Stark, Presiding
KES Analysis Inc.

8:30

The Tomas Hirschfeld Award in NIRA
Sponsored by Bran + Luebbe Analyzing Technologies, Inc.
Presented to
Charles E. Miller
of
University of Washington
by
Arnold G. Grushkin, President
Bran + Luebbe Analyzing Technologies, Inc.

8:50 (520) **Award Address: Near Infrared Spectroscopy of Synthetic Polymers**—C.E. MILLER, University of Washington, B.E. Eichinger

9:10 (521) **The NIR Experience: How Can the Process Industry Benefit from It?**—H MARTENS, Martens Analysis, Inc.

9:30 (522) **Global Calibration Methods for Predicting Properties from Near Infrared Spectra**—S.M. BUCO, Statistical Resources, Inc., J.G. Montalvo, Jr.

9:50 (523) **Comparisons of NIR Calibration Methods**—L.G. WEYER, Hercules Research Center

10:10 RECESS

10:25 (524) **Vibrational Assignments of Weak Features in the C-H Stretching Fundamental and Overtone Regions for Selected Hydrocarbons**—P.R. GRIFFITHS, University of Idaho, J.M. Olinger

10:45 (525) **Near-IR Spectrometry Is Easy with the BENDS**—R.A. LODDER, University of Kentucky

11:05 (526) **Effect of Wavelength Drift on Prediction Errors in the NIR**—E.H. BAUGHMAN, Amoco Corporation, G.H. Vickers, D.M. Mayes

11:25 (527) **Near-Infrared Spectroscopy in the Chemical Industry: Renaissance at Last**—H.W. SIESLER, University of Essen

11:45 (528) **The Problem of Reference Data and the Certification of Near Infrared Reflectance Spectroscopy**—F.E. BARTON, II, USDA/ARS

Separations of Pharmaceutical Interest

Tuesday Morning, Room 1E08
M.J. Levitt, Presiding
Biodecision Laboratories

8:30 (529) **Enantiomeric Resolution of N-[4,4-di(3-methyl-thien-2-yl)-but-3-enyl] Nipecotic Acid by Reversed-Phase Chiral High Performance Liquid Chromatography**—A.M. RUSTUM, Abbott Laboratories, L. Gutierrez

8:50 (530) **New Polymeric Columns for Simultaneous Reversed Phase and Ion-Exchange Chromatography of Pharmaceutical Formulations**—P. WILLIAMS, Dionex Corporation, J.A. Statler

9:10 (531) **The Use of Supercritical Fluid Extraction in the Analysis of Drugs from Complex Matrices**—J.V. SMITH, Hewlett-Packard Company, W.J. Sanders

9:30 (532) **Biochemical Separations with Two New HPLC Ion-Exchange Columns**—N.F. NELSON, Interaction Chemicals Inc., N. Kitagawa

9:50 (533) **TG-FTIR Analysis of Pharmaceuticals**—R.M. CARANGELO, Advanced Fuel Research, P. Solomon, D. Gravel, M. Baillargeon, G. Vail, F. Baudais

10:10 RECESS

10:25 (534) **New Polymeric Achiral and Chiral Reagents for Off-Line Solid Phase Derivatizations of Alcohols in HPLC-UV/FL**—I.S. KRULL, Northeastern University, C.X. Gao, A. Trogen

10:45 (535) **Detection and Selectivity Enhancement of Pharmaceutical Compounds Through Automated Derivatization Methods**—F. LAI, Varian Instrument Group, T.L. Sheehan, G. Mayer

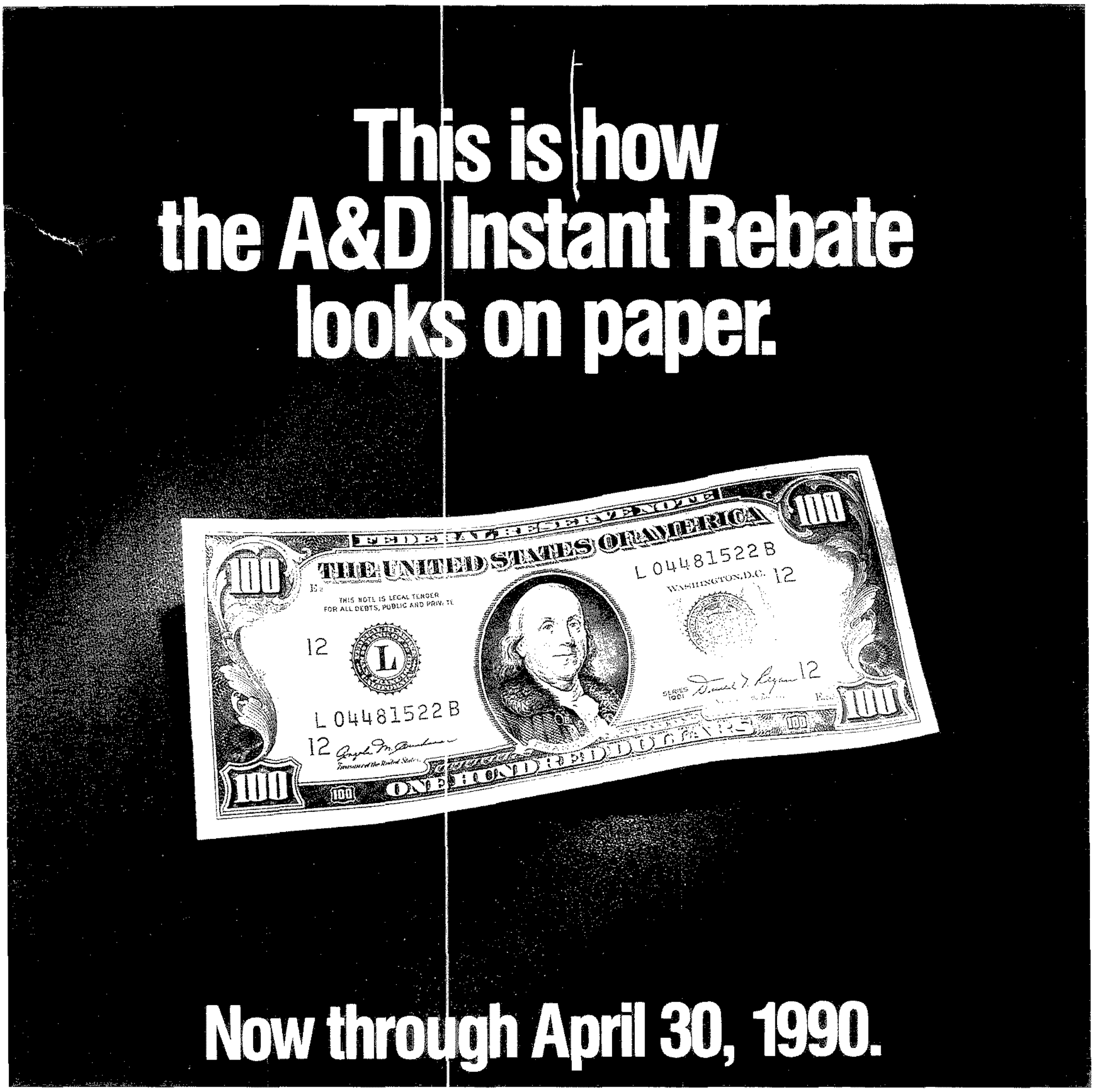
This is how
the A&D Instant Rebate
looks on paper.
FEDERAL RESERVE NOTE
THE UNITED STATES OF AMERICA
100
L 04481522 B
WASHINGTON, D.C.
12
THIS NOTE IS LEGAL TENDER FOR ALL DEBTS, PUBLIC AND PRIVATE
L
ONE HUNDRED DOLLARS
Now through April 30, 1990.

Right now, our analytical balances look better than ever.

Because right now, A&D is giving an instant rebate with each one sold.

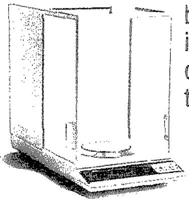

Buy an ER Series analytical balance and your company gets an instant rebate of $50. Buy one from our FR Series and the rebate jumps to $100.

Just be sure to place your order by April 30, 1990.

Even without the rebate, picking up an A&D analytical balance is a smart move. Not just because of our automatic calibration, ease-of-use, and wireless-remote options, but because of A&D's own technological breakthroughs. All of which can help you save money now. And down the road, too, thanks to our remarkable dependability.

Call 800-726-3364 today for the dealer nearest you.

Because while this offer looks good on paper, it looks even better in person.

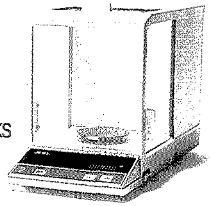

Distributed in Canada by Johns Scientific Inc.
800-268-4440

A&D ENGINEERING, INC.
1555 McCandless Drive, Milpitas, CA 95035 (408) 263-5333

CIRCLE 7 ON READER SERVICE CARD

11:05 (536) **Automation of Pre-Column Derivatization with PITC for the Analysis of Amino Acids from Protein Hydrolyzates and Physiological Fluids**—M. MEYS, Waters Chrom. Div. Millipore Corp., S.A. Cohen, T.L. Tarvin

11:25 (537) **Automated Pre-Column Derivatization of Amino Groups of Toxicologically and Biologically Relevant Compounds**—M. STEINWAND, Bodenseewerk Perkin-Elmer GmbH, W. Vogel, C. Gonner

11:45 (538) **Applicability of a Photochemical Reaction Unit in HPLC-Trace Analysis of Drugs**—R. KUPFERSCHMIDT, ICT GmbH, C. Wolf, R.W. Schmid

Supercritical Fluid Extraction

Tuesday Morning, Room 1E15
G.A. Pearse, Jr., Presiding
LeMoyne College

8:30 (539) **Clean Extractions from Nasty Matrices Using Supercritical Fluids**—D.C. LOCKE, Queens College, CUNY, J. Cai, E. Wolfe, K.R.R. Mahanama, S. Tewani

8:50 (540) **SFE - Strategy for Successful Extractions**—C.R. KNIPE, Hewlett-Packard Company, L.G. Randall, J. Smith, W. Pipkin

9:10 (541) **Solvent Elimination SFE/SFC for Trace Analysis of Analytes in Volatile Solvents**—J.L. HEDRICK, VA Polytech. Instit. & State Univ., L.T. Taylor

9:30 (542) **Extending the Range of Petrochemical Analysis by SFC/SFE**—D.E. KNOWLES, Lee Scientific, A.F. Rynaski

9:50 (543) **Supercritical Fluid Extraction of Organochlorine Pesticides from Fish Tissue**—W.S. MILES, Hewlett-Packard Company, L.G. Randall

10:10 RECESS

10:25 (544) **Supercritical Fluid Extraction Coupled to Gas Chromatography for the Analysis of Pesticide Residues in Natural Matrices**—B.J. MURPHY, Lee Scientific, N.L. Porter, B.E. Richter

10:45 (545) **Supercritical Extraction of Two Classes of Environmentally Important Compounds from a Soil Matrix Using Off Line Capillary Gas Chromatography FID and Mass Spectral Analysis**—H.M. McNAIR, VA Polytechnic Inst. & State Univ., J.O. Frazier

11:05 (546) **New Applications of Integrated Intelligent Instruments in Trace Organic Analysis**—S.A. LIEBMAN, Geo-Centers, Inc., R.A. Fifer, S. Lurcott, J.C. Watkins, E.J. Levy, M.B. Wasserman

11:25 (547) **Automated Modifier Module for SFC-SFE, Applied to Polar Organics**—T.W. RYAN, Computer Chemical Systems, Inc., S.G. Yocklovich, S. Lurcott, E.J. Levy, S.A. Liebman

11:45 (548) **Supercritical Fluid Extraction for the Rapid Determination of Polychlorinated Dibenzo-*p*-Dioxins and Dibenzofurans in Municipal Incinerator Fly Ash**—N. ALEXANDROU, University of Waterloo, J.B. Pawliszyn

SYMPOSIUM

Recent Advances in High Molecular Weight Mass Spectrometry - arranged by A.G. Sharkey of University of Pittsburgh

Tuesday Afternoon, Room 1A08
A.G. Sharkey, Presiding
University of Pittsburgh

1:30 (549) **Applications of Matrix Assisted UV-Laser Desorption - Ionization Mass Spectrometry**—F. HILLENKAMP, University of Muenster

2:05 (550) **Capillary Electrophoresis and Electrospray Ionization-Mass Spectrometry and Tandem Mass Spectrometry of Large Biomolecules**—R.D. SMITH, Battelle Pacific Northwest Labs.

2:40 (551) **High-Resolution, Time-of-Flight Mass Spectrometry**—A. BENNINGHOVEN, University of Muenster

3:15 RECESS

3:30 (552) **Protein Sequence Analysis: New Methods and Instrumentation**—J. SHABANOWITZ, University of Virginia, D.F. Hunt

4:05 (553) **Time-of-Flight SIMS of Polymers**—D.M. HERCULES, University of Pittsburgh

SYMPOSIUM

Laboratory Accreditation and Standardization: Perspectives on Europe in 1992 (EC'92) - arranged by H.S. Hertz of National Institute of Standards & Technology

Tuesday Afternoon, Room 1D01
H.S. Hertz, Presiding
National Institute of Standards & Technology

1:30 (554) **The Roles of U.S. Science, Technology, Government, and Industry in Preparing for 1992**—T. MURRIN, Department of Commerce

2:15 (555) **The CEN Role in Progress Toward EC'92**—H. PLISSART, European Committee for Standardization (CEN)

3:00 RECESS

3:15 (556) **Perspectives on Laboratory Accreditation**—A. WILLIAMS, The Government Chemist

4:00 (557) **U.S. Industrial Concerns on Laboratory Accreditation and Standardization**—P.D. LAFLEUR, Eastman Kodak Company

4:45 **Panel Discussion**

SYMPOSIUM

Quality and Productivity with Chromatographic Methods (Part II) - arranged by J.Q. Walker of IBM Corporation

Tuesday Afternoon, Room 1A23
J.Q. Walker, Presiding
IBM Corporation

1:25 **Introductory Remarks**—J.Q. WALKER

1:30 (558) **HPLC Column/Substrate Selection**—J.J. KIRKLAND, E.I. du Pont de Nemours & Co., Inc.

2:05 (559) **SFC Column/Method Development**—L.T. TAYLOR, VA Polytechnic Inst. & State University

2:40 (560) **When Chromatography Is Not the Best Method**—R.P.W. SCOTT, Dexsil Chemical Corporation

3:15 RECESS

3:30 (561) **Multidimensional Gas Chromatography via Hyphenated Techniques**—B.M. GORDON, R.J. Reynolds Tobacco Company, W.M. Coleman III

4:05 **Round Table Discussion: Troubleshooting Instrument and Method Problems**

SYMPOSIUM

Charles N. Reilley Award - arranged by F.C. Anson of California Institute of Technology

Tuesday Afternoon, Room 1A06
F.C. Anson, Presiding
California Institute of Technology

1:30 **Introductory Remarks**—F.C. ANSON

1:35

1990 Charles N. Reilley Award
will be presented to
Jean-Michel Saveant
of
Universite de Paris VII
by
Barry Miller, AT&T Bell Laboratories
President, Society for Electroanalytical Chemistry

1:40 (562) **Award Address: Electrochemical Approach to Electron Transfer Chemistry - A Few Examples**—J.M. SAVEANT, Universite de Paris VII

2:15 (563) **The Characterization of Metal Chelates - DNA Interactions by Electrochemical and ECL Methods**—A.J. BARD, University of Texas, Austin, M.T. Carter, M. Rodriquez

2:50 (564) **Recent Mechanistic Studies by Cyclic Voltammetry**—D.H. EVANS, University of Delaware

3:25 RECESS

3:40 (565) **Reorganizational and Other Factors for Electron Transfer Rates at Two-Immiscible Liquid and Semiconductor-Liquid Interfaces**—R.A. MARCUS, California Institute of Technology

4:15 (566) **New Electrochemical Microstructures, New Views of Dynamics**—L.R. FAULKNER, University of Illinois

SYMPOSIUM

Williams-Wright Award - arranged by G.L. Richmond of University of Oregon

Tuesday Afternoon, Room 1A07
G.L. Richmond, Presiding
University of Oregon

1:30 **Coblentz Society Annual Membership Meeting. Report of Activities and Plans for 1990-1991**—K. KALASINSKY, President, Coblentz Society

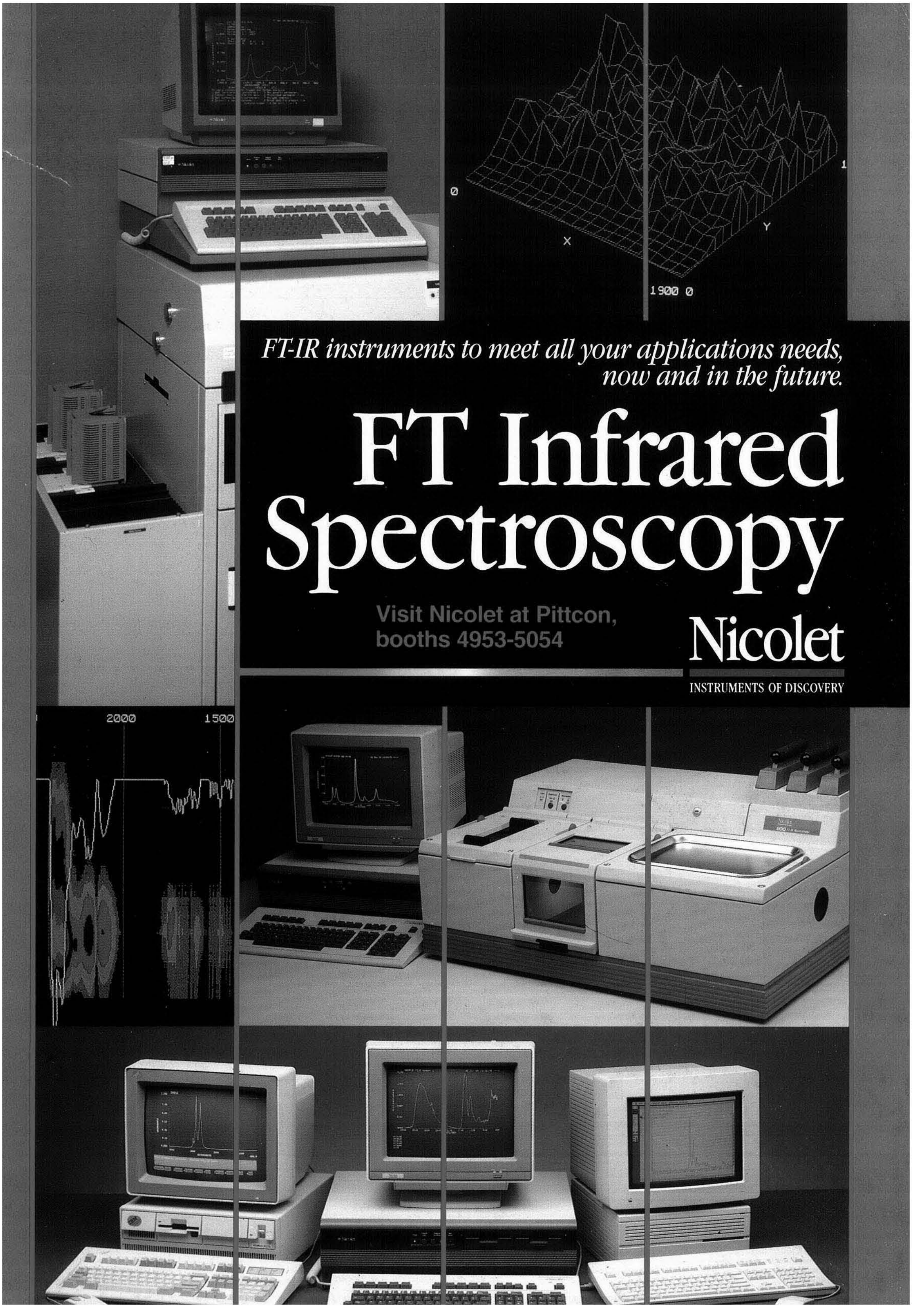
0
1
X
Y
1900 0
2000
1500

FT-IR instruments to meet all your applications needs, now and in the future.

FT Infrared Spectroscopy

Visit Nicolet at Pittcon, booths 4953-5054

Nicolet

INSTRUMENTS OF DISCOVERY

New System 800

Shaping the future of FT-IR spectroscopy

The Nicolet System 800 sets new standards for performance and adaptability. This new system provides the excellent stability, resolution, repeatability, signal-to-noise performance, and high-speed data collection and processing capabilities required in the demanding research environment.

Advanced System 800 capabilities and features include a new ultra-stable interferometer design and sophisticated dynamic alignment system for superior stability and data quality; highest throughput optical design, ultra-high-output sources, and ultra-quiet electronics train for superior S/N performance; optical bench communications, on-screen optical bench configuration status, and an on-board optical bench computer for complete instrument control; and a fully expandable optical path for experimental versatility.

System 800 supports the full range of experiments, including FT-Raman, Emission, Microspectroscopy, GC/FT-IR, SFC/FT-IR, and more. Multiple beam paths allow several different experiments or applications to be simultaneously configured.

System 800 offers the superior problem-solving capabilities and adaptability required in today's research laboratories.

CIRCLE 161 ON READER SERVICE CARD

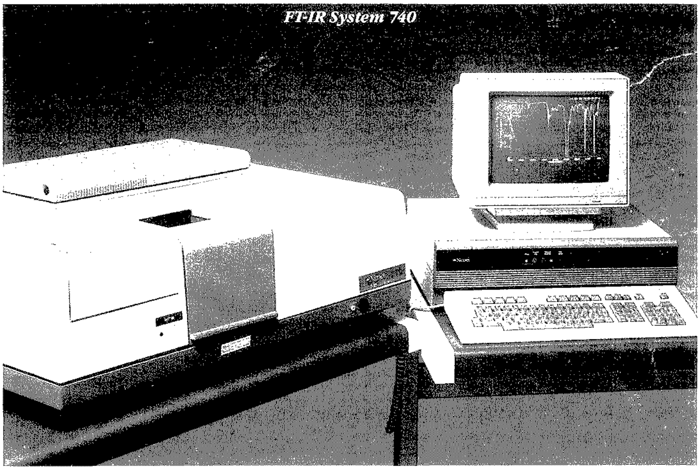
FT-IR System 740

700 Series FT-IR Systems

The Nicolet 700 Series instruments provide exceptional stability, sensitivity, and spectral processing capabilities for demanding applications. Advanced integrated system design and automation provide rapid and accurate spectral measurements and configuration flexibility, regardless of operator experience.

Users can select from an extensive range of beamsplitters and detectors to optimize coverage for near-IR, mid-IR, or far-IR. The System 740 model also includes automatic system optimization using advanced chemometric techniques. 700 Series instruments have been designed to work with Nicolet's proven accessories and auxiliary modules, including those for GC/FT-IR, SFC/FT-IR, TGA/FT-IR, IR microspectroscopy, and microbeam analytical techniques.

CIRCLE 162 ON READER SERVICE CARD

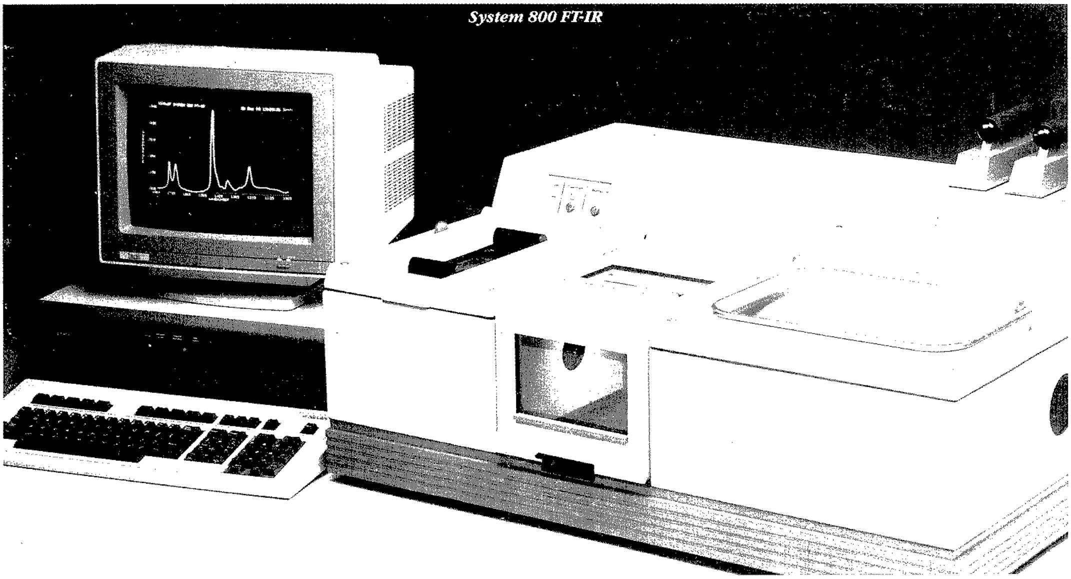
System 800 FT-IR

Nicolet FT-Raman

The Nicolet FT-Raman Spectroscopy System incorporates innovative design features and significant performance advantages over other available instrumentation.

FT-Raman spectroscopy is now a viable technique that offers important advantages over the traditional dispersive technique, making Raman spectroscopy applicable to a wider range of sample types. Two important advantages include the profound decreases in fluorescence and thermal decomposition effects. Further advantages include the inherent throughput, multiplex, and wavenumber accuracy advantages, and the ability to collect high-resolution Raman spectra in a short time. *Nicolet has optimized all design aspects of this FT-Raman system in order to fully realize these intrinsic FT spectroscopy advantages.*

Features of the Nicolet FT-Raman system include:

- The proprietary Nic-Notch™ filter system performs very efficient Rayleigh line supression, allowing measurement of Raman shifts very close to the Rayleigh line.
- Simultaneous collection of Stokes data and anti-Stokes data.
- Excellent sensitivity.
- Sampling versatility and convenience.
- Both FT-Infrared and FT-Raman spectra can be acquired on the same sample with the same Nicolet system in only a few minutes. Since these two techniques give complementary information, this is one of the principle advantages of the Nicolet FT-Raman instrument.

The Nicolet FT-Raman system provides the highest quality data, while offering experimental versatility, convenience, and ease-of-use. This system offers the vibrational spectroscopist formidable capabilities for solving challenging research problems.

CIRCLE 168 ON READER SERVICE CARD

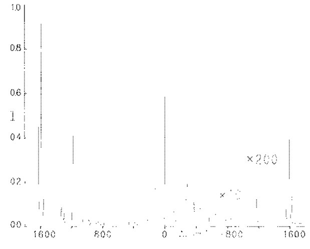

FT-Raman spectrum of 1,4-Bis(2-methylstyryl) benzene, both Stokes and anti-Stokes regions, shows excellent Rayleigh line rejection and signal-to-noise performance, and Raman shifts within 75 cm⁻¹ of the Rayleigh line.

Nicolet IR Microspectroscopy

Nicolet offers a complete line of IR microscope products, from the most advanced research level to routine IR microsampling. The range of microscope offerings includes the Research IR-Plan®, the Analytical Microscope with redundant aperturing®, and the Laboratory Microscope for routine single-aperture operation. Nicolet's microspectroscopy advantages include the patented 20-hour MCT-A detector, 18-bit signal digitization, optimal hardware configuration, unique multi-dimensional mapping software, and extensive applications and service support. These features place the Nicolet IR Microspectroscopy system in the forefront of the industry.

In the example below, an x,y motorized stage controlled by the FT-IR was used to automatically collect the data necessary to delineate the distribution of a coating on a metal substrate. The mapping software shows how a component of the coating varies in concentration with x,y position as the spectroscopist rotates the displayed image on the FT-IR monitor.

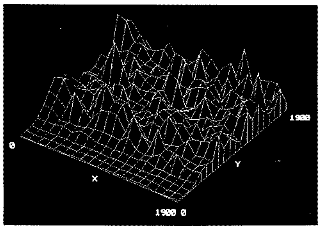

Axonometric profile of coating distribution on steel, produced with the Nicolet Multi-dimensional Analysis software.

CIRCLE 169 ON READER SERVICE CARD

Nicolet SFC/FT-IR System

This system combines the unique separation capabilities of supercritical fluid chromatography (SFC) with the specificity and sensitivity of FT-IR spectroscopy. SFC is a rapidly growing technique for separating samples that are difficult to analyze by gas or liquid chromatography. The Nicolet SFC/FT-IR interface provides the capability to instantly analyze separated components in real time as they elute from the SFC column. This interface maintains chromatographic performance and allows eluents to be analyzed by both the FT-IR spectrometer and the FID detector in the SFC instrument. Supercritical fluid CO_2, which has excellent infrared transparency, is used as the mobile phase to limit interfering spectroscopic absorbances. Comprehensive Nicolet SID™ (Specific Infrared Detection) software performs an extensive range of interactive data manipulation functions.

Applications. SFC/FT-IR is especially well-suited for the analysis of samples that are non-volatile, temperature-sensitive, or of high molecular weight. Thus, the Nicolet SFC/FT-IR system is of particular interest in such applications as polymers, fuels, foods, pharmaceuticals, flavors and fragrances, petrochemicals, biomolecules, and natural products.

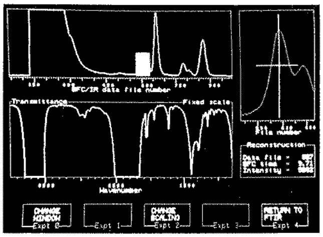

Multi-window SFC/FT-IR display.

CIRCLE 170 ON READER SERVICE CARD

Integrated GC/FT-IR System

for routine separation and indentification.

Excellent sensitivity and resolution without compromising chromatographic quality.

Nicolet SID™ (Specific Infrared Detector) software provides simplified, automatic, real-time operation designed for the chromatographer as well as the spectroscopist.

Exclusive Aldrich-Nicolet on-line gas-phase library for effective search and identification.

Integrated control of GC autosamplers and chromatographic functions such as temperature programming.

Easy, fast switching between GC-IR and other experiments.

CIRCLE 171 ON READER SERVICE CARD

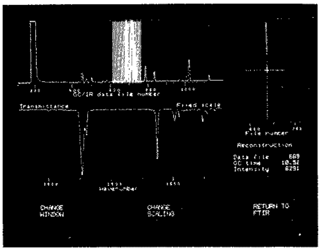

Multi-window GC/FT-IR display.

FT-IR Analyzers

A family of of rugged, compact FT-IR analyzers featuring integrated sample handling and software tailored to meet the needs of specific analyses.

8210 Oil Analyzer: The simplest, most reliable, most efficient way to analyze oil samples. The 8210 features simple one-button operation, and requires no operator interpretation.

CIRCLE 165 ON READER SERVICE CARD

The 8210 is pre-programmed for simultaneous quantitative analysis of oxidation (carbonyls), sulfation, nitration, water content, soot, coolant, and fuel dilution.

8220 Gas Analyzer: Routine gas analysis for industrial process monitoring, ambient air monitoring, and quality control.

- Excellent sensitivity: ppb to % levels
- Multicomponent analysis
- Powerful quantitative software
- Simple one-button operation

The 8220 is versatile enough for wide-ranging applications, yet dedicated in design for easy operation by inexperienced operators. The 8220 is designed specifically for repetitive gas analysis applications, where the speed, sensitivity, and specificity of FT-IR are required.

CIRCLE 166 ON READER SERVICE CARD

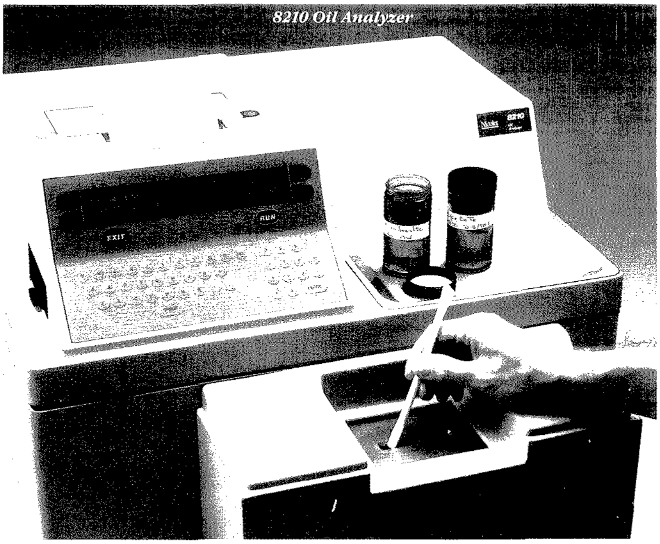
8210 Oil Analyzer

ECO-8S FT-IR for Semiconductor Wafer Analysis. The ECO-8S provides efficiency and versatility in performing semiconductor wafer analytical measurements, including quantitative carbon and oxygen determination, boron and phosphorus in silicate glass (BPSG) analysis, and epitaxial thickness measurement.

The ECO-8S can be equipped with microspectroscopy capabilities for wafer contaminant measurements.

CIRCLE 167 ON READER SERVICE CARD

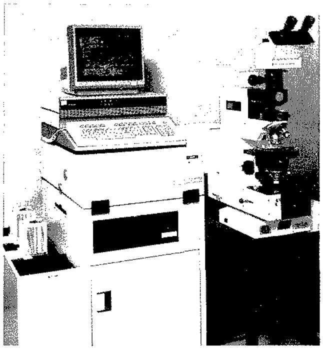

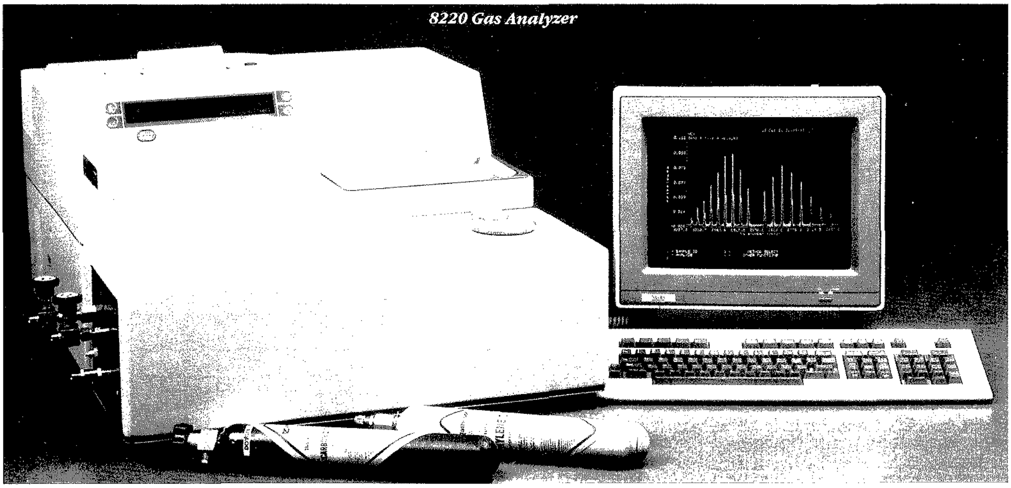
8220 Gas Analyzer

500 Series FT-IR

Compact, cost-effective instruments providing reliable, trouble-free operation.

The Nicolet 500 Series is Nicolet's "workhorse" family, providing excellent performance and value, along with the versatility to be configured to fit particular needs. These instruments incorporate many of the technical innovations of Nicolet's research systems while providing economy and ease-of-use for industrial QA/QC, academic, and multi-user laboratories. Excellent performance is achieved through advanced optical design and signal processing electronics. The 500 Series optical bench is available in several versions, with sampling and resolution options available to allow a wide variety of experiments.

Choice of data systems. The 500 Series instruments can be configured with a choice of popular computers, each with powerful yet easy-to-use FT-IR system software.

500 FT-IR Spectrometer

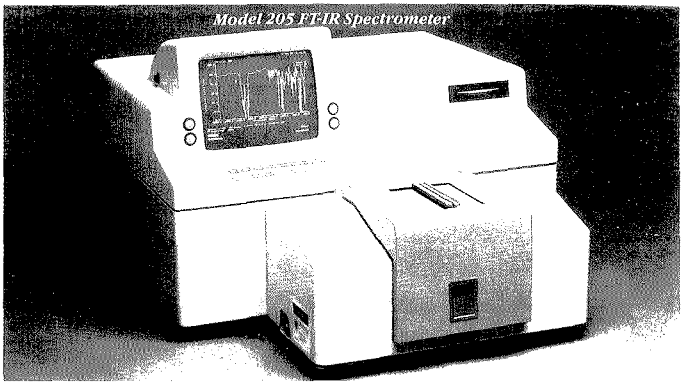
Model 205 FT-IR Spectrometer

The 500 configuration features the Nicolet 620 Spectroscopy Workstation with the Nicolet Advantage™ software package, offering proven versatility, performance, and ease-of-use.

500P system with IBM PS/2. For users desiring IBM compatibility, the 500 Series instruments can be configured with an IBM PS/2 MicroChannel™ system using either the Model 50 or Model 80 and Nicolet's PC/IR software, providing elegant operational simplicity and advanced chemometric tools.

500M configuration with Apple Macintosh II Computer, featuring the revolutionary new Nicolet software that makes FT-IR easier than ever.

CIRCLE 163 ON READER SERVICE CARD

Model 205

Low-cost FT-IR spectrometer

The new Model 205 FT-infrared spectrometer is designed to meet the practical needs of the routine analytical laboratory, the environmental laboratory, and the teaching laboratory. This new instrument provides all the essential features of a modern analytical instrument within a single compact, integrated package. Emphasis is on ease-of-use, without compromise of key capabilities that are important to the user.

The Model 205 incorporates a sealed, desiccated optical bench with a rugged, field-proven interferometer; a high-performance computer with fast, high-resolution graphics displayed on a built-in monitor; a touch-sensitive pushbutton control panel with full-function keyboard; and a flexible sample compartment featuring a unique sample mounting system that permits the use of plug-in, pre-aligned accessories. All spectroscopic functions are simple pushbutton control operations.

CIRCLE 164 ON READER SERVICE CARD

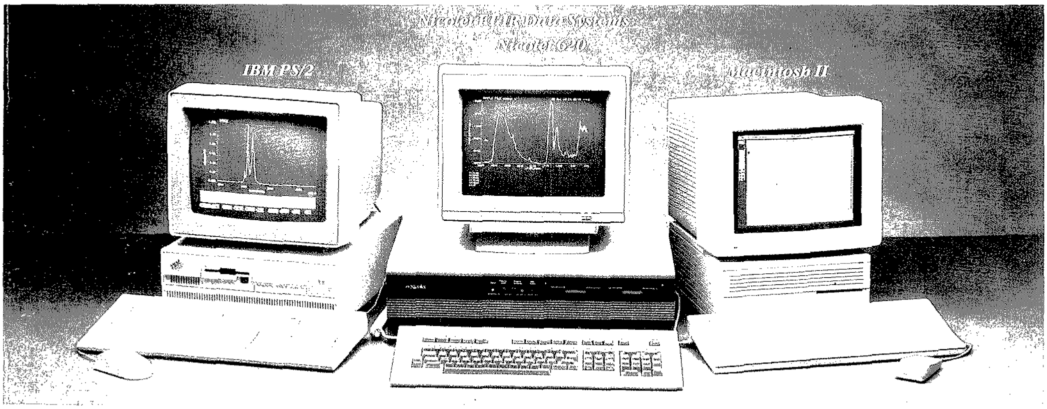
Nicolet FT-IR Data Systems

Nicolet TGA/FT-IR

The Nicolet TGA/FT-IR system couples FT-IR with thermogravimetric analysis, and is designed and optimized for the Du Pont TGA instruments. The resulting system combines the positive identification power of FT-IR with the qualitative and quantitative weight-loss information from TGA. Used with Nicolet's Specific Infrared Detection (SID™) software, this system provides a remarkably sensitive and selective means for analyzing evolved gases from the TGA instrument. The TGA/FT-IR package includes a unique heated flow cell and the SID software with communication of temperature, time, and derivative data from the TGA system.

TGA/FT-IR has been found to be beneficial in solving a wide variety of complex chemical analysis problems such as determining decomposition pathways and studying the thermal stability of materials. In the example here the Contour Display of the SID™ software is used to elucidate otherwise undetectable IR species.

CIRCLE 172 ON READER SERVICE CARD

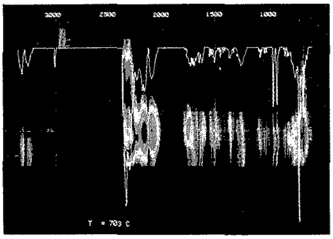

TGA/FT-IR contour display.

Nicolet FT-IR

Spectral Libraries and Search Software for Rapid Identification

Nicolet offers the largest commercially available on-line data base of high-quality FT-IR spectra, along with easy-to-use software for rapid and accurate spectral search, comparison, and identification.

Many FT-IR spectrometer users benefit from using Nicolet's large, general-purpose libraries include the Nicolet-Aldrich Condensed Phase Library of solids and liquids; The Nicolet Vapor Phase Library, particularly useful for GC-IR work; and the Nicolet-Sigma Biochemical Library. These are complemented by specialty libraries, including surfactants, industrial coatings, forensics libraries including drugs and paint chips, the Nicolet-Sigma steroids collection, and several polymer libraries. Search software includes easy-to-use routines that perform rapid and accurate identification using sophisticated match algorithms.

The combination of these features gives Nicolet users the best problem-solving tools for confidently identifying unknowns and verifying suspected chemicals.

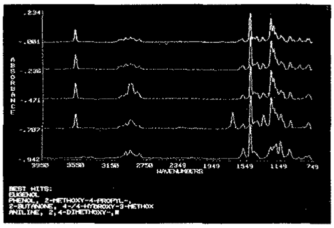

```
BEST HITS:
EUGENOL
PHENOL, 2-METHOXY-4-PROPYL-,
2-BUTANONE, 4-/4-HYDROXY-3-METHOX
ANILINE, 2,4-DIMETHOXY-,
```

Library search display. Unknown (top, green) overlaps best matches for direct comparison.

Nicolet Worldwide Sales and Support Centers

U.S.A. Corporate Headquarters: 5225-1 Verona Road / Madison, WI 53711 / TEL: 608/271-3333 / FAX: 608/273-5046
U.S.A. Eastern Region: 4720-F Boston Way / Lanham, MD 20706 / TEL: 301/459-2940 / FAX: 301/731-5761
U.S.A. Southern Region: 5251 Westheimer / Suite 470 / Houston, TX 77056 / TEL: 713/622-0982 / FAX: 713/622-0987
U.S.A. Central Region: 1834 Walden Office Square / Suite 100 / Schaumburg, IL 60173 / TEL: 312/397-5200 / FAX: 312/397-6519
U.S.A. Western Region: 215 Fourier Avenue / Fremont, CA 94539 / TEL: 415/490-8870 / FAX: 415/490-8063
Canada: 1-1200 Aerowood Drive / Mississauga, Ontario L4W 2S7 / Canada / TEL: 416/625-8302 / FAX: 416/625-3670
United Kingdom: Budbrooke Road / Warwick CV34 5XH / United Kingdom / TEL: 0926-494111 / FAX: 0926-494452
France: Z.I. Les Gatines / 44, Rue Pierre Curie / B.P. 40 / 78370 Plaisir, France / TEL: 1-30-81-30-81 / FAX: 1-30-55-95-63
West Germany: Senefelderstrasse 162 / D-6050 Offenbach am Main / West Germany / TEL: 069-837001 / FAX: 069-844411
Belgium and Netherlands: Avenue Paul Hymanslaan 105 Bte.22 / 1200 Brussels / Belgium / TEL: 02-762-2511 / FAX: 02-763-2180
Japan (Osaka): Ryokuchi-Eki, Bldg. 6F / 4-1, 2-Chome, Terauchi / Toyonaka, Osaka-PRF. / 560-Japan / TEL: 06-863-1550 / FAX: 06-863-1096
Japan (Tokyo): 1-2, 1-Chrome, Higashiyama / Meguro-ku, Tokyo, 153 / TEL: 03-715-2551 / FAX: 03-791-2580
Nicolet Analytical Instruments International Sales: 5225-1 Verona Road / Madison, WI 53711 / TEL: 608/271-3333 / TWX: 910-286-2736 (Nicolet MDS B) / FAX: 608/273-5046 / TLX: 170326 (NICOLET ANALYT)

To complement these direct Nicolet subsidiaries, Nicolet maintains a network of representative organizations in countries throughout the world.

Nicolet
INSTRUMENTS OF DISCOVERY

169-7044-00 8/89

Leak-tight Valves & Fittings for Analytical Instrument Applications

The leak-tight technology of the SWAGELOK Companies is built into all the products you see here.

They work with each other to give you design flexibility. You can select sizes, shapes, materials and ratings to handle *your* service conditions.

They're all manufactured to the same standards of precision and quality control. You can count on consistent tolerances, compatible end connections, and reliable seals.

They're available locally from Authorized Sales and Service representatives. You can save money through efficient purchasing, controlled inventories, and on-time delivery.

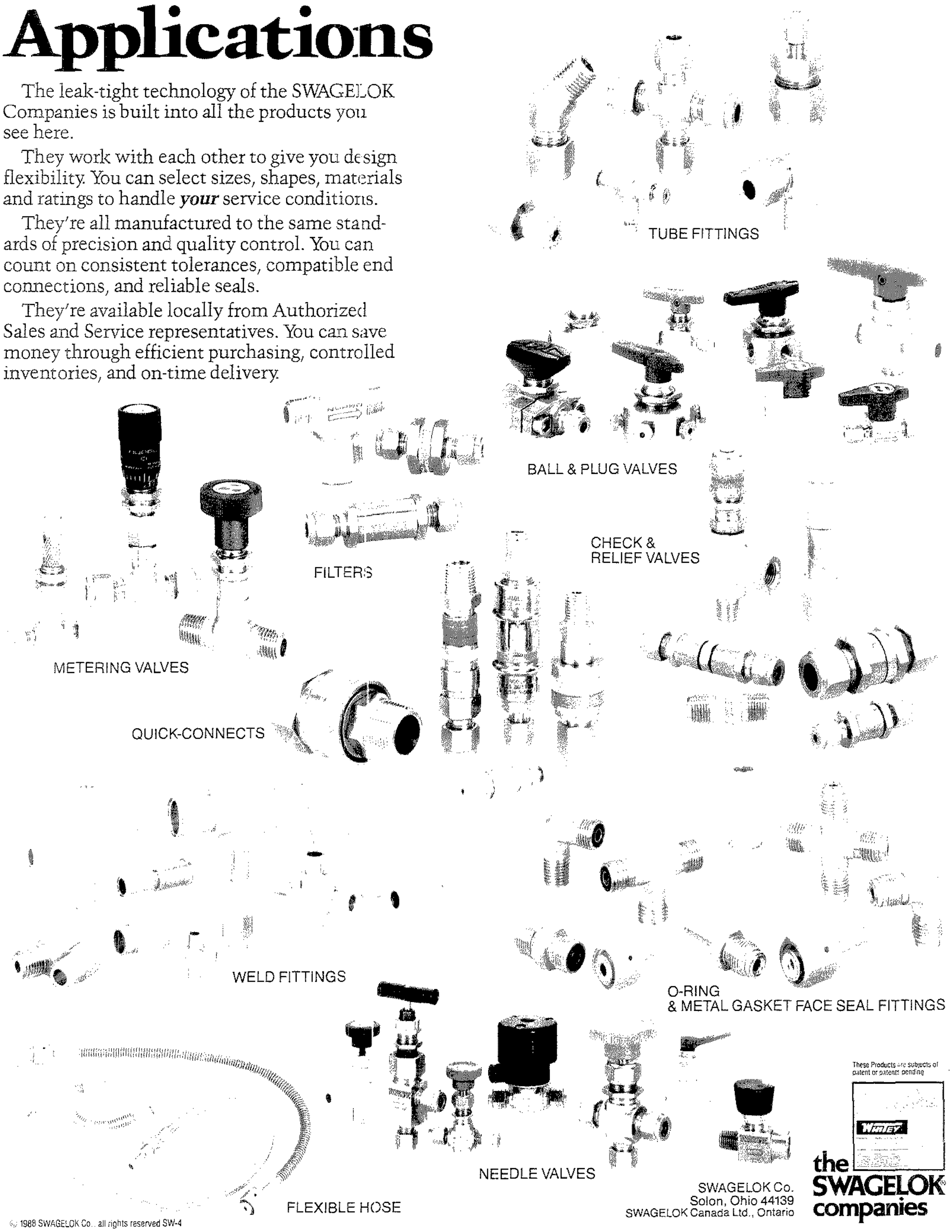
TUBE FITTINGS
BALL & PLUG VALVES
FILTERS
CHECK & RELIEF VALVES
METERING VALVES
QUICK-CONNECTS
WELD FITTINGS
O-RING & METAL GASKET FACE SEAL FITTINGS
NEEDLE VALVES
FLEXIBLE HOSE

These Products are subjects of patent or patents pending

the SWAGELOK companies

SWAGELOK Co.
Solon, Ohio 44139
SWAGELOK Canada Ltd., Ontario

© 1988 SWAGELOK Co., all rights reserved SW-4

See us at Pittsburgh Conference -- Booth #5204 & 5303. CIRCLE 158 ON READER SERVICE CARD

1:45

1990 Williams-Wright
Industrial Spectroscopist Award
Presented to
John F. Rabolt
of
IBM Almaden Research Center
by
Kathryn Kalasinsky

1:55 (567) **Award Address: Spectroscopic Characterization of Thin Film Molecular Assemblies: From FTIR to FT-Raman**—J.F. RABOLT, IBM Almaden Research Center

2:30 (568) **Fourier Transform Raman Spectroscopy from the Visible to the Infrared**—D.B. CHASE, E. I. du Pont de Nemours & Co., Inc

3:05 RECESS

3:20 (569) **Tuneable Resonance Raman in the Near Infrared**—B. SWANSON, Los Alamos National Laboratories

3:55 (570) **IR Hole Burning as a Possible Analytical Method**—H. STRAUSS, University of California-Berkeley

4:30 (571) **Exploring Molecular Organization at Metal Surfaces**—V.M. HALLMARK, IBM Almaden Research Laboratory

Atomic Spectroscopy—Insights and Analysis

Tuesday Afternoon, Room 1E15
J.J. Tice, Presiding
Georgia Pacific Corp.

1:30 (572) **Use of Fourier Transforms to Discern Peak Shape Differences Between Standards and Samples**—J.M. HARNLY, USDA, NCL

1:50 (573) **The Analysis of Uranium in Natural Water by Chelation IC Sample Pretreatment for Inductively Coupled Argon Plasma Emission Spectroscopy**—R.M. MANABE, Thermo Jarrell Ash, J. Schmelzel, J. Riviello

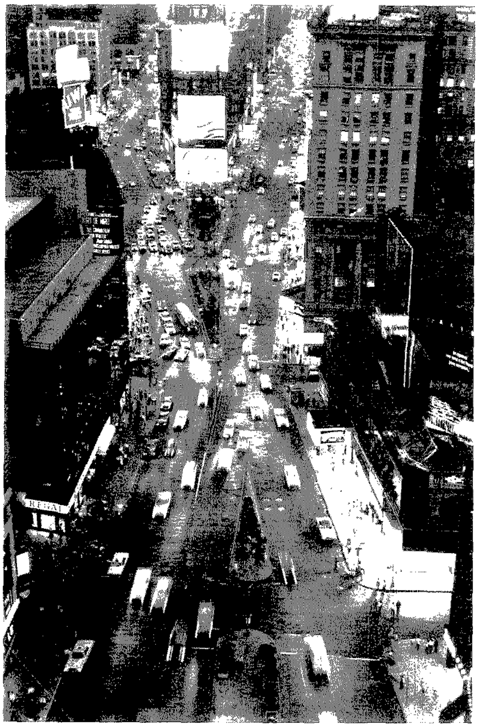

2:10 (574) **Quantum State Distributions of Excimer Laser (193 nm) Produced Oxygen Atoms**—B.E. FORCH, US Army Ballistic Research Lab., C.N. Merrow, A.W. Miziolek

2:30 (575) **A Study of Signal to Noise Ratio in Electrothermal Atomizer Laser Excited Atomic Fluroescence with a 500 Hertz Excimer Pumped Dye Laser**—R.L. IRWIN, University of Connecticut, D.J. Butcher, G.T. Wei, R.G. Michel

2:50 (576) **Dv-X$_\alpha$ Study of Electronic and Vibrational Structure of MgF$_2$:V^2** —J.H. YU, Anhui University, Y.Q. Lu

3:10 RECESS

3:25 (577) **Determination of P$^+$, Pd and Rh in Autocatalysts**—J. BOZIC, Inco Limited, W. Flora, S. Maggs

3:45 (578) **Qualitative Considerations Used in the Spectrometric Wear-Metal Evaluation of Borderline Engines and Transmissions**—D. COX, Department of the Army, R. Chazell

4:05 (579) **LIF Spectroscopy and Vibrational Spectra of $^{39}K_2$ Dimer Excited by 4579 Å Line of Ar Laser**—Y.Q. LU, Anhui Instit. Optics & Fine Mech., Y.C. Zhang, J.H. Yu

4:25 (580) **Selection of Internal References for Bulk Analysis of Alloys by Glow Discharge Emission Spectrometry (GD-ES)**—P. HUNAULT, Jobin Yvon (ISA), A. Le Marchand

4:45 (581) **Dv-X$_\alpha$ Study of a Kinetical on Reaction ($^1A_1$) SiH$_2$ + H$_2$ — SiH$_4$**—Y.L. TONG, Anhui Instit. Optics & Fine Mech., Y.Q. Lu

Environmental Water Analysis I

Tuesday Afternoon, Room 1E19
D.R. Weill, III, Presiding
Shady Side Academy

1:30 (582) **Chloramine Depletion in Covered Reservoirs**—M. BARRIOS, City of Austin Water/Wastewater Utility, P. Stone

1:50 (583) **Atomic Absorption Studies of Sodium - Determination of Sodium in Metropolitan Area Tap Water**—B.K. PERKINS, Grambling State University

2:10 (584) **Electrochemical Investigation of Metal Binding Capability of Microcystis Capsule in Aquatic Systems**—J.L. PLUDE, University of Wisconsin, Oshkosh, D. Parker, O. Schommer, J. Lauerhaas

2:30 (585) **Ion Chromatographic Determination of Chlorite, Chlorate, Bromate, and Iodate in Drinking Water Treated by Alternate Disinfection Processes**—R.J. JOYCE, Dionex Corporation, M. Harrold, J.D. Pfaff, C.A. Brockhoff

2:50 (586) **Effects of Sample Composition on Chemical Oxygen Demand Analysis**—P.M. WALDRON, Ionics, Incorporated, K.M. Queeney

3:10 RECESS

3:25 (587) **Method Validation for Pesticide Determination in Water and Soil Using Quantitative Thermospray Liquid Chromatography/Mass Spectrometry**—R.A. BETHEM, Enseco-Cal Lab., J.W. Cornacchia, R.A. Kornfeld, K.P. Matuszak, S. Teng

3:45 (588) **Interaction of Aqueous Chlorine and Chloroamine Solutions with the Keto Compounds of the Tricarboxylic Acid Cycle. A Source for Mutagens**—M. RAHI, University of Cincinnati, K. Jayasimhulu, H. Zimmer

4:05 (589) **Ecosystem Shift in Lake Kinnerent, Israel**—J.D. PAZ, Reeco, M. Gofen

4:25 (590) **Determination of Haloforms in Kuwaiti Drinking Water by GC/ECD**—F. ABU-DAGGA, Kuwait Inst. for Scientific Res., T. Saeed, R. Abu-Tabanja

4:45 (591) **CAWA - Computer Aided Water Analysis**—H.J. STAN, Technical University of Berlin, J. Lipinski

Food Analysis

Tuesday Afternoon, Room 1E20
N.R. Dando, Presiding
Aluminum Company of America

1:30 (592) **Organic Acids Separations in Food Products**—D.W. TOGAMI, Interaction Chemicals Inc., L. Treat-Clemons, D.J. Hometchko

1:50 (593) **A New Alternative to the Kjeldahl Method: A Pyro-Chemiluminescent Nitrogen/Protein Analyzer for Foods**—E.M. FUJINARI, Antek Instruments, Inc., L.O. Courthaudon, A.J. Britten

2:10 (594) **Analytical Characterization of the Products of Nonenzymatic Glycosylation of Lysozyme**—H. DAUN, Rutgers, The State Univ. of NJ, R.B. Leslie, S.H. Hwang, M. Trebilcock-Guzman

2:30 (595) **Culinary Spectroscopy - Part III - Chemically Correct Cooking**—G.J. DEMENNA, Libra Labs, Inc.

2:50 (596) **Fully Automated Liquid Chromatographic Analysis of Contaminants in Food Products Using On-Line Dialysis Sample Preparation**—M.M.L. AERTS, State Inst. for Quality Control, H. Lingeman, U.A.T. Brinkman

3:10 RECESS

Discover new solutions

So picture a choice of three.

1 An automated system for QA and other high-throughput jobs.

- Large capacity: 40 samples and 4 different buffers
- Includes data management and method programming

2 A compact, integrated research unit with multimode injection

- 30-kV dual-polarity power
- Reproducible analyses with as little as 2 µl of sample

3 A versatile on-column UV detector

- ideal for low-cost modular systems and special applications

All three give you femtomole sensitivity with samples you can't easily separate any other way. And affordability that may surprise you.

Phone today **(800)228-4250.**

CIRCLE 80 ON READER SERVICE CARD

See at PittCon.

See all of Isco's new instruments for CE, SFE, and LC at Pittsburgh Conference, **Booth 4153.**
Seminars and demos daily.

Isco, Inc., P.O. Box 5347, Lincoln NE 68505

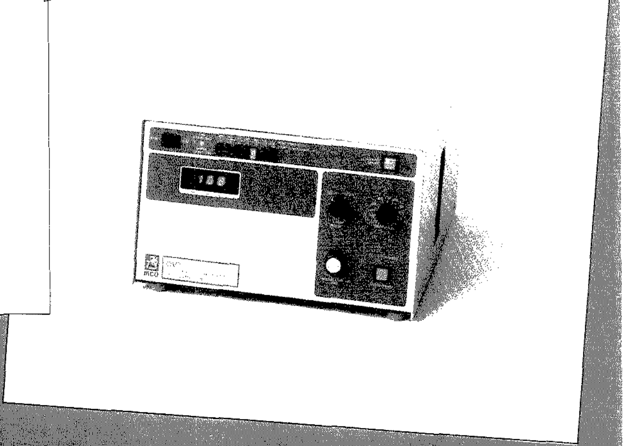

Hadamard Spectrometry

Tuesday Afternoon, Room 1E20
N.R. Dando, Presiding
Aluminum Company of America

3:25 (597) **Improvements in Hadamard Transform Raman Spectrometry**—A.P. BOHLKE, Kansas State University, J.M. Jarvis, J.S. White, R.M. Hammaker, W.G. Fateley

3:45 (598) **Multichannel Hadamard Transform Raman Microscopy**—P.J. TREADO, University of Michigan, M.D. Morris

4:05 (599) **Instrumental Design of Stationary Mask Hadamard Transform Spectrometers**—J.S. WHITE, Kansas State University, R.M. Hammaker, W.G. Fateley

4:25 (600) **Hadamard-Transform Infrared Microspectroscopic Compositional Mapping - Discussion and Preliminary Results**—R.G. MESSERSCHMIDT, Connecticut Instrument Corp., D. Kuehl

4:45 (601) **A Stationary Hadamard Transform Interferometer**—J.D. TATE, Kansas State University, B. Curnutte, Jr., J.M. Jarvis, J.S. White, R.M. Hammaker, W.G. Fateley

Gas Chromatography—Techniques

Tuesday Afternoon, Room 1E21
J.L. Glajch, Presiding
E. I. du Pont de Nemours & Co., Inc.

1:30 (602) **Optimization of Gas Chromatographic Separations Using Dissimilar Injection Solvents**—J.R. BERG, Varian Instrument Group, C.K. Huston, Jr.

1:50 (603) **An Empirical Scheme for the Classification of Gas Chromatographic Stationary Phases Based on Solvatochromism**—P.W. CARR, University of Minnesota, J. Li, A. Dallas

2:10 (604) **Detector Specific Applications of Analytical Pyrolysis**—T.P. WAMPLER, CDS Instruments, J.W. Washall

2:30 (605) **Retention Indices for Oxygen- and Nitrogen-Containing Species Using Selective Gas Chromatographic Detectors**—S.D. ANDERSON, Wright Research & Develop. Center, E.M. Steward, J.L. Moler, R.B. Howard

2:50 (606) **Identification and Confirmation of Unknown Compounds Using Atomic Emission Detection in Gas Chromatography**—J.J. SULLIVAN, Hewlett-Packard Company, B.D. Quimby

3:10 RECESS

3:25 (607) **Sources of Error in Purge and Trap Analysis of Volatile Organic Compounds**—J.W. WASHALL, CDS Instruments, T.P. Wampler

3:45 (608) **Utilization of Micro-Packed Capillary Columns for the Characterization of Carbon-Based Adsorbents**—W.R. BETZ, Supelco, Inc., J.K. Crissman, Jr.

4:05 (609) **Compound-Independent Calibration Using Gas Chromatography with Atomic Emission Detection - Application to Pesticide Analysis**—P.L. WYLIE, Hewlett-Packard Company

4:25 (610) **Gas Chromatography - Capillary Versus Packed Columns: A Mixed State of Affairs**—B. DIEHL, Applied Automation, Inc., R. George, R. Dahlgren

4:45 (611) **Marine Fatty Acids—A Wealth of Information**—O. GRAHL-NIELSEN, University of Bergen

HPLC—In the Life Sciences

Tuesday Afternoon, Room 1E06
C.T. Santasania, Presiding
Supelco, Inc.

1:30 (612) **Resolution of Racemic Drugs on a Chiral AGP Column**—J. HERMANSSON, ChromTech AB

1:50 (613) **Microbore HPLC Separations of Transfer Ribonucleic Acids**—V.T. REMCHO, III, VA Polytechnic Inst. & State Univ., H.M. McNair

2:10 (614) **Analysis of Glutamine and Asparagine Residues in Protein**—F.F. SHIH, USDA, ARS, So. Regional Res. Ctr.

2:30 (615) **Effects of Pore Size, Particle Size, and Surface Area on the Binding Capacity of Various Ion Exchange Matrices for IgM and Other Large Proteins Under Various Chromatographic Conditions**—D.R. NAU, J. T. Baker Inc.

2:50 (616) **HPLC Techniques for Purification of Monoclonal Antibodies from Ascites**—R.G. HATCH, Rainin Instrument Company, Inc., W.C. Holberg, III

3:10 RECESS

3:25 (617) **On-Line Process Monitoring of Saccharomyces Fermentation by High-Performance Liquid Chromatography**—J.T. GOTSICK, Rainin Instrument Company, Inc., R.F. Benson

3:45 (618) **Peptide Mapping by LC - An Overview**—M.W. DONG, The Perkin-Elmer Corporation, F.L. Vandemark

4:05 (619) **Recovery of Biologically Active Substances After HPLC Separation**—G. ROZING, Hewlett-Packard GmbH, M. Prange, G. Kamperman, G. Curtis

4:25 (620) **Chromatographic Evaluation of HPLC Columns for Bioseparations**—G. ROZING, Hewlett-Packard GmbH, A. Prange

4:45 (621) **Separation and Quantitation of Metallothioneins (MT-I and MT-II) by HPLC and AAS (The Application of Photodiode Array Detector)**—L.W. XIA, Hunan Medical University, C.L. Xiao, S.X. Liang, B.M. Chen, Y. Xia

HPLC—Stationary Phases II

Tuesday Afternoon, Room 1E16
C. Conroy, Presiding
Biotage, Inc.

1:30 (622) **An Alternative Stationary-Mobile Phase Combination for Chemically Suppressed Ion Chromatography of Anions**—M.T. BUNKER, Hamilton Company, D.P. Lee

1:50 (623) **HPLC Characteristics of Immobilized Artificial Membranes**—J.A. PERRY, Regis Chemical Company, L.J. Glunz

2:10 (624) **Study of the Scalability of the Separation of Pharmaceutical Compounds Using pH Stable Stationary Phases**—C. CONROY, Biotage, Inc., T. Sawyer

2:30 (625) **Standardization of Reversed Phase Packings in HPLC**—R.E. MAJORS, EM Science

2:50 (626) **HPLC on Wide Pore Silicas with a Narrow Pore Size Distribution**—H.J. RITCHIE, Shandon Scientific Ltd., P. Ross, D.R. Woodward

3:10 RECESS

3:25 (627) **Advantages of Multiphase Pellicular Ion Exchange Columns for Ion Chromatography**—R.E. KISER, Dionex Corporation, J. Stillian

3:45 (628) **A Cation Exchange Chromatography Column for the Simultaneous Quantitation of Alkali Metals, Alkaline Earths, and Amines**—M.E. POTTS, Dionex Corporation, J. Stillian, C. Pohl, L.A. Woodruff, C.R. Deveza

4:05 (629) **An Extraordinary HPLC Medium and Its Applications: Alumina-Based Reversed Phase**—T. SAWYER, Biotage, Inc., C. Conroy

4:25 (630) **A Novel HPLC Phase for Analysis of Basic Compounds**—T.L. ASCAH, Supelco, Inc., J. Wilson

4:45 (631) **Evaluation of Ion Exchangers for Single Column Ion Chromatography**—S.V. ROSE, Chrompack Inc., J.P. Crombeen

Near-IR Processes

Tuesday Afternoon, Room 1E13
H.S. Gold, Presiding
E. I. du Pont de Nemours & Co., Inc.

1:30 (632) **On-Line Monitoring the BTU Content of Natural Gas with a Near-IR Fiber Optic System**—C.W. BROWN, University of Rhode Island, S.M. Donahue, S.C. Lo, B. Caputo

1:50 (633) **Closed Loop Control of Moisture Content in the Manufacturing Process Utilizing Near Infrared Reflectance**—R.W. WEEDON, Bran+Luebbe Analyzing Tech.

2:10 (634) **Applications of Near Infrared Spectroscopy for At- and On-Line Analysis in the Petrochemical and Polymer Industries**—L. McDERMOTT, L T Industries, Inc

2:30 (635) **System Performance of a Remote Sensing NIR Statistical Spectrophotometer for Process Monitoring**—D.A. LEFEBRE, Guided Wave, Inc.

2:50 (636) **Near-Infrared Spectroscopy On-Line: Chemistry in a Pipe**—F.A. DETHOMAS, NIRSystems, Inc.

3:10 RECESS

Flow Analysis

Tuesday Afternoon, Room 1E13
H.S. Gold, Presiding
E. I. du Pont de Nemours & Co., Inc.

3:25 (637) **Solute Focussing in Flow Injection Analysis**—B.F. JOHNSON, University of Cincinnati, J.G. Dorsey

3:45 (638) **Acid-Base Titrations by Discontinuous Programmed Flow Analysis (DFA)**—J.D. PETTY, Ionode Pty. Ltd., R.M. Peachey, D.R. Sweatman

4:05 (639) **Automatic Dilution Apparatus for Segmented-Flow Analyzers**—S.C. COVERLY, Bran+Luebbe, F. Kawamoto, T. Tochimoto

4:25 (640) **Flow Injection Analysis-Atomic Absorption Spectrophotometric Determination of Ammonia Cyanide and Thiosulfate by Continuous Dissolution of Solid Silver Chloride**—A.S. ATTIYAT, Yarmouk University, M. Kharoaf, F. Esmadi

Bells and whistles aren't everything...

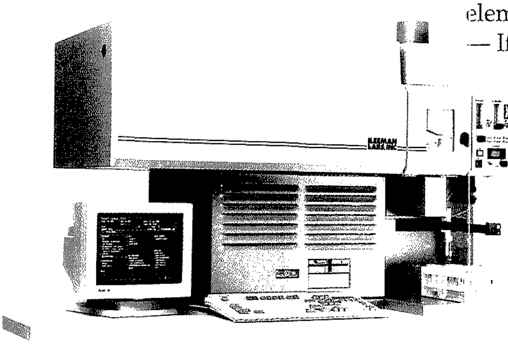

PS900: PS Series performance without the bells and whistles.

If you need the multielement (72 elements) analysis of ICP — If you need a fast problem-solving instrument with top analytical performance — But if you don't have the sample load (or budget) to justify all the bells and whistles — **Then you need Leeman's new PS900 ICP/Echelle Spectrometer.** You don't have to keep using slow, limited flame AA just because you only have a few samples a day.

Look into Leeman's new **PS900**, a powerful ICP/Echelle Spectrometer that's had some expensive (but expendable) fat trimmed off, leaving plenty of muscle for superb multielement analysis — at a price far lower than a fancy new AA — or other ICP.

The **PS900**: a sequential air path ICP/Echelle Spectrometer with precise manual argon and power controls. Monochrome monitor running powerful **PS** software. Autosampler optional.

Looking for an ICP?

...but they sure are nice.

If you need more than bare bones —If your sample load is pushing your capacity — **Then you need PS900's big brothers:**

PS1000 (and 1000UV): Sequential air path or purged ICP/Echelle Spectrometer. The fastest sequential available.

PS2000 (and 2000UV): Simultaneous air path or purged ICP/Echelle Spectrometer.

PS3000 (and 3000UV): Combination Sequential/Simultaneous air path or purged ICP/Echelle Spectrometer.

PS1000 and above: Computer-controlled argon and power. Color monitor. Large capacity data storage. Built-in voltage regulator. Autosampler optional.

Whichever sequential you choose — PS900 or PS1000 — either can be upgraded to a combination PS3000 when your sample load grows.

Get more information now — circle the reader service number or call Leeman's Sales Department directly.

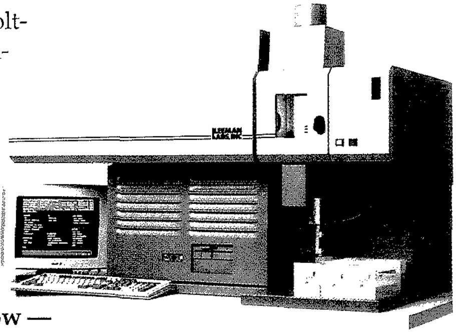

Only one photo for PS1000, PS2000, PS3000? Because of Leeman's unique optical design, you can't tell the simultaneous, sequential or combination apart by looking. They're all compact, benchtop units.

LEEMAN LABS, INC

55 Technology Drive
Lowell, MA 01851
(508)454-4442
FAX (508)452-7429

See us at Pittcon, booth 4709. CIRCLE 98 ON READER SERVICE CARD

Must reading for any professional in any major chemistry field...

JOURNAL
OF THE
AMERICAN
CHEMICAL
SOCIETY

The most frequently cited chemical publication throughout the world, this biweekly journal delivers:

- original research articles that cover every key area in the field of chemistry
- up-to-the-minute communications
- authoritative information with direct application to your own work
- a subscription value unmatched by JACS' "competitive" journals!

EDITOR: Allen J. Bard, University of Texas, Austin

1990 Rates	**ACS Members**** 1 Year	2 Years	**Nonmembers** 1 Year
US	$75	$135	$630
Canada & Mexico	$131	$247	$686
Europe*	$191	$367	$746
All other countries*	$236	$457	$791

*Air service included
**Member rates are for personal use only
For nonmember rates in Japan, contact Maruzen Co., Ltd.

Order your own subscription to the number one chemical journal today!

Call Toll Free 1-800-227-5558 (U.S. only).
In D.C. and outside the U.S.: (202) 872-4363.
Telex: 440159 ACSP UI or 89 2582 ACSPUBS
Cable Address: JEICHEM

For more information or to subscribe, contact:

American Chemical Society
Marketing Communications Department
1155 Sixteenth Street N.W.
Washington D.C. 20036

Now Monthly!

For Those Involved in the Vital Field of Surface and Colloid Chemistry

Langmuir

The ACS Journal of Surfaces and Colloids

Langmuir is a monthly journal of broad coverage that brings together research from all aspects of the field: ultra-high vacuum surface chemistry and spectroscopy, heterogeneous catalysis, all aspects of interface chemistry involving fluids, and disperse systems.

***Langmuir* publishes peer-reviewed research in:**
*** "Wet" Surface Chemistry * "UHV" Surface Chemistry**
*** Disperse Systems * Electrochemistry**
*** Surface Structure; tunneling electron microscopy**

EDITOR
Arthur W. Adamson, University of Southern California

ASSOCIATE EDITORS
A.T. Hubbard, University of Cincinnati
R.L. Rowell, University of Massachusetts

1990 Rates	ACS Members* 1 year	2 years	Nonmembers 1 year
U.S.	$58	$104	$429
Can. & Mex.	$70	$128	$441
Europe**	$78	$144	$449
All Other Countries**	$85	$158	$456

* For personal use only.
** Air service included.
For nonmember rates in Japan, contact Maruzen Co., Ltd.

For more information or to subscribe, write:

American Chemical Society
Marketing Communications Dept.
1155 Sixteenth Street, NW
Washington, DC 20036

In a hurry?

Call Toll Free (800)227-5558 (U.S.), or (202)872-4363 in D.C. and outside the U.S., or Fax your order at (202)872-4615.

697 IC Pump
690 Ion Chromatograph
698 Autosampler
POWER
Metrohm
Metrohm

Ion chromatography with system – quite simply with Metrohm.

IC 690:
Highly sensitive conductivity detector with electronic compensation of the background conductivity

IC 697 Pump:
Built and optimised for IC

IC 698 Autosampler:
For routine analysis: holds up to 64 samples

IC columns:
For all requirements; Metrohm SUPER-SEP for exacting ion analyses, e.g. the simultaneous determination of mono- and divalent cations (according to Schomburg)

IC twin system:
Opens up new possibilities, e.g. parallel anion and cation analysis

IC evaluation:
With recorder, integrator or PC

IC service:
Well over a hundred fully developped applications together with reprints, IC literature as well as advice, application assistance and customer service. The world over.

Ion analysis — quite simply with Metrohm

Ω Metrohm
Measurement in Chemistry
Worldwide with Metrohm

METROHM Ltd.
CH-9101 Herisau Switzerland
Phone 071 / 53 11 33
Telefax 071 / 52 11 14
Telex 88 27 12 metr ch

Brinkmann
INSTRUMENTS, INC.
Cantiague Rd., Westbury, New York 11590
(516) 334-7500 (800) 645-3050

CIRCLE 108 ON READER SERVICE CARD

Planar Chromatography

Tuesday Afternoon, Room 1E12
J.B. Callis, Presiding
University of Washington

1:30 (641) **Mechanistic Study of Microwave-Assisted Acid Hydrolysis of Peptides on TLC Plates**—Y. DU, Stevens Institute of Technology, D.C. Shelly

1:50 (642) **Effects of Solute Focusing on Zone Shape in Column - Planar Separations**—D.C. SHELLY, Stevens Institute of Technology, V.L. Antonucci

2:10 (643) **Quantitative Analysis of a Chloroquinolin-Ethenyl Derivative Using Thin Layers Impregnated with Di-*p*-Toluyl Tartaric Acid**—N. GRINBERG, Merck & Co., Inc., G. Bicker, P. Tway, R. Sblendorio

2:30 (644) **Vapor Pretreatment of the Stationary Phase in Planar Chromatography**—K.C. VAN HORNE, Jones Chromatography USA, Inc., T.J. Good

2:50 (645) **Paper Withdrawn**

3:10 RECESS

3:25 (646) **A Novel Thin Layer Chromatography Product - A Separation Technology Breakthrough**—D.D. BLEVINS, Analytichem International, D.F. Hagen, S.J. St. Mary, V. Dixit

3:45 (647) **The Quantitative and Qualitative Application of Near Infrared Spectroscopy to Thin Layer Chromatography**—D.M. MUSTILLO, College of St. Elizabeth, E.W. Ciurczak

4:05 (648) **Direct Quantitation of Phospholipids Separated by Two Dimensionally Developed Thin Layer Chromatography**—K. LAM, Shimadzu Scientific Instr., Inc., M. Nakatani, F. Tsuji, K. Shinya, D. Sequera

4:25 (649) **Zeolites as New Adsorbents for Separation of Direct Dyes by Thin Layer Chromatography**—S.K. SRINIVASULU, Vikram University, B. Srinivas

Raman Spectroscopy

Tuesday Afternoon, Room 1E08
R.S. McDowell, Presiding
Los Alamos National Lab.

1:30 (650) **Transient Raman Study of the Chemical Reactions: OH Oxidation of Simple Aromatics**—G.N.R. TRIPATHI, University of Notre Dame

1:50 (651) **Raman Spectroscopy of Carbon Materials: Frequency Shifts and Resonance Effects Over a 351nm - 1064nm Laser Wavelength Range**—R.L. McCREERY, The Ohio State University, Y. Wang

2:10 (652) **FT-Raman Studies of Metal Carbonyl Complexes and Protein-Metal Carbonyl Conjugates**—S. BARNETT, McGill University, A.A. Ismail, H. Buijs

2:30 (653) **UV-Resonance Raman Excitation Profiles of Tryptophan in Solution and in the Cu-Protein Azurin**—J. SWEENEY, University of Pittsburgh, S.A. Asher

2:50 (654) **UV Resonance Raman and UV Absorption Difference Spectroscopy of Myoglobins: Titration Behavior of Individual Tyrosine Residues**—P.J. LARKIN, University of Pittsburgh, J. Teraoka, S.A. Asher

3:10 RECESS

3:25 (655) **Analysis of NiO-Coated and Bare Ceramic Surfaces (Si_3N_4 and SiC) and of Lubricating Carbonaceous Layers Formed Thereon by Raman and Auger Electron Spectrometries During Friction and Wear**—J.L. LAUER, Rensselaer Polytechnic Institute, S.R. Dwyer, L.P. DuPlessis

3:45 (656) **FT-Raman Investigation of Compounds in a Complex Matrix**—J. BELLO, SPEX Industries, Inc., F.J. Purcell

4:05 (657) **Fourier Transform Raman Spectroscopy of Industrial Samples**—J.A. GRAHAM, Hercules Incorporated

4:25 (658) **Signal Enhancement Methods for NIR/FT-Raman Spectroscopy**—R.A. LARSEN, The Perkin-Elmer Corporation, D.W. Schiering, R. Bennett, D.J. Cutler

4:45 (659) **Remote Micro-Raman Cartography by the RLFO (Raman Laser Fiber Optics) Method Using a Multichannel Spectrometer**—N.Q. DAO, Laboratoire de Chimie, O. Sqalli, P. Plaza, M. Jouan

Spectral Absorption: Fluorescence—Chemical Applications

Tuesday Afternoon, Room 1E18
J.E. Paterson, Presiding

1:30 (660) **Evaluation of Near Infrared Dyes for Analytical Applications**—G. PATONAY, Georgia State University, A. Sexton, M. Shepherd, L. Strekowski

1:50 (661) **Studies of Chemically Modified Cyclodextrin Complexes Using Fluorescence Probes**—J.B. ZUNG, Emory University, I.M. Warner

When You Need R.I.
Choose a Company That Knows R.I.

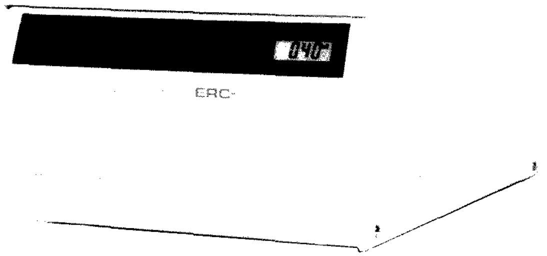

Whether you use refractive index detection every day, or only occasionally, you need a sensitive and stable instrument. When you need R.I., choose a company that *really* knows R.I. - **Erma ERC.**

The new **ERC-7515** R.I. detector combines all the sensitivity, low noise and minimum drift performance of the ERC-7512 with more advanced automation and ergonomic design.

The **automated auto-zero** function is controlled optically *and* electronically, eliminating the need for manual zeroing. The new cabinet requires less bench space, features a large **LCD display** of recorder and integrator output and easy access to controls.

Erma has been building the most refined and easy to use R.I. detectors for 10 years. Anspec provides service and support that's just a phone call away. 1-800-521-1720.

ERC
ERMA INC.
ANSPEC

The Anspec Company Inc.▲ Box 7730 Ann Arbor, MI 48107▲ 800-521-1720 ▲ Fax 313-665-6402 *See Us at PittCon Booth 5515*

CIRCLE 3 ON READER SERVICE CARD

NEW

THE MERCK INDEX Eleventh Edition

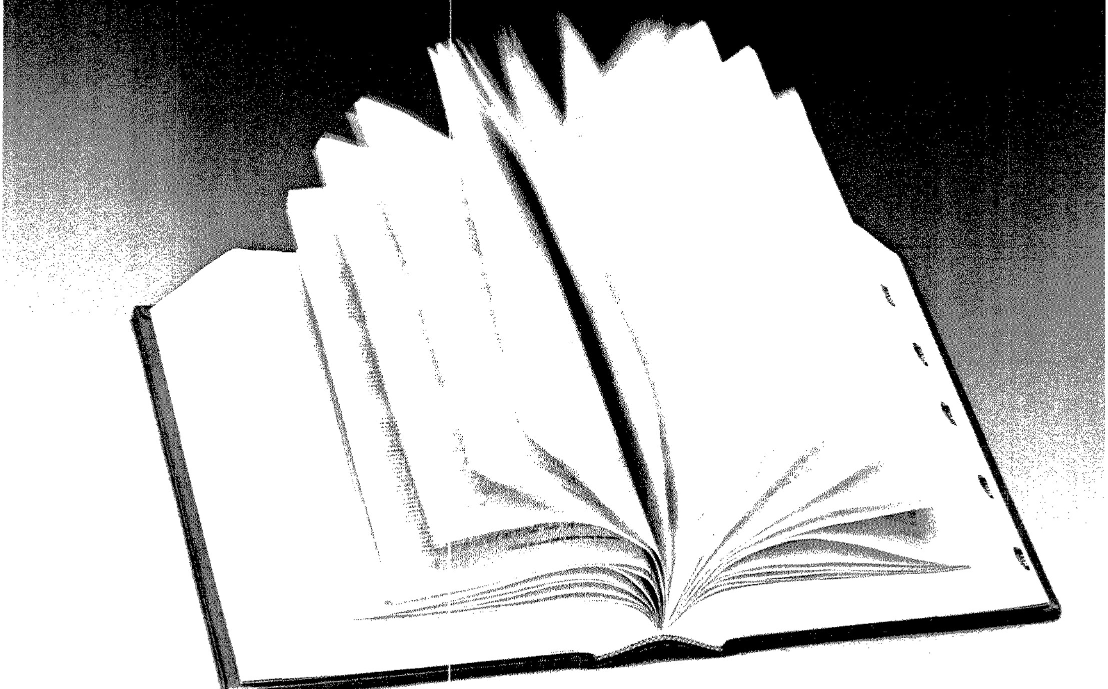

Keeping pace with chemistry and biochemistry...
for over 100 years

Since 1889, *The Merck Index* has provided pertinent, authoritative information of interest to scientists the world over. Now we are pleased to present the newly published Eleventh/Centennial Edition. This special leather-bound edition provides expanded coverage of therapeutically important biotechnology products, agriculturals and compounds of environmental impact, and features an entirely new therapeutic category/bioactivity index as well as CAS Registry Number indices. And you'll find information on more than 10,000 significant drugs, chemicals, and natural substances.

To order, call toll-free 1-800-999-3633, extension 750 (VISA or MasterCard only) or complete the coupon.

NEW

THE
CENTENNIAL
EDITION

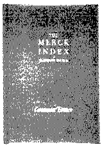

Merck & Co., Inc., a research-intensive company, publishes *The Merck Index* as a non-profit service to the scientific and medical communities.

CIRCLE 106 ON READER SERVICE CARD

Enclosed is my payment for $35.00 for the Eleventh/Centennial Edition of THE MERCK INDEX. I will not be charged for shipping.

☐ Check enclosed. Make check payable to Merck & Co., Inc. ☐ VISA ☐ MasterCard

Card No. __________ Exp. Date __________

Signature __________

Name __________

Address __________

City __________

State __________ Zip __________

Please allow four to six weeks for delivery.

Merck & Co., Inc.
Professional Handbooks
Department 750
P.O. Box 2000
Rahway, NJ 07065-0901

2:10 (662) **Development of a Lanthanide Ion Probe Technique for the Determination of Metal-Ligand Complex Formation Constants**—W. SUSETYO, University of Georgia, L.A Carreira, D.M. Grimm, L.V. Azarraga

2:30 (663) **Lifetime Studies of Metal-Humic Complexes**—F.E. KNIGHT, University of Georgia, W. Susetyo, L.A. Carreira, L.V. Azarraga

2:50 (664) **Fluorescence Properties - Molecular Structure Correlations for Polycyclic Aromatic Hydrocarbon (PAH) Solute Probes Used in Analytical Chemistry**—S.A. TUCKER, University of North Texas, W.E. Acree, Jr., A.I. Zvaigzne, K.W. Street, Jr., J.C. Fetzer

3:10 RECESS

3:25 (665) **Dual Fluorescence UV-Vis Detection in HPLC**—J.G. WANGSGAARD, Lenear Instruments Corporation, D.J. Bornhop, L. Hlousek

3:45 (666) **Effect of Reversed Micelles on Peroxyoxalate Chemiluminescence Reaction and Analytical Implication**—N. DAN, Seton Hall University, M.L. Grayeski

4:05 (667) **Spectrophometric Solvent Extraction Method for Quantitation of Lauroamphocarboxyglycinate**—M. TSAO, Ciba Vision Corporation, R. Dandridge, G. Scott

4:25 (668) **Pentachloronitrosyliridate as a New Reagent for Spectrophotometric Determination of Diethylstilbestrol**—Y.B. QU, Institute of Precious Metals

4:45 (669) **Spectrophotometric Investigation of Zinc(II) and Cadmium(II) Dithizonates in Aqueous Medium**—B. KUMAR, University of Delhi, H.B. Singh, R.L. Sharma, M. Katyal

Supercritical Fluid Extraction—Chromatography

Tuesday Afternoon, Room 1E10
V. Berry, Presiding
SepCon Separations Consultants

1:30 (670) **Thermionic Ionization Detection (TID) for Capillary Supercritical Fluid Chromatography (SFC)**—E.R. CAMPBELL, Lee Scientific, B.E. Richter

1:50 (671) **The Evaluation of a He-HEMIP as an Element Selective Detector for SFC**—C.B. MOTLEY, VA Polytechnic Inst. & State Univ., G. Long

2:10 (672) **Photoionization Detection in Mixed Mobile Phase Supercritical Chromatography**—M.S. DAVIS, University of Massachusetts, P.C. Uden

2:30 (673) **SFC-MS Using MAGIC Interface**—D.M. BURDETTE, Georgia Institute of Technology, R.F. Browner, G.U. Holzer

2:50 (674) **Solubility and Matrix Effects in Supercritical Extraction**—S. MITRA, USEPA, N.K. Wilson

3:10 RECESS

3:25 (675) **Quantitative SFE Coupled to High Resolution Gas Chromatography**—J.M. LEVY, Suprex Corporation, A. Rosselli, D. Boyer, K. Cross, R. Ravey, P. Zimmerman

3:45 (676) **Coupled Solid Phase Extraction and Supercritical Fluid Extraction**—G.C. SLACK, VA Polytechnic Inst. & State Univ., H.M. McNair

4:05 (677) **Combined Supercritical Fluid Extraction and Chromatography with FTIR Identification**—K.L. NORTON, University of Idaho, R. Fuoco, P.R. Griffiths

4:25 (678) **Supercritical Fluid Extraction/Cryogenic Collection Fraction/Supercritical Fluid Chromatography (SFE/CCF/SFC) for Quantitative Analysis**—M. ASHRAF-KHORASSANI, Suprex Corporation, M.L. Kumar, G.W. William, D.S. Koebler

4:45 (679) **An Electrochemical Detection System for Supercritical Fluid Chromatography**—M. DI MASO, McGill University, W.C. Purdy, S.A. McClintock

Wednesday, March 7, 1990

SYMPOSIUM

Catastrophic Environmental Problems - arranged by R.S. Danchik of Aluminum Company of America

Wednesday Morning, Room 1D01
R.S. Danchik, Presiding
Aluminum Company of America

8:30 **Introductory Remarks**—R.S. DANCHIK

8:35 (680) **Environmental Monitoring and Assessment Programs—Moving Towards the 21st Century**—J.H. SKINNER, US Environmental Prot. Agency

9:15 (681) **Acid Rain: An Unresolved Issue**—H.C. MARTIN, Atmospheric Environment Service

9:55 RECESS

10:10 (682) **To be announced**

10:50 (683) **Stratospheric Ozone Depletion—Latest Developments in Scientific Understanding**—M.J. KURYLO, National Aeronautics and Space Administration (NASA)

DEPENDABLE CONTINUITY

SHAKER BATH

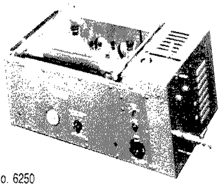

Cat No. 6250
To provide immersed agitation at controlled temperatures. Available in two sizes, table model or floor model, to meet a wide range of requirements. Variable speed, stroke, and temperature featured in all models.

STIRRERS

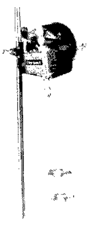

Cat. No. 7225 (w/o agitator)
The **Eberbach** Con-Torque stirrer with high torque output, is designed to stir highly viscous materials such as resins. Hollow spindle concept utilized in **Eberbach** Stirrer line assures additional gripping of agitator and facilitates changing containers. Available from 1/70 thru 1/10 hp.

RECIPROCATING SHAKERS

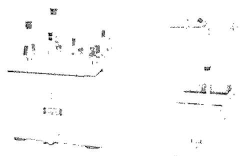

Cat No. 5850
For general purpose shaking with a reciprocating (back and forth) action. Wide range of accessories available. Speeds from 20 to 240 excursions per minute.

WARING CONTAINERS

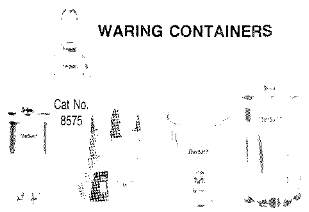

Cat No. 8581 · Power Unit · Cat No. 8470 · Cat No. 8520

Glass, stainless steel, and aluminum containers available in capacities from 1000 ml to 3 ml. Commercial one quart Blendor Power units to include an explosion proof power unit will accept all **Eberbach** containers. Replacement blending assemblies and components available.

ANALYTICAL ELECTRO-ANALYSIS APPARATUS

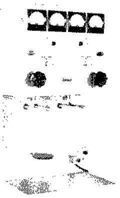

Cat no. 1000 (w/o platinum)
Apparatus for determining copper, lead, antimony, cadmium, nickel, and zinc, by the electro-deposition process. Apparatus also available for high speed determinations and the separation of metals by the mercury cathode technique.

ACCENT ON PERFORMANCE

Cat No. 8017
with 8020 Container

BLENDER POWER UNIT—EXPLOSION PROOF

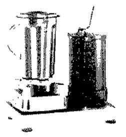

Eberbach's new blender power unit, catalog No. 8017, solves the hazard problem of blending mixtures containing volatile solvents. It features an explosion proof 1½ H.P. single phase motor with automatic reset thermal protection. Motor provides free running spindle speed of 11,500 RPM. The heavy duty motor is UL approved for Class I, Group D and Class II, Group E, F, and G operation. Accommodates the Waring Gallon Size container, Eberbach catalog No. 8020, and with the addition of an adapter will accommodate standard size Eberbach and Waring Containers.

Eberbach
CORPORATION
ANN ARBOR, MICHIGAN

Booth #4232 at the Pittsburgh Conference CIRCLE 56 ON READER SERVICE CARD

Wallgårds, Malmö

Remote fiber-optic sensing is moving into the process plant.

New Model 300 double-beam analyzer for process and research applications.

Guided Wave is the industry leader for process-monitoring systems based on remote NIR-VIS-UV spectroscopy and single-strand fiber-optics. Faster, simpler and less expensive to maintain, these systems eliminate the need for handling or preparation of samples and can operate in hazardous environments.

Guided Wave analyzers are used for research, process development and process monitoring in the chemical, petrochemical, polymer, textile, pharmaceutical and food industries.

With the double-beam Model 300, users can tailor remote in-line monitoring systems for specific process requirements. A unique multiplexing capability enables high-speed multi-component analysis at up to 8 remote sampling points — with no degradation of performance. The Model 300 has the highest signal-to-noise ratio of any NIR instrument. It offers unmatched stability and precision. And it includes powerful, user-friendly software for faster application development and simpler customization.

Dedicated customer support ensures efficient performance.

Guided Wave has achieved its position as industry leader on the basis of state-of-the-art fiber-optics technology, dedicated customer support and a long-term commitment to process monitoring.

Our engineers can help you develop methods and applications. A complete training program and continuous technology updates ensure that you get the full benefit of your investment in Guided Wave systems.

The top-of-the-line Model 300 and the laboratory-pilot plant Model 260 can make in-line process monitoring a reality in your process plant. For more information, contact Guided Wave today.

Guided Wave, Inc., 5190 Golden Foothill Parkway,
El Dorado Hills, CA 95630, USA.
Fax (916) 939-4307. Tel. (916) 939-4300.

Guided Wave International AB, Karbingatan 22,
S-252 66 Helsingborg, Sweden.
Fax Int. + 46 42 20 18 28. Tel. Int. + 46 42 20 10 25.

CIRCLE 70 ON READER SERVICE CARD

SYMPOSIUM

Chromatography and Mass Spectrometry in Studies on Human Diseases - **arranged by E. Jellum of University of Oslo**

Wednesday Morning, Room 1A07
E. Jellum, Presiding
University of Oslo

8:30 **Introductory Remarks**—E. JELLUM

8:35 (684) **Advanced Instrumentation and Strategies for Profiling Body Fluids**—C.C. SWEELEY, Michigan State University

9:10 (685) **Chromatography and Mass Spectrometry for Studies on Diseases Related to Steroid Metabolism**—C.H.L. SHACKLETON, Children's Hospital Med. Center.

9:45 (686) **Chromatography and Mass Spectrometry in Studies on Diseases Related to Fat and Lipid Metabolism**—A. KUKSIS, University of Toronto

10:20 RECESS

10:35 (687) **The Use of Chromatography, Mass Spectrometry and Stable Isotopes in Clinical Studies**—P.V. FENNESSEY, University of Colorado

11:10 (688) **GC-MS, HPLC and Capillary Zone Electrophoresis for Diagnosis of Metabolic Disorders**—E. JELLUM, University of Oslo

SYMPOSIUM

International Regulatory Issues of Chiral Drugs - **arranged by A.F. Fell of University of Bradford**

Wednesday Morning, Room 1A23
A.F. Fell, Presiding
University of Bradford

8:30 **Introductory Remarks**—A.F. FELL

8:35 (689) **Chiral Drugs: Regulatory Issues in Europe**—E.J. ARIENS, University of Nijmegen

9:10 (690) **Chiral Drugs: Regulatory Issues in the USA**—C.S. KUMKUMIAN, Food and Drug Administration

9:45 (691) **The Developoment and Validation of Chiral Methodology for Drug and Bioanalytical Studies**—I.W. WAINER, St. Jude Children's Res. Hospital

10:20 RECESS

10:35 (692) **Chiral Drugs: An Industrial Analytical Perspective**—R. BOPP, Lilly Research Laboratories, T.J. Wosniack, E.C. Jensen

11:10 (693) **Biological Aspects of Chirality: Contributions to Improved Drug Development and Use**—J. CALDWELL, St. Mary's Hospital Med. School

SYMPOSIUM

1990 Pittsburgh Spectroscopy Award - **arranged by J. Kerkhoff of Aluminum Company of America**

Wednesday Morning, Room 1A08
J. Kerkhoff, Presiding
Aluminum Company of America

8:30 **Introductory Remarks**—J. KERKHOFF

8:35

Presentation of the
1990 Pittsburgh Spectroscopy Award
to
Professor Charles B. Harris
of
University of California, Berkeley
by
John W. Novak, Chairman
Spectroscopy Society of Pittsburgh

8:45 (694) **Award Address: Probing Chemical Reactions in Liquids on the Femtosecond Timescale**—C.B. HARRIS, Univ. of California-Berkeley

9:25 (695) **Femtosecond Coherent Processes in Molecules and Solids**—C.V. SHANK, Univ. of California-Berkeley

10:05 RECESS

10:20 (696) **Femtosecond IR Studies of Chemical and Biological Photo Processes**—R.M. HOCHSTRASSER, University of Pennsylvania

11:00 (697) **Non-Linear View of Molecules Bonded to Surfaces**—Y.R. SHEN, Univ. of California-Berkeley

POSTER FORUM

ALL DAY WEDNESDAY - 8:30 AM to 5:00 PM

These paper numbers (949-960) appear out of sequence because of the All Day status of *this Poster Forum.*

New Horizons in Planar Chromatography—Session I—Applications - **arranged by J.C. Touchstone of University of Pennsylvania**

Wednesday, Room 1C01
J.C. Touchstone, Presiding
University of Pennsylvania

8:30 **Introductory Remarks**—J.C. TOUCHSTONE

8:40 (949) **Qualitative and Quantitative Determination of Canabinoids in Urine by TLC**—T. SEIK, Analytic Biochemistries, W.A. Dunn

9:10 (950) **Clinical Applications of Planar Chromatography in Drug Analysis**—S.H.Y. WONG, University of Connecticut

9:40 (951) **Comparison of HPLC and TLC in Chiral Separations**—D.W. ARMSTRONG, University of Missouri-Rolla

10:10 RECESS

10:30 (952) **Direct Assay of Glycolipid Glycosyltransferase on TLC**—R.K. YU, Virginia Commonwealth University

11:00 (953) **Diphasic Planar Chromatogrpahy of Lipids**—J.C. TOUCHSTONE, University of Pennsylvania, J.G. Alvarez

11:30 (954) **Kinetic Analysis of Artifactual Phenomena Occurring in TLC**—N. GRINBERG, Merck Sharp and Dohme

12:00 RECESS

New Horizons in Planar Chromatography—Session II—Instrumentation in Planar Chromatography - **arranged by J.C. Touchstone of University of Pennsylvania**

Wednesday, Room 1C01
J.C. Touchstone, Presiding
University of Pennsylvania

1:30 **Introductory Remarks**—J.C. TOUCHSTONE

1:40 (955) **Two Dimensional Quantitative Analysis in Planar Chromatography**—D. SEQUERA, Shimadzu Scientific Instr. Inc.

2:10 (956) **Analysis of Planar Chromatograms by Fast Atom Bombardment Mass Spectrometry**—K.L. BUSCH, Georgia Institute of Technology, S.M. Brown, H.H. Schurz

2:40 (957) **Quantitative Analysis in Planar Chromatography by Multiwavelength Video Densitometry**—P. ALDRIDGE, University of Washington, D. Burns, J.B. Callis

3:10 RECESS

3:30 (958) **Recent Developments in Isotope Scanning and Related Topics in Planar Chromatography**—H. FILTHUTH, Laboratorium Prof. Berthold

4:00 (959) **Imaging and Quantitation of Two Dimensional TLC with the Ambis Radioanalytic Imaging System**—L. HOOK, Ambis Systems

4:30 (960) **Betascope: Direct Imaging and Analysis of Radiolabelled Surfaces**—D.L. STANTON, Betajem Corporation, D.E. Sullivan, J.E. Stanchfield

Capillary Electrophoresis

Wednesday Morning, Room 1E06
L. Bottomley, Presiding
Georgia Inst. of Technology

8:30 (698) **Design Criteria for an Automated High-Performance Electrophoresis System**—J.D. OLECHNO, Dionex Corporation, R. Rubin, J.T.K. Pang, M. Love

8:50 (699) **Clinical Application of Capillary Electrophoresis with Concentration Gradient Detection**—J.B. PAWLISZYN, University of Waterloo, K. Chan

9:10 (700) **Electroanalytical Detection of Underivatized Amino Acids and Oxalyl Thiolesters in Capillary Electrophoresis**—C.E. ENGSTROM-SILVERMAN, Penn State University, A.G. Ewing

Run with the best . . .

Innovative chromatography products that provide high performance and exceptional value.

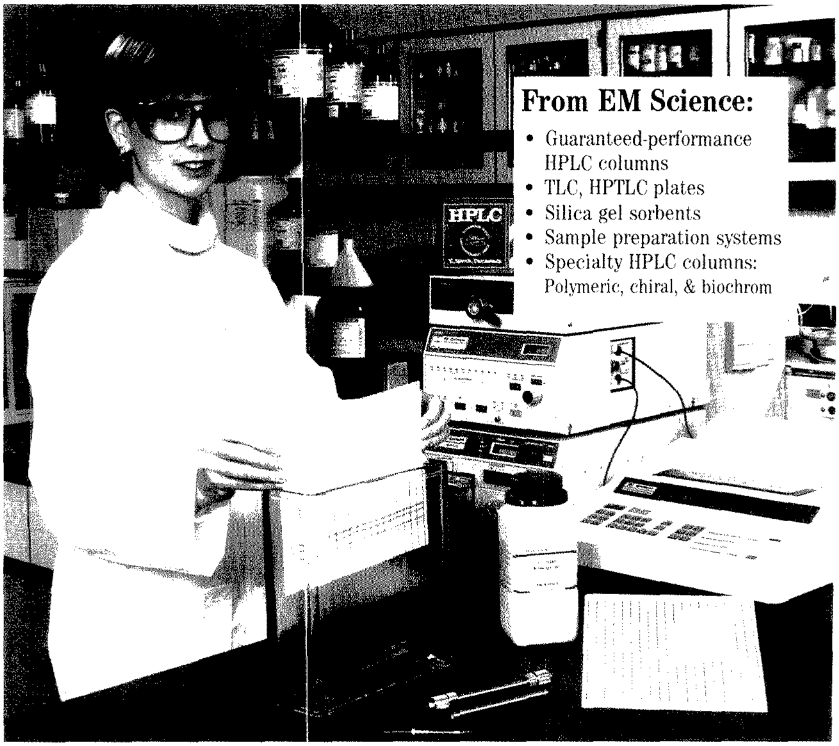

From EM Science:

- Guaranteed-performance HPLC columns
- TLC, HPTLC plates
- Silica gel sorbents
- Sample preparation systems
- Specialty HPLC columns: Polymeric, chiral, & biochrom

Turn to EM Science for the best performance, value, and innovation in chromatography products. All EM Science chromatography products provide reproducibility you can depend on . . . and the economy you'll appreciate.

EM SCIENCE
A Division of EM Industries, Inc.
P.O. Box 70 480 Democrat Road
Gibbstown, NJ 08027
(609) 354-9200 (800) 222-0342
Associate of E. Merck, Darmstadt, Germany

Find out what's new in innovative chromatography products. Call or write today for this new, FREE bulletin.

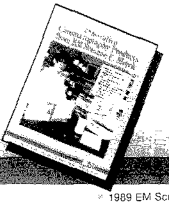

We have service down to a science.

© 1989 EM Science

HPLC Columns	TLC	Sorbents	Sample Prep	Specialty HPLC Columns
Circle # 206	*Circle # 207*	*Circle #208*	*Circle #209*	*Circle #210*

EMS-908

See us at Pitcon booth 3653-3654

9:30 (701) **Direct Injection of Cytoplasmic Samples from Single Nerve Cells onto an Electrophoresis Capillary**—T.M. OLEFIROWICZ, Penn State University, S.J. Stranick, A.G. Ewing

9:50 (702) **A Potency Assay for Commercial Insulin Samples Using Capillary Zone Electrophoresis**—M.A. LOOKABAUGH, USFDA, M. Biswas, D. Woodford, I.S. Krull

10:10 RECESS

10:25 (703) **Application of Capillary Zone Electrophoresis for the Rapid Determination of Amino Acids and Peptides with Fluorescence Detection**—J.T.K. PANG, Dionex Corporation, J.D. Olechno, P. Newton, D. Kramer

10:45 (704) **Capillary Isotacophoresis with Concentration Gradient Detection**—T. McDONNELL, University of Waterloo, J.B. Pawliszyn

11:05 (705) **Separation of Antibiotics by Capillary Electrophoresis**—A. WAINWRIGHT, Dionex Corporation

11:25 (706) **Advancement on Capillary Electrophoresis Hardware: A Microprocessor-Controlled Capillary Column Cleaning Device**—N.A. GUZMAN, Princeton Biochemicals, Inc., L. Hernandez, J.P. Advis

11:45 (707) **Applications of Capillary Gel Electrophoresis in Biochemical Research**—A. PAULUS, Ciba-Geigy Ltd., E. Gassmann, H. Walther

Electrochemistry—Detectors

Wednesday Morning, Room 1E10
S.G. Weber, Presiding
University of Pittsburgh

8:30 (708) **Integrated Pulsed Amperometric Detection in Liquid Chromatography**—W.R. LACOURSE, Iowa State University, D.C. Johnson

8:50 (709) **A New Electrochemical Detector for HPLC**—W. HACKER, Hewlett-Packard GmbH, L. Huber, T. Doerr

9:10 (710) **Recent Developments in Conductivity Cell Design for Ion Chromatography**—P.G. ALDEN, Waters Chrom. Div. Millipore Corp., A.L. Heckenberg, R. Lawrence III, P. Jandik, J. Krol, J. Romano

9:30 (711) **A New Multimode Detector for Ion Chromatography**—R.D. ROCKLIN, Dionex Corporation, T. Tullsen, M. Beher-Leon, C. Bryant

9:50 (712) **Flow Injection Analysis in Combination with Ion Selective Electrode Detection**—J.A. PERSSON, Tecator AB

10:10 RECESS

10:25 (713) **The Use of a Reductive Amperometric Detector for Ion Chromatography**—A.F. PALUS, EG&G Princeton Applied Research

10:45 (714) **Determination of Sulphate in Water Using Flow Injection Analysis and In-Line Preconcentration**—M. KARLSSON, Tecator AB, J.A. Persson

11:05 (715) **A Square-Wave Voltammetric Detection System for Anion Chromatography**—T.L. RULICK, Youngstown State University, J.R. Einfalt, D.W. Mincey

11:25 (716) **Comparison of Kel-F Oil and Kel-F Wax Carbon Paste Electrodes for LC-EC**—J. WANGSA, Miami University, N.D. Danielson

Gas Chromatography—Environmental I

Wednesday Morning, Room 1E15
G. Fritz, Presiding
Los Alamos National Laboratory

8:30 (717) **The Application of Wide-Bore Capillary Gas Chromatography to the Environmental Testing Laboratory**—P.R. LOCONTO, Nanco Laboratories, S. Easter, A. Gaind

8:50 (718) **The Development of a Wide-Bore Fused Silica Capillary Column for the Rapid Separation of Volatile Organics in Drinking Water (EPA Method 502.2)**—J. HUBBALL, Quadrex Corp., E. Bozzi, J.B. Lipsky, G. McLean

9:10 (719) **New Quick Screen Methods for Environmental Analyses**—K. KLATT, J&W Scientific, D. Miller

9:30 (720) **Quality Assurance Studies for Collection of Whole Air Samples in Stainless Steel Canisters, for Volatile Organic Compound Determinations**—B.B. KEBBEKUS, New Jersey Instit. of Tech., G. Dai, W.Ji

9:50 (721) **Optimization of Sample Introduction Parameters for Automated Trace Analysis of Pesticides by Capillary GC**—Z. PENTON, Varian Instrument Group

10:10 RECESS

10:25 (722) **A Unitized Gas Chromatographic System for the Determination of Pesticides and PCB's**—A.K. VICKERS, O. I. Analytical, K. Davis

10:45 (723) **Fast Analysis of Hazardous Waste Material Using Wide Bore Capillary Columns: Quick Turnaround Methods**—S.B. COLE, Supelco, Inc., I.D. DeGraff, M.J. Keeler, L.M. Sidisky

11:05 (724) **Analysis of Trace Level (sub ppb) Vapor Phase Atmospheric Pollutants by Narrow-Bore Capillary Gas Chromatography**—E. WOOLFENDEN, Perkin-Elmer Ltd.

11:25 (725) **Determination of ppb Level Atmospheric Impurities in Ultra-High Purity Gases Using GC HID**—K. MAGUIRE, Scott Specialty Gases, G. Bean, R.B. Denyszyn

11:45 (726) **Improved Methods for Field GC Analysis for Priority Pollutants**—M.S. YOUNG, Cambridge Analytical Associates, D.M. Mauro

HPLC—Chiral Separations

Wednesday Morning, Room 1E19
R.E. Majors, Presiding
EM Science

8:30 (727) **Novel Chiral Separation Techniques Based on Surfactants**—W.L. HINZE, Wake Forest University, R.W. Williams, Jr., Y. Suzuki

8:50 (728) **Normal Phase HPLC: Cyclodextrin Based Stationary Phases for Chiral Separation**—J.D. DUNCAN, University of Missouri-Rolla, D.W. Armstrong

9:10 (729) **(S)-Hydroxypropyl-β-Cyclodextrin: A New Chiral Liquid Chromatographic Stationary Phase**—A.M. STALCUP, University of Missouri-Rolla, D.W. Armstrong, S.C. Chang, J. Pitha

9:30 (730) **Separation of Enantiomeric Pairs on Chiral Stationary Phases by Overloaded Elution Chromatography**—S. JACOBSON, University of Tennessee, S. Golshan-Shirazi, G. Guiochon

9:50 (731) **Pharmaceutically Active Glutarimides by HPLC and Chiral Stationary Phases**—A. KAMALIZAD, Analytical Research Inst. of VA, H.M. McNair

10:10 RECESS

10:25 (732) **The Determination of Chemical and Enantiomeric Purity of Acid Chlorides in Pharmaceutical Analysis by High Performance Liquid Chromatography**—K.A. BONDONNA, Squibb Institute for Med. Res., T.V. Raglione, M. Jemal, W. Thompson

10:45 (733) **A New Polymeric Achiral Reagent Containing the 3,5-Dinitrophenyl Tag for Off-Line Derivatizations of Amines and Alcohols in HPLC-UV/EC**—A.J. BOURQUE, Northeastern University, C.X. Gao, D. Schmalzing, I.S. Krull

11:05 (734) **A New Method for the Separation of Drug Enantiomers by Automated Precolumn Formation of Diastereomers**—H. GOETZ, Hewlett-Packard GmbH, F. Steiner

11:25 (735) **A New Robust Stationary Phase for Chiral Chromatography**—B. MONAGHAN, Shandon Scientific Ltd., R.J. Dolphin, B. Kaur

11:45 (736) **HPLC Analyses of Optically Active Compounds Using a New Optical Rotation Detector**—H. SUZUKI, Showa Denko K.K., T. Tokieda, H. Watanabe, J.D. MacFarlane, S. Moriguchi

HPLC—Pharmaceutical Applications

Wednesday Morning, Room 1E21
P. Brown, Presiding
University of Rhode Island

8:30 (737) **Measurement of Ibuprofen in Human Whole Blood by Reversed-Phase Ion-Paired HPLC Using a pH Stable Polymeric Column**—A.M. RUSTUM, Abbott Laboratories

8:50 (738) **Reversed-Phase High Performance Liquid Chromatography Determination of Verapamil in Human Plasma**—A.M. RUSTUM, Abbott Laboratories

9:10 (739) **Separation of Atrazine, Simazine, and Their Degradation Products by Reversed-Phase, Paired-Ion HPLC with Photo-Diode Array Detection**—J.D. STUART, University of Connecticut, W. Qian, A.S. Mason, R.W. Spencer, J.A. Poland, J.C. Hogan, Jr.

9:30 (740) **Isolation and Purification of Lecithin by High Performance Liquid Chromatography Using Two Types of Preparative Systems**—J.V. AMARI, University of Rhode Island, P.R. Brown, C.M. Grill

9:50 (741) **Assaying Low Level Impurities in Lovastatin: An Application of High-Low Chromatography**—A.L. HOUCK, Merck Inc., D.K. Ellison

10:10 RECESS

10:25 (742) **The Use of Size Exclusion Chromatography and Sedimentation Field Flow Fractionation for the Characterization of Liposomes**—M. MERCORELLI, R.W. Johnson Pharm. Res. Institute, J. Womble, A. Greenberg, F. DeLuccia, P.A. Lane

10:45 (743) **The High Performance Liquid Chromatographic Determination of Clomiphene Citrate Isomers in Solid Pharmaceutical Dosage Forms**—H. AHMAD, Barr Laboratories, Inc., R. B. Kirsch

11:05 (744) **Versatility of Latex-Based Multi-Phase Cation Exchange HPLC Columns: From Inorganic Cations to Polar and Ionic Pharmaceutical Compounds**—M.A. REY, Dionex Corporation, R. Slingsby, C. Pohl

11:25 (745) **Bioanalytical and Pharmaceutical Applications of a Novel Polybutadiene Coated Alumina Stationary Phase**—P.T. JEDRZEJEWSKI, VA Polytech Instit. & State Univ., C.M. Conroy, L.T. Taylor

11:45 (746) **Development of Chemiluminescence Detector for HPLC and Its Biomedical Applications**—S. HIGASHIDATE, Japan Spectroscopic Co., Ltd., H. Goto, M. Sakamoto, K. Hibi, M. Senda, W. Kottcamp

WHAT CAN YOU DO WITH
THE VESTEC 201?

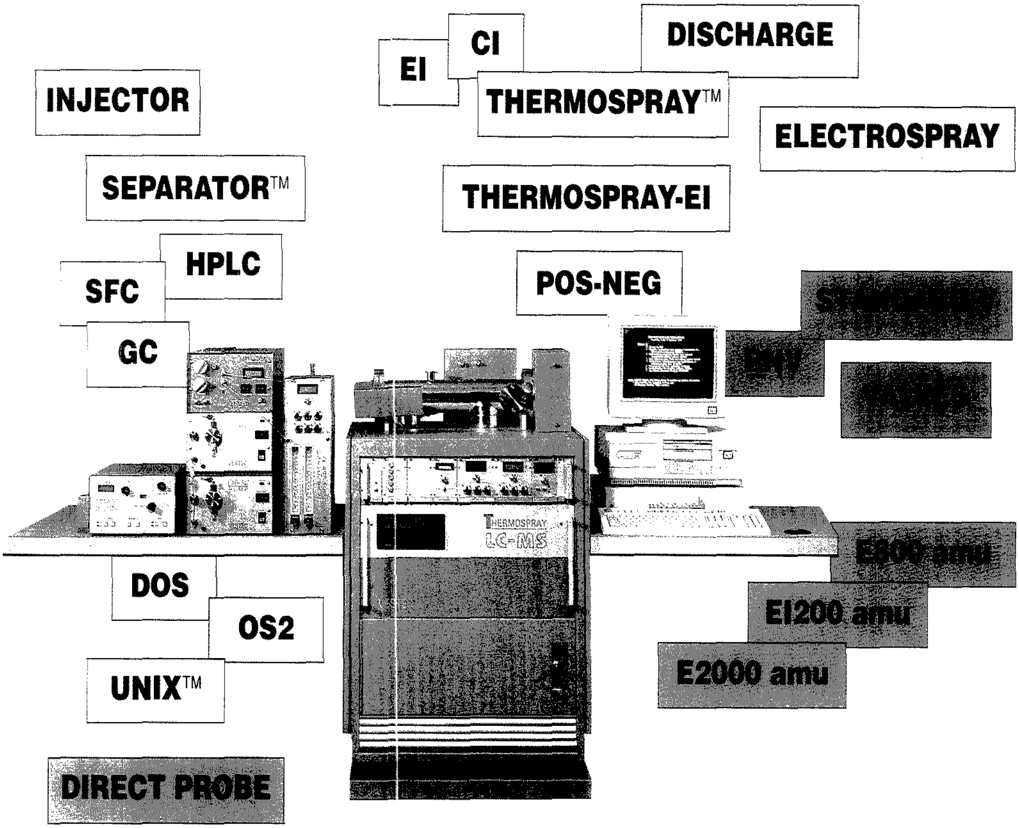
DISCHARGE
CI
EI
INJECTOR
THERMOSPRAY™
ELECTROSPRAY
SEPARATOR™
THERMOSPRAY-EI
HPLC
SFC
POS-NEG
GC
THERMOSPRAY
LC-MS
E800 amu
DOS
EI200 amu
OS2
E2000 amu
UNIX™
DIRECT PROBE

WHAT CAN'T YOU!

You can find out virtually everything you've ever wanted to know about a sample with the 201 LC-MS system—from trace analysis, peak purities and identification of unknowns to quantitative analysis. How do we give you all this power in a routine lab instrument? We've applied our technology in designing a system so flexible it can be upgraded into the ultimate LC detector. The Vestec 201 represents a relatively inexpensive yet equally powerful alternative to the more time-, labor- and cost-intensive mass spectrometry techniques, such as MS/MS. Challenge us with an unknown and see for yourself!

SEPARATOR™ and Thermospray™ are trademarks of Vestec Corporation
UNIX™ is a trademark of AT&T.

VESTEC
CORPORATION
9299 Kirby Drive, Houston, Texas 77054, 713-796-9677

© Copyright 1990 Vestec Corporation

CIRCLE 189 ON READER SERVICE CARD

HPLC—Stationary Phases III

Wednesday Morning, Room 1E16
T. Hanai, Presiding
Health Research Foundation

8:30 (747) **Comparison of Reversed Phase Packings Developed for the Analysis of Basic Compounds**—R.F. MEYER, YMC Inc., R.S. Cooley

8:50 (748) **New Silica Based Polar Bonded Phase Exhibiting Reduced Hydrogen Bonding Interference**—Y.L. CHEN, J&W Scientific, G. Luehr, M. Wareing

9:10 (749) **Comparison of Various Polymer-Based Stationary Phase HPLC Columns with Unisphere-PBD Columns**—P.T. JEDRZEJEWSKI, VA Polytech Instit. & State Univ., J. Via, C.M. Conroy, L.T. Taylor

9:30 (750) **Durability of PBD Unisphere Alumina Reverse Phase HPLC Columns with Extreme pH Mobile Phases**—E.S. MARTIN, Alcoa Laboratories, C.M. Conroy, L.F Wieserman

9:50 (751) **Solvent-Exchangeability of Reversed-Phase Polymer HPLC Columns**—T. OKAMOTO, Ibaraki Research Laboratory, N. Shumizu, T. Aoyama, M. Matsui

10:10 RECESS

10:25 (752) **New Aromatic Derivatized Cyclodextrin Bonded Phase for Normal Phase Chromatography**—M.L. HILTON, University of Missouri-Rolla, D.W. Armstrong

10:45 (753) **A New Alkaline Stable Silica-Based Reversed-Phase Stationary Phase**—A.M. STALCUP, University of Missouri-Rolla, D.W. Armstrong, D. Day

11:05 (754) **The Synthesis of New Chemically Bonded Stationary Phases for HPLC Using Reduced Silica**—J.J. PESEK, San Jose State University, J. Sandoval

11:25 (755) **Efficiency of the Silylation of Controlled Pore Glass Measured by Chemical Derivatization and ESCA**—R. GNANASEKARAN, Mansfield University, T.A. Dang

11:45 (756) **Separation of Nucleic Acids and Oligonucleotides Using New Tentacle-Type Ion-Exchangers**—C. JANSEN, E. Merck, W. Muller

ICP/AES—Instrumental Concepts

Wednesday Morning, Room 1E13
M.L. Ruschak, Presiding
Aluminum Company of America

8:30 (757) **Studies of Solvent Introduction into Ar and He HEMIPs**—K.A. McCLEARY, VA Polytech Instit. & State Univ., G. Long

8:50 (758) **Doughnut Shaped High Power Microwave Induced Plasma Source for Trace Element Analysis**—D. BASS, Hitachi Instruments, Inc., M. Koga, T. Okumoto, Y. Okamoto, M. Uasuda, S. Murayama

9:10 (759) **Reduction of Breakdown Threshold in Laser Induced Plasmas**—V. MAJIDI, University of Kentucky

9:30 (760) **Characterizing Phosphate Rock Using ICP**—F.E. PATRICK, IMC Fertilizer Inc., J.E. Gibson, P.E Kandetzki

9:50 (761) **Application of Optical Fibers in ICP Spectroscopy**—J.E. GOULTER, Spectro Analytical Instru., Inc., S.F. Zhu, H. de Laffolie

10:10 RECESS

10:25 (762) **A New Instrumental Concept for Multielement Analysis of Environmental Materials - Polyscan Spectroanalyzers**—Y. NOURI, Jobin Yvon (ISA), Y. Lang, A. Le Marchand, I.B. Brenner

10:45 (763) **Information Based Expert Systems for Atomic Emission Spectroscopy**—R.S. POMEROY, University of Arizona, J.D. Kolczynski, M.B. Denton

11:05 (764) **Enhancing Limits of Detection by ICP-AES**—A. LE MARCHAND, Jobin Yvon (ISA), Y. Lang, I.B. Brenner

11:25 (765) **Improvement in the Reproducibility of ICP-AES Measurements Using Optical Feedback Power Regulation**—M.W. ROUTH, Applied Research Laboratories, D. Rupp, W. Vogel, D.F. Sermin, W.J. Kinsey

11:45 (766) **Analytical Implications of Using a Water-Cooled Low-Flow Torch in ICP Emission**—M.T.C. DELOOS-VOLLEBREGT, Delft University of Technology, J.J. Tiggelman, D.A. Yates

Infrared IV—Apparatus and Techniques B: Applications

Wednesday Morning, Room 1E18
D.W. Mayo, Presiding
Bowdoin College

8:30 (767) **Infrared Spectroscopy of Moving Solids**—R.W. JONES, Iowa State University, J.F. McClelland

8:50 (768) **Some Recent Developments in Sampling Techniques**—N.J. HARRICK, Harrick Scientific Corporation, M. Milosevic

9:10 (769) **Key Considerations for the Adaptation of FTIR to Process Monitoring**—J.P. COATES, Nicolet Instrument Corporation, D.A. Huppler, M.E. Meyers

9:30 (770) **The Customization of FTIR Analyzers to Meet Specific or Dedicated Chemical Applications**—J.P. COATES, Nicolet Instrument Corporation, M.P. Fuller

9:50 (771) **The Design and Performance of a State-of-the-Art FTIR System**—K. KRISHNAN, Bio-Rad, Digilab Division, D.B. Johnson, J.L. Leonardi

10:10 RECESS

10:25 (772) **Developments and Applications of Vibrational Reflection-Absorption Spectroscopy**—T.H. PAI, Mississippi State University, V.F. Kalasinsky, K.S. Kalasinsky

10:45 (773) **A Comparison of Monolayer Structure at Air-Solid and Air-Liquid Interfaces Using Infrared Reflectance Spectroscopy**—R.A. DLUHY, Battelle Memorial Institute

11:05 (774) **Applying FT-Spectroscopy to a Variety of Emission Techniques**—R. RUBINOVITZ, Bruker Instruments, Inc., R. Kenton, A. Simon

11:25 (775) **The Use of Infrared Active Probe Molecules for the Structural Analysis of Adsorbed Proteins**—M.P. FULLER, Nicolet Instrument Corporation, M.C. Garry, B.R. Singh

11:45 (776) **Rapid Verification of Identity and Concentration of Drug Formulations Using Mid Infrared Spectroscopy**—D.A.C. COMPTON, Bio-Rad, Digilab Division, J.A. Ryan, S.V. Compton, M.A. Brooks

Near Infrared—Applications and Data Processing

Wednesday Morning, Room 1E20
B.J. Sparr, Presiding
Aluminum Company of America

8:30 (777) **Qualitative & Quantitative Analysis of Algin & Xanthan Gums Using Near Infrared Reflectance Spectroscopy**—H.N. DANG, Bran+Luebbe Analy. Tech., Inc.

8:50 (778) **NIR Spectrophotometric Measurement of Water Content in Intact Leaves of Higher Plants**—D. SEQUERA, Shimadzu Scientific Instr., Inc., K. Harada, K. Furusawa, T. Ichikawa, T. Nishimura, R. Patch

9:10 (779) **Determination of Refractive Index via Near Infrared Spectroscopy Utilizing a Single Strand Fiber Optic Probe**—E.W. CIURCZAK, College of St. Elizabeth, D. Honigs

9:30 (780) **Diagnosing Malignancies Using Near Infrared**—S.M. MONAT

FOR SPECTRA-PHYSICS DETECTOR CIRCLE 156 →

9:50 (781) **Determination of Octane Number in Gasoline Relating Fuel Performance to Chemical Structure**—P.J. BRIMMER, NIRSystems, Inc.

10:10 RECESS

10:25 (782) **Anticipatory Control with Near Infrared: Strategy and Implementation**—C. KRADJEL, Bran+Luebbe Analyzing Tech.

10:45 (783) **Applications of Discriminant Analysis to Real-World Samples**—J. DUCKWORTH, Galactic Industries Corporation, D. Kuehl

11:05 (784) **Instrument Transparency: The Key for Universal Training Libraries in NIR Analysis**—A. LORBER, Negev Ctr. for Nuclear Research, I. Landa

11:25 (785) **Is There a Best Way to Analyze NIR Data?**—K.H. NORRIS, P. Williams

11:45 (786) **Performance Evaluation of Near-Infrared Diode-Array Spectrophotometers**—E. STARK, KES Analysis Inc.

Personal Computer Networking Solutions for Laboratory Data Management

Wednesday Morning, Room 1A06
A.S. Nakagawa, Presiding
Analytical Systems, Inc.

8:30 (787) **LIMS Using AppleTalk and the Macintosh**—J. HEFTER, GTE Laboratories Incorporated, D.M. Koffman

8:50 (788) **OS/2 Based Instrument Data-Stations Using Standard Software Packages**—J.L. CAWLEY, Northwest Analytical, Inc., L.K. Halvorsen, F.J. Barberis

9:10 (789) **Integrated Networking in the UNIX Environment**—N. RAMAN, Hewlett-Packard Company, N. Rathnam, D. Pearce

9:30 (790) **A New Generation of Chromatography Workstations**—T. ROONEY, Spectra-Physics, Inc., C. Chell, R. Bell

9:50 (791) **The Value of a MS DOS ChemStation to Increased Productivity in Environmental Analyses**—S.B. LEWIS, Hewlett-Packard Company, W.J. Sanders

10:10 RECESS

Post Analysis Data Processing

Wednesday Morning, Room 1A06
A.S. Nakagawa, Presiding
Analytical Systems, Inc.

10:25 (792) **Applications of PC-Based Relational Data Bases in Chromatography**—S. BURGESS, Spectra-Physics, Inc., C.W. Crandell, C. Chell, T. Rooney

10:45 (793) **Superflow II - A New Software for Flow Injection Analysis**—J.A. PERSSON, Tecator AB

11:05 (794) **Automatic Programming in a Push-Button Environment**—R.E. KLEBBA, Nicolet Instrument Corporation

11:25 (795) **Spectral Comparison Software for Materials Checking**—J. SELLORS, Perkin-Elmer Limited, R.A. Spragg

11:45 (796) **Concurrent Library Identification of Spectra Using Parallel Processing**—M. PIERCE, VG MassLab Ltd., M. Tan, I. Butler, J. Mitchell, P. D'Arcy, D. Pudvah

Remote Chemical Vapor Sensing

Wednesday Morning, Room 1E08
R.T. Kroutil, Presiding
U. S. Army Chemical Research

8:30 (797) **Recursive Digital Filtering of Infrared Emission Spectra**—S.D. BROWN, University of Delaware

8:50 (798) **Rapid Signal Processing Techniques for FTIR Remote Sensing**—G.W. SMALL, University of Iowa

9:10 (799) **Design of a Real Time Passive Infrared Remote Sensor with a Digital Signal Processor**—R.J. COMBS, U. S. Army Chemical Reserach, J.T. Ditillo, R.L. Gross, R.B. Knapp

9:30 (800) **Breadboard Demo of Non-Moving FTIR Concept**—W.K. WONG, SSG, Inc.

9:50 (801) **Laser Remote Sensing of Chemical Vapors**—J.P. CARRICO, SRI International

10:10 RECESS

10:25 (802) **Design of an FTIR Remote Analyzer for Monitoring Industrial Atmospheres**—R.N. HUNT, Mobay Corporation, R.L. Sandridge

10:45 (803) **Remote FTIR Study of Fugitive Emissions at a Chemical Waste Water Treatment Site**—R.H. KAGANN, TECAN, R. DeSimone, O.A. Simpson

11:05 (804) **Qualitative and Quantitative Analysis of Target Analytes Using Remote Detection FTIR**—J. DEMIRGIAN, Argonne National Labortory, S. Spurgash

WHEATON ANOTEC INORGANIC MEMBRANE FILTRATION

Wheaton Filtration Apparatus and ANOTEC Membrane Filters Offer Clearly Superior Results.

Wheaton has been an OEM supplier of high quality filtration apparatus to major membrane filter manufacturers for over 10 years. Now you can purchase these items from the source. In addition, we offer these revolutionary inorganic membrane filter products from Anotec Separations. Tested and compared against other leading membrane filters, ANODISC™ filter discs, and ANOTOP® and ANOTOP® Plus disposable syringe filters provide significant advantages:

- Better, more precise particle retention in 0.2, 0.1, and 0.02 μm sizes
- High porosity and well defined pore structure for higher flow rates even with difficult samples
- Wider range of chemical compatibility for use with aqueous solutions and organic solvents

WHEATON
WHEATON

WHEATON
Manufacturers Since 1888
1501 N. Tenth Street
Millville, NJ 08332, USA
Call Toll-Free: 1-800-225-1437, Ext. 3089
TLX: 55-1295 (WHEATON US)
FAX: 1-609-825-1368

Anotec Separations, which is a part of the Alcan Group of Companies, is a licensed user of the trademarks ANOTEC, ANOTOP, and ANODISC.

CIRCLE 202 ON READER SERVICE CARD

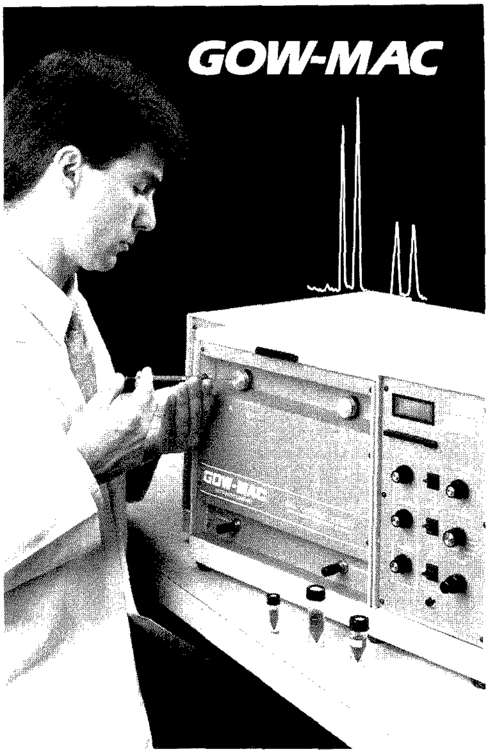

The GOW-MAC Series 580 Gas Chromatograph Lets You Set the Specifications

Custom modifications insure optimum performance for your dedicated applications

☐ Select one of seven different detector options for isothermal analyses

☐ Specific TC detectors designed for corrosion, trace, preparative scale, and high O_2 content analysis

☐ Select either packed, capillary, or widebore capillary columns

☐ Complete selection of manual or automatic valves for gas/liquid sampling, backflush, column switching, and series bypass operations

☐ Select injection ports for either gas or liquid samples

Send your specifications to P.O. Box 32, Bound Brook, New Jersey 08805 or call 201/560-0600, FAX: 201/271-2782 and we will provide a Gas Chromatograph custom tailored for the job.

GM GOW-MAC INSTRUMENT CO.

The World's Leading Manufacturer of Thermal Conductivity Detectors

CIRCLE 65 ON READER SERVICE CARD **PITTCON BOOTH #4903**

11:25 (805) **On-Site Measurements of Volatile Organic Compounds (VOCs) Using a Mobile Fourier Transform Spectrometer System**—M.L. SPARTZ, Kansas State University, M.R. Witkowski, R.M. Hammaker, W.G. Fateley, R.E. Carter, M. Thomas, D.D. Lane, B.J. Fairless, T. Holloway, J.L. Hudson, D.F. Gurka

11:45 (806) **Remote Sensing Using Long Path Ultraviolet Spectroscopy**—D.H. STEDMAN, University of Denver, S.E. McLaren

Spectral Fluorescence and Absorption

Wednesday Morning, Room 1E12
C.W. Gardner, Presiding
Bacharach, Inc.

8:30 (807) **Deep UV Raman Spectroscopy of Synthetic Polymers**—F. GHIAMATI, University of Rhode Island, R. Manoharan, W. H. Nelson

8:50 (808) **Effect of β-Cyclodextrin on Mucochloric Acid**—I.R. POLITZER, Xavier University, K.T. Crago, W. Benjamin, T. Hampton, J. Joseph, W.E. Coleman

9:10 (809) **Studies of Organized Bile Salt Media: Mixed Micelles and Lyotropic Phases**—K. WU, Duke University, L.B. McGown

9:30 (810) **Limits of Resolution in Multifrequency Phase-Resolved Fluorescence Spectroscopy**—D.W. MILLICAN, Duke University, L.B. McGown

9:50 (811) **Comparison of the Relative Effectiveness of Beta-Cyclodextrin Media as Luminescence Enhancement Agents**—W.L. HINZE, Wake Forest University, R. Frankewich, K.N. Thimmaiah

10:10 RECESS

10:25 (812) **Wavelength Selection and Nonlinear Response in Multivariate Spectroscopic Assays**—V.G. GREGORIOU, East Carolina University, P.J. Gemperline

10:45 (813) **Quantitative Analysis with a High Duty Cycle Solid State Random Wavelength Access Near-Infrared System**—D.L. WETZEL, Kansas State University, A.J. Eilert

11:05 (814) **Chemometrics in Fluorescence Spectroscopy**—J.N. MILLER, Loughborough University of Tech.

11:25 (815) **Measurement of Perylene in the Soil and Water of Earth Surface Using the Synchronous Fluorescence Quenching Method**—S. YANG, Anhui Inst. Optics & Fine Mech., Y. Zhu

POSTER PRESENTATIONS

Poster Papers will be on display from 9:30 AM - 4:00 PM Wednesday and Thursday. Authors will be available from 2:00 PM - 4:00 PM each day

Poster Session III

Wednesday and Thursday, Room 1A01

Poster Session IV

Wednesday and Thursday, Room 1B01

SYMPOSIUM

ASTM E-42—Recent Advances in Surface Analysis - arranged by S.R. Bryan of BP Research

Wednesday Afternoon, Room 1A08
S.R. Bryan, Presiding
BP Research

1:30 **Introductory Remarks**—S.R. BRYAN

1:35 (939) **Challenges to Quantitation of AES and XPS**—N.R. ARMSTRONG, University of Arizona

2:10 (940) **A Technique for Performing Angle-Resolved Auger Electron Spectroscopy and Angle-Resolved Electron Energy Loss Spectroscopy**—G.B. HOFLUND, University of Florida

2:45 (941) **The Use of XPS and Scanning Auger for Studying Mechanical and Tribological Properties of Ceramics**—D.D. HAWN, Dow Chemical, B.M. Dekoven, E.A. Ness

3:20 RECESS

3:35 (942) **Quantitative Analysis of Semiconductors by Secondary Ion Mass Spectrometry**—D.S. SIMONS, Nat'l. Inst. of Standards & Tech.

4:10 (943) **Applications of a Direct Imaging Time-of-Flight Instrument**—B. SCHUELER, Charles Evans & Associates

Batch 341
Batch

TAKE PERFORMANCE FROM LAB TO LINE
WITH NIRSYSTEMS FIBER OPTICS

See us
at Pittcon
Booth 5304.

Now you can use near-infrared spectroscopy in-line, at the batch reactor, in a sidestream, or for manual inspection.

Here are the right tools: advanced new fiber-optic systems from NIRSystems. They offer true transmission, reflectance and interactance measurements of fluids, suspensions and solid materials in process.

For on-line use, we package our laboratory-accurate Model 6500, 5500 and 5000 spectrophotometers with fiber-optic modules in NEMA 4X enclosures. The instruments are effectively isolated from the process environment.

Our new fiber-optic bundle Interactance Immersion probe solves process design problems with its single-hole mount and variable (1-20mm) path.

For manual testing and at-line quality control, our new hand-held single fiber-optic wand is the right solution. It performs true transmission and interactance measurements with the speed and accuracy you've come to expect from NIR analysis.

Whether your application is petrochemical, chemical, polymer, pharmaceutical or textile, we'll help you take it from the lab to the line.

Call NIRSystems today at 800-343-2036.

NIRSystems™
A Perstorp Analytical Company

CIRCLE 121 ON READER SERVICE CARD

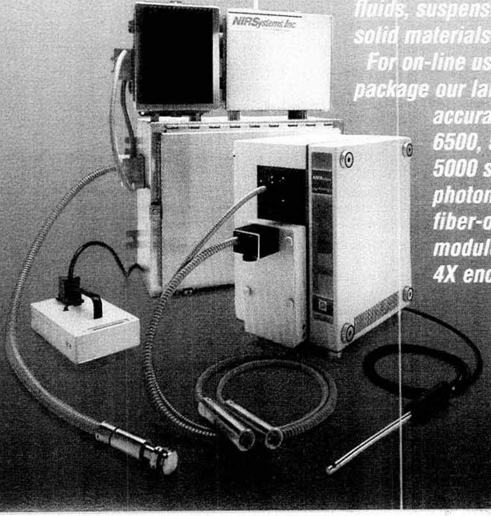

SYMPOSIUM

Characterization and Analysis of Chiral Compounds - arranged by J.A Feldman of Duquesne University and V.S. Venturella, Anaquest

Wednesday Afternoon, Room 1A23
J.A. Feldman, Presiding
Duquesne University

1:30 **Introductory Remarks**—J.A. FELDMAN

1:35 (944) **Characterization of Naturally Occurring and Synthetically Produced Chiral Compounds**—A. BROSSI, National Institutes of Health

2:10 (945) **Supercritical Fluid Chromatographic Analysis of Chiral Compounds**—K.E. MARKIDES, Brigham Young University

2:45 (946) **Chirality of Isoflurane—Supportive Data for Method Validation**—V.S. VENTURELLA, Anaquest

3:20 RECESS

3:35 (947) **Computer-Aided Strategies for Optimization in Chiral HPLC**—A.F. FELL, University of Bradford

4:20 (948) **Coupled-Column Systems for Bioanalysis of Chiral Drugs and Metabolites**—I.W. WAINER, St. Jude Children's Res. Hospital

SYMPOSIUM

Selectivity in Capillary Electrophoresis - arranged by D.J. Rose of Hewlett-Packard Laboratories

Wednesday Afternoon, Room 1D01
D.J. Rose, Presiding
Hewlett-Packard Laboratories

1:30 **Introductory Remarks**—D.J. ROSE

1:35 (961) **Selectivity in Capillary Zone Electrophoresis (CZE)**—R.A. HARTWICK, Rutgers University

2:10 (962) **Selectivity in Micellar Electrokinetic Capillary Chromatography (MECC)**—M.J. SEPANIAK, University of Tennessee, D. Swaile, A.C. Craig, R. Cole

2:45 (963) **Selectivity in Capillary Gel Electrophoresis**—D.J. ROSE, Hewlett-Packard Laboratories, R.R. Holloway

3:20 RECESS

3:35 (964) **Selectivity and Resolution in Capillary Isoelectric Focussing**—S. HJERTEN, University of Uppsala

4:10 (965) **Selectivity in Capillary Isotachophoresis**—F.S. STOVER, Monsanto Co.

SYMPOSIUM

James L. Waters First Annual Symposium Recognizing Pioneers in the Development of Analytical Instrumentation: Gas Chromatography - arranged by J.F. Coetzee of University of Pittsburgh

Wednesday Afternoon, Room 1A06
J.F. Coetzee, Presiding
University of Pittsburgh

1:30 **Introductory Remarks**—J.F. COETZEE

1:35 **Introduction—James L. Waters, Waters Business Systems**

1:40 (966) **The Evolution of Gas Chromatography and Gas Chromatographic Instrumentation**—L.S. ETTRE, The Perkin-Elmer Corporation

2:20 (967) **The Emergence of Gas Chromatography**—K.P. DIMICK

3:00 RECESS

3:15 (968) **The Story of the Electron Capture Detector and Its Role in "Green Politics"**—J.E. LOVELOCK, Consultant

3:55 (969) **Evolution of Gas Chromatography Detectors: From Universal to Selective**—A. ZLATKIS, University of Houston

Advanced Topics in Chemical Computing

Wednesday Afternoon, Room 1E08
P. Kutzenco, Presiding
American Cyanamid Co.

1:30 (970) **Comparison of a Neural Network with Rule-Building Expert Systems**—P.de B. HARRINGTON, Ohio University

1:50 (971) **Carbon-13 Nuclear Magnetic Resonance Spectrum Simulation of Benzenes and PAHs**—G.P. SUTTON, Penn State University, P.C. Jurs

2:10 (972) **Testing the Limits of a Novel Algorithm Used for Chemical and Pharmaceutical Research**—J.K. DRENNEN, University of Kentucky, R.A. Lodder

2:30 (973) **High-Speed 2-D Molecular Graphics**—C.A. JAMES, Hewlett-Packard Company

2:50 (974) **Standard Molecular Geometry Interchange Format for Computational Chemistry**—R. LYSAKOWSKI, Digital Equipment Corporation

3:10 RECESS

3:25 (975) **On-Site Software Identification of Unknown Environmental Pollutants**—A. LINENBERG, Sentex Sensing Technologies, Inc., R.K. Davis

3:45 (976) **A Cross Correlation Technique to Enhance Jansson's Method for Deconvolution of Noisy Chromatographic Data**—P.B. CRILLY, The Univ. of Tennessee-Knoxville

4:05 (977) **False Color Data Imaging: A New Technique for Analyzing Complex Chromatographic Data Sets**—B.K. LAVINE, Clarkson University, A. Stine, R. Gunderson, L. Helfend

4:25 (978) **Reducing Noise in Transmission Spectra, Using Maximum Likelihood**—L.K. DeNOYER, Spectrum Square Associates, J.G. Dodd

4:45 (979) **Data Handling Methods for a Portable Gas Analyzer**—P. HARRIS, Atomic Energy of Canada Limited, N.P. Reynolds, A.C. Vikis

Atomic Absorption—Analytical Procedures II

Wednesday Afternoon, Room 1E10
R.A. Kramer, Presiding
Aluminum Company of America

1:30 (980) **Kinetic Studies of Analyte Atomization in Slurry-Electrothermal Atomic Absorption Spectrometry**—K.W. JACKSON, State University of New York, H. Qiao

1:50 (981) **Procedures for Testing Furnace AAS Instrumentation and Methods**—W. SLAVIN, The Perkin-Elmer Corporation, G.R. Carnrick, I. Shuttler, G. Schlemmer, J. Schickli, S. McIntosh

2:10 (982) **Direct Multielement Analysis of Powders Using Fast Sequential AA and a Solid Sample Atomizer**—J.M. CARTER, Analyte Corporation, A.E. Bernhard, H.L. Kahn

2:30 (983) **Multielement Analysis of Undissolved Titanium and Nickel-Base Alloys by Fast Sequential Atomic Absorption**—H.L. KAHN, Mars Company, A.E. Bernhard, E. Edin, T. Sciutto

2:50 (984) **Improving AA Analysis with Fast Sequential Multielement Techniques**—W. BATIE, Analyte Corporation, A.E. Bernhard, H.L. Kahn

3:10 RECESS

3:25 (985) **Use of a Sequential Atomic Absorption Spectrophotometer in a Production Laboratory**—M. KLICK, GPU Nuclear Corporation, D.D. Frymoyer

3:45 (986) **On-Line Photo-Oxidation Followed by Hydride Reduction Atomic Absorption Spectrophotometry for the Detection of Chromatographically Separated Arsenic Species**—D.A. KALMAN, University of Washington, R.H. Atallah

4:05 (987) **Water Lead Analysis - A Comparative Study Between Delves Cup and Graphite Furnace Methods**—Y.S. LEE, Univ. of District of Columbia, B.A. Serrano, J.B. Thomas, Jr.

4:25 (988) **The Application of a New Atomic Absorption System to Biological Analysis**—R.G. GREY, GBC Scientific Equip. Pty. Ltd., P.R. Liddell, M.W. Tikkanen

4:45 (989) **Palladium as a Matrix Modifier for the Graphite Furnace Atomic Absorption Spectrometric Determination of Lead in Human Whole Blood**—V.A. GRANADILLO, Universidad del Zulia, R.A. Romero

Electrochemistry—Detectors and Sensors

Wednesday Afternoon, Room 1E18
R.L. McCreery, Presiding
The Ohio State University

1:30 (990) **Microband Electrochemical Detector for HPLC**—J.M. ZADE II, Shimadzu-Kansas Res. Laboratory, R. Mitchel, T. Kuwana

1:50 (991) **LCEC Carbohydrates Sensor**—J. MARIOLI, Shimadzu-Kansas Res. Laboratory, J.M. Zade II, T. Kuwana

2:10 (992) **Separation and Identification of Isoflavones with High Performance Liquid Chromatography-Electrochemical Thermospray Mass Spectrometry (LCEC-MS)**—S.A. WORST, Ohio University, H.D. Dewald

2:30 (993) **Trace Oxygen Measurement in Inert Gases Using AC Polarographic Operation of a Zirconia Electrolyte Sensor**—E. GUTHRIE, J&W Scientific, D. Rittenhouse, S. Woodward

2:50 (994) **The Application of HPLC with Electrochemical Detection for Stability Determination of Iodine-Containing Organic Compounds**—S.K. GOZO, Quad Pharmaceuticals, Inc., J.A. Feldman

3:10 RECESS

3:25 (995) **New HPLC Methods for Quantitative and Sensitive Analysis of Neurotransmitters**—S.V. ROSE, Chrompack Inc., J.P. Crombeen

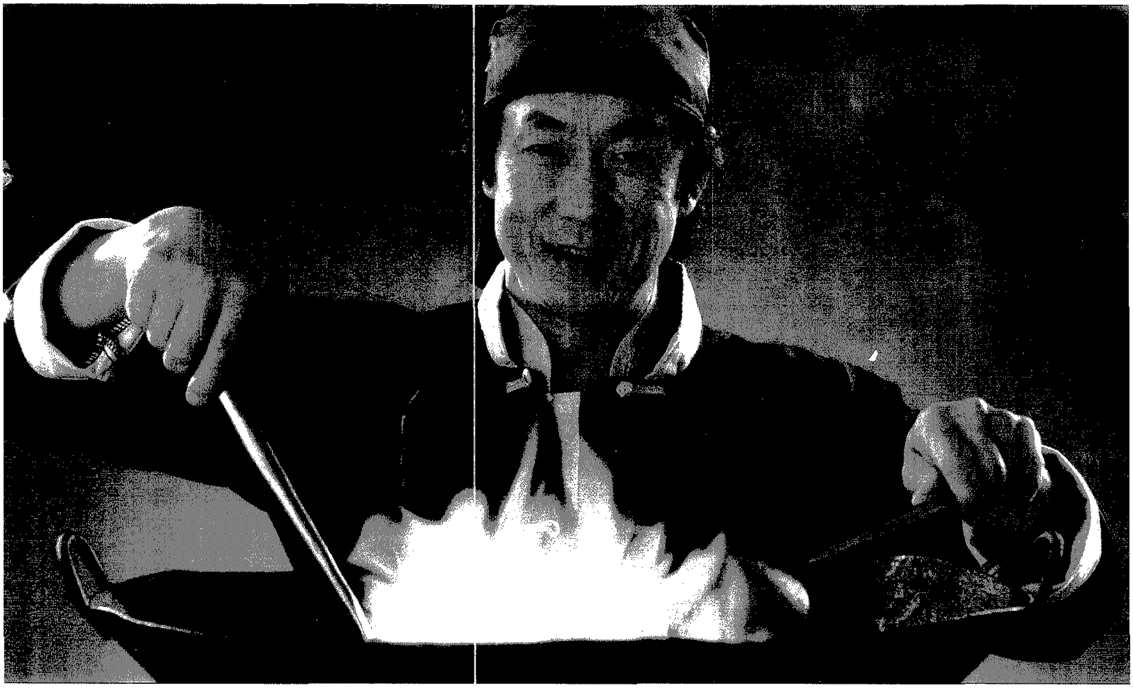

WHO KNOWS MORE ABOUT HEATING AND STIRRING?

Thermolyne manufactured their first hot plate more than 45 years ago, and since then we've developed the industry's most complete line of hot plates, stirrers and stirring hot plates. You can now choose from four distinct top plate materials, and an assortment of sizes and styles. In 1990, we expand the list with our **NEW** Remote Control Cimarec™ giving you convenient operation (up to 6 feet away) with our performance engineered ceramic top units.

So when you want to know more about heating and stirring, call the experts at Thermolyne: **1-800-553-0039**

Or write Barnstead | Thermolyne, 2555 Kerper, Dubuque, IA 52001.

Because you don't want to stir up trouble in your wok!

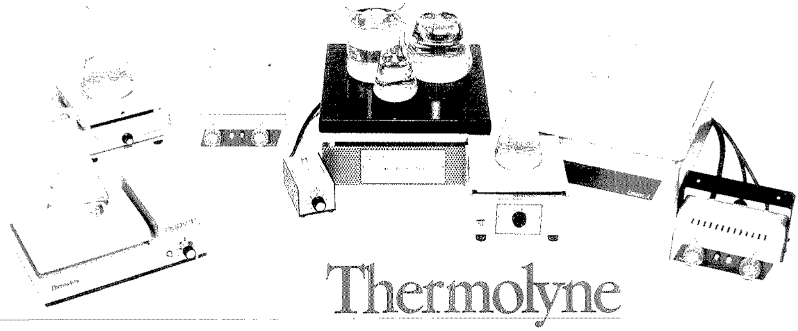

Thermolyne

For a **FREE** detailed catalog, circle reader service card no. 18.

We'll put all the latest advances in the chemical sciences right in your hands... And you won't need to lift a finger!

AMERICAN CHEMICAL SOCIETY STANDING ORDER PLANS

The ACS has a simple way to ensure that your library always has the chemistry titles your patrons require. It's called the ACS Standing Order Plans.

With ACS Standing Order Plans, you can save the time you'd otherwise spend on literature searches and purchase order details . . . and make certain that your library has the titles your patrons want—when they need them.

AS EASY AS 1-2-3

You can select from three Standing Order Plans—choose one or all or a combination . . . whatever best suits your patrons' needs!

1. **By Series:**
Advances in Chemistry Series
ACS Symposium Series
ACS Monographs
Professional Reference Books
All ACS Series

2. **By Single Title:**
ACS Abstract Books
ACS Directory of Graduate Research
College Chemistry Faculties

3. **By Subject:**
Analytical • Agricultural/Agrochemical • Biological • Biotechnology • Carbohydrate • Cellulose/Paper/Textile • Colloid/Surface • Computers in Chemistry • Electronic Materials • Environmental/Chemical Health and Safety • Food/Flavor • Energy/Fuel/Petroleum/Geochemistry • Industrial/Chemical Engineering • Inorganic • Materials Science • Medicinal/Pharmaceutical • Nuclear • Organic • Polymer/Applied Polymer Science • Physical Chemistry

PLUS FIVE NEW SUBJECT AREAS . . . Chemical Information • Directories • History • Non-Technical • Toxicology!

25 TO CHOOSE FROM!

You tell us which Standing Order Plan (or Plans) you'd like—1, 2, 3, or a combination. Your one-time order assures prompt, automatic delivery of each new title in the plan or plans you've chosen as soon as it's published. We'll send you an invoice with your shipment. You'll have thirty days to examine each new book and (if you decide for any reason) to return it for full credit. And you may modify or cancel your Standing Order Plan at any time. It's that easy!

Make sure your chemistry resources are always complete—don't overlook a single book from the world's most respected publisher in the chemistry field. Enroll in ACS Standing Order Plans today.

Write to American Chemical Society, 1155 Sixteenth Street, N.W., Washington, DC, 20036. Or call us TOLL FREE (800) 227-5558.

CALL 800-638-6360

AND

GET TO THE CORE

YOUR DIRECT LINE TO A SPECIALTY GAS PROFESSIONAL

Call a Specialty Gas Professional at MG's new 800-638-6360 number for data and recommendations that relate to 150 gases required for pivotal research, development, and production applications.

We can discuss your specialty gas needs in terms of purity requirements, gas distribution systems, hazardous gas instrumentation, and MG systems designed to control toxic waste—any area where process gases are integral components in your application.

For meaningful results on your call, use the checklist provided and we'll get to the core of your problem.

MG SPECIALTY GAS CHECKLIST

Application Relates to
- ☐ Analytical Instrumentation
- ☐ Atmosphere Requirements
- ☐ Chemical Processing/Intermediate
- ☐ Research
- ☐ Medical Diagnostics
- ☐ Other (specify)

Which of the following do you use in your process?
- ☐ Zero Grade Gases
- ☐ Liquid Helium
- ☐ Emissions Gases
- ☐ Gas Blenders
- ☐ Research Grade Gases
- ☐ Carrier Gases
- ☐ Calibration Gases
- ☐ Gas Regulating Equipment

How many cylinders do you use per month:
0–3 ☐ 3–10 ☐ 10–40 ☐ Greater than 40 ☐

Technically Speaking is our Best Means of Communication. Call: 800-638-6360. Ask for our Technical Representative, Specialty Gas. MG Industries, P.O. Box 945, Valley Forge, PA 19482, or FAX your request to 215-630-5600.

OUR LEADERSHIP WORKS.

MG

SPECIALTY GAS

CIRCLE 116 ON READER SERVICE CARD

3:45 (996) **An Enzyme Sensor for the Determination of Inosine and Hypoxanthine in Aqueous Solutions**—S.D. HAEMMERLI, University of New Orleans, A.A. Suleiman, O. Fatibello-Filho, G.G. Guilbault

4:05 (997) **Amperometric Biosensors with Polymeric Electron-Transfer Relays**—P.D. HALE, Brookhaven National Laboratory, T. Inagaki, H.I. Karan, H.S. Lee, T.A. Skotheim, Y. Okamoto

4:25 (998) **Use of Electropolymerized Films in Biosensors to Stabilize the Enzyme, Prevent Fouling and Screen Out Interferences**—R.J. GEISE, Rutgers, The State Univ. of NJ, A.M. Yacynych, J. Adams, N. Barone, S. Rao

4:45 (999) **Use of Multichannel Bioanalyzer for the Assay of Glucose, Lactate, and Uric Acid in Whole Blood and Plasma**—T.T. HSU, Industrial Tech. Res. Institute, J.C. Chen, Z.S. Chow, T. Chang, M.C. Wu, K.P. Hsiung, C.N. Yang, L.J. Wang

Gas Chromatography—Environmental II

Wednesday Afternoon, Room 1A07
M.E. McNally, Presiding
E. I. du Pont de Nemours & Co., Inc.

1:30 (1000) **Comparison of Field- and Laboratory-Based Gas Chromatographs with PID Detectors to Monitor for the Aromatics at Two Gasoline Contaminated Sites**—C. WOOD, HNU Systems Inc., J.D. Stuart, M.J. Lacy

1:50 (1001) **Automatic On-Line Air Monitoring with Enrichment Down to the ppb-Level**—U.K. GOEKELER, ES Industries

2:10 (1002) **Analysis of Volatile Organic Compounds by Capillary Gas Chromatography, Using Purge and Trap Without Cryofocusing**—R.E. SHIREY, Supelco, Inc., S.A. Hazard

2:30 (1003) **Optimization and Evaluation of a Gas Chromatographic Column and System for the Analysis of Organic Contaminants in Water**—R.H. KOLLOFF, Hewlett-Packard Company, S.S. Stafford, N.G. Chechik, R.D. DeVeaux, K.J. Hyver

2:50 (1004) **Methodology for Reduced Detection Levels of Poly-Nitroaromatics in Drinking Water**—C.A. ASOWATA, U.S. Army Environ. Hyg. Agency, C.J. Stern, M.A. Hable

3:10 RECESS

3:25 (1005) **Analyzing Volatile Drinking Water Contaminants by Capillary Gas Chromatography**—N.H. MOSESMAN, Restek Corporation, C.R. Vargo

3:45 (1006) **Sample Preparations for Drinking Water Analysis Using Solid Phase Adsorbent Cartridges: An Alternative to Liquid/Liquid Extraction**—L. NOLAN, Supelco, Inc., S.B. Cole

4:05 (1007) **Automatic On-Line Monitoring of Volatiles in Water: Prevention of Water Pollution**—U.K. GOEKELER, ES Industries

4:25 (1008) **Development of Analytical Reference Standards for the Analysis of Organic Compounds in Drinking Water by Liquid-Solid Extraction and Capillary Column Gas Chromatography/Mass Spectrometry**—K.H. KIEFER, Supelco, Inc., J.L. Vonada, R.M. Whitehill, J.K. Crissman, Jr.

4:45 (1009) **Rapid Isolation of Volatile Organics from Water Samples with Gas Elimination Device Constructed from Microporous Hollow-Fibers**—J.B. PAWLISZYN, University of Waterloo

HPLC—In the Life Sciences II

Wednesday Afternoon, Room 1E06
H. McNair, Presiding
Virginia Polytechnic Institute & State University

1:30 (1010) **Automated HPLC Amino Acid Analysis by Pre-Column Derivatization**—R. SPATZ, E. Merck, T. Nogami, H. Iwabuchi, H. Kaji

1:50 (1011) **Blank-Subtracted Standard Addition Applied to Analysis of Catecholamine Metabolites in Urine**—R. SPATZ, E. Merck, Y. Yamada, K. Deguchi, T. Nogami, Y. Nomura

2:10 (1012) **Improving DABS Amino Acid Analysis Speed and Sensitivity**—M.E. TERRY, Beckman Instruments, Inc., R. Bae, J. Mayhew

2:30 (1013) **A Sensitive HPLC Assay for D-Cycloserine Human Plasma**—L.A. KOSOBUD, G. D. Searle & Co., M.S. Chang, G.L. Schoenhard

2:50 (1014) **Automated Solid Phase Extraction and HPLC Injection of Theophylline from Serum**—B.D. HOLDEN, Zymark Corporation, B.G. Lightbody, J. Tomlinson

3:10 RECESS

3:25 (1015) **Liquid Chromatography as a Tool in Defining the Abnormality in the Levels of Catecholamines and Tryptophan Metabolites in Patients with Neurological Disorders**—G.A. QURESHI, Karolinska Institute, S. Baig

3:45 (1016) **Plasma Amino Acid Profile in Patients Undergoing Liver Transplantation - An HPLC Study Based on Pre-Column Derivatization of OPA with Amino Acid and Presence of 2-Mercaptoethanol**—G.A. QURESHI, Karolinska Institute, A.F. Qureshi, B.G. Ericzon, J. Bergstrom, C.G. Groth

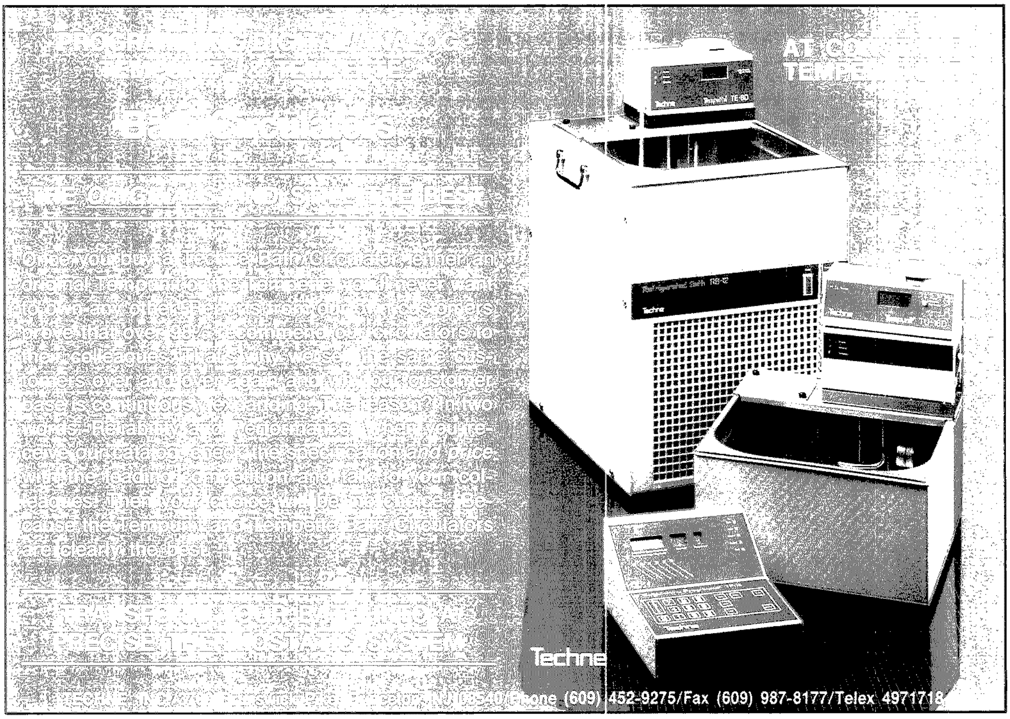

(609) 452-9275/Fax (609) 987-8177/Telex 4971718

CIRCLE 174 ON READER SERVICE CARD

GET TO THE POINT!

CD-Bonn

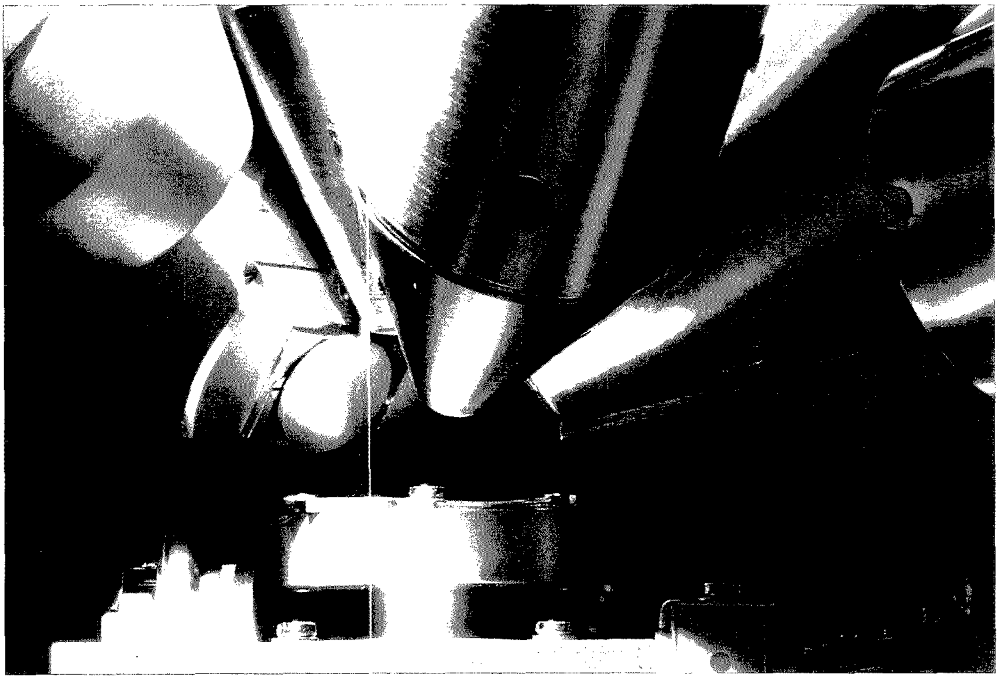

190.0.61 23.003.02

With MAX – the Multi-Method System for High Precision Surface Analysis

When several different surface analysis methods are required to solve a problem, MAX holds the key to success. All excitation sources point to the same spot on the sample.

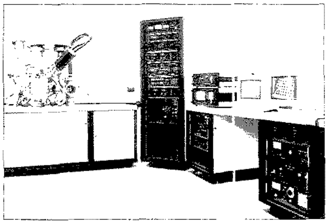

As an analysis proceeds step by step, one technique after another is applied, in the same system, without moving either sample or source.

- X-ray Photoelectron Spectroscopy (XPS) • Scanning Auger Electron Spectroscopy (SAM) • Ion Scattering Spectroscopy (ISS) • Secondary Ion Mass Spectrometry (SIMS) • Sputtered Neutral Mass Spectrometry (SNMS)

To find out how MAX can help you to "Get to the point", contact us at: (412) 327-5700.

Visit us at Booth 1128, Level 1
PITTSBURGH CONFERENCE
Javits Convention Center, N.Y.C.
March 5–8, 1990

■ LEYBOLD VACUUM PRODUCTS INC. LAS GROUP
5700 Mellon Road, Export, PA 15632

■ LEYBOLD AG
Bonner Strasse 498, D-5000 Cologne 51, West Germany

LH
LEYBOLD

Innovative Vacuum Technology

A Degussa Company

CIRCLE 90 ON READER SERVICE CARD

4:05 (1017) **Determination of Oxalic Acid in Human Plasma by Ion Exclusion Chromatography with a Reaction Detector**—R. HORIKAWA, Toyama Med. & Pharm. University, K. Kitazawa, Y. Aoki, T. Tanimura

4:25 (1018) **The Use of Chromatographic Methods for the Purification of Proteins from Complex Mixtures**—D. JOSIC, Institut fur Molekularbiologie, W. Hofmann, W. Reutter, J. Reusch, K. Gottschall

4:45 (1019) **Evaluation of HPLC Systems for Separation of Biopolymers**—G. ROZING, Hewlett-Packard GmbH, F. Strohmeier, M. Herold, G. Curtis

LC; GC-MS

Wednesday Afternoon, Room 1E16
C. Fenselau, Presiding
University of Maryland

1:30 (1020) **The Determination of Peptide and Protein Molecular Weights by On-Line Ion Spray Liquid Chromatography/Mass Spectrometry**—J. HENION, Cornell University, E. Huang, J.J. Conboy

1:50 (1021) **Enhanced Sensitivity and Quantitative Performance with Particle Beam LC/MS**—A. APFFEL, Hewlett-Packard Company, P.C. Goodley, D.E. McIntyre

2:10 (1022) **Quantitative Particle Beam LC/MS**—R.C. WILLOUGHBY, Extrel Corporation, P. Sanders, E.W. Sheehan

2:30 (1023) **Environmental Applications of Particle Beam LC/MS**—A. APFFEL, Hewlett-Packard Company, P.C. Goodley, D.E. McIntyre

2:50 (1024) **Particle Beam LC-MS with an Ion Trap Detector**—J.A. KOROPCHAK, Southern Illinois University, C. Chavez

3:10 RECESS

3:25 (1025) **Renaissance of Time-of-Flight Mass Spectrometry in GC-MS: Time Array Detection**—J.T. WATSON, Michigan State University, J. Allison, C.G. Enke, J.F. Holland

3:45 (1026) **Optimization of Ion Source Parameters for GC-Time-of-Flight Mass Spectrometry**—B. GARDNER, Michigan State University, R. Tecklenburg, J.T. Watson, J.F. Holland

4:05 (1027) **Evaluation of a New Micro Jet Separator for GC/MS Analysis of Volatile Organics with Megabore Capillary Columns**—J.D. MARTIN, Roy F. Weston, Inc., P.D. Perkins

4:25 (1028) **Developments in Continuous Flow FAB LC-MS**—C.C. STACEY, Waters Chrom. Div. Millipore Corp., M.P. Balogh, T.A. Dourdeville, W.E. Greene, L.M. Mallis

4:45 (1029) **Different Approaches to Chromatographic Methods Development for LC-MS**—M.P. BALOGH, Waters Chrom. Div. Millipore Corp., E.G. Cassis, C.C. Stacey

Laser Mass Spectrometry; FTMS

Wednesday Afternoon, Room 1E21
F.W. McLafferty Presiding
Cornell University

1:30 (1030) **Multiphoton Ionization Mass Spectrometry of Small Biological Molecules and Polymers Using Pulsed Laser Desorption/Volatilization from Liquid Matrices into Supersonic Beams**—D.M. LUBMAN, University of Michigan, L. Li

1:50 (1031) **Selective Mass Spectrometry by Single-Photon Ionization from a Molecular Hydrogen Laser Source**—J.W. FINCH, University of Arizona, M.B. Denton

2:10 (1032) **IR and UV Laser Experiments in an FTMS**—L.M. NUWAYSIR, Univ. of California, Riverside, C.L. Wilkins

2:30 (1033) **Laser Probe Mass Spectrometry**—D.A. WEIL, Nicolet, J. Hoerning, J.E. Campana

2:50 (1034) **Laser Desorption Fourier Transform Mass Spectrometry for Analysis of Thin-Layer Chromatograms and Electropherograms**—J.C. DUNPHY, Oak Ridge National Labortory, R.L. Hettich, M.V. Buchanan, K.L. Busch

3:10 RECESS

3:25 (1035) **Isotopic Imaging by Ion Microscopy: A New Approach for Intracellular Diffusible Element Analysis**—S. CHANDRA, Cornell University, P.F. Clardy, G.H. Morrison

3:45 (1036) **New Techniques for Fourier Transform Mass Spectrometry**—R.D. CODY, Nicolet

4:05 (1037) **Investigation of Detection Limits Using a High Sensitivity Detector on a Quadrupole Mass Spectrometer**—J. PEREL, Phrasor Scientific, Inc., J.F. Mahoney, K. Faull, N. Pascoe

4:25 (1038) **FTMS and External Ion Production, A Major Step Ahead**—C. RADLOFF, Spectrospin AG, P. Grossmann, H.P. Kellerhals, F. Laukien, J. Wronka

The agony. The ecstasy.

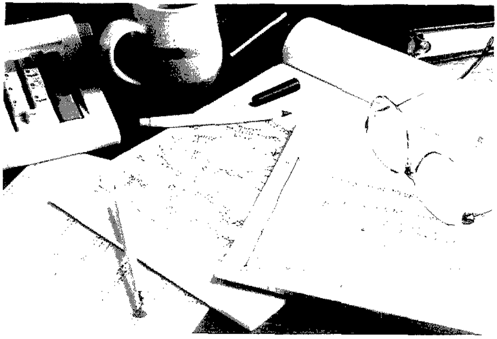

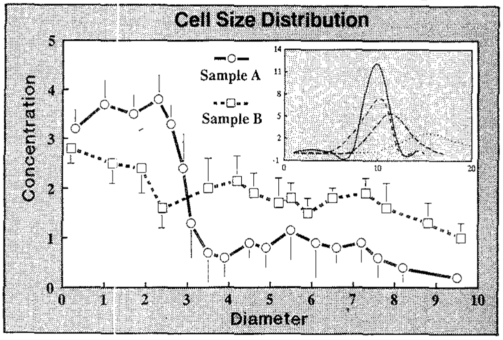

We know it takes a lot of work to produce good scientific data. Which is why you owe it to yourself to check out SlideWrite Plus. You see, our powerful presentation graphics software for the IBM PC and compatibles can turn the data you worked so hard to capture into high impact charts, graphs, slides and overheads — and do it all *in minutes.*

SlideWrite Plus gives you powerful graphing features, full drawing capability, flexible labeling with 16 great fonts, and *extremely* high quality output on printers, plotters, and cameras. And that's just for starters. It's no wonder SlideWrite Plus tied for first place in a recent *PC Week* poll!

Call us for a free demo diskette right now. We'll show you how SlideWrite Plus can help your results *get* results.

Call for your FREE full-featured trial diskette!
(408) 749-8620

Advanced Graphics Software
333 West Maude Ave., Sunnyvale, CA 94086

SlideWrite Plus™ We make your data look terrific.

CIRCLE 9 ON READER SERVICE CARD

SURE THINGS

Trust Parker quality throughout your operation.

You've learned to be certain of Parker column end fittings and valves for critical chromatography applications.

Now extrapolate.

You will enjoy all that quality and accuracy, all that craftsmanship and performance in the total Parker line for all your analytical, laboratory and instrumentation applications.

Parker's complete line includes compression, welded and face-seal fittings, sizes from 1/16″ to 1″ O.D., in a broad range of materials and configurations. It also includes a full line of needle, ball, bellows, check valves and filters, plus sample cylinders, transfer coils, and more.

All Parker. All sure things. Contact the Instrumentation Divisions or your independent Parker Distributor.

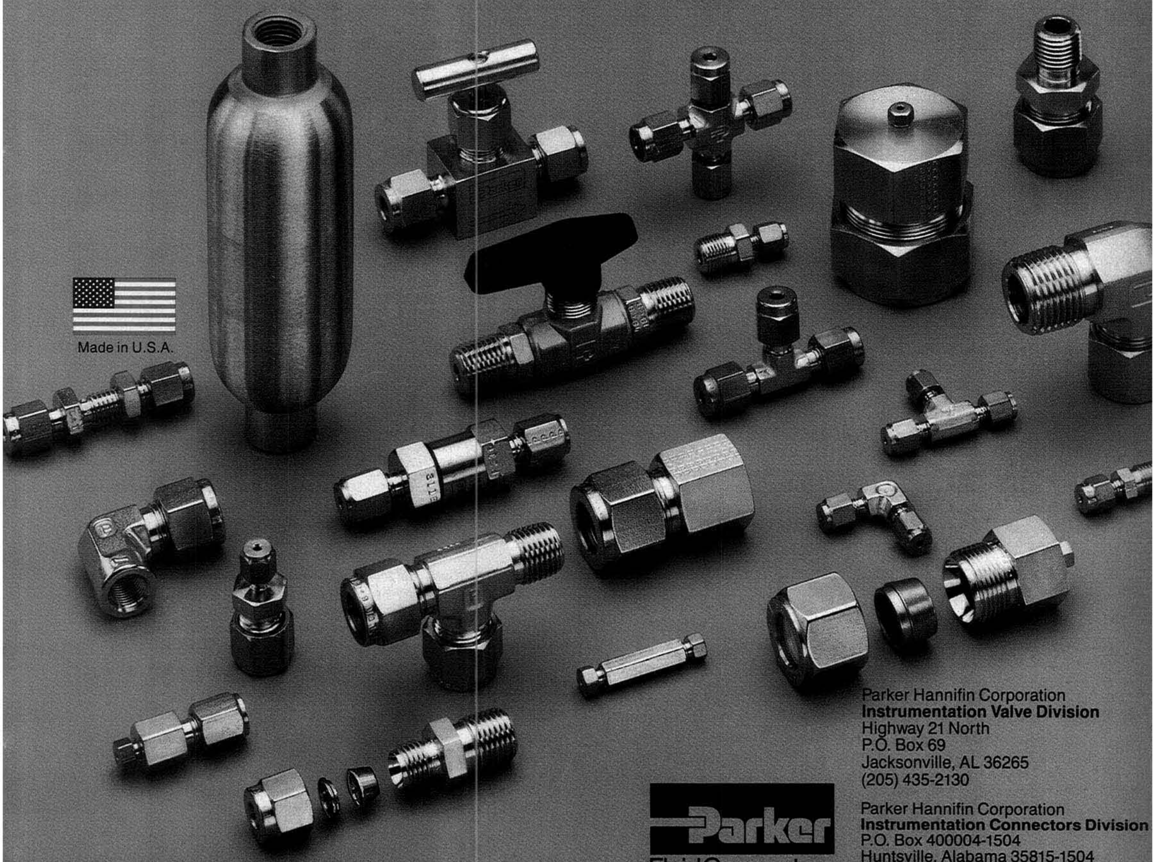

Parker Hannifin Corporation
Instrumentation Valve Division
Highway 21 North
P.O. Box 69
Jacksonville, AL 36265
(205) 435-2130

Parker Hannifin Corporation
Instrumentation Connectors Division
P.O. Box 400004-1504
Huntsville, Alabama 35815-1504
(205) 881-2040

Parker
FluidConnectors

CIRCLE 148 ON READER SERVICE CARD

-926

Microseparations

Wednesday Afternoon, Room 1E15
H. Hatano, Presiding
Health Research Foundation

1:30 (1040) **Particle Separations by Capillary Electrophoresis**—H.K. JONES, Battelle, Pacific Northwest Lab., N.E. Ballou

1:50 (1041) **Multidimensional Micro HPLC/CZE**—W.H. WILSON, VA Polytechnic Inst. & State Univ., H.T. Rasmussen, H.M. McNair

2:10 (1042) **A New, Fully Automated Instrument for Capillary Electrophoresis**—S.R. WIENBERGER, Spectra-Physics Corporation, L. Hellinger

2:30 (1043) **Packed Microbore and Capillary Columns for LC and SFC**—M.V. PISERCHIO, Keystone Scientific, Inc., R.A. Henry, D.C. Shelly

2:50 (1044) **Dedicated Instrumentation for Microbore and Packed Capillary GC**—A.D. BASHALL, Carlo Erba Instruments/Fisons, A. Trisciani, F. Andreolini

3:10 RECESS

3:25 (1045) **A Comparison of Efficiency, Resolution and Concentration, and Mass Detection Limits Among Three Different Microchromatographic Techniques**—J.A. MACCHIA, Spectra-Physics, Inc., S. Yarbro, S.R. Weinberger

3:45 (1046) **New Polymeric Microbore Columns for Biological Molecules**—P. NEWTON, Dionex Corporation, J. Thayer

4:05 (1047) **A Universal Microbore Packed Column for GC, SFC, LC, and IC**—Y. LIU, Dionex Corporation, C. Pohl, F. Yang

4:25 (1048) **Newly Developed Semi-Microbore Gradient HPLC System**—S. FUJIMOTO, Shimadzu Corporation, S. Maruyama, K. Saito, A. Nakamoto

4:45 (1049) **Investigation of Short Narrow Bore Columns in HPLC**—G.H. XIE, Institute of Chemistry, Y. He

New Atomic Spectroscopy Instrumentation; X-ray Fluorescence

Wednesday Afternoon, Room 1E12
E. McClendon, Presiding
Midwest Research Institute

1:30 (1050) **Determination of Relative Ion Yields of Insulating Materials by Radio Frequency - Glow Discharge Mass Spectrometry**—D.C. DUCKWORTH, Clemson University, R.K. Marcus

1:50 (1051) **Characterization of the First-Stage Expansion in an ICP-MS Interface**—D.M. CHAMBERS, Indiana University, P. Yang, G.M. Hieftje

2:10 (1052) **Theta Pinch Discharges for Elemental Analysis: What Parameters Really Matter?**—A. SCHEELINE, University of Illinois, D. Miller

2:30 (1053) **Design and Application of a New Radio Frequency (RF) Powered Glow Discharge Atomic Emission Spectrometer for the Direct Analysis of Nonconducting Samples**—M.R. WINCHESTER, Clemson University, R.K. Marcus

2:50 (1054) **Introduction of Aqueous Samples into a Glow Discharge Device via a Particle Beam Interface**—C.M. STRANGE, Clemson University, R.K. Marcus

3:10 RECESS

3:25 (1055) **Improvements in Sensitivity and Resolution in Wavelength Dispersive X-ray Fluorescence Spectrometry**—J.A. ANZELMO, Fisons Instruments, B. Boyer, R. Yellepeddi, D. Bonvin

3:45 (1056) **Identification of Television Picture Tube Panel Glass Composition by On-Line X-ray Fluorescence**—M.A. CHENOWETH, Thomson Consumer Electronics, H.J. Peresie

4:05 (1057) **Total Reflection X-ray Fluorescence Analysis of Ultrapure Reagents at the Sub ng/mL Level**—A. PRANGE, GKSS, GmbH, K. Kramer, U. Reus

4:25 (1058) **A New Fundamental Parameters Software Package for Bulk and Multi-Layered Samples**—P. BROUWER, Philips Analytical, G.T.J. Kuiperes

4:45 (1059) **Semiquantitative Analysis in Wavelength-Dispersive XRF Spectrometry Using the Fundamental Parameters Program**—G. PLATBROOD, Laborelec

Pattern Recognition and Signal Processing Techniques for Organic Spectroscopic Analysis

Wednesday Afternoon, Room 1E20
K.K. Trischan, Presiding
Aluminum Company of America

1:30 (1060) **Interactive Fast PLS/PCR for Improved NIR Analysis in On-Line Applications**—A. LORBER, Negev Ctr. for Nuclear Research, L. McDermott

1:50 (1061) **Raw Materials Testing by Pattern Recognition Techniques Using Near Infrared Reflectance Spectra**—N.K. SHAH, East Carolina University, P.J. Gemperline

2:10 (1062) **Neural Networks and the Interpretation of Infrared Spectra**—S.M. DONAHUE, University of Rhode Island, C.W. Brown, R. Kumaresan

2:30 (1063) **Determination of Protein in Wheat from Near-Infrared Spectra Using Artificial Neural Networks**—J.R. LONG, East Carolina University, P.J. Gemperline

2:50 (1064) **Advanced Pattern Recognition Principles for FTIR Remote Sensing**—T.F. KALTENBACH, University of Iowa, G.W. Small, R.T. Kroutil, J.T. Ditillo, W.R. Loerop

3:10 RECESS

3:25 (1065) **Applications of Auto-By-Cross Correlation Detection in Flowing Streams**—E. VOIGTMAN, University of Massachusetts, M.E. Johnson

3:45 (1066) **Statistical Evaluation of Intercomparison Data Obtained with Different Analytical Methods**—D.L. MacTAGGART, University of Idaho, S.O. Farwell

4:05 (1067) **Getting Slopes from Noisy Data and Detecting Outlying Data**—M. MOEN, University of Alberta, K. Griffin, A.H. Kalantar

4:25 (1068) **Calibration Transfer in Quantitative Analysis Using FTIR**—R.A. SPRAGG, Perkin-Elmer Limited, R.E. Aries, D.P. Lidiard

4:45 (1069) **Identification of Maturity Factors by Partial-Least-Squares Target Rotation of Diffuse Reflectance Infrared Spectroscopic Profiles Acquired on Extracts of Coals and Sediments**—A.A. CHRISTY, University of Bergen, O.M. Kvalheim, B. Dahl, K. Oygard, T.V. Karstang

Preparative LC

Wednesday Afternoon, Room 1E19
A. Stalcup, Presiding
University of Missouri

1:30 (1070) **High Performance Preparative Chromatography of Proteins Using Silica-Based Bonded Phases in Radial-Flow Columns**—V. SAXENA, Sepragen Corporation, N.T. Miller

1:50 (1071) **Packing of Preparative HPLC Columns by Sedimentation**—T. WANG, Rutgers University, R.I. Robinson, R.A. Hartwick, N.T. Miller, D.C. Shelley

2:10 (1072) **Liquid Chromatographic Preparative Packing Utility as a Function of Particle Shape**—J.A. PERRY, Regis Chemical Company, T.J. Szczerba

2:30 (1073) **True Countercurrent Chromatography - Its Preparative Applications in Natural Products Research**—Y.W. LEE, Research Triangle Institute, Z. Lee

2:50 (1074) **Paper Withdrawn**

3:10 RECESS

3:25 (1075) **The Use of Cartridge Columns for Analytical and Preparative HPLC**—E.T. BUTTS, Whatman Manufacturing Inc., J.D. Barbosa, L. Lane, J.J. McNicholas, P.R. Levison

3:45 (1076) **Enantiomeric Separation of Biologically Important Materials Using Centrifugal Partition Chromatography**—R. MENGES, University of Missouri-Rolla, D.W. Armstrong

4:05 (1077) **Effects of Mobile Phase Composition on the Adsorption of Proteins to Anion-Exchange Cellulose**—P.R. LEVISON, Whatman Paper Ltd., D.W. Toome, E.T. Butts

4:25 (1078) **Performance of Anion-Exchange Cellulose Using Radial Flow Column Chromatography**—L. LANE, Whatman Manufacturing Inc., M.L. Koscielny, E.T. Butts, P.R. Levison

4:45 (1079) **Capacity and Kinetics of Protein Adsorption by Anion-Exchange Celluloses. Influence of Molecular Mass and pH**—P.R. LEVISON, Whatman Paper Ltd., D.W. Toome, S.E. Badger, D. Carcary, E.T. Butts

Thermal Analysis for Process Monitoring

Wednesday Afternoon, Room 1E13
C. Bates, Presiding
Aluminum Company of America

1:30 (1080) **Applications of Simultaneous DSC/FTIR**—D.J. JOHNSON, Bio-Rad, Digilab Division, D.A.C. Compton

1:50 (1081) **TGA/FTIR as a Tool for Measuring Low Levels of Volatiles from Organic Materials**—C.L. GRAY, Oneida Research Services, D.A.C. Compton, D.J. Johnson

2:10 (1082) **The Use of Thermogravimetric Analysis to Understand Results Obtained from Combustion Analysis**—J. DEZWAAN, The Upjohn Company

2:30 (1083) **The Analysis of Smelting Grade Aluminas for Adsorbed and Gibbsitic Moisture by Differential Scanning Calorimetry and Thermogravimetry**—C. BATES, Alcoa Technical Center

2:50 (1084) **Sulfonation of Aniline - Thermodynamic Study Using an Automated Laboratory Reactor/Calorimeter**—R.J. FALK, Contraves Industrial Prod. Div.

3:10 RECESS

3:25 (1085) **Correlation of Dielectric Cure Index to Degree of Cure for Hercules 3501-6 Graphite Epoxy**—D.R. DAY, Micromet Instruments, Inc., D.D. Shepard

3:45 (1086) **A New Phase Transition in Brominated Carbon Fibers**—D.D.L. CHUNG, State University of New York, C.T. Ho

Don't Rely on Gas Cylinders for your Analytical Instrument Gas!

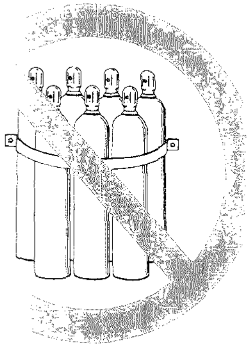

...eliminate the need for expensive, inconvenient gas cylinders of unknown quality, by converting compressed air into gas pure enough for even your most sensitive analytical instrumentation.

Balston Dryer units utilize existing House Air and Clean Air Packages are supplied complete with an air compressor, so whether you've got an existing source of reliable compressed air or not, with Balston Purification Products you never have to worry about running out of gas again.

So whether your requirement is for dry, CO_2-free air for an FT-IR, Zero Air for an FID, clean, dry air for an NMR, or any other gas requirement, Balston Purification Products can provide a safe, reliable, convenient, and economical alternative to high pressure gas cylinders.

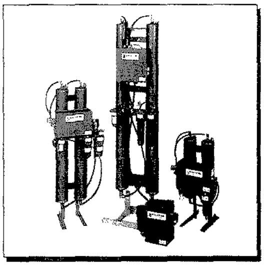

- Less expensive than Nitrogen
- CO_2 removal to 2 ppm
- Pressure dew point below -100°F

CIRCLE 13 ON READER SERVICE CARD

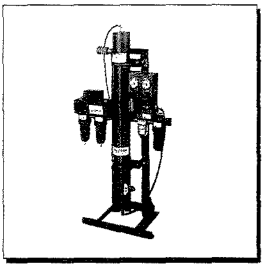

- Eliminate expense and inconvenience of bottled nitrogen
- Nitrogen purity to 99%
- CO_2 levels to less than 10 ppm

CIRCLE 16 ON READER SERVICE CARD

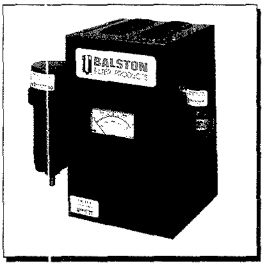

- Use existing Compressed Air
- Total hydrocarbons less than 0.1 ppm
- No particles larger than 0.01 µm

CIRCLE 14 ON READER SERVICE CARD

Call today for complete information and prices -
or use the convenient coupon!

Call Toll-Free
800-343-4048
In Massachusetts, 617-861-7240

FILTER PRODUCTS

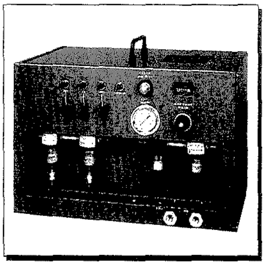

- 99.99% removal of 0.1 µm oil, water, dirt
- Generates 12 SCFM of pure, compressed air
- Pressure dew point below -100°F

CIRCLE 15 ON READER SERVICE CARD

Mail to: Balston, Inc.
P.O. Box C, Lexington, MA 02173

Yes! Please send me data sheets and price lists for the applications checked below:

☐ CO_2-free air for FT-IR purge gas
☐ Zero Grade Air for FID's
☐ Dry air to -100°F for Spectrometers
☐ Nitrogen from compressed air

Name
Title or Department
Company
Address
City
State, Zip
Telephone (include area code)

AD ACHEM 02/90

Super Quiet Deuterium Lamps

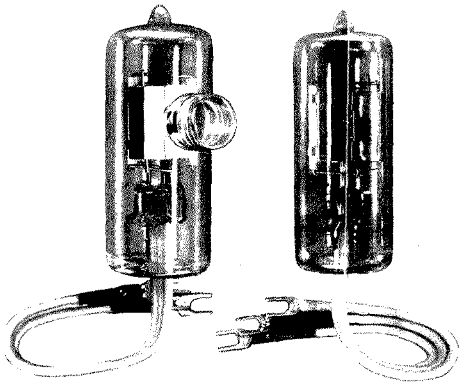

[illegible]

FEATURES

- 3 times longer life .... 1500 hours, minimum
- Extremely low noise .... 0 05%p-p, maximum
- High stability .... ±0.5%/hour, maximum
- Rugged construction

These new Hamamatsu deuterium lamps with indirectly heated cathodes provide three times longer life. Operating time is increased from 500 hours for conventional lamps to over 1500 hours. You get noise-free light of high intensity throughout a year's operation. Saves taking your instrument down three times a year.

An indirect heater coil is placed inside a metal cylinder which supports the cathode. This prevents movement of the cathode, periodic output shifting and flaking off of the oxide coating on the cathode. Eliminates hot spots while increasing lamp life. Noise is reduced to 0.5% p-p, maximum.

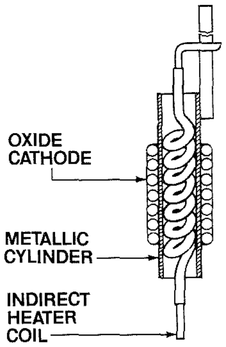

Your choice of silica window or high efficiency UV glass with characteristics similar to conventional deuterium lamps, or synthetic fused silica window for applications requiring high intensity below 200 nm wave length. Operation levels: 7.0V, 1A or 1.7V, 3.3A.

The end-user price is approximately $150 compared with $100 for conventional lamps. With three times longer life, the annual lamp replacement cost is reduced approximately 50%. Instrument down time for lamp replacement is reduced 66-2/3%.

For Application Information
CALL 800-524-0504
In New Jersey Call 201-231-0960

HAMAMATSU CORPORATION • 360 FOOTHILL ROAD, P.O. BOX 6910, BRIDGEWATER, NJ 08807 • PHONE: 201/231-0960

UNITED KINGDOM: Hamamatsu Photonics UK Ltd. (phone: 44 1367 6384) • FRANCE: Hamamatsu Photonics France (phone: [1] 49 75 56 80)
ITALY: Hesa S. P. A. (phone: [02] 34.92.679) • W. GERMANY: Hamamatsu Photonics Deutschland GmbH (phone: 49 8152 3750)
SWEDEN, NORWAY, FINLAND: Hamamatsu Photonics Norden AB (phone: 46 760 32190) • JAPAN: Hamamatsu Photonics K.K. (phone: [0534] 52 2141)

© 1990, Hamamatsu Corporation

See us at the Pittsburgh Conference, New York City, March 5–8th. CIRCLE 75 ON READER SERVICE CARD

RF POWER
As You Like It.

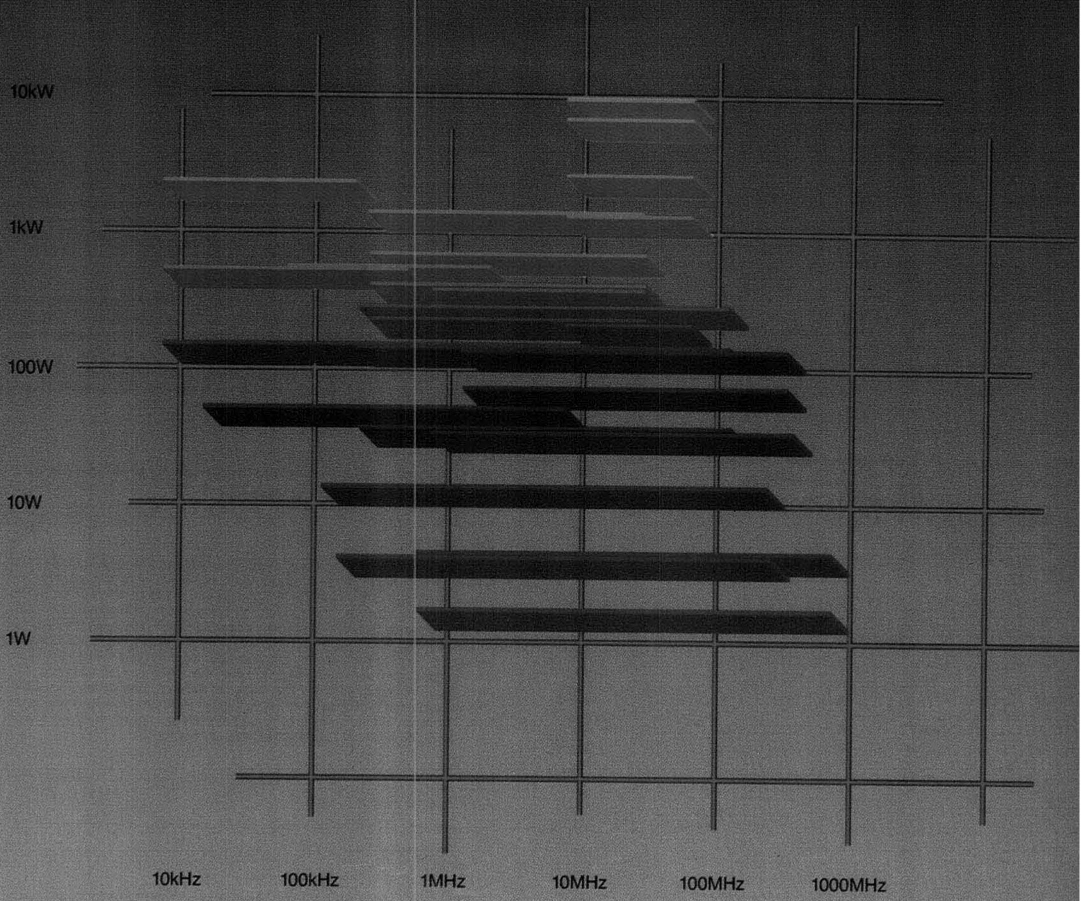

All solid state. Unconditionally stable. Compact. Tremendously versatile. Whatever your need for RF Power, ENI offers you a choice of Class A power amplifiers unsurpassed in quality. Our wide line spans a frequency spectrum from 10kHz to 1GHz with power outputs that range from 300 milliwatts to over 4000 watts.

These units can be driven by virtually any signal source. They're completely broadband and untuned, amplifying inputs of AM, FM, TV, SSB, and pulse modulations with minimum distortion. Their unconditional stability and fail-safe design make them impervious to severe mismatch conditions, and capable of delivering rated power to any load impedance from an open to a closed circuit.

For our latest catalog, please contact us at any of the offices listed below.

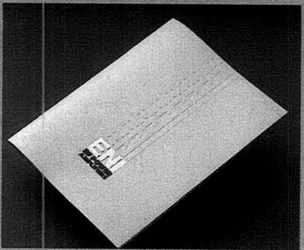

ENI

VISIT US AT PITTCON BOOTH #1754.

U.S. HEADQUARTERS: ENI, 100 Highpower Road, Rochester, NY 14623-3498 USA,
Tel: (716) 427-8300, Tlx: 671 1542 ENI UW, Fax: (716) 427-7839
SANTA CLARA, CA: Tel: (408) 727-0993, Fax: (408) 727-1352
TOKYO, JAPAN: Tel: 0425 229011, Fax: 0425 222636
OSAKA, JAPAN: Tel: 06 367-0823, Fax: 06 367-0827
WELWYN GARDEN CITY, UK: Tel: (0707) 371558, Fax: (0707) 339286
STUTTGART, WEST GERMANY: Tel: 7156-2 10 95, Fax: 7165-4 9372

CIRCLE 48 ON READER SERVICE CARD

4:05 (1087) **Solid State Conversion of the Racemic Mixture of MK571 to the Racemic Compound**—S. GHODBANE, Merck Sharpe & Dohme Res. Labs., J. McCauley

4:25 (1088) **Heat Capacity of Plastic Marble Substitutes**—S.R SAUERBRUNN, E. I. de Pont de Nemours & Co., Inc., P.S. Gill, T.A. Blazer, J.W. Furry

4:45 (1089) **A New Robust and High Performance Ceramic Sensor for Differential Scanning Calorimetry**—T.A. KEHL, Mettler Instrumente AG, L. Meier, G. van der Plaats

Thursday, March 7, 1990

SYMPOSIUM

Bomem-Michelson Award - arranged by D.W. Vidrine of Measurex Corporation

Thursday Morning, Room 1A08
D.W. Vidrine, Presiding
Measurex Corporation

8:30

Presentation of the
1989 Bomem-Michelson Award
by
Dr. Henry Buijs
Bomem Company
to
Professor William Klemperer
Harvard University

8:45 (1090) **Award Address: Models for Interstellar Chemistries**—W. KLEMPERER, Harvard University

9:25 (1091) **Free Radical Catalysis: From Electronic Structure to Stratospheric Ozone Depletion**—J. ANDERSON, Harvard University

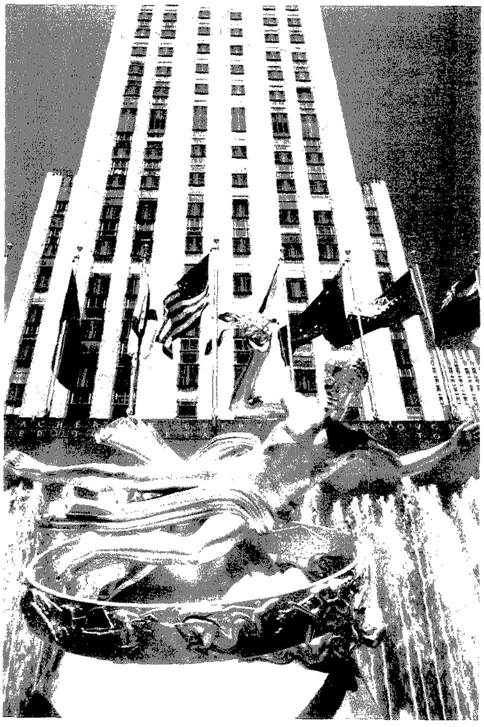

10:05 RECESS

10:20 (1092) **Exotic Molecules in the Interstellar Gas**—P. THADDEUS, Harvard University

11:00 (1093) **Building a Better Universe Through Chemistry: Molecules in Distant Galaxies**—J. BLACK, University of Arizona

SYMPOSIUM

Information Technology: Integrating the Laboratory into the Corporation - arranged by R.R. Mahaffey of Eastman Kodak Company

Thursday Morning, Room 1D01
R.R. Mahaffey, Presiding
Eastman Kodak Company

8:30 **Introductory Remarks**—R.R. MAHAFFEY

8:35 (1094) **Keynote Address: Responsibility for Innovation**—J.J. HALLETT, TRAC, Inc.

9:20 (1095) **An Architecture for a Comprehensive LIMS**—R.D. McDOWALL, Wellcome Research Laboratories, D.C. Matthes

9:50 RECESS

10:10 (1096) **Building a Second General LIMS for Commercial Laboratory Operations**—R. AMANO, Analytical Technologies, Inc., J. Shelton, J.H. Taylor, Jr.

10:40 (1097) **Exploiting the Corporate Database**—G. JONES, Wessex Water Services Ltd.

11:10 (1098) **Development of an Analytical Information Management Strategy for Eastman Kodak Company**—A.P. UTHMAN, Eastman Kodak Company

SYMPOSIUM

Women in Science: A Blueprint for Progress - organized by Robin L. Garrell of University of Pittsburgh

Thursday Morning, Room 1A06

This symposium will focus on identifying key factors in our educational system and our society that constrain the progress of women in science. The goal is to establish a blueprint for eliminating barriers to women's participation and progress in science-related fields, by creating educational and corporate environments that foster their success. Locally and federally supported educational programs, and changing corporate hiring and employment practices are among the specific mechanisms for progress that will be discussed. Speakers will include Professor Allen Wigfield from the University of Maryland, Dr. Margaret A. Cavanaugh from the National Science Foundation, Ms. Jolie Solomon from the Wall Street Journal, and a representative from the President's Task Force on Women, Minorities, and the Handicapped in Science and Technology, whose final report will be issued in early 1990.

Analysis of Fuels

Thursday Morning, Room 1E18
E. Ladner, Presiding
U.S. Dept. of Energy, PETC

8:30 (1104) **Pyrolysis GC/MS and Pyrolysis GC/FTIR/FID Studies of a Series of Eocene-Age, Indonesia Coals**—W.M. ZUNIC, University of South Carolina, G.C. Calvert, J.R. Durig, T.A. Moore

8:50 (1105) **Studies of Peats as Adsorbents for Hydrocarbons in Waste Water Runoff**—M.S. ROLLINS, University of South Carolina, W.M. Zunic, G.D. Calvert, J.R. Durig, A.D. Cohen

9:10 (1106) **A Comparison Study of Methods for the Hydroxyl Content of Coal**—A. WELLS, U.S. Department of Energy, R. Frank, E. Frommell

9:30 (1107) **The Determination of Oxygenated Species in Coal Derived Liquid Fuels by GC-OFID**—R.B. HOWARD, Wright Research & Develop. Center, E.M. Steward, S.D Anderson, J.L. Moler

9:50 (1108) **The Determination of Nitrogen-Containing Compounds in Shale and Coal Derived Liquid Fuels by GC-CLD**—J.L. MOLER, Wright Research & Develop. Center, E.M. Steward, S.D. Anderson, R.B. Howard

10:10 RECESS

10:25 (1109) **Group Type Separation of Crude Oils, High Boiling and Low Boiling Petroleum Products with High Performance HPLC**—S.V. ROSE, Chrompack Inc., J.P. Crombeen

10:45 (1110) **Adsorptive Effects in Trace Analysis of Explosives by Capillary GC, ECD**—G.A. REINER, VA Polytechnic Inst. & State Univ., H.M. McNair

11:05 (1111) **A Gas Chromatograph Based Explosive Vapor Generator for Use in the Evaluation of Portable Explosive Vapor Detection Systems**—G.A. REINER, VA Polytechnic Inst. & State Univ., C.L. Heisey, H.M. McNair

11:25 (1112) **FTIR Study of Surface Activity of Catalysts in Diffuse Reflectance (DRIFT) Reactor**—C.V. PHILIP, Texas A&M University, R.G. Anthony

See us at PITTCON '9[illegible]
Booths 1041 thru 1044

ANALYTICAL EXCELLENCE

XR400

EDXRF SPECTROMETER

ANALYTICAL EXCELLENCE

- Are you concerned with chemical analysis in a quality control environment?
- Is accurate, precise quantitative elemental analysis your problem?
- Have you considered the EDXRF solution?
- EDXRF delivers rapid analysis for all elements from Na to U.
- EDXRF handles solid, powder and liquid samples with equal ease.
- For many types of analysis a single calibration standard is more than adequate.
- The simplicity of the ED X-ray spectrum ensures that an unambiguous QUALITATIVE analysis is available for every specimen.
- To find out more, write today for a full color brochure and detailed application notes.

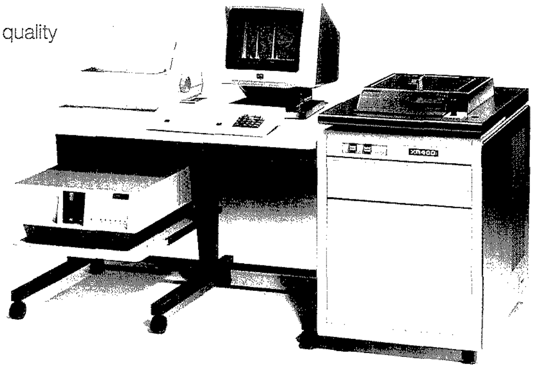

CIRCLE 96 ON READER SERVICE CARD

1985 1986 1987

Link
ANALYTICAL

Link Analytical Limited,
Halifax Road, High Wycombe
Bucks HP12 3SE,
England
Tel: 0494 442255
Telex: 837542LINK HWG
Fax: 0494 [illegible]4129

Link Analytical (France) S.A.R.L.
9 Rue Fernand Leger,
Centre Val Courcelle,
91190 Gif Sur Yvette, France
Tel: (1) 6907 7802
Telex: 603849S · LINK
Fax: (1) 6907 4469

Link Analytical Inc,
240 Twin Dolphin Drive,
Suite D,
Redwood City,
California 94065 USA
Tel: (415) 595-5465
Fax: (415) 595 5589

Link Nordiska AB
Kyrkvägen 4, Box 1153,
S-181, Lindingö,
Sweden.
Tel: 08-767 9170
Telex: 12645 SPECTAB
Fax: 08-767 5776

Link Analytical, (Aus) Pty. Ltd.
P.O. Box 7,
Pennant Hills,
N.S.W. 2120,
Sydney, Australia.
Tel: 2-8753130
Fax: 02-4841667

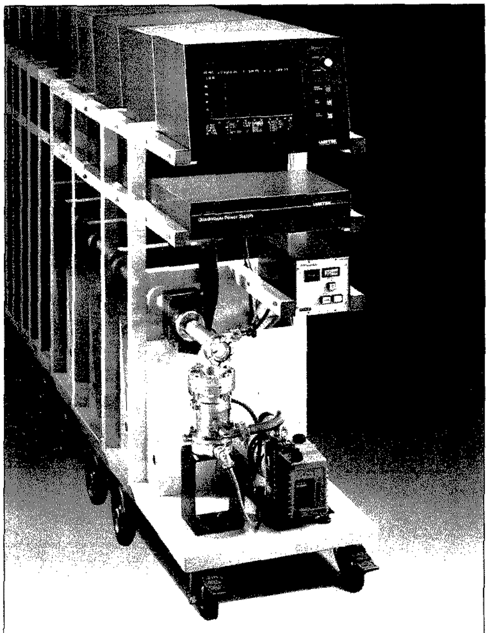

Now quadrupole gas analysis, to go! Now, in addition to high performance rack-mount and bench models, Ametek can also offer you a mobile Dycor™ Quadrupole Gas Analyzer.

A perfect, go-anywhere, microprocessor-based mass spectrometer that can handle all your gas analysis, process monitoring, or leak detection applications.

And tell you in a glance at the high resolution display—exactly what's in your sample, off-gas, or vacuum system.

Standard Features

☐ 1-100 AMU Mass Range ☐ Faraday Cup Detector ☐ 100% Front Panel Control ☐ High-Resolution CRT Display ☐ Graph or Tabular Data Display ☐ RS232 Computer Interface ☐ 5 x 10^{-12} Torr Minimum Detectable Partial Pressure ☐ Background Subtraction

Optional Features

☐ 1-200 AMU Mass Range ☐ Pressure vs Time Display ☐ Graphics Printer For Hard Copy ☐ Electron Multiplier ☐ 5 x 10^{-14} Torr Minimum Detectable Partial Pressure ☐ Sample System For Higher Pressures

For literature, contact AMETEK, Thermox Instruments Division, 150 Freeport Road, Pittsburgh, PA 15238. Tel: (412) 828-9040.

AMETEK
THERMOX INSTRUMENTS DIVISION

See us at Booth #4907. CIRCLE 5 ON READER SERVICE CARD

11:45 (1113) **Field Testing and Quality Evaluation of Aviation Fuels by Near Infrared Spectroscopy and Multivariate Statistics**—M.J. LYSAGHT, Univ. of Washington, J. I. Kelly, J.B. Callis

---

Capillary Electrophoresis

Thursday Morning, Room 1E21
A.G. Ewing, Presiding
Penn State University

8:30 (1114) **Structural Analysis of RNase T1 Native and Site-Directed Mutants by Capillary Electrophoresis**—J.E. WIKTOROWICZ, Applied Biosystems Inc., J.C. Colburn

8:50 (1115) **Free Solution Separation of Double and Single Stranded Nucleic Acids Using Counter-Migration Capillary Electrophoresis**—A.M. CHIN, Applied Biosystems Inc., J.C. Colburn

9:10 (1116) **Applications of Fluorescence Detection in Capillary Electrophoresis of Biological Molecules**—S. MORING, Applied Biosystems, R. Weinberger, J.E. Wiktorowicz, E. Sapp

9:30 (1117) **High Sensitivity Absorbance and Fluorescence Detectors for Capillary Electrophoresis**—E. SAPP, Applied Biosystems, R. Weinberger, S. Moring

9:50 (1118) **An Evaluation of Several Sodium Alkyl Sulfates as Micellar Phases for MECC**—H.T. RASMUSSEN, VA Polytechnic Inst. & State Univ., H.M. McNair

10:10 RECESS

10:25 (1119) **An Extended Model for the Retention of Ionic Solutes in Micellar Electrokinetic Capillary Chromatography**—M.G. KHALEDI, North Carolina State University, J.K. Strasters

10:45 (1120) **Instrumental Methods of Electroosmotic Flow Control in Capillary Zone Electrophoresis**—S.C. SMITH, North Carolina State University, M.G. Khaledi

11:05 (1121) **Influence of Peptide Structure and Buffer Composition on Peptide Mobility in Capillary Electrophoresis**—R. PALMIERI, Beckman Instruments, T. Akiyama, L. Holladay, K. Ulfelder

11:25 (1122) **Fluorescence Detection in Capillary Electrophoresis**—L.A. SAARI, SpectroVision, Inc., A.M. DeFeo, T.J. Cetto

11:45 (1123) **Monitoring Tryptic Maps and Preparative Separations with Capillary Electrophoresis**—E. GASSMANN, Ciba-Geigy Ltd., A. Paulus, M. Faupel

---

Characterization of Polymers and Coatings Using Thermal Analysis

Thursday Morning, Room 1E19
G. Armstrong, Presiding
Aluminum Company of America

8:30 (1125) **Characterization of Thin Films and Coatings by DMA**—W.J. SICHINA, DuPont Instruments, P.S. Gill

8:50 (1126) **Use of a Multimode DMA to Investigate the Glass Transition Phenomenon**—R.B. CASSEL, The Perkin-Elmer Corporation

9:10 (1127) **Stress Relaxation of Polymer Coated Metals**—J.C. TEROSKY, III, E. I. du Pont de Nemours & Co., Inc., W.J. Sichina

9:30 (1128) **Torsional Braid Analysis (TBA): A Technique for Characterizing the Cure and Properties of Thermosetting Systems**—J.K. GILLHAM, Princeton University, J.B. Enns

9:50 (1129) **Dielectric Analysis of Thermoplastics and Thermosets**—W.J. SICHINA, DuPont Instruments, C.L. Jaworski, P.S. Gill,

10:10 RECESS

10:25 (1130) **Characterization of Polymers by Thermal Stimulated Current and Relaxation Map Analysis Spectroscopy**—J.P. IBAR, Solomat Instrumentation, P. Denning, T.R. Thomas, A. Bernes, C. de Goys, J.R. Saffell, P. Jones, C. Lacabanne

10:45 (1131) **Dielectric Analysis of Polymeric Materials**—C.L. MARCOZZI, E. I. du Pont de Nemours & Co., Inc., W.J. Sichina, P.S. Gill

11:05 (1132) **Thermal and Mass Spectrometric Analyses of Polycarboxylic Acids Used as Durable Press Reactants for Cotton: Catalyst Effects**—B.J. TRASK-MORRELL, USDA, ARS, SR Research Center, B.A. Kottes Andrews

11:25 (1133) **Glass Transitions of High Impact Plastic**—S.R. SAUERBRUNN, E. I. du Pont de Nemours & Co. Inc., L.C. Thomas, T.A. Blazer

11:45 (1134) **Physical Ageing in Polymers Compared by DSC, DMTA, DETA, and TSD Measurements**—R.E. WETTON, Polymer Laboratories Ltd., R.D.L. Marsh, G.M. Foster, D. Loeb, P. Newbatt

Introducing

BAIRD ENVIRONALYSIS+

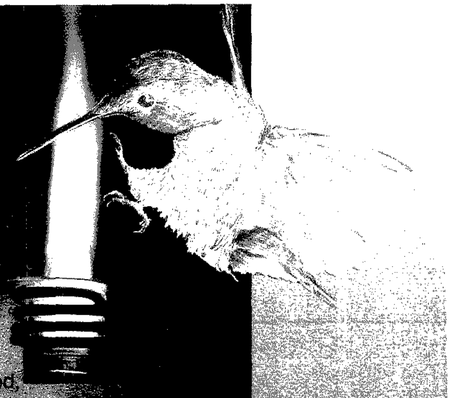

Speed and Precision for the Analytical Laboratory

For the chemist concerned with environmental analysis of water and waste, Baird has designed Environalysis+, the most carefully coordinated, modular ICP laboratory system available — the instruments and software you need to make the fastest, most delicate determinations possible (and make government requirements routine).

Meet or exceed EPA and CLP detection sensitivities.

The new 60-channel BAIRD ICP-2000 is assured to determine the 25 EPA-approved elements in ppb quantities better than those listed in *Method 200.7* for water and wastes analysis. In tandem with the BAIRD UDX Ultrasonic Nebulizer, it also meets the CLP sensitivity requirements for As, Se, Pb, and Tl — comprehensively and *simultaneously* accommodating every CLP analyte except Hg. Could this mean the end of expensive, one-sample-at-a-time graphite furnace AA? Yes.

Automate multielement determinations and save on per-sample cost.

The BAIRD ICP-2000 works with a variety of random-access autosamplers having a wide range of sample/size capacities. Q.C. check and recheck can be at any preselected intervals, and, in the event of a Q.C. [illegible] the choice of action, including repeat analysis, is inherent in the program's software. Standardization and restandardization are routine. This tightly controlled automation is in complete compliance with all government requirements, including the CLP protocol for quality assurance and control.

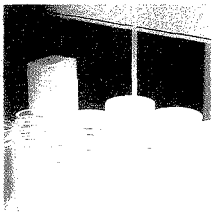

Produce reports as quickly and easily as your analyses.

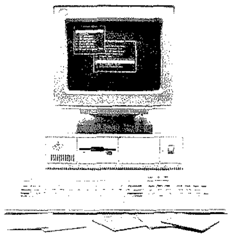

BAIRD Plasmacomp® software is fully compatible with a variety of packages that routinely generate reports required by the CLP on CLP-specified forms, as well as the computer-deliverables described by *Statement of Work 788.* And Plasmacomp's many diverse options are easily customized to meet all the needs of any ICP analytical laboratory.

Write or call today for complete information on Environalysis+.
Baird Corporation, Analytical Instruments Division,
125 Middlesex Turnpike, Bedford, MA 01730.
Telephone (617) 276-6163.

See BAIRD Environalysis+ in action at the 1990 Pittsburgh Conference, Booth 4331.

IMO

BAIRD ICP

CIRCLE 22 ON READER SERVICE CARD

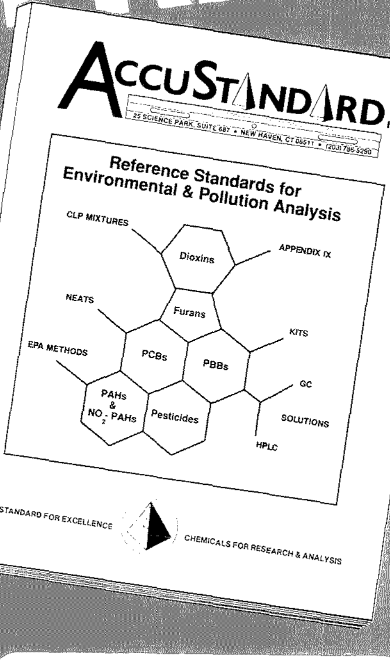
AccuStandard INC.
25 SCIENCE PARK, SUITE 687 • NEW HAVEN, CT 06511 • (203) 786-5290
Reference Standards for Environmental & Pollution Analysis
CLP MIXTURES
APPENDIX IX
NEATS
KITS
EPA METHODS
GC
SOLUTIONS
HPLC
Dioxins
Furans
PCBs
PBBs
PAHs & NO_2-PAHs
Pesticides
THE STANDARD FOR EXCELLENCE
CHEMICALS FOR RESEARCH & ANALYSIS

NEW! FREE!

Write/phone/fax today for your Free copy of this comprehensive guide of Reference Standards for Environmental and Pollution Analysis!

- CLP mixtures
- Appendix 9 solutions
- EPA methods
- Over 500 Carcinogens, Mutagens, Teratogens, etc.
- Plus, much more!

Order your Free copy today.
Ask about AccuStandard's 24-hour shipment from stock.

AccuStandard, Inc.
25 Science Park, Suite 687, New Haven, CT 06511.
Telephone: (203) 786-5290.
Telex: 643-998. FAX: (203) 786-5449.

CIRCLE 1 ON READER SERVICE CARD

Electrochemistry: Voltammetry

Thursday Morning, Room 1E10
J.F. Rusling, Presiding
University of Connecticut

8:30 (1135) **In Situ Laser Activation of Carbon Ultramicroelectrodes**—T.G. STREIN, Penn State University, A.G. Ewing

8:50 (1136) **Effect of pH and Electrochemical Treatment on the Voltammetry of Catechols at Carbon Ring Electrodes**—H.A. FISHMAN, Penn State University, A.G. Ewing

9:10 (1137) **Electroanalytical Studies of Sodium Chloride as a Lewis Buffer for Room Temperature Chloroaluminate Molten Salts**—J.T. MALOY, Seton Hall University, T.J. Melton, J. Joyce, J.A. Boon, J.S. Wilkes

9:30 (1138) **Pulse Techniques for the Determination of Midazolam**—A.J. RIBES, State Univ. of NY at Buffalo, J.G. Osteryoung

9:50 (1139) **Host-Guest Interactions of α -Cyclodextrin with *p*-Nitrophenol Studied with Pulse Voltammetry**—M.J. NUWER, State Univ. of NY at Buffalo, J.G. Osteryoung, O. Perez de Marquez

10:10 RECESS

10:25 (1140) **Determination of Lead, Stannous, and Stannic Ions in Zinc-Iron Plating Solution by On-Line Voltammetry**—H. KURAYASU, Sumitomo Metal Industries, Ltd., Y. Inokuma

10:45 (1141) **Microwave Digestion of High Organic Matter Content Drinking Water to Permit the Electrochemical Determination of Aluminum**—A.J. MORONTA, Universidad del Zulia, J.E. Tahan, R.A. Romero

11:05 (1142) **Determination of Antimony in Arsenous Oxide by Polarographic Adsorptive Complex Wave of Antimony(III)-Morin**—N. LI, Peking University, Y. Xu

11:25 (1143) **A Study on the Electrochemical Behavior and the Electrode Reaction Mechanism of Cadmium(II)-KI-Ethyl Violet System**—Y. ZHANG, Central Iron & Steel Res. Inst., M. Yan

11:45 (1144) **Polarographic Behavior of the Nitrophenol Compounds - Application of PPP-SCF-MO in Analytical Chemistry**—X. WANG, Zhejiang Educational College, S. Ye

Environmental Water Analysis II

Thursday Morning, Room 1E15
W.R. Sharpe, Presiding
Clarion State University

8:30 (1145) **Automated Determination of Free & Total Cyanide in Wastewater Using Photodissociation and Gas Dialysis Followed by Ion Chromatographic Determination**—R.J. JOYCE, Dionex Corporation, Y. Liu

8:50 (1146) **Application of an Automated Random Access Analyzer in a Reservoir Eutrophication Study**—J.J. NOTTE, North Jersey District Water Supply Commission

9:10 (1147) **A New Sample Injection Technique for Total Organic Carbon (TOC) Analyzer**—N. TON, Rosemount Analytical, Y. Takahashi, K. Lines

9:30 (1148) **Application of Microextraction and GC/MS to Determination of Organics in Environmental Water Samples**—A. GOLDBERG, USEPA, J.M. Soroka, D. Lillian

9:50 (1149) **New, High Speed, Automatic Evaporation Workstation**—J.P. HELFRICH Zymark Corporation, B. Johnson, D. Friswell

10:10 RECESS

10:25 (1150) **Solid Phase Extraction Procedure for Base/Neutral and Acid Extractables in EPA Method 625**—D. ROOD, J&W Scientific, J. Knitter

10:45 (1151) **Microscale Solid Phase Extraction Method Using Fused Silica Optical Fibers**—J.B. PAWLISZYN, University of Waterloo, R. Belardi, A. Egerhazi

11:05 (1152) **Determination of Low Level Organic Carbon (<100 ppb) in Ultra-Pure Waters**—B. DULANEY-TRAVIS, Shimadzu Scientific Instr., Inc., Y. Morita, A. Seidoh, S. Sumi, H. Matsuhisa

11:25 (1153) **Ammonium Vanadate Titration of Trace Uranium in Natural Water by Using a New Ultrasensitive Vanadate Indicator**—Y. LI, Y. Tang

11:45 (1154) **Characterization of Inorganic Pollutants in Water of River Betwa at Mandideep, Madhya Pradesh**—P.K. SHRIVASTAVA, Pollution Control Board, A. Desmukh

Gas Chromatography—Instrumentation I

Thursday Morning, Room 1A07
M. Margosis, Presiding
US Food and Drug Administration

8:30 (1155) **Unique, Fully Automatic Instrumentation for On-Line Coupled LC/Capillary GC**—A.D. BASHALL, Carlo Erba Instruments/Fisons, F. Munari

Can You Measure Leadership With A Spectrometer?

No. But You Can Measure It In Spectroscopy.

A decade of leadership continues into the 1990's. From our inception as Analect in 1980 to our current presence as Laser Precision Analytical, we're maintaining our position of innovation and reliability.

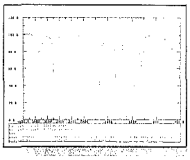

Spectra of cocaine base for forensic applications.

Calling ourselves the leader is easy. But actually being one requires something more. Like putting all the most sought after features of FT-IR into our instrumentation. And delivering repeatable results. Year after year.

Measure our claim for yourself. Just look at the extensive list of innovations and capabilities we've built into our instruments.

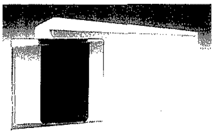

The unique and patented TRANSEPT® wedges.

The patented TRANSEPT® interferometer is an excellent example. It withstands unavoidable vibrations, shocks and temperature swings to continually provide accurate, repeatable results. And combining this durability with a permanently aligned optical system that uses corner cube reflectors creates drift-free performance in both resolution and signal to noise.

Noise? No problem. You can't get much more noise and vibration than in the process environment. And we're there everyday providing reliable on-line composition data and a rapid payback on the equipment.

Since flexibility is also a sought after quality in FT-IR, we use a modular design to build instruments perfectly suited for your specific applications (and we're the only company that does). But let's say your applications change. What then?

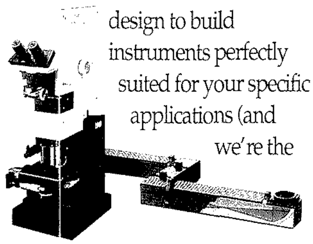

Our patented OPTIBUS® allows the FT-IR and the MICRO-XAD^{PLUS} to adapt to your work environment.

Don't worry. The same modular design that created the right instrument for you in the first place also allows us to modify or upgrade your unit when a new configuration is needed.

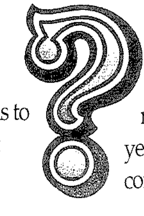

How can we help with your application?

And our patented OPTIBUS® optical conduit keeps the instrument just as flexible on the bench. Instead of adapting your work to your FT-IR, put our FT-IR wherever it's most convenient.

At Laser Precision Analytical, we also build our reputation into a full line of peripherals and accessories. GC/FT-IR. TGA/FT-IR. TLC/FT-IR. You can count on sample compartment accessories such as ATR, DRIFTS, and gas cells that incorporate the same high quality optics and precision tolerances as our spectrometers. We've got **the** microscope built for FT-IR.

Once you've developed your applications, a powerful and complete software library is there to automate routine functions. From simple single keystrokes to sophisticated command line operation, our full-featured basic package, expansion programs, and extensive spectral libraries are there to make sure your data can be fully utilized.

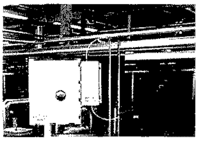

You can count on our instruments no matter how noisy the environment.

Call us. We'll listen to your current application requirements and put our ten years of FT-IR experience at your command. We've seen virtually every application you can imagine. And chances are we have a solution for you.

(800) 326-2328

LASER PRECISION ANALYTICAL

17819 Gillette Ave.
Irvine, CA 92714

CIRCLE 100 ON READER SERVICE CARD

Electrochemistry
and Biochemistry:
A Growing
Relationship

Although biochemists have long appreciated the value of electrochemical techniques, at EG&G Princeton Applied Research, we're taking the relationship to its next level.

With our Model 273 potentiostat, you can now investigate biochemical systems using microelectrodes at low current levels *or* at high scan rates!

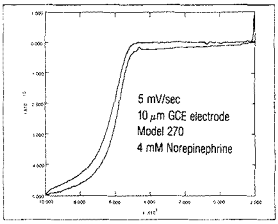

Using our Model 270 software, you can measure currents at 8 picoamps—or lower! And there's no need for extra hardware—our software takes the superb technical specifications of the Model 273 to their limits and beyond.

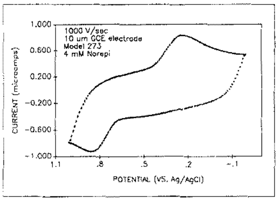

Are you studying kinetics? The Model 273 has the analog specifications to let you run at scan rates of up to 10,000 volts per second!

Electrochemistry and biochemistry. Through our applications research and technical support, we're dedicated to making this relationship grow. For more information call us at **1-800-274-PARC.**

EG&G PARC

P.O. BOX 2565 • PRINCETON, NJ 08543-2565
(609) 530-1000 • TELEX: 843409 • FAX: (609) 883-7259

Circle 57 for literature. Circle 58 for Sales Rep.

The National Institute of Standards and Technology has developed a series of SRM's to serve as calibrants, test mixtures, and standardization materials for Quality Control of analytical instrumentation and methodology.

MEASUREMENTS and STANDARDS are important to everyone who needs quality. NIST has over 1,000 Standard Reference Materials that can help you calibrate instruments and check on measurement accuracy. For more information phone or write for a free catalog.

Telephone (301) 975-OSRM (6776)
FAX (301) 948-3730

STANDARD REFERENCE MATERIAL PROGRAM

Building 202, Room 204
National Institute of Standards
and Technology
Gaithersburg, MD. 20899

CIRCLE 123 ON READER SERVICE CARD

HELLMA®

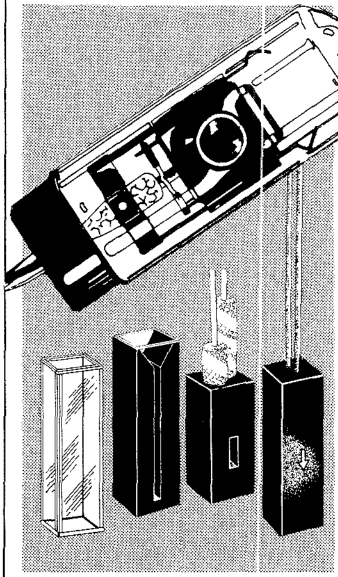

Your one stop for Cells and D_2 Lamps.

A full line of quality cells:
- Stock and custom
- Dye laser

Plane Optics
UV light sources for all major instruments:
- D_2 and Hg.

CUV-O-STIR
- Mini-magnet cuvette stirrer
- Variable speed
- Multiple cell capability.

HELLMA® Box 544, Borough Hall Station, Jamaica, NY 11424
(718) 544-9534 or (718) 544-9166.

See us at PittCon Booth #3153–3155. CIRCLE 71 ON READER SERVICE CARD

CETAC U-5000 ULTRASONIC NEBULIZER

For Superior Limits of Detection

Several years ago, CETAC TECHNOLOGIES began research on an ultrasonic nebulizer that would provide today's chemist with a faster, more sensitive, stable, and reliable method of obtaining vastly improved detection limits. They succeeded.

SUPERIOR ANALYTICAL PERFORMANCE When used in conjunction with an ICP, the CETAC ULTRASONIC NEBULIZER will allow the analyst to achieve significant improvement in detection limits.

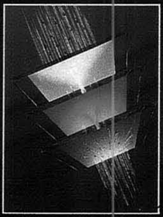

HOW THE U-5000 WORKS A peristaltic pump delivers the sample to the transducer face which is vibrating at 1.40 MHz. Instantly, the sample is nebulized into an extremely fine aerosol mist and swept away by the argon carrier gas. The dense aerosol mist then enters a "U" shaped tube which is heated to a temperature determined to best aid the desolvation process. The water component is then "stripped" away through condensation, thus resulting in a dry aerosol dense in analyte being introduced into the plasma.

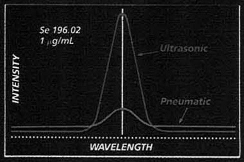

STABLE, RELIABLE PERFORMANCE Superior reliability and precision resulting from an air-cooled transducer and thermostatically controlled desolvation.

SAMPLE HANDLING FLEXIBILITY Whether your analysis needs call for the analysis of selenium in dolphin livers or arsenic in water, the U-5000 can do the job.

IMPORTANT FACTS ON THE MOST IMPORTANT INSTRUMENT IN YOUR LAB

- Installation can be performed in as little as fifteen minutes.
- Perfect for food, environmental, clinical, pharmaceutical analyses.
- Extremely cost effective.
- Total size of just 11¼" high X 17" wide X 13" deep.
- Total weight of just 35 pounds.

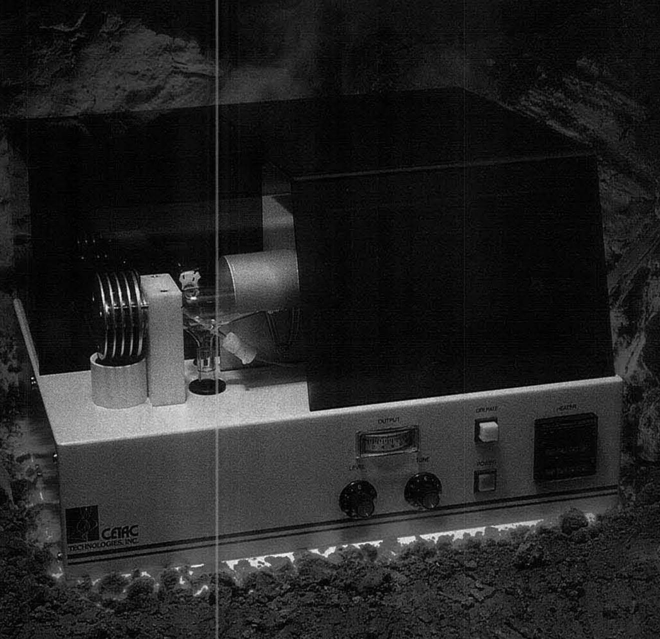

CETAC
TECHNOLOGIES, INC.
Expanding The Scope Of Measurement.

P.O. Box 31118
302 South 36th Street
Omaha, NE USA 68131
(402) 346-4345
FAX: (402) 346-9256

CIRCLE 36 ON READER SERVICE CARD

8:50 (1156) **Automatic Sampling System for High Temperature Capillary GC Ensuring Discrimination Free Injections Over the Full Boiling Point Range (0 to +800° C)**—A.D. BASHALL, Carlo Erba Instruments/Fisons, F. Munari, S.Trestianu

9:10 (1157) **A Septumless Gas Chromatography Injector Assembly**—G. MOLLER, University of California, M.L. Tracy

9:30 (1158) **A New Helium Ionization Detector Application for Gaseous Electronics Chemicals**—S.D. STEARNS, Valco Instrument Co. Inc., C.J. Meyer

9:50 (1159) **A New Combination PID/FID for Gas Chromatography**—K. DAVIS, O. I. Analytical

10:10 RECESS

10:25 (1160) **SCP Emission Detector - A Powerful Detector System for Gas Chromatography**—B. PLATZER, Graz University of Technology, A. Grillo, M. Michaelis, E. Leitner, R. Gross, G. Knapp, A. Schalk, H. Sinabell

10:45 (1161) **Flame Infrared Emission (FIRE): A Versatile, New, Element-Specific Detector for Gas Chromatography**—M.A. BUSCH, Baylor University, S. Ravishankar, D.C. Tilotta, K.W. Busch

11:05 (1162) **Improvements in a Flame Photometric Detector for Determination of Sulfur and Phosphorous Compounds**—A.W. BERGER, HNU Systems Inc., J.N. Driscoll

11:25 (1163) **New Sulfur-Selective Detector for Gas and Supercritical Fluid Chromatography: Principles of Operation and Applications**—R.S. HUTTE, Sievers Research, Inc., N.G. Johansen, M.F. Legier

11:45 (1164) **A New Approach to Flame Ionization Detection Using Water as the Source of Hydrogen**—A. LINENBERG, Sentex Sensing Technology, Inc., R.K. Davis

HPLC—Environmental and Solubility

Thursday Morning, Room 1E16
S.S. Oliverio, Presiding

8:30 (1165) **Separation of Chlorhexidine Breakdown Products Including 4-Chloroaniline in Surgical Scrubs Containing Chlorhexidine**—J.F. MOELLMER, Deseret Medical, Inc., M. Hoang, M.A. Khan

8:50 (1166) **Determination of Nicotine and Cotinine in Saliva Samples Using HPLC**—S. BRENDECKE, Los Alamos National Laboratory, D. Gilbert

9:10 (1167) **A New Approach for Effective Sampling and Simultaneous Derivatization of Airborne Aliphatic Amines**—K. JEDRZEJCZAK, Ontario Ministry of Labour, V.S. Gaind

9:30 (1168) **Determination of Arsenate in Wastewater and Environmental Samples by On-Line Ion Chromatography**—D. CAMPBELL, Dionex Corporation, S. Stone, S. Carson

9:50 (1169) **Improved Determination of Alkanolamines in Surface Finishing, Chemical and Environmental Samples by Ion Chromatography**—D. CAMPBELL, Dionex Corporation, S. Heberling, S. Carson

10:10 RECESS

10:25 (1170) **Pesticides in Drinking Water - Fulfilling Legal Requirements for LC Methodology Using Diode Array Detection**—E.M. KEIL, Bodenseewerk Perkin-Elmer GmbH, G. Kurz, M. Steinwand

10:45 (1171) **Identification and Determination of Pesticides in the Part Per Trillion Range Using Diode-Array Detection and Microbore HPLC**—R. SCHUSTER, Hewlett-Packard GmbH, L. Huber

11:05 (1172) **Structure-Activity-Retention Relationship Studies Using Micellar Liquid Chromatography**—E.D. BREYER, North Carolina State University, J.K. Strasters, M.G. Khaledi

11:25 (1173) **Application of Micellar Liquid Chromatography to the Problem of Measuring the Hydrophobicity of Organic Compounds**—J.H. HAN, Clarkson University, B.K. Lavine, A.J.I. Ward

11:45 (1174) **Development and Evaluation of a Rapid Microscale Method for the Determination of Partition Coefficients by HPLC**—H. FORD, JR., National Cancer Institute, NIH, C.L. Merski, J.A. Kelley

HPLC—Multiwavelength Detectors

Thursday Morning, Room 1E06
S. Tomellini, Presiding
University of New Hampshire

8:30 (1175) **Effects of Noise and Drift on Spectral Peak Purity Analysis in UV-VIS LC Detection**—A.D. LONG, Spectra-Physics, Inc., L. Hellinger, V. Nau

8:50 (1176) **Applications for a Multi-Dimensional, Low Inertia Scanning UV-Vis Detector for Liquid Chromatography**—L. HELLINGER, Spectra-Physics, Inc. V. Nu, S. Weinberger

9:10 (1177) **Confirmation of Peak Identity of Routine Liquid Chromatographic Analysis**—A.F. POILE, The Perkin-Elmer Corporation, A. Cole, N.B. Hetherington, M. Upton

9:30 (1178) **Spectral Matching: A Critical Analysis of the Capabilities and Limitations of Diode Array Detection in HPLC**—H.J.P. SIEVERT, Hewlett-Packard Company

9:50 (1179) **Reliable, Real Time Detectors in Coelution in HPLC**—B. ARCHER, Beckman Instruments, Inc., T. Hill, L.S. Ramos

10:10 RECESS

10:25 (1180) **Peak Purity Assessment Using LC Diode Array Detection**—G.J. SCHMIDT, The Perkin-Elmer Corporation, E.M. Keil, M. Steinwand

10:45 (1181) **The Application of an FID/Transport Detector for HPLC**—B.E. TURNER, Applied Chromatography Systems, Ltd.

11:05 (1182) **A Critical Comparison of Chromatographic Plotting and Integration Methods for Photodiode Array Detector Data and High Performance Liquid Chromatography**—M.E. ADASKAVEG, Varian Instrument Group, T.L. Sheehan, L. Giradina, J.J. Robinson, F. Lai

11:25 (1183) **A Novel Optical Design for a New Diode Array HPLC Detector**—M.N. MUNK, LDC Analytical, Inc.

11:45 (1184) **Multi-Method Compatible Full Spectral Scanning UV-Visible Detector**—J.G. WANGSGAARD, Linear Instruments Corporation, D.J. Bornhop, L. Hlousek

Mass Spectrometry Ion Sources

Thursday Morning, Room 1E13
J.T. Watson, Presiding
Michigan State University

8:30 (1185) **High Mass Range Operation of Ion Trap Mass Spectrometers**—J.E.P. SYKA, Finnigan MAT, R. Kaiser, J.N. Louris, G.C. Stafford, Jr., R.G. Cooks, P. Hemberger

8:50 (1186) **Recent Advances in Ion Trap Technology**—J.N. LOURIS, Finnigan MAT, R. Kaiser, S. Kirkish, G.C. Stafford, Jr., J.E.P. Syka, D. Tucker, M. Weber-Grabau

9:10 (1187) **New Thermospray Ion Source for Enhanced Performance and Convenience**—S. HANSEN, Hewlett-Packard Company, P.C. Goodley, K. Imatani

9:30 (1188) **Real-Time Control of Sample Voltage in Plasma Bombardment Sputtered Neutrals Mass Spectrometry for High Resolution Depth Profiling**—B.J. HALL, Charles Evans and Associates, J.C. Huneke, H.E. Buriecci

9:50 (1189) **Mass Spectrometry in Supersonic Molecular Beams**—A. AMIRAV, Tel-Aviv University, A. Danon

10:10 RECESS

10:25 (1190) **Atmospheric Pressure Ionization for SFE/SFC/MS Identification of Anabolic and Estrogenic Drugs**—J. HENION, Cornell University, R. Huopalahti, E. Huang, J.J. Conboy

10:45 (1191) **One Ion Source—Many Solutions: The Atmospheric Pressure Ion Source for High Performance Liquid Chromatography Supercritical Fluid Chromatography, and Capillary Zone Electrophoresis Mass Spectrometry with Practical Applications in Drug Metabolism, Protein Sequencing, Biotechnology Quality Control, and Industrial Polymer Analysis**—T. COVEY, Sciex

11:05 (1192) **Detection of Small Biological Molecules Using VUV Ionization and an Atmospheric Pressure Glow Discharge in Atmospheric Pressure Ionization Mass Spectrometry**—D.M. LUBMAN, University of Michigan, I. Sofer

11:25 (1193) **Atmospheric Pressure Ionization of Perfluorocarbons, Freons, and Chlorofluorocarbons by Ion Mobility Spectrometry and IMS/MS**—G.A. EICEMAN, New Mexico State University, R.M. Randall, L. Garcia, A.P. Snyder, D.A. Blyth, D.B. Sholf, C.S. Harden

11:45 (1194) **Instrumental Effects on Bacterial Taxonomy by Pyrolysis-Mass Spectrometry**—P.de B. HARRINGTON, Ohio University, S.J. DeLuca, E.W. Sarver, K.J. Voorhees

New Spectrometer Designs

Thursday Morning, Room 1E12
A.S. Manocha, Presiding
PPG Glass R&D

8:30 (1195) **Optimizing Data Acquisition for Quantitation with a Solid State Spectrometer Operating in the Near-IR**—D.L. WETZEL, Kansas State University, A.J. Eilert

8:50 (1196) **Application of a Feedback-Controlled Piezoelectric Transducer for Mirror Stabilization in a Step-Scanning Interferometer**—J.H. PERKINS, University of Idaho, B. Lerner, P.R. Griffiths

9:10 (1197) **Improved Performance and Sensitivity of a Research-Grade Quadrupole Mass Spectrometer System**—K. IMATANI, Hewlett-Packard Co., S. Mazer, S. Hansen, H. Loucks

9:30 (1198 **A Highly Corrected Molecular Fluorescence Spectrometer**—L.E. BOWMAN, Michigan State University, S.R. Crouch

9:50 (1199 **The Barrel Ellipsoid Infrared Sampling Accessory for Remote Diffuse Reflectance and Emission Measurements**—G.L. POWELL, Martin Marietta Energy Systems, M. Milosevic, N.J. Harrick

10:10 RECESS

10:25 (1200 **Design of a High Performance UV-VIS-NIR Instrument**—R. FRANCIS, Varian Techtron Pty. Ltd., C. Porter, J. Steensrud

BUILDING AN AA SPECTROMETER THIS GOOD REQUIRED SOME BRILLIANT THINKING.

YOURS.

We listened to your suggestions. Then we made our new Model 3100 AA Spectrometer easier to operate, added new features, and kept it affordable. For superior performance, we developed a new high dispersion optical system and ASIC-based microprocessor electronics. We also added an optional Enhanced Data System with data handling and automation capabilities. Of course, we retained the reliability of its predecessors. For more information on the AA you helped to create, call toll-free 1-800-762-4000.

PERKIN ELMER

The Perkin-Elmer Corporation, Norwalk, CT 06859-0012

CIRCLE 142 ON READER SERVICE CARD

10:45 (1201) **Dual Beam FTIR: Increased Sensitivity for Surface Studies**—S WEIBEL. Mattson Instruments, Inc., D.R Mattson, P. Faguy

11:05 (1202) **Characterization Studies in Fast Scan Fourier Transform Ion Mobility Spectrometry (FT-IMS)**—R.H. ST. LOUIS, Washington State University, W.F. Siems, H.H. Hill, Jr.

11:25 (1203) **Fourier Transform Infrared Spectropolarimeter Design**—D.B. CHENAULT, University of Alabama-Huntsville, R.A. Chipman

11:45 (1204) **A Novel Approach to Spectropolarimeter Instrumentation and Applications**—Y. YOSHIDA, Japan Spectroscopic Co., Ltd., T. Takakuwa, N. Sakayanagi, A. Wada, H. Okahana, W W. Kottkamp

Optical Methods—Biomedical Applications

Thursday Morning, Room 1E08
V.S. Venturella, Presiding
Anaquest

8:30 (1205) **Laser-Induced Ionization Spectroscopy of Small Biological Molecules in Supersonic Beams**—D.M. LUBMAN, University of Michigan, L. Li

8:50 (1206) **Fluorescence-Detected Circular Dichroism for Homogeneous Immunoassay**—C.K. WILLIAMSON, Duke University, L.B. McGown

9:10 (1207) **Elucidating Protein Conformation with the Aid of Circular Dichroism**—K. KORKIDIS, SPEX Industries, Inc.

9:30 (1208) **Ultrasensitive Detection of Nucleic Acids with Chemiluminescence**—I. BRONSTEIN, Tropix, Inc., J.C. Voyta, K. Lazzari, O.J. Murphy

9:50 (1209) **Activation of Cells in Suspension or Attached to Surfaces, Monitored by Continuous Fluorescence Ratio Measurements of Their Cytoplasmic Ca^{++} and pH Changes**—E.R. SIMONS, Boston University, L. Brennan, J. Schonhorn, J. Bernardo, H. Koshi, B. Variano

10:10 RECESS

10:25 (1210) **A Photon Counting, Near-Infrared Fluorimeter for the Analysis of Ultratrace Levels of Toxicants, Microbiological Disease Agents and Disease Markers**—G. MOLLER, University of California, M.L. Tracy

10:45 (1211) **Analysis of Intracellular Metabolites: Novel Approaches Using A New Fluorescence Spectrometer**—S.R. HUCKINS, Perkin-Elmer Ltd., A.T. Rhys-Williams

11:05 (1212) **The Kinetic Characterization of Alkaline Phosphatase Isozymes**—W.H. LEWIS, JR., Virginia Commonwealth University, S.C. Rutan

11:25 (1213) **Automatic Drug Dissolution Testing with Multicomponent Analysis of UV Spectra**—S.C. LO, University of Rhode Island, S.M. Donahue, C.W. Brown

Powder Characterization

Thursday Morning, Room 1E20
J.R. Thompson, Presiding
Aluminum Company of America

8:30 (1215) **The Adaptation of FIA for the Determination of Phosphate in Phosphate Ore**—F.E. PATRICK, IMC Fertilizer Inc., J.E. Gibson, M.G. Cipollone

8:50 (1216) **A New Method for the Automatic and Selective Determination of Total Organic Carbon in Soils, Sediments, and Rocks**—B. LAVETTRE, Carlo Erba Instruments/Fisons, M. Baccanti, B. Colombo

9:10 (1217) **Characterization of Actinide Oxide Powders and Pellets**—J.C. CLAYTON, Westinghouse Electric Corp.

9:30 (1218) **A New Approach to Particle Sizing by Dynamic Light Scattering**—P.J. FREUD, Leeds & Northrup Co., M.N. Trainer

9:50 (1219) **Recycling of Spent Sand into a Construction Material**—A.P. CONNER, PG&E

10:10 RECESS

Particle Size Analysis

Thursday Morning, Room 1E20
J.R. Thompson, Presiding
Aluminum Company of America

10:25 (1220) **Particle Size Analysis of Uniform Latex Particles by Photon Correlation Spectroscopy**—S. MOHANRAJ, Seradyn, Inc.

10:45 (1221) **Particle Size Measurement by Linear System Modelling and Inversion of Scattered Light**—M.N. TRAINER, Leeds & Northrup Co., P.J. Freud, E.L. Weiss

11:05 (1222) **Submicron Grading of Diamond Particles by Dynamic Light Scattering**—W.J. DONEY, E. I. du Pont de Nemours & Co., Inc., N.F. Bailey

11:25 (1223) **Improved Pore Diameter and Pore Volume Resolution in Mercury Porosimetry Analysis**—A. THORNTON, Micromeritics Instrument Corp., M. Kane

Complete reaction systems...

featuring...
EZESEAL™
Stirred Autoclaves and Pressure Vessels

- Easy opening closure using metallic Double Delta Seal
- Interchangeable vessel volumes
- 50, 100, 300, 500 and 1,000 ml sizes available up to 3300 psi
- Complete with speed and temperature control
- Exclusive packless MagneDrive® mixer
- Transparent Vessels available in various sizes and pressures to 50 psi

For further information write factory or call toll free:
1-800-458-0409
Autoclave Engineers Group
2930 W. 22nd St.
Box 4007, Erie, PA 16512 USA

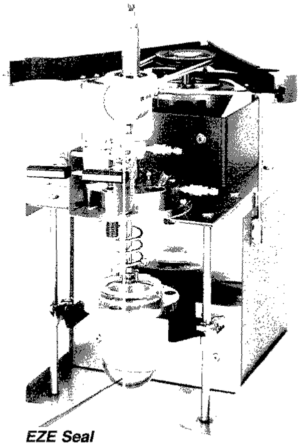

EZE Seal is now available with Transparent Reaction Vessels add-on package.

Autoclave Engineers

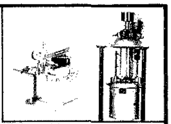

High and low pressure reactors and vessels

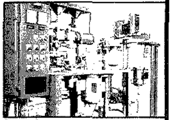

Reaction control and real time monitoring

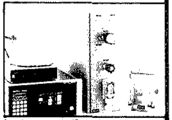

Instrumentation for measurement, control and automation

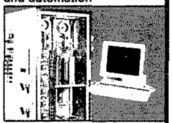

Micro-scale bench top reaction system – BTRS

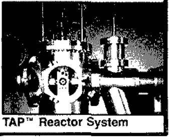

TAP™ Reactor System

CIRCLE 8 ON READER SERVICE CARD

Ammonium
Acetic
OPTIMA
Nitric Acid
Sulfuric
OPTIMA
A468-1
Nitric Acid
OPTIMA
Hydrofluoric
Hydrochloric
OPTIMA
FisherScientific

Expect more from FisherChemical Optima™ Acids and TraceMetal Acids ...and get less:

Less aluminum, less cadmium, less lead, less mercury...

Move up to Fisher acids

Why settle for "high purity" when you can get the world's highest purity? Choose the acids that offer the most by providing the least: FisherChemical Optima Acids for the lowest metal content and highest purity available anywhere...and FisherChemical TraceMetal Acids, for exceptionally low metal content and incomparable value.

Fisher Optima Acids—
The first acids good enough to be Optima

FisherChemical's new Optima Acids offer the lowest metal content of any acids available. Most metals are present in concentrations of less than one part per billion, and many are in the parts per trillion range, as indicated on the certificate of analysis supplied with each bottle. Optima Acids are the obvious choice for environmental testing, plasma analysis, electronic research...any application that demands the utmost purity and precision.

Each step in the creation of Optima Acids ensures the lowest level of metals in the acids you receive. Optima Acids are double-distilled in Teflon* or pure quartz stills at temperatures below the boiling point of the acid, then packaged in Teflon bottles that have undergone a hot acid leaching process. And every stage of production and packaging takes place in Class 100 clean room environments.

Fisher TraceMetal Grade Acids—exceptional value

FisherChemical's new TraceMetal Acids provide extraordinary purity at a lower cost and are ideal for many applications that require extremely low metal content. TraceMetal Acids are produced with low metal content in mind; the competition's so-called "metal-analyzed acids" are simply lot-selected ACS acids. TraceMetal Acids far surpass the purity of these products...and in fact are as pure as, or even purer than, many competitors' top-of-the-line acids...yet cost considerably less.

Careful sub-boiling distillation...ICP analysis... specially-treated containers designed to maintain exacting specifications...and a Certificate of Analysis with each bottle are the keys to TraceMetal Acid purity.

Select Optima or TraceMetal Acetic, Hydrochloric, Hydrofluoric, Nitric, Perchloric, Sulfuric Acids and Ammonium Hydroxide.

*Teflon is a registered trademark of E.I. du Pont de Nemours & Co., Inc.

Expect more from FisherChemical

FisherChemical

Fisher Scientific

Excellence in Serving Science...Since 1902

PITTCON BOOTH NUMBERS 4704, 4718, 4804 CIRCLE 62 ON READER SERVICE CARD

11:45 (1224) **Refractive Index Effects on the Laser-Diffraction Particle Size Analysis**—O.T IGUSHI, Horiba, Ltd., Y. Togawa, J. Ukon, K. Matsuda, K. Hara

Sampling—Sample Preparation—General

Thursday Morning, Room 1E11
N.C. Radcliffe, Presiding
PPG Industries, Inc.

8:30 (1225) **Sample Preparation Using Polymer-Based Solid Phase Extraction**—R.M. PATEL, Interaction Chemicals Inc., D.J. Hometchko

8:50 (1226) **Extraction of a Wide Variety of Compounds Using Thermal Stripping and Thermal Desorption**—S.A. HAZARD, Supelco, Inc., W.R. Betz

9:10 (1227) **Automated Sampling in Karl Fischer Coulometry: A System Overview**—G. BALOCK, EM Science

9:30 (1228) **A New Concept of Automatic Sample Handling and Preparation for Steel Plant Laboratories**—G. HAWICKHORST, Herzog Maschinenfabrik GmbH, P. Schubert

9:50 (1229) **Instrumental Solutions for Fully Automatic SFE-Capillary GC**—A.D. BASHALL, Carlo Erba Instruments/Fisons, G. Mapelli, C. Borra, S. Trestianu

10:10 RECESS

Biological Sequences and Profiles

Thursday Morning, Room 1E11
N.C. Radcliffe, Presiding
PPG Industries, Inc.

10:25 (1230) **High Resolution DNA Separations on Pellicular Ion Exchange Resins**—J. THAYER, Dionex Corporation, P. Newton

10:45 (1231) **Chemiluminescent Imaging of DNA in Electrophoretic Agarose Gels**—D. WILLIS, SymBiotech, Inc., P. Gray, R. Werba, R.W. Coughlin, E.M. Davis

11:05 (1232) **Peptide Mapping: A Comparison of Capillary Electrophoresis and Liquid Chromatography**—J. THAYER, Dionex Corporation, A. Wainright, J.D. Olechno, M. Weitzhandler

11:25 (1233) **Data Evaluation Techniques for Routine Peptide Mapping**—J.V. POSLUSZNY, Applied Biosystems, Inc., D. Wickham, A. Nip

11:45 (1234) **Determination of Modified Oligonucleotides in DNA Using MicroHPLC and Online FAB MS**—M. LINSCHEID, ISAS-Institut fur Spektrochemie, W. Lenhart

SYMPOSIUM

Applications of Microdialysis in Biological Systems - **arranged by B.G. Hoebel of Princeton University**

Thursday Afternoon, Room 1A06
J. Justice, Presiding
Justice Innovations, Inc.

1:30 (1235) **Introduction to Microdialysis as a Biological Sampling Technique for the Analytical Chemist: Amino Acids, Peptides and Biogenic Amines in Brain, Blood and Other Tissues**—U. UNGERSTEDT, Karolinska Institute

2:05 (1236) **Analytical Issues in Microdialysis and Applications to Drug Abuse**—J.B. JUSTICE, Emory University, H.O. Pettit, M.Z. Pan

2:40 (1237) **Prospects for Microdialysis and Capillary Electrophoresis**—L. HERNANDEZ, Princeton University, N. Joshi, B.G. Hoebel

3:15 RECESS

3:30 (1238) **Microdialysis Studies of Neural Recovery and Sparing of Functions After Brain Damage**—T.E. ROBINSON, University of Michigan

4:05 (1239) **Comparison Between Single-Channel and Multi-Channel Coulometric Analysis of Brain Monoamine Metabolism**—I. ACWORTH, ESA, Inc., P.H. Gamache, M.L. Lynch

SYMPOSIUM

Polymer Characterization in Food Packaging Applications - **arranged by J.P. Auses of Aluminum Company of America**

Thursday Afternoon, Room 1A23
J.P. Auses, Presiding
Aluminum Company of America

1:30 **Introductory Remarks**—J.P. AUSES

1:35 (1240) **Advanced Analytical Techniques for Polymer Surface Characterization**— L. SHADOFF, Dow Chemical Company

FAST, ACCURATE
TRACE MOISTURE ANALYSIS
State-of-the-Art
Silicon Chip Technology

Saturation to Dry Down in Fifteen Seconds
Continuous Monitoring or Spot Check
Fully Temperature Controlled Sensors Available
Vacuum to 275 Atmospheres
Exclusive "PUSH-PURGE" Diagnostic Feature
Standard on all Models

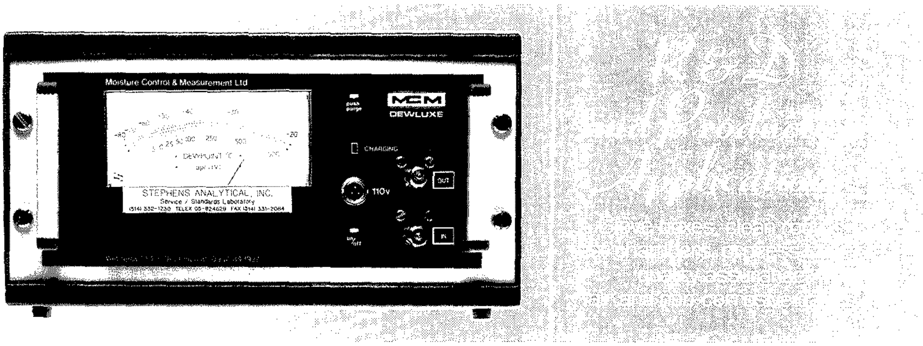
Moisture Control & Measurement Ltd
MCM
DEWLUXE
push purge
CHARGING
110v
OUT
IN
on off
DEWPOINT °C
STEPHENS ANALYTICAL, INC.
Service / Standards Laboratory

MCM Si-Grometers Render Obsolete Aluminum Oxide, Electrolytic and Chilled Mirror Technologies.

STEPHENS

STEPHENS ANALYTICAL, INC.
An Associate Company of the Stephens group
P.O. Box 1126
Champlain, New York 12919-1126
Tel.: (514) 332-1230 • Fax: (514) 331-2084
Tlx.: 05 824 629

SEE US AT THE PITTSBURGH CONFERENCE BOOTH NO. 2138 CIRCLE 180 ON READER SERVICE CARD

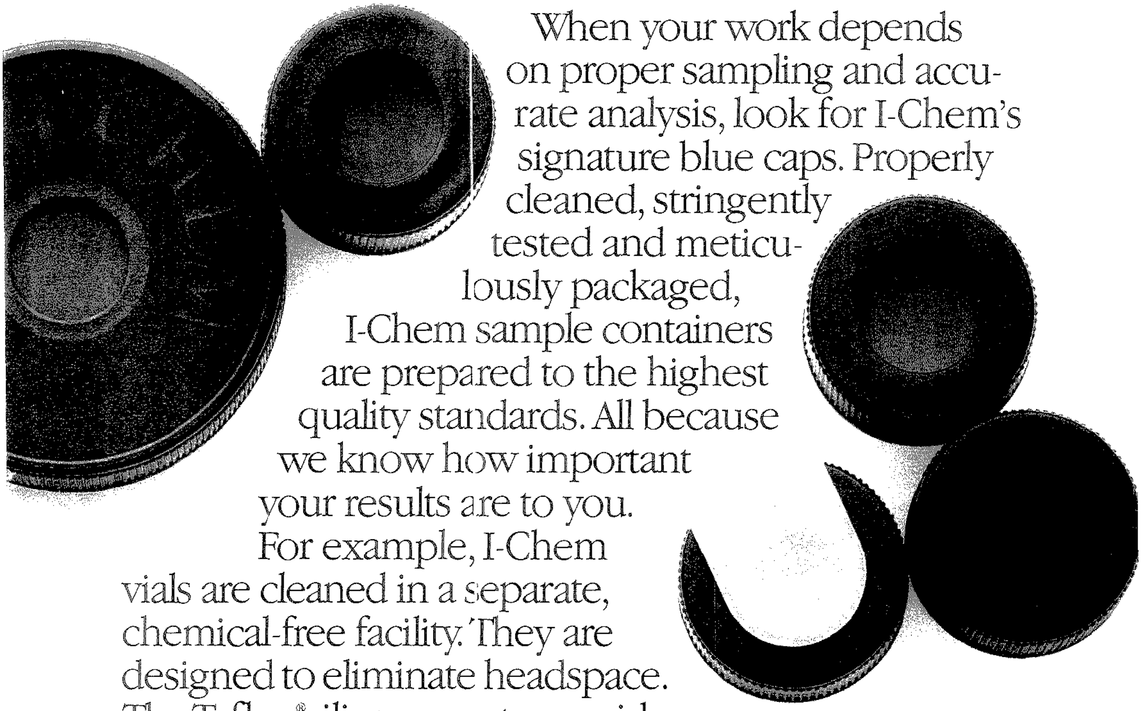

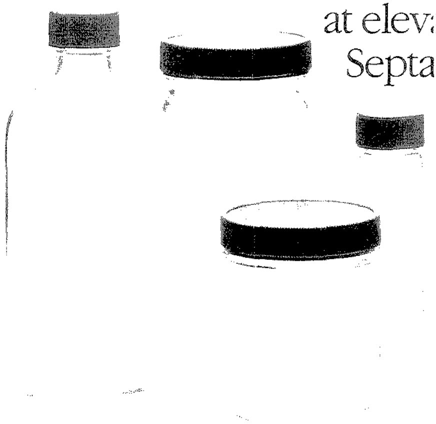

I-Chem. Quality that will be reflected in your results.

When your work depends on proper sampling and accurate analysis, look for I-Chem's signature blue caps. Properly cleaned, stringently tested and meticulously packaged, I-Chem sample containers are prepared to the highest quality standards. All because we know how important your results are to you.

For example, I-Chem vials are cleaned in a separate, chemical-free facility. They are designed to eliminate headspace. The Teflon®-silicone septa provide a strong, tight seal. The proprietary blue cap won't crack at elevated temperatures. And our unique Septa-Gard™ protects your volatiles and reduces contamination.

Let your results reflect your high standards. Contact I-Chem for a free catalog today.

I-CHEM

***Chemists in the container business.*™**

Hayward, CA (800) 443-1689 (800) 262-5006 In Calif.
New Castle, DE (800) 553-3696
Also available through your CMS, Fisher or VWR representative.

"Chemists in the container business," Septa-Gard and Septa Jar are trademarks of I-Chem Research, Inc. Teflon is a registered trademark of DuPont.

CIRCLE 78 ON READER SERVICE CARD

2:10 (1241) **Capillary Rheometry in Characterization of Coextrusion Polymers**—C. BATES, Alcoa Technical Center

2:45 (1242) **Control of Aluminum Can Production Using Sensory Analyses and Analytical Chemistry Measurements**—D.J. EHNTHOLT, Arthur D. Little, Inc., D.A. Kendall, E.V. Miseo

3:20 RECESS

3:35 (1243) **Material Selection Criteria in Food Can Coatings Development**—T.R. MALLEN, The Valspar Corporation, L. Landauer

4:10 (1244) **Evaluation of the Organic Vapor Barrier and Sorption Characteristics of Polymer Films and Their Relationship to Product Quality**—J.R. GIACIN, Michigan State University, R.J. Hernandez

SYMPOSIUM

Selective Detectors for Gas Chromatography—Practical Aspects - arranged by G.D. Dupré of Exxon Research & Engineering Co.

Thursday Afternoon, Room 1D01
G.D. Dupré, Presiding
Exxon Research & Engineering Co.

1:30 **Introductory Remarks**—G.D. DUPRÉ

1:35 (1245) **The Oxygen - Specific O-FID for Determination of Oxygenated Compounds in Petroleum Systems**—J.C. FROHNE, Veba Oel AG

2:10 (1246) **The Hall Electrolytic Conductivity Detector (HECD) for Selective Element Analyses**—C.W. BAYER, Georgia Tech. Research Institute

2:45 (1247) **The Sulfur - Specific Chemiluminescence Detector (SCD) Advances in Sulfur Component Speciation**—R.L. SHEARER, Shell Development Company

3:20 RECESS

3:35 (1248) **Thermionic Ionization Detectors in Gas Chromatography**—P.L. PATTERSON, Detector Eng. & Tech., Inc.

4:10 (1249) **The Atomic Emission Detector for Gas Chromatography—Twelve Years of Industrial Experience**—J.S. MARHEVKA, 3M Company, D.F. Hagen, J.W. Miller

Atomic Absorption—Instrumentation

Thursday Afternoon, Room 1E10
D.A. Wilson, Presiding
Aluminum Company of America

1:30 (1250) **The Analysis of Biological Samples by Laser Enhanced Ionization in a Graphite Tube Furnace with Probe Atomization**—D.J. BUTCHER, University of Connecticut, S. Sjostrom, R.L. Irwin, G. Michel

1:50 (1251) **Optimization of Graphite Furnace Design and Operation**—J.A. HOLCOMBE, University of Texas at Austin, O.A. Guell

2:10 (1252) **Continuum Source AAS with a Pulsed Light Source and Diode Array Detector**—G.P. MOULTON, University of Maryland, T.C. O'Haver, J.M. Harnly

2:30 (1253) **A Comparison of Hollow Cathode Lamps in Graphite Furnace Atomic Absorption Spectroscopy**—D. BASS, Hitachi Instruments, Inc., G.D. Rayson

2:50 (1254) **Extended Calibration Range in Graphite Furnace Atomic Absorption Spectrometry Using Partial-Peak Methods**—T.W. BRUEGGEMEYER, USFDA, F.L. Fricke

3:10 RECESS

3:25 (1255) **Hollow Anode Discharge - Graphite Furnace Atomic Emission Spectrometry**—J.M. HARNLY, USDA, NCL, D.L. Styris, N.E. Ballou

3:45 (1256) **Enhancement of Sensitivity in Flame Atomic Absorption Spectrometry (FAAS) Using a New Atom Concentrator Tube Accessory**—E. SALADINO, Varian Associates, J. Moffett

4:05 (1257) **Extending the Calibration Range of Conventional Flame AAS by Continuous Flow Techniques**—J.F. TYSON, University of Massachusetts, S.R. Bysouth, E. Debrah, S.G. Offley

4:25 (1258) **Optimization of Glow Discharge Emission Spectrometry (GD-ES) for Surface and Depth Profile Analysis**—H. HOCQUAUX, Unieux Research Center, P. Hunault

4:45 (1259) **A Novel Method for AAS**—G. LI, Hunan Institute of Analy. & Test.

Clinical Fluorescence

Thursday Afternoon, Room 1E08
S. Morris, Presiding
IGEN

1:30 (1260) **Competitive Particle Concentration Fluorescence Immunoassays for Femtomole Detection of Small Molecules**—L.D. TABER, Eli Lilly and Company, J.R. Sportsman

1:50 (1261) **Versatile Luminescence Optrode Measurement System**—M.A. RUBERTO, Stevens Institute of Technology, D.C. Shelly

2:10 (1262) **Tb-Containing Latex Beads for Multi-Fluorescence Labeling of Proteins**—C.Y. GUO, University of Missouri, R. Shankar, Y. Al-Roumi, R.N. Thomas, S. Pickup, J.E. Kuo

2:30 (1263) **Protein Labeling with Fluorescent Silica Microspheres**—C.Y. GUO, University of Missouri, R. Shankar, Y. Al-Roumi, S. Pickup, J.E. Kuo

2:50 (1264) **New Fluorescence Immunoassays for Cyclosporins**—M. FRENCH, Loughborough University of Tech., J.N. Miller, N.J. Seare, M. Yacoub

3:10 RECESS

Surface Characterization of Materials

Thursday Afternoon, Room 1E08
L. Salvati, Jr., Presiding
Perkin Elmer Corporation

3:25 (1265) **Voltammetric Pulse Techniques for Investigation of Early Stages of Corrosion**—M. DONTEN, State Univ. of NY at Buffalo, J.G. Osteryoung

3:45 (1266) **The Effect of Processing Conditions on the Dielectric Properties of an FR-4 Glass/Epoxy Circuit Board Resin**—D.D. SHEPARD, Micromet Instruments, Inc., D.R. Day

4:05 (1267) **Characterizing Metal-Matrix Composites**—D.D.L. CHUNG, State University of New York, J.M. Chiou

4:25 (1268) **Comparison of Effective Dispersion Between Anionic and Nonionic Surfactants Upon Normal and Reverse Phase Silicas by Time-of-Transition Particle Size Analysis**—G.S LONG, Rainin Instrument Company, Inc., R.F. Benson

4:45 (1269 **A Combined ESCA/SIMS Investigation of Surface Modified Polymer Materials**—L. SALVATI, JR., Perkin Elmer Corporation, G.L. Grobe, III, J.G. Newman

Electrochemistry

Thursday Afternoon, Room 1E15
J.T. Maloy, Presiding
Seton Hall University

1:30 (1270) **Bicontinuous Microemulsions: New Media for Electroanalytical Chemistry**—M.O. IWUNZE, University of Connecticut, A. Sucheta, J.F. Rusling

1:50 (1271) **Sensitivity of Membrane Electrodes**—K.L. CHENG, Univ. of Missouri-Kansas City, T.M. Chang

2:10 (1272) **Solid Composite Reference Electrodes (SCRE) for Nonaqueous Solvent and Instrumental Applications**—Y. DENG, University of Connecticut, B.R. Shaw

2:30 (1273) **Anion-Selective Electrodes Based on Extracted-Metal Complexes of Triisobutylphosphine Sulphide**—M. VALIENTE, Univ. Autonoma de Barcelona, M. Munoz, S. Daunert, W. Dunaway, L.G. Bachas

2:50 (1274) **Automated Determination of Trace Metals in Nuclear Power Plant Cooling Waters by Stripping Potentiometry**—L. RENMAN, University of Gothenburg, D. Jagner

3:10 RECESS

3:25 (1275) **Determination of Gallium and Arsenic in GaAs Crystals by Precise Coulometric Titration Methods**—A. OKADA, Toshiba Corporation, N. Hirate

3:45 (1276) **Autotitrator Applications in Environmental Treatment Systems to Control Chlorine Emissions from a Chlorine Plant**—T.G. ANGELINI, PPG Industries, Inc.

4:05 (1277) **Binding of Metals to Melanin Studied by the Electrochemical Quartz Crystal Microbalance**—M. HEPEL, State Univ. of NY at Potsdam, W. Janusz

4:25 (1278) **An Inexpensive Computer-Based AC Impedance and High Frequency AC Electrochemical Measurement System**—P. HE, Fudan University, X. Chen

4:45 (1279) **Electrochemistry and Photoelectronic Spectroscopy of Vinyl Triflates**—K. ASHLEY, San Jose State University

Environmental; Pesticide Analysis Methods

Thursday Afternoon, Room 1E19
S.H. Peterson, Presiding
Westinghouse STC

1:30 (1280) **Use of Immobilized Enzyme Reactors for Pesticide Residue Analysis**—R.K. TRUBEY, E. I. du Pont de Nemours & Co. Ltd.

1:50 (1281) **Chlorinated Pesticide Analysis Using Capillary Gas Chromatography**—C.R. VARGO, Restek Corporation, N.H. Mosesman

2:10 (1282) **Model DNA/Carcinogen Ion-Molecule Reactions to Estimate the Carcinogenic Potential of Environmental Contaminants**—J.A. FREEMAN, University of Florida, J.V. Johnson, R.A. Yost, D.W. Kuehl

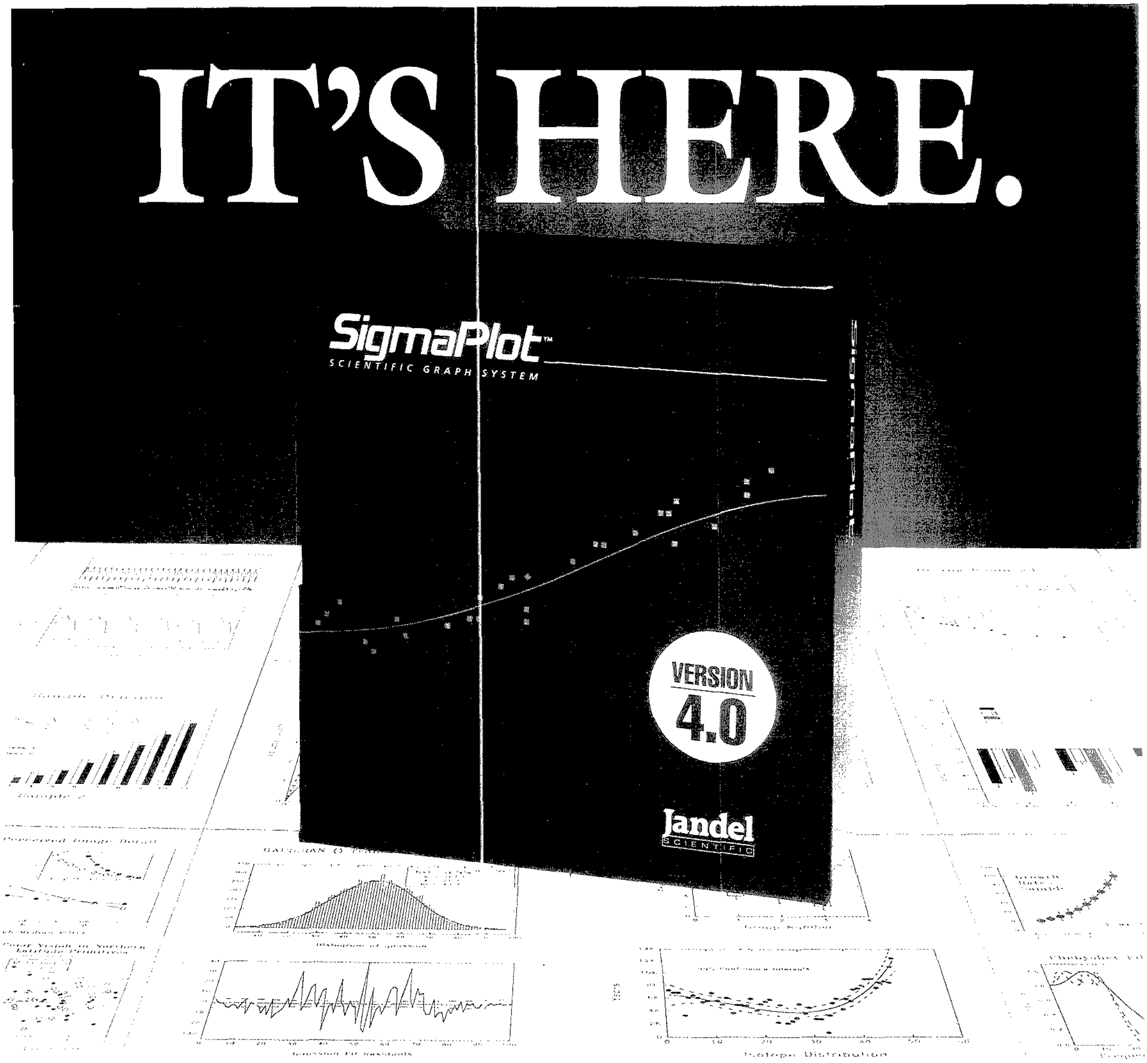

Introducing SigmaPlot™ 4.0.

The powerful new version of the world's finest PC software for the production of publication-quality scientific charts and graphs...on your own IBM® or compatible personal computer.

Used by over 10,000 scientists.

SigmaPlot, Version 3.1, is the software of choice worldwide for creating graphics for scientific papers and poster sessions. It was selected "Editor's Choice" by *PC Magazine* for its outstanding output. Now, Jandel's new SigmaPlot Version 4.0 gives you all of the advantages of 3.1...and much, much more.

Designed with the scientist in mind.

SigmaPlot 4.0 is elegant and easy to use...with its pull-down menu interface, mouse and keyboard support, novice prompting, and full context-sensitive interactive help. Input data directly from the keyboard, or from Lotus 123®, or ASCII files, into SigmaPlot's *huge* worksheet - 16,000 columns by 65,000 rows. Version 4.0's full mathematical transform language lets you plot mathematical functions or transform data. SigmaPlot 4.0 also gives you highly sophisticated non-linear curve fitting...and error bars that are complemented by confidence intervals and quality control lines.

Outstanding plot output.

Extremely high-quality output is given, a result of extraordinary control over the appearance of your graphs. With SigmaPlot 4.0 you have outstanding page layout control, as well as control over individual width, color and position of independent graphic elements. You also have more fonts, more scales, and more graph types to work with. Not to mention multiple axes, Greek, mathematical and European characters, descriptive statistics, and much more. You can easily export graphs into WordPerfect® 5.0, Pagemaker®, Ventura Publisher® and many other programs. And SigmaPlot outputs to plotters, slide makers, dot matrix printers, Postscript™ and HP Laserjet™ printers.

Affordable and fully supported.

Priced under $500, SigmaPlot 4.0 is well within reach of any research facility. And, like all Jandel products, SigmaPlot 4.0 comes with a money-back guarantee and the full technical support of Jandel's experts. It's what you'd expect from the leader in software for scientists. Find out how much you can do with SigmaPlot 4.0.
Call today for a FREE brochure:
1-800-874-1888 (inside CA 415-924-8640).

65 Koch Road • Corte Madera, CA 94925
1-800-874-1888 (inside CA or Canada 415-924-8640)
FAX: 415-924-2850 • TELEX: 4931977

SCIENTIFIC
"Microcomputer Tools for the Scientist"

In Europe: RJA Handels GmbH
Grosser Mühlenweg 14A, 4044 Kaarst 2, FRG
Phone: 2101/666268 • FAX: 2101/64321

CIRCLE 87 ON READER SERVICE CARD

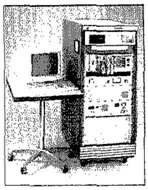

CIRCLE 211

Questor I High-Speed Process Analyzer

Over 98.5% uptime, monitoring hundreds of process streams in production plants, pilot plants and process research facilities worldwide. Fast and accurate, it replaces multiple instruments to boost efficiency and provide rapid payback. Easy communications with control and host computers, enclosures for classed environments, ready-to-use statistical packages, menu-driven software and applications support from EXTREL process engineers. Call EXTREL Corp. at (412) 963-7530.

NEW HTE-400 High-Transmission Environmental GC/MS

For low detection limit **524 and 525 drinking water requirements,** a high transmission 3/4-inch quadrupole and ion source, coupled to a unique geometry detection system employing a dual sector ESA. Includes full software support for all EPA methods. Avoids matrix, self CI and automatic gain control problems of ion trap detector systems. Call EXTREL Corp. at (412) 963-7530.

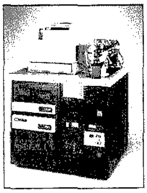

CIRCLE 212

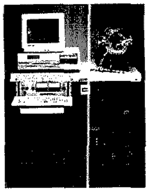

CIRCLE 213

Glow Discharge Mass Spectrometer (GD/MS)

The EXT-1000 Glow Discharge Quadrupole Mass Spectrometer performs complete major and trace elemental analyses of metals and alloys. Simple one-step sample preparation, sub ppm detection limits and minimal matrix effects. Easy to calibrate and remains stable over long periods of time. For more information, contact EXTREL Corp. at (412) 963-7530.

2001 Fourier Transform Mass Spectrometer

EXTREL's new easy-to-use 2001 provides affordable analytical FT/MS®. Ultra-high resolution better than 1,000,000 at $^{m}/_{z}$ 131, accurate mass measurements better than 2 ppm, high-resolution multistage MS with accurate mass measurement, high mass range and low detection limits. The revolutionary SWIFT™ method provides unprecedented experimental versatility and ease of use, and the menu-driven FT/MS® software is the most powerful in the industry. Prices start at $299,000. Call EXTREL FTMS at (608) 273-8262.

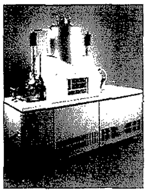

CIRCLE 214

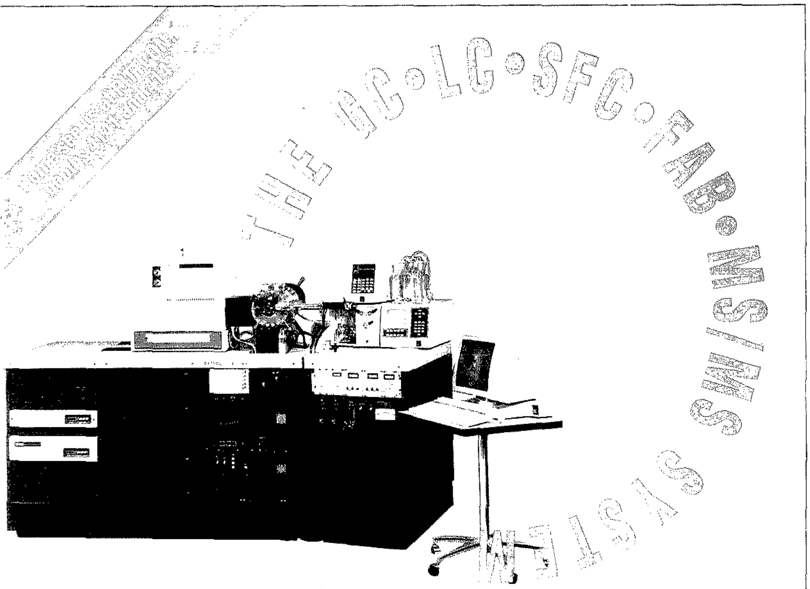

EXTREL ELQ 400-3 Triple Quadrupole MS

Perform more high-level analyses with EXTREL's ELQ 400-3 than with any other triple quadrupole. The key is *flexibility*. The ELQ 400-3 provides **the widest array of inletting and ionization techniques in the industry.** Choose LC, GC, SFC or probes ... choose EI, CI or our new FAB system for ThermaBeam™ particle beam MS. Plus, you can switch inletting techniques in minutes without venting.

The ELQ 400-3 also has a full compliment of pumping options and mass ranges up to 4000 u. And our new 2000 data system provides automatic data batching for better processing and color graphics for better on-screen display.

Flexibility. Quality. Stability. Once again, EXTREL pushes technology just a little further — giving you more in a mass spectrometer.

For more information on the ELQ 400-3 Triple Quadrupole MS, use the reader service card or cal EXTREL today.

575 EPSILON DRIVE • PITTSBURGH PA 15238 • (412) 963-7530 • TELEX 812 316 • FAX (412) 963-6578

CIRCLE 217 ON READER SERVICE CARD

Laser Probe FT/MS®

New surface probe instrument combines the power of EXTREL's 2001 FT/MS® system with laser ablation and sample viewing for solving tough materials characterization problems. A versatile, easy-to-use industrial problem solver for analysis of advanced materials: semiconductors, adhesives, polymers, biopolymers, catalysts, ceramics, superconductors and fibers. Features high resolution, accurate mass measurement, simultaneous measurement of all ions, and MS/MS. Call EXTREL FTMS at (608) 273-8262.

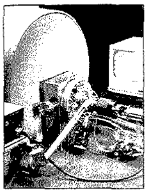

CIRCLE 215

Finnigan Rehab Kits

Update and rehabilitate old Finnigan systems, like the 3200 Series, to full capability with these Rehab Kits. Easy to install, increased mass ranges, manual and/or full computer control. Backed by EXTREL service support, Finnigan Rehab Kits are the most economical way to have a "new" mass spectrometer. For price list and specifications, contact EXTREL Corp. at (412) 963-7530.

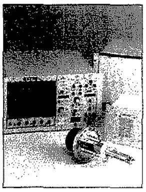

CIRCLE 216

American Chemical Society publications offer:

• Reliable and Accurate Research • Techniques • Trends • Discoveries • Reviews • Developments • And much more!

Take advantage of the most current chemical research and general scientific reporting available — from the many respected researchers worldwide.

Use the postage-paid order card below to order your 1990 subscriptions.

F.W. McLafferty, Editor; Cornell Univ.
Monthly offering short, critical reviews written by scientists active in the research described.

	U.S.	Canada & Mexico	Europe	All Other Countries
Members				
One Year	$ 24	$ 31	$ 33	$ 36
Two Years	$ 43	$ 57	$ 61	$ 67
Nonmembers	$127	$134	$136	$139

George H. Morrison, Editor; Cornell Univ.
The world's foremost publication in the vital field of measurement science. Semi-monthly.

	U.S.	Canada & Mexico	Europe	All Other Countries
Members				
One Year	$ 29	$ 64	$ 96	$118
Two Years	$ 49	$ 119	$ 183	$227
Nonmembers	$ 59	$ 94	$ 186	$208

NOW WEEKLY!

Hans Neurath, Editor; Univ. of Washington.
Results of original research in all recognized or developing areas of biochemistry. Weekly.

	U.S.	Canada & Mexico	Europe	All Other Countries
Members				
One Year	$ 85	$174	$278	$345
Two Years	$153	$331	$539	$673
Nonmembers	$690	$779	$883	$950

BIOCONJUGATE CHEMISTRY*

NEW JOURNAL!

Claude F. Meares, Editor; Univ. of California, Davis
Six times a year, chemists, biochemists, and molecular biologists will find the most important research in conjugate chemistry in one publication—Bioconjugate Chemistry.

	U.S.	Canada & Mexico	Europe	All Other Countries
Members				
One Year	$ 29	$ 35	$ 39	$ 43
Two Years	$ 52	$ 64	$ 72	$ 80
Nonmembers	$249	$255	$259	$263

BIOTECHNOLOGY PROGRESS*

NEW JOURNAL!

Jerome S. Schultz, Editor; Univ. of Pittsburgh
Bimonthly, this publication will focus on the application of fundamental chemical and engineering principles to biological phenomena and to processor product design.

	U.S.	Canada & Mexico	Europe	All Other Countries
ACS/AIChE				
Members	$ 25	$ 31	$ 34	$ 39
Nonmembers	$250	$256	$259	$ 264

Michael Heylin, Editor
Chemical newsweekly and the official publication of the ACS that all members receive as part of their dues.

	U.S.	Canada & Mexico	Europe*	All Other Countries*
Nonmembers				
One Year	$ 60	$ 93	$127	$169
Two Years	$108	$174	$242	$326

Surface Delivery All Countries: 1 Year, $93; 2 Years, $174
** Air service delivery*

Lawrence J. Marnett, Editor; Vanderbilt Univ.
Bimonthly international journal for scientists needing the most current research in the highly active field of toxicology.

	U.S.	Canada & Mexico	Europe	All Other Countries
Members				
One Year	$ 46	$ 52	$ 57	$ 60
Two Years	$ 82	$ 94	$104	$110
Nonmembers	$269	$275	$280	$283

Josef Michl, Editor; Univ. of Texas, Austin
Reviews of research in various areas of chemistry that eliminate the need to scan scores of articles concerning particular fields. 8 issues per year.

	U.S.	Canada & Mexico	Europe	All Other Countries
Members				
One Year	$ 26	$ 42	$ 59	$ 70
Two Years	$ 46	$ 78	$112	$134
Nonmembers	$225	$ 241	$258	$269

Leonard V. Interrante, Editor; Rensselaer Polytechnic Institute
This bimonthly journal gives direction in the fundamentals of materials preparation, characterization, and processing science and technology.

	U.S.	Canada & Mexico	Europe	All Other Countries
Members				
One Year	$ 49	$ 57	$ 65	$ 69
Two Years	$ 88	$104	$120	$128
Nonmembers	$299	$307	$315	$319

Benjamin J. Luberoff, Editor
Stimulating, personal monthly helping chemists and engineers arrive at innovative solutions to real problems.

	U.S.	Canada & Mexico	Europe	All Other Countries
Members				
One Year	$ 39	$ 48	$ 52	$ 55
Two Years	$ 66	$ 84	$ 92	$ 98
Nonmembers				
Personal	$ 69	$ 78	$ 82	$ 85
Institutional	$299	$308	$312	$315

John W. Larson, Editor; Lehigh Univ.
A bimonthly journal covering all aspects of the transformation, utilization, formation, and production of fuels and non-nuclear energy in addition to studies of fuel structure and properties.

	U.S.	Canada & Mexico	Europe	All Other Countries
Members				
One Year	$ 48	$ 55	$ 59	$ 62
Two Years	$ 86	$ 100	$108	$114
Nonmembers	$ 294	$301	$305	$308

1990

Please enter my subscription(s) for the following:

Title __________ 1 yr. $________ 2 yrs. $________
Title __________ 1 yr. $________ 2 yrs. $________
(If you wish to enter more than two subscriptions, please use a separate piece of paper and mail with this coupon in an envelope.)

Name ____________________
Company __________ Title __________
Address ☐ Home ☐ Business ____________________
City __________ State ____ ZIP ______
☐ Payment enclosed. (Payable to American Chemical Society)
☐ Bill Me ☐ Bill Company
☐ Charge my ☐ VISA/MasterCard ☐ Diners Club/Carte Blanche
Card No. ____________________
Expires ________ Signature ____________________

☐ I am an ACS Member ☐ I am not an ACS Member
☐ Please send me information on how to become an ACS member

Member rates are for personal use only. All journal subscriptions are based on a calendar year. Subscriptions to ANALYTICAL CHEMISTRY, CHEMICAL & ENGINEERING NEWS (nonmembers only), CHEMTECH, and ENVIRONMENTAL SCIENCE & TECHNOLOGY will start the month the order is placed and expire one year later unless subscriber specifies otherwise.

Foreign payment must be made in U.S. dollars by international money order, UNESCO coupons, or U.S. bank draft. Orders accepted through your subscription agency. For nonmember rates in Japan contact Maruzen Co., Ltd.

Air Service Delivery included in all rates listed for countries outside the U.S., Canada, and Mexico.

In a Hurry?
Call TOLL FREE (800)227-5558 (U.S. only) and charge your order!
In D.C. and outside the U.S. call (202)872-4363.
Telex: 440159 ACSPUI OR 89 2582 ACSPUBS
FAX: (202) 872-4615

5471L

[illegible]

William H. Glaze, Editor; Univ. of North Carolina, Chapel Hill

Published monthly for those engaged in environmental study and maintenance through the application of chemical principles.

	U.S.	Canada & Mexico	Europe	All Other Countries
Members				
One Year	$ 36	$ 50	$ 65	$ 72
Two Years	$ 61	$ 89	$119	$133
Nonmembers				
Personal	$ 67	$ 81	$ 96	$103
Institutional	$276	$290	$305	$312

[illegible]

Donald R. Paul, Editor; Univ. of Texas, Austin

This monthly provides timely reports on original work in the broad field of chemical engineering and industrial chemical research.

	U.S.	Canada & Mexico	Europe	All Other Countries
Members				
One Year	$ 55	$ 73	$ 84	$ 94
Two Years	$ 99	$135	$157	$177
Nonmembers	$372	$390	$401	$411

[illegible]

M. Frederick Hawthorne, Editor; Univ. of California, L.A.

Biweekly journal publishes fundamental studies, experimental and theoretical, in all phases of inorganic chemistry.

	U.S.	Canada & Mexico	Europe	All Other Countries
Members				
One Year	$ 82	$120	$146	$170
Two Years	$147	$223	$275	$323
Nonmembers	$612	$650	$676	$700

[illegible] **NOW MONTHLY!**

Irvin E. Liener, Editor; Univ. of Minnesota

Monthly reporting on original research into the chemical aspects of agriculture and food.

	U.S.	Canada & Mexico	Europe	All Other Countries
Members				
One Year	$ 25	$ 41	$ 52	$ 61
Two Years	$ 45	$ 77	$ 99	$117
Nonmembers	$204	$220	$231	$240

[illegible]

Allen J. Bard, Editor; Univ. of Texas, Austin

Most quoted biweekly journal of the widest possible interest to research workers and students in all areas of chemistry.

	U.S.	Canada & Mexico	Europe	All Other Countries
Members				
One Year	$ 75	$131	$191	$236
Two Years	$135	$247	$367	$457
Nonmembers	$630	$686	$746	$791

BUSINESS REPLY MAIL

FIRST CLASS PERMIT NO. 10094 WASHINGTON, D.C.

POSTAGE WILL BE PAID BY ADDRESSEE

AMERICAN CHEMICAL SOCIETY
Attn: Marketing Communications Department
1155 Sixteenth Street, N.W.
Washington, D.C. 20077-5768

NO POSTAGE
NECESSARY
IF MAILED
IN THE
UNITED STATES

[illegible]

Bruno J. Zwolinski, Editor; Texas A&M Univ.

This quarterly journal is primarily concerned with the presentation of data of lasting value.

	U.S.	Canada & Mexico	Europe	All Other Countries
Members				
One Year	$ 30	$ 35	$ 37	$ 40
Two Years	$ 54	$ 64	$ 68	$ 74
Nonmembers	$207	$212	$214	$217

George W.A. Milne, Editor; National Institutes of Health

Quarterly reporting on new R&D, concepts, systems and programs in all areas of information and computers relative to chemistry.

	U.S.	Canada & Mexico	Europe	All Other Countries
Members				
One Year	$ 18	$ 22	$ 24	$ 26
Two Years	$ 32	$ 40	$ 44	$ 48
Nonmembers	$108	$112	$114	$116

[illegible]

Philip S. Portoghese, Editor; Univ. of Minnesota

Monthly publishing on the relationship of chemistry to biological activity including rapid communication of major advances in drug design and development.

	U.S.	Canada & Mexico	Europe	All Other Countries
Members				
One Year	$ 42	$ 63	$ 81	$ 93
Two Years	$ 75	$117	$153	$177
Nonmembers	$329	$350	$368	$380

[illegible]

Clayton H. Heathcock, Editor; Univ. of California, Berkeley

Biweekly offering critical accounts of original work and interpretive reviews of existing data that presents new viewpoints.

	U.S.	Canada & Mexico	Europe	All Other Countries
Members				
One Year	$ 56	$ 98	$134	$162
Two Years	$100	$184	$256	$312
Nonmembers	$428	$470	$506	$534

[illegible] **NOW BIMONTHLY!**

David R. Lide, Jr., Editor; National Institutes of Standards & Technology

Published bimonthly with Am. Inst. of Physics and NIST presenting critically evaluated data on physical and chemical properties.

	U.S.	Canada & Mexico	Europe	All Other Countries
Members (ACS, AIP affiliated societies)	$ 70	$ 85	$105	$105
Nonmembers	$325	$340	$360	$360

[illegible]

Mostafa A. El-Sayed, Editor; Univ. of California, L.A.

Biweekly. Experimental and theoretical research on fundamental aspects of physical chemistry and chemical physics.

	U.S.	Canada & Mexico	Europe	All Other Countries
Members				
One Year	$ 70	$126	$178	$217
Two Years	$126	$238	$342	$420
Nonmembers	$670	$726	$778	$817

[illegible] **NOW MONTHLY!**

Arthur W. Adamson, Editor; Univ. of Southern California

Broad coverage of all areas of fundamental surface and colloid science, wet surface chemistry, UHV surface chemistry, disperse systems, electrochemistry. Monthly.

	U.S.	Canada & Mexico	Europe	All Other Countries
Members				
One Year	$ 58	$ 70	$ 78	$ 85
Two Years	$104	$128	$144	$158
Nonmembers	$429	$441	$449	$456

[illegible] **NOW BIWEEKLY!**

Field H. Winslow, Editor; AT&T Bell Laboratories

Biweekly publication of original material on all fundamental aspects of polymer chemistry.

	U.S.	Canada & Mexico	Europe	All Other Countries
Members				
One Year	$ 57	$ 95	$121	$144
Two Years	$102	$178	$230	$276
Nonmembers	$553	$591	$617	$640

[illegible]

Dietmar Seyferth, Editor; M.I.T.

Interdisciplinary approach to organometallic chemistry; synthesis; structure and bonding; reactivity and mechanism; applications in organic, inorganic, polymer, solid state chemistry and materials science. Monthly.

	U.S.	Canada & Mexico	Europe	All Other Countries
Members				
One Year	$ 59	$ 80	$ 98	$110
Two Years	$106	$148	$184	$208
Nonmembers	$521	$542	$560	$572

*Indicates periodicals printed on acid-free paper.

TAKE A PEAK AT OVONYX™ MULTILAYERS—
YOU'LL NEVER LOOK AT CRYSTALS AGAIN.

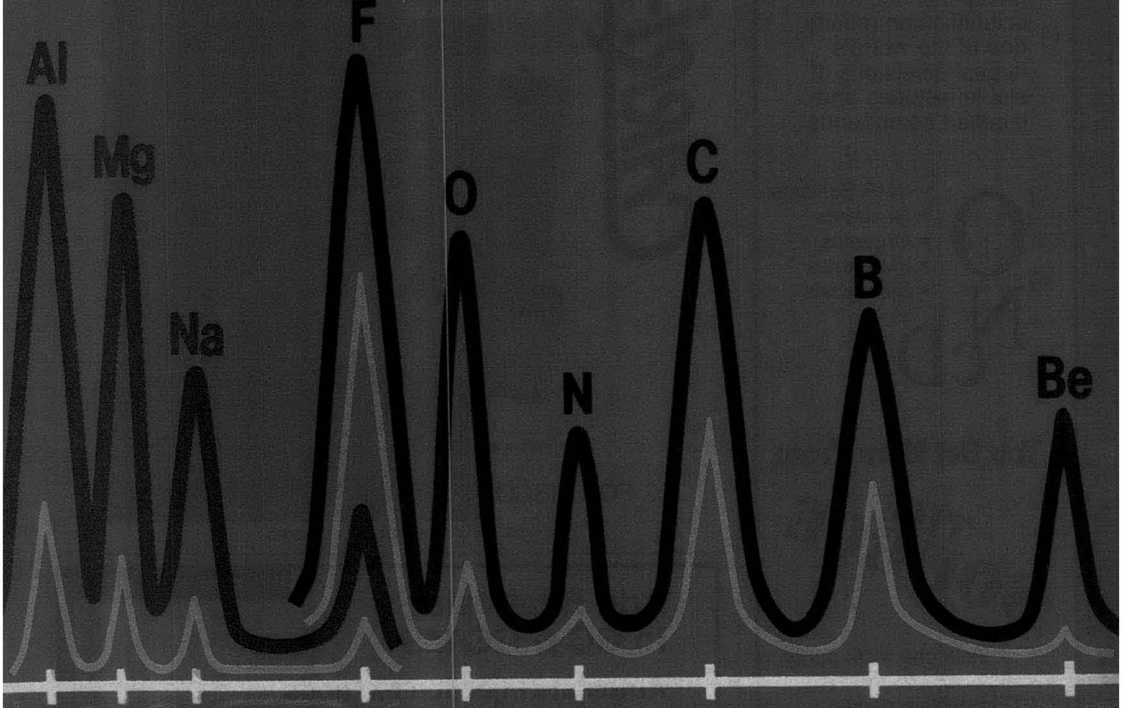

Peak intensities 2 to 20 times higher.

When it comes to light element X-ray analysis, Ovonyx multilayers are fast replacing yesterday's Acid Phthalate crystals and Langmuir-Blodgett pseudo-crystals in WD XRF and EPMA spectrometers. With peak intensities 2 to 20 times higher than those of crystals, Ovonyx multilayers offer reflectivities previously unobtainable for light elements. So your X-ray measurements can be faster *and* more accurate.

Standardized or customized.

Ovonyx multilayers have been designed for almost every WDXRF spectrometer in use, both old and new. We can also custom design multilayers to meet your particular research requirements.

So before you look into replacing your crystals, look into Ovonyx. And take advantage of today's technology.

Call us today for details at 1-800-366-1299.

■ OVONYX™
▬ CRYSTALS

OVONYX™

Ovonic Synthetic Materials Co., Inc.
A Subsidiary of Energy Conversion Devices, Inc.
1788 Northwood Drive
Troy, MI 48084
(313) 362-1290
FAX (313) 362-4043

© 1989, Ovonic Synthetic Materials Co., Inc., Troy, MI

CIRCLE 127 ON READER SERVICE CARD

Make
THE SOURCE
Your Source for
STABLE ISOTOPES

Isotec Inc. offers the scientific community one of the world's largest selections of stable isotopes and labelled compounds

^{18}O ^{15}N ^{13}C D

- NMR Solvents
- Reagents
- Organics
- Inorganics
- Biologicals

You Get More From THE SOURCE

- > 99% chemical purity
- High isotopic enrichment
- Competitive prices
- Fast delivery

Plus . . .

metal stable isotopes, helium-3 and other noble gas isotopes, other enriched stable isotopes, multiply-labelled compounds and custom synthesis

Call or write for your NEW complete price list today!

ISOTEC INC.
A Matheson, USA Company

3858 Benner Road, Miamisburg, OH 45342
(513) 859-1808 (800) 448-9760
Telex: 288278 Fax: (513) 859-4878

PittCon Booth #1843
CIRCLE 82 ON READER SERVICE CARD

CARRi-MED

THE NEW CARRI-MED CSL is the rheometer that meets all of your rheology measurement needs in one instrument. It's simple to use, versatile and accurate. The CSL offers sensitivity for both product research and applications uses. Our software enables Flow, Creep, Dynamic, Controlled Shear Rate and Low Shear Rate measurements, with analysis. Geometries include: Cone & Plate, Plate & Plate and Concentric Cylinder fixtures. CARRI-MED CSL is the most advanced and versatile rheometer on the market today.

Exclusively from
Mitech Corporation
1780 ENTERPRISE PKWY.
TWINSBURG, OHIO 44087
PH:216-425-1634 FAX:216-425-9254

. . . FOR VISCOUS FLUIDS MEASUREMENT

CIRCLE 117 ON READER SERVICE CARD

Pittsburgh Conference 2453

Add Real Value
to GC & GC/MS

Automate Injection Methods

LEAP's CTC A200S
Autosampler

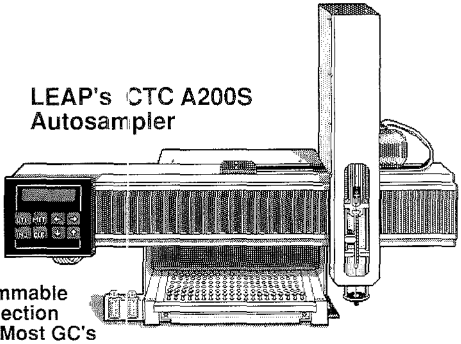

- Programmable
- Dual Injection
- Fits on Most GC's
- Variable Injection Rates

LEAP Technologies

P.O. Box 3220
Chapel Hill, NC
27515
Tel 800 229-8814
FAX 919 929-8956

CIRCLE 102 ON READER SERVICE CARD

A BRIEF ANALYSIS OF OUR NEW ICP-MS.

TERRIFIC.

ICP-MS technology took a giant leap forward with the introduction of the ELAN 5000. A product of the joint venture between SCIEX and Perkin-Elmer, the ELAN 5000 combines speed, ease of use and reliability into the next generation ICP-MS. With its small footprint, advanced computer, powerful software and single-button control of the vacuum system and ICP, the ELAN 5000 meets your demanding productivity and analytical requirements. For literature or more information, call toll-free 1-800-762-4000. The ELAN 5000. You have to use it to believe it.

PERKIN ELMER SCIEX

The Perkin-Elmer Corporation, Norwalk, CT 06859-0012

CIRCLE 143 ON READER SERVICE CARD

2:30 (1283) **A New Bonded Stationary Phase for the Separation of Volatile Halogenated Hydrocarbons for Environmental Application**—J. DE ZEEUW, Chrompack International b.v., D. Zwiep

2:50 (1284) **Applications of Electron-Capture and Sulfur-Chemiluminescence Detection in Supercritical Fluid Chromatography**—H.C.K. CHANG, VA Polytech Instit. & State Univ., L.T. Taylor

3:10 RECESS

3:25 (1285) **Application of Membrane Separation in the Determination of Phenolic Compounds by Flow Injection Analysis**—M.R. STRAKA, Alpkem Corporation, B. Karlberg

3:45 (1286) **Automation of GFAAS Analyses for EPA Contract Laboratory Samples**—G.R. DULUDE, Thermo Jarrell Ash Corporation, D.L. Pfeil, J.J. Sotera

4:05 (1287) **New Low Maintenance On-Line Total Organic Carbon Monitor for Water**—R. GODEC, Sievers Research, Inc.

4:25 (1288) **Stand-Alone Monitor for the Measurement of Sulfur-Containing Compounds in the Atmosphere**—R.L. BRENNER, University of Denver, D.H. Stedman, M.F. Legier

4:45 (1289) **A New Indicator and Test Paper for the Semiquantitative Determination of Carbaryl in Traces in Water**—H.S. RATHORE, Aligarh Muslim University, S.K. Saxena

Gas Chromatography—Instrumentation II

Thursday Afternoon, Room 1A08
C Schonhardt, Presiding
Perkin-Elmer Corporation

1:30 (1290) **Benefits of Using Guard Columns in Capillary Gas Chromatography**—C.M. Ross, Restek Corporation, D.M. Shelow

1:50 (1291) **A New, Novel Splitter Sleeve for Capillary Gas Chromatographs**—P.H. SILVIS, Restek Corporation, J.W. Walsh, D.M. Shelow, C.R. Vargo

2:10 (1292) **The Reality of 0.18mm ID Fused Silica Capillary Columns**—D.M. SHELOW, Restek Corporation, N.H. Mosesman, C.R. Vargo

2:30 (1293) **Applications of Automated Microsampling from Subnatents, Supernatents, and Small Volumes**—J.R BERG, Varian Instrument Group, C.K. Huston, Jr.

2:50 (1294) **Ideal Sample Injection: A Tool for Increasing Laboratory Productivity**—M. UEDA, Shimadzu Corporation, S. Miyoshi, S. Tanabe, S.D. Cubbedge

3:10 RECESS

3:25 (1295) **A New GC and SFC Element Specific Detector**—G. KNAPP, Graz University of Technology, A. Grillo, R. Gross, E. Leitern, M. Michaelis, B. Platzer, A. Schalk

3:45 (1296) **The Oxygen Specific Detector O-FID Practical Benefits for Naphtha, Gasoline, Flavor, and Fragrance Samples**—U.K. GOEKELER, ES Industries

4:05 (1297) **Double-Focusing Liquid On-Column Injection in Capillary Gas Chromatography**—C. BRYDEN, Hercules Inc.

4:25 (1298) **An Inert, Flexible Alternative to Glass Lined Stainless Steel Tubing**—R.D. ORMSBY, Restek Corporation, P.H. Silvis, J.W. Walsh

4:45 (1299) **Architecture and Design of a PC-Based Integrator for Chromatography**—G.T. PAUL, The Perkin-Elmer Corporation

HPLC—Instrumentation

Thursday Afternoon, Room 1E06
T.L.C de Souza, Presiding
Pulp & Paper Research Institute of Canada

1:30 (1300) **Evaluation of Biocompatible PEEK Columns for the Separation and Purification of Biopolymers**—D.L. GOODING, SynChrom, Inc., M.P. Nowlan

1:50 (1301) **Computer-Aided Optimization of HPLC Separations**—F. STEINER, Hewlett-Packard GmbH, A. Drouen

2:10 (1302) **Interactive, User-Directed, Computer-Assisted HPLC Methods Development**—F.F QI, University of New Hampshire, S.A. Tomellini

2:30 (1303) **Multi-Parameter Optimization in LC**—T.H. JUPILLE, LC Resources Inc., D.C. Lommen, J.W. Dolan, L.R. Snyder

2:50 (1304) **The Use of a Near Infrared Detector for Normal Phase HPLC**—T DICKENSON, College of St. Elizabeth, E.W. Ciurczak

3:10 RECESS

3:25 (1305) **LC Degassing Techniques: A Review and New Inexpensive Method**—V. BERRY, SepCon Separations Consultants, J. Fay

3:45 (1306) **Performance and Potential of Series-Coupled Columns in Liquid Chromatography**—R.A. HENRY, Keystone Scientific, Inc., J. Garver, R. Romesburg

4:05 (1307) **A New, Low Loss, Variable Volume Autosampler for Liquid Chromatography**—J.C. HODGIN, Alcott Chromatography, Inc., P.Y. Howard, M. Medley, K.C Cater, J. Thompson

4:25 (1308) **Do New Guaranteed 5% Phenylmethylsilicone Columns Provide Enhanced Chromatographic Properties When Compared to Conventional Capillary Columns**—P.J. SCHRYNEMEECKERS, CH2M Hill

4:45 (1309) **New Pyrene Column for Environmental Analysis**—J.D. MacFARLANE, JM Science Inc., N. Tanaka, M. Araki, S. Kubota

HPLC—Systems and Validation

Thursday Afternoon, Room 1A07
A.F. Fell, Presiding
University of Bradford

1:30 (1310) **Advantages of a Multi-Tasking Spectral Data System for Simultaneous Quantitative and Qualitative Analysis in Liquid Chromatography**—R. WEISZ, Spectra-Physics, Inc., C. Chell, D. Smith

1:50 (1311) **Design and Applications of an Advanced System for HPLC Methods Development**—J. SCHAEFER, Beckman Instruments, Inc.

2:10 (1312) **A User-Friendly Quality Control System with an Integrated Autosampler**—J.L. LINDAHL, Beckman Instruments, Inc., S.J. Luchetti, L.L. Robison

2:30 (1313) **An Advanced System Suitability Software Package**—S.P. HARRINGTON, Waters Chrom. Div. Millipore Corp., R.T. Hsu

2:50 (1314) **The Integrated LC Comes of Age?**—A. COLE, Perkin-Elmer Ltd., A.T. Rhys-Williams, A.F. Poile, N.B. Hetherington

3:10 RECESS

3:25 (1315) **Developing Robust LC Methods Using a Computer-Controlled LC System**—A. VITALI, Perkin-Elmer Italiana S.P.A., M.W. Dong, F.L. Vandemark, A.F. Poile

3:45 (1316) **An Instrumental Response to Increased Pressures for Improved Data Quality in Liquid Chromatography**—A. COLE, Perkin-Elmer Ltd., M. Upton, A.F. Poile

4:05 (1317) **Design Implications and Advantages of a Totally Integrated Liquid Chromatograph**—J. WELLAND, Perkin-Elmer Ltd., D.W. Bradwell, A.F. Poile

4:25 (1318) **System Suitability Testing in an Integrated Liquid Chromatograph**—A. COLE, Perkin-Elmer Ltd., A.F. Poile, A.T. Rhys-Williams

Analogic Announces A World Class NMR Spectroscopy System

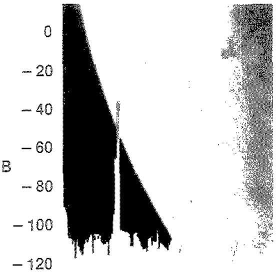

Unsurpassed Dynamic Range, Symmetric Broadband RF Design

Analogic, the world leader in precision signal acquisition and processing, announces a new NMR spectroscopy system, incorporating the latest advances in RF and digital technology. The ANMR9200 spectroscopy system is designed to meet the critical requirements of RF stability and purity as well as the computational requirements of today's 2-D experiments.

Basic features of the ANMR9200 NMR spectroscopy system include:

- ■ Unique patented sample loading and spinner mechanism
- ■ Comprehensive decoupling capability
- ■ Flexible Pulse-programming
- ■ Complete control of RF signal
- ■ Fully computerized shim system
- ■ 32-bit floating point data system with powerful enhancements
- ■ Deuterium lock system with frequency offset capability
- ■ Proven 16-bit A/D converter

And all of this in a compact, affordable package!

Analogic's ANMR9200 NMR system is available as a complete spectrometer or as a console replacement for existing high field NMR magnet systems. Contact us today for further information and availability. For superior spectroscopy performance, the world is turning to Analogic.

For Further Information: Analogic Corporation,
8 Centennial Drive., Peabody MA 01961
Tel: (508) 977-3000, X3312, Telex: 94-9307,
Intl Telex: 681-7021, Fax: (508) 531-0567

ANALOGIC®
The World Resource
for Precision Signal Technology

CIRCLE 11 ON READER SERVICE CARD

.003%

WE'RE STILL NOT SATISFIED. For every 100,000 reagents, high-purity solvents, and chromatography products we shipped last year, we received only three valid customer complaints. But as far as we're concerned, that's still three too many. For a free catalog, call **1-800-222-0342.**

EM SCIENCE
We have service down to a science.

A Division of EM Industries, P.O. Box 70, 480 Democrat Road, Gibbstown, NJ 08027
Associate of E. Merck, Darmstadt, W. Germany

CIRCLE 54 ON READER SERVICE CARD

At the cutting edge of weighing technology... Johnson-Precisa

- User-friendly programmable
- Automatic calibration
- Analog and digital outputs
- 3-year warranty
- World-wide sales and service

For detailed information, write or call Johnson Scale Co.
P.O. Box 1329
West Caldwell, NJ 07006
Tel: (201) 226-2100
FAX: (201) 882-8068

If you're about to place a balance order...STOP. Are you sure you're buying the latest in microelectronics and weighing technology? Like you'll find in Swiss-made Johnson-Precisa balances. Designed to give you easier, more reliable results. In weighing ranges starting at 0.01 mg, to 12,000 g.

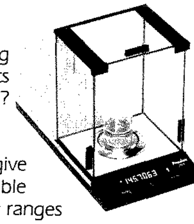

ConF USR
User configuration

Unit 1 g
Unit 1, grams

15.02.89 D.M.Y
Day, month and year

15.34.50 H.M.S
Hours, minutes, seconds

CAL AUT
Automatic calibration

Print St
Print a stable weight

Tone response to button pressed
Sound on

Johnson PRECISA
The Balance People™

CIRCLE 85 ON READER SERVICE CARD

SAMPLE PREPARATION BOMBS FOR TRACE METAL ANALYSIS

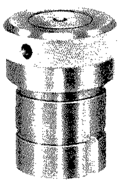

Available in a variety of sizes and styles, our teflon-lined **Acid Digestion Bombs** are designed for microwave and convection heating. Use them to treat inorganic samples in HF, HCl and other strong mineral acids.Or to digest organic samples in strong alkali or oxidizing acid at elevated temperatures and pressures.

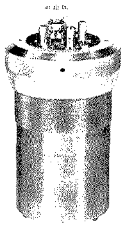

Our **Oxygen Combustion Bombs** decompose any combustible solid or liquid — quickly and completely. The sealed bomb contains and converts materials to a soluble form while allowing complete recovery of all elements. Now available in a new longer-lasting material for high halogen-containing substances.

For complete details ask for our free Brochure #4700.

PARR INSTRUMENT COMPANY
211 Fifty-Third Street
Moline, IL 61265
309-762-7716
Telex: 270226
Fax: 309-762-9453

CIRCLE 146 ON READER SERVICE CARD

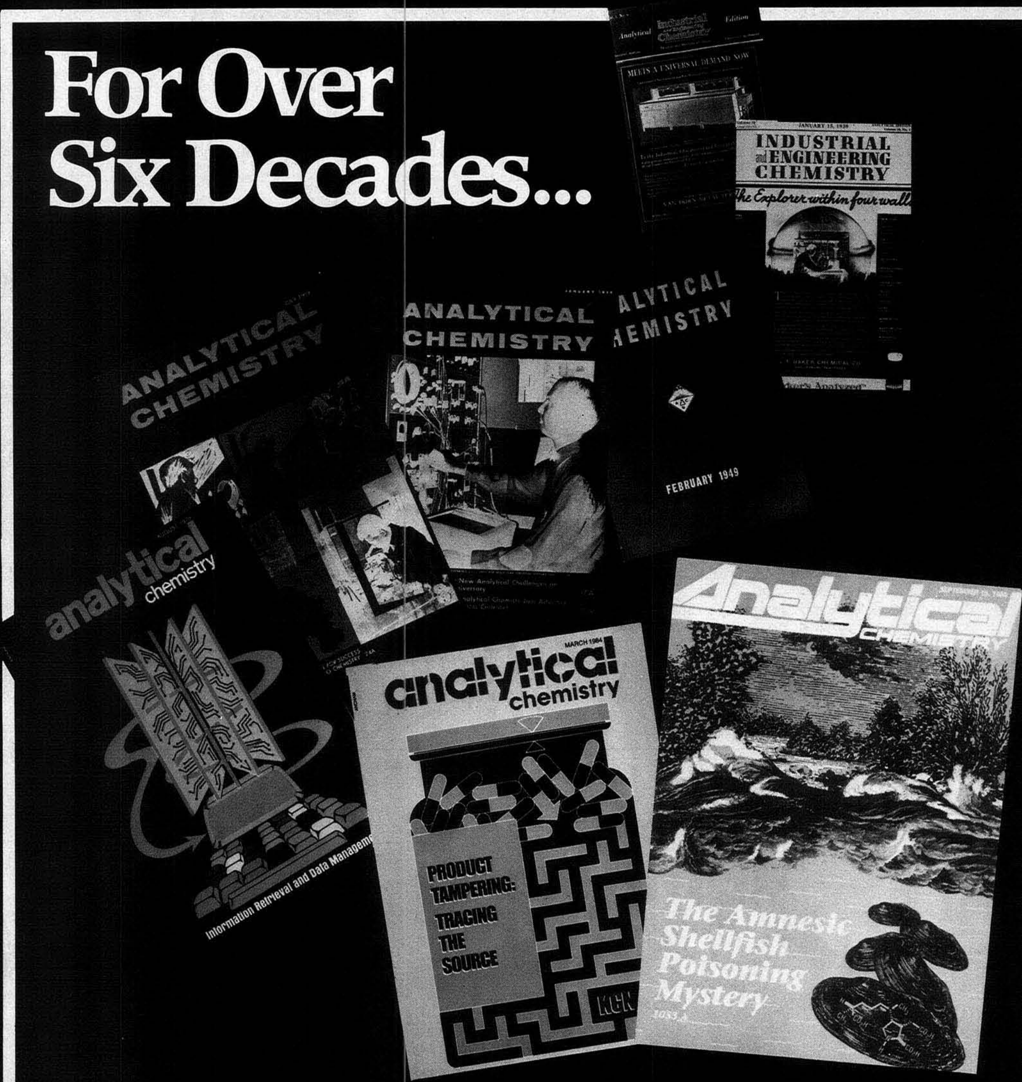
INDUSTRIAL and ENGINEERING CHEMISTRY
ANALYTICAL CHEMISTRY
FEBRUARY 1949
analytical chemistry
Information Retrieval and Data Management
MARCH 1984
PRODUCT TAMPERING: TRACING THE SOURCE
Analytical CHEMISTRY
The Amnesic Shellfish Poisoning Mystery

For Over Six Decades...

The Leader in the Field.

ANALYTICAL CHEMISTRY, the world's foremost publication in the vital field of measurement science, comes to you semi-monthly packed with *more* research articles, special features and application papers.

Keeping pace with the changes has continued to make *ANALYTICAL CHEMISTRY* the pinnacle of publications in the field . . . for over 6 decades.

For your personal subscription:

CALL TOLL FREE (800) 227-5558 (U.S. only)
Outside U.S. (202) 872-4363

Telex: 440159 UI
89 2582 ACSPUBS

American Chemical Society
1155 16th St., NW
Washington, DC 20036

4:45 (1319) **An Integrated Approach to Instrument Control, Data Acquisition and Presentation in Liquid Chromatographic Analysis**—M. UPTON, Perkin-Elmer Ltd., N.B. Hetherington, A.T. Rhys-Williams, A.F. Poile

Infrared V—Hyphenated Techniques and Infrared-Raman

Thursday Afternoon, Room 1E18
R.J. Jacobsen, Presiding
IR-ACTS

1:30 (1320) **Detection Limits for Organic Compounds Examined by Light Pipe GC/FTIR**—K.D. KEMPFERT, Nicolet Instrument Corporation, F.J. Weesner

1:50 (1321) **A Comparison of Methods for Spectral Coaddition of Gas Chromatography/Fourier-Transform Infrared Spectroscopy Data**—D.S. BLAIR, Sandia National Laboratories, K.J. Ward

2:10 (1322) **Novel GC-FTIR Techniques in the Analysis of Methoxymethanol**—R.A. JOHNSON, U. S. Army Missile Command

2:30 (1323) **An Evaluation of Mass Spectrometry and Fourier Transform Infrared Quantitation Techniques for Environmental Analysis**—D.F. GURKA, U. S. Environ. Protection Agency, I. Farnham, R. Titus

2:50 (1324) **Enhanced Characterization of Natural Products with Combined GC/FTIR/MS Using Selected Wavelength Chromatography, Extracted Ion Profiles, and Specialized Spectral Libraries**—R.J. LEIBRAND, Hewlett-Packard Company

3:10 RECESS

3:25 (1325) **LC-FTIR: Dynamics within the Particle Beam Interface**—K.R. EDMAN, Georgia Institute of Technology, R.F. Browner, J.A. de Haseth

3:45 (1326) **Specific Advantages in Combining TG/FTIR with GC/FTIR and GC/MS in the Analysis of Complex Samples**—G.L. McCLURE, The Perkin-Elmer Corporation, R.B. Cassel, A.J. Patkin

4:05 (1327) **Variable-Pressure Infrared and Raman Spectroscopic Studies of Orientationally-Disordered Solids**—N.T. KAWAI, McGill University, I.S. Butler, D.F.P. Gilson

4:25 (1328) **Resonance Raman, FTIR, and Vibrational Circular Dichroism Studies of Azide Binding in Hemoglobin and Myoglobin**—P.J. LARKIN, University of Pittsburgh, S.A. Asher, R.W. Noble, T.B. Freedman, L.A. Nafie, B.A. Springer, S.G. Sligar

4:45 (1329) **FTIR and Raman Characterization of Molecular Interactions at Chromatographic Surfaces**—M.R. O'GRADY, VA Polytechnic Inst. & State Univ., C.M. Conroy, L.T. Taylor, R.A. Henry, L.F. Wieserman

Mass Spectrometry General/Data Systems

Thursday Afternoon, Room 1E13
S.K. Viswanadham, Presiding
University of Pittsburgh

1:30 (1330) **High Sensitivity NCI-MS Analysis of Selected Drugs**—S. MAZER, Hewlett-Packard Company, P.C. Goodley

1:50 (1331) **Chloride Attachment Negative Ion Mass Spectra of Sugars by LC-APE Mass Spectrometry**—K. OGAN, Hitachi Instruments, Inc., F. Nakajima, T. Mimura, Y. Kato

2:10 (1332) **An Instrument Specification Sample Mixture for Dynamically Coupled Gas Chromatographic/Mass Selective Detection Systems**—M.L. PERRY, VA Polytechnic Inst. & State Univ., G.A. Reiner, H.M. McNair

2:30 (1333) **Determination of Gas-Phase Metal-Ligand Bond Strengths by Low-Energy Collision-Induced Dissociation**—R.H. SCHULTZ, University of Utah, P.B. Armentrout

2:50 (1334) **Chemical Structural Investigation of Benzoguanamine-Formaldehyde Resins by Field Desoprtion Mass Spectrometry**—H. SUGITANI, Hitachi Chemical Co. Ltd., M. Fukasawa, T. Ezure

3:10 RECESS

3:25 (1335) **Management and Improvement of a Mass Spectral Database: Strategies for Quality Control, and Generation of Better Search Algorithms**—S.G. LIAS, Nat'l. Inst. Standards & Tech., S.E. Stein

3:45 (1336) **Use of Correlation Analysis of Mass Spectrometry**—K.G. OWENS, Drexel University, J.P. Reilly

4:05 (1337) **High-Speed Acquisition of Mass Spectra Using an Unmodified Quadrupole Mass Spectrometer**—C.A. JAMES, Hewlett-Packard Company

4:25 (1338) **A Program of Identification of Functional Groups from Mass Spectra**—Q. HONG, Dalian Inst. of Chemical Physics, D. Zhu, B. Yang, C. Xu

4:45 (1339) **An Interactive Rule Generation System for Mass Spectrum/Substructure Correlation**—B. YANG, Dalian Inst. of Chemical Physics, D. Zhu, J. She, Q. Hong, P. Liu, C. Xu, P. Lu

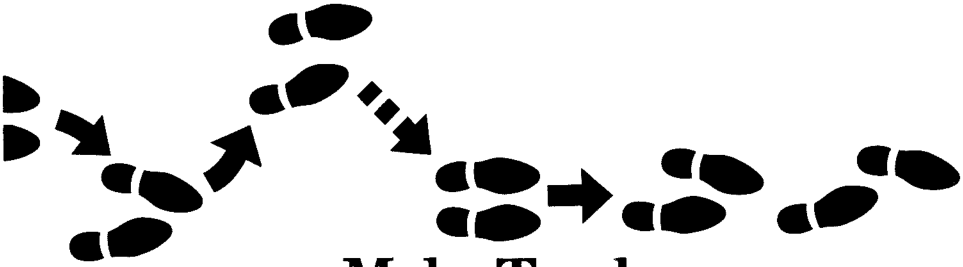

Make Tracks
to our booth at the Pittsburgh Conference.
You'll be taking steps in the right direction.
Booth No. 1829
See the new and revolutionary Aquatest MS analyzer featuring
modular technology for today's changing laboratory needs...PLUS,
Aquatest Pyrolysis Unit I and Photovolt 577 Gloss & Reflectance Meter.

PHOTOVOLT
Division of Seradyn, Inc.
A Subsidiary of
Mitsubishi Kasei Corporation
1200 Madison Avenue • Indianapolis, IN 46225 U.S.A.

For more information or a demonstration call toll-free: 1-800-222-5711. In Indiana, call collect: 317-266-2075.
FAX: 1-317-266-2991 • TELEX: 8102601940.

CIRCLE 137 ON READER SERVICE CARD

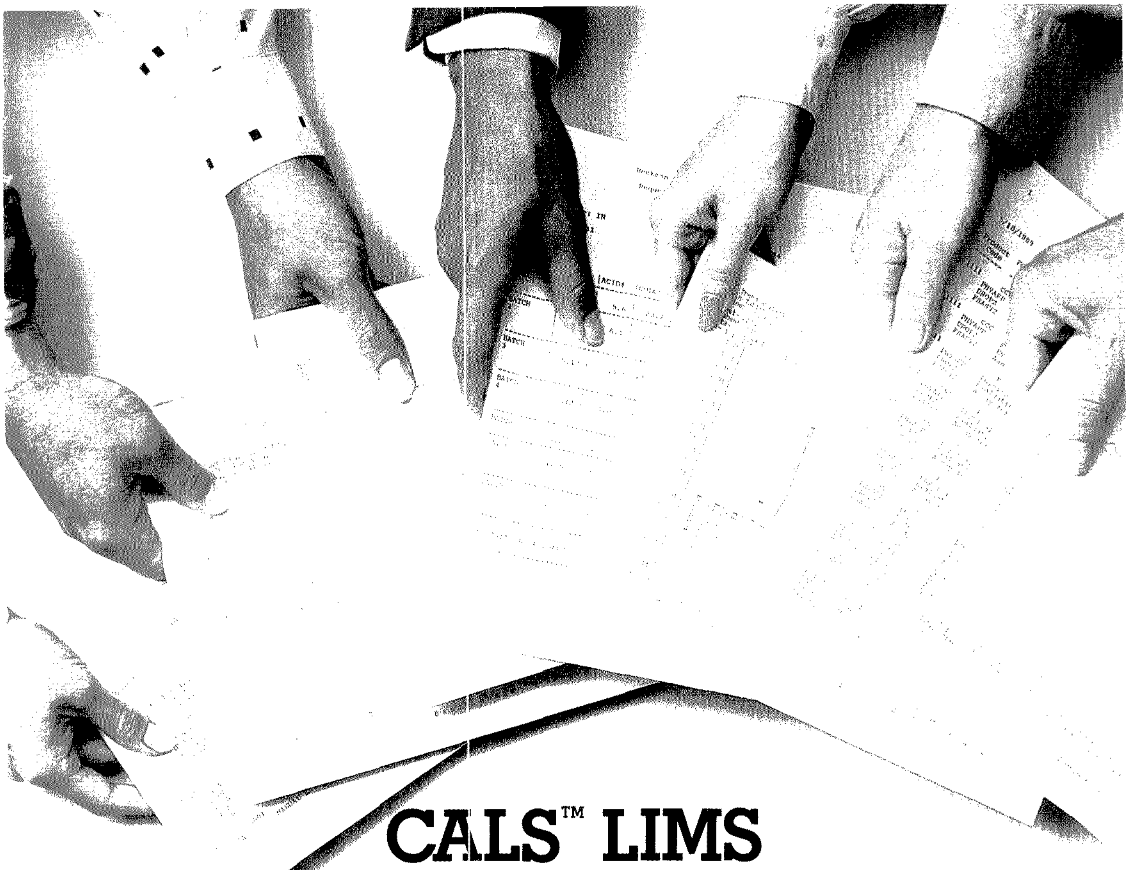

CALS™ LIMS
We do it all.

CALS has grown into the most versatile and capable LIMS available today. Because every lab has unique requirements, we have made CALS a flexible program that can be tailored to fit your own lab needs.

CALS can do it all. And can do it better ... beginning with a software program that put lab automation at your fingertips — CALS has added one capability after another, many of them exclusive.

Lab Manager™, the heart of the CALS family of products, is a fully-functional LIMS that manages your samples and converts your data into valuable information.

There is *PeakPro™* ... to automate chromatography labs. Then options like *ICMS* ... for instrument calibration and maintenance schedules. And *IDAS* ... a system that connects the LIMS with your instruments to schedule testing and collect results. This greatly increases productivity and reduces transcription errors. And the Stability option, to schedule, manage and report all stability testing and shelf life studies.

Exciting new capabilities have been developed ... like a powerful and easy-to-use transaction processor that links CALS to your other computer systems. And *BIOASSAY* ... to help laboratories in pharmacokinetics and drug metabolism studies. There is also *AUTOLOG*, to schedule routine samples automatically, reducing tedious log-in functions found in the process industries.

Today, as testimony to the usefulness — and uniqueness — of CALS, you will find it installed in over 300 laboratories around the world. CALS users find that Beckman is always there to back them with effective training courses, technical support and service, and with the Beckman Software Enhancement and Maintenance (SEAM) program that keeps their systems up-to-date with the very latest enhancements.

For more information on the most up-to-date, most complete LIMS available anywhere, call
(201) 818-8900 or write to Beckman Instruments, Inc.,
90 Boroline Road, Allendale, NJ 07401

See us at PittCon, Booth #5005

BECKMAN

CALS, Lab Manager and PeakPro are registered trademarks of Beckman Instruments, Inc.

CIRCLE 28 ON READER SERVICE CARD

New Instrumentation for Chromatography

Thursday Afternoon, Room 1E16
R. Hamilton, Presiding
Millipore Corporation

1:30 (1340) **Surface-Enhanced Raman Spectroscopy as a Detector for High Performance Liquid Chromatography and Flow Injection Analysis**—N.J. POTHIER, University of Rhode Island, R.K. Force

1:50 (1341) **A Laser-Induced Photoionization Detector for Liquid Chromatography**—V.L. McGUFFIN, Michigan State University, J.W. Judge

2:10 (1342) **Specific Nitrogen Gas Chromatography Detectors Based on Chemiluminescence**—L.O. COURTHAUDON, Antek Instruments, Inc., E.M. Fujinari, A.J. Britten

2:30 (1343) **A Flexible Automatic Liquid Handling System for the Automation of Liquid Chromatography and Routine Spectrophotometers**—M. RETZIK, Hitachi Instruments, Inc., H. Kaji, G. Hirata

2:50 (1344) **The Determination of Deuterium by GC-MIP Atomic Emission Spectrometry**—S.R. GOODE, University of South Carolina, J.J. Gemmill

3:10 RECESS

3:25 (1345) **Chromatographic Interfaces and Applications of an Extended Range Supercritical Fluid Extractor/Accumulator**—S.G. YOCKLOVICH, Computer Chemical Systems, Inc., T.W. Ryan, S. Lurcott, B.L. Bergman, E.J. Levy

3:45 (1346) **Automated Sampling of Process Water Streams for Analysis by Purge and Trap Gas Chromatography**—R.G. WESTENDORF, Tekmar Company, M. Mason-Helm

4:05 (1347) **Design and Performance of an Automatic Static Headspace Analyzer**—R.G. WESTENDORF, Tekmar Company, H.J. Lehan

4:25 (1348) **Recent Developments for Enhancement of GC-FTIR Sensitivity**—D.E. ROBERTS, Mattson Instruments, Inc.

4:45 (1339) **An Interactive Rule Generation System for Mass Spectrum/Substructure Correlation**—B. YANG, Dalian Inst. of Chemical Physics, D. Zhu, J. She, Q. Hong, R. Liu, C. Xu, P. Lu

New Instrumentation—General

Thursday Afternoon, Room 1E21
H.Y. Aboul-Enein, Presiding
King Faisal Specialist Hospital

1:30 (1350) **CHEMFET Sensors and Biotelemetry**—J. McCARTHY, McGill University, W.C. Purdy

1:50 (1351) **Improved Density Measurements with High Resolution Helium Pycnometry**—R.W. CAMP, Micromeritics Instrument Corp., W.P. Hendrix, Jr., T. Sibert

2:10 (1352) **New Advances in Automated Ion Testing: Development of a Combination Flow Injection Analysis/Segmented Microcontinuous Flow Analysis System for the Analytical Lab**—M.R. STRAKA, Alpkem Corporation

2:30 (1353) **Linear Titrations of Thioethers**—J.A. LYNCH, University of Tennessee at Chattanooga, R.I. Breazeale, S.T. Holder, J.W. Thomte, E.T. Lane

2:50 (1354) **Simultaneous Nitrogen and Sulfur Analysis**—J.R. CRNKO, Antek Instruments, Inc. R.D. Brooks

3:10 RECESS

3:25 (1355) **A Random Access Medical Analyzer Used for Traditional Industrial Chemical Analysis**—P.M. WEST, Eli Lilly and Company

3:45 (1356) **Evaluation of a Commercially Available POA Autosampler: Comparison to Conventional Manual and Automated Purge and Trap/GC/MS Instruments**—J.M. SOROKA, USEPA, A. Goldberg, R. Coismain, D. Lillian

4:05 (1357) **Reinforced Nafion Tube Devices for Drying and Dialysis**—J. KERTZMAN, Perma Pure Products, Inc.

4:25 (1358) **Beam Induced Damage in Organic Targets**—M. CHOLEWA, The University of Melbourne

4:45 (1359) **A New Type of Instrument for Quickly Determining the Molecular or Fiber Orientation of Poly(vinyl alcohol) Film or Nonwoven Fabrics by Use of Microwave Method**—S. OSAKI, Kanzaki Paper Mfg. Co., Ltd.

Novel Separation Extraction Detection Techniques

Thursday Afternoon, Room 1E11
G.L. Vassilaros, Presiding
Crucible Materials Corporation

1:30 (1360) **The Impact of Derivatized Cyclodextrins on Chromatographic Separations**—D.W. ARMSTRONG, University of Missouri-Rolla

1:50 (1361) **Advantages of the Use of Size Exclusion Chromatography and a Diode Array Detector to Identify UV-Cure Initiators**—N.L. HESSEFORT, PRA Labs, P.A. Frisbie

NEW GENERATION TIME-OF-FLIGHT SIMS
TFS SURFACE ANALYZER

Now you can simultaneously image with high mass resolution!

Surface Microanalysis of:
- Polymers
- Pharmaceuticals
- Semiconductors
- Biomolecules
- Ceramics

Applications In:
- Organic Microanalysis
- Tissue Targeting
- Wafer Contamination
- Particle Analysis

CHARLES EVANS & ASSOCIATES
SPECIALISTS IN MATERIALS CHARACTERIZATION
301 Chesapeake Dr., Redwood City, CA 94063
(415) 369-4567 Telex 172747 FAX (415) 369-7921
See us at PittCon in booth 3209

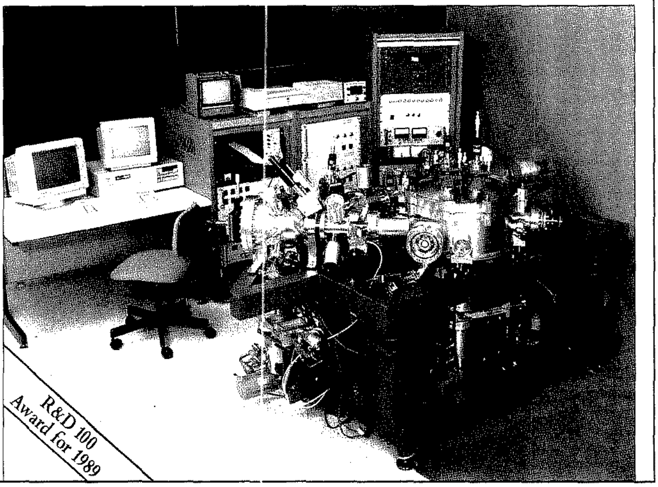

CIRCLE 52 ON READER SERVICE CARD

THE MORE
FEATURES AN
ICP SPECTROMETER
HAS THE MORE
IT COSTS
RIGHT?

WRONG.

Using your valuable input, we made our Plasma 1000 and Plasma 2000 the fastest, most accurate ICP emission spectrometers in the industry. Better yet, we made them more affordable. Both models offer a high-resolution scanning optical system, powerful computer and high speed monochromators. They also come with a computer-controlled ICP which provides total automation of RF power, gas flows and sample uptake. For literature or more information, call toll-free 1-800-762-4000. We gave you just what you wanted — more features for less money.

PERKIN ELMER

The Perkin-Elmer Corporation, Norwalk, CT 06859-0012

CIRCLE 144 ON READER SERVICE CARD

Dry, sterilize or bake to perfection–automatically!

Blue M's combination gravity oven and dry-air sterilizer line operates in a temperature range from +20 C above ambient to 300 C. New solid-state, electronic Pro-Set II® control delivers main temperature control and independent overtemperature protection. It's capable of maintaining oven temperature to ±0.5 C. Setpoints are adjustable to 1 C resolution.

See your laboratory distributor for full details or write for your copy of the Blue M scientific equipment catalog today. Lindberg/Blue M, A Unit of General Signal, 304 Hart Street, Watertown, WI 53094. Phone 414-261-7000 • FAX 414-261-0925.

1389A

LINDBERG/BLUE M
A UNIT OF GENERAL SIGNAL

CIRCLE 92 ON READER SERVICE CARD

New from Elsevier and the American Society for Mass Spectrometry!

FREE SAMPLE COPIES AVAILABLE

JOURNAL OF THE AMERICAN SOCIETY FOR MASS SPECTROMETRY

EDITOR-IN-CHIEF:
Michael L. Gross, *University of Nebraska – Lincoln*
ASSOCIATE EDITORS:
Kelsey D. Cook, *University of Tennessee*
Simon Gaskell, *Baylor Medical College*
Gary L. Glish, *Oak Ridge National Laboratory*
R.S. Houk, *Iowa State University*

The Journal of the American Society for Mass Spectrometry publishes refereed, original research papers from all fields of scientific inquiry in which mass spectrometry can play a role, including developments in both fundamentals and applications. Contributors investigate new instrumentation and methods, present new discoveries in ion chemistry, and develop problem-solving strategies. The Journal also publishes *Short Communications*, which contain ideas for which some experimental or theoretical justification is presented (usually to be followed by a full paper), and *Accounts and Perspectives*, including brief review articles and reflections on the state of research in mass spectrometry.

ISSN 1044-0305
1990, Volume 1 (six issues)
Subscription rate $235.00 (outside USA, add $24.00 for postage)
Send North American sample copy requests and all subscription orders to
Elsevier Science Publishing Co., Inc., P.O. Box 882, Madison Square Station, New York, NY 10159
Send all other sample copy requests to **Elsevier Science Publishers**, P.O. Box 211, 1000 AE Amsterdam, The Netherlands
For fastest service when subscribing or requesting a sample issue, call **(212) 633-3950**, or FAX your request to **(212) 633-3990.**

D5AY ELSEVIER 1/90

CIRCLE 50 ON READER SERVICE CARD

2:10 (1362) **Quantitative Structure-Retention Relationship Studies of Odor-Active Aliphatic Compounds with Oxygen-Containing Functional Groups**—L.S. ANKER, The Pennsylvania State Univ., P.C. Jurs, P.A. Edwards

2:30 (1363) **Supercritical Fluid Extraction of Organics from Water Matrix Samples**—J.B. PAWLISZYN, University of Waterloo, M. Colquhoun, N. Alexandrou

2:50 (1364) **Comparison of Column Extraction Methods for Oxygenated Fatty Acids in Mammary Tissue Based on Analysis by Capillary GC-MS**—E.M. YUREK, Michigan State University, C.C. Sweeley, C.W. Welsch, J.T. Watson

3:10 RECESS

3:25 (1365) **Application of Liquid Chromatography in Overcoming Ligand Instability in Commercial, Chelated Iron-Hydrogen Sulfide Oxidation Process Catalysts**—D. McMANUS, ARI Technologies, Inc.

3:45 (1366) **The Use of a Hollow Fibre Liquid Supported Membrane for Separation and Concentration of Vanadium in Low Level Samples**—M. VALIENTE, Univ. Autonoma de Barcelona, M. Munoz, C. Palet

4:05 (1367) **Applications of Fully Automated Sample Preparation with Liquid-Solid Extraction**—B. PICHON, Gilson Medical Electronics S.A., A. El Sayed

4:25 (1368) **Optical Isomer Separations on Microcrystalline Tribenzoylcellulose**—R. WERNICKE, Riedel-de Haen AG

4:45 (1369) **Qualitative Separation of Metal Ions in Tube Well Water Samples by Thin Layer Partition Chromatography**—R.B. KHARAT, Institute of Science, L. Deshmukh

On-Line; In-Line; Quality Control; Process Analysis

Thursday Afternoon, Room 1E12
M. Feldman, Presiding
E. I. du Pont de Nemours & Co., Inc.

1:30 (1370) **Statistical Methods for Monitoring and Maintenance of NIR Calibrations**—M.J. BLACKBURN, Cargill, Inc., J.T. McDonald, N.J. Weeks, III

1:50 (1371) **Evaluation of Globally-Based Near Infrared Calibrations on In-Process Agricultural/Feed Samples**—J.T. McDONALD, Cargill, Inc., M.J. Blackburn

2:10 (1372) **On-Line Process Analysis of Nylon-Barrier Multilayer Extrusions**—D.W. VIDRINE, Measurex Corporation, D. Marrow

2:30 (1373) **Applications of Near-Infrared Spectroscopy for the Analysis of Pulp and Paper**—P.J. BRIMMER, NIRSystems, Inc.

2:50 (1374) **Application of Fiber-Optic (Spectro)Photometry to the Monitoring of Uranium and Plutonium in Nuclear Fuel Process Streams**—J. BURCK, Kernforschungszentrum Karlsruhe, K. Kramer, W. Konig

3:10 RECESS

3:25 (1375) **Continuous HCl Monitoring in Stack Gas Incinerators**—G. POPPE, Bran-Luebbe Analyzing Tech., Inc.

3:45 (1376) **Stack Effluent Analysis Using On-Line Mass Spectrometry**—L. KEPHART, Extrel Corporation, S.N. Ketkar, J.D. Buchner

4:05 (1377) **Coupling FIA with an Ion-Selective Electrode for an On-Line Determination of Trace Levels of Chloride in 20% Caustic**—K. HOOL, Dow Chemical Company, E.D. Yalvac

4:25 (1378) **Ammonia Production Control Using Process Mass Spectrometry**—C.[illegible] WEAVER, Extrel Corporation, G.D. Cessna

4:45 (1379) **On-Line Micro-Distillation Apparatus for Segmented-Flow Analyzers**—S.C. COVERLY, Bran+Luebbe, M. Sahn

Spectrometric Instrumentation and Techniques

Thursday Afternoon, Room 1E20
A.J. Sharkins, Presiding
Aluminum Company of America

1:30 (1380) **Collinear Photothermal Deflection Spectroscopy with Light-Scattering Samples**—J.D. SPEAR, Lawrence Berkeley Laboratory, R.E. Russo, R.J. Silva

1:50 (1381) **Near Infrared Laser Diode Intracavity Spectroscopy: A New Versatile Analytical Tool**—G. PATONAY, Georgia State University, D. Andrews-Wilberforce, [illegible] Hicks

2:10 (1382) **Development of a High Performance Scanning Fluorescence Detector for Use with HPLC**—J.G. WANGSGAARD, Linear Instruments Corporation, D.J. Bornhop, L. Hlousek

2:30 (1383) **Advantages and Disadvantages of Remote Fiber Optic Sensing for Fluorescence**—K.J. RUBELOWSKY, SPEX Industries, Inc., W.S. Slutter, R. Kaminsky

2:50 (1384) **Advantages of Simultaneous Dual Wavelength Frequency Domain Fluorescence**—J.R. MATTHEIS, SLM Instruments, Inc., V. Tyagi, S. Grossman

It's A Dirty Job, But We Can Handle It.

"The sample is almost water...

Just a little dirty...but that's today's river water for you...

Tomorrow's samples are in... Great... Sewage, sludges and solids.

Oh well... my Purge & Trap system and I can handle almost anything."

Seem familiar?...Very!

Samples:
Water, Sludges, Soils & Air Tubes

Automation:
16 Sample Discrete Purging

Concentration:
Quantitative Trapping
Rapid Desorption
Trace Water removal

Separation:
Complete Systems with the Worlds Leading GC (HP)

Real world samples place tough demands on your equipment. O I Analytical designs and manufactures the most complete line of systems for environmental analyses in the world. Recognizing the fact that sampling and detection systems are intimately coupled has resulted in designing these components to work as a system, not a collection of parts.

Anyone can offer pieces and parts, but O I Analytical provides an entire system backed by field support and on-site repair and training.

Detection:
4420 Electrolytic Conductivity Detector (ELCD)
4430 Photoionization Detector (PID)
4440 ELCD/PID Tandem (no transfer lines)
4450 PID/FID Tandem (great for fuels analysis)

Support: Complete System Support and Training

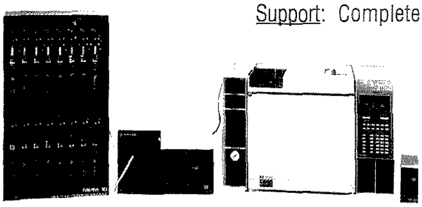

The real world is full of surprises. Compatibility of Lab Equipment shouldn't be one of them. For the fundamental solution...Call (409) 690-1711

O·I·Analytical

CIRCLE 134 ON READER SERVICE CARD

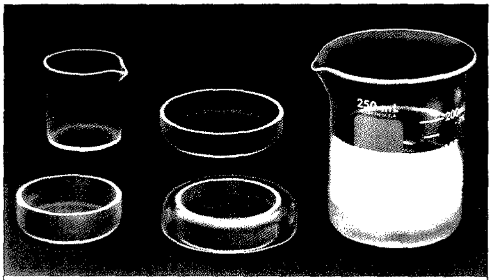

AVOID LABWARE CONTAMINATION

With High Purity Molded Fused Quartz Labware

PYROQUARTZ™ beakers and Petri dishes permit bacteriological, mycological and other laboratory work to be performed virtually free of vessel-source leaching contamination that can cause spurious results.

Orders of magnitude more pure than conventional laboratory glassware, PYROQUARTZ™ permits ultra-controlled environments free of contaminants found in conventional laboratory ware (see chart below).

Typical Analysis, ppm

Material	Al	Na	P	B
Pyroquartz™	15	<1	<1	<1
Borosilicate	14,800	35,500	30	38,200
96% Silica	1,000	25	10	11,000

Let us quote your labware for critical requirements. Our patented powder forming, high temperature sintering technology produces labware noted for high purity, chemical inertness, high temperature stability and thermal shock resistance.

PYROMATICS®

SILICA TECHNOLOGY
P.O. Box 764, 3985 Ben Hur Avenue
Willoughby, OH 44094
Phone: (216) 951-3985
Telex: 980374
FAX: (216) 951-8728

VISIT PYROMATICS BOOTH 6132 PITTSBURGH CONFERENCE

CIRCLE 140 ON READER SERVICE CARD

ACS Software

High-quality software programs for the personal computer that meet the standards you expect from the ACS

For information about ACS SOFTWARE, call TOLL FREE (800) 227-5558 or write to:

American Chemical Society,
Marketing Communications Dept.,
1155 Sixteenth Street, N.W.,
Washington, D.C. 20036

3:10 RECESS

3:25 (1385) **Measurement of Fluorescence Lifetimes for Multicomponent Systems at Submillisecond Rates**—K.M. SWIFT, SLM Instruments, Inc., G.W Mitchell

3:45 (1386) **Performance of a Miniature Diode Array Spectrometer**—J.T BROWNRIGG, American Holographic, Inc., C.S. Hatch, T.L. Mikes

4:05 (1387) **A Remote Fiber Optical Process Photometer System**—H. DANIGEL, Ciba-Geigy AG, G. Michel

4:25 (1388) **Novel Approaches to Total Fluorescence Spectroscopy Using a New Fluorescence Spectrometer**—S.R. HUCKINS, Perkin-Elmer Ltd., A.T. Rhys-Williams

4:45 (1389) **Measurement of Fluorescence Lifetimes by a Stroboscopic Optical Boxcar Technique**—D.R. JAMES, Photon Technology Int'l. Inc., W.R. Ware

Friday, March 8, 1990

SYMPOSIUM

User-Manufacturer Information Exchange Symposia

These symposia consist of overview lectures, presentations by panelists from vendor companies, and open question and answer sessions among the audience and panelists. Four UMIX will be offered:

Chromatography Data Systems, organized by E.J. Kikta, Jr.

Inductively Coupled Plasma Spectroscopy, organized by J.E. Paterson

Liquid Chromatography-Mass Spectrometry, organized by L.K. Wong

Near Infrared Spectroscopy, organized by E. Baughman

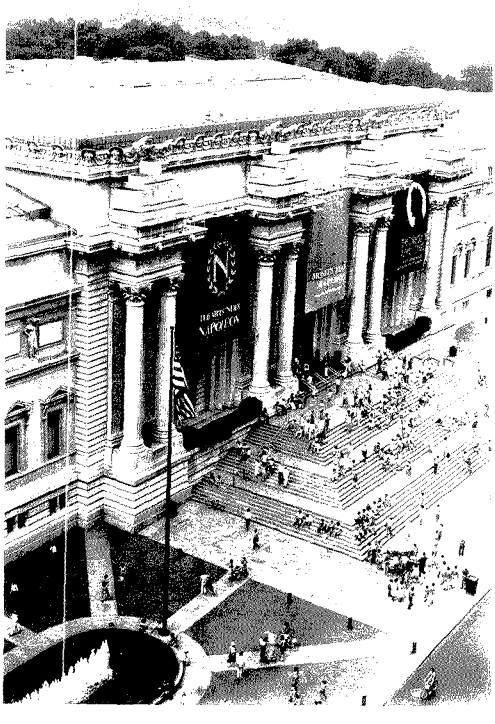

SOLUTIONS *Number 3*

An Update on the State of the Art in Separations Technology

ew detector combines conductivity and amperometry.

The Dionex PED (Pulsed Electrochemical Detector) is the first to offer conductivity and amperometry measurements in one powerful detector. Both techniques are strong alternatives to low-wavelength UV and refractive index detection for non-chromophoric compounds. For many compounds, these electrochemical methods are often more sensitive and specific than UV.

PED is the perfect complement to UV. When used in series with UV, PED virtually guarantees that anything eluted from the column will not be missed. Together, PED and UV provide the most universal detection scheme short of mass spectrometry.

Pulsed Electrochemical Detection

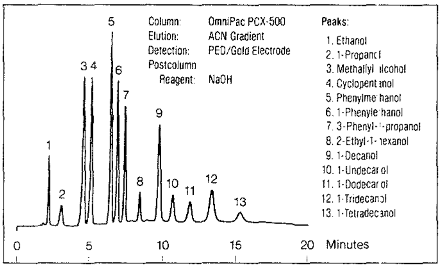

Pulsed amperometric capabilities allow selective detection of alcohols.

Detection of Amines and Inorganic Cations with PED

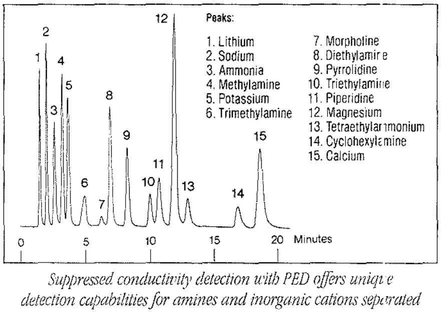

Suppressed conductivity detection with PED offers unique detection capabilities for amines and inorganic cations separated on the new OmniPac™ column.

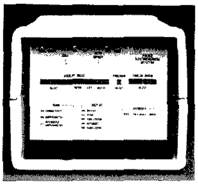

Detection With and Without Chemical Suppression

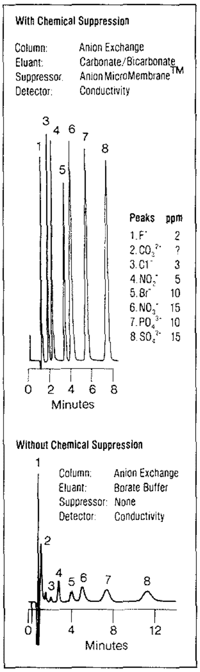

Chemically suppressed conductivity detection dramatically improves signal-to-noise ratio, lowering minimum detection limits by as much as an order of magnitude over conventional conductivity detectors.

In the pulsed amperometry mode, PED excels in detecting alcohols, amines, thiols, sulfides, and carbohydrates. In the conductivity mode, PED will detect virtually any ionic or ionizable compound, including inorganic ions, carboxylic acids, and amines.

Dionex's patented chemical suppression technology expands the conductivity detection capabilities of PED to give unmatched sensitivity and specificity. Chemical suppression increases analyte response by at least tenfold.

It suppresses background noise by chemically reducing eluant conductivity. It converts OH and H+ into water, providing the greatest linearity and widest dynamic range available for conductivity detection.

or complete information or to discuss your application, contact your local Dionex representative or (in U.S.A.) call 1-800-227-1817, ext. 42.

DIONEX

A BETTER SOLUTION

Dionex Corporation, P.O. Box 3603, Sunnyvale, CA 94088-3603. **Canada** Dionex Canada, Ltd., (416) 855-2551. **England** Dionex (UK) Ltd., (0276) 691722, **West Germany** Dionex GmbH, (06126) 6036, **France** Dionex S.A., (1) 46216666, **Italy** Dionex S.r.l., (06) 3792979, **Netherlands** Dionex B.V., (076) 714800

©1989 Dionex Corporation

SEE US AT PITTCON — BOOTH # 5520 CIRCLE 42 ON READER SERVICE CARD

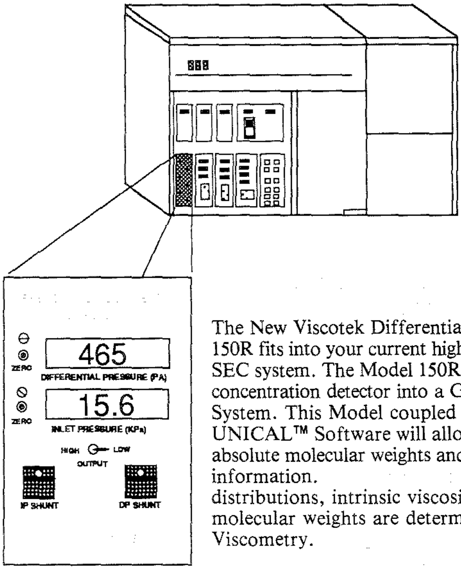

The New Viscotek Differential Viscometer Model 150R fits into your current high temperature GPC/SEC system. The Model 150R converts your plain concentration detector into a GPC-VISCOMETRY System. This Model coupled with Viscotek's UNICAL™ Software will allow you to determine absolute molecular weights and polymer branching information.
distributions, intrinsic viscosities and accurate molecular weights are determinable using GPC-Viscometry.

1032 Russell Drive, Porter, Texas U.S.A. 77365
(713) 359-5966 Fax: (713) 359-4336 Telex: 9102400852

CIRCLE 195 ON READER SERVICE CARD

Who is Quantum Analytics?

Quantum Analytics
Rents
State-of-the-art
Analytical Instruments

Call 800-992-4199
to rent your next instrument
from

363-D Vintage Park Drive • Foster City, CA 94404
Phone (415) 570-5656 or (800) 992-4199 • Fax (415) 570-6087

CIRCLE 150 ON READER SERVICE CARD

Plenum Books
UPDATES IN ANALYTICAL CHEMISTRY

MODERN ANALYTICAL CHEMISTRY
Series Editor: **David Hercules**

ION CHROMATOGRAPHY
by **Hamish Small**

Small details the major chromatographic modes for separating ionic species and illuminates the close connections between their practical implementation and such fundamentals as ion exchange equilibria and selectivity, complexation, and chelation.
0-306-43290-0/288 pp./ill./1989/$49.50

LIQUID CHROMATOGRAPHY/ MASS SPECTROMETRY
Techniques and Applications
by **Alfred L. Yergey, Charles G. Edmonds, Ivor A. S. Lewis,** and **Marvin L. Vestal**

This guide to techniques in liquid chromatography/mass spectrometry presents selected applications which illustrate the power of liquid chromatography/mass spectroscopy for materials not readily analyzed by other methodologies.
0-306-43186-6/316 pp./ill./1989/$65.00

COMPUTER-ENHANCED ANALYTICAL SPECTROSCOPY
Volume 2
edited by **Henk L. C. Meuzelaar**

This new volume presents discussions of remote IR sensing, deconvolution and signal processing methods that have been extended to UV/VIS and GC/MS applications; novel factor analysis techniques in the areas of UV/VIS and IR spectroscopy; and uses of expert systems in IR, NMR, and MS.
0-306-43276-5/313 pp. + index/ill. 1990/$65.00

SPECTROSCOPY OF SEMICONDUCTOR MICROSTRUCTURES
edited by **Gerhard Fasol, Annalisa Fasolino,** and **Paolo Lugli**

Volume 206 in the NATO ASI Series: Series B: Physics.
0-306-43378-8/proceedings/650 pp. + index/1990/$125.00

Visit Plenum at booth No. 1704 at the Pittsburgh Conference!

PLENUM PUBLISHING CORPORATION
233 Spring Street, New York, NY 10013-1578
Telephone orders:
212-620-8000/1-800-221-9369

CIRCLE 138 ON READER SERVICE CARD

A MEASURE OF SUCCESS

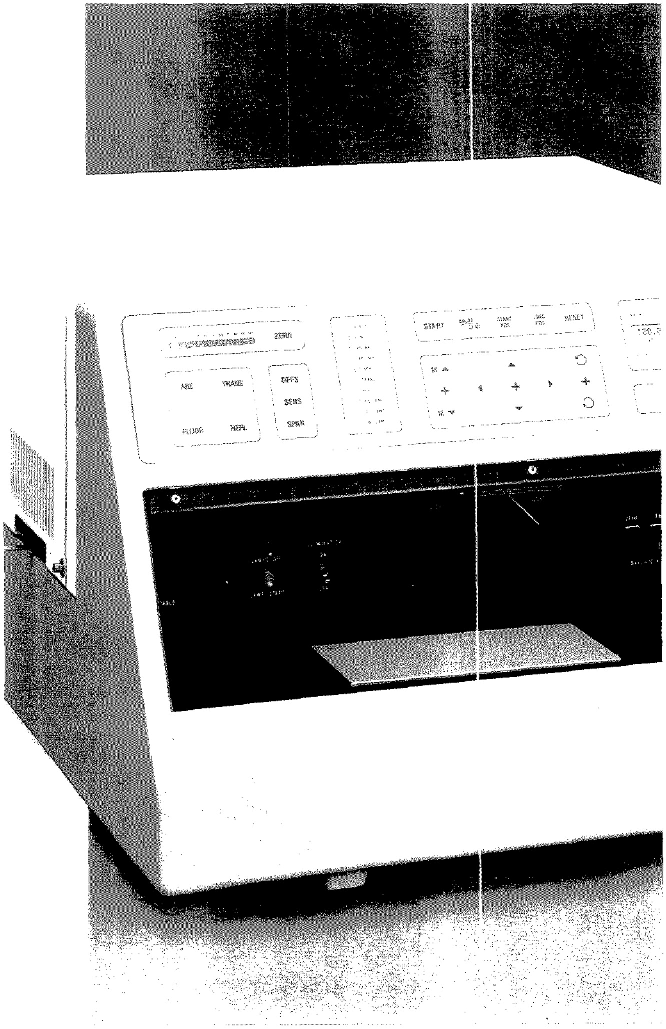

Modern Thin-Layer Chromatography combines precision, speed and versatility.

Measure your benefits of state of the art densitometry using the CAMAG TLC Scanner II:

Precision: Positively identify substances or determine whether a fraction is pure by recording in-situ spectra.

Speed: Obtain a plain language analysis report with quantitative results on 30 samples, within 1–3% relative standard deviation, in less than 3 minutes.

Versatility: Scan chromatograms by absorbance or fluorescence, at any wavelength between 190 and 800 nm. Combine with your personal computer and CAMAG's proprietary software.

Call us at (800) 334-3909, in NC (800) 476-1815 for technical information. Let us show you how CAMAG Scanner II and other CAMAG instruments can become your measure of analytical success.

CAMAG

Leading the World in Modern Thin-Layer Chromatography

CAMAG Scientific Inc. · P.O. Box 563 · Wrightsville Beach, NC 28480 · Telephone (919) 343-1830 · Fax (919) 343-1834

CIRCLE 32 ON READER SERVICE CARD

THE AMERICAN CHEMICAL SOCIETY PRESENTS . . .

25 Unique Sources of Archival-Quality Chemistry Research and News

ACCOUNTS OF CHEMICAL RESEARCH
Editor, Fred W. McLafferty
Cornell University
12 issues a year. ISSN 0001-4842
Member **$24** Nonmember **$127**

ANALYTICAL CHEMISTRY
Editor, George H. Morrison
Cornell University
24 issues a year. ISSN 0003-2700
Member **$29** Nonmember **$59**

BIOCHEMISTRY
Editor, Hans Neurath
University of Washington
*51 issues a year. ISSN 0006-2960
Member **$85** Nonmember **$690**

☛ **BIOCONJUGATE CHEMISTRY** *New in 1990!*
Editor, Claude F. Meares
University of California, Davis
The unifying medium of conjugation chemistry. BIOCONJUGATE CHEMISTRY will emphasize the joining of two different molecular functions by chemical or biological means.
6 issues a year. ISSN 1043-1802
Member **$29** Nonmember **$249**

☛ **BIOTECHNOLOGY PROGRESS** *New in 1990!*
Editor, Jerome S. Schultz
University of Pittsburgh
Jointly published with the American Institute of Chemical Engineers, this established journal offers *new, bimonthly access* to significant research in process development, product development, and equipment/instrumentation design for the biotechnology industry.
6 issues a year. ISSN 8756-7938
Member **$25** Nonmember **$250**

CHEMICAL & ENGINEERING NEWS
Editor, Michael Heylin
51 issues a year. ISSN 0009-2347
Nonmember **$60**

☛ **CHEMICAL RESEARCH IN TOXICOLOGY**
Editor, Lawrence J. Marnett
Vanderbilt University
For the latest original findings, in primary research, on the toxicological effects of chemical agents.
6 issues a year. ISSN 0893-228X
Member **$46** Nonmember **$269**

CHEMICAL REVIEWS
Editor, Josef Michl
University of Texas, Austin
8 issues a year. ISSN 0009-2665
Member **$26** Nonmember **$225**

Rates are valid through December 31, 1990.

☛ **CHEMISTRY OF MATERIALS**
Editor, Leonard V. Interrante
Rensselaer Polytechnic Institute
This new, international journal provides a molecular-level perspective at the interface of chemistry, chemical engineering, and materials science.
6 issues a year. ISSN 0897-4756
Member **$49** Nonmember **$299**

CHEMTECH
Editor, Benjamin J. Luberoff
12 issues a year. ISSN 0009-2703
Member **$39** Nonmember (Pers.) **$69**
Nonmember (Inst.) **$299**

☛ **ENERGY & FUELS**
Editor, John W. Larsen
Lehigh University
A practitioner's guide to the chemistry of fossil fuels—from formation to methods of utilization.
6 issues a year. ISSN 0887-0624
Member **$48** Nonmember **$294**

ENVIRONMENTAL SCIENCE & TECHNOLOGY
Editor, William H. Glaze
University of North Carolina, Chapel Hill
12 issues a year. ISSN 0013-936X
Member **$36** Nonmember (Pers.) **$67**
Nonmember (Inst.) **$276**

INDUSTRIAL & ENGINEERING CHEMISTRY RESEARCH
Editor, Donald R. Paul
University of Texas, Austin
12 issues a year. ISSN 0888-5885
Member **$55** Nonmember **$372**

INORGANIC CHEMISTRY
Editor, M. Frederick Hawthorne
University of California, Los Angeles
26 issues a year. ISSN 0020-1669
Member **$82** Nonmember **$612**

JOURNAL OF AGRICULTURAL AND FOOD CHEMISTRY
Editor, Irvin E. Liener
University of Minnesota
*12 issues a year. ISSN 0021-8561
Member **$25** Nonmember **$204**

JOURNAL OF THE AMERICAN CHEMICAL SOCIETY
Editor, Allen J. Bard
University of Texas, Austin
26 issues a year. ISSN 0002-7863
Member **$75** Nonmember **$630**

JOURNAL OF CHEMICAL AND ENGINEERING DATA
Editor, Bruno J. Zwolinski
Texas A&M University
4 issues a year. ISSN 0021-9568
Member **$30** Nonmember **$207**

JOURNAL OF CHEMICAL INFORMATION AND COMPUTER SCIENCES
Editor, George W.A. Milne, N.I.H.
4 issues a year. ISSN 0095-2338
Member **$18** Nonmember **$108**

JOURNAL OF MEDICINAL CHEMISTRY
Editor, Philip S. Portoghese
University of Minnesota
12 issues a year. ISSN 0022-2623
Member **$42** Nonmember **$329**

THE JOURNAL OF ORGANIC CHEMISTRY
Editor, Clayton H. Heathcock
University of California, Berkeley
26 issues a year. ISSN 0022-3263
Member **$56** Nonmember **$428**

JOURNAL OF PHYSICAL AND CHEMICAL REFERENCE DATA
Editor, David R. Lide, Jr.
National Institute of Standards & Technology
*6 issues a year. ISSN 0047-2689
Member **$70** Nonmember **$325**

THE JOURNAL OF PHYSICAL CHEMISTRY
Editor, Mostafa A. El-Sayed
University of California, Los Angeles
26 issues a year. ISSN 0022-3654
Member **$70** Nonmember **$670**

LANGMUIR
Editor, Arthur W. Adamson
University of Southern California
*12 issues a year. ISSN 0743-7463
Member **$58** Nonmember **$429**

MACROMOLECULES
Editor, Field H. Winslow
AT&T Bell Laboratories
*26 issues a year. ISSN 0024-9297
Member **$57** Nonmember **$553**

ORGANOMETALLICS
Editor, Dietmar Seyferth
Massachusetts Institute of Technology
12 issues a year. ISSN 0276-7333
Member **$59** Nonmember **$521**

For subscription information write:
American Chemical Society
Marketing Communications Dept.
1155 Sixteenth Street, N.W.
Washington, D.C. 20036 U.S.A.

Call toll free 1-800-227-5558.
In Washington, D.C. and outside the U.S. call 202-872-4363.
Telex: 440159 ACSP UI or 89 2582 ACSPUBS. **FAX:** 202-872-4615.

For nonmember rates in Japan contact:
Maruzen Co., Ltd.,
3-10 Nihonbashi 2-Chome, Chuo-ku,
Tokyo 103, Japan

*Frequency change in 1990.

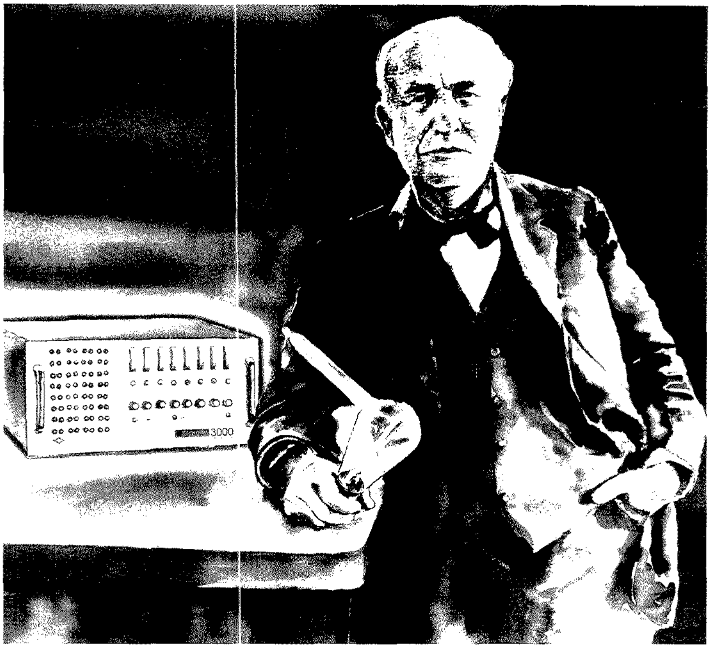

"With CAMILE*, I'd have seen the light sooner."

If you need to automate laboratory processes, you really have only one choice: the CAMILE* System from The Dow Chemical Company. CAMILE is the only completely integrated, personal computer-based data acquisition and control system designed specifically for research.

From our tradition of great laboratory and engineering science, we have designed the CAMILE System to improve our scientists' ability to optimize reactions and processes on a research scale and increase their research productivity.

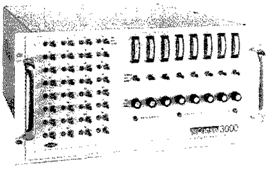

And now, with the development of the latest CAMILE software, automating your lab process has been made even easier by using Question & Answer and Report Generation functions.

With the power and flexibility to interface with a wide range of laboratory equipment, including balances, chromatographic integrators, and other intelligent lab equipment, the CAMILE System is the complete answer to lab automation.

Call 1-800-252-1977 to learn how the CAMILE System can help you view laboratory and pilot plant automation in a better light.

Camile®

The Dow Chemical Company • CAMILE Products • 1607 Building • Midland, MI 48674

*Trademark of The Dow Chemical Company

CIRCLE 35 ON READER SERVICE CARD

A long-awaited unifying medium for virtually any practitioner of conjugation chemistry

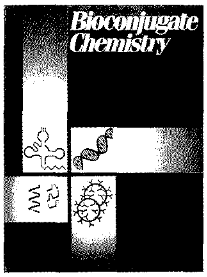

Bioconjugate Chemistry

Premiering January/February 1990.
Editor: Claude F. Meares,
University of California, Davis

Centralized Access Is Here!

In *bimonthly* issues, **Bioconjugate Chemistry** will bring together important research findings in the fast-developing discipline of conjugation chemistry. Now—*in a single, time-saving source*—you'll find information which otherwise might be scattered throughout broader-focus scholarly journals.

The central theme of **Bioconjugate Chemistry** *is the joining of two different molecular functions by chemical or biological means.* This includes:

Conjugation of . . .
antibodies (and their fragments)
nucleic acids and their analogs (α-anomers, phosphonates, . . .)
liposomal components
other biologically active molecules (receptor-binding proteins, hormones, peptides, . . .)

with each other or with any molecular groups that add useful properties . . .
drugs, radionuclides, toxins, fluorophores, photoprobes, inhibitors, enzymes, haptens, ligands, etc.

There is *no* journal with this precise focus published today.

The Leading Edge In Biomedical Advances

Bioconjugate Chemistry will publish research at the core of many biotechnology enterprises, as well as of specific interest to biomedical firms, drug companies, and chemical laboratories.

Topics will emphasize the *chemical* aspects of *conjugate preparation and characterization* . . . *in vivo* applications of conjugate methodology . . . *molecular biological* aspects of antibodies, genetically engineered fragments, and other immunochemicals . . . and the relationships between conjugation chemistry and the biological properties of conjugates.

Guided by a "Who's Who" in the Field

Editor: Claude F. Meares, *Univ. of Calif., Davis*

1990 Editorial Advisory Board

V. Alvarez, *Cytogen Corp.*
L. Arnold, *Gen-Probe*
R. W. Atcher, *Argonne Natl. Labs*
R. W. Baldwin, *Univ. of Nottingham, England*
T. Bumol, *Eli Lilly & Co.*
K. Chang, *Immunomedics*
G. David, *Hybritech, Inc.*
P. B. Dervan, *California Inst. of Tech.*
D. Dolphin, *Univ. of British Columbia, Canada*
T. W. Doyle, *Bristol - Myers*
R. E. Feeney, *Univ. of California, Davis*
D. Fitzgerald, *Natl. Inst. of Health*
J. M. Frincke, *Hybritech, Inc.*
A. Fritzberg, *NeoRx Corp.*
W. F. Goeckler, *Dow Chemical Co.*
D. Goodwin, *Stanford Univ.*
E. Haber, *E.R. Squibb and Sons, Inc.*
T. Hara, *Inst. for Biomedical Res., Japan*
R. Haugland, *Molecular Probes, Inc.*
J. Hearst, *Univ. of California, Berkeley*
N. Heindel, *Lehigh Univ.*
C. Helene, *Museum National D'Histoire Naturelle, France*
E. Hurwitz, *Weizmann Inst. of Science, Israel*
D. Johnson, *Abbott Labs*
D. Kaplan, *Dow Chemical Co.*
B. A. Khaw, *Massachusetts Genl. Hospital*
K. Krohn, *Univ. of Washington*
P. Miller, *Johns Hopkins Univ.*
H. Nagasawa, *Univ. of Minnesota, Minneapolis*
P. Nielsen, *Univ. of Copenhagen, Denmark*
A. Oseroff, *Tufts New England Medical Ctr.*
M. Ostrow, *The Liposome Co., Inc.*
G. Pietersz, *Univ. of Melbourne, Australia*
R. Reisfeld, *Scripps Clinic & Res. Fnd.*
S. Rocklage, *Salutar, Inc.*
J. Rodwell, *Cytogen Corp.*
P. Schultz, *Univ. of California, Berkeley*
P. Senter, *Oncogen*
S. Srivastava, *Brookhaven Natl. Lab.*
P. E. Thorpe, *Imperial Cancer Res. Fund, England*
G. Tolman
A. Tramontano, *Scripps Clinic & Res. Fnd.*
J. Upeslacis, *Lederle Lab.*
R. S. Vickers, *Sterling Drug Co.*
E. S. Vitetta, *Univ. of Texas, Dallas*
S. Wilbur, *NeoRx Corp.*
M. Wilchek, *Weizmann Inst. of Science, Israel*
M. Zalutsky, *Duke Univ.*

Attention Prospective Contributors!

With its exclusive, focused readership, Bioconjugate Chemistry will attract the specific audience of experts whom you want to reach, and is committed to prompt publication of manuscripts.

For information on submitting your original work, please contact
Dr. Claude F. Meares,
Department of Chemistry,
University of California, Davis, CA 95616
(916/752-3360).

Are you using the right chromatography column for your application?

Chrompack helps you with a full range of Tailor-made columns.
Optimized and guaranteed for a specific application field.

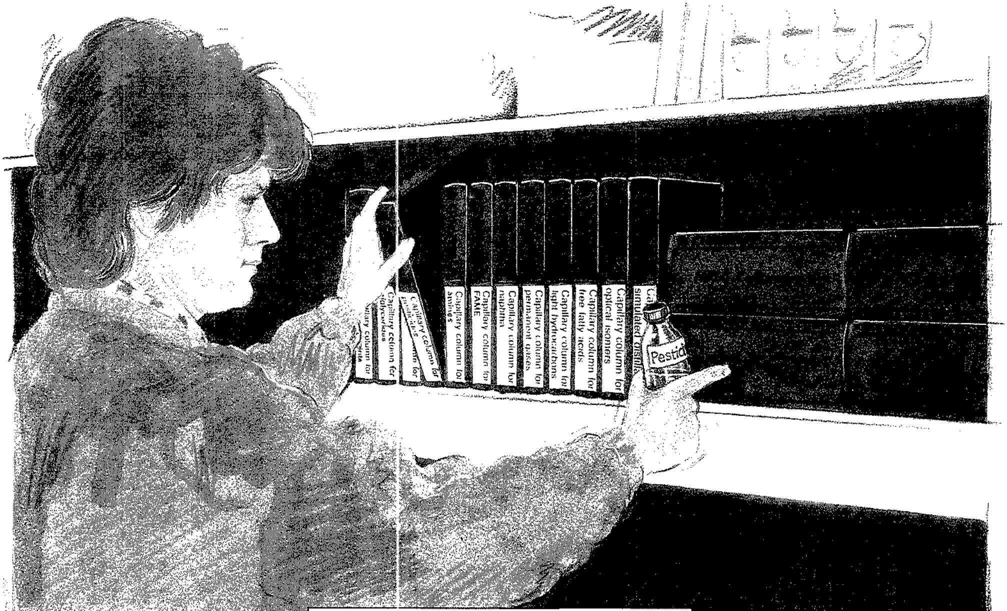
Capillary column for amines
Capillary column for FAME
Capillary column for naphtha
Capillary column for permanent gases
Capillary column for light hydrocarbons
Capillary column for free fatty acids
Capillary column for optical isomers
simulated distilla
Pestic

Tailor-made GC columns are available for:

- Amines
- C_1-C_{10} Hydrocarbons
- C_4-C_{12} Hydrocarbons
- Dioxins
- Fatty Acid Methyl Esters
- Free Fatty Acids C_2-C_{24}
- Gasoline fuels
- Glycols
- Halocarbons (EPA 624)
- PCB's
- Optical isomers
- N_2, O_2, CO, CO_2, C_1-C_3
- Permanent gases
- Pesticides
- Simulated distillation
- Triglycerides
- Volatiles in Spirits

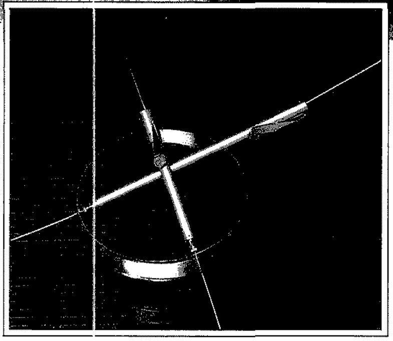

Tailor-made HPLC columns are available for:

- Anions
- Aromatic acids
- Carbohydrates
- Cations
- Large biomolecules
- Optical isomers
- Organic acids
- Pesticides
- Petroleum products
- Polyaromatic hydrocarbons

CHROMPACK

Chrompack Inc.
1130 Route 202, Raritan NJ 08869
Tel: toll free (800) 526-3687-New Jersey (201) 722-8930
Telex 833290, Fax (201) 722-8365

Free leaflets are available for all Tailor-made columns, showing a number of specific applications. Chrompack columns are pretested and guaranteed.

FROM CHROMATOGRAPHERS – FOR CHROMATOGRAPHERS

P25336

CIRCLE 34 ON READER SERVICE CARD

New Products

Most of the products in this section will be shown at the Pittsburgh Conference. Future NEW PRODUCTS sections of ANALYTICAL CHEMISTRY will include more instrumentation and equipment from this year's conference.

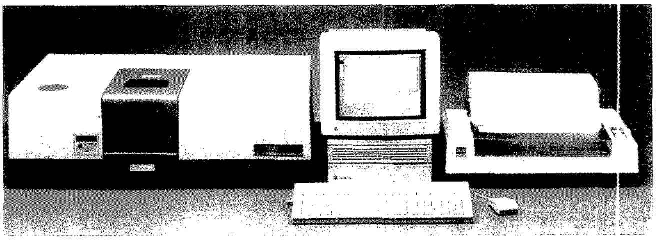

Model 510M FT-IR system includes a Macintosh II computer and a software package with pull-down menus and on-line help screens. Data or spectra can be transferred to word processing or other software packages for further analysis. Nicolet 402

Electrophoresis. Capillary electrophoresis systems feature femtomole detection sensitivity and multiple sample injection modes. The automated system includes a 40-position autosampler, computer-based control over all separation parameters, and complete data management. Isco 412

Titration. DL-12 autotitrator is designed for automation of routine laboratory acid–base titrations and for educational use. All control and calculation functions are programmed into the instrument. Mettler Instrument Corp. 413

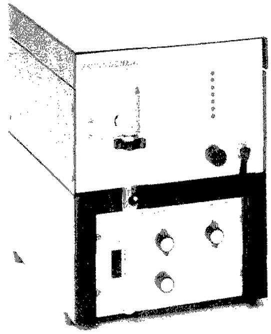

Model 8901 prescreener for organics in water prevents overloading of concentrators, autosamplers, and GC columns. The unit features a built-in flame ionization detector and dilution meter. Envirochem 408

Fraction collector. Vanderkamp VK3000 stores 10 different programs, each capable of taking up to 10 samples at intervals ranging from 3 min to 16 h. A keyboard lock feature prevents unauthorized interference with the collection program. VanKel Industries 414

Transilluminators. Spectroline variable-intensity UV transilluminators feature sensitivity of 1–2 ng DNA and complete intensity control from 100% down to 20% of the typical peak irradiance of 8000 $\mu W/cm^2$. A built-in cooling fan protects DNA from heat damage and maintains constant irradiance over a prolonged period. Spectronics Corp. 415

MS. Auditor I is a 650-amu quadrupole-based process mass spectrometer that is suitable for environmental gas monitoring and control. The system features continuous spectra monitoring, fully interactive controls, and a PC/AT-based data system. Leybold Inficon 416

Workstation. LabData 200 can simultaneously acquire, analyze, and report data from a variety of analytical instruments. Software packages are available for chromatography; thermal analysis; MS; and atomic, UV–vis, and IR spectroscopies. Laboratory Data Systems 417

Nitrogen. Heraeus Macro N provides automatic quantitative nitrogen or protein analysis of samples weighing up to 2 g without the need for wet chemical digestion. A built-in sample feeder allows unattended analysis of 90 samples. UIC 421

Proteins. System 100 is an LC-based protein purification system that is suitable for research, process scale-up, QC, or production applications. A program mode allows for creation, storage, and editing of up to nine user-designated protocols. Genex Corp. 422

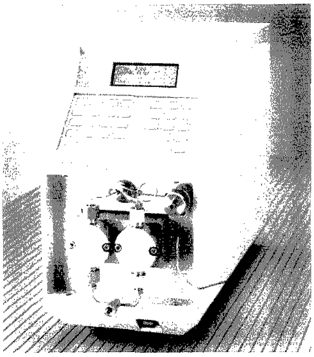

ConstaMetric 3500 provides flow programming and gradient control of up to three accessory pumps for quaternary high-pressure gradients. Up to 65 gradient files can be stored in the internal memory. LDC Analytical 409

For more information on listed items, circle the appropriate numbers on one of our Readers' Service Cards

---

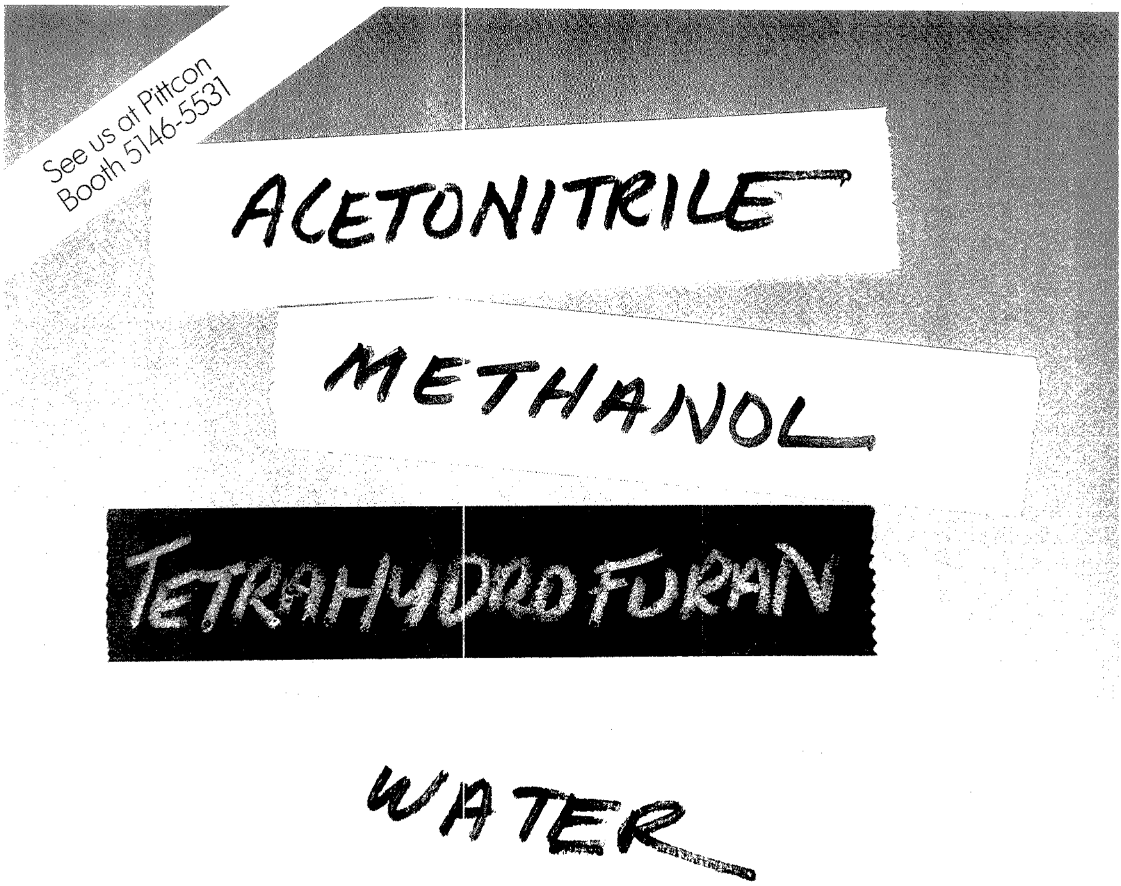

See us at Pittcon
Booth 5146-5531

One filter fits all.

The new Millex®-LCR Filter Unit is compatible with all common aqueous or organic-based HPLC solvents—from water to methanol to tetrahydrofuran.

Its special membrane produces no organic or inorganic contaminants. So risk of introducing unwanted variables and artifacts into your work is eliminated.

Particulates are reduced below detectable limits, which keeps frits from plugging and extends column life.

Test the HPLC-certified Millex-LCR Filter Unit yourself. Send in the coupon, or call 800-225-1380 (in Mass., call 617-275-9200) for a free sample and technical brief.

Try the Millex-LCR Unit. Free.

Send to: Joe Peters
Millipore Corporation
80 Ashby Road
Bedford, MA 01730

Name ______
Title ______
Co./Inst. ______
Department ______
Address ______
City ______
State ______ Zip ______
Phone ( ) ______ Best time to call ______

PA 900008 © 1990 Millipore Corporation

CIRCLE 110 ON READER SERVICE CARD

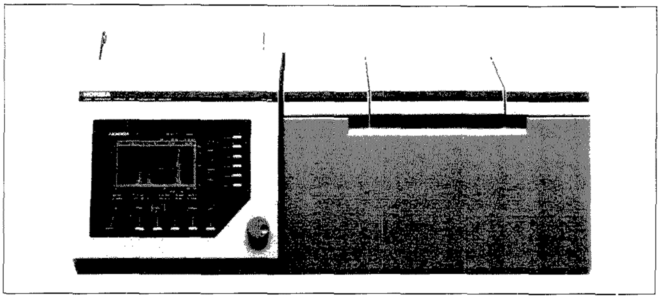

LA-500 is a laser diffraction-based particle size distribution analyzer that covers the particle size range of 0.1–200 μm. Up to 24 sets of data can be stored in memory or downloaded to an independent computer. Horiba Instruments 405

Sample preparation. SmartPREP is an automated sample preparation system for LC, GC, and SFC. The system includes a versatile reporting package and a compact robot that can be equipped with a variety of integrated robotic peripherals. Source For Automation 418

FT-IR. Sirius research-grade FT-IR spectrometer features resolution of 0.09 cm^{-1} and is compatible with all conventional sampling accessories, including IR microscopes. Software is available for Unix, Macintosh, or IBM-compatible data systems. Mattson Instruments 419

Optical luminometers. ILA 911 system is a single-well counter designed for the manual entry of test tubes into the light detection housing; ILA 912 is an automated version capable of processing up to 220 test tubes. Both systems can be used with any chemiluminescent or bioluminescent reaction. Tropix 420

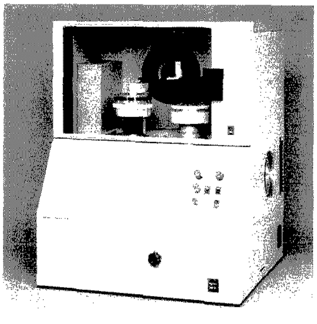

Quanta 4000 capillary electrophoresis system allows multiple unattended analyses and automatically cleans the capillaries after each run. Waters Chromatography Division of Millipore 403

Photometric analysis. Orbeco-Hellige Model 980 absorbance colorimeter features plug-in filters, a wavelength range of 390–800 nm, and concentration readings in three ranges. Results can be displayed as percent transmittance or in absorbance units. Orbeco Analytical Systems 423

Carbon dioxide. $CO_2$001 removal dryer removes CO_2 and H_2O from compressed air used for FT-IR and NMR spectrometers and other laboratory instruments. Features include CO_2 removal to < 1 ppm, maximum output of 18 L/min, and dew point of < −70 °C. Jun-Air 441

Sampler. Model CLS-300 samples corrosive and viscous liquids directly from a chemical distribution line, performs particulate measurements, and returns the sample to the pressurized source from which it was taken. Hydraulic isolation is used to remove bubbles from the sampled fluid for observation of particulate content. Particle Measuring Systems 425

Clinical analysis. Electra 900C is designed to perform chromogenic tests as well as standard clot testing. The system features random access testing, automatic disposal of used cuvettes, patient data storage, and in-lab printout. Medical Laboratory Automation 426

Digitizing system. Un-Plot-It uses a PC, plotter, and optical pen to automatically read graphic data from paper into a computer in (x,y) ASCII format. The system features accuracy of 0.002 in. and sensitivity adjustment for variable line thickness and darkness. Silk Scientific 427

LC. Gynkotek M480G high-precision pump features pulse-free eluent delivery, flow gradients for microbore to semipreparative applications, behind-seal washing, and an automatic independent maintenance reminder. Flow rates range from 1 μL/min to 8 mL/min. Analytical Sales and Services 428

Detector. Argon-ion laser Dawn Model F can be used on line as a GPC detector for determining absolute number, weight, and z-average molecular weights and sizes, or off line for determining absolute weight-averaged molecular weights, root mean square radii, and the second virial coefficient. Wyatt Technology Corp. 429

ICP. Spectro-ICP Model M is a sequential ICP spectrometer with direct wavelength drive that selects wavelength with an accuracy of 0.0008 nm. Wavelengths below 190 nm are accessible via nitrogen purge. Spectro Analytical Instruments 430

Electrophoresis. Spectraphoresis 1000 capillary electrophoresis system features multiwavelength detection, on-the-fly spectra, and an autosampler that accommodates 80 samples. Fiber optics are used to detach the optical sensor from the detector body, permitting independent thermostatting of the entire capillary. Spectra-Physics 433

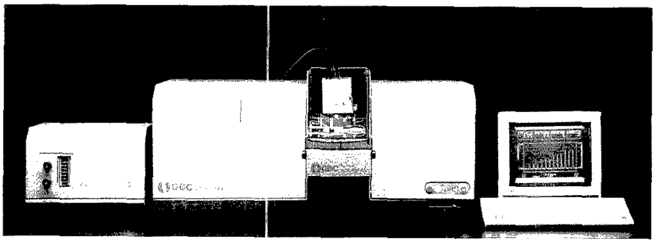

GBC 904 atomic absorption spectrometer features double-beam optics and a built-in disk drive that provides storage for methods, results, signal graphics, calibration graphs, report headings, notes, and sample labels. GBC Scientific Equipment Pty. Ltd. 404

The good news is you can get absolute macromolecular analysis in minutes.

There is no bad news.

EXCEPT, perhaps, that you haven't discovered us sooner. Using one of our DAWN® laser light scattering instruments, you'll learn more about your macromolecules in minutes than you've learned in years. A lot more!

You could, for example, couple our DAWN Model F detector to your existing Size Exclusion Chromatography line to determine *absolute* molecular weights, sizes, distributions and molecular conformations of almost *any* polymer without resorting to column calibrations, reference standards or "fudge factors." And, there's more good news...

The batch-mode DAWN Model B is the most perfect instrument ever conceived for time-dependence studies. You can study reaction and polymerization phenomena in real time. You can even control the temperature for high, ambient or *below* ambient environments for thermoplastics or biopolymers.

Ease of Use

Maybe you're familiar with old-fashioned light scattering instruments—how hard they are to use and maintain. Not ours. Wyatt Technology started with the theory of light scattering, threw out the stepper motors, refractive index-matching baths, photomultiplier tubes, swing-arms and all the other features that make light scattering the bane of a chemist's existence. The result is a line of instruments so elegant, so advanced, that they are a pleasure to use.

Imagine an innovative optical instrument with no lenses, mirrors or prisms (which often require realignment and cleaning). Imagine unpacking a laser light scattering photometer, and being up-and-running within 60 minutes! Imagine a multi-angle instrument with no moving parts. Imagine turn-key software solutions, and computer-programmers who implement your suggestions.

Imagine no more. We're here to prove the power of light scattering to solve your toughest problems. The DAWNs make tens-of-thousands of measurements in the time that it used to take to make one. Our multi-angle geometry produces the root-mean-square (rms) radius of your molecules *instantly,* not after hours of data collection. You won't make any of the arbitrary assumptions about the molecular shape, distribution or homogeneity required by other techniques. This is, after all, a real world—not one populated by perfectly spherical molecules with Gaussian distributions.

More Good News

At Wyatt Technology we've been producing state-of-the-art instruments for over seven years, and we continue to back our products with training, seminars, consulting and the finest customer service in our industry.

Jump light years ahead of the competition; call us at (805) 963-5904 for a complete information package. With case histories, application notes, a sample-running laboratory, and a long list of delighted customers to confirm our good news, it won't take us long to show you just how much you've been missing!

Wyatt Technology
CORPORATION
820 East Haley Street • Santa Barbara, CA 93103
Tel: (805) 963-5904 • Fax: (805) 965-4898

© 1990 Wyatt Technology Corporation

PittCon Booth #1048 CIRCLE 200 ON READER SERVICE CARD

Register today for this popular Hands-on ACS Short Course to be held at Virginia Tech, Blacksburg, VA

High Performance Liquid Chromatography: Theory and Practice

Two sessions in 1990!
Monday-Thursday, April 23-26
(HPTP9004)
Monday-Thursday, December 3-6
(HPTP9012)

This unique four-day laboratory-lecture course will provide you with the training you need to effectively and efficiently work with this important analytical method. Through lectures and the do-it-yourself learning experience, you will

☐ solve separation problems
☐ perform qualitative and quantitative analyses
☐ interpret and "troubleshoot" from chromatograms
☐ operate and maintain state-of-the-art HPLC systems

Faculty: Dr. Harold McNair, Professor of Chemistry, Virginia Tech, together with guest lecturers from industry, instrument companies, and universities.

For details on this course, mail in the coupon below or call the Continuing Eduction Short Course Department TOLL FREE (800) 227-5558, and ask for ext. 4370.

American Chemical Society, Dept. of Continuing Education, Meeting Code VPI90040, 1155 Sixteenth Street, N.W., Washington, DC 20036

YES! Please send me information on the *High Performance Liquid Chromatography: Theory and Practice* (VPI90040) course to be held at Virginia Tech in Blacksburg, VA:

Name ______________________
Title ______________________
Organization ______________________
Address ______________________
____
City, State, Zip ______________________
VPI90040

NEW PRODUCTS

FAB. Cesium ion source, suitable for static and flow FAB, can be focused to a small spot size with infinite focal length. The system operates between 0 and 12 kV at current densities between 0 and 10 $\mu A/cm^2$; for higher voltage operation, the source can be floated and referenced to a mass spectrometer ionization source voltage. Phraser Scientific 431

XRF. Simultix system 3550 is a multichannel X-ray fluorescence spectrometer that allows determination of elements ranging from boron to uranium. Samples can be analyzed for up to 40 elements at a time at a rate of one sample per minute. Rigaku/USA 432

Sample preparation. ML 1200 microwave laboratory system is designed for digestion of samples for atomic absorption and ICP spectrometry as well as wet chemical analysis. The system includes a programmable microwave unit, a heavy-duty vessel capping module, a high-power exhaust module, and an acid fumes absorption module. GT Instruments 434

Elemental analysis. TraceLab can be used to analyze aqueous samples for Ag, As, Cd, Bi, Co, Cu, Fe, Ga, Hg, In, Ni, Mn, Pb, Sb, Se, Sn, Ti, U, and Zn. Detection limits are in the range 0.01 to 1 ppb, and analysis times are typically 1–3 min. Radiometer America 435

Pyrolysis. Pyroprobe 2000 prepares solid samples such as polymers, composites, and fibers for analysis by GC, MS, or FT-IR. The platinum filament and heated interface can be independently programmed in steps containing an initial temperature, heating rate, and final temperature. CDS Instruments 436

Particle size. Elzone 282-PC particle size analyzer features macro commands covering data acquisition, processing, and output; automatic blockage detection/clearance within the analysis; and integral dual sample stands for instant switching of size range. Particle Data 437

Color measurement. MiniScan is a battery-operated portable color measurement system that offers user-selectable color scales, indices, and observers. Color values are stored in memory for output to a printer or computer. HunterLab 438

FT-IR. Collegian is an FT-IR spectrometer designed specifically for academic use. The system, which features spectral resolution of 0.5 cm^{-1} and fast data acquisition times, can be controlled by any IBM PC/AT-compatible computer. Midac Corp. 439

LC/MS. Separator, which interfaces a liquid chromatograph to an electron ionization mass spectrometer, includes an interface with a vaporizer/nebulizer chamber, a diffusion cell, flow controllers, and associated electronics; a pumping system; and a two-stage momentum separator. Vestec 440

Thin films. RBS-400 analytical end station for Rutherford backscattering spectrometry is a complete hardware and software system designed to be used with an electrostatic accelerator to quantitatively and nondestructively measure the thickness of thin films. Charles Evans & Associates 424

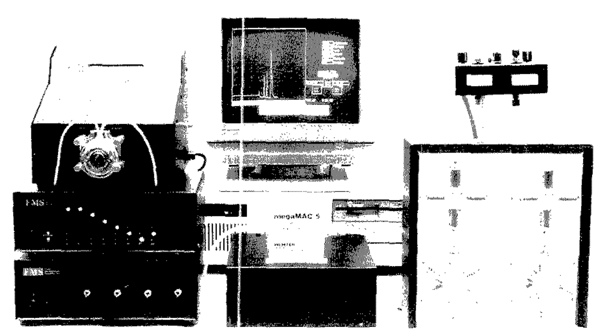

AutoMAC is an automated membrane affinity chromatography system that purifies and harvests multigram quantities of monoclonal antibodies or other proteins in 1 h or less. Flow rates range from microliters to liters per minute. Memtek 406

Purer filtration begins with a purer microfilter.

Introducing Whatman microfiltration devices.

Whatman microfiltration products represent the state of the art in microfiltration technology, and feature these unique advantages:

- *All* devices are fusion-sealed. Absolutely no sealants, adhesives or releasing agents are used, thus ensuring a purer filtrate.
- *All* devices offer a wide range of pore sizes and media, the most advanced materials, and the greatest possible selection to meet each of your application needs.
- *All* devices are smaller and lighter in weight, with an effective filtration area equivalent to larger devices.
- *All* devices give you the very finest in filtration – and more. With every purchase, you get instant access to Whatman sales, service, and technical support.

POLYCAP TF is just one of 36 new and exciting Whatman microfiltration devices. For more information about POLYCAP TF and other Whatman devices, call our Technical Service Representative or your local authorized laboratory distributor. We'll help you find a Whatman microfiltration device to fit your specific needs.

POLYCAP™ TF
Disposable Filter Device

POLYCAP TF is manufactured with a solvent-resistant, hydrophobic PTFE membrane. The entire Whatman line features a wide choice of filter media and pore sizes.

Easy to identify: *All* Whatman devices are stamped on the housing to allow fast, accurate product identification.

Chemical-resistant housing: *All* Whatman devices are manufactured from chemical-resistant polypropylene.

Compact: *All* Whatman devices feature an incredibly efficient design that provides a large effective filtration area in a smaller size.

Stepped hose barb connections fit a number of tubing sizes.

The advantages filter through.

Whatman®

POLYCAP™ is a trademark of Arbor Technologies, Inc., USA.

CIRCLE 198 ON READER SERVICE CARD

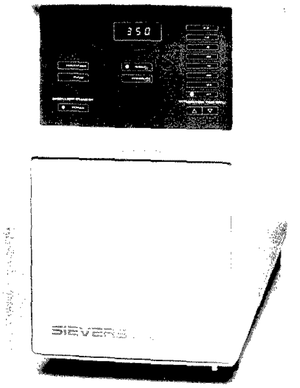

Model 350 sulfur chemiluminescence detector for GC and SFC is based on the chemiluminescence reaction of SO and ozone. The detector is suitable for total sulfur analysis and individual component analysis of complex matrices. Sievers Research 401

LC. Büchi 684 fraction collector, designed for preparative-scale LC, features remote-control capability and a distribution plate that allows the use of any collection vessels, including evaporation flasks. Up to 12 L can be collected using standard-size tubes. Anspec 442

Software

IR. Cascade uses artificial intelligence to interpret near-IR spectral data. The software classifies an unknown sample and then selects the proper calibration to predict quantitative results, without operator intervention. Bran+Luebbe Analyzing Technologies 445

Chemical information. Centrum provides chemical publishing and information-handling capabilities designed for scientists, technical support staff, and research management. The software features an icon-based user interface. Polygen Corp. 446

Graphics. SlideWrite Presenter designed for the IBM-PC and compatible computers, allows users to take text and graphics and create slide show presentations directly on the computer. The package includes a screen capture program to capture text and graphics screens from programs such as Lotus 1-2-3 and WordPerfect. Advanced Graphics Software 447

Information management. LIMS Extender Graphics System (LEGS) allows automatic downloading of data from any LIMS system for specialized, user-definable data analysis, graphing, and reporting. Telecation Associates 448

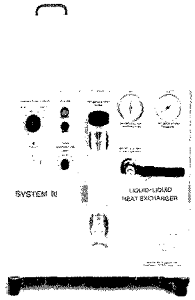

System III is a water-to-water recirculating chiller that provides cool, clean recirculating fluid to water-cooled equipment. Circulating fluid is stable to at least ±1.0 °C over a user-adjustable range of 5 °C to 40 °C. Neslab Instruments 407

CLASSIFIED
HELP WANTED

GAS CHROMATOGRAPHY. Field Service Technician for Analytical Instruments includes installation, servicing, and customer training; involves extensive travel. Experience in Gas Chromatography required. Send Resume to: **ES Industries, Suite 3, 701 Cooper Road, Voorhees, NJ 08043.**

HELP WANTED ADS

ROP display at ROP rates. Rate based on number of insertions within contract year. Cannot be combined for frequency.

Unit	1-Ti	6-Ti	12-Ti
1″ (25 mm)	$190	$170	$160
	24-Ti	48-Ti	72-Ti
	$150	$140	$130

CALL OR WRITE JANE GATENBY

ANALYTICAL CHEMISTRY
500 Post Road East
P.O. Box 231
Westport, CT 06880
203-226-7131
FAX: 203-454-9939

LABORATORY SERVICE CENTER

MRL
(201) 731-1776
FAX (201) 731-1778
ANALYSIS SERVICES
R & D / QA / FAILURE ANALYSIS
ESCA•AES•SEM•EDS•WDS•XRD
MATERIALS RESEARCH LABORATORIES, Inc.
SCHOOLHOUSE PLAZA, SUITE 1E
720 KING GEORGES POST ROAD
FORDS, NJ 08863

USE LABORATORY SERVICE CENTER

FREE DATA, FAST

To quickly amass data on all of the products you need, consult the Lab Data Service section on our *Analytical Chemistry* reader reply card insert.

Laboratory Service Center (Equipment, Materials, Services, Instruments for Leasing), Maximum space — 4 inches per advertisement. Column width, 2-3/16″; two column width, 4-9/16″. Artwork accepted. No combination of directory rates with ROP advertising. Rates based on number of inches used within **12** months from first date of first insertion. Per inch: 1″ — **$165; 12″ — $160; 24″ — $155; 36″ — $150; 48″ — $145.**

CALL OR WRITE JANE GATENBY

ANALYTICAL CHEMISTRY
500 Post Road East
P.O. Box 231
Westport, CT 06880
203-226-7131/FAX: 203-454-9939

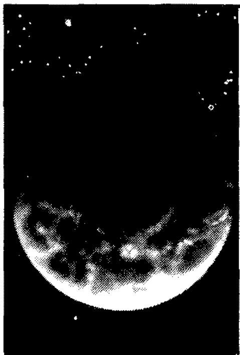

JANAF THERMOCHEMICAL TABLES

Third Edition

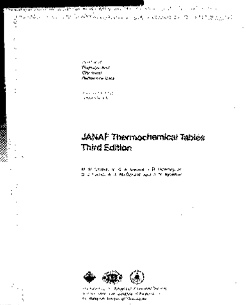

A Major Supplement from JOURNAL OF PHYSICAL AND CHEMICAL REFERENCE DATA

Presenting Reliable Data Utilized by Chemists, Chemical Engineers, and Materials Scientists from Around the World for Over 25 Years

JOURNAL OF PHYSICAL AND CHEMICAL REFERENCE DATA is very pleased to publish the Third Edition of the JANAF THERMOCHEMICAL TABLES.

Since the first version appeared 25 years ago, the JANAF THERMOCHEMICAL TABLES have been among the most widely used data tables in science and engineering.

You'll find:

- Reliable tables of thermodynamic properties of substances of wide interest
- A highly professional approach with critical evaluations of the world's thermochemical and spectroscopic literature
- A concise and easy-to-use format

This Third Edition presents an extensive set of tables including thermodynamic properties of more than 1800 substances, expressed in SI units. The notation has been made consistent with current international recommendations.

There is no other reference source of thermodynamic data that satisfies the needs of such a broad base of users.

Order your 2-volume set of the JANAF THERMOCHEMICAL TABLES today! You'll get over 1890 pages of valuable information that is crucial to your research—in two hardback volumes.

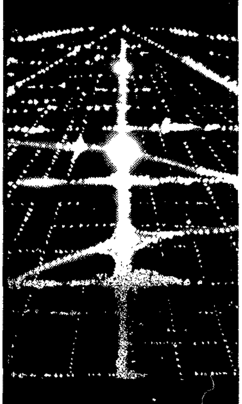

Editors:
M.W. Chase, Jr.
National Institute of Standards and Technology
C.A. Davies
Dow Chemical U.S.A.
J.R. Downey, Jr.
Dow Chemical U.S.A.
D.J. Frurip
Dow Chemical U.S.A.
R.A. McDonald
Dow Chemical U.S.A.
A.N. Syverud
Dow Chemical U.S.A.

SUBSCRIPTION INFORMATION

The JANAF THERMOCHEMICAL TABLES, THIRD EDITION is a two-volume supplement of *Journal of Physical and Chemical Reference Data.*

1896 pages, 2 volumes, hardcover
ISBN 0-88318-473-7
Supplement Number 1 to Volume 14, 1985

U.S. & Canada	$130.00
All Other Countries	$156.00
(Postage included.)	

All orders for supplements must be prepaid.

Foreign payment must be made in U.S. currency by international money order, UNESCO coupons, U.S. bank draft, or order through your subscription agency. For rates in Japan, contact Maruzen Co., Ltd. Please allow four to six weeks for your copy to be mailed.

For more information, write **American Chemical Society**, Marketing Communications Department, 1155 Sixteenth Street, NW, Washington DC 20036.

In a hurry? Call TOLL FREE 800-227-5558 and charge your order!

Published by the **American Chemical Society** and the **American Institute of Physics** for the **National Institute of Standards and Technology**

INDEX TO ADVERTISERS IN THIS ISSUE

CIRCLE INQUIRY NO.	ADVERTISERS	PAGE NO.
7	*A&D Engineering, Inc.	155A
1	*AccuStandard, Inc. The Robert A. Paul Advertising Agency Inc.	204A
9	Advanced Graphics Software, Inc.	194A
5	Ametek, Inc. Richardson, Thomas & Bushman, Inc.	202A
11	Analogic Corporation	223A
3	The Anspec Company, Inc. JJ&K Advergraphics	172A
8	Autoclave Engineers Group Altman-Hall Associates	210A
20	Bacharach Coleman Instruments Skutski & Associates, Inc.	141A
22	Baird Corporation W. J. Hearn & Compnay, Inc.	203A
13–16	Balston, Inc. Gillett Brown & Associates	197A
25, 26	*Beckman Instruments, Inc. AC&R Advertising, Inc.	113A
28	*Beckman Instruments, Inc. Techmarketing	227A
30	*Bio-Rad Chemical Division Robert Anthony	151A
32	*Camag Scientific, Inc.	237A
36	Cetac Technologies, Inc. Rosenfield-Lane, Inc.	207A
34	*Chrompack Inc.	241A
38	Delsi/Nermag Instruments	128A
40	*Dialog Information Services, Inc. HL&S Partners Inc.	143A
42	*Dionex Corporation Rainoldi, Kerzner & Radcliffe	233A
35	Dow Chemical/Camile Bradford-La Riviere, Inc.	239A
56	Eberbach Corporation	174A
57, 58	*EG&G Princeton Applied Research Market Force	206A
50	Elsevier Science Publishing Company, Inc.	230A
206–210	*EM Science	177A
54	*EM Science Tallant LaPointe & Partners, Inc.	224A
48	ENI Quinlan, Foels & Company	199A
52	Charles Evans & Associates	228A
211–217	Extrel Blattner/Brunner, Inc.	216A
60	Finnigan MAT Corporation Lena Chow, Inc.	127A

CIRCLE INQUIRY NO.	ADVERTISERS	PAGE NO.
62	*Fisher Scientific Tech-Ad Associates	211A
63	Gelman Sciences	131A
182–186	*Gilson Medical Electronics, Inc.	110A–111A
220–233	**Gilson Medical Electronics SA	110A–111A
65	*Gow-Mac Instrument Company Scientific Marketing Services, Inc.	186A
70	Guided Wave International AB	175A
75	Hamamatsu Corporation Ketchum/Mandabach & Simms	198A
71	*Hellma Cells, Inc. Dansco Advertising	206A
73	*Hewlett-Packard Company Brooks Communications	107A
78	*I-Chem Research Lena Chow, Inc.	213A
80	*Isco, Inc. Farneaux Associates	167A
82	*Isotec, Inc.	220A
87	*Jandel Scientific	215A
85	Johnson Scale Company The Sanford Solarz Company	224A
100	*Laser Precision Analytical	205A
102	Leap Technologies	220A
94	*Leco Corporation	OBC
98	Leeman Labs, Inc. JRJ Communications	169A
90	*Leybold Vacuum Products, Inc. CD Werbeagentur GmbH	193A
92	*Lindberg/Blue M Fensholt Incorporated	230A
96	Link Analytical	201A
114	*Mattson Instruments, Inc. Cunningham & Welch Design Group	108A
106	Merck & Company, Inc. William Douglas McAdams, Inc.	173A
112	*Merck Sharp & Dohme Isotopes BGH Advertising Associates, Inc.	138A
108	*Metrohm Ltd. Ecknauer + Schoch Werbeagentur ASW	171A
111	*Mettler Instrument Corporation Gilbert, Whitney & Johns, Inc.	117A
116	MG Industries Wright Associates, Inc.	191A
110	*Millipore Corporation Mintz & Hoke	243A
117	*Mitech Corporation	220A
123	*National Institute of Standards & Technology	206A

INDEX TO ADVERTISERS IN THIS ISSUE

CIRCLE INQUIRY NO.	ADVERTISERS	PAGE NO.
118, 119, 161–173	*Nicolet Analytical Instruments	135A, 157A–164A
121	*NIRSystems Barrett Advertising	187A
132	*Ohaus Corporation Ballotta Napurano & Company, Inc.	147A
134	O. I. Analytical	231A
130	*Omega Engineering, Inc. Media Business House	IFC
125	*On-Site Instruments	116A
127	Ovonic Synthetic Materials Company, Inc. Ross & Associates	219A
148	*Parker Hannifin Corporation Amundsen/Beier, Inc.	195A
146	*Parr Instrument Company FBA Marketing Communications	224A
142–144	Perkin-Elmer Corporation Keiler Advertising	209A, 221A, 229A
136	Pharmacia LKB Biotechnology Media Services	144A
137	Photovolt/Division of Seradyn, Inc. Garrison, Jasper, Rose & Company, Inc.	226A
138	Plenum Publishing Corporation Plenum/Da Capo Advertising	234A
140	Pyromatics Ashby, Dillon Inc.	232A
150	Quantum Analytics	234A
152	Rheodyne, Inc. Bonfield Associates	120A
160	Siemens Analytical X-Ray Instruments, Inc.	115A
154–156	*Spectra-Physics	137A, 181A–184A
180	*Stephens Analytical, Inc.	212A
158	*The Swagelok Companies Falls Advertising Company	165A
174	*Techne, Inc. Brunswick Advertising	192A
178	*Tekmar Company Kenyon Hoag Associates	114A
18	Thermolyne	189A
176	Tracor Atlas	133A
44	The University of Dayton Research Institute	116A
187	*Valco Instruments Company, Inc. Technical Advertising Associates	153A
204	*Varian Lanig Associates	122A
193	VCH Publishers, Inc.	119A
189	Vestec Corporation Barbeau-Hutchings Advertising, Inc.	179A
191	VG Instruments, Inc. Bryce Advertising	149A
195	Viscotek	234A
198	Whatman GrossTownsendFrankHoffman Inc.	247A
202	*Wheaton The Wheaton Agency	185A
200	Wyatt Technology Corporation	245A

Classified advertising section, see page 248A.
Directory section, see page 248A.
** See ad in ACS Laboratory Guide.*
*** Company so marked has advertisement in Foreign Regional edition only.*
Advertising Management for the American Chemical Society Publications

CENTCOM, LTD
President
James A. Byrne
Executive Vice President
Benjamin W. Jones
Clay S. Holden, *Vice President*
Robert L. Voepel, *Vice President*
Joseph P. Stenza, *Production Director*

500 Post Road East
P.O. Box 231
Westport, Connecticut 06880
(Area Code 203) 226-7131
Telex No.643310
FAX: 203-454-9939

ADVERTISING SALES MANAGER
Bruce E. Poorman

ADVERTISING PRODUCTION MANAGER
Jane F. Gatenby

SALES REPRESENTATIVES

Philadelphia, PA . . . Patricia O'Donnell, CENTCOM, LTD., GSB Building, Suite 405, 1 Belmont Avenue, Bala Cynwyd, Pa. 19004. Telephone: 215-667-9666, FAX: 215-667-9353

New York, NY . . . John F. Raftery, CENTCOM, LTD., 60 East 42nd St., New York, N.Y. 10165. Telephone: 212-972-9660

Westport, CT . . . Edward M. Black, CENTCOM, LTD., 500 Post Road East, P.O. Box 231, Westport, Ct. 06880. Telephone: 203-226-7131, Telex 643310, FAX: 203-454-9939

Cleveland, OH . . . Bruce E. Poorman, John C. Guyot, CENTCOM, LTD., 325 Front St., Suite 2, Berea, Ohio 44017. Telephone: 216-234-1333, FAX: 216-234-3425

Chicago, IL . . . Michael J. Pak, CENTCOM, LTD., 540 Frontage Rd., Northfield, Ill. 60093. Telephone: 708-441-6383, FAX: 708-441-6382

Houston, TX . . . Michael J. Pak, CENTCOM, LTD. Telephone: 708-441-6383

San Francisco, CA . . . Paul M. Butts, CENTCOM, LTD., Suite 1070, 2672 Bayshore Frontage Road, Mountain View, CA 94043. Telephone: 415-969-4604

Los Angeles, CA . . . Clay S. Holden, CENTCOM, LTD., Newton Pacific Center, 3142 Pacific Coast Highway, Suite 200, Torrance, CA 90505. Telephone: 213-325-1903

Boston, MA . . . Edward M. Black, CENTCOM, LTD. Telephone: 203-226-7131

Atlanta, GA . . . John F. Raftery, CENTCOM, LTD. Telephone: 212-972-9660

Denver, CO . . . Paul M. Butts, CENTCOM, LTD. Telephone: 415-969-4604

United Kingdom

Reading, England . . . Malcolm Thiele, Technomedia Ltd., Wood Cottage, Shurlock Row, Reading RG10 OQE, Berkshire, England. Telephone: 073-434-3302, Telex #848800, FAX: 073-434-3848

Lancashire, England . . . Technomedia Ltd., c/o Meconomics Ltd., Meconomics House, 31 Old Street, Ashton Under Lyne, Lancashire, England. Telephone: 061-308-3025

Continental Europe . . . Andre Jamar, International Communications, Inc., Rue Mallar 1, 4800 Verviers, Belgium. Telephone: (087) 22-53-85, FAX: (087) 23-03-29

Tokyo, Japan . . . Sumio Oka, International Media Representatives Ltd., 2-29 Toranomon, 1-Chome Minato-ku Tokyo 105 Japan. Telephone: 502-0656, Telex #22633, FAX: 591-2530

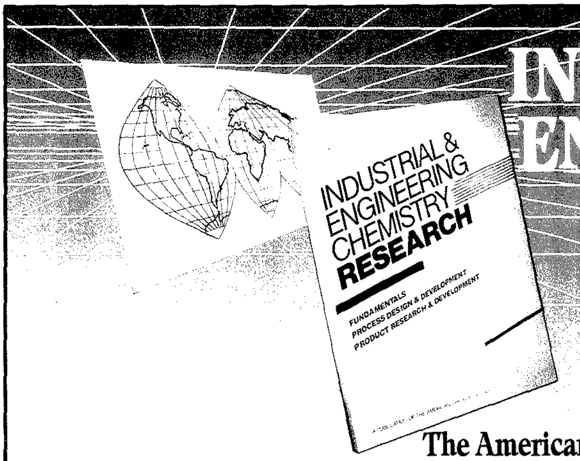
INDUSTRIAL & ENGINEERING CHEMISTRY RESEARCH
FUNDAMENTALS
PROCESS DESIGN & DEVELOPMENT
PRODUCT RESEARCH & DEVELOPMENT

INDUSTRIAL & ENGINEERING CHEMISTRY RESEARCH*

Published Monthly!

The American Chemical Society offers you *the* interdisciplinary research journal in the broad field of chemical engineering and industrial chemistry.

INDUSTRIAL & ENGINEERING CHEMISTRY RESEARCH publishes original, state-of-the-art research findings from around the world.

Quality Information That Gives You The Leading Edge

Each monthly issue of I&EC RESEARCH gives you access to new ideas . . . new techniques . . . new procedures—research that could prove crucial to you and your work.

In this one professional journal you will find reports on—
● fundamental and theoretical aspects of chemical engineering ● recent work on design methods and their applications ● current and future products involving chemical engineering processes ● process design and development ● new technologies ● special updates on timely symposia ● specially selected topics

I&EC RESEARCH helps you meet today's intense challenges in chemical technology with the most timely, innovative research. The editorial team and editorial advisory board are members of your profession—and reflect the broad spectrum of areas covered by the journal.

Start your subscription TODAY. Don't miss a single issue of I&EC RESEARCH!

*I&EC RESEARCH covers all the areas previously addressed by the three I&EC quarterlies: *Fundamentals*, *Process Design & Development*, and *Product Research & Development*.

Volume 29 (1990) **ISSN 0888-5885** **CODEN:IECRED**	U.S.	Canada & Mexico	Europe Air Service Included	All Other Countries Air Service Incl.
ACS Members				
One Year	$ 55	$ 73	$ 84	$ 94
Two Years	$ 99	$135	$157	$177
Nonmembers	$372	$390	$401	$411

Member rates are for personal use only. Subscriptions are based on a calendar year. Foreign payment must be made in U.S. currency by international money order, UNESCO coupons, or U.S. bank draft, or order through your subscription agency. For nonmember rates in Japan, contact Maruzen Co., Ltd.
This publication is available in mocrofilm, microfiche, and the full text is available online on STN International.

In a hurry?
CALL TOLL-FREE in the U.S. at **800-227-5558**, D.C. and outside the U.S. call 202-872-4363 for credit card orders, or write: **American Chemical Society,** Marketing Communications Department, 1155 16th Street, NW, Washington, D.C. 20036

Editor
Donald R. Paul
Univ. of Texas, Austin

Senior Editor
J.A. Seiner
PPG Industries

Editorial Advisory Board:
D.R. Bauer
Ford Motor Co.

K.F. Jensen
Univ. of Minnesota

C.J. King
Univ. of California, Berkeley

H. Leidheiser, Jr.
Lehigh Univ.

O. Levenspiel
Oregon State Univ.

N.N. Li
Allied-Signal Inc.

M. Morari
California Institute of Tech.

J.P. O'Connell
Univ. of Florida

J.F. Roth
Air Products and Chemicals, Inc.

D.M. Ruthven
Univ. of New Brunswick, Canada

J.J. Siirola
Eastman Kodak Co.

C.M. Starks
Cimarron Technical Assoc.

V.W. Weekman, Jr.
Mobil R&D Corp.

Analytical CHEMISTRY

EDITOR: **GEORGE H. MORRISON**

ASSOCIATE EDITORS: **Catherine C. Fenselau, Georges Guiochon, Walter C. Herlihy, Robert A. Osteryoung, Edward S. Yeung**

Editorial Headquarters
1155 Sixteenth St., N.W.
Washington, DC 20036
Phone: 202-872-4570
Telefax: 202-872-6325

Managing Editor: Sharon G. Boots

Associate Editors: Louise Voress, Mary Warner

Assistant Editors: Grace K. Lee, Alan R. Newman

Editorial Assistant: Felicia Wach

Contributing Editor: Marcia Vogel

Director, Operational Support: C. Michael Phillippe

Head, Production Department: Leroy L. Corcoran

Art Director: Alan Kahan

Designers: Amy Meyer Phifer, Robert Sargent

Production Editor: Elizabeth E. Wood

Circulation: Claud Robinson

Editorial Assistant, LabGuide: Joanne Mullican

Journals Dept., Columbus, Ohio

Associate Head: Marianne Brogan

Journals Editing Manager: Joseph E. Yurvati

Associate Editor: Rodney L. Temos

Advisory Board: Bernard J. Bulkin, Michael S. Epstein, Renaat Gijbels, William S. Hancock, Thomas L. Isenhour, James W. Jorgenson, Peter C. Jurs, Alan G. Marshall, Lawrence A. Pachla, John F. Rabolt, Debra R. Rolison, Ralph E. Sturgeon, Shigeru Terabe, George S. Wilson, Mary J. Wirth, Richard N. Zare
Ex Officio: Sam P. Perone

Instrumentation Advisory Panel: Daniel W. Armstrong, Bruce Chase, Thomas L. Chester, R. Graham Cooks, L. J. Cline Love, Sanford P. Markey, Brenda R. Shaw, Gary W. Small, R. Mark Wightman

Published by the
AMERICAN CHEMICAL SOCIETY
1155 16th Street, N.W.
Washington, DC 20036

Publications Division

Director: Robert H. Marks

Journals: Charles R. Bertsch

Special Publications: Randall E. Wedin

Manuscript requirements are published in the January 1, 1990 issue, page 89. Manuscripts for publication (4 copies) should be submitted to ANALYTICAL CHEMISTRY at the ACS Washington address.

The American Chemical Society and its editors assume no responsibility for the statements and opinions advanced by contributors. Views expressed in the editorials are those of the editors and do not necessarily represent the official position of the American Chemical Society.

AUTHOR INDEX

Abruña, H. D., 274
Ashcom, G. S., 314

Bachas, L. G., 314
Baisden, P. A., 298
Ballistreri, A., 279
Bjerga, J. M., 226
Bontempelli, G., 293

Caton, J. E., Jr., 253
Cha, S. K., 274
Cook, C. E., 244
Cotter, R. J., 248
Crouch, S. R., 304

Daunert, S., 314

Einhorn, J., 287
Emnêus, J., 263

Fang, Q. C., 244
Farnia, G., 293
Fassett, J. D., 240
Fenselau, C. C., 248
Fleming, G. S., 253
Fraser, D. J. J., 308

Garcia, M. E., 253
Garozzo, D., 279
Giuffrida, M., 279
Gorton, L., 263
Gregg, B. A., 258
Griest, W. H., 253
Griffiths, P. R., 308

Hardy, M. R., 248
Harmon, S. H., 253
Heller, A., 258

Impallomeni, G., 279
Ito, Y., 244

Kingston, H. M., 240
Kinoshita, T., 311

Lee, Y. C., 248
Lee, Y. W., 244
Lopez-Nieves, M., 304

Malosse, C., 287
Mayo, S., 240
Meyerhoff, M. E., 314
Miaw, C. L., 268
Montaudo, G., 279

Nagaki, H., 311
Nakamura, T., 311
Norton, K. L., 308

Ohki, Y., 311
Owlia, A., 268

Pack, T. W., 244
Palmer, C. E. A., 298
Papas, A. N., 234

Rusling, J. F., 268
Russo, R. E., 298

Sandonà, G., 293
Schenley, R. L., 253
Schiavon, G., 293
Silva, R. J., 298
Simpson, R. C., 248
Small, G. W., 226

Tomkins, B. A., 253
Torres, R. A., 298
Tougas, T. P., 234
Townsend, R. R., 248
Treese, C. A., 253

Varughese, K., 318
Voyksner, R. D., 244

Walker, R. J., 240
Wang, J., 318
Wentzell, P. D., 304

Zotti, G., 293

Automated Selection of Library Subsets for Infrared Spectral Searching

Joanne M. Bjerga and Gary W. Small*

Department of Chemistry, The University of Iowa, Iowa City, Iowa 52242

A method for decreasing the time required to perform a standard library search is described based on principal components analysis of infrared spectra. Principal components analysis calculates a new set of axes and coordinates which reduce the dimensionality of the original data space. Spectra are projected onto a principal plane where they are represented by a single point in a two-dimensional space. The angle of the point in the plane representing the unknown spectrum is determined, and only those library spectra with similar angles in the same plane are searched by use of the Euclidean distance metric. The principal components analysis was based on 2000 spectra in the EPA vapor phase infrared library. The plane angle procedure accurately selects a subset of spectra around the unknown which contains the 15-20 nearest matches as obtained by a previous Euclidean distance search of all 2000 spectra. The selection of the appropriate principal plane to use for a particular unknown spectrum is also discussed. The methodology is tested with intralibrary searches and with searches of laboratory data.

INTRODUCTION

The availability of digitized infrared spectral libraries has led to the development of computer-based algorithms for determining the similarity between spectra. Given a suitable spectral library, the identity of an unknown compound can often be elucidated by comparing the spectrum of the unknown to each spectrum in the library. The early research in infrared library searching was devoted to determining the best methods for representing spectra (i.e., full intensity data or peak representation) and the corresponding optimal spectral comparison algorithms for those representations (*1-3*). Quantitative measures for assessing the quality of proposed library searches have also been developed (*4, 5*). Subsequently, additional spectral representations have been offered based on peak tables (*6*), width-enhanced binary peak representations (*7*), Karhunen-Loeve transformations (principal components analysis) (*8-10*), Fourier encoding (*11*), the utilization of the phase components of the inverse fast Fourier transform (*12*), cross correlation (*13*), and odd moments of the cross correlation integral (*14*). Of these, only two proposed searches (*12, 13*) take more time than what is considered the standard library search, the Euclidean distance metric. The remainder have reduced the time required to perform library searching by deresolving the spectra (fewer points per spectrum) and/or representing the spectra in an alternate (compressed) format that can be utilized with a faster spectral comparison algorithm.

The increased size of infrared spectral libraries and the corresponding increased time required to perform searches have motivated the development of less time-consuming search algorithms. An alternative approach to simplifying the spectral representation is to develop a methodology that will select a subset of the spectral library likely to contain the spectra most similar to the unknown. Significant savings in searching time can be realized by only comparing the unknown to similar spectra. To realize these time savings, however, the subset selection or "prefilter" methodology must be implemented rapidly.

Relatively little work has been reported on prefilter strategies for infrared library searches. Anderegg and Pyo (*15*) developed a methodology for selecting the subset of the library most likely to contain a particular functionality (i.e. spectral feature). Wang and Isenhour (*10*) developed a search prefilter based on factor analysis of the time-domain representation of 900 members of a spectral library. Optimal search results depended on the number of points included in the factor analysis and the number of principal components included in the implementation of the prefilter. In this case, the projection of each library entry onto the principal components was used in the searching procedure. In this example, a data compression technique was used to select the library subset and to form the basis for the library comparisons.

Alternatively, a reduced spectral representation could be used for selecting a subset of the library, with the subsequent library search of the subset being performed with full-spectral data. Rather than requiring a new algorithm for searching the library, this approach would require only a fast prefilter capable of properly selecting the subset. The advantages of a full-spectral comparison would be retained, but the overall search speed would be increased. The function of this prefilter would be to define the subset of the spectral library that is most likely to include those spectra most similar to the target spectrum, i.e., the "hits" produced by a standard full-spectral searching procedure. Once the subset has been defined, conventional searching could commence. In this paper, a prefilter of this type is introduced based on principal components analysis. The subsequent library search is performed by use of the standard full-spectrum Euclidean distance metric.

EXPERIMENTAL SECTION

Data Preparation. A visual inspection of 3296 members of the EPA vapor phase infrared spectral library was undertaken to identify members of the library containing spectral anomalies. The 348 spectra judged anomalous were not included in this work. Of the remaining 2948 spectra, 2000 were randomly selected to form the spectral library for this work.

The spectra in the EPA library are stored at 2-cm^{-1} resolution from 4003 to 450 cm^{-1}. There are 1842 points per spectrum. In order to simplify the computations, the spectra were deresolved to 32 cm^{-1}. The spectra were deresolved in two steps, from 2 to 8 cm^{-1} and then from 8 to 32 cm^{-1}. Each step required four spectral points to be replaced by one. The points in the deresolved spectra were taken as the middle points in a series of nine-point Savitzky-Golay smooths (*16*) taken across the input spectrum. The smoothing procedure was performed to minimize discontinuities in the deresolved spectra. After smoothing, each 32-cm^{-1} spectrum is represented by only 115 points. The spectra were then normalized to reduce the effects of concentration.

Experimental Data. Ten laboratory spectra were used to test the performance of the prefilter. The compounds are (1) methylene chloride, (2) ethyl acetate, (3) 1-penten-3-ol, (4) 2-methylcyclohexanone, (5) vinyl acetate, (6) 3-pentanone, (7) acetyl acetone, (8) cyclohexanol, (9) butyric acid, and (10) 2-propyl-

0003-2700/90/0362-0226$02.50/0 © 1990 American Chemical Society

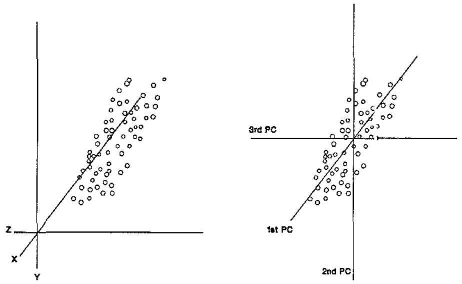

Figure 1. "Cloud" of data points represented in three dimensions (left). The same set of data points after principal components analysis has been applied (right). The origin is located in the center of the data, and the first principal component is parallel to the greatest amount of variance in the data.

pentanoic acid. The spectra were collected from a gas chromatography (GC)/Fourier transform infrared (FTIR) system consisting of a Hewlett-Packard 5890-A GC equipped with a 15 m by 0.322 mm i.d. DB 5 capillary column. The GC was coupled to an IBM M98 FTIR spectrometer equipped with a medium-range Hg:Cd:Te detector. Interferograms (2048 points) were collected and transferred by serial communications link to a Prime 9955 interactive computer system operating at the Gerard P. Weeg Computing Center at the University of Iowa. The compounds designated by the numbers **1** and **9** were single-scan spectra, i.e., no interferograms were coadded prior to Fourier transformation. For the spectra of compounds **2** through **8**, six interferograms were coadded and Fourier transformed. The spectrum of compound **10** was obtained by coadding five interferograms before Fourier transformation. The remaining computations reported here were performed on the Prime system with software implemented in FORTRAN 77. Plots were generated by use of the TELLAGRAF interactive graphics system (Integrated Software Systems Corp., San Diego, CA). A Hewlett-Packard 7475A digital plotter was used as the output device.

Principal Components Computation. Principal components analysis (PCA) has been described in the literature several times (*17–20*). The main goal of PCA is to reduce the dimensionality of experimental data and thus simplify the analysis being performed. As an example, a set of infrared spectra can be considered as points in a coordinate system, where each of the coordinate axes corresponds to a specific spectral resolution element. Due to the presence of sparsely populated spectral regions and to the occurrence of relatively wide spectral bands, the distribution of points in the space is not spherically symmetric. Stated differently, the same information could be closely approximated with fewer points if an alternate (i.e., smaller) set of coordinate axes were available. The principal components of a data set are these alternate axes. In the analysis of a set of spectra, an $m \times n$ data matrix, $\mathbf{X}$, would be formed, where m designates the number of spectra and n designates the number of data points per spectrum.

In performing PCA, $\mathbf{X}$ is decomposed as

$$\mathbf{X} = 1 \cdot \bar{x} + \mathbf{T} \cdot \mathbf{P} + \mathbf{E} \qquad (1)$$

where $\bar{x}$ is the average spectrum, $\mathbf{P}$ is an $f \times n$ principal components matrix, $\mathbf{T}$ is an $m \times f$ matrix containing the scores for each of the projections of spectra onto the principal components, and $\mathbf{E}$ is an $m \times n$ matrix of residuals. The term, f, designates the number of principal components (i.e. axes) used to represent the data. Rows of the $\mathbf{P}$ matrix define the principal axes, while columns of the $\mathbf{T}$ matrix contain the coordinates (scores) of each of the spectra onto the principal axes.

Figure 1 illustrates graphically the action of PCA in three dimensions. The "cloud" of data points is long and wide, but not very deep. Also, the cloud of data points is not oriented parallel to any of the axes of the space in which the data are plotted. PCA would yield three principal components defining a new data space, i.e. three alternate axes and associated coordinates along these axes for each data point. The first principal component describes the axis containing the largest variance in the data cloud. The second principal component would describe the axis containing the second largest variance in the data cloud and be orthogonal to the first principal component. The third and last principal component would describe the remaining variance in the data cloud and be orthogonal to both the first and second principal components. In this example, it may be possible to describe the data space adequately by use of the first and second principal components only, as the third accounts for such a small percentage of the variance in the data. In cases of higher dimensionality, it is common to use fewer principal components than required to explain 100% of the total data variance. Several methods have been described in the literature for choosing the most informative principal components (*10, 19, 21*).

The original data space is a matrix of observations (rows) and variables (columns) which have been measured. In the case of infrared spectra, the observations are compounds, and the variables are absorbance intensities at discrete wavelengths. In the work performed here, the rows of the data matrix used as the basis for the principal components analysis were the 2000 randomly selected spectra, and the 115 columns were the absorbance values of each spectrum at 32-cm^{-1} intervals between 4003 and 450 cm^{-1}.

The initial step in conventional PCA is to form the correlation matrix of the data matrix. This matrix is diagonalized to compute the entire set of principal components. However, with a large data matrix, an alternative computational method is desirable. The NIPALS (Nonlinear Iterative PArtial Least Squares) algorithm of Wold (*16*) was selected as it is designed to compute the principal components one at a time. As a first step, the average spectrum across the 2000 spectra is calculated and subtracted from each spectrum. By subtraction of the average spectrum from each row of the data matrix, the subsequent principal components will be centered; i.e., the origin of the principal axes will be at the center of the data.

The first principal component is computed by fitting a least-squares line through the centered data matrix, in such a way as to account for the greatest amount of variance in the data. Each observation is projected onto the first principal component to obtain the coordinate of each original data point on this new axis. After the information corresponding to the first principal component is subtracted from the data matrix, the second principal component is calculated in the same way. This process is repeated until the desired number of principal components have been computed. For the library of 2000 spectra, the first 23 principal components were computed to form the basis for the prefilter work.

Euclidean Distance Metric. The Euclidean distance or least-squares metric is widely used to compare infrared spectra. Each spectrum is treated as a vector of n dimensions, where n is the number of resolution elements. The absorbance intensity at each resolution element is represented by x_k for $k = 1$ to $k = n$. The geometric distance $d_{i,j}$ between two spectra $\mathbf{x}_i$ and $\mathbf{x}_j$, is calculated by

$$d_{i,j} = [\sum_{k=1}^{n} (\mathbf{x}_{i,k} - \mathbf{x}_{j,k})^2]^{1/2} \qquad (2)$$

where $\mathbf{x}_i$ is a vector representing the target spectrum and $\mathbf{x}_j$ is a vector representing a spectrum in the library. The smaller the value of $d_{i,j}$, the more similar the spectra. To speed the computation, the square root in eq 2 is usually not taken, producing a metric that is technically the squared Euclidean distance.

Developing new library searching algorithms is not as difficult as developing universally accepted criteria for evaluating the results. As in a previous study (*5*), the ability to reproduce the results of a full-spectrum Euclidean distance search will serve as the basis for evaluating the performance of the spectral prefilter.

Prefilter Benchmarks. Of the 2000 spectra used in the principal components computation, 200 were randomly selected for use in designing the prefilter methodology. A Euclidean distance search of the 2000-member (at 32 cm^{-1}) subset of the EPA library was conducted for each of these 200 target spectra. The 20 nearest matches for each of the target spectra were subsequently used as a reference point for evaluating the performance of the prefilter. Since the target spectra are members of the library being searched, the target and first nearest match were the same.

Ten spectra collected in our laboratory and 100 EPA library spectra not included in the principal components analysis were also used to test the performance of the prefilter. If the prefilter performs well for compounds not included in the PCA, then the compounds included in the PCA can be considered to be representative and can provide a basis for much larger libraries. It would be impractical to recompute the principal components each time a new spectrum is added to a library.

RESULTS AND DISCUSSION

Overview of Prefilter Design. The library search prefilter implemented in this work is based on the construction of one or more "distance lists" that serve to index the spectra in an infrared library. The distance lists contain two entries for each library spectrum: (1) the spectrum identification number and (2) a "distance" that describes the position of that spectrum in the data space defined by the library. The lists are sorted based on the distance values and stored with the library. When an unknown spectrum is searched, one of the stored lists is selected and the corresponding distance for the unknown spectrum is computed. By use of a binary search, the list is then inspected for the position at which the computed distance would be inserted. Only those library spectra with distances "nearby" are included in the actual search. Spectral comparisons in the search are performed in a standard manner, employing a metric such as the Euclidean distance.

The distance lists employed here are derived from projections of the library spectra onto the computed principal components of the library. The design and testing of these distance lists, the selection of the best list to use for a given unknown spectrum, and the actual selection of the library subset to search are discussed below.

Construction of Distance Lists. *Projection Magnitude Prefilter.* As an initial prefilter, the projection magnitudes of spectra onto a hyperplane formed by two or more principal components were tested. A distance list was constructed consisting of the sorted projection magnitudes of the 2000 library spectra onto the plane formed by the first and second principal components. The spectral identification numbers corresponding to each element in the distance list were also stored. The 200 test spectra included in the PCA calculations were used to evaluate the projection magnitude distance list. For each of these target spectra, the position of the spectrum in the distance list and the corresponding positions of the previously determined 20 nearest matches defined a subset (i.e. a range of entries) of the library. The best possible result would be obtained if the target and its 20 nearest matches were found in a range of 21 positions in the list of sorted projection magnitudes. While the use of only two principal components makes obtaining a range this small unlikely, the size of the range is the best criterion by which to judge the prefilter. The average range of library entries required to include the 20 nearest matches was 976, corresponding to a reduction of almost 50% in the library size. However, because the target spectrum is not always in the center of the range, implementation of this prefilter would require searching perhaps as many as 976 compounds on either side of the target, producing almost no reduction in search time. As the number of principal components used for the projection magnitude calculation was increased, the average range also increased. Clearly, the projection magnitude by itself does not adequately provide a basis for a spectral prefilter.

Plane Angle Prefilter. The failure of the projection magnitude as a prefilter was attributed to a lack of directional information. Two library entries may have similar projection magnitudes onto a principal plane, but they may lie in opposite directions. On the basis of this reasoning, the angle of the projection vector in the principal plane was then tested. Figure 2 depicts the projection magnitude and plane angle distances graphically. The plane angles for the 2000 member library in the plane formed by the first and second principal components were calculated and sorted. The average range of plane angles required to reproduce the list of 20 nearest matches was 456, a great improvement over the projection magnitude prefilter. However, compounds of small projection magnitude onto this plane might have some of the 20 hits projecting onto the opposite side of the origin, resulting in a large range of plane angles. Therefore, it was judged important to incorporate the projection magnitude information into the implementation of the plane angle prefilter.

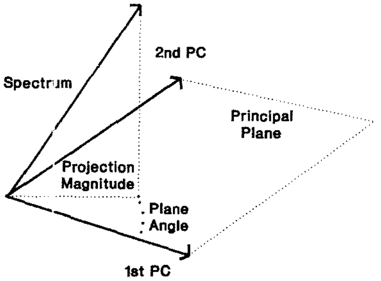

Figure 2. Projection magnitude and plane angle represented graphically.

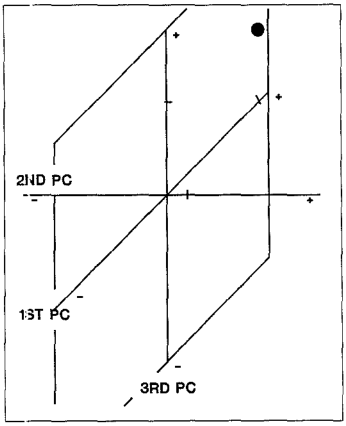

Figure 3. Representation of a point in a three-dimensional principal components space. The actual location of the point is best estimated in two dimensions by its location in the plane formed by the first and third principal components, where the values of its coordinates are the greatest.

Combining Plane Angle and Projection Magnitude Information. In order for the plane angle prefilter to be effective, the projection of the target spectrum must be far enough from the origin of the plane so that potential nearest matches will lie on the same side of the origin (i.e. have a small distribution of plane angles). This is most easily accomplished in the prefilter calculations by utilizing the plane onto which the target spectrum has the largest projection magnitude. Computationally, this is determined easily by finding the two principal components for which the target spectrum has the largest scores.

Figure 3 illustrates further the rationale for the selection of the plane containing the two largest scores of the target spectrum. The coordinates of a point in a three-dimensional space are marked on each of the axes, and the point itself is represented by the circle. The magnitude of the projection of the point onto the first and third principal components is clearly greater than the projection onto the second principal component. The point lies closer to the plane formed by the first and third principal components (the 1–3 plane), and the location of the projection of the point onto this plane, in two dimensions, closely approximates the location of the point in three dimensions. Points in the three-dimensional space near the circle will be characterized by a small distribution of angles in the 1–3 plane. Thus, the implementation of the plane angle prefilter will use the two largest scores to approximate the location of the spectrum in the reduced space spanned by the principal components.

Selection of Which Principal Components To Include. Considering that f principal components give rise to a possible $f!/(2(f-2)!)$ principal planes (1–2, 1–3, 1–4, etc.), it is important to choose the plane to use in the prefilter calculation from among only those planes deemed "significant". Previous library searching enhancement strategies relying on PCA have selected the significant principal components via several strategies (*10*). One method is to plot the total percent variance explained vs principal component number and look for the point at the which the slope of the curve approaches zero. A second method plots the log of the individual percent variance explained vs principal component number, searching for a sharp drop in the curve. Another method calculates the mean of the percent variance explained over all principal components and selects those that explain more than the mean variance as significant (*21*). In the current work, the algorithm used to generate the principal components calculates them one at a time, making it inappropriate to test for significance by use of the latter method. Plots of percent variance explained and log percent variance explained vs principal component number were examined, but no definitive conclusions could be reached regarding which principal components to include.

Theoretically, 115 principal components would be needed to explain 100% of the variance in the data. Previous principal components based library searching strategies have used the number of principal components required to explain 85% (*9*) and 90% (*10*) of the data variance. If 115 principal components were required to implement the prefilter, the purpose of computing the principal components in order to reduce the dimensionality of the problem would be defeated. It is generally accepted that the last principal components model the noise in the data and are therefore not useful. The goal is to use the minimum number of principal components in order to obtain satisfactory results.

In this study, 23 principal components were calculated, accounting for 88.96% of the variance in the data. Each principal component explains a fraction of the data variance. This explained variance can be computed from the reduction in the sum of the squares of the data values caused by subtracting the contribution of the principal component. Thus, each principal component has an associated sum-of-squares value that corresponds to the amount of information it explains.

Given that the prefilter strategy is based on projecting spectra onto the principal planes, it was hypothesized that a plot of the "areas" of the principal planes might indicate which planes would contain the greatest information. By multiplication of the sum-of-squares values for two principal components, a value is obtained that is analogous to the area of the plane formed by those principal components. These areas are plotted in the upper plot of Figure 4 for each of the 253 planes that can be formed with 23 principal components. It is clear from this figure that approximately the first 30 planes have the greatest areas. If the same 253 planes are ranked by decreasing area, the top nine planes are the 1–2 through the 1–10 planes. The plane formed with the first and 23rd principal components ranks 34th.

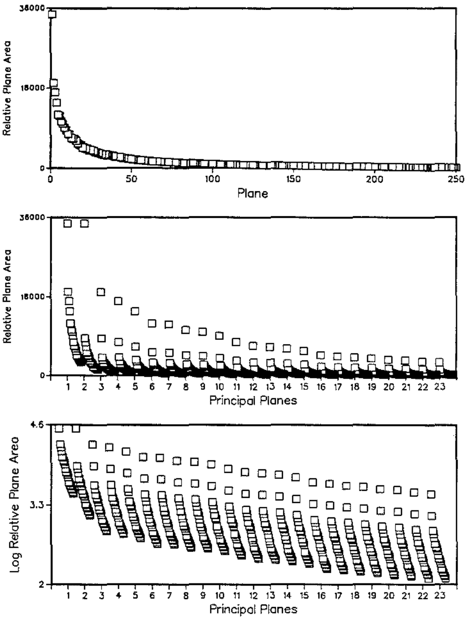

Figure 4. Top: Relative principal plane area vs plane number. Of the 253 possible planes, the first 30 contain by far the greatest area. Middle: Relative principal plane area organized by principal components used to form them. As an example, for $x = 1$, the squares represent all principal planes formed with the first principal component. The first and second principal components clearly form the planes with the largest areas. Bottom: log of relative principal plane area also organized by principal components used to form them. This plot gives a greater separation of the plane areas, but it is still clear that those planes formed with the first principal component contain the greatest relative area.

The center plot in Figure 4 is a plot of plane area vs principal components used in the area calculation. In the plot, for $x = 1$, all planes formed with the first principal component are represented. For $x = 2$, all planes formed with the second principal component are represented, etc. It is noteworthy that the area of any plane formed with the first principal component will be greater than the area of planes formed by combinations of (1) the second with ≥12th principal components and (2) ≥3rd with ≥6th principal components.

The bottom plot in Figure 4 shows the log of plane area vs principal components used in the area calculation. Once again, it is clear that the planes formed by use of either the first or second principal components have by far greater area and, based on the percent variance explained by each of them, greater information content.

Evaluation of Prefilter. *Test of 200 Compounds Included in PCA.* Two hundred compounds were randomly selected from the spectra included in the principal components analysis. The scores of these spectra onto the principal components were calculated as the principal components analysis was being performed.

It is not clear exactly how many principal components are statistically significant based on Figure 4, especially since not all 115 possible principal components were computed. Therefore, the performance of the prefilter was tested by using from 2 to all 23 calculated principal components.

For each target spectrum, the following steps were taken: (1) the two largest scores were determined (for the specified number of principal components); (2) the plane angles of all

Table I. Results of 200 Searches Using All Planes Possible

	no. of searches out of 200 (±500 plane angles)			
no. of hits	5[a]	10	15	23
20	185	187	183	178
19	10	5	11	15
18	3	3	3	5
17	–	3	2	2
16	2	1	–	–
⋮				
12	–	1	1	–

[a] Number of principal components.

Table II. Results of 200 Searches Using 1-Planes

	no. of searches out of 200 (±500 plane angles)			
no. of hits	5[a]	10	15	23
20	181	180	179	177
19	12	11	13	14
18	4	3	1	2
17	1	5	5	6
16	2	–	–	–
⋮				
12	–	1	2	1

[a] Number of principal components.

Table III. Results of 200 Searches Using All Planes Possible

	no. of searches out of 200			
no. of hits	5[a]	10	15	23
	(±500 plane angles)			
10	197	193	193	192
9	2	5	4	6
8	–	2	3	2
7	1	–	–	–
	(±400 plane angles)			
10	194	191	189	188
9	5	6	4	4
8	–	3	5	5
7	–	–	2	3
6	1	–	–	–
	(±300 plane angles)			
10	180	181	180	175
9	15	13	10	11
8	3	3	6	7
7	1	2	3	5
6	–	1	1	2
5	–	–	–	–
4	1	–	–	–

[a] Number of principal components.

2000 members of the library included in the principal components analysis were calculated in the plane indicated in part 1; (3) the plane angles were sorted along with their spectral identification numbers; and (4) the position in the list of the target and its 20 nearest matches were determined. By use of the above procedure, the average range in the list of the 200 targets and their corresponding 20 nearest matches was computed based on the use of 2 to 23 principal components. These results are plotted at the top of Figure 5, with the error bars defined by the 90% confidence interval. As the number of principal components is increased, i.e., the number of planes from which to select increases, the average range of plane angles required to span all 20 nearest matches decreases. In this first set of cases, the first "hit" is the target itself. The average range decreases until 10–11 principal components are included, at which point the average levels off at approximately 330. Most of the target spectra have their largest scores onto the first through tenth principal components and will therefore not benefit much by including more principal components.

As noted previously, the planes formed with the first principal component have by far the greatest area as a group. The ability of these planes alone to form the basis for the spectral prefilter was also tested. For each target spectrum, the largest score onto a specified number of principal components was determined. If the largest score was on the first principal component, the second largest score was determined, and the corresponding plane was used for the prefilter. If the largest score was not on the first principal component, that principal component along with the first principal component would form the basis for the prefilter. Steps 2–4 were then followed as described above. The average range required to include all 20 nearest matches is plotted at the bottom of Figure 5. As in the case where all planes were used, the average range decreases as the number of principal components increases up to around 10. The average also levels off around 330, but the error bars defining the 90% confidence interval are slightly larger. These results indicate that the plane angle in the plane formed by the principal components where the target spectrum has its largest scores can function as a prefilter for a conventional Euclidean distance search.

In the previous section, the ranges of plane angles required to encompass 20 hits were reported. As mentioned, the plane angle of the target is not always in the middle of the range, and is often at the beginning or end of the plane angle range. Any implementation scheme must take this observation into account. To use the prefilter in an actual library search, a range of plane angles around the position of the target spectrum must be defined. This range serves as the library subset to be searched. Initially, ±500 plane angles (i.e., ±25% of the number of library entries) was chosen as a reasonable range in which the nearest matches should be found, as the average range reached a minimum around 325.

Although the average range required to span the 20 nearest matches leveled off around 10–11 principal components, the implementation of the plane angle as a prefilter using the largest two scores on the principal components of the target compound was tested at 5, 10, 15, and 23 principal components.

Thus, for each of the 200 spectra, the position in the appropriate list of plane angles was found, and the range of ±500 spectra in the list was interrogated for the presence of the 20 nearest matches determined through the Euclidean distance search of the full 2000-member library. Table I lists the number of searches (out of 200) that return a specified number of the 20 nearest matches when the ±500 range is inspected. The results are listed by the number of principal components used in selecting the best list of plane angles. All possible planes were considered for the specified number of principal components. For example, in 185 of the 200 cases, each of the 20 nearest matches was found in the ±500 range when the plane angle list was selected from among all planes formed by the first five principal components. An additional 10 cases produced 19 of the 20 nearest matches. All 200 searches obtained at least 16 of the 20 nearest matches when this prefilter strategy was used. Analogously, when all planes formed by the first 10 principal components were used in selecting the list of plane angles, all 20 nearest matches were found in the ±500 range in 187 of the 200 cases.

Table II lists the analogous information when only the planes formed with the first principal component are considered. Figure 6 displays the results in Tables I and II graphically in the form of two clustered bar graphs. The upper plot is based on the data in Table I, while the lower plot is

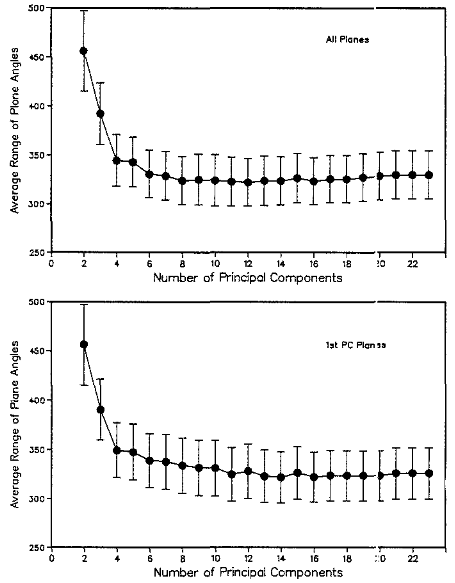

Figure 5. Average range of library entries required to obtain all of the top 20 nearest matches as defined by a Euclidean distance search of the 2000 member library. The top plot depicts the results obtained when all of the planes formed by the specified number of principal components are utilized, while the bottom plot displays the results obtained when only the planes formed with the first principal component are used. Little difference is observed between the two sets of results.

Table IV. Results of 200 Searches Using 1-Planes

no. of hits	no. of searches out of 200			
	5^a	10	15	23
	(±500 plane angles)			
10	196	193	193	193
9	3	6	3	4
8	–	1	4	3
7	1	–	–	–
	(±400 plane angles)			
10	191	189	190	191
9	8	9	2	1
8	–	2	4	4
7	–	–	3	3
6	1	–	1	1
	(±300 plane angles)			
10	178	178	179	177
9	17	16	12	13
8	3	2	3	3
7	1	3	4	5
6	–	1	2	2
5	–	–	–	–
4	1	–	–	–

[a] Number of principal components.

based on the data in Table II.

Tables III and IV display the analogous information when only the first ten nearest matches are considered. Out of 200 targets, 197 return all of the top 10 nearest matches when a range of ±500 plane angles is specified for five principal components, all possible planes. If the range is reduced to ±400, 194 searches return all of the top 10 nearest matches. If the range is further reduced to ±300, 180 searches return all of the top 10 nearest matches, and 195 searches will return at least 9 of the top 10 nearest matches. Thus the number of searches obtaining the 20 nearest matches at a range of ±500 is comparable to the number of searches obtaining the 10 nearest matches at a range of ±300. Similar results are obtained when only the planes formed with the first principal component are considered, as shown in Table IV.

Table V. Results of 100 Test Spectra Using All Planes

no. of hits	no. of searches out of 100 (±500 plane angles)			
	5^a	10	15	23
21	96	91	87	90
20	1	6	7	6
19	2	–	1	2
18	–	–	2	1
17	1	1	1	–
16	–	1	1	1
15	–	–	–	–
14	–	1	1	–

[a] Number of principal components.

Table VI. Results of 100 Test Spectra Using All Planes

no. of hits	no. of searches out of 100 (±300 plane angles)			
	5^a	10	15	23
11	91	88	86	87
10	7	9	9	8
9	1	1	1	2
8	–	–	1	1
7	1	2	3	2

[a] Number of principal components.

Test of 100 Library Spectra Not Included in PCA. To test the plane angle prefilter further, 100 EPA spectra not included in the PCA calculations were randomly selected. A Euclidean distance search of the 2000 member subset of the EPA library was performed at 32 cm^{-1} to obtain a list of 20 nearest matches. In order to implement the prefilter, the following steps were taken: (1) the target spectrum was deresolved as before to 32 cm^{-1}; (2) the deresolved spectra were projected onto each of the principal components to obtain the corresponding scores; (3) the two largest scores were determined among the specified number of principal components; (4) the plane angles of the target and 2000 member subset were calculated; (5) the plane angles were sorted along with their spectral identification numbers; and (6) the list of sorted plane angles was inspected to determine the location of the target and its 20 nearest matches. The results of this experiment are summarized in Table V and displayed graphically in Figure 7. In these searches, the top hit is not the target, as the target is not included in the subset of the EPA library searched. Therefore, the ranges must include the nearest matches and the target (i.e. for 20 nearest matches, 21 plane angles will result). By use of five principal components, 96 out of 100 searches returned all of the top 21 hits, using all possible planes and a range of ±500 plane angles. All 100 searches returned 17 of the top 21 hits when the 22 planes formed with the first principal component were used. Table VI shows the results for including the top 10 nearest matches. The range of plane angles on either side of the target is ±300 as that range was previously shown to be adequate. By use of five principal components, 91 searches include all top 10 nearest matches, while 98 out of 100 include at least the top 9 nearest matches. It is clear that the prefilter functions comparably for spectra not included in the principal components analysis.

Test of Prefilter with Experimental Spectra. The experimental GC/FTIR spectra were collected at 8-cm^{-1} resolution. These spectra were deresolved as described previously in order

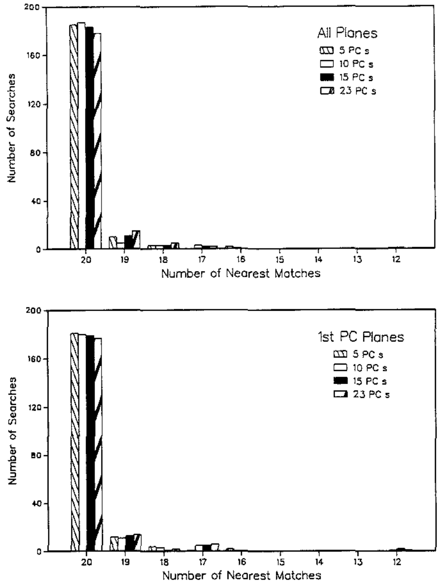

Figure 6. Histograms indicating the number of searches (out of 200) for which the indicated number of nearest matches (out of 20) were obtained when the prefilter methodology was employed. The top histogram displays the results obtained when all planes formed by the specified number of principal components were used, while the bottom histogram displays the results obtained through the use of only planes formed with the first principal component. Little difference is noted between the two sets of results.

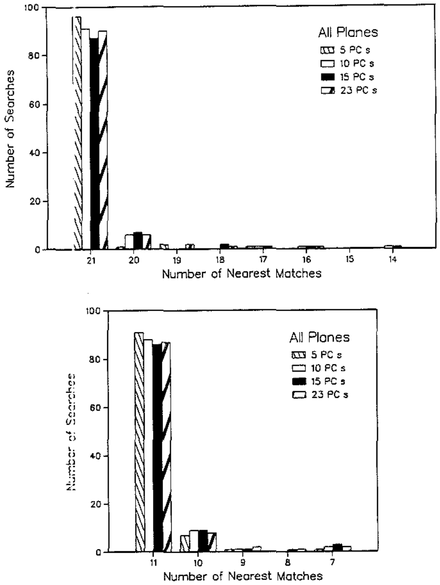

Figure 7. Histograms indicating the search results obtained when the prefilter methodology was applied to the 100 library spectra not included in the PCA. The results are displayed in a manner analogous to Figure 6. The displayed results are equivalent to those obtained for spectra included in the PCA.

Table VII. Results for 10 Experimental Spectra Using All Planes

no. of hits	no. of searches out of 10 (±500 plane angles)			
	5^a	10	15	23
21	7	7	8	8
20	1	1	1	1
19	2	1	1	1
18	–	1	–	–

[a] Number of principal components.

Table VIII. Results for 10 Experimental Spectra Using All Planes

no. of hits	no. of searches out of 10 (±300 plane angles)			
	5^a	10	15	23
11	7	8	9	9
10	–	–	–	–
9	$2^{b,c}$	–	–	–
8	1^d	$2^{b,d}$	1^d	1^d

[a] Number of principal components. [b] 1-Penten-3-ol. [c] 2-Propylpentanoic acid. [d] 2-Methylcyclohexanone.

to use the 32-cm^{-1} EPA library. The same steps in testing the prefilter were then followed as described above for the group of 100 EPA spectra. The results are summarized in Table VII for the ability to include the 20 nearest matches within the range of ±500 plane angles on either side of the position of each target spectrum in the chosen plane. By use of 5, 15, or 23 principal components, 19 out of 21 hits were returned for all of the experimental spectra. Table VIII lists the results for the top 10 nearest matches using a plane angle range of ±300 entries. The best results were obtained with either 15 or 23 principal components, where 9 of 10 searches obtained all of the top 10 nearest matches, while the remaining search returned 7.

It is interesting to note that the performance of the prefilter increases as the number of principal components increases. In the previous sections, five principal components were capable of producing the best results. The key difference between the experimental spectra and the library spectra used previously is the presence in the experimental spectra of significantly higher noise. The increased variation in these spectra appears to cause the spectral information to be distributed across a larger number of principal components. By including more principal components in the selection of the plane to use for the prefilter calculation, it appears that a more accurate representation can be made of the orientation of the experimental spectrum in the data space defined by the library spectra.

As indicated in Table VIII, the prefilter calculation works significantly worse for the case of 2-methylcyclohexanone than for the other nine experimental spectra. In this case, 3 of the 11 nearest spectral matches are not present in the range of ±300 plane angles. Inspections of the experimental spectra and the lists of nearest matches have not revealed a clearcut reason for this anomalous result. This case remains under study in our laboratory.

Computational Speed. Finally, the question of computational cost of the prefilter must be weighed against the benefits. The principal components analysis as well as the plane angle distance list computations would be performed only once for a given library. Searching an unknown spectrum would require first that the unknown spectrum be projected onto each of the principal components. Each projection calculation is equal to one Euclidean distance calculation in terms of the number of computations required. Thus, assuming that the binary search of the chosen distance list is negligible, the computational cost of the prefilter is f spectral comparisons, where f is the number of principal components used.

The only other cost of the prefilter is the increased disk space required to store the sorted distance lists. Given the decreased cost and increased capacity of computer disk drives, this storage requirement is judged insignificant in most cases. If storage space were a concern, the prefilter strategy could be implemented adequately by use of only those planes formed with the first principal component.

Weighed against these costs of the prefilter are significant benefits in terms of reducing the number of spectral comparisons required. On the basis of the testing performed here, a 50% savings in searching time can be realized if the 20 nearest matches are sought (±500 plane angles used), and a 70% savings can be realized if only the first 10 nearest matches are desired (±300 plane angles used).

CONCLUSIONS

It has been shown that principal components analysis of a vapor phase infrared spectral library can form the basis for a reliable prefilter for standard Euclidean distance searching. As few as five principal components are capable of providing excellent results. The principal components need only be recomputed occasionally as deemed necessary by the addition of significant numbers of new library members not already represented in the original PCA data matrix. Alternatively, a strategy of carefully selecting the spectra to be included in the principal components analysis could be employed where only one spectrum from a given class or subclass of compounds would be represented.

While the work described here was based on a specific infrared spectral library, we know of no reason why these prefiltering concepts could not be used with other libraries or with other types of spectral data. The number of principal components to use in the selection of the best plane for the prefilter calculation does appear to be an experimental variable, however. The results presented here indicate that the number of principal components to use is related to the noise level in the unknown spectrum. It would appear that this variable needs to be optimized for each specific application in order to define an acceptable trade-off between the performance of the prefilter and the number of computations required.

Papers describing the development of library searching algorithms often include great detail regarding the hit lists or spectra in order to rationalize their results. In this paper, no attempt has been made to qualitatively evaluate the results of the Euclidean distance metric used as the benchmark for the prefilter. It may be that the nearest matches not within the specified plane angle ranges are not similar to the target spectrum. However, since the prefilter was developed specifically for the Euclidean search, the results are left to stand on their own merit.

Finally, if one calculates the plane angles for each of the 200 spectra included in the development of the prefilter for all possible planes, it is found that selecting the plane based on the two largest principal components scores does not always produce the minimum range of plane angles. Therefore, an improvement in the prefilter methodology may be realized with the development of an alternative method for selecting the principal plane to use for a particular target spectrum.

LITERATURE CITED

(1) Rasmussen, G. T.; Isenhour, T. L. *Appl. Spectrosc.* **1979**, *33*, 371–376.
(2) Tanabe, K.; Tamura, T.; Hiraishi, J.; Saeki, S. *Anal. Chim. Acta* **1979**, *112*, 211–218.
(3) Erickson, M. D. *Appl. Spectrosc.* **1981**, *35*, 181–184.
(4) Kwiatkowski, J.; Riepe, W. *Frezsenus' Z. Anal. Chem.* **1980**, *302*, 300–303.
(5) Delaney, D. F.; Warren, F. V., Jr.; Hallowell, J. R., Jr. *Anal. Chem.* **1983**, *55*, 1925–1929.
(6) Lowry, S. R.; Huppler, D. A. *Anal. Chem.* **1983**, *55*, 1288–1291.
(7) Warren, F. V., Jr.; Delaney, M. F. *Appl. Spectrosc.* **1983**, *37*, 172–181.
(8) Williams, S. S.; Lam, R. B.; Isenhour, T. L. *Anal. Chem.* **1981**, *55*, 1117–1121.
(9) Hangac, G.; Wieboldt, R. C.; Lam, R. B.; Isenhour, T. L. *Appl. Spectrosc.* **1982**, *36*, 40–47.
(10) Wang, C. P.; Isenhour, T. L. *Appl. Spectrosc.* **1987**, *41*, 185–195.
(11) Azarraga, L. V.; Williams, R. R.; deHaseth, J. A. *Appl. Spectrosc.* **1981**, *35*, 466–469.
(12) Kawata, S.; Noda, T.; Minami, S. *Appl. Spectrosc.* **1987**, *41*, 1176–1184.
(13) Powell, L. A.; Hieftje, G. M. *Anal. Chim. Acta* **1978**, *100*, 313–327.
(14) Yu, J.; Friedrich, H. B. *Appl. Spectrosc.* **1987**, *41*, 869–874.
(15) Anderegg, R. J.; Pyo, D. *Anal. Chem.* **1987**, *59*, 1914–1917.
(16) Savitsky, A.; Golay, M. J. E. *Anal. Chem.* **1964**, *36*, 1627–1639.
(17) Wold, H. In *Multivariate Analysis*; Krishnaiah, P. R., Ed.; Academic Press: New York, 1966; Vol. 1.
(18) Lyttkens, E. In *Multivariate Analysis*; Krishnaiah, P. R., Ed.; Academic Press: New York, 1966; Vol. 1, pp 335–350.
(19) Malinowski, E. R.; Gowery, D. G. *Factor Analysis in Chemistry*; Wiley-Interscience: New York, 1980.
(20) Wold, S.; Albano, C.; Dunn, W. J., III; Edlund, U.; Esbensen, K.; Geladi, P.; Hellberg, S.; Johansson, E.; Lindberg, W.; Sjostrom, M. In *Mathematics and Statistics in Chemistry*, Kowalski, B. R., Ed.; D. Reidel Publishing Co.: Boston, MA, 1984.
(21) Kaiser, H. F. *Educ. Psychol. Meas.* **1960**, *20*, 141.

RECEIVED for review July 14, 1989. Accepted November 8, 1989.

Anal. Chem. **1990**, *62*, 234–239

Accuracy of Peak Deconvolution Algorithms within Chromatographic Integrators

Andrew N. Papas*,[1]

U.S. Food & Drug Administration, Winchester Engineering and Analytical Center, Winchester, Massachusetts 01890

Terrence P. Tougas[1]

Chemistry Department, University of Lowell, University Avenue, Lowell, Massachusetts 01854

The soundness of present-day algorithms to deconvolve overlapping skewed peaks was investigated. From simulated studies based on the exponentially modified Gaussian model (EMG), chromatographic peak area inaccuracies for unresolved peaks are presented for the two deconvolution methods, the tangent skim and the perpendicular drop method. These inherent inaccuracies, in many cases exceeding 50%, are much greater than those calculated from ideal Gaussian profiles. Multiple linear regression (MLR) was used to build models that predict the relative error for either peak deconvolution method. MLR also provided a means for determining influential independent variables, defining the required chromatographic relationships needed for prediction. Once forecasted errors for both methods are calculated, selection of either peak deconvolution method can be made by minimum errors. These selection boundaries are contrasted to method selection criteria of present data systems' algorithms.

INTRODUCTION

Chromatographers have developed efficient columns for the separation of complex mixtures, yet many times additional efficiency reveals partially resolved coeluting bands not seen with older generation columns or instrumentation. With complex sample matrices such as biological, agricultural, or natural products separations, it may not be possible to avoid overlapping peaks. According to Giddings (*1*), a chromatogram must be approximately 95% vacant to provide a 90% probability that a given component of interest will appear as an isolated component. In many cases either pure standards are not available or the external standard's "background" does not match that of the analytes; in these cases the accuracy of the peak area deconvolution software is very critical. Even though it is recommended that all quantitative analyses involve base line resolved peaks to avoid problems (*2*), this is not always possible. In these situations, chromatographers rely on their intelligent integrator/data system to reliably and accurately quantitate their analyte.

Chromatographic peaks can be characterized by a Gaussian profile when there is no instrumental distortion. However, it has been shown many times that any number of extracolumn processes lead to peak asymmetry (*3–6*). Some feel that as a result of too many undefined causes for tailing, no unique analytical functional form can be used for such peaks (*7–9*). Despite this argument, a single representative mathematical function has been pursued vigorously.

Due to extracolumn effects that distort the ideal Gaussian profile, true chromatographic peaks are better represented by an asymmetric profile. Models that have been applied to real data include the following: a combination Gaussian/triangle/exponential decay (*10*); a combination Cauchy and Gaussian (*11, 12*); a combination Gaussian–hyperbolic–exponential decay (*9*); a bi-Gaussian (*13, 4*), Poisson (*13, 4*); a cam-driven analog peak (*14*); a Binomial (*6*); and a Gram–Charlier (*15*). Theoretical and experimental work has been done by Pauls and Rogers (*16*), Grushka (*17*), Maynard (*18*), and others on demonstrating exponential decay which justifies the use of an exponentially modified Gaussian (EMG) model, a convolution of a Gaussian profile with an exponential decay. In limited studies by Foley (*19, 20*), this model was shown to be valid for over 90% of the real data analyzed. Even though only 90% of the real data tested can be adequately described by the EMG model, leaving 10% uncharacterized, it would appear that the EMG is the best proposed model to mimic real chromatographic data.

A recent publication (*21*) reviewed the development and operation of electronic integrators and commercial data systems over the span of 30 years. All peak deconvolution methods appropriate for single-dimensional data were presented and scrutinized. The most *reliable* and simple peak area deconvolution methods found were the perpendicular drop method (PD) and the tangent skim method (TS), even though both are inherently inaccurate (*22, 23*). Recently, empirical geometric peak moment calculations for paired overlapped EMG peaks (*25*) have been published, applicable only to chromatographic peaks that fit the EMG profile. Over 20 years have passed, yet no better reliable mathematical peak deconvolution has been found for single-dimensional peaks of no known profile. As a result, tangent skim and perpendicular drop are the only two peak deconvolution methods currently used by electronic integrators.

When the resolution of two overlapping tailed peaks decreases, the perpendicular drop method becomes very inaccurate for the smaller peak; dropping a perpendicular makes the smaller peak grossly overestimated whereas the larger peak is underestimated. Under these conditions, the tangent skim method appears to be more appropriate. Criteria for deciding whether to use either tangent skim or perpendicular drop are not well defined. A general rule of thumb employs the peak height ratio, and a value of 10:1 has been suggested as the decision point. Recent studies indicate very real and large differences exist among manufacturers, leading to large differences in peak quantitation (*25, 26*). This work delineates peak conditions necessary for applying a tangent skim. Unfortunately, tangent skim methods are not available on some commercial data systems (*25*), forcing all peaks to be deconvoluted by the PD method.

This paper numerically assesses the accuracy of the two peak deconvolution methods under controlled conditions. Multiple linear regression (MLR) is then used to assess the dependence of each specified chromatographic factor on the observed error, where minimized error is suggested for method selection. To demonstrate correct peak deconvolution method

---

[1] Present address: Polaroid Corp., Film Imaging Research, Bld. W4, 1265 Main St., Waltham, MA 02254.

0003-2700/90/0362-0234$02.50/0 © 1990 American Chemical Society

selection, published method selection criteria for several commercial algorithms are compared to the MLR results, critically assessing the validity of peak deconvolution method selection criteria within present-day integrators.

EXPERIMENTAL SECTION

A Pascal program (Turbo Pascal, Borland International, Inc., Scotts Valley, CA) written to generate EMG-based chromatograms is based on the EMG polynomial approximation (*26*). This was an adaption from previous work (*29*), where the current simulations were performed on an IBM-PC compatible computer.

Several families of paired unresolved asymmetric peaks were stimulated. (To ensure simplicity and to avoid any confounding effects, only paired peaks are considered.) The degree of tailing for an EMG peak is characterized by its τ/σ ratio, where σ is the Gaussian standard deviation and τ is the EMG exponential decay constant. Four chromatographic factors are considered in groups: the (ratioed) peak standard deviation ratio ($[(\sigma^2 + \tau^2)_a/(\sigma^2 + \tau^2)_b]^{1/2}$), the peak resolution ($(t_1 - t_2)/(\sigma^2 + \tau^2)^{1/2}$) the peak asymmetry ratio (τ/σ), or the peak area ratio (A/B). Each is varied systematically, while the others remain constant. Peak accuracy was calculated by calculating the percent of the true peak area with the net peak area determined for both peak deconvolution methods. This percent error was tabulated along with the simulation chromatographic conditions and EMG peak shape parameters (τ/σ, resolution, area ratio, and $[(\sigma^2 + \tau^2)_a/(\sigma^2 + \tau^2)_b]^{1/2}$. Peak height ratios ($H_a/H_b$) were recorded for statistical analysis. One representative chromatogram was computer-simulated as described elsewhere (*30*) and quantitated by two integrators. These results were compared to tabulated errors for confirmation.

BMDP's subprogram 1R (BMDP Statistical Software, Los Angeles, CA) was used for the least-squares multiple linear regression (MLR). For each deconvolution method, a model of the dependent variable accuracy is considered a function of five primary variables (resolution, variance ratio, area ratio, peak asymmetry, and peak height ratio) as well as all 20 two-way interaction and factor-squared terms.

Selection of the best model was performed manually by backward elimination, where all variables—including all cross terms—were introduced and insignificant terms were eliminated one by one. Model selection was based on three criteria: the smaller s^2, the largest (reduced) R^2, and random residual plots. (R^2 is the sum of squares due to regression divided by the total corrected sum of squares and explains the proportion of total variation about the mean accounted for by the regression model. The value of s^2, the variance about the regression, measures the error with which any observed value of the response variable could be predicted from the dependent variable values using the proposed regression model. Random-looking residual plots are prerequisite to satisfy regression model assumptions.) All graphs were performed in Lotus 1-2-3 (Version 2.01, Lotus Development Corp., Cambridge, MA).

RESULTS AND DISCUSSIONS

There are four peak parameters that were systematically varied in each independent set or family of chromatograms: peak area ratio, resolution, τ/σ ratio, and peak variance ratio. The first family of chromatograms constrained paired peaks that vary in peak variance (for the EMG, the variance is ($\sigma^2 + \tau^2$)) while remaining constant in ratioed peak area (10:1), peak asymmetry (τ/σ), and in peak resolution ($R = 1.0$). Each family is simulated at each of three peak asymmetry (τ/σ) levels: 0.0, 2.0, and 4.0. Figure 1a shows the chromatograms of $\tau/\sigma = 4.0$, part b shows the chromatograms of $\tau/\sigma = 2.0$, and part c shows the chromatograms of $\tau/\sigma = 0.0$. Each plot contains eight paired chromatograms. In all cases, the paired peaks begin at a standard deviation ratio of 8:1 (large peak ratioed to the small peak) on the left and decrease by 1 for each paired chromatogram. Thus each plot contains paired chromatograms sequenced at a standard deviation ratio of 8:1, 7:1, 5:1, 4:1, 3:1, 2:1, and 1:1, from left to right.

Even though the index of peak separation (resolution) is calculated to be 1.0 in all cases, it is obvious that the peak separation is not constant as peak asymmetry increases. This would also happen in reverse if instead of the true variance ($\sigma^2 + \tau^2$) being used in the resolution equation, only σ^2 were used, excluding τ^2. This was discussed previously (*23, 29*) and is graphically depicted here.

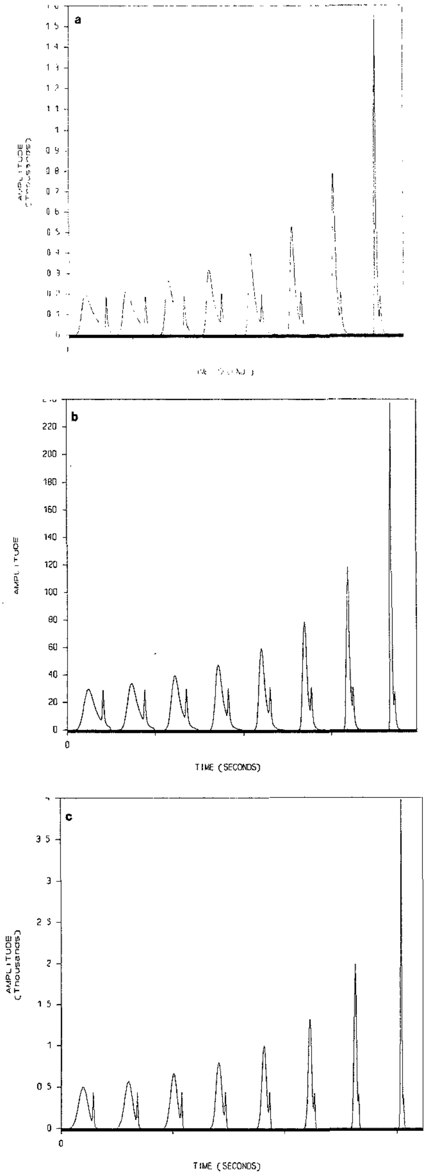

Figure 1. (a) Chromatograms of constant resolution ($R = 1.0$), peak area ratio (10:1), and asymmetry ($\tau/\sigma = 4.0$) obtained while the standard deviation ratio was varied from 8:1 to 1:1. (b) Same conditions as in part a except peak asymmetry changed; $\tau/\sigma = 2.0$. (c) Same conditions as in part a except peak asymmetry changed; $\tau/\sigma = 0.0$.

Note the peak height ratio in each case. As the peak width ratio decreases from 8:1 to 1:1 (left to right) in Figure 1, the peak height ratio (the larger's height divided by the second

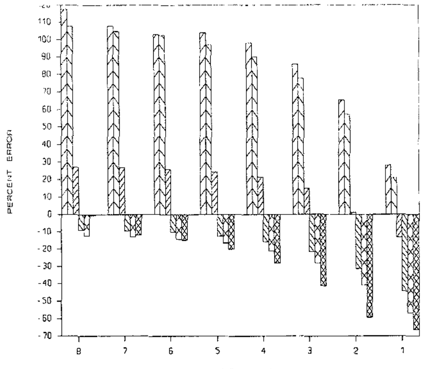

Figure 2. Peak area errors for the two peak deconvolution methods at variance ratios of 8:1, 7:1, 6:1, 5:1, 4:1, 3:1, 2:1, and 1:1. Positive errors are for the perpendicular drop method at τ/σ = 4, 2, 0 followed by negative errors for the tangent skim.

peak's height) varies roughly from 1:1 to 10:1. A selection of peak deconvolution methods based on peak height ratio would select the TS method for *lower* ratios and the PD method for *higher* ratios for minimum error. Looking ahead, the opposite decision is reached by many commercial algorithms (i.e. selecting TS for higher ratios and PD for low ratios).

The percent error for the smaller peak in the chromatograms of Figure 1 is presented in Figure 2 where the abscissa is the peak standard deviation ratio, or the width of the larger peak to the smaller. At each standard deviation ratio are six bar graphs, a pair for each τ/σ ratio: 4.0, 2.0, and 0.0, respectively. Each pair consists of the percent error for the perpendicular drop (positive errors) deconvolution method (of the larger peak) and the percent error for the tangent skim peak (negative errors) deconvolution method. Experimental verification of these errors was accomplished by inputting the simulated chromatograms of Figure 1a to two representative integrators through an interrupt driven digital-to-analog converter. Peak areas were quantitated for both the PD and TS methods, and percent errors were then calculated. Agreements were within 1%–4% of those values manually calculated in Figure 2.

The perpendicular drop results in positive errors, and the tangent skim always results in negative errors, due to the nature of the "base line". The perpendicular drop method will gain more area from the larger (first) peak than it loses from the second peak, whereas the straight line tangent skim will always account for less of the true underlying curve "base line" (base lines are relative; here the *base line* is actually the first peak's profile). There are much larger errors, both positive and negative, for the asymmetric peaks in any situation compared to Gaussian peaks. Of course, since it is the tail overlap of the first asymmetric EMG into the second peak, a combination of EMG followed by a Gaussian peak will result in the exact errors reported here. Only in the case of three or more peaks will the second peak's asymmetry affect its error by either deconvolution method.

By plotting the percent error as in Figure 2, it is easy to graphically determine which method results in minimum error for specific chromatographic conditions. It appears that some threshold point exists for switching from one method to another to minimize peak error, depending on the peaks' τ/σ ratio and standard deviation ratio (at these fixed conditions of resolution equaling 1.0 and an area ratio of 10:1). In the next two studies the effect of changing resolution and changing peak area ratios was examined.

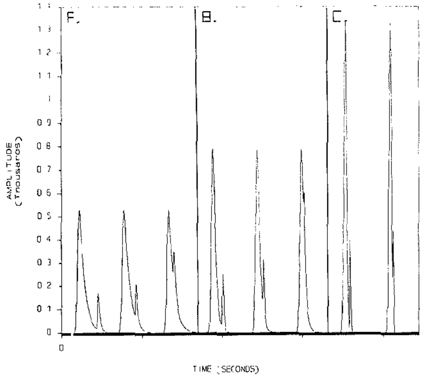

Figure 3. Chromatograms at three levels of resolution, R = 1.5, 1.0, and 0.5, for a fixed variance ratio of 3:1 and a peak area ratio of 10:1. Values of τ/σ; (A) 4.0, (B) 2.0, (C) 0.0.

The chromatograms in Figure 3 depict changes in resolution for the three τ/σ levels resulting in eight sets of overlapping peaks. For all paired peaks, the area ratio is fixed at 10:1 and the standard deviation ratio is fixed at 3.0. In figure 3A, chromatograms of τ/σ = 4.0 are presented at a resolution of 1.5, 1.0, and 0.5. In Figure 3B, τ/σ = 2.0, and in Figure 3C, τ/σ = 0.0 (or Gaussian peaks). The third Gaussian situation at a resolution of 0.5 is not presented; at this resolution and peak width ratio, there is only one fused peak or shoulder peak. No tangent skimming is possible, and therefore this case is not included in further studies.

As the resolution decreases in Figure 3A–C and the peak overlap increases, the relative peak height ratio decreases regardless of the peak asymmetry. The amount of peak area from the larger "solvent" peak underlying the smaller peak increases as resolution decreases. A perpendicular drop peak area assignment at lower resolution would include more of the larger peak's area, making a skim separation intuitively more appropriate, as verified below. Resolution should therefore be influential in selecting a peak deconvolution method. What information does the peak height ratio convey? A decrease in the peak height ratio indirectly representing a loss in resolution would select the TS method. Any algorithm selection based solely on peak height ratios would pick the TS method at *low* ratios and the PD method at *high* ratios for minimal error. This is again the exact opposite decision reached by many algorithms that rely strictly on peak height ratios to select a peak deconvolution method.

Errors for the chromatograms presented in Figure 3 are reported in Figure 4. As the resolution decreases from left to right, the PD errors increase dramatically (published elsewhere (23)), whereas the TS errors increase very little. The peak asymmetry only amplifies this effect. It is clear that errors from a wrong peak separation method will become acute as the resolution decreases, exceeding 200% at a resolution of 0.5. At this standard deviation ratio (8:1), TS is more appropriate for all levels of peak asymmetry at all resolution levels considered, including Gaussian peaks.

When the standard deviation ratio is changed, method selection is not as clear-cut. In Figure 5, errors are presented for the same conditions as in Figure 4, except the standard deviation ratio has been changed to 3:1. In a comparison of Figures 5 and 6, the errors incurred at a lower standard deviation ratio are less severe. Because the paired peaks are closer in peak width, the contribution of the larger peak's underlying tail is less. At a resolution of 1.5, the two methods are equally inaccurate. But at lower resolution, use of the TS

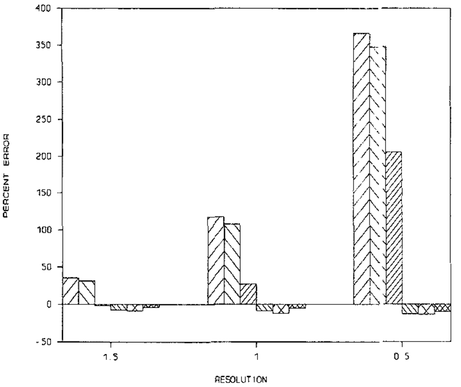

Figure 4. Peak errors at standard deviation ratio of 8:1 at resolution of 1.5, 1.0, and 0.5. At each resolution level are positive PD errors for τ/σ = 4, 2, 0 followed by the negative errors for τ/σ = 4, 2, 0.

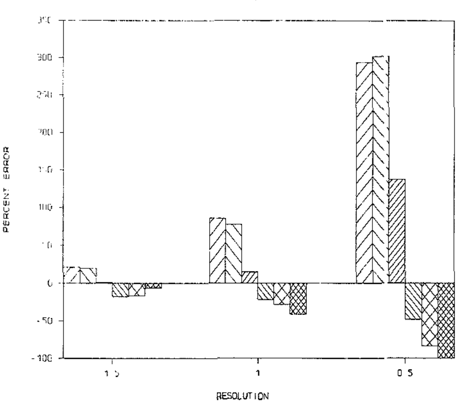

Figure 5. Peak errors incurred at a variance ratio of 8:1 while the resolution was changed from 1.5 to 0.5. Positive PD errors for τ/σ = 4, 2, 0 are followed by the negative errors for τ/σ = 4, 2, 0.

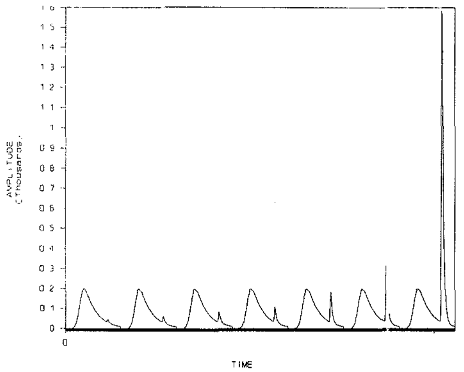

Figure 6. Chromatogram of paired peaks changing in peak area ratio, from 100:1 to 1:0 at τ/σ = 4.0, variance ratio = 8:1, and R = 1.0.

method results in less error for both symmetric and asymmetric peaks. Even for Gaussian peaks, less error is incurred with the TS method than with the PD method at lower resolution.

The last variable considered is the change in area ratio. In Figure 6, paired peaks are presented at a fixed peak asymmetry (τ/σ = 4.0), a fixed resolution (1.0), and a fixed standard deviation ratio (8:1). (This is the case of minimal error for TS and largest error for PD from Figure 2.) For seven paired peaks, the area ratios are 100:1, 50:1, 30:1, 20:1, 10:1, 5:1, and 1:1. (Although this chromatographic situation of sharp and wide peaks may not occur in isocratic systems, it can occur where mixed retention mechanisms exist. Area ratios of 100:1 represent a 1% impurity level, commonly encountered.)

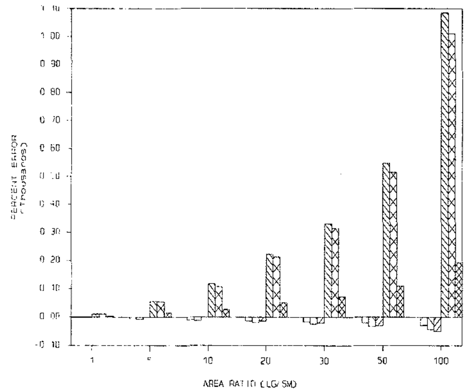

Figure 7. Peak errors incurred while the area ratio was changed, at variance ratio of 8:1 and resolution of 1.0. Negative TS errors for τ/σ = 4, 2, 0 are followed by the positive errors for τ/σ = 4, 2, 0.

Table I. Peak Errors Incurred upon Changing the Area Ratio[a]

area ratio	% error TS	% error PD
1	-11.66	3.54
5	-33.1	21.5
10	-47.7	28.1
20	-64.9	50.9
30	-77.8	67.9
50	-87.8	101.8
100	-99.8	155.8

[a] With a variance ratio of 1:1 and resolution of 1.0.

The peak area errors for both PD and TS are presented in Figure 7 for the chromatograms of Figure 6. As expected, the PD percent errors at larger peak area ratios are multiplicative; when PD is used a 10% error at peak area ratio of 1:1 becomes a 100% error at an area ratio of 10:1 and a 1000% error at 100:1. This linear effect is found for each peak asymmetry level. If one projects this relationship beyond the range considered, a 0.1% impurity (not uncommon) would have a 10 000% error with the PD separation method, under these conditions. Much smaller errors are incurred with the tangent skim. Varying the area ratio at fixed asymmetry and resolution only demonstrates relative error changes for the unresolved peak. The *amount* of underlying peak area does not change; its *relative* contribution to the unresolved peak's area changes.

Peak height ratios in Figure 7 also vary proportionally to the peak area ratio; as the area ratio decreases from 100:1 to 1:1, the peak height ratio also decreases proportionally, from 10:1 to 0.1:1. This only occurs because of the fixed asymmetry and resolution. Thus the peak height ratio does not provide any new information here; its change is proportional to the change in peak area and cannot contribute much information for method selection.

Most of the conditions studied thus far have demonstrated less error with the use of the TS peak deconvolution method.

Table II. Summary of MLR Models[a]

Asymmetric Peaks

$$\text{(predicted) \% error}_{\mathrm{PD}} = 173.36 + 2.24((\tau/\sigma)A) - 27.4342((\tau/\sigma)R_s) + 3.85((\tau/\sigma)\sigma^{1/2}) + 1.9714(A\sigma^{1/2}) - 2.37(Ah_p) - 22.27(R_s\sigma^{1/2}) - 11.03\sigma^{1/2}$$

$$\text{\% error}_{\mathrm{TS}} = -59.78 + 33.25R_s^2 + 6.36\sigma^{1/2} - 2.79h_p - 3.70(R_s\sigma^{1/2})$$

Gaussian Peaks

$$\text{\% error}_{\mathrm{PD}} = 354.34 - 391.20R_s + 5.85\sigma^{1/2} - 24.58h_p + 31.90(\sigma^{1/2}h_p) + 0.9939(h_p\sigma^{1/2})$$

$$\text{\% error}_{\mathrm{TS}} = -38.53 + 4.70\sigma^{1/2} - 16.85h_p + 12.92R_sh_p$$

[a] Interaction terms are expressed as factor 1 × factor 2, for example $(\tau/\sigma)A$ is the interaction term for τ/σ and peak area ratio.

Table III. Published Tangent Skim Peak Deconvolution Method Selection Criteria

HP3390/2/6/GENIE	first derivative on *front* side of beginning peak
SP4200/4270	first peak must be asymmetric; second peak must be *greater* than a minimum resolution from first
Varian Vista 400	*user-entered* peak height ratio of first/second peak
Perkin-Elmer LC100	*user-entered* peak height ratio of first/second peak
Dynamic Solutions	*user-entered* peak height ratio of first/second peak
Labtech Chrom	*user-entered* peak height ratio of first/second peak
Nelson Analytical	not specified; capable of nonlinear tangent skim

In Table I, errors incurred by using the TS and PD methods for badly tailed peaks ($\tau/\sigma = 4.0$) are presented for different peak area ratios. Here, the PD errors are less than the TS errors in all cases. From the results of Figures 2, 5, and 6, it appears that the TS method results in minimum errors for peaks that are significantly different in peak width regardless of peak asymmetry and for poorly resolved peaks regardless of asymmetry.

Multiple Linear Regression Model Building. In the discussions above, influential factors that affect the percent error became apparent. Most important was the standard deviation ratio and the peak separation or resolution. The remaining factors appeared important in some cases, while not in others. This information cannot be directly used to choose the best peak deconvolution method on the basis of minimum error because of the number of variables, noted nonlinearities, and conditional dependencies. A multivariable approach was needed. Multiple linear regression (MLR) was used to build linear models to predict the peak area percent error for both peak deconvolution methods using any and all factors described above.

Regression analysis required using the peak deconvolution method as a grouping variable, leading to two regression models, TS/EMG and PD/EMG. Later, all asymmetric peaks were deleted from the data file, and models were built for the remaining Gaussian peaks, the PD/Gaussian and the TS/Gaussian models, as these were the conditions under which many algorithms were developed. Thus there are four regression models, two PD percent error prediction models and two TS percent error prediction models, seen in Table II.

There are certain constraints of MLR that reduced the data set. This occurred when most data were confined to a small data space and a few points lay far away (very large peak area errors). These points became very influential and weighted the regression toward them, leading to nonrandom residual plots. This occurred in the PD/Gaussian model where the negative error values were too influential and in the PD/EMG model where three values exceeded 500%.

Both models involving tangent skim are relatively simple. Both only require knowledge of the *resolution* the *standard deviation ratio*, and the *peak height ratio*. This simplicity stems from the dependent variable being modeled. Here the percent error is only the difference between the straight line skim and the underlying curved true base line. This relative error varies as the two peaks come closer together or move apart; it varies as the standard deviation ratio widens; and it varies as the size of the first grows or shrinks. Only one interaction term (the resolution and peak height interaction in the percent error/TS/Gaussian model) is significant.

The percent error/TS/EMG model with four independent variables (*resolution squared, standard deviation ratio, peak height ratio*, and one interaction term—resolution times standard deviation) can explain 89.5% of the variance about the mean within the dependent variable. Adding more cross terms led to small increments in R^2, but residual plots became more ordered. The percent error/TS/Gaussian model with three terms (standard deviation, peak height, and resolution times peak height) explains 95.6% of the variance about the mean. There is no peak asymmetry term, τ/σ, in either model.

The perpendicular drop models are rather complex and nonlinear in peak relationship factors, evidenced by the numerous cross terms. Even with seven independent variables (τ/σ times area ratio, τ/σ times resolution, τ/σ times standard deviation, area ratio times standard deviation, area ratio times peak height resolution times standard deviation, and standard deviation times peak height), the asymmetric percent error/PD/EMG model can only account for 90.7% of the variance about the mean. With all collinear single factors removed by the MLR process, the resultant model is full of exceptions rather than rules. (An interaction term accounts for cases where the effect of A depends on what C or D is also present.) Also note that all five variables are required to predict the PD error. This was the best model that met the three criteria of small s^2, highest (reduced) R^2, and random residual plots.

For the percent error/PD/Gaussian model, one first-order term and four product terms explain 98.8% of the variance (standard deviation, peak height, and resolution times peak height). Here the same three terms needed for the TS models are required, resolution, standard deviation ratio, and peak height ratio. It would appear that these three are the common denominator or parameters required for minimizing peak error, as predicted from the simulation chromatograms above. Note that building a model based solely on the peak height ratio resulted in $R^2 < 0.5$ in all cases, in large s^2 values, and in nonrandom residual plots. Peak height ratios alone are thus demonstrated to be a poor prediction of errors incurred by choice of deconvolution method.

From a potential of 25 independent variables (5 first-order terms, 10 second-order terms, and 10 two-way interaction terms), all four regression models minimally require knowledge of the standard deviation ratio, peak height ratio, and peak resolution These were the same three variables found significant in discussing the error graphs. Note that three independent variables are needed for method selection and that the same three variables are needed for Gaussian peaks as well as symmetric peaks. MLR models also include significant cross terms, pointing out nonlinearities in the multidimensional response surface, not easily recognized when one is examining the error graphs. By using these prediction models with calculated peak relationship values (resolution, peak height and width ratios, etc.), a chromatographer (or algorithm) could calculate error that would be incurred with either peak deconvolution method. Method selection would then be a matter of comparing and minimizing errors.

From the most recent integrator owner's manuals, 10 algorithms' tangent skim criteria are listed in Table III, where the default method is the perpendicular drop. One manufacturer, capable of nonlinear tangent skimming, does not inform chromatographers of its selection criteria, nor does it describe the type or manner of performing the nonlinear skim. This vendor was excluded from related work (27) due to inconsistent performance that could not be favorably altered and is evaluated here by other means.

The manufacturer of the integrator capable of nonlinear tangent skimming assured the chromatographer that it was most accurate. When simulated chromatograms the same as Figure 1 were applied to this integrator, only one of the eight cases was nonlinear tangent skimmed. The remainder were PD separated. (The one case that was skimmed was not at the most decisive case to perform TS peak deconvolution (standard deviation of 8:1), but at a less obvious case, at standard deviation of 5:1.) Since selection criteria were not provided, an aimless search for effective peak parameters was not undertaken. If the algorithm were truly accurate, the largest standard deviation ratioed chromatograms would have been skimmed and the smallest would have been PD separated. This selection criterion does not compare to the MLR results.

Four manufacturers base their TS selection on a user-specified peak height ratio. No standard deviation ratio is required, nor is peak resolution. Method selection is not automatic and relies on the chromatographer to make a decision solely on the peak height ratio. On the basis of the percent error plots (Figures 2, 4, 5, and 7) it was demonstrated that the peak height ratio alone is not a sufficient criterion for accurately predicting the appropriate deconvolution method. Through MLR model building, peak height ratios were found to be one of three variables required to predict peak area error; alone, the peak height ratio accounted for only 50% of the variance, not a useful predictive model. In short, peak height ratios alone are not enough information with which to select a peak deconvolution method, either manually or in an automatic algorithm. Using the approach suggested by the MLR model in conjunction with this type of integrator would require manual determination of peak height ratios, standard deviation ratios, and resolution. This would be followed by selection of integrator parameters that force the appropriate peak deconvolution method. As a practical matter, the latter would probably require extensive and undesirable use of timed chromatographic events.

One manufacturer bases the deconvolution criteria on the rising portion of the peak. It does not take into account the peak resolution, the standard deviation ratio, or the peak height ratio. In cases where the TS is clearly the best choice, the shallower peaks (higher standard deviation ratios) require the TS. These shallower peaks also have a smaller rate of change on the peak's front side, contradictory to this algorithm's selection rule.

The last remaining algorithm considers peak asymmetry and resolution. With this integrator, the resolution criterion contradicts our observations; i.e. as resolution decreases it is less likely that tangent skimming will be selected. Simulations above show the opposite; with less resolution, tangent skimming leads to minimum error and should be preferred.

CONCLUSIONS

It was shown through analysis of error graphs that the standard deviation ratio and resolution were important in predicting the minimum error for either method. In MLR model building, this was confirmed for all cases, with the inclusion of the peak height ratio factor. This was true for either the PD or TS method, for asymmetric and for Gaussian peak profiles. To evaluate commercial algorithms, these prediction criteria were compared to those of commercial algorithms. None satisfactorily matched the criteria found in the simulation studies. Unfortunately, these two peak deconvolution methods may remain the only peak deconvolution methods available to chromatographers for some time.

This situation would not be deleterious if all manufacturers followed the same albeit incorrect selection rules; comparison of one laboratory's chromatographic quantification would match that of another. Unfortunately this is not the case; any given example of overlapping chromatographic peaks would be deconvoluted differently, leading to potentially large discrepancies not attributed to the physical separation. A laboratory could be disqualified from a collaborative study and possibly discredited not because of its analytical technique but due to its choice of data system. Quality assurance testing of electronic integrators would inform analytical chemists exactly how their integrators are performing peak quantitation with chromatography typically encountered.

LITERATURE CITED

(1) Davis, J. M.; Giddings, J. C. *Anal. Chem.* **1983**, *55*, 418.
(2) Subcommittee E-19.08 Task Group on Liquid Chromatography for the ASTM. *J. Chromatogr. Sci.* **1981**, *19*, 338.
(3) Kirkland, J. J.; Yau, W. W.; Stoklosa, H. J.; Diiks, C. H. *J. Chromatogr. Sci.* **1977**, *15*, 303.
(4) Giddings, J. C. *Anal. Chem.* **1963**, *35*, 1999.
(5) Kucera, E. *J. Chromatogr.* **1965**, *19*, 235.
(6) Mc Williams, I. G.; Bolton, H. C. *Anal. Chem.* **1969**, *41*, 1762.
(7) Buys, T. S.; de Clerk, K. *Anal. Chem.* **1972**, *44*, 1274.
(8) Jonsson, J. A. *Chromatographia* **1980**, *13*, 273.
(9) Chesler, S. N.; Cram, S. P. *Anal. Chem.* **1973**, *45*, 1354.
(10) Chesler, S. P.; Cram, S. P. *Anal. Chem.* **1971**, *43*, 1922.
(11) Fraser, R. D. B.; Suzuki, E. *Anal. Chem.* **1966**, *38*, 1770.
(12) Fraser, R. D. B.; Suzuki, E. *Anal. Chem.* **1969**, *41*, 37.
(13) Buys, T. S.; de Clerk, K. *Anal. Chem.* **1972**, *44*, 1274.
(14) Grushka, E.; Myers, M. N.; Schettler, P. D.; Giddings, J. C. *Anal. Chem.* **1969**, *41*, 889.
(15) Grubner, O. *Anal. Chem.* **1971**, *43*, 1934.
(16) Pauls, R. E.; Rogers, L. B. *Anal. Chem.* **1977**, *49*, 625.
(17) Grushka, E.; Myers, M. N.; Giddings, J. C. *Anal. Chem.* **1970**, *42*, 21.
(18) Maynard, V.; Grushka, E. *Anal. Chem.* **1972**, *44*, 1427.
(19) Foley, J. P. *Anal. Chem.* **1987**, *59*, 1984.
(20) Foley, J. P.; Dorsey, J. G. *J. Chromatogr. Sci.* **1984**, *22*, 234.
(21) Papas, A. N. *CRC Crit. Rev. Anal. Chem.* **1989**, *4*, 20.
(22) Hancock, H. A.; Dahm, L. E.; Muldoon, J. F. *J. Chromatogr. Sci.* **1970**, *8*, 57.
(23) Foley, J. P. *J. Chromatogr.* **1987**, *384*, 301.
(24) Jeansonne, M. S.; Foley, J. P. *J. Chromatogr.* **1989**, *461*, 149.
(25) Chidester, David, American Cyanamid, personal correspondence, 1987.
(26) Papas, A., unpublished data, 1986.
(27) Delaney, M. F., personal communications, 1986.
(28) Foley, J. P.; Dorsey, J. G. *Anal. Chem.* **1983**, *55*, 730.
(29) Papas, A. N.; Delaney, M. F. *Anal. Chem.* **1987**, *59*, 54A.
(30) Papas, A. N. Ph.D. Thesis, University of Lowell, 1989.
(31) Kirkland, J. J.; Yau, W. W.; Stoklosa, H. J.; Diiks, C. H. *J. Chromatogr. Sci.* **1977**, *15*, 303.

RECEIVED for review June 8, 1989. Accepted November 8, 1989.

Measurement of Vanadium Impurity in Oxygen-Implanted Silicon by Isotope Dilution and Resonance Ionization Mass Spectrometry

Santos Mayo

Semiconductor Electronics Division, National Institute of Standards and Technology, Gaithersburg, Maryland 20899

John D. Fassett,* Howard M. Kingston, and Richard J. Walker

Inorganic Analytical Research Division, National Institute of Standards and Technology, Gaithersburg, Maryland 20899

The combined analytical capabilities of isotope dilution, laser-induced resonance ionization spectroscopy, and mass spectrometry, integrated in the resonance ionization mass spectrometry technique (RIMS), have been evaluated as a tool for quantitative elemental impurity analysis of SIMOX (separation by implanted oxygen), a new silicon-based material prepared by oxygen implants. The vanadium impurity content was measured in the top crystalline SIMOX film and the oxygen-synthesized buried oxide layer in commercial wafers, resulting in 0.14 μg/g ± 20%, or 1.7 × 10^{15} atoms/cm^3. A similar analysis on the substrate bulk shows about 30 times lower vanadium impurity levels. The origin of this contamination may be linked to the oxygen implant, although no modeling for it is offered here. The sensitivity of RIMS to vanadium is in the pg/g range. The accuracy of results is limited by the uncertainty in the blank, in view of the low total vanadium content in the specimen.

INTRODUCTION

The purpose of this work was to evaluate the integrated use of isotope dilution (ID), laser-induced resonance ionization spectroscopy (RIS), and mass spectrometry (MS), as ID–RIMS, for quantitative ultrasensitive elemental analysis of SIMOX, a silicon-based semiconductor material. Vanadium was chosen for this evaluation because it is a contaminant element possibly introduced during the manufacturing process. In addition, it is an element for which the selectivity of RIMS is highlighted because of titanium and chromium isobaric interferences.

SIMOX (separation by implanted oxygen) material constitutes an important step in the actual development of an emergent technology aimed at creating silicon-on-insulator materials for improved microelectronic device fabrication. This technology may eventually provide radiation-hardened, high-performance, electrically insulated, crystalline silicon thin films, structurally bonded to regular substrate wafers appropriate for very large scale and ultralarge scale device integration (*1*). Commercial SIMOX wafers are fabricated by implantation of atomic oxygen in Czochralski-grown silicon wafers at energies in the 150–200-keV range and at temperatures between 520 and 620 °C, with total ion fluence in the 10^{18} oxygen/cm^2 range. By subsequent thermal treatment, the implanted oxygen forms a buried silica layer that provides electrical separation between the top crystalline silicon film and the substrate (*2*, *3*). Thoughout this paper we refer to the top crystalline film as "the film", the buried silica layer as "the layer", and the silicon substrate as "the substrate".

Measurement of transition-metal impurities in SIMOX films is critical because dislocation sites and structurally damaged regions are effective gettering centers for heavy metals in silicon (*4*, *5*). There have been reports linking transition-metal contamination to the oxygen implantation process (*6*, *7*). The origin of the contamination introduced in implanted wafers is still an open question. To minimize such contamination, some parts of the implanter that are exposed to interactions with the accelerated oxygen beam are lined with ultrapure silicon. Ultrasensitive measurement is required to understand the impurity inclusion mechanism into the implanted film.

The elemental analysis of semiconductor materials has been dominated by secondary ion mass spectrometry (SIMS). This technique not only has good sensitivity, but also provides information about the spatial distribution of an element in an electronic material or device. For instance, SIMS has been used to study implant profiles in semiconductor materials down to concentrations in the 10^{15} atom/cm^3 range (*8*, *9*). As with most direct analysis techniques, signal intensities are both matrix and instrument dependent, so quantitative analysis depends on suitability and availability of primary or secondary standards. Furthermore, the relative sensitivities among elements can be highly variable. Chemical analysis avoids many of the problems of direct analysis—the analyte can be concentrated from relatively large amounts of sample material, and the matrix can be chemically eliminated. However, contamination in the chemical processing, "blank", can hinder the measurement. Recently, a procedure titled "chemical SIMS" has been published, which combines the two analytical methods and uses isotope dilution for accurate, quantitative analysis (*10*), although depth profiling capability is lost. Gallium arsenide has been analyzed, and sensitivities for impurities such as Zn have been claimed to be a 1000-fold better than for direct SIMS analysis.

Neutron activation analysis has also been applied to the determination of subnanogram quantities of contaminants in semiconductor materials. The detection limits for trace elements in silicon and silica vary from the μg/g to the pg/g range for a variety of elements in the periodic table (*11*, *12*). The main advantage of this technique is the lack of sample preparation for bulk analysis. However, for film analysis some sample preparation is needed in order to separate it from the substrate, and consequently, some blank interference due to processing is likely.

RIMS combines the elemental selectivity of resonance ionization spectroscopy with the mass selectivity of mass spectrometry. For the resonance ionization spectrometry, we used a single-color, two-photon resonance ionization scheme with photon energy just halfway above the analyte ionization energy. This scheme allows pumping the atom from its ground or initial state to the corresponding excited state with one photon, and ionizing it with the second photon. There are three main atomization techniques generally used for RIS analysis of solids: laser ablation (*13*, *14*), ion sputtering (*15*, *16*), and thermal evaporation (*17*). The first two may be used

This article not subject to U.S. Copyright. Published 1990 by the American Chemical Society

for direct analysis without specimen preparation. The direct analysis of iron in SIMOX by resonance ionization has been reported using sputter atomization (*18*). This experiment utilized the selectivity of the RIS process to its fullest advantage since SIMS is hampered by the interference from the dimer silicon ion on the major iron isotope at $m/e = 56$. Direct quantitative analysis by RIMS, like SIMS, depends upon availability of suitable standards. Such standards are generally very difficult to find or prepare for ultratrace impurity levels.

Atomization by thermal evaporation has been extensively used in combination with resonance ionization. Chemical processing of the sample is required to prepare it for loading on the resistively heated filament. Since ID-RIMS requires specimen dissolution, it is well suited to thermal evaporation, although sputter atomization for ID samples has been reported (*19*). The great advantage of the ID-RIMS technique is that it can be used independently of standards. The major disadvantage of thermal evaporation is the inherent duty cycle mismatch when pulsed laser beams are used.

In the following sections we describe the methodology developed for sample preparation and isotope dilution as well as for isotope ratio measurements with the RIMS instrumentation. We present results for representative SIMOX samples.

EXPERIMENTAL SECTION

The ID technique for quantitative analysis is based on measurement of the isotopic composition of a sample as a mixture of the analyte with a known amount of an enriched isotope tracer called the spike (*20, 21*). The resulting isotopic ratio in the mixture, $R = {}^{50}\mathrm{V}/{}^{51}\mathrm{V}$, is measured, and the analyte concentration in the sample, C_s, is then calculated. An enriched ^{50}V tracer from Oak Ridge National Laboratory was used.

Reagents. High-purity acids, produced by sub-boiling distillation at NIST (*22*) and stored in Teflon bottles, were used in this work.

Isotopic Spike. The spike solution was prepared in dilute HNO_3 and stored in a Teflon bottle. Its concentration was calibrated by thermal ionization mass spectrometry (TIMS) using high-purity natural vanadium, which has an isotopic mixture of 0.25% ^{50}V and 99.75% ^{51}V. The measured TIMS ratio was 0.5647 ± 0.0011 (1σ, 15 determinations).

SIMOX Film Plus Layer Specimen Preparation. These specimens were prepared in air-filtered clean hoods from commercial ⟨100⟩ SIMOX wafers, 100 mm in diameter and about 0.8 mm thick. The silicon wafers were implanted with 150-keV oxygen ions at constant temperature in the 520 and 620 °C range to a total fluence of 1.7×10^{18} atoms/cm^2. Rectangular plates, 1.587 cm wide and 3.175 cm long, were cut from them with a diamond saw and were first cleaned in a boiling ammonia-hydrogen peroxide solution, subsequently boiled in a hydrochloric acid-hydrogen peroxide solution (*23*), and stored in clean plastic boxes. No residual contamination from the saw was expected in the plates after this cleaning. Each plate was dipped in HF for 30 s to remove the native oxide film (estimated 2-3 nm thick) just prior to specimen preparation. All containers and tools used were made of FEP Teflon previously boiled in 1:1 HCl-water and HNO_3-water solutions. After weighing, the plate was soaked in about 6 g of HF with very gentle heating to help remove the film from the substrate due to dissolution of the buried silica layer. The substrate was removed from the solution, rinsed with water added to the solution, and dried, and the weight of the removed material was measured with 1-μg sensitivity. Typically, the removed sample weighed about 600 μg. About 0.1 g of HNO_3 was then added to the solution to dissolve the silicon. The amount of spike added was estimated to yield ratios compatible with error multiplication factors of about 2 as explained below. The solution was evaporated at sub-boiling temperatures to a drop of about 5-μL volume for RIMS analysis.

SIMOX Silicon Substrate Specimen Preparation. The remaining substrate plate was etched with HF plus one drop of nitric acid to remove the surface, and this solution was discarded. The plate was thoroughly rinsed and etched again by floating it with its back face in contact with about 5 g of HF plus one drop of dilute nitric acid at low temperatures to remove a small substrate layer. The amount of silicon removed was typically about 10 mg. The resulting solution containing the bulk silicon was spiked and evaporated at sub-boiling temperatures to about a 10-μL drop for RIMS analysis.

Blank Sample Preparation. Blank samples were prepared simultaneously with every specimen, using the same amounts of acids as used to prepare specimens. The blanks were spiked to have isotope ratios, $^{50}\mathrm{V}/^{51}\mathrm{V}$, of about 0.3. They served to monitor the vanadium content in the acids in addition to accidental contamination in the specimen preparation routine, plus the residual vanadium in the rhenium filament material. Independently, large quantities (about 80 g) of the acids used were analyzed to monitor their vanadium content. They were spiked and evaporated at sub-boiling temperatures to a 5-μL drop for RIMS analysis.

Filament Preparation. Single U-shaped, float-zone purified rhenium ribbon filaments were used to evaporate the specimen. The ribbon is 0.075 cm wide, 0.0025 cm thick, and about 1 cm long, spot-welded to 0.1-cm-diameter insulated wires. The part of the flat ribbon where the specimen is deposited is about 0.6 cm long. Filaments are first baked at temperatures in the 2200 °C range for 30 min in a 133-μPa (10^{-6} Torr) vacuum, cooled in a 13.3-μPa (10^{-7} Torr) vacuum, and immediately used for RIMS work. The specimen is deposited on the filament by using a 5-μL pipet with a disposable Teflon tip. The solution is evaporated by heating with infrared light. To reduce the oxides, a thin graphite film is deposited on the dried sample via an ethanol slurry. The graphite enhances the vanadium atomic fraction evaporated from the hot filament (*24*). Because the RIMS scheme relies on the laser ionization of thermally emitted neutral atoms, the filament temperature used for vanadium atomization is set at the lowest possible value compatible with proper signal yield and persistence. This condition allows for a steady RIMS signal. We have adopted the practice of preparing a small number of filaments at a time, keeping them in a vacuum, and using them shortly after taking them out of the vacuum in order to minimize the loading blank contributed by incipient corrosion occurring in the insulated wires when stored in the laboratory atmosphere for a long period.

RIMS Apparatus. The RIMS facility used at the National Institute of Standards and Technology (NIST) has been described elsewhere (*25*). Briefly, the system uses a tunable dye laser pumped by a Nd-YAG rod excited with two flashlamps placed in an afocal double-elliptical pump cavity and Q-switched at 10 Hz. After frequency doubling, the laser beam was about 3 mJ per pulse with the wavelength in the 297.8-nm region, with about 7-ns pulse duration.

The SIMOX specimen was thermally evaporated in a 13.3-μPa (10^{-7} Torr) vacuum (Langmuir-type evaporation) at temperatures in the 1200-1500 °C range. The laser beam, about 0.1 cm in diameter, is directed parallel to the long leg of the U-shaped filament, passing 0.1 cm from the front surface where the specimen was deposited. An electrostatic ion-optics system collects and focuses the ions, injecting them into the entrance slit of a 60°, 6 in. radius of curvature magnetic analyzer. A multidynode electron multiplier located by the exit slit on the focal plane of the mass spectrometer is used as an ion detector. The corresponding signal is used for both digital and analog computerized data processing (*26*).

Data Acquisition Routine. The isotope ratio was measured by a computer-controlled RIMS apparatus programmed to select the proper laser wavelength and magnetic fields for the two vanadium isotopes. The signal from the ion detector was processed by a fast transient digitizer with 8-bit resolution. The peaks corresponding to the two vanadium isotopes were measured in blocks of six data pairs, and the isotope ratio R was calculated. The software includes a statistical routine to average peak intensity fluctuations, subtract background, and calculate twice the standard deviation of the mean of the R data. The blocks of six data pairs were repetitively collected until the error in R reached the level desired by the operator. The typical data collection period per specimen was about 150 min. When the amount of total vanadium loaded on the filament is below the 50-pg range, enhancement of the RIMS signal can be achieved by modulating the filament temperature synchronously with the laser pulse. This

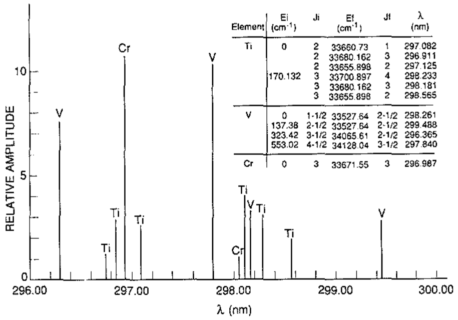

Element	Ei (cm^{-1})	Ji	Ef (cm^{-1})	Jf	λ (nm)
Ti	0	2	33660.73	1	297.082
		2	33680.162	3	296.911
		2	33655.898	2	297.125
	170.132	3	33700.897	4	298.233
		3	33680.162	3	298.181
		3	33655.898	2	298.565
V	0	1-1/2	33527.64	2-1/2	298.261
	137.38	2-1/2	33527.64	2-1/2	299.488
	323.42	3-1/2	34065.61	2-1/2	296.365
	553.02	4-1/2	34128.04	3-1/2	297.840
Cr	0	3	33671.55	3	296.987

Figure 1. Titanium, vanadium, and chromium spectroscopic information used to select the proper RIS scheme for vanadium to minimize isobaric interference. The laser-induced transitions are indicated in the table.

enhances the thermal emission of the analyte atomic species, yielding larger RIMS signals without consuming analyte material between the laser pulses (*27*).

RESULTS AND DISCUSSION

Isotope Dilution Analysis. The accuracy of the ID technique relies on the analyte equilibration in the mixture; i.e., the specimen and spike atoms are in an identical chemical state. When this condition is satisfied, quantitative separation of the analyte is not required, and sources of systematic errors (e.g., blank and isobaric interferences) can be assessed.

Due to limitations in vanadium enrichment, we used a spike with low isotopic enrichment, which still is appropriate for precise ID measurements in view of the low ^{50}V natural isotopic abundance. The error in the determination of C_s is dependent on the error in measuring R through a multiplication factor. Thus, the amount of spike added to the specimen must be carefully gauged to optimize R for minimization of the error multiplication factor (*28*). This is especially true for a technique such as RIMS where ratio measurement precision is at the percent level. Thus, we aimed at producing ID ratios in the 0.2–0.3 range where, for our experimental conditions, the error multiplication factor is about 2, and we strove to collect 1000–10000 ^{50}V ions (3–1% counting uncertainty).

Chemical Treatment of Samples. One of the key aspects of this work is the ability to dissolve and spike the samples with a minimum of chemical manipulation. In this case, this is possible because the chemical characteristics of the material being analyzed are suitable and because RIMS is used to discriminate instrumentally against the elemental isobaric interferences of titanium and chromium. Thus, no special chemical separations were required to remove these elements from the sample prior to measurement.

The substrate can be neatly separated by etching the film plus layer material because the HF is free of any oxidizing agent. The acids used are reduced to a small volume by gentle heating. In this process much of the silicon is vaporized as SiF_4 (boiling point, −86 °C), although visible deposits did remain in the preparation. Any residual silicon matrix did not interfere with the vanadium measurement.

As mentioned above, the ID technique requires chemical equilibration between the spike and sample isotopes. Because the oxidation state of vanadium in solution is dependent on pH, the strongly acidic nature of the solution used to dissolve the sample causes the vanadium in the sample (and spike) to be in a high oxidation state (*29*). Recent ID experiments show that the conditions we used here produce results indistinguishable from those achieved by using the very severe perchloric acid digestion procedure previously applied (*30*).

Although a minimum of chemical manipulation was done on these samples, it is the contamination introduced in this processing that limits the sensitivity of the measurement. The contamination originates principally in the HF and from the rhenium filaments used to vaporize the samples. The loading blank was evaluated by depositing small quantities of spike on representative filaments in the same manner as for the samples. The loading blank is typically less than 10 pg.

RIMS of Vanadium. Resonance ionization requires atomization of the element of interest, and thermal vaporization has been shown to be broadly applicable. Vanadium has a number of low-energy excited levels that will be populated according to a Boltzmann distribution (*31*). Although this distribution of the atom population fractionally reduces the vanadium that is accessible with the use of a single resonance ionization scheme, the number of possible schemes increases because of the larger availability of initial states. We have chosen a scheme that utilizes the resonant transition between the initial 4F $J = 4^1/_2$ (553.02 cm^{-1}) level and 4D $J = 3^1/_2$ (34 128.04 cm^{-1}) level. At 1550 °C we calculate this initial level to be the highest populated, containing 23.9% of the atoms leaving the filament.

The RIS scheme used for vanadium here is a two-photon, single-color one (1 + 1), which has been shown to be efficient for a wide range of elements. We have examined the spectroscopy for vanadium, as well as for chromium and titanium, the elements that have specific isobaric interferences. Figure 1 shows schematically the spectroscopic data taken by loading microgram quantities of each element on filaments and scanning the laser wavelength under similar conditions while the major isotopes of each element (^{48}Ti, ^{51}V, ^{52}Cr) were monitored. The peaks were all ascribed to 1 + 1 resonance ionization schemes as shown in the insert. The wavelength used for the vanadium at 297.8 nm corresponds to a region where titanium and chromium isobaric interferences are negligible. The background is taken at 297.9 nm, which is significantly away from the resonant transitions of all three elements. These data also show the RIMS selectivity for vanadium titanium, and chromium species.

Good elemental selectivity is crucial to the success of this technique since no chemical separation of interfering elements is used. Furthermore, without selective ionization, the loading blanks of titanium and chromium are just as important as those of vanadium. The expected magnitude of these interferences can be estimated from thermal ionization vanadium blank measurements. In one blank measurement the TIMS titanium interference was 180–420 pg equivalent of vanadium, and in a second blank measurement the interference was 80–200 pg equivalent. Similarly, the chromium interferences were respectively 4–5 pg equivalent and 20–50 pg equivalent of vanadium. The ranges of interferences indicate that the TIMS signals of V, Ti, and Cr change relative to each other. Thus, considerable time must be spent to measure such interferences, and as the correction becomes large, accuracy is degraded, making quantification of results very difficult. These interferences impose a limit to high sensitivity measurements of vanadium by TIMS. Such a limit does not exist with RIMS.

Resonance ionization and thermal ionization signal intensities were compared by using the same experimental arrangements. The ratio of RIMS to TIMS ion signal in our instrument ranged from 23 at 1100 °C with 24 RIMS-generated vanadium ions/s to 2.1 at 1275 °C where the RIMS-generated vanadium was 38 000 ions/s. These figures are consistent with the small ionized fraction generated by thermal vaporization and the overall resonance ionization efficiency. From the Saha–Langmuir equation, we calculate the vanadium ion to atom ratio as 4.1 × 10^{-7} evaporated from a rhenium

Table I. Typical RIMS Results for Vanadium in ⟨100⟩ p-SIMOX Wafer Annealed in Argon at 1300 °C for 6 h after 200-keV Oxygen was Implanted at 620 °C to 1.7 × 10^{18} atom/cm^2 Fluence[a]

	SIMOX		
	film	substrate	blank
W_s	662 μg	15.98 mg	12.8 g
W_{sp}	11.45 mg	11.45 mg	5.73 mg
R	0.263	0.353	0.287
±RSD	1.8%	3.7%	4.4%
C_s	0.14 μg/g	3.0 ng/g	5.5 pg/g
±RSD	3.4%	10%	8.8%
at/cm^3	1.7 × 10^{15}	3.6 × 10^{13}	
HF	10 g	4.45 g	9.94 g
HNO_3	2.3 g	2.5 g	2.8 g
total acids	12.3 g	7 g	12.8 g

[a] The spike concentration is 19.543 ng/g. W_s and W_{sp} respectively are the sample and spike weight. R and RSD are the isotope ratio and standard deviation. C_s, RSD, and at/cm^3 are the vanadium concentration, standard deviation, and atomic density. HF and HNO_3 are the amount of acids employed.

filament at 1100 °C. The laser ionization efficiency is calculated from the duty cycle, which is determined by the time the evaporated vanadium takes to fill the laser photoionization volume in front of the hot filament. Here we assume the photoionization efficiency is equal to 1. Considering the population of the vanadium initial state used for our RIMS scheme, the overall resonance ionization efficiency would be 1.7 × 10^{-5}. Based on these assumptions, the theoretical RIMS/TIMS signal ratio is 41 (1.7 × 10^{-5}/4.1 × 10^{-7}), which agrees fairly well with our experimental result. The two techniques are comparable in sample utilization efficiency. However, the high selectivity and low background of RIMS allow quantification of smaller sized samples.

Isotope effects must be considered in any RIMS measurements. Although our laser bandwidth is expected to be much broader than energy level shifts between isotopes in this region of the periodic table, anomalous effects have been reported for other elements. The small, natural V isotopic ratio is difficult to measure with high precision. Thus, we have measured the spike ratio both by RIMS, 0.5472 ± 0.0069 (1σ, $n = 9$), and by thermal ionization, 0.5647 ± 0.0011 (1σ, $n = 15$), obtaining values that differ by 3.2%. Here n is the number of times the experiment was repeated on separately loaded filaments. This difference could be caused either by a photoionization isotopic effect or another instrumental discrimination effect. Isotopic bias will have little effect on ID measurements as long as it is constant for all isotopic measurements used in the calculation of the ID results. We used the TIMS calibration of the spike, which introduced a systematic error of about 2% in determining sample concentration measured by RIMS.

Quantitative Results. We measured the vanadium content in film and substrate from six different samples cut from three commercial SIMOX wafers supplied by EATON/IBIS[2]. Two wafers were unannealed, and one was annealed in argon at 1300 °C for 6 h after the 200-keV oxygen implant. We observed scattering in the individual results with a factor of 2 with respect to the average of the six samples set, probably due to factors such as implant homogeneity and sample preparation reproducibility. However, we are not able to detect marked differences in the samples as a function of the postimplant thermal treatment. The question of a possible vanadium contamination introduced by the annealing furnace atmosphere has not been addressed here. Table I shows a typical result obtained in a ⟨100⟩ p-SIMOX wafer implanted with 200-keV oxygen at 620 °C to 1.7 × 10^{18} cm^{-2} fluence and postannealed in argon at 1300 °C for 6 h. The symbols in the first column correspond to the sample weight, spike weight, isotope ratio, vanadium concentration, and amounts of acids employed. Once the ratio was measured, the concentration was calculated and an error in C_s estimated. For both the film and substrate, it is seen that the blank is a significant fraction of the total vanadium measured. However, since a larger amount of substrate was analyzed, its lower vanadium content could be determined. The concentration of the vanadium in the film plus layer after subtracting the blank contribution was 0.14 μg/g or 1.7 × 10^{15} atom/cm^3 with an estimated uncertainty of 20%. The concentration in the silicon substrate was 3.0 ng/g or 3.6 × 10^{13} atom/cm^3 with an estimated uncertainty of 20%. These results clearly show that the comparatively high contamination in the film plus layer is likely due to the SIMOX fabrication process via oxygen implantation, as has been pointed out previously.

CONCLUSIONS

We have evaluated ID–RIMS for quantitative measurement of vanadium in SIMOX material. Because of the relatively small amount of film material available to prepare the specimen, the blank interference may become a limiting factor for a more general application of this technique. Due to the specimen preparation technique used, both the top crystalline silicon film and the silica-synthesized buried layer are included in a single sample. However important it may be to know the impurity content in the film alone, subsequent thermal treatments involved in device preparations cause impurity diffusion and redistribution through the film/layer interface. Thus, for the purpose of this work, the mixture of the top silicon film plus the buried silica layer in a single sample does not alter the validity of the results.

The ID–RIMS sensitivity to vanadium is within a few parts per trillion, and the analytical reproducibility is within the error uncertainty as demonstrated by the acid blank analysis, which consistently was 3–4 pg/g. We consider RIMS an appropriate technique for research-oriented semiconductor elemental trace analysis, provided that the wet chemistry involved is well understood. Our present vanadium results link contamination to the oxygen implant process since the vanadium content in the substrate is substantially lower. Other transition elements such as iron, chromium, nickel, and copper are possibly present in the films as a consequence of implant processing (*32*), and it will be useful to develop RIMS schemes for these elements. The overall applicability of RIMS for semiconductor characterization can be expected to improve with technical advances in higher repetition rate tunable lasers. This may significantly reduce the data collection time, while at the same time increasing sample utilization efficiency.

ACKNOWLEDGMENT

We are indebted to B. Cordts, IBIS Corp., Danvers, MA, for supplying SIMOX wafers for this investigation. We also thank W. Robert Kelly for helpful discussions on error propagation in isotope ratio measurement.

Registry No. Vanadium, 7440-62-2.

LITERATURE CITED

(1) Lee, C. T.; Burns, J. A. *IEEE Electron Devices Lett.* **1988**, *9*, 235–237.
(2) Pinizzotto, R. F. *J. Vac. Sci. Technol.* **1984**, *A2*, 597–598.
(3) Lam, H. W.; Pinizzotto, R. F. *J. Cryst. Growth* **1983**, *63*, 554–558.
(4) Kamins, T. I.; Chiang, S. Y. *J. Appl. Phys.* **1985**, *58*, 2559–2563.
(5) Delfino, M.; Jaczynski, M.; Morgan, A. E.; Vorst, C.; Lunnon, M. E.; Malliot, P. *J. Electrochem. Soc.* **1987**, *134*, 2027–2030.
(6) Hemment, P. L. F. *Vacuum* **1979**, *29*, 439–442.
(7) Cordts, B., Ibis Corp., personal communication, 1988.
(8) Stevie, F. A.; Kelly, M. J.; Andrews, J. M.; Rumble, W. *Secondary Ion Mass Spectrometry SIMS V*; Proceedings of the 5th International Conference, Washington, DC, 1985; Benninghoven, A., Colton, R. J., Simons, D. S., Werner, H. W., Eds.; Springer Verlag: New York, 1986; pp 327–330.
(9) Ehrstein, J. R.; Downing, R. G.; Stallard, B. R.; Simons, D. S.; Fleming, R. F. *Semiconductor Processing, ASTM Special Technical Publication*

850; Gupta, D. C., Ed.; American Society for Testing and Materials: Philadelphia, PA, 1984; pp 409–425.
(10) Tanaka, T.; Kurosawa, S. *J. Electrochem. Soc.* **1986**, *133*, 416–420.
(11) Lindstrom, R. M. *Microelectronic Processing: Inorganic Materials Characterization*; Caspar, L. A., Ed.; ACS Symposium Series 295; American Chemical Society: Washington, DC, 1986; pp 294–307.
(12) Schmidt, P. F.; Pearce, C. W. *J. Electrochem. Soc.* **1981**, *128*, 630–637.
(13) Piepmeier, E. H. *Analytical Applications of Lasers*, Piepmeier, E. H., Ed.; J. Wiley: New York, 1986; Chapter 19.
(14) Kronert, U.; Becker, St.; Hilberath, Th.; Kluge, H.-J.; Schultz, C. *Appl. Phys.* **1987**, *A44*, 339–345.
(15) Donohue, D. L.; Christie, W. H.; Goeringer, D. E.; McKown, H. S. *Anal. Chem.* **1985**, *57*, 1193–1197.
(16) Kimock, F. M.; Baxter, J. P.; Pappas, D. L.; Koprin, P. H.; Winograd, N. *Anal. Chem.* **1984**, *56*, 2782–2791.
(17) Travis, J. C.; Fassett, J. D.; Lucatorto, T. B. *Resonance Ionization Spectroscopy 1986*; Hurst, G. S., Morgan, C. G., Eds.; Institute of Physics Conference Series 84; Institute of Physics: Bristol, U.K., 1987; pp 91–96.
(18) Young, C. E.; Pellin, M. J.; Calloway, W. F.; Stein, H. J.; Tsao, S. S. *Resonance Ionization Spectroscopy 1988*; Lucatorto, T. B., Parks, J. E., Eds.; Institute of Physics Conference Series 94; Institute of Physics: Bristol, U.K., 1989; pp 205–206.
(19) Moore, L. J.; Spaar, M. T.; Taylor, E. H.; Parks, J. E.; Beekman, D. W. *Resonance Ionization Spectroscopy 1988*; Lucatorto, T. B., Parks, J. E., Eds.; Institute of Physics Conference Series 94; Institute of Physics: Bristol, U.K., 1989; pp 273–276.
(20) Heumann, K. G. *Int. J. Mass Spectrom. Ion Phys.* **1982**, *45*, 87–110.
(21) Heumann, K. G. *Inorganic Mass Spectrometry*; Adams, F., Gijbels, R., Van Grieken, R., Eds.; J. Wiley: New York, 1987; Chapter 7.
(22) Paulsen, P. J.; Beary, E. S.; Bushee, D. S.; Moody, J. R. *Anal. Chem.* **1988**, *60*, 971–975.
(23) Kern, W.; Deckert, C. A. *Thin Film Processes*; Vossen, J. L., Kern, W., Eds.; Academic Press: New York, 1978; Chapter V-1, pp 401–496.
(24) Studier, M. H.; Sloth, E. N.; Moore, L. P. *J. Phys. Chem.* **1962**, *66*, 133–134.
(25) Fassett, J. D.; Moore, L. J.; Travis, J. C.; Lytle, F. E. *Int. J. Mass Spectrom. Ion Phys.* **1983**, *54*, 201–216.
(26) Fassett, J. D.; Walker, R. J.; Travis, J. C.; Ruegg, F. C. *Int. J. Mass Spectrom. Ion Phys.* **1987**, *75*, 111–126.
(27) Fassett, J. D.; Moore, L. J.; Shideler, R. W.; Travis, J. C. *Anal. Chem.* **1984**, *56*, 203–206.
(28) Crouch, E. A.; Webster, R. K. *J. Chem. Soc., London* **1963**, *Part I*, 118–131.
(29) Clark, R. J. H. *Comprehensive Inorganic Chemistry*; Bailar, J. C., Emeleus, H. J., Nyholm, R., Trotman-Dickerson, A. F., Eds.; Pergamon Press: Oxford, U.K., 1973; Chapter 34.
(30) Fassett, J. D.; Kingston, H. M. *Anal. Chem.* **1985**, *57*, 2474–2478.
(31) Fassett, J. D.; Travis, J. C.; Moore, L. J.; *Applications of Laser Chemistry and Diagnostics*; Harvey, A. B., Ed.; Proceedings SPIE 482, 1984; pp 36–43.
(32) Jastrebski, L.; Ipri, A. C. *IEEE Electron Device Lett.* **1988**, *9*, 151–153.

RECEIVED for review July 5, 1989. Accepted October 18, 1989.

Certain commercial equipment, instruments, or materials are identified in this paper in order to adequately specify the experimental procedure. Such identification does not imply recommendation or endorsement by the National Institute of Standards and Technology, nor does it imply that the materials or equipment identified are necessarily the best available for the purpose.

Application of Countercurrent Chromatography/Thermospray Mass Spectrometry for the Identification of Bioactive Lignans from Plant Natural Products

Yue Wei Lee,* Robert D. Voyksner, Terry W. Pack, and C. Edgar Cook

Research Triangle Institute, P.O. Box 12194, Research Triangle Park, North Carolina 27709

Q. C. Fang

Institute of Materia Medica, Chinese Academy of Medical Sciences, Beijing, China

Yoichiro Ito

Laboratory of Technical Development, National Heart, Lung, and Blood Institute, Bethesda, Maryland 20892

The versatility and resolving power of countercurrent chromatography (CCC) has been demonstrated with a newly developed analytical high-speed planet centrifuge system. Interfacing countercurrent chromatography with mass spectrometry (MS) provides a new analytical methodology that integrates the advantages of countercurrent chromatography with the low detection limit and identification capability of mass spectrometry. In this paper the capability of thermospray CCC/MS is demonstrated in identifying and validating the bioactive and structurally known lignans from a crude extract of *Schisandra rubriflora* Rhed et Wils, a traditional Chinese herbal medicine for treatment of hepatitis.

INTRODUCTION

The development in the 1980s of modern countercurrent chromatography (CCC) instrumentation based upon the fundamental principles of liquid–liquid partition has caused a resurgence of interest in this separation science. The advantages of liquid–liquid extraction—the process for separating a multicomponent mixture according to its differential solubility in two immiscible solvents—have long been recognized. In spite of the limitations of the traditional countercurrent distribution methods that prevailed in the 1950s and 1960s, liquid–liquid extraction was used successfully to fractionate commercial insulin into two subfractions differing by only one amide group out of a molecular weight of 6000 (*1*).

In recent years, significant improvements have been made to enhance the performance and efficiency of countercurrent methods (*2*). The newly developed high-speed CCC technique utilizes a particular combination of coil orientation and planetary motion to produce a unique hydrodynamic phenomenon in the unilateral phase distribution of two immiscible solvents in a coiled column. The hydrodynamic properties can effectively be applied to perform a variety of countercurrent chromatographies, including true countercurrent (*3*)

---

* Author to whom correspondence should be addressed.

0003-2700/90/0362-0244$02.50/0 © 1990 American Chemical Society

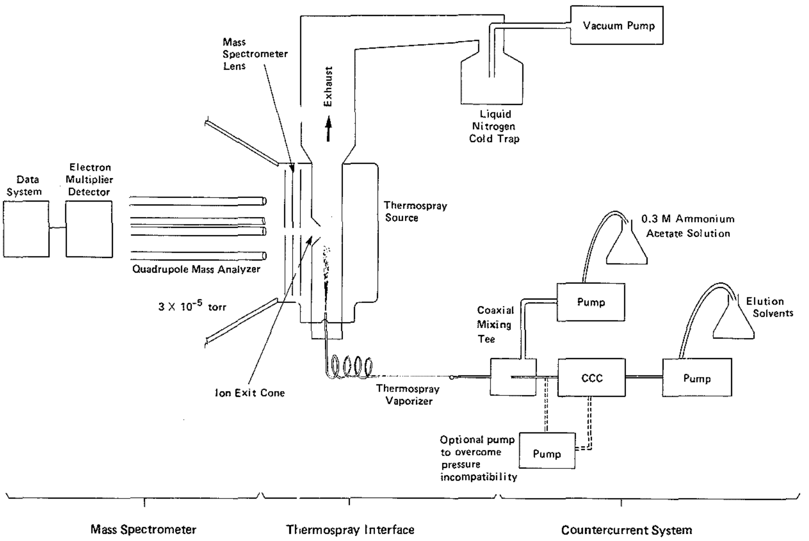

Figure 1. Schematic diagram of the CCC/thermospray MS system.

and foam countercurrent methods (*4*). More recently, a 2000-rpm high-speed CCC has been developed, which performs, separations with speeds and resolutions approaching those achieved by HPLC (*5*).

High-performance liquid chromatography coupled with mass spectrometry (HPLC/MS) represents one of the most rapidly advancing analytical techniques. Many different approaches have been developed in combining HPLC with MS, with their advantages and disadvantages extensively reviewed (*6–9*). Thermospray HPLC/MS (*10, 11*) is one technique that can handle a high quantity of aqueous solvent at conventional flow rates while providing a soft means of ionization (*12, 13*). The versatility of thermospray HPLC/MS is evidenced in numerous applications of environmental and clinical analyses (*14–18*).

The interface of countercurrent chromatography with thermospray mass spectrometry initially appeared incompatible due primarily to the pressure limitation imposed on the couuntercurrent system. A 6000-psi back-pressure commonly generated from the thermospray vaporizer often exceeds the pressure limitation of the Teflon fitting connected to CCC and causes solvent leakage. The newly developed high-speed CCC system not only provided improved efficiency but also could withstand the back-pressure, thus enabling the coupling of CCC with thermospray MS.

Interfacing countercurrent chromatography with thermospray mass spectrometry provides a new analytical methodology. This combination enhances the versatility of countercurrent chromatography with the specific detection and sensitivity of mass spectrometry.

The two-phase solvent system commonly employed in CCC offers distinct advantages by allowing the interface to be operated with the use of an aqueous mobile phase. The high-percentage aqueous condition with a volatile buffer provides the best thermospray/MS sensitivity (*12*) without the losses in resolution typically observed in HPLC when the mobile phase is switched to higher aqueous percentages.

The CCC/MS technique has been initially applied in the analysis of plant alkaloids from *Vinca minor* (*19*). This paper describes the application of thermospray CCC/MS in the identification of bioactive and structurally known lignans from a crude extract of *Schisandra rubriflora* Rhed et Wils, a traditional Chinese herbal medicine for treatment of hepatitis.

EXPERIMENTAL SECTION

Reagents and Materials. Ethanol and *n*-hexane used for preparation of the two-phase solvent systems were of glass-distilled chromatographic grade, purchased from Burdick and Jackson Laboratories, Inc., Muskegon, MI. Experiments were performed with a two-phase solvent system composed of *n*-hexane, ethanol, and water with a volume ratio of 6:5:5. The two-phase solvent system was prepared by thoroughly equilibrating the solvent mixture in a separatory funnel at room temperature followed by filtration and degassing with a 5-μm filter.

The *Schisandra* sample was kindly provided by Professor Chen Y. Y. at the Institute of Materia Medica, Chinese Academy of Medical Sciences, Meijing, China. The ethanolic extract of the kernels of *S. rubriflora* was filtered and concentrated to provide the crude sample for CCC/MS study.

Analytical High-Speed CCC. A recently developed analytical high-speed planet centrifuge equipped with a multilayer coil column of 0.85 mm i.d. poly(tetrafluoroethylene) (PTFE) tubing was employed. The system is capable of revolution at 2000 rpm with a 5-cm radius (*3*). A Waters 6000A HPLC pump (Waters Associates, Milford, MA) was used for the mobile phase. UV detection was achieved with an ISCO Model 1840 (Lincoln, NE) variable wavelength UV–vis absorbance detector. The column was first filled with the stationary phase (upper phase); then the mobile phase (lower phase) was pumped at 0.8 mL/min while the column was spun at 1500 rpm. The sample solution was injected when clean mobile phase (lower phase) was eluted.

Thermospray CCC/MS. In our system, shown in Figure 1, the effluent from the CCC, operating at 0.8 mL/min, was introduced into a Waters 6000A pump through a zero dead volume tee fitted with a reservoir. The waters pump was necessary to achieve the solvent pressure required for thermospray. Since the pressure in CCC fluctuates, the thermospray Waters pump was operated at 0.7 mL/min with the reservoir providing extra solvent or venting excess solvent from the CCC system. The effluent from the Waters pump was mixed coaxially (*20*) with 0.3 M ammonium acetate added at 0.3 mL/min to provide the volatile buffer for ion evaporation ionization. This solvent system (total of 1 mL/min) passed through a UV detector (254 nm) and into the thermospray interface. At lower CCC flow rates (0.3–0.6 mL/min) the pressure drop across the thermospray vaporizer was sufficiently low to permit direct coupling of the CCC effluent (lower phase) to the thermospray interface without the use of the auxiliary pump. Postcolumn addition of buffer and UV detection of the

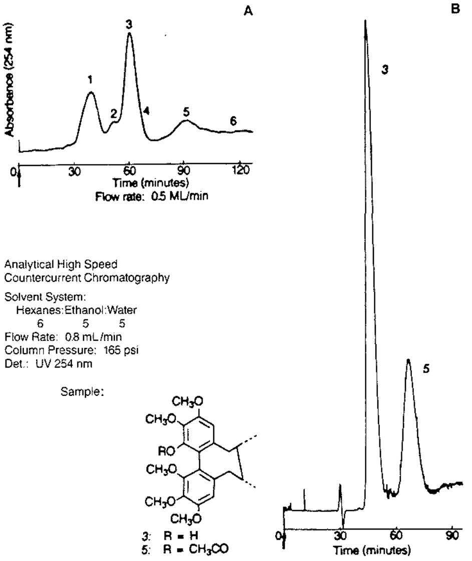

Figure 2. (A) CCC/UV chromatogram of the crude extract of the bioactive lignans of *Schisandra rubriflora*. (B) CCC/UV chromatogram for analysis of standard of schisanhenol and schisanhenol acetate.

CCC effluent were maintained as described above.

The thermospray interface (Vestec, Houston, TX) was installed on a Finnigan 4500 quadrupole mass spectrometer. The interface included a temperature controller and readout. The temperature zones monitored were the vaporizer, source, and aerosol (just pass the ion exit cone). Electrical cartridge heaters were used in the source, and the vaporizer was directly heated. The thermospray interface was operated at a source temperature of 250 °C and a vaporizer temperature to maximize the HPLC solvent clusters (about 170 °C). The solvent cluster has been shown to comaximize with the analyte being analyzed (*14*). This interface did not require any splitting of the LC effluent. The large volume of solvent was pumped out of the source with a liquid nitrogen cold trap prior to a mechanical rough pump. Both negative and positive ion detection using ion evaporation ionization and filament on chemical ionization (CI) were employed for the analysis of the herb medicine. The filament was operated at 1000 V with a 0.15-mA emission current. The mass spectrometer was scanned from m/z 180 to 600 in 2 s. The mass calibration of the quadrupole was verified with poly(propylene glycol) (average MW 1000).

RESULTS AND DISCUSSION

Countercurrent chromatography (CCC) based on the principle of liquid–liquid partition provides a number of distinct advantages, particularly in dealing with crude natural products (*21, 22*). We have successfully applied the high-speed CCC system in the separation of plant alkaloids, plant indole hormones, and herbicides. Recently, the study of *Schisandra rubriflora* Rhed et Wils has led to the identification of a number of bioactive lignans (*23*). Because of structural similarities, these bioactive lignans require extensive effort in isolation and identification following either conventional or off-line HPLC mass spectrometry procedures. An efficient thermospray CCC/MS spectrometric system that integrates the versatility of countercurrent chromatography with the specific detection capability of mass spectrometry has been developed in this laboratory. This new analytical technique has been successfully demonstrated in our preliminary study with a mixture of plant alkaloids (*19*) and further applied in the identification of bioactive lignans of *Schisandra*.

Table I. Lignans from *Schisandra* Detected in Thermospray CCC/MS along with Their Tentative Identification

peak no.	lignan ID	RT, min	rel peak area, %	spectra m/z (rel intens)
1	pregomisin	27	21	$[M + H]^+$ 391 (100) $[M + NH_4]^+$ 408 (70)
2	*meso*-dihydroguaiaretic acid	37	13	$[M + H]^+$ 331 (8) $[M + NH_4]^+$ 348 (100)
3	schisanhenol	54	54	$[M + H]^+$ 403 (98) $[M + NH_4]^+$ 420 (100)
4	schisanhenol B	52	<0.1	$[M + H]^+$ 387 (100) $[M + NH_4]^+$ 404 (12)
5	schisanhenol acetate	82	10	$[M + H]^+$ 445 (4) $[M + NH_4]^+$ 462 (100)
6	deoxyschisandrin	87	2	$[M + H]^+$ 417 (55) $[M + NH_4]^+$ 434 (100)

The CCC/UV chromatogram for the crude ethanolic extract of the bioactive lignans of *Schisandra* shows four distinct peaks (Figure 2A). Peaks 3 and 5 were postulated to be schisanhenol and schisanhenol acetate on the basis of CCC/UV retention time (Figure 2B). Thermospray CCC/MS was used to confirm this identification and to identify the minor components present in the extract. The thermosray spectra acquired for the bioactive components of *Schisandra* were very simple. They exhibited $[M + H]^+$ and $[M + NH_4]^+$ ions with no significant fragmentation. The negative ion spectra for these lignans were 10–100 times less intense. Only spectra for the major components (schisanhenol and schisanhenol acetate) were recorded. The negative ion spectra primarily showed $[M - H]^-$ ions and loss of CH_3CO for schisanhenol acetate. Selected ion chromatograms for the $[M + H]^+$ or $[M + NH_4]^+$ ion of the possible lignans from *Schisandra* indicated six components to be present (Figure 3). Due to statistical fluctuations normally observed in ionization for thermospray and the low concentrations of sample entering the MS, the ion chromatograms appear spiky with ion currents not greatly above detection limits. The major CCC/UV components present in the extract were confirmed to be schisanhenol (Figure 4B) and schisanhenol acetate (Figure 4A) on the basis of their identical thermospray spectra and retention times compared to the standards for these two components. The thermospray spectra of other components tentatively identified in Figure 3 are given in Table I along with their retention times and relative percentages. The minor bioactive lignans such as schisanhenol B (4) and deoxyschisandrin (6) were not sufficiently separated by CCC from schisanhenol or schisanhenol acetate, respectively, under UV detection. However, since they exhibited different characteristic ions, CCC/MS enabled the detection and acquisition of "clean" spectra of these trace components that coeluted with the major components in the sample.

Thermospray CCC/MS total ion current chromatograms presented a different picture of the relative abundances of the bioactive lignans compared to HPLC/UV. The thermospray CCC/MS response factors were determined to be more uniform for the various lignans compared to the UV response factors, enabling a more accurate estimate of the relative percentages of each lignan (Table I). Thermospray CCC/MS showed the main active lignans from *Schisandra* were schisanhenol (54%), pregomisin (21%), *meso*-dihydroguaiaretic acid (13%), and schisanhenol acetate (10%). The possibility of identifying more than six lignans exists, since nonpolar lignans having high partition coefficients in the stationary phase were not eluted under the current mobile-phase conditions.

CCC/MS offers a number of advantages to the chemist. The absence of column packing eliminates the complications

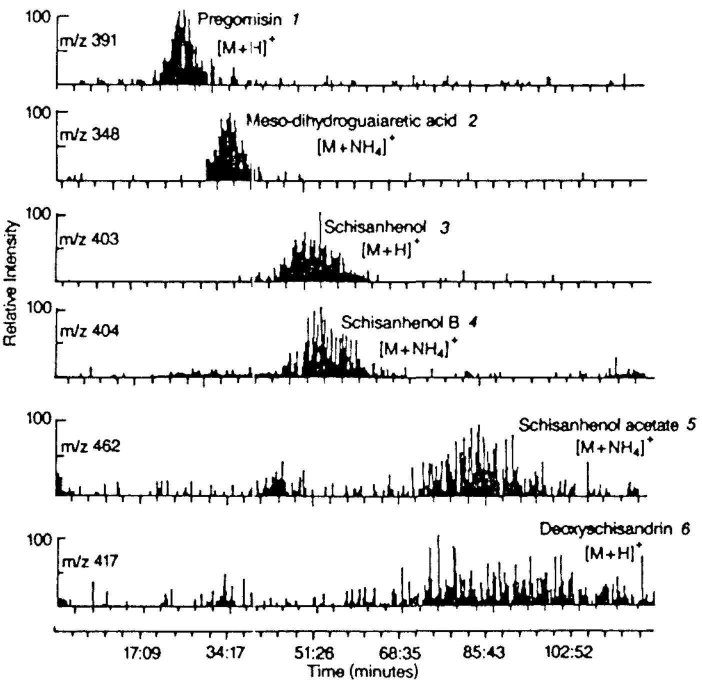

Figure 3. Thermospray CCC/MS $[M + H]^+$ or $[M + NH_4]^+$ selected ion chromatogram for all the lignans from *Schisandra* detected. The ion chromatograms presented for each lignan were normalized to 100% relation intensity. The identities of the peaks are presented in Table I.

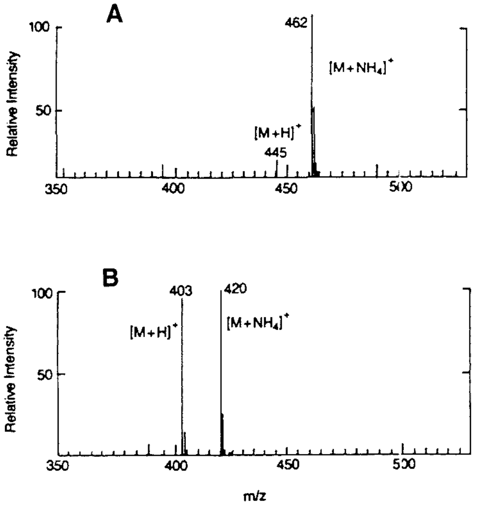

Figure 4. Thermospray CCC/MS spectra of (A) schisanhenol acetate MW 444 and (B) schisanhenol MW 402.

arising from column asorption, deactivation, and contamination often observed in HPLC. The coupling of CCC to thermospray MS is also suited for preparative work in which information on the purity as well as the identification of each component can be easily obtained. Because the two-phase solvent system that can be employed for CCC is unlimited, coupling of CCC to MS provides a complementary methodology to HPLC/MS in solving problems dealing with water-soluble compounds, polypeptides, and proteins.

There are also a number of shortcomings with CCC/MS. Namely, the peak widths in CCC are sufficiently wider (often greater than 10 min) so that the concentration of material eluting into the MS within a given scan is very low. This shortcoming is evident in Figure 3, resulting in very weak and jagged thermospray ion chromatograms (especially for the late-eluting components). Other shortcomings, including the relatively long analysis times and lack of gradient elution capabilities, hinder a wide acceptance of CCC/MS. Nevertheless, the coupling of CCC to MS is in its early stages, and new refinements are continually being made. Thick wall tubing and connections that withstand the high back-pressure (~600 psi) of thermospray MS will make CCC/MS more convenient and easy to use. An analytical CCC system capable of operating at 4000 rpm is being developed in the laboratory of Technical Development at the U.S. National Institutes of Health (*24*), which should increase the chromatographic resolution of the technique and therefore improve thermospray MS response. The feasibility of using two aqueous nonimmiscible solvent systems for separation of polypeptides and proteins is also being investigated.

ACKNOWLEDGMENT

The authors express their appreciation to Robert Bowman of the National Heart, Lung, and Blood Institute for the loan of some equipment.

Registry No. Pregomisin, 66280-26-0; *meso*-dihydroguairetic acid, 112867-79-5; schisanhenol, 69363-14-0; schisanhenol B, 102681-52-7; schisanhenol acetate, 75629-14-0; deoxyschisandrin, 61281-38-7.

LITERATURE CITED

(1) Hams, J. I.; Sanger, F.; Naughton, M. A. *Arch. Biochem. Biophys.* **1956**, *65*, 427.
(2) Ito, Y. *CRC Crit. Rev. Anal. Chem.* **1986**, *17*, 65.

(3) Lee, Y. W.; Cook, C. E.; Ito, Y. *J. Liq. Chromatogr.* **1988**, *11*, 37-53.
(4) Ito, Y. *J. Liq. Chromatogr.* **1985**, *8*, 2131.
(5) Lee, Y. W.; Ito, Y.; Fang, Q. C.; Cook, C. E. *J. Liq. Chromatogr.* **1988**, *11*(1), 75-89.
(6) Vestal, M. L. *Science* **1984**, *226*, 275-281.
(7) Covey, T. R.; Lee, E. D.; Bruins, A. D.; Henion, J. D. *Anal. Chem.* **1986**, *58*, 1451A-1461A.
(8) Games, D. E. *Adv. Mass Spectrom.* **1986**, *104*, 323-342.
(9) Voyksner, R. D. High Performance Liquid Chromatography/Mass Spectrometry. *In Analytical Aspects of Drug Testing*; Deutsch, D. G., Ed.; J. Wiley and Sons: New York, 1989; Chapter 7, pp 173-202.
(10) Blakely, C. R.; Carmody, J. J.; Vestal, M. L. *J. Am. Chem. Soc.* **1980**, *102*, 5931-5933.
(11) Blakely, C. R.; McAdams, M. J.; Vestal, M. L. *J. Chromatogr.* **1978**, *158*, 261-276.
(12) Blakely, C. R.; Carmody, J. J.; Vestal, M. *Anal. Chem.* **1980**, *52*, 1636-1641.
(13) Blakely, C. R.; Vestal, M. L. *Anal. Chem.* **1983**, *55*, 750-754.
(14) Voyksner, R. D.; Haney, C. A. *Anal. Chem.* **1985**, *57*, 991-996.
(15) Conchillo, A.; Casas, J.; Messequer, A.; Abian, J. *Biomed. Environm. Mass Spectrum* **1988**, *16*, 339-344.
(16) Bellar, T. A.; Budde, W. L. *Anal. Chem.* **1988**, *60*, 2076-2083.
(17) Watson, D.; Taylor, G. W.; Murray, S. *Biomed. Environ. Mass Spectrom.* **1986**, *13*, 65-69.
(18) Barcelo, D. *Biomed. Environ. Mass Spectrom.* **1988**, *17*, 363-369.
(19) Lee, Y. W.; Voyksner, R. D.; Fang, Q. C.; Cook, C. E.; Ito, Y. *J. Liq. Chromatogr.* **1988**, *11*(1), 153-171.
(20) Voyksner, R. D.; Bursey, J. T.; Pellizzari, E. I. *Anal. Chem.* **1984**, *56*, 1507-1514.
(21) Martin, D. G.; Mizsak, S. A.; Nielsen, J. W. *J. Antibiot.* **1986**, *39*, 603.
(22) Martin, D. G.; Peltonen, R. E.; Nielsen, J. W. *J. Antibiot.* **1986**, *39*, 721.
(23) Wang, H. J.; Chen, Y. Y. *Acta Pharm. Sin.* **1985**, *20*, 832-835.
(24) Ito, Y. Laboratory of Technical Development, NIH, Bethesda, MD, private communication.

RECEIVED for review July 10, 1989. Accepted October 25, 1989.

Adaptation of a Thermospray Liquid Chromatography/Mass Spectrometry Interface for Use with Alkaline Anion Exchange Liquid Chromatography of Carbohydrates

Richard C. Simpson* and Catherine C. Fenselau

Department of Chemistry and Biochemistry, University of Maryland, Baltimore County, Baltimore, Maryland 21228

Mark R. Hardy, R. Reid Townsend, and Yuan C. Lee

Department of Biology, Johns Hopkins University, Baltimore, Maryland 21218

Robert J. Cotter

Department of Pharmacology, Johns Hopkins University, Baltimore, Maryland 21205

An interface is described that allows the direct coupling of high-performance alkaline anion exchange liquid chromatography with thermospray mass spectrometry. A membrane suppressor is used to remove nonvolatile alkaline salts from the mobile phase after the chromatographic process is completed and prior to introduction into the mass spectrometer. Examples are given of both isocratic and gradient separations of a three-component test mixture of N-acetylated mono- and disaccharides, followed by on-line mass spectral data acquisition. Sensitivity studies show minimum detection limits for the test compounds to be in the microgram range.

INTRODUCTION

Various high-performance liquid chromatography (HPLC) techniques have been developed to facilitate carbohydrate analyses in an effort to better understand their role in biochemical processes. Some of these methods require precolumn derivatization of the sugars to enable or enhance detection (*1, 2*). Many of the techniques utilize reverse-phase (i.e. alkyl bonded phases) (*3, 4*) or normal-phase (i.e. amino bonded phases) (*5, 6*) separation mechanisms. Additionally, cation exchange HPLC has also been used for the resolution of various saccharides (*7, 8*). Most recently anion exchange HPLC, employing an alkaline mobile phase and electrochemical detection, has been successfully used for the resolution of sacchrides (*9, 10*). Work by Hardy and Townsend (*11*) indicates that alkaline anion exchange HPLC permits efficient resolution of underivatized saccharide positional isomers which is not possible to achieve with previous normal- or reverse-phase approaches.

Our laboratories are actively engaged in developing direct interfacing between alkaline anion exchange HPLC and mass spectrometry (MS), with the end goal being application of the interface to analyses of carbohydrates by HPLC/MS. The combination of excellent chromatographic resolution and mass spectral structure information could substantially contribute to the role of HPLC/MS in carbohydrate chemistry. This paper describes our initial efforts in the successful development of an interface to allow on-line coupling of alkaline anion exchange HPLC of underivatized N-acetylated saccharides with thermospray mass spectrometry.

EXPERIMENTAL SECTION

Materials. *N*-Acetylglucosamine (GlcNAc), *N*-acetylmannosamine (ManNAc), *N*-acetyllactosamine (LacNAc), glucose, sucrose, lactose, and stachyose were obtained from Sigma Chemical Co. (St. Louis, MO) and used without further purification. Doubly distilled deionized water was produced in-house and used for all solutions and reagents. All other chemicals were of reagent grade purity.

Apparatus. The HPLC was a Model 114M binary gradient system (Beckman, Berkeley, CA). The system utilized a Rheodyne 7125 injection valve (Cotati, CA) fitted with either a 20- or 250-μL sample loop. The alkaline mobile phase was either 10 or 100 mM NaOH. The variable-wavelength UV detector was a Model 757 fitted with a high-pressure flow cell (Applied Biosystems, Ramsey, NJ). The booster HPLC pump was a Spectroflow 400 dual piston pump, also purchased from Applied Biosystems. An AS-6 ana-

0003-2700/90/0362-0248$02.50/0 © 1990 American Chemical Society

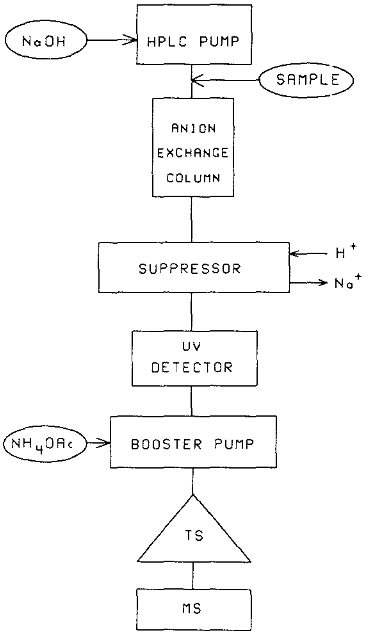

Figure 1. Schematic diagram of integrated anion exchange HPLC/MS system: TS, thermospray interface; MS, mass spectrometer.

lytical anion exchange column (250 × 4.6 mm, 10-μm polymeric packing), an AMMS anion micromembrane suppressor, and regenerant delivery system were obtained through Dionex Corp. (Sunnyvale, CA). A Corning low-level sodium ion selective combination electrode was purchased from VWR scientific (Bridgeport, NJ). A 10-μL mixing chamber was supplied by The Lee Co. (Westbrook, CT).

The mass spectrometer was a MS80RF magnetic instrument equipped with a thermospray interface (Karatos Analytical, Ramsey, NJ). Data collection and reduction were performed with DS-90 software on a Data General S/120 computer (Kratos). The mass spectrometer was calibrated over the appropriate mass ranges with a poly(ethylene glycol)/0.1 M ammonium acetate solution. The scan rate was held at 3 s/decade and a resolution of 1500 was used throughout the entire study. To minimize base-line noise due to low molecular weight mobile phase components, the low-mass cut-off was set at 125 amu.

The thermospray parameters were optimized for the mobile phase composition and flow rate. Typical temperatures were 190 °C for the vaporizer, 125 °C for the probe, 200 °C for the source block, and 250 °C for the vapor jet.

Integrated System. A schematic of the integrated system is shown in Figure 1. The HPLC pump delivers the NaOH mobile phase through the analytical anion exchange column at a flow rate of 1 mL/min. The column effluent is directly passed through the suppressor for the removal of Na^+ from the mobile phase. The suppressor is continuously regenerated with 70 mN H_2SO_4, which is supplied by the regenerant delivery system pressurized with He to 25 psi. This pressure resulted in a regenerant flow rate of 10 mL/min.

The mobile phase, which is now free of Na^+ and mildly acidic, passes through the variable-wavelength UV detector for conventional UV monitoring. After exiting the UV detector, the mobile phase is directed into one arm of a "T" fitting. The second arm of the "T" fitting is connected to a reservoir of 0.6 M ammonium acetate, which serves as the thermospray ionization reagent. The base of the "T" fitting is connected to the inlet check valve of the booster pump.

The booster pump, which is of the dual piston design, is set at a flow rate of 1.2 mL/min. Thus all of the mobile phase (at 1 mL/min) is delivered through the inlet check valve and the remaining difference (0.2 mL/min) is supplied by the 0.6 M ammonium acetate solution. The resulting combined mobile phase/ammonium acetate solution is then 0.1 M in ammonium acetate, which is in the proper concentration range to assist in the thermospray ionization process. To reduce dispersion of the resolved chromatographic bands, the pulse damper in the booster pump is bypassed and the combined mobile phase/ammonium acetate solution is pumped at a flow rate of 1.2 mL/min from the booster pump outlet check valve through a 10-μL mixing chamber into the thermospray interface and subsequently into the mass spectrometer.

Table I. Efficiency of Na^+ Removal

method of analysis: low-level sodium ion selective electrode
suppressor: Dionex AMMS
regenerant: 70 mN H_2SO_4 at 10 mL/min
NaOH flow rate: 1 mL/min

[NaOH], mM	residual [Na^+], μM	[NaOH], mM	residual [Na^+], μM
blank	10	70	19
10	30	100	13
40	18		

RESULTS AND DISCUSSION

The direct interfacing of alkaline anion exchange HPLC to thermospray mass spectrometry requires removal of nonvolatile NaOH from the mobile phase prior to introduction into the mass spectrometer. Incorporation of an anion micromembrane suppressor into the system between the HPLC column outlet and mass spectrometer accomplishes this removal. The micromembrane suppressor achieves Na^+ removal through a dialysis or ion replacement process, with Na^+ passing out of the mobile phase, through the membrane, and into the regenerant solution where it is swept to waste. In turn, H^+ is transported from the regenerant solution, through the membrane, and into the mobile phase. Thus the alkaline mobile phase is rendered slightly acidic and the OH^- mobile phase component is converted to water. To maximize the efficiency of Na^+ removal, the regenerant solution was used at the maximum concentration (70 mN H_2SO_4) and delivered at the maximum pressure (25 psi, corresponding to 10 mL/min) recommended by the manufacturer. Table I presents quantitative results concerning the efficiency of Na^+ removal by the micromembrane suppressor. The measurements, obtained by using a low-level sodium ion selective electrode, demonstrate the ability of the suppressor to efficiently remove Na^+ over a wide concentration range in the mobile phase. The implication of these results is that the mobile phase concentration of NaOH may be substantially varied to obtain the desired chromatographic resolution of analytes yet still be removed prior to entry into the mass spectrometer.

A major obstacle to interfacing with the thermospray mass spectrometer is the limit on the maximum operating pressure of the micromembrane suppressor. The manufacturer sets a maximum operating pressure of 100 psi, above which the membrane will rupture or the suppressor assembly will leak. Unfortunately the back pressure generated by the operating thermospray interface is approximately 600–700 psi. Therefore the suppressor cannot be directly connected to the thermospray interface. Placement of a booster pump (*12*) between the suppressor and the thermospray interface provides the required pressure drop between the two components. Since the booster pump requires more liquid than is being supplied by the mobile phase, the mobile phase may exit the suppressor and enter the booster pump at essentially atmospheric pressure. The volumetric difference between the mobile-phase flow rate and the set booster pump flow rate (0.2 mL/min) is provided by the 0.6 M ammonium acetate

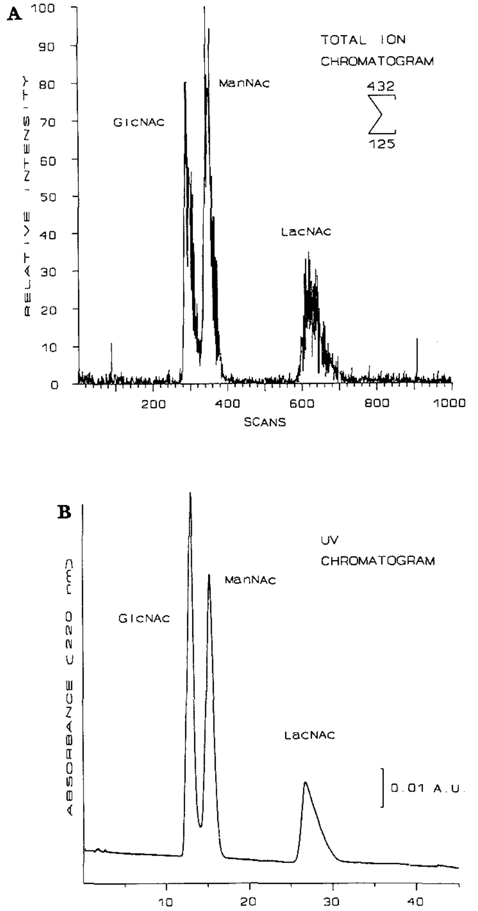

Figure 2. Isocratic separation of model compounds (100 μg each): mobile phase, 10 mM NaOH; (A) total on chromatogram (432–125 amu), (B) UV chromatogram (220 nm).

solution. The resulting ammonium acetate solution/mobile phase mixture becomes 0.1 M in ammonium acetate, which is in the proper concentration range to assist in the thermospray ionization process.

The dead volume within the booster pump pulse damper was shown to cause excessive extracolumn band broadening of the chromatographic peaks. Therefore to maintain the chromatographic resolution the pulse damper was removed from the flow path, allowing the ammonium acetate/mobile phase mixture to exit the booster pump at high pressure directly from the outlet check valve. To assist in the mixing of the ammonium acetate solution and the mobile phase, a 10-μL mixing chamber is placed in the flow path between the booster pump and the thermospray interface. The integrated system allows the temperature parameters for the thermospray interface to be adjusted just as in conventional thermospray mass spectrometry.

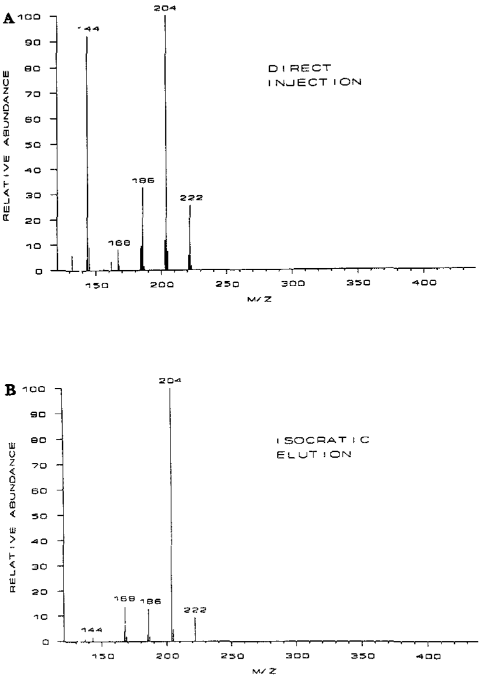

Figure 3. Thermospray mass spectra of GlcNAc (100 μg): (A) direct injection spectrum; (B) isocratic elution spectrum (at peak apex).

The model compounds used in this study are GlcNAc and ManNAc (epimeric monosaccharides), and LacNAc (a disaccharide with a β(1,4) linkage). The isocratic anion exchange separation of the model compounds is illustrated in Figure 2. The chromatography easily resolves all three components, including the two epimeric monosaccharides. An excellent correlation of quality between the total ion and 220-nm UV chromatograms was noted. With the suppressor placed before the UV detector, background absorbance due to NaOH is reduced and wavelengths down to 200 nm may be used, resulting in improved UV sensitivity.

The noise present in the total ion chromatogram is quite noticeable and is attributed to two causes. The primary source was found to be pressure pulsations from the booster pump. Even though the pump is of the dual piston design, removal of the pulse dampner from the flow path does introduce pressure pulsations of large enough amplitude to be detected by the thermospray mass spectrometer. In an attempt to reduce the pulsations, narrow bore Tefzel tubing was used as the transfer line between the booster pump and thermospray inlet. Although Tefzel is flexible and exhibits some elasticity, its use did not significantly reduce the noise relative to that obtained with a rigid stainless steel transfer line.

The secondary noise source is incomplete mixing of the mobile phase and ammonium acetate reagent. Use of a larger volume mixing chamber, such as 500 μL, between the booster pump and thermospray interface does provide a slight decrease in the noise. However due to increased extracolumn void volume, the decrease in noise is at the expense of chromatographic resolution. Thus the use of a 10-μL mixing chamber represents a compromise.

Figure 3 presents a comparison of the thermospray mass spectra of GlcNAc obtained by the conventional direct-injection technique and by isocratic elution through the integrated anion exchange HPLC/MS system. The spectra are similar to each other, indicating that the anion exchange chromatography and sodium removal do not adversely affect the mass spectrum obtained. Some of the primary features

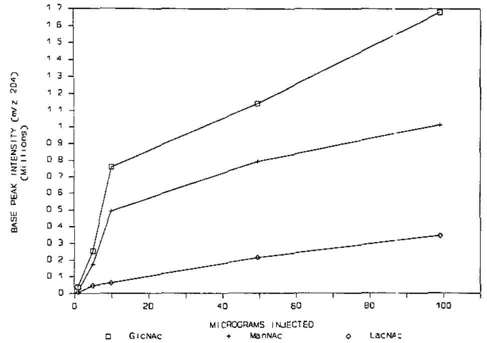

Figure 4. Sugar response curves. Intensity of the base fragment (*m/z* 204) was measured for each sugar.

of the GlcNAc mass spectra are $[MH]^+$ at *m/z* 222, $[MH - 18]^+$ at *m/z* 204, $[MH - 2 \times 18]^+$ at *m/z* 186 and $[MH - 3 \times 18]^+$ at *m/z* 168. Each loss of 18 probably corresponds to loss of a water molecule. The fragment at *m/z* 144 may be due to two losses of water and loss of acetamide, originating from the *N*-acetyl moiety, from the ammonium adduct of the molecular ion.

The direct injection and HPLC/MS spectra for ManNAc also exhibit the same degree of similarity to each other. As one may expect, the GlcNAc and ManNAc epimers yield identical mass spectra. Thus on the basis of mass spectral information alone, no differentiation of the species is possible. However, the integrated HPLC/MS system demonstrates its ability to combine chromatographic resolution and mass spectral information, thus resulting in less ambiguous data. In the case of LacNAc there is somewhat less correlation between the isocratic and direct injection spectra, although the major ions are still observed in each. The major differences between the isocratic elution and direct injection spectra are variations in relative ion intensities as well as absence of low-intensity high mass fragments in the isocratic spectrum. Optimization of the thermospray temperatures may improve the correlation of relative ion intensities. The lack of low-intensity high mass fragments in the isocratic spectrum may be attributed to sample dilution within the volume of the eluted chromatographic peak.

A study was conducted to determine the sensitivity and response of the system to each of the model sugars. Varying quantities of each model compound, ranging from 1 to 1000 μg each, were isocratically chromatographed, and the intensity of the base fragment (*m/z* 204) was observed for each compound. The results are depicted graphically in Figure 4. The response curves were found to be linear in the 10–100 μg range. Sample loadings above approximately 200 μg of each component begin to show negative deviation from linearity. This deviation is accompanied by substantial deterioration in the chromatographic peak shapes due to the column overloading. The minimum detection limit for each compound (at a signal to noise ratio of 2:1) is approximately 0.5 μg for GlcNAc and ManNAc and 1 μg for LacNAc. These values correspond to approximately 2.5 nmol of each compound.

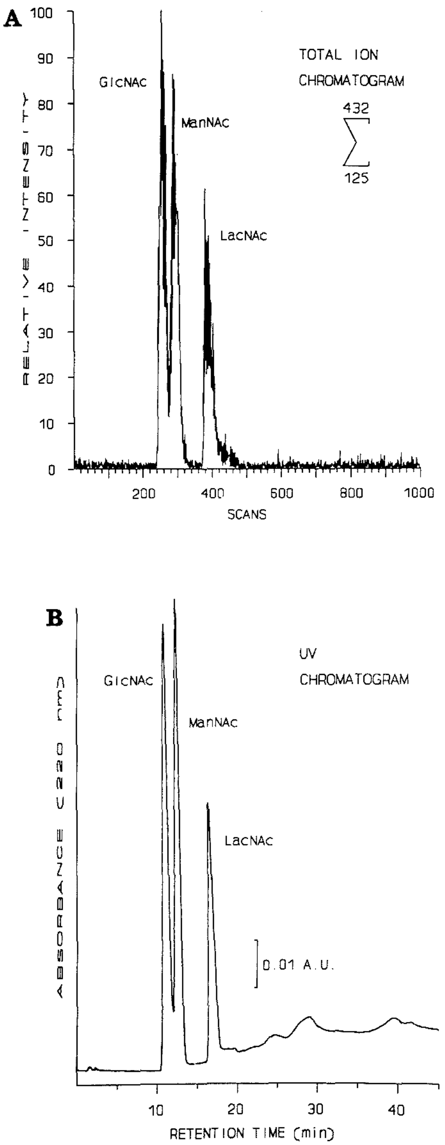

Figure 5. Gradient separation of model compounds (100 μg each): (A) total ion chromatogram (432–125 amu), (B) UV chromatogram (220 nm); mobile phase A, 10 mM NaOH; mobile phase B, 100 mM NaOH; flow rate, 1 mL/min; gradient profile, isocratic at 0% B for 8 min, ramp to 20% B over 4 min, ramp to 100% B over 11 min, isocratic at 100% B for remainder of run.

An additional demonstration of the flexibility of the integrated system is its ability to perform gradient separations, as shown in Figure 5. Excellent resolution of all three compounds is maintained while reducing the analysis time. The gradient also results in improved peak shapes, especially for LacNAc, and nearly doubles the detector response due to the sharper peak profiles. The relative base-line noise level in the gradient total ion chromatogram is less than that noted in the isocratic total ion chromatogram. This is due to the increased detector response in the gradient mode due to increased analyte concentration within the compressed chromatographic bands, which is a result of the gradient elution process. However the absolute intensity of the noise is the same as that observed in the isocratic total ion chromatogram. The mass spectrum of each compound obtained during gradient elution is essentially identical with that obtained during isocratic elution. In addition, the LacNAc spectrum exhibits some of the low-intensity high mass fragments (ex: *m/z* 366) not seen

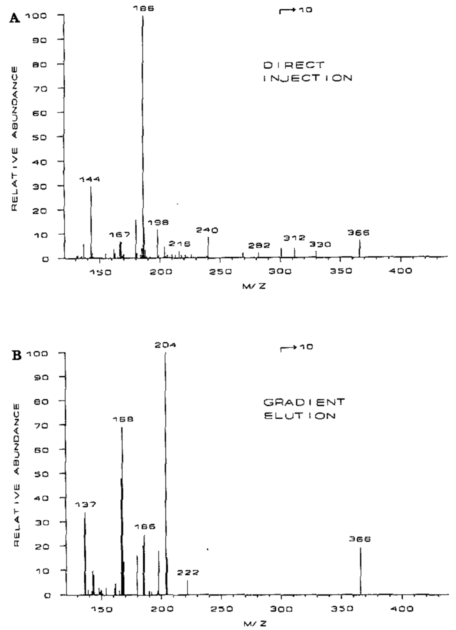

Figure 6. Thermospray mass spectra of LacNAc (100 μg): (A) direct injection spectrum; (B) gradient elution spectrum (at peak apex). The intensity of the spectra is magnified 10-fold above *m/z* 300.

at similar sample loadings in the isocratic mass spectrum. This can be attributed to the higher concentration of analytes in the chromatographic bands due to the compressed bandwidths obtained through gradient elution. Figure 6 illustrates a comparison of the thermospray mass spectra of the disaccharide LacNAc obtained by direct injection thermospray MS and gradient elution through the integrated HPLC/MS system. Again there is some similarity between the spectra obtained in each mode, although differences do exist. No protonated molecular ion is observed in either spectrum. Some of the primary features of the spectra are $[MH - 18]^+$ at *m/z* 366, $[MH - 3 \times 18]^+$ at *m/z* 330, $[MH - 4 \times 18]^+$ at *m/z* 312, a protonated GlcNAc fragment ($[GlcNAcH]^+$) at *m/z* 222, $[GlcNAcH - 18]^+$ at *m/z* 204, $[GlcNAcH - 2 \times 18]^+$ at *m/z* 186, $[GlcNAcH - 3 \times 18]^+$ at *m/z* 168, an ammonium adduct of galactose ($[GalNH_4]^+$) at *m/z* 198 and $[GalNH_4 - 18]^+$ at *m/z* 180. The fragment at *m/z* 144 may be due to loss of two water molecules and loss of acetamide, originating from the *N*-acetyl moiety, from the ammonium adduct of GlcNAc. No assignments have been made to fragments at *m/z* 302, 282, 268, and 240. The major differences between the two spectra are the lower intensity for the higher mass fragments at *m/z* values of 330, 312, 302, 282, 268, and 240 when the interface is used. Realizing that in direct injection thermospray MS the sample is introduced in a narrow concentrated band and recalling that chromatography is inherently a dilution process, we postulate that the LacNAc has been sufficiently diluted within the chromatographic band such that the higher mass fragments are not observed. Indeed if higher concentrations of LacNAc are injected into the HPLC/MS system, the fragments at *m/z* 366, 330, 312, and 240 do appear.

A disadvantage of the current system is the apparent inability of neutral unmodified sugars, such as glucose, sucrose, lactose, etc., to transit the suppressor. The fact that GlcNAc does transit the length of the suppressor while a large neutral sugar, such as stachyose (molecular weight 666) does not, indicates size alone is not the determining factor. The process is most likely much more complex, possibly involving both molecular size and charge considerations. Our experience generally indicates that amino sugars, and N-acetylated amino sugars will successfully transit the length of the suppressor assembly, while unmodified neutral sugars will not. Although this limitation may initially appear to be a serious disadvantage, such is not necessarily the case. Our ultimate goal is the application of the current method to the analyses of sugars obtained from tryptic digests of glycoproteins and glycopeptides. The vast majority of these saccharides contain amino or N-acetylated amino sugars. Thus the present method would be very amenable to this type of assay. Previous work by Hardy and Townsend (*11*) has demonstrated the use of alkaline anion exchange HPLC for such analyses, providing good resolution of the sugar analytes. The mass spectrometric detection of these analytes should not be more prone to deleterious interferences in this type of analysis than in any other, providing chromatographic resolution is maintained.

LITERATURE CITED

(1) Muramoto, K.; Goto, R.; Kamiya, K. *Anal. Biochem.* **1987**, *162*, 435-442.
(2) Takemoto, H.; Hase, S.; Ikenaka, T. *Anal. Biochem.* **1985**, *145*, 245-250.
(3) Rajakyla, E. *J. Chromatogr.* **1986**, *353*, 1-12.
(4) Tomiya, N.; Kurono, M.; Ishihara, H.; Tejima, S.; Endo, S.; Arata, Y.; Takahashi, N. *Anal. Biochem.* **1987**, *163*, 489-499.
(5) Koizumi, K.; Utamura, T.; Kubota, Y.; Hizukuri, S. *J. Chromatogr.* **1987**, *409*, 396-403.
(6) Blanken, W. M.; Bergh, M. L. E.; Koppen, P. L.; Van den Eijnden, D. H. *Anal. Biochem.* **1985**, *145*, 322-330.
(7) Derler, H.; Hormeyer, H. F.; Bonn, G. *J. Chromatogr.* **1988**, *440*, 281-286.
(8) Haginaka, J.; Nomura, T. *J. Chromatogr.* **1988**, *447*, 268-271.
(9) Reim, R. E.; VanEffen, R. M. *Anal. Chem.* **1986**, *58*, 3203-3207.
(10) Hardy, M. R.; Townsend, R. R.; Lee, Y. C. *Anal. Biochem.* **1988**, *170*, 54-62.
(11) Hardy, M. R.; Townsend, R. R. *Proc. Natl. Acad. Sci. U.S.A.* **1988**, *85*, 3289-3293.
(12) Lee, Y.-W.; Voyksner, R. D.; Fang, Q.-C.; Cook, C. E.; Ito, Y. *J. Liq. Chromatogr.* **1988**, *11*, 153-171.

RECEIVED for review August 21, 1989. Accepted October 30, 1989. The authors acknowledge financial support of this work through NSF Grants DCB8509638 and BBS8610589, NIH Grants GM21248, DK31376, and DK09970, and a Dionex Corp. Postdoctoral Fellowship.

Anal. Chem. 1990, 62, 253-257

Determination of Regulatory Organic Compounds in Radioactive Waste Samples. Semivolatile Organics in Aqueous Liquids

Bruce A. Tomkins,* John E. Caton, Jr., G. Scott Fleming, Manuel E. Garcia,[1] Sara H. Harmon, Robert L. Schenley, Cheryl A. Treese,[2] and Wayne H. Griest

Organic Chemistry Section, Analytical Chemistry Division, Oak Ridge National Laboratory, Oak Ridge, Tennessee 37831-6120

The regulatory semivolatile organic compounds present in radioactive aqueous waste samples are extracted and concentrated in a small-scale version of a standard EPA procedure normally used for groundwaters. Decontamination is sufficient to permit analysis of the extract in a conventional gas chromatography/mass spectrometry laboratory. The performance of the modified procedure, based on surrogate standards, matrix spikes and matrix spike duplicates, and blanks, is comparable to that of the standard method. The modified procedure was applied to a variety of aqueous radioactive waste tank samples. Only 12 of the EPA Appendix VIII compounds were present, and none in concentrations exceeding the reporting limit (500 or 2500 μg/L). The most common semivolatile present was tributyl phosphate, an organic extractant commonly used in radiochemical processing, at 2000–30000 μg/L.

The U.S. Environmental Protection Agency (EPA) mandated closure and decommissioning of Department of Energy nuclear waste storage tanks requires the chemical characterization of highly radioactive aqueous liquids to determine their regulatory status and to select appropriate treatments and disposal. In a previous paper (*1*), the characterization of volatile organic compounds, which can be removed from aqueous samples using an inert sparge gas, was described. The characterization must also include semivolatile organic compounds, which cannot be sparged from aqueous samples, but can be readily extracted and concentrated by using liquid–liquid extraction procedures.

The EPA identifies the regulatory semivolatile organic compounds in its Appendix VIII and describes their quantitation in *nonradioactive* wastes in its Solid Waste Manual 846 (SW-846) (*2*). Specifically, EPA Method 3510, "Separatory Funnel Liquid-Liquid Extraction" (*2*), of SW-846 describes the extraction and concentration of the compounds of interest, while Method 8270, "Gas Chromatography/Mass Spectroscopy (GC/MS) for Semivolatile Organics: Capillary Column Technique" (*2*), covers the identification and quantitation of these compounds. Unfortunately, the direct application of these procedures to the characterization of the aforementioned waste would result in the contamination of the GC/MS instrument and would expose laboratory staff to unsafe levels of radiation.

This paper describes modifications to EPA Method 3510 that not only permit the operator to use much smaller volumes of radioactive waste as the sample, thereby reducing his radiation exposure, but also produce a final extract that is essentially uncontaminated by radioactivity. The performance of the modified procedure, based upon the usual surrogate standards, matrix spikes, and blanks, is comparable to that achieved for nonradioactive groundwater using conventional EPA methods.

EXPERIMENTAL SECTION

Sample Collection. The aqueous radioactive waste samples were collected as described in detail elsewhere (*3*). Briefly, a small vacuum pump was used to draw the sample from a particular depth in the waste tank into a precleaned 250-mL widemouth jar (I-Chem, Hayward, CA). Approximately 15–25 mL of headspace was left in the jar. All samples were screened and tagged in the field for α and β/γ radiation before transferring to a lead pig and shipping to the analytical laboratory.

Surrogates, Spikes, and Internal Standards. An ampule of Acid Surrogate Standard Mix–CLP (Supelco, Inc., Bellefonte, PA, part no. 4-8875) was diluted to exactly 10 mL with Purge & Trap methanol (Baxter Healthcare Corp., Burdick & Jackson Division, Muskegon, MI), then transferred to a 20-mL screwcap vial supplied with a solid cap and Teflon liner. The concentration of each acid surrogate, viz. 2-fluorophenol, phenol-d_5; and 2,4,6-tribromophenol, was 200 μg/mL. An ampule of Base-Neutrals Surrogate Standard Mix–CLP Supelco, part no. 4-8925) was treated similarly. The concentration of each base-neutral surrogate, viz. nitrobenzene-d_5, 2-fluorobiphenyl, and 4-terphenyl-d_{14}, was 100 μg/mL. These surrogate mixtures were replaced at least every other week.

Two separate matrix spike stock solutions were prepared, one for acid and the other for base–neutral species. The acid stock solution contained ca. 10 mg/mL of the following species: phenol, 2-chlorophenol, 4-chloro-3-methylphenol, 4-nitrophenol, and pentachlorophenol. The base–neutral stock solution contained ca. 5 mg/mL of the following species: 1,4-dichlorobenzene; *N*-nitrosodipropylamine; 1,2,4-trichlorobenzene; acenaphthene; 2,4-dinitrotoluene; and pyrene. The neat matrix spikes were purchased from Supelco. A 200-μL aliquot of each stock was placed in the same volumetric flask and diluted to exactly 10 mL with Purge & Trap grade methanol (Baxter). The diluted matrix spike solution contained 100 μg/mL of each base–neutral matrix spike and 200 μg/mL of each acid matrix spike. This working solution was replaced at least monthly.

Supelpreme-HC Internal Standards Mix (Supelco, part no. 4-8902) was added to the finished extract. This mix contains 4 mg/mL each of the following components in methylene chloride: acenaphthene-d_{10}; chrysene-d_{12}; 1,4-dichlorobenzene-d_4; perylene-d_{12}; and phenanthrene-d_{10}. This mixture was not diluted and was usually replaced at least every 3 to 4 weeks.

Extraction Procedure. The liquid–liquid extractions for semivolatile organic compounds were performed after gross α and β/γ activity measurements were completed. This information was needed to determine how much sample could be taken safely for extraction in a radiochemical hood.

A 20-mL aliquot of aqueous sample was transferred to a 40-mL volatile organics analysis (VOA) vial (Shamrock Glass, Co., Seaford, DE, part no. 6-06K). These vials are precleaned according to EPA 40 CFR 136 and EPA 40 CFR 141 and are used as received. The natural pH of the sample was determined with wide-range pH paper. Three distinct cases were observed: (a) pH > 10; (b) pH < 2; (c) pH $\sim$ 6–9. The sample pH determined the order in which the acid and base–neutral fractions were extracted:

Sample pH $>$ 10. One-milliliter aliquots of the acid and base–neutral surrogates (all samples) and matrix spike (matrix

---

* To whom correspondence should be addressed.

[1] Present address, Environmental Compliance Division, Oak Ridge National Laboratory, Oak Ridge, TN 37831-6222.

[2] Present address, Hewlett-Packard Co., P.O. Box 22940, One Energy Center, Suite 200, Pellissippi Parkway, Knoxville, TN 37932.

0003-2700/90/0362-0253$02.50/0 © 1990 American Chemical Society

spike and matrix duplicate samples only) were added to the sample. The sample was then extracted 3 times with 5 mL of methylene chloride (High Purity, B & J Brand, Baxter) by mixing sample and solvent *gently*, end over end, at least 30 times. In a smaller number of cases, the two layers formed an emulsion which did not break within approximately 5–10 min. In these cases, the mixture was centrifuged briefly (normally about 1–2 min was sufficient) in a benchtop clinical laboratory centrifuge to break the layers. The methylene chloride layer contaminated with aqueous sample was retrieved from the VOA vial with a Pasteur pipet and transferred to a disposable 10-mL polypropylene syringe barrel equipped with an Acrodisc CR, 0.45-μm porosity, Teflon membrane filter in a disposable assembly (Gelman Sciences, Inc., Ann Arbor, MI, part no. 4404). The methylene chloride layer dripped from the filter free of water into a second 40-mL VOA vial. All methylene chloride extract layers were pooled.

The pH of the sample was adjusted to <2 with 12 N hydrochloric acid, sealed, and then shaken once or twice *gently*. Some bubbling was observed; the pressure was relieved by cracking the seal slightly. When the bubbling had ceased, the sample was extracted as before.

The methylene chloride layers from the acid and base–neutral extractions were pooled, then concentrated under dry, flowing nitrogen to approximately 2–4 mL. The sample was concentrated further to exactly 1 mL in a volumetric flask using dry, flowing nitrogen, transferred to a crimp-top vial, spiked with 10 μL of the Supelpreme-HC Internal Standard Mix, and sealed.

Sample pH < 2. The sample was spiked with surrogates and, where necessary, matrix spike and extracted as before. The pH was later adjusted to >10 with 1 M sodium hydroxide solution. The subsequent extraction and concentration steps were identical with those described above.

Sample pH ~ 6–9. The sample was rendered basic (pH > 10) with 1 M sodium hydroxide solution, then extracted as other samples with pH > 10.

Two 100-μL aliquots of the final methylene chloride extract were drawn for gross α and β radiochemical screening. The samples were checked further for radioactive contamination by using standard probe and smear techniques and then transferred to a conventional laboratory for quantitation of semivolatile organics by GC/MS (described below).

Method Performance Evaluation. Method performance was evaluated through the use of matrix spikes, matrix spike duplicates, and water blanks. A matrix spike and spike duplicate pair and blank accompanied each lot of samples (usually three to six aqueous radioactive liquids) prepared daily.

Gas Chromatographic Screening. All of the extracts were screened by gas chromatography to identify those that either required dilution or contained little organic matter and would not require GC/MS analysis (see below). A Hewlett-Packard Model 5840 gas chromatograph was equipped with a Model 7671A automatic sampler (Hewlett-Packard) and a Megabore DB-5 fused silica column (0.53 mm i.d. × 30 m, 1.5-μm film thickness, J & W Scientific, Folsom, CA). The column oven was programmed from 35 °C (hold for 4 min) to 270 °C (hold for 30 min) at 10 °C/min. The inlet and flame ionization detector temperatures were 270 and 290 °C, respectively. The autosampler injected a single 1.6-μL aliquot from each extract. The instrument was not calibrated quantitatively, but multicomponent standards of 20 and 4 μg/mL concentrations were run with each set to verify sensitivity. The standards included the acid and base–neutral target compound list (TCL) constituents specifically named by the EPA Contract Laboratory Program (CLP), as well as additional compounds selected from Appendix VIII.

GC/MS Identification and Quantitation. The final identification and quantitation of the semivolatile organic analytes were performed by using SW-846 Method 8270, "Gas Chromatograph–Mass Spectrometric Analysis for Semivolatile Organics: Capillary Column Technique", as described in ref 2.

Supplementary Semivolatile Appendix VIII Standards and Organic Extractant Standards. Standards containing additional semivolatile organic compounds listed in Appendix VIII, such as pesticides, chlorinated aromatics, nitrogen heterocyclics, and aromatic amines, were prepared using neat materials purchased from either the Aldrich Chemical Co. (Milwaukee, WI) or Chem Service, Inc. (West Chester, PA), in 95% or greater purity. In addition, Mr. James Botts, the Group Leader of the Transuranium Analysis Laboratory, Oak Ridge National Laboratory, Oak Ridge, TN, provided small samples of organic extractants commonly used in radiochemical processing. All materials were used as received, and diluted in B & J Brand methylene chloride (Baxter) to 20 mg/L.

RESULTS AND DISCUSSION

The aqueous radioactive waste samples described in this paper have been stored in underground waste storage tanks with headspace for up to 40 years. The major radionuclides present are the usual products of uranium fission, vis. ^{137}Cs and ^{90}Sr, exhibiting activity up to 6 × 10^5 and 1 × 10^4 Bq/mL, respectively. Other radionuclides, such as ^{60}Co, ^{233}U, and tritium, were commonly observed, but at hundred-fold less activities.

A number of inorganic anions and cations were also observed in the aqueous waste samples. The sample pH ranged between 0.5 and 13, with the great majority exceeding 8. Nitrate and sulfate were the dominant anions with concentrations up to 31 000 and 83 000 mg/L, respectively. The concentrations of sodium and potassium have not yet been measured but are expected to range from micrograms per liter to grams per liter. The major cation measured was uranium (up to 4000 mg/L). Lower concentrations of ten RCRA target metals were occasionally observed, particularly chromium and mercury.

The very high radiation fields limited access to the tank contents and the high specific activity of the tanks precluded the collection of samples by using the standard EPA protocols. Compromise procedures had to be utilized, as described in detail elsewhere (*3*).

Each sample was subjected to a variety of organic, inorganic, and radiochemical characterizations, each with its own requirement for holding time and minimum sample volume. In all cases the extraction of the semivolatile organics followed the determination of the regulatory target volatile organics and was performed in most cases within 14 days of receipt of sample. This arrangement satisfied the EPA SW-846 holding time for aqueous samples analyzed for semivolatiles.

The collection and conventional liquid–liquid extraction of 1-L samples (volume specified by EPA SW-846 Method 3510) bearing the stated activity was judged extremely hazardous to both the team sampling the radioactive waste storage tank and the analyst performing the sample preparation (*4*). For that reason, the sample volumes taken for semivolatile organic extraction were scaled back by a factor of 50. A 20-mL sample volume contained the maximum level of radiation, based on the activity of ^{137}Cs, which could be handled individually using a "Contamination Zone" radiochemical hood. The risk of radiation exposure and contamination was therefore reduced to more manageable and safer levels, but at the expense of analytical sensitivity. Given the hostile nature of the samples, the exchange between operator safety and method sensitivity was acceptable. The reporting limits were 50-fold those of the conventional SW-846 method, viz. 500–2500 μg/L.

The liquid–liquid extraction of even small volumes of aqueous radioactive waste proved challenging. Vigorous mixing of sample and methylene chloride extraction solvent invariably resulted in a stable emulsion. Gentle mixing, in which the sample vial was turned end-over-end, provided good mixing and easy separation of the layers. Sometimes even the end-over-end mixing produced emulsions which ultimately had to be broken by centrifugation. The methylene chloride layer was drawn from the bottom of the VOA vial using a disposable Pasteur pipette.

Other examples of complicating sample behavior included buffering, NO$_x$ formation, and precipitation. While most basic samples were acidified to pH <2 with the addition of ap-

Table I. Summary of Semivolatile Surrogate and Matrix Spike Recoveries for Radioactive Aqueous Waste Tank Samples

compound name and QC acceptance limits[a]	recovery data, %, for real samples				recovery data, %, for blanks			
	no. of samples	mean	std dev	RSD, %	no. of samples	mean	std dev	RSD, %
			Surrogates					
nitrobenzene-d_5 (35–114)	67	70	15	21	8	65	18	28
2-fluorobiphenyl (43–116)	67	64	14	22	8	58	13	23
terphenyl-d_{14} (33–141)	67	88	17	19	8	85	18	21
phenol-d_5 (10–94)	63	53	12	23	8	49	12	24
2-fluorophenol (21–100)	63	48	11	24	8	42	8	19
2,4,6-tribromophenol (10–123)	63	71	17	24	8	69	14	20
			Acid Matrix Spikes					
phenol (12–89)	10	40	9	22				
2-chlorophenol (27–127)	10	43	7	17				
4-chloro-3-methylphenol (23–97)	10	55	19	34				
4-nitrophenol (10–80)	10	69	31	46				
pentachlorophenol (9–103)	8	74	32	44				
			Base–Neutral Matrix Spikes					
1,4-dichlorobenzene (36–97)	14	50	10	20				
N-nitrosodi-*n*-propylamine (41–116)	14	66	10	15				
1,2,4-trichlorobenzene (39–98)	14	53	12	22				
acenaphthene (46–118)	14	64	13	21				
2,4-dinitrotoluene (24–96)	14	71	18	25				
pyrene (26–127)	14	78	12	15				

[a] Quality Control Acceptance Limits for surrogates taken from SW-846, Method 8270 (*2*). Quality Control Limits for matrix spikes taken from ref 5.

Table II. Semivolatile Organic Compounds Quantitated in Aqueous Radioactive Tank Samples[a]

	concentration of semivolatile organic compound in µg/L for the tank and aqueous sample shown													
	T-2			T-9	TH-4	W-6	W-7	W-8	W-9	W-10		W-3		
	L-038	L-039	L-112	L-047	L-056	L-079	L-082	L-087	L-090	L-094	L-095	L-016	L-017	L-018
compound (reporting limit, µg/L)														
2-nitrophenol (500)	170	200	180	*	*	*	*	*	*	*	*	*	*	53
2,4-dichlorophenol (500)	100	140	*	*	*	*	*	*	*	*	*	*	*	*
2,4,5-trichlorophenol (2500)	99	110	120	*	*	*	*	*	*	*	*	*	*	*
bis(2-ethylhexyl)phthalate (500)	200	300	280	*	*	*	*	*	*	*	*	*	*	*
di-*n*-butyl phthalate (500)	*	*	24	*	*	*	*	17	20	*	*	60	48	230
di-*n*-octyl phthalate (500)	*	*	*	*	*	*	*	*	*	*	*	49	80	*
acenaphthene (500)	*	*	*	*	42	*	*	*	*	*	*	*	*	*
naphthalene (500)	*	*	*	*	110	*	*	28	*	*	20	*	*	*
phenanthrene (500)	*	*	*	*	56	*	*	*	*	*	*	*	*	*
fluoranthene (500)	*	*	*	*	*	*	*	*	*	*	*	*	*	33
pyrene (500)	*	*	*	*	*	*	*	*	*	*	*	*	*	60
benzoic acid (2500)	*	*	*	400	*	290	1900	*	*	400	2900	*	*	*
Tentatively Identific Compounds (TIC)														
tributyl phosphate (E)[b]	20000	20000	20000	30000	20000	*	*	20000	10000	2000	*	30000	30000	30000
dibromonitrophenol (E)[b]	*	*	*	*	*	*	700	700	*	*	*	*	*	*

[a] Asterisk indicates not observed; concentration below the reporting limit. [b] (E) Concentration estimated from the response factor of the nearest internal standard in the gas chromatogram.

proximately 1–2 mL of 12 N hydrochloric acid, a few required up to approximately 7 mL of the concentrated acid. This behavior suggests that the sample matrix possessed significant buffering capacity which had to be overcome before the extractions could proceed. Samples that were initially acid exhibited little to no such buffering capacity and could be rendered basic easily using 1 M sodium hydroxide In other cases, the sample foamed during the acidification step, and a brown gas was generated. This behavior suggests that significant concentrations of nitrite were present and that nitrous oxides were generated during this part of the sample preparation. Both situations provide unwanted yet unavoidable, complications in the analytical procedure. The generation of nitrous oxides is particularly undesirable because these highly reactive species may affect the integrity of the sample and may combine with analytes of interest. Precipitates also were observed upon the acidification of a few samples.

The methylene chloride layers had to be reasonably dry before concentration using the nitrogen blow-down procedure, otherwise two layers would be obtained from the concentration step. Not even experienced operators could remove only methylene chloride from the extraction vial; a little aqueous sample was always transferred as well. The aqueous contamination was successfully removed by simply passing the methylene chloride layer through a disposable filtration assembly containing a Teflon filter. Methylene chloride passed freely through the filter, while water was retained by virtue of its greater surface tension. The syringe barrel and filtration assembly were thrown away after each sample, eliminating possible cross-contamination. The filter contributed only a small level of hydrocarbon contamination, and this did not interfere with the regulatory compound measurements. The extracts were reduced in volume to 1.0 mL by evaporation under dry flowing nitrogen.

The internal standard was added to each concentrated extract immediately after sealing the crimp-top vial. The addition at this point was critical, since aliquots would necessarily be withdrawn for the radiochemical screening. On several occasions, the pale yellow concentrate turned a deep orange upon addition of the internal standard. The reason for the color change is under investigation, but we suspect that a complexation reaction with traces of coextracted metals may have occurred.

In most cases, the final methylene chloride extract was virtually, although not entirely, free of α and β/γ radiation. Hence, the two major fission products, ^{137}Cs (β and γ emitter) and ^{90}Sr (β emitter) were almost entirely removed by using a simple liquid–liquid extraction employing methylene chloride. Such a result suggests that the two fission products are usually present as uncomplexed entities and are therefore insoluble in the organic solvent. In a few cases, a significant quantity of α radiation was observed in the final extract. We suggest, but cannot prove at present, that an organic complexing agent was present in those aqueous samples and that some radionuclide was carried into the organic layer via its associated ligand. In most cases, the specific activity of the original sample was reduced by 3 or more orders of magnitude in the final concentrated extract. This concentrate could be safely analyzed in a conventional GC/MS laboratory.

The recovery of the six surrogate standard compounds for 67 real samples and 8 blanks is summarized in Table I. The recovery data for the acid surrogates taken from four real samples were invalidated by apparent laboratory error and are not included in the calculations. Overall, the mean recoveries calculated for the real samples are well within the Quality Control Acceptance Limits for each compound specified for groundwater samples by EPA SW-846 (*2*). Although the applicability of these Quality Control Acceptance Limits to aqueous radioactive waste samples is not clear, they are useful for comparison purposes. The precision of the recovery measurements, expressed by the relative standard deviation, is approximately 20%. These conclusions held for the surrogates quantitated in the eight blanks as well. The recovery data obtained for the real and blank sample matrices were virtually indistinguishable, demonstrating the ruggedness of the sample preparation method.

Seven pairs of matrix spike and matrix spike duplicate recoveries were evaluated, also shown in Table I. While all of the available base-neutral matrix spike data were used, two pairs (total four samples) of acid matrix spike data were invalidated either by errors in the sample preparation laboratory or by matrix effects which the existing extraction procedure could not overcome. An additional pair of recovery values for pentachlorophenol was also deleted because the measured recovery exceeded 150%. The problem was traced to an erratic peak shape produced during the GC/MS analysis. The mean recovery values for both the acid and base–neutral matrix spikes fell within accepted quality control limits defined by the EPA Contract Laboratory Program (CLP) (*5*); there are no Quality Control Acceptance Limits for matrix spikes listed in EPA SW-846. The standard deviation and relative standard deviation of the base–neutral matrix spikes were almost identical with those observed for the surrogates. These two parameters tended to be somewhat greater for the acid matrix spikes. Possible reasons for the weaker precision include the following: (a) the pH of the final extract was insufficient to permit quantitative removal of the smaller, more acidic phenols, notably 4-nitrophenol, and (b) reliable quantitation of at least one species by GC/MS, viz. pentachlorophenol, is historically difficult. The modified procedure clearly worked as well as that defined by EPA Method 3510 on the basis of surrogates and matrix spikes. The agreement between a matrix spike and its companion matrix spike duplicate was typically between 10 and 20%.

The method blanks (eight in all) were all free of TCL compounds except for traces (110 and 170 μg/L, respectively) of di-*n*-butyl and di-*n*-octyl phthalates detected in one blank. Low levels of hydrocarbons contributed by the Teflon membrane filter were found in all blanks and samples (typically at 100–200 μg/L), but they did not interfere with the quantitation of the TCL analytes.

Table II summarizes the semivolatile organic compounds quantitated in the aqueous liquids from radioactive waste tanks. Twelve species were identified in 14 tank samples, but of these, only one, benzoic acid, was observed at levels exceeding the reporting limit (2500 μg/L), and even then only

Table III. Results of GC–MS Analysis of Supplementary Semivolatile Appendix VIII and Other Organic Compounds as Tentatively Identified Compounds (TICs) (All Prepared at 20 mg/L Solution Concentration)

compound	est concn as TIC, mg/L
Semivolatiles Supplementary Standard	
N-nitrosodimethylamine	ND[a]
N-nitrosodiethylamine	11
benzenethiol	13
acetophenone	19
2,6-dichlorophenol	12
1,4-naphthoquinone	8
2-naphthylamine	6
4-aminobiphenyl	8
benz[*c*]acridine	12
dibenz[*a,j*]acridine	9
p-dioxane	ND
pentachloroethane	11
N-dimethyl-1,1-phenethylamine	ND
hexachloropropene	7
1,4-diphenylenediamine	ND
1,2,4,5-tetrachlorobenzene	11
2,4-diaminotoluene	ND
pentachlorobenzene	12
1,2-diphenylhydrazine	ND
pentachloronitrobenzene	6[b]
benzidine	ND
hexachlorophene	ND
Pesticides Standard	
α-BHC	14
β-BHC	12
γ-BHC	13
δ-BHC	11
Heptachlor	14
Aldrin	15
Heptachlorepoxide	12
Endosulfan I	22
DDE	27
Dieldrin	22
Endrin	19
Endosulfan II	19
DDD	20
Endrin Aldehyde	15
Endosulfan Sulfate	18
Methoxychlor	15
Dibutylchlorendate	ND
Mirex	ND
DDT	ND
Extractants Standard	
diethylbenzene	20
2-thenoyltrifluoroacetone	6
tributyl phosphate[c]	26
di-*s*-butyl phenylphosphonate	ND
2,5-di-*tert*-butylhydroquinone	10

[a] Mass spectrometer may have begun collecting data too far into gas chromatography trial and may have missed these very early eluting compounds. [b] Pentachlorophenol was detected, suggesting decomposition in the gas chromatograph or mass spectrometer. [c] Not identified by machine search; spectrum manually identified.

once. We postulate the following mechanism to explain the presence of these entities: Toluene present in the waste tank may have been oxidized radiolytically to benzoic acid and various phenols, which in turn reacted with nitrate and chloride also present in the waste. The phthalates are omnipresent in the environment; low concentrations (less than 200 μg/L) were also detected in two of the eight analytical blanks. Polycyclic aromatic hydrocarbons such as naphthalene are known constituents of liquid scintillation cocktails. Toste et al. (*6–8*) has also reported the presence of small concentrations of phthalates and various phenols in aqueous radiochemical waste.

Table II includes the "tentatively identified compounds" (TICs) which were actually observed in 14 liquid samples. The most frequently occurring and most concentrated TIC was tributyl phosphate, which was present at levels ranging from 2000 to 30 000 μg/L. The prevalence of this compound is not surprising because it is one of the most common extracting agents used in radiochemical processing.

A limited evaluation was made of the ability of the GC/MS instrument to identify and estimate other Appendix VIII compounds which might be present in the semivolatile organic extracts. In addition, the evaluation was extended to certain nonregulatory compounds such as extractants, chelators, and complexing agents unique to the nuclear industry which are highly likely to be present in the waste tank extracts. These compounds would be reported in the GC/MS analysis of the semivolatiles as TICs, and the concentration data would be estimates only. For this purpose, four sets of supplementary standards were prepared at 20 mg/L each in methylene chloride. After the addition of the semivolatiles internal standards, these supplementary standards were analyzed as described in EPA Method 8270. The results are listed in Table III. The identifications and estimates were quite successful, considering that the identifications were made by machine (with the exception of tributyl phosphate, which was not included in the spectral library) with operator approval, and the concentrations were estimated based upon the response factor of the nearest eluting internal standard, the normal procedure for TICs. A wide range of compounds, including nitrosamines, aromatic amines, chlorinated aromatics, nitrogen heterocyclics, and pesticides were correctly identified and estimated. Exceptions apparently arose from very early eluting species, which were either missed (e.g., *N*-nitrosodimethylamine and dioxane) or may not have eluted from the column (e.g., some of the aromatic amines and hydrazines) under the conditions used. It is possible that sample residues present in the gas chromatographic inlet and/or column may have prevented the elution of some of the more polar species. In general, there was a good probability that additional Appendix VIII compounds would be identified and estimated if they were present in the extracts at milligram per liter concentrations.

The performance of this modified EPA methodology, as defined by surrogate standards, matrix spikes, and blanks, shows that semivolatile organic compounds present in highly radioactive samples can be isolated confidently by using modified and smaller-scale technology than that recommended for nonradioactive samples. The resulting extracts are essentially nonradioactive, and the required determinations may be performed by GC/MS analysis in a conventional analytical laboratory.

ACKNOWLEDGMENT

The authors express their appreciation to the staff of the High Radiation Level Analytical Laboratory, Oak Ridge National Laboratory, for providing the radiochemical characterization and inorganic analysis data presented in this paper. The authors also acknowledge Ms. Nancy R. Sweat-Pope and Mr. William F. Fox, health physicists and members of the Environmental Compliance Division, Oak Ridge National Laboratory, for their advice concerning the proper handling of the radioactive waste samples which were discussed in this work. Mr. James L. Botts, Group Leader of the Transuranium Analysis Laboratory, Oak Ridge National Laboratory, provided small samples of organic extractants used in radiochemical processing. Ms. Linda L. Kaiser, Mr. Christopher B. Scott, and their co-workers designed and executed the sampling plan described in this work.

LITERATURE CITED

(1) Tomkins, B. A.; Caton, J. E., Jr.; Edwards, M. D.; Garcia, M. E.; Schenley, R. L.; Wachter, L. J.; Griest, W. H. *Anal. Chem.* **1989**, *61*, 2751–2756.

(2) *Test Methods for Evaluating Solid Waste. Volume 1B, Laboratory Manual Physical/Chemical Methods*; SW 846; Third Edition; United States Environmental Protection Agency, Office of Solid Waste and Emergency Response: Washington, DC, November 1986.

(3) Autrey, J. W.; Costanzo, D. A.; Griest, W. H.; Keller, J. M.; Kaiser, L. L.; Nix, C. E.; Tomkins, B. A. *Sampling and Analysis of the Inactive Waste Storage Tank Contents at ORNL*; ORNL/RAP-53, Environmental and Health Protection Division, Oak Ridge National Laboratory: Oak Ridge, TN, August 1989.

(4) Operating Guide for Radiochemical Laboratories at Various Activity Levels: Procedure No. A-7. In *Procedures and Practices for Radiation Protection: Health Physics Manual*; Oak Ridge National Laboratory: Oak Ridge, TN, July 1, 1987.

(5) *USEPA Contract Laboratory Program: Statement of Work for Organic Analysis, Multi-Media, Multi-Concentration, S. O. W. 787*; Oak Ridge National Laboratory: Oak Ridge, TN, 1987.

(6) Toste, A. P.; Pahl, T. R.; Lucke, R. B.; Myers, R. B. In *Twenty-Fourth Hanford Life Series Sciences Symposium: Health & Environmental Research on Complex Organic Mixtures*; CONF-851027, UC-11; Gray, R. H., Chess, E. K., Mellinger, P. J., Riley, R. G., Springer, D. L., Eds.; Richland, WA, 1987; p 41.

(7) Toste, A. P.; Lechner-Fish, T. J.; Hendren, D. J.; Scheele, R. D.; Richmond, W. G. *J. Radioanal. Nucl. Chem.* **1988**, *123*, 149–166.

(8) Toste, A. P.; Hara, F. T.; Hendren, T. J.; Matsuzaki, C. L.; Molton, P. M.; Robertson, D. E.; Scheele, R. D.; Thomas, C. W.; Widrig, D. L. *Chemical and Radiochemical Analyses of Hanford Radioactive Wastes*; Pacific Northwest Laboratory: Richland, WA, unpublished work, 1987.

RECEIVED for review August 17, 1989. Accepted November 2, 1989. Oak Ridge National Laboratory is operated by Martin Marietta Energy Systems, Inc., under Contract DE-AC05-84OR21400 with the U.S. Department of Energy.

Anal. Chem. 1990, 62, 258–263

Cross-Linked Redox Gels Containing Glucose Oxidase for Amperometric Biosensor Applications

Brian A. Gregg and Adam Heller*

Department of Chemical Engineering, University of Texas at Austin, Austin, Texas 78712

Oxidoreductases, such as glucose oxidase, can be electrically "wired" to electrodes by electrostatic complexing or by covalent binding of redox polymers so that the electrons flow from the enzyme, through the polymer, to the electrode. We describe two materials for amperometric biosensors based on a cross-linkable poly(vinylpyridine) complex of $[Os(bpy)_2Cl]^{+/2+}$ that communicates electrically with flavin adenine dinucleotide redox centers of enzymes such as glucose oxidase. The uncomplexed pyridines of the poly(vinylpyridine) are quaternized with two types of groups, one promoting hydrophilicity (2-bromoethanol or 3-bromopropionic acid), the other containing an active ester (*N*-hydroxysuccinimide) that forms amide bonds with both lysines on the enzyme surface and with an added polyamine cross-linking agent (triethylenetetraamine, trien). In the presence of glucose oxidase and trien this polymer forms rugged, cross-linked, electroactive films on the surface of electrodes, thereby eliminating the requirement for a membrane for containing the enzyme and redox couple. The glucose response time of the resulting electrodes is less than 10 s. The glucose response under N_2 shows an apparent Michaelis constant, $K_m' = 7.3$ mM, and limiting current densities, j_{max}, between 100 and 800 $\mu A/cm^2$. Currents are decreased by 30–50% in air-saturated solutions because of competition between O_2 and the Os(III) complex for electrons from the reduced enzyme. Rotating ring disk experments in air-saturated solutions containing 10 mM glucose show that about 20% of the active enzyme is electrooxidized via the Os(III) complex, while the rest is oxidized by O_2. These results suggest that only part of the active enzyme is in electrical contact with the electrode.

INTRODUCTION

Enzyme-based biosensors are being used in an increasing number of clinical, environmental, agricultural, and biotechnological applications (*1–4*). Ideally, the high selectivity of enzymes, when coupled with modern electrode technology, should result in an electrochemical sensor capable of detecting the concentration of a single biochemical species in a medium containing a diverse mixture of other compounds. Amperometric enzyme electrodes (*5*) require some form of electrical communication between the electrode and the active site of the redox enzyme. However, the measurement of a current proportional to the concentration of the enzyme substrate is complicated by the fact that the active site is often located deep inside an insulating protein shell. Thus, redox enzymes such as glucose oxidase do not exchange electrons with simple metal electrodes (*6–9*). Historically, electrical communication between enzyme and electrode has been achieved through the use of diffusing mediators. The first mediator employed for flavin adenine dinucleotide (FAD)–enzyme electrodes was the natural substrate of the flavin-linked oxidases, O_2 (*10–15*). For example, the reaction of glucose oxidase (GO) is

$$\text{GO–FAD} + \text{glucose} \rightarrow \text{GO–FADH}_2 + \text{gluconolactone} \quad (1)$$

$$\text{GO–FADH}_2 + O_2 \rightarrow \text{GO–FAD} + H_2O_2 \quad (2)$$

and the first commercial amperometric glucose sensors measured either the decrease in O_2 concentration at an oxygen electrode (*15*) or the increase in H_2O_2 concentration at a platinum electrode. The H_2O_2 formed in such sensors degrades the enzyme (*16*). Nature alleviates this problem through the use of the highly active enzyme catalase, which catalyzes the disproportionation of the H_2O_2 to water and oxygen. Furthermore, the electrode current depends on the concentration of *both* enzyme substrates, i.e., glucose *and* O_2. Measurement of the H_2O_2 concentration requires both a highly catalytic electrode (e.g., Pt) and a potential (ca. 0.7 V vs SCE) substantially positive of the reversible potential for the $FAD/FADH_2$ couple ($E° \approx -0.4$ V vs SCE) (*17*). This may result in large spurious currents due to a number of easily oxidized species in the system to be measured. Because of this problem, selective membranes were required to maintain the specificity of the enzyme electrode.

The more recent devices have employed small diffusing electron mediators (Ox/Red) such as ferrocenes (*18, 19*), quinones (*20*), ruthenium amines (*21*), components of organic metals (*22–27*), and octacyanotungstates (*28*). In such electrodes, reaction 1 above is followed by

$$\text{GO–FADH}_2 + 2\text{Ox} \rightarrow \text{GO–FAD} + 2\text{Red} + 2H^+ \quad (3)$$

where the reduced form of the mediator (Red) is subsequently electrooxidized. Catalase can be added to such a system to protect the enzyme from H_2O_2. The potential at which these electrodes operate is only slightly positive of the formal potential of the mediator, and a highly active noble metal electrode is not required for the reaction. Thus, spurious currents due to competing species may be reduced. Still, in an oxygen-containing medium, there is a competition between the oxidized form of the mediator (Ox) and oxygen for the reduced form of the enzyme ($GO–FADH_2$) (eqs 2 and 3). Thus, the electrode current is independent of the oxygen concentration only insofar as the mediator competes effectively with O_2.

Many enzyme electrodes require that the enzyme be confined to the proximity of the electrode surface by a membrane. Diffusion of substrate and product through such a membrane controls the (usually slow) response time of these electrodes. The required membrane seal also increases the cost of these electrodes. Furthermore, the small mediators commonly employed in the recent devices eventually diffuse through the membranes and are lost. Recently, a polymeric redox "wire" based on the poly(vinylpyridine) (PVP) complex of $Os(bpy)_2Cl$ (abbreviated POs^+) has been introduced (*29*). The "wire" electrically connects the enzyme to the electrode yet, by virtue of its molecular size, remains confined behind the membrane. This polycationic redox polymer forms electrostatic complexes with the polyanionic glucose oxidase in a manner mimicking the natural attraction of some redox proteins for enzymes, e.g., cytochrome *c* for cytochrome *c* oxidase (*30*). We report here a method for bonding a similar redox polymer to the enzyme and immobilizing the enzyme/polymer compound on an electrode in one step. The need for a membrane is eliminated in the resulting electrode. To simultaneously "wire" and immobilize the enzyme, we quaternize the PVP backbone with either the bromoacetic or bromopropionic acid ester of *N*-hydroxysuccinimide (NHS). The NHS esters react rapidly with primary amines, e.g., lysines on the enzyme surface, to

0003-2700/90/0362-0258$02.50/0 © 1990 American Chemical Society

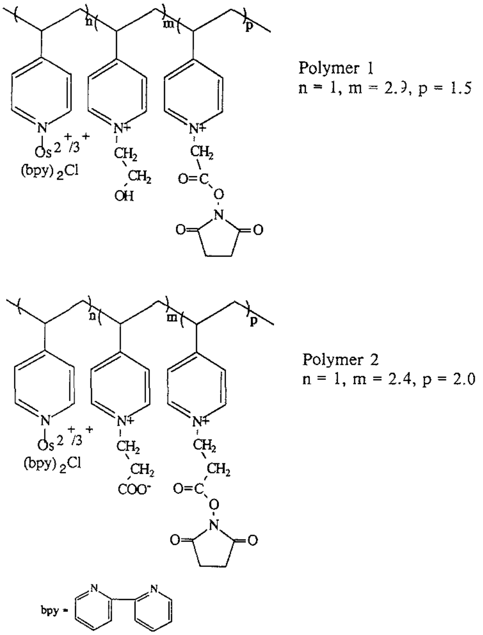

Figure 1. Structures of the two cross-linkable, redox gel-forming polymers.

form amide bonds (*31*). In the presence of an enzyme and a cross-linking agent (triethylenetetraamine, trien) this polymer forms, on the surface of an electrode, an insoluble, cross-linked film containing covalently bound enzyme. The resulting electrode is simple to make, fast, and rugged. We report the synthesis of two derivatives of this polymer and the electrochemical characterization of several polymer/glucose oxidase electrodes as a function of temperature and the concentrations of glucose, other sugars, and oxygen. We also describe a convenient method for quantifying the relative rates of eqs 2 and 3 in our system by rotating ring disk voltammetry.

EXPERIMENTAL SECTION

Chemicals. Glucose oxidase [EC 1.1.3.4] from *Aspergillus niger* (Sigma, catalog no. G-8135), catalase [EC 1.11.1.6] (Sigma, catalog no. C-100), Na-HEPES (sodium 4-(2-hydroxyethyl)-1-piperazineethanesulfonate) (Aldrich), and K_2OsCl_6 (Johnson Matthey) were used as received. Poly(vinylpyridine) (PVP, Polysciences, MW 50 000) was purified 3× by dissolution in methanol, filtration, and precipitation with ether.

Polymers. The structure of the polymers reported here is shown in Figure 1. The poly(vinylpyridine) complex of the $Os(bpy)_2Cl_2$ was synthesized as previously reported (*32*) and purified by precipitation from ethyl acetate. The resulting polymer was quaternized in warm (ca. 60 °C) dimethylformamide (DMF) under N_2 with either bromoethanol (Aldrich) or a mixture containing equimolar amounts of triethylamine and 3-bromopropionic acid (Aldrich) for 2 h. (The polymer compositions shown in Figure 1 assume that these materials reacted quantitatively with the poly(vinylpyridine) backbone.) After the initial partial quaternization, a slight excess of either the bromoacetic or bromopropionic acid ester of *N*-hydroxysuccinimide (NHS) (synthesized from the respective acid chloride and NHS essentially by the method of Pollak et al. (*33*)) was added, and the solution was further warmed for ca. 2 h. The resulting solution was then cooled and poured into rapidly stirred acetone, and the precipitate was filtered, washed with acetone, and stored in a desiccator.

The polymer quaternized with bromoethanol and the bromoacetic acid ester of NHS (polymer 1, POs^+–EtOH–C_2NHS) has a formula weight of 1878 g/repeat unit, assuming the composition shown in Figure 1. This corresponds to ca. 0.8 μmol of active ester groups per milligram of polymer. The polymer quaternized with bromopropionic acid and the bromopropionic acid ester of NHS (polymer 2, POs^+–EtCOO$^-$–C_3NHS) has approximately 1.0 μmol of active ester groups per milligram of polymer.

Electrodes. A representative electrode film was prepared as follows: An electrode consisting of a gold disk, 4.7 mm in diameter, surrounded by a platinum ring, was polished first with 0.3-μm alumina and then with 0.05-μm alumina, sonicated, rinsed with water, and dried in air. Aliquots (4 μL each) of the following solutions were then applied to the gold disk: 10 mg/mL glucose oxidase solution in 10 mM HEPES buffer, pH 7.2; 8 mM trien in the same buffer solution; and a freshly made solution of 10 mg/mL polymer 2 in H_2O. The solutions were briefly mixed on the electrode surface; the electrode was then dried in a vacuum dessicator containing a beaker of H_2O for at least 30 min. Similar films were made on glassy carbon, graphite, and platinum electrodes of various sizes.

Equipment. Electrochemical measurements were performed with a Princeton Applied Research 175 universal programmer, a Model 173 potentiostat, and a Model 179 digital coulometer. The signal was recorded on a Kipp and Zonen X-Y-Y′ recorder. A conventional single-compartment electrochemical cell was used with an aqueous saturated calomel reference electrode (SCE) (0.226 V vs a normal hydrogen electrode (NHE)) and a platinum counter electrode. The rotating ring disk experiments were performed with a Pine Instruments AFMSRX rotator, MSRS speed control and RDE4 bipotentiostat, and either a glassy carbon disk/platinum ring electrode (GC/Pt RRDE) or a gold disk/platinum ring electrode (Au/Pt RRDE), both from Pine Instrument Co.

RESULTS AND DISCUSSION

Enzyme Immobilization and Film Formation. The immobilization of enzymes has been the subject of extensive recent work (*2*, *34*, *35*) because heterogeneous catalysis has advantages over homogeneous catalysis and also because, in some cases, enzymes are stabilized by immobilization (*36*–*39*). The observed stabilization has been attributed both to the protection against attack by proteases that is afforded by the polymeric support and to the physical confinement of the enzyme's peptide chains that can retard thermal denaturation. Polymers containing *N*-hydroxysuccinimide (NHS) esters have been commonly used as coupling agents for affinity chromatography (*40*) and for the immobilization of a number of enzymes (*33*).

Recently, Foulds and Lowe (*41*) have reported the entrapment of glucose oxidase in films of ferrocene-containing polypyrrole. In these electrodes both direct current and indirect (O_2-mediated) current were observed. Hale et al. (*42*) described a biosensor based on the adsorption of glucose oxidase onto a mixture of carbon paste and a ferrocene-containing siloxane polymer. Here we report the covalent binding of glucose oxidase in an electrically conducting, hydrophilic, cross-linked redox gel on the surface of an electrode. The NHS ester chemistry was incorporated in the previously developed PVP-based polycationic redox polymer (POs^+) (*29*, *32*) by quaternizing some of the uncomplexed pyridines of POs^+ with bromoacetic or bromopropionic acid esters of NHS. To provide solubility in water to the resulting polymer, the remaining free pyridines were quaternized with either 2-bromoethanol or 3-bromopropionic acid (Figure 1).

Active NHS esters are highly specific for primary amines; they also slowly hydrolyze in aqueous solution (*33*). Thus, the two reactions of importance are the aminolysis and the hydrolysis of these active ester groups on the polymer chain. The cross-linked polymer is formed on the surface of the electrode by the addition of a few microliters of a fresh solution of the polymer to a solution of the enzyme and the cross-linking agent (trien) followed by evaporation of the solvent. It is feasible to use the enzyme as the only cross-linking agent.

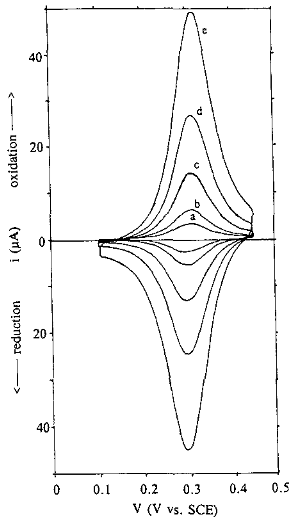

Figure 2. Cyclic voltammograms of a cross-linked film consisting of polymer **2**, glucose oxidase, and triethylenetetraamine on glassy carbon in the absence of glucose: 0.1 M HEPES buffer at pH 7.1; scan rates (mV/s), (a) 10, (b) 20, (c) 50, (d) 100, (e) 200.

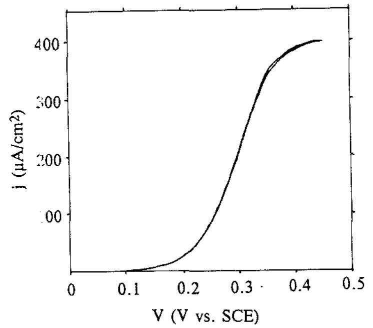

Figure 3. Cyclic voltammogram of the film shown in Figure 2 under N_2 after addition of 40 mM glucose: scan rate, 5 mV/s; rotation rate, 1000 rpm.

This requires, however, a high concentration of enzyme and results in an electrode exhibiting slow charge-transfer kinetics. Polymer/GO/trien films have been prepared on glassy carbon, graphite, gold, and platinum electrodes; the electrode characteristics were not noticeably affected by the nature of the conducting substrates. In systems where the enzyme is free to diffuse, platinum or glassy carbon electrodes often cause irreversible adsorption or denaturation of the enzyme (*43*). Apparently the enzyme in the cross-linked polymer films is protected from the deactivating influence of the electrode surface.

Electrochemical Characterization of the Polymer/Enzyme Film. In the absence of glucose oxidase in the polymer film, the current density resulting from direct electrooxidation of glucose (30 mM) is less than the background current (<10 nA/cm²) in the range 0–0.5 V vs SCE. Cyclic voltammetric waves at different scan rates of a thin layer of polymer 2/GO/trien on a glassy carbon electrode are shown in Figure 2 in a solution containing 0.1 M HEPES buffer titrated to pH 7.1 with HCl (ionic strength, 0.17 M). In the absence of glucose, the enzyme gives no response and only the polymer electrochemistry is observed. The electrode exhibits the classical features of a kinetically fast redox couple strongly bound to an electrode surface (*44*). At a scan rate of 200 mV/s the difference in the reduction and the oxidation peak potentials is less than 20 mV, showing that charge transfer and counterion movement through the film, as well as charge transfer from the film to the electrode, are rapid (*44*). Integration of the charge passed on either reduction or oxidation of the polymer leads to a value of $\Gamma \approx 10^{-9}$ mol/cm² of redox active centers on the surface. The symmetrical surface waves and fast kinetics seen in Figure 2 show that the presence of the enzyme does not appreciably affect the electrochemistry of the osmium polymer film. Later results will show that, conversely, the presence of the polymer does not appreciably affect the specificity or the activity of the enzyme.

Catalytic Oxidation of Glucose with Polymer/Enzyme Films. Upon addition of glucose (40 mM) to the solution, a catalytic oxidation wave is observed and the reduction peak is eliminated (Figure 3). Thus, glucose oxidase is reduced by the glucose penetrating the gel (eq 1), electrons are transferred from the reduced enzyme to the Os(III) sites (eq 3), and the electrons are then transferred through the osmium polymer film to the electrode surface. The absence of a reduction wave shows that, at this scan rate (5 mV/s), the film is homogeneously maintained in the reduced state by the transfer of electrons from GO–$FADH_2$ to the Os(III) complex (eq 3). This is also evidenced by the almost complete lack of hysteresis between the forward and the reverse scans. At faster scan rates (data not shown) a hysteresis appears and, eventually, a reduction wave is also observed. Thus, at fast scan rates, the film is no longer completely reduced by enzyme-mediated electron transfer from glucose in the time required for the scan. The appearance of the hysteresis and the reduction wave is a function of substrate concentration, scan rate, film composition and thickness, and ionic strength.

The temperature dependence of a film of polymer 2/GO/trien was investigated from 14 to 40 °C in a solution containing 0.1 M HEPES, catalase, and 30 mM glucose under a nitrogen atmosphere. Thirty millimolar glucose is many times the apparent Michaelis constant of the electrode (see below) and is close to the saturation level for substrate. The electrode was rotated at 500 rpm (the results were independent of rotation rate above ca. 300 rpm), and the potential was held at 0.35 V vs SCE. Over this range, the current exhibits a smooth exponential increase with temperature. An Arrhenius plot of this data (Figure 4) gives an activation energy for the rate-determining step in these films under such conditions of 11.1 kcal/mol.

Glucose Response and Apparent Michaelis Constant of the Enzyme Electrodes. The glucose response curves of films on rotating disk electrodes were measured at 2000 rpm (fast rotation rates were required to prevent concentration polarization at low glucose concentration) and 0.45 V vs SCE. Aliquots of a 1 M solution of glucose were injected into the cell (solution volume 100 mL) while the current was monitored. The current stabilized in ca. 10 s, i.e., in the time required to reach a uniform glucose concentration throughout the cell. Thus, an upper limit on the response time of these enzyme electrodes is 10 s.

The glucose response curves measured under N_2 are consistent with those expected for Michaelis–Menten kinetics. Castner and Wingard (*45*) have shown that enzymes immobilized on rotating disk electrodes, under conditions where the enzymatic reaction is rate controlling, follow the Eadie–Hofstee form of the Michaelis–Menten equation:

$$j_{ss} = j_{max} - K_m'(j_{ss}/C^*) \qquad (4)$$

where j_{ss} is the steady-state current density, j_{max} is the maximum current density under saturating substrate conditions

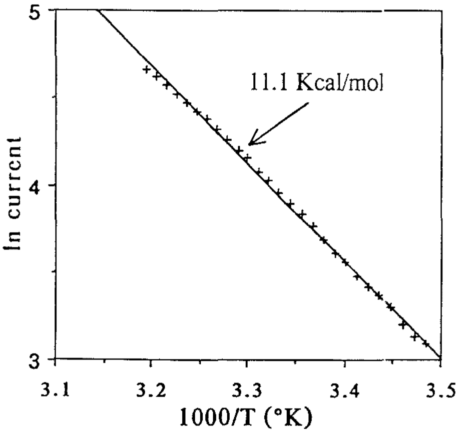

Figure 4. Arrhenius plot of the steady-state catalytic current of a polymer **2**/glucose oxidase/trien film on a gold disk electrode: 0.1 M HEPES at pH 7.1, 30 mM glucose, N_2 atmosphere, catalase added to solution. The electrode was rotated at 500 rpm and held at 0.35 V vs SCE.

(this is related to the V_{max} measured in homogeneous solution), K_m' is the apparent Michaelis constant (which can differ substantially from that measured in homogeneous solution and is not an intrinsic property of the enzyme, but of the system), and C^* is the concentration of glucose in solution. The glucose response data (Figure 5a) were plotted in an Eadie–Hofstee type plot (Figure 5b) giving a straight line with a slope equal to the negative of the apparent Michaelis constant (K_m' = 7.3 mM) and an intercept equal to $j_{max} \approx 565$ $\mu A/cm^2$. The K_m' measured for a number of films varied only slightly; j_{max}, however, varied from ca. 100 to 800 $\mu A/cm^2$ depending on film thickness, composition, and temperature. The apparent Michaelis constant, K_m', characterizes the enzyme electrode, not the enzyme itself. It is a measure of the substrate concentration range over which the electrode response is approximately linear. Castner and Wingard (*45*) obtained values of K_m' for glucose oxidase electrodes of 6, 14, and 36 mM for glucose oxidase immobilized with derivatized albumin, allylamine, and a silane, respectively.

Competition between Oxygen and the Redox Polymer. A comparison of glucose response curves measured under N_2 and under air is shown in Figure 6. There was no catalase present in either the film or the solution. The decrease in catalytic current density in air-saturated solutions can be explained by the competition between O_2 and the Os(III) complex for electrons from the reduced enzyme (eqs 2 and 3). Thus, the response of the present polymer/enzyme electrode is still dependent on the oxygen concentration, although this dependence is less than that for an electrode measuring either O_2 or H_2O_2. Improvements in the redox polymer would be expected to further decrease the oxygen sensitivity of these electrodes.

When O_2 is competing with the redox couple for the oxidation of the enzyme, it is important to quantify the relative rates of the two competing reactions (eqs 2 and 3). This was achieved by rotating ring disk voltammetry. The enzyme-containing polymer film was deposited only on the disk of a rotating ring disk electrode (RRDE). The disk electrode was either Au or glassy carbon, i.e., a material with a high overpotential for oxidation of H_2O_2, while the ring was Pt, a good catalyst for the oxidation of H_2O_2. The measurement was conducted by placing the electrode in a HEPES solution through which air was being continuously bubbled and that contained at first, no sugar. There was no catalase either in the film or in solution. The electrode was rotated at 1000 rpm while the ring was biased at 0.7 V vs SCE. After stabilization of the background current (ca. 10 min), the disk potential was stepped from 0.1 V (polymer in the Os(II) state) to 0.45 V

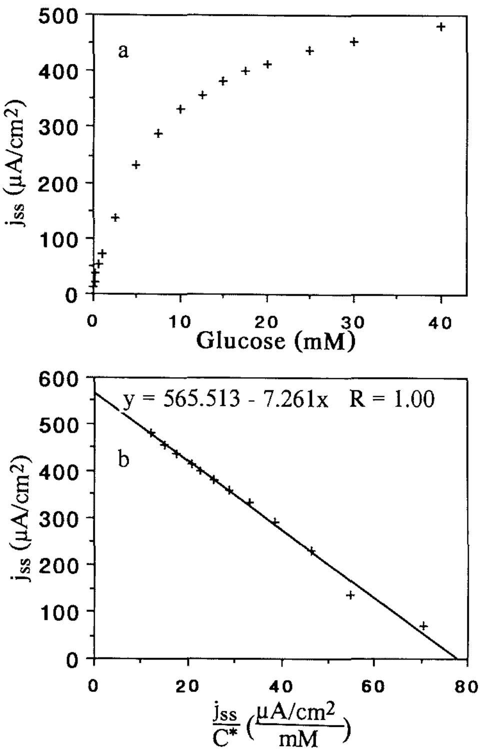

Figure 5. (a) Steady-state glucose response curve of the film shown in Figure 4 under N_2 at 37.5° C: ω = 2000 rpm, V = 0.45 V vs SCE. (b) Eadie–Hofstee type plot of the data in a. The best fit equation is shown.

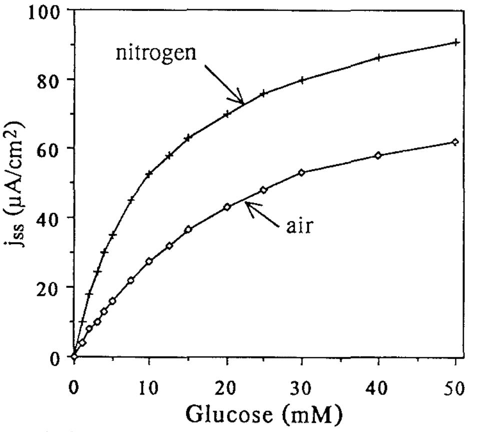

Figure 6. Steady-state glucose response curves under N_2 and under air of a film composed of polymer **1**/glucose oxidase/trien: no catalase in the film or in solution, T = 23 °C, ω = 2000 rpm, V = 0.45 V vs SCE.

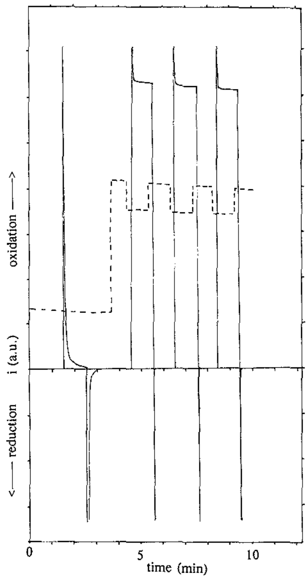

Figure 7. Rotating ring disk experiment with a polymer **2**/glucose oxidase/trien film on a glassy carbon disk surrounded by an uncoated platinum ring. The solid line is the disk current (disk potential was either 0.1 or 0.45 V), and the dashed line (offset by ca. 0.2 min) is the ring current (ring potential was 0.7 V). Conditions: air-saturated HEPES buffer (0.1 M) at pH 7.1; no catalase in the film or in solution. At $t \approx$ 1.5 min the disk potential was stepped from 0.1 to 0.45 V; at $t \approx$ 2.5 min it was stepped back to 0.1 V. At $t \approx$ 4 min glucose was injected to a concentration of 10 mM. At $t \approx$ 4.5 min the disk voltage was stepped from 0.1 to 0.45 V; at $t \approx$ 5.5 min it was stepped back to 0.1 V. The cycle was repeated twice more.

(polymer in the Os(III) state) and then back (Figure 7). The disk showed only charging current; i.e., no steady-state current was observed. Furthermore, the ring current, as expected, showed no change upon stepping the potential of the disk. Upon addition of 10 mM glucose (i.e., a value close to K_m', in the normal operational range of the electrode), the ring current increased because of the oxidation of H_2O_2 formed by the enzyme bound to the disk. The increase in ring current upon addition of glucose (while the polymer is in its inactive, Os(II), state) is a measure of the activity of the enzyme immobilized in the redox polymer. This mode of operation is similar to that of a peroxide-measuring glucose sensor. Stepping the disk potential from 0.1 to 0.45 V now resulted in a steady-state disk current and a substantial and reversible (upon stepping back to 0.1 V) decrease in the ring current. Thus, the increase in the polymer-mediated oxidation of glucose (disk current) resulted in the decrease of the oxygen-mediated oxidation of glucose (ring current). After subtraction of the background, this decrease in ring current upon oxidation of the polymer was measured to be ca. 20% of the total. Since the percentage of the total H_2O_2 that is collected at the ring is a function only of the geometry of the derivatized RRDE, the 20% decrease in ring current upon oxidation of the polymer corresponds to the percentage of the active enzyme that is directly oxidized by the polymer rather than by the competing O_2.

Selectivity and Stability of the Enzyme Electrode. The selectivity of these enzyme electrodes was briefly examined by holding the potential at 0.45 V while fructose, galactose, and ethylene glycol were added sequentially at concentrations of 10 mM. These substances, individually or collectively, had no measurable effect on the electrode current (i.e., less than 1 nA). Addition of 10 mM glucose led to a current of 9.3 μA. These results, and the high activity of the immobilized enzyme (as seen from the large j_{max}), suggest that the glucose oxidase covalently bound in these redox polymer films retains much of its native selectivity and activity.

Preliminary tests of these electrodes in solutions containing ascorbate (a common interferent) have shown that the current due to ascorbate oxidation is apparently inversely proportional to the surface coverage of the polymer film. Thus, the redox polymer is an advantageously poor electrocatalyst for the oxidation of ascorbate. When stored dry, without precautions, in the laboratory ambient, the electrodes showed no deterioration over the course of 3 weeks. Longer tests are in progress.

CONCLUSIONS

A simple and effective method for immobilizing redox enzymes on electrodes while simultaneously electrically connecting them to the electrode is described. The resulting cross-linked, enzyme-containing films are stable, selective, and highy active for the catalytic oxidation of glucose. Although the glucose-related current density from these electrodes is high, O_2 can still competitively oxidize a significant fraction of the enzymes. This technique for immobilization and electrical connection of redox enzymes appears to be promising for a number of enzyme electrode applications.

LITERATURE CITED

(1) Wise, D. L., Ed. *Applied Biosensors*; Butterworths: Boston, 1989.
(2) Mosbach, K., Ed. *Methods in Enzymology*; Academic Press: New York, 1987; Vol. 137.
(3) Luong, J. H. T.; Mulchandani, A.; Guilbault, G. G. *Trends Biochem.* **1988**, *6*, 310–316.
(4) Higgins, I. J. *Biotec* **1988**, *2*, 3–8.
(5) Bartlett, P. N.; Whitaker, R. G. *Biosensors* **1987/1988**, *3*, 359–379.
(6) Hill, H. A. O. *Pure Appl. Chem.* **1987**, *59*, 743–748.
(7) Degani, Y.; Heller, A. *J. Phys. Chem.* **1987**, *91*, 1285–1289.
(8) Degani, Y.; Heller, A. *J. Am. Chem. Soc.* **1988**, *110*, 2615–2620.
(9) Degani, Y.; Heller, A. In *Redox Chemistry and Interfacial Behavior of Biological Molecules*; Dryhurst, G., Niki, K., Eds.; Plenum Press: New York, 1987.
(10) Clark, L. C., Jr.; Lyons, C. *Ann. N.Y. Acad. Sci.* **1962**, *102*, 29–45.
(11) Clark, L. C., Jr.; Spokane, R. B.; Homan, M. M.; Sudan, R.; Miller, M. *Trans Am. Soc. Artif. Intern. Organs* **1988**, *34*, 259–265.
(12) Jönsson, G.; Gorton, L. *Anal. Lett.* **1987**, *20*, 839–855.
(13) Ianniello, R. M.; Yacynych, A. M. *Anal. Chem.* **1981**, *53*, 2090–2095.
(14) Masor, M. *Biotec* **1988**, *2*, 49–53.
(15) Updike, S. J.; Hicks, G. P. *Nature* **1967**, *214*, 986–988.
(16) Tse, F. H. S.; Gough, D. A. *Biotechnol. Bioeng.* **1987**, *29*, 705–713.
(17) Stankovich, M. T.; Schopfer, L. M.; Massey, V. *J. Biol. Chem.* **1978**, *253*, 4971.
(18) Green, M. J.; Hill, H. A. O. *J. Chem. Soc., Faraday Trans. 1* **1986**, *82*, 1237–1243.
(19) Cass, A. E. G.; Davis, G.; Green, M. J.; Hill, H. A. O. *J. Electroanal. Chem. Interfacial Electrochem.* **1985**, *190*, 117–127.
(20) Kulys, J. J.; Čėnas, N. K. *Biochim. Biophys. Acta* **1983**, *744*, 57–63.
(21) Crumbliss, A. L.; Hill, H. A. O.; Page, D. J. *J. Electroanal. Chem. Interfacial Electrochem.* **1986**, *206*, 327.
(22) Kulys, J. J.; Samalius, A. S.; Swirmickas, J. S. *FEBS Lett.* **1980**, *114*, 7.
(23) Čėnas, N. K.; Kulys, J. J. *Bioelectrochem. Bioenergy* **1981**, *8*, 103.
(24) Kulys J. J.; Čėnas, N. K. *Biochim. Biophys. Acta* **1983**, *744*, 57.
(25) Albery, W. J.; Bartlett, P. N.; Cass, A. E. G.; Craston, D. H.; Haggett, B. G. D. *J. Chem. Soc., Faraday Trans. 1* **1986**, *82*, 1033.
(26) Albery, W. J.; Bartlett, P. N. *J. Elctroanal. Chem. Interfacial Electrochem.* **1985**, *194*, 211.
(27) Albery, W. J.; Bartlett, P. N.; Craston, D. H. *J. Electroanal. Chem. Interfacial Electrochem.* **1985**, *194*, 223.
(28) Taniguchi, I.; Miyamoto, S.; Tomimura, S.; Hawkridge, F. M. *J. Electroanal. Chem. Interfacial Electrochem.* **1988**, *240*, 33.
(29) Degani, Y.; Heller, A. *J. Am. Chem. Soc.* **1989**, *111*, 2357–2358.
(30) Hazzard, J. T.; Moench, S. J.; Erman, J. E.; Satterlee, J. D.; Tollin, G. *Biochemistry* **1988**, *27*, 2002–2008.
(31) Anderson, G. W.; Zimmerman, J. E.; Callahan, F. M. *J. Am. Chem. Soc.* **1964**, *86*, 1839–1842.
(32) Pishko, M. V.; Katakis, I.; Lindquist, S.-E.; Ye, L.; Gregg, B. A.; Heller, A. *Angew. Chem.*, in press.
(33) Pollak, A.; Blumenfeld, H.; Wax, M.; Baughn, R. L.; Whitesides, G. M. *J. Am. Chem. Soc.* **1980**, *102*, 6324–6336.
(34) Mosbach, K., Ed. *Methods in Enzymology*; Academic Press: New York 1987; Vol. 135 and 136.
(35) Trevan, M. D. *Immobilized Enzymes*; Wiley and Sons: New York, 1980.
(36) Klibanov, A. M. *Anal. Biochem.* **1979**, *93*, 1–25.

(37) Martinek, K.; Klibanov, A. M.; Goldmacher, V. S.; Berezin, I. V. *Biochim. Biophys. Acta* **1977**, *485*, 1–12.
(38) Martinek, K.; Klibanov, A. M.; Goldmacher, V. S.; Tchernysheva, A. V.; Mozhaev, V. V.; Berezin, I. V.; Glotov, B. O. *Biochim. Biophys. Acta* **1977**, *485*, 13–28.
(39) Torchilin, V. P.; Maksimenko, A. V.; Smirnov, V. N.; Berezin, I. V.; Klibanov, A. M.; Martinek, K. *Biochim. Biophys. Acta* **1978**, *522*, 277–283.
(40) Schnaar, R. L.; Lee, Y. C. *Biochemistry* **1975**, *14*, 1535–1541.
(41) Foulds, N. C.; Lowe, C. R. *Anal. Chem.* **1988**, *60*, 2473–2478.
(42) Hale, P. D.; Inagaki, T.; Karan, H. I.; Okamoto, Y.; Skotheim, T. A. *J. Am. Chem. Soc.* **1989**, *111*, 3482–3484.
(43) Bowden, E. F.; Hawkridge, F. M.; Blount, H. N. In *Comprehensive Treatise of Electrochemistry*; Srinivasan, S., et al., Eds.; Plenum: New York, 1985; Vol. 10.
(44) Murray, R. W. *Electroanal. Chem.* **1984**, *13*, 191–368.
(45) Castner, J. F.; Wingard, L. B., Jr. *Biochemistry* **1984**, *23*, 2203–2210.

RECEIVED for review June 19, 1989. Accepted November 7, 1989. We gratefully acknowledge the financial support for this research from the Office of Naval Research, Contract No. N0014-88-K-0401, the Texas Advanced Research Program, and the Robert A. Welch Foundation.

Flow System for Starch Determination Based on Consecutive Enzyme Steps and Amperometric Detection at a Chemically Modified Electrode

J. Emnéus and L. Gorton*

Department of Analytical Chemistry, University of Lund, P.O. Box 124, S-221 00 Lund, Sweden

A flow injection system is described for the determination of the total glucose content of starch. The starch is sequentially hydrolyzed on-line in two immobilized enzyme reactors for complete degradation to glucose. The first reactor contains a thermostable α-amylase, Termamyl, and is operated at 60 °C. The second reactor contains amyloglucosidase and is operated at room temperature. The detection is based on the electrochemical oxidation of the hydrogen peroxide formed after the complete oxidation of the produced glucose in a third reactor containing coimmobilized mutarotase and glucose oxidase. Rectilinear calibration curves for starch (expressed as glucose) were obtained between 10 μM and 0.6 mM, using an injection volume of 160 μL. The sample throughput was 15 h^{-1}.

INTRODUCTION

The determination of the glucose content of starch is a tedious process when performed in the traditional batchwise mode. The various steps are time-consuming, involving the addition of hydrolyzing chemicals (including soluble enzymes), pH regulation, and incubation, followed by the actual glucose analysis. Several attempts have been made to decrease the time necessary for this analysis. Various starch hydrolyzing enzymes, mainly amyloglucosidase but also α-amylase, have been immobilized in reactors and used in flow injection systems, FIA (*1–4*). In the systems, using only immobilized amyloglucosidase, a range of 90% to complete hydrolysis of soluble starch to glucose has been reported.

In the present paper, an extention of previously published systems aimed at a FIA system for on-line, complete hydrolysis and analysis of native starch is reported. A thermostable α-amylase, Termamyl, is contained in one reactor, operated at 60 °C, in which the starch is partially hydrolyzed to α-limit dextrin and oligosaccharide fractions. These are in turn totally hydrolyzed to glucose in a second reactor containing immobilized amyloglucosidase, operating at room temperature. The glucose is then oxidized in a third reactor with coimmobilized glucose oxidase and mutarotase. The hydrogen peroxide formed is electrocatalytically oxidized at a Pd/Au-modified graphite electrode (*5*, *6*).

EXPERIMENTAL SECTION

Enzymes and Enzyme Reactors. One milliliter of a suspension of a thermostable α-amylase, EC 3.2.1.1, from *Bacillus licheniformis*, Termamyl 120L, Novo Industri A/S, Bagsvaerd, Denmark (*7*), was added to 1 mL of a 0.1 M citrate buffer at pH 6.7. This solution was transferred to dialysis tubing and dialyzed for 48 h against the same buffer to remove the dark brown compounds present. The activity of the Termamyl suspension is expressed as 120 KNU g^{-1} of solution; 1 KNU (kilo Novo unit) is expressed as the amount of enzyme which breaks down 5.26 g of starch (Merck, Amylum Solubile Erg. B. 6, Batch 9947275) per hour (*7*). The density of the suspension was found to be 1.22 g mL^{-1}, which means that 1 mL should contain 146.4 KNUs. After 48 h the volume in the dialysis tubing containing the enzyme had increased to 4 mL and the dark brown color had virtually disappeared. This solution was immobilized on 330 mg of glutaraldehyde-activated, aminopropyl silanized, controlled pore glass, CPG, Serva catalog no. 44811, particle size 75–125 μm, pore size 2869 Å, according to a previously published procedure (*8*, *9*). The reaction was allowed to continue for 12 h at reduced pressure and at 4 °C. The immobilization efficiency was 80% expressed as the ratio between the absorbance at 280 nm of the clear enzyme solution after and before immobilization. The enzyme glass was packed into a reactor with a 2.7 mm i.d. and a total length of 8.7 cm. Throughout the experiments a volume of 500 μL was used. When not in use the reactor was filled with 0.1 M acetate buffer at pH 5.0 and kept at 4 °C.

A 375-mg portion of amyloglucosidase, AMG, EC 3.2.1.3, from *Aspergillus niger*, 100 U mg^{-1}, Merck catalog no. 1332, was dissolved in 2.0 mL of 0.1 M acetate buffer at pH 5.0, transferred to dialysis tubing, and dialyzed against the same buffer overnight. After dialysis the pH of the solution containing the enzyme, 3.9 mL, was changed to 7.0 and was immobilized on 500 mg of glutaraldehyde-activated, aminopropyl silanized CPG, Serva catalog no. 44770, particle size 125–180 μm, pore size 729 Å, as above. The immobilization efficiency, expressed as above, was 99%. The enzyme glass was packed into a reactor with 2.7 mm i.d. and a total length of 13 cm. Throughout the experiments a fixed volume of 740 μL was chosen. When not in use it was stored at 4 °C filled with 0.1 M acetate buffer at pH 5.0.

A 9.5-mg portion of glucose oxidase, GOx, EC 1.1.3.4, from *Aspergillus niger*, SERVA catalog no. 22738, 270 U mg^{-1}, and 200

© 1990 American Chemical Society

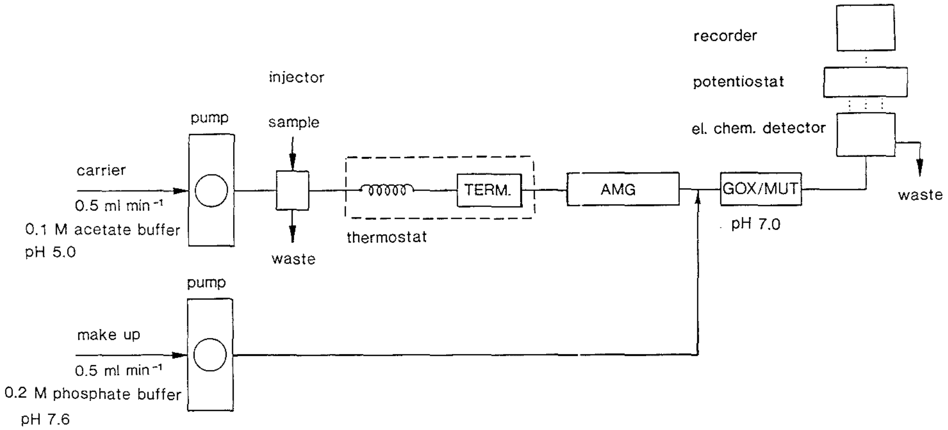

Figure 1. FIA system for starch analysis.

μL of a solution of mutarotase, MUT, EC 5.1.3.3, from porcine kidney dissolved in 3.2 M ammonium sulfate, Sigma catalog no. M-4007, were added to 1.4 mL of a 0.1 M phosphate buffer at pH 7.0. This solution was dialyzed overnight against a large surplus of the same phosphate buffer in order to remove the ammonium ions that would otherwise interfere in the immobilization process. The purified enzyme solution, 3.0 mL, was added for coupling with 150 mg of CPG 10, Serva catalog no. 44752, particle size 37–74 μm, pore size 379 Å, that had previously been aminopropyl silanized and glutaraldehyde activated as above. The immobilization efficiency was essentially total (<1% remained) measured as above. The GOx/MUT-glass was filled into a reactor, 2.7 mm i.d., 4 cm length, and 235 μL volume. When not in use it was filled with a 0.15 M phosphate buffer at pH 7.0 and stored at 4 °C.

The various parts of the FIA system are depicted in Figure 1. A LC pump, Model 2150, LKB Bromma, Sweden, delivered a 0.1 M acetate buffer at pH 5.0, at a constant flow rate of 0.5 mL min^{-1}. Before startup, this solution was degassed for 5 min under reduced pressure to prevent the appearance of microbubbles in the flow system. Samples were injected into this stream with a pneumatically operated injection valve, Cheminert type SVA, Kemila, Stockholm, Sweden. A flow-through thermostat, Model 5101, Tecator, Höganäs, Sweden, was inserted between the injector and the reactor containing immobilized Termamyl. This reactor was thermally insulated to maintain the temperature set by the thermostat. A peristaltic pump, Gilson minipuls 2G, delivered an additional flow of 0.20 M phosphate buffer at pH 7.6, at a constant flow rate of 0.5 mL min^{-1} to raise the pH of the sample stream from pH 5.0 to 7.0 before passing through the GOx/MUT reactor. This solution was saturated with oxygen at 40 °C and then cooled to room temperature in order to increase the oxygen concentration necessary for reaction (*3*), see below, but not saturate the carrier with gas. The oxygen content was 0.7 mM in this solution. Beyond the mixing point and in the GOx/MUT reactor the oxygen level will then be at least 0.35 mM. Teflon tubing, 0.5 mm i.d., with Altex screw couplings connected the various parts of the flow system. All buffers were prepared from ultrapure water and p.a. chemicals. Kathon CG, 50 μL L^{-1}, containing 1.125% methylchloroisothiazolinone and 0.375% methylisothiazolinone, was also added as a preservative to all solutions to prevent growth in the flow system.

The three-electrode flow-through cell was of the confined wall jet type and has been described earlier (*10*). The hydrogen peroxide formed in the GOx/MUT reactor was detected at a graphite electrode on the 0.0731 cm^2 flat surface of which, a catalytic layer, 400 Å, of sputtered Pd/Au (40:60, w/w) was deposited (*6*). The applied potential was in all experiments +600 mV vs the Ag/AgCl (0.1 M KCl) reference electrode used in the cell. It was previously found that by covering graphite electrodes with a layer of vacuum sputtered Pd/Au, the overvoltage of the electrochemical oxidation of hydrogen peroxide is decreased and a mass transport controlled current is obtained at potentials more positive than about +400 mV at pH 7.0 (*5, 6*). This means that higher currents are obtained and that the response will not vary with time, which might be the result when using a solid Pt-disk electrode operated at the same potential.

A personal computer, ABC 815, Luxor, Sweden, an A/D converter, and a TTL-I/O card were used with a homemade computer program, written in BASIC II, for controlling the sampling and the injection in the FIA system. The computer program was also used for evaluation of the peak time, the peak height, and the integrated peak areas by coupling the computer to the outlet of the potentiostat. The data acquisition sampling frequency was set by the need for evaluation of the peak time, height, and area.

A gel permeation chromatography column, GPC, Ultropac, TSK G4000PW, LKB Bromma, Sweden, was used for the separation of fractions according to their molecular weights of the investigated starches and also for investigating the effect of passing through the Termamyl and AMG reactors on the starch. In these experiments a LC injector, Model 724065, Valco, Switzerland, with a 100-μL loop and a refractive index, RI, detector, Model 2142, LKB Bromma, Sweden, were used.

Solutions of D-glucose, BDH catalog no. 10117, α-D-glucose, Sigma catalog no. G-5000, maltose, Sigma catalog no. M-5885, Lintner starch, Sigma catalog no. S-2630, and Zulkowsky starch, Merck catalog no. 1257, were prepared daily by dissolving appropriate amounts in 0.1 M acetate buffer, pH 5.0. To dissolve the Lintner starch, the solution had to be heated to 90 °C for 1 min. The starch preparations were allowed to dry over phosphorus pentaoxide in a desiccator, since the water content of these were found to vary with the temperature and humidity in the laboratory. The water content of the starches after drying was determined by Karl Fischer titrations and found to be 8% for the Lintner and 4% for the Zulkowsky starch. The weight loss after 12 h at 110 °C and the ash content after 2 h at 600 °C were 4% and 5%, respectively, for the Lintner and 4% and 12% for the Zulkowsky starch. The maximum starch content of the Lintner and Zulkowsky preparations was then taken as the weight of the commercial powder minus the water and the ash contents. The starch concentrations given below are, however, expressed as if consisting of glucose only, where every glucose unit is given the mean molecular weight of 162.14 g mol^{-1}. Maximum conversion to glucose should therefore be 87% of Lintner and 84% of Zulkowsky starch, respectively.

The amperometric response was checked by measuring solutions of hydrogen peroxide, appropriately diluted from a stock solution, Perhydrol, Merck catalog no 7209, and standardized by titrations against permanganate.

Detection Principle. The immobilized thermostable α-amylase, Termamyl, attacks randomly the α-1,4 linkages within the starch molecule yielding smaller polymer and oligomer fractions. The anomeric configuration is preserved when the α-1,4 linkages are hydrolyzed. If the reaction is allowed to proceed to completion, the following reaction is valid (*11*):

$$\text{starch} \xrightarrow{\alpha\text{-amylase}} \alpha\text{-limit dextrins} + \text{maltose} \; (+ \text{maltotriose}) \qquad (1)$$

The pH optimum for the reaction of soluble Termamyl varies with temperature and is between 5 and 7 at 37 °C and 6.8 at 95 °C (*7, 12*). No values were available for immobilized Termamyl.

The products formed in the Termamyl reactor are further hydrolyzed to glucose in a second reactor by the action of immobilized AMG. It attacks only the terminal, nonreducing ends of the starch molecule and its degradation products, splitting off one glucose unit at a time. Inversion of the anomeric configuration of the glycolytic bond takes place, so that the glucose unit split off appears in its β-form. AMG attacks the α-1,4 linkages of glucose polymers, of oligomers, and of maltose (dimer). AMG can also attack α-1,6 linkages of glucose polymers if the next linkage in the chain is of the α-1,4 type. The turnover rate is faster for larger fragments than for oligo- and dimers and also for α-1,4 bonds compared to α-1,6 bonds (*11*). The pH optimum for immobilized AMG is between 4 and 4.5 (*13*) as compared with soluble AMG which has an opimum at 4.5 (*13*)

$$\begin{array}{l} \text{starch} \\ \alpha\text{-limit dextrins} \\ \text{maltodextrins} \\ \text{maltooligosaccharides} \end{array} + nH_2O \xrightarrow{\text{AMG}} \begin{array}{l} (n-x)\beta\text{-D-glucose} + \\ x\alpha\text{-D-glucose} \end{array} \qquad (2)$$

The glucose formed in reaction 2 is then oxidized in the presence of molecular oxygen to gluconate and hydrogen peroxide by immobilized GOx contained in a third reactor

$$\beta\text{-D-glucose} + O_2 + H_2O \xrightarrow{\text{GOx}} \text{D-gluconate} + H^+ + H_2O_2 \qquad (3)$$

The main reaction product formed by the action of AMG is β-D-glucose. However, some α-D-glucose is expected to be formed. If the terminal reducing end of the chain is in the α-anomeric configuration, this glucose unit will appear as α-D-glucose. Spontaneous mutarotation of β-D-glucose to α-D-glucose will also take place during the passage of the sample from the second reactor to the third reactor. To make this portion of the glucose oxidizable, GOx was coimmobilized with MUT, catalyzing the following reaction:

$$\alpha\text{-D-glucose} \overset{\text{MUT}}{\leftrightarrow} \beta\text{-D-glucose} \qquad (4)$$

Coimmobilized GOx and MUT on CPG with glutaraldehyde have been successfully used at pH 7 (*14*). The hydrogen peroxide formed in the GOx/MUT reactor is transported to the Pd/Au-modified graphite electrode and is there electrocatalytically oxidized (*5*). The net reaction is

$$H_2O_2 \rightarrow O_2 + 2H^+ + 2e^- \qquad (5)$$

The applied electrode potential, +600 mV, is well within the range to guarantee that the current is controlled by the mass transport of hydrogen peroxide (*5, 6*).

RESULTS AND DISCUSSION

Performance of the GOx/MUT Reactor. The conversion efficiency of the GOx/MUT reactor was checked by injecting 160-μL samples containing equal concentrations of either H_2O_2, D-glucose, or freshly prepared α-D-glucose, into the FIA system depicted in Figure 1 (omitting the Termamyl and AMG reactors and the thermostat). The sample volume, 160 μL, is sufficiently small for the whole sample plug to be diluted by the carrier, so that the detector will register the sample as a peak. The amperometric responses, both the peak heights and the integrated areas under the peaks, to H_2O_2, D-glucose, and α-D-glucose were exactly the same up to a glucose concentration of 0.5 mM, where the concentration of dissolved oxygen in the carrier solution starts to limit reaction 3. The response (peak area) to H_2O_2 was also found to be equal when omitting the GOx/MUT reactor from the system. This indicates that H_2O_2 undergoes no reaction in the GOx/MUT reactor. These results reveal that the conversion efficiency of the glucose to form H_2O_2 is 100% and that the two coimmobilized enzymes are fully active so that reactions 3 and 4 can proceed.

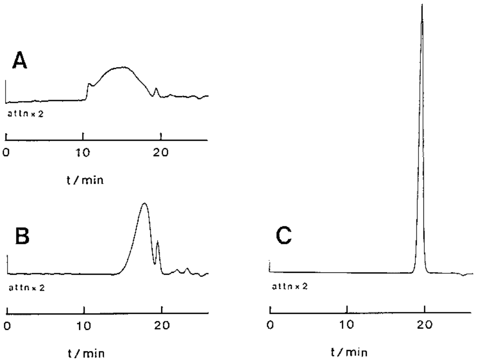

Figure 2. Gel permeation chromatograms of 2.5 mM (A) Lintner starch, (B) Zulkowsky starch, and (C) glucose.

Performance of the AMG Reactor. In a previous report (*1*) it was found that about 90% of a Lintner starch sample, corrected for its water content, could be detected as glucose after passage through an AMG reactor equivalent to the one used in this report. The glucose detection system used was based on a reactor with immobilized glucose dehydrogenase, which, like GOx, acts only on β-D-glucose.

In this report, the GOx is coimmobilized with MUT in order to be able also to detect glucose in the α-anomeric configuration. As a result, a somewhat higher conversion efficiency was obtained for Lintner and Zulkowsky starch. However, 100% is not reached. Even when three AMG reactors were used in series, only a very minute increase in the conversion efficiency could be detected. Maltose on the other hand is totally converted to glucose in a single AMG reactor. This reveals a very high activity of the immobilized AMG since the turn-over rate for the hydrolysis of maltose is up to 10 times lower than for larger oligo- and polyglucans (*11*).

If soluble AMG is added to the starch samples and hydrolysis is allowed to proceed for at least 4 h before injection into the FIA system, 100% of the glucose could be detected. This clearly indicates that AMG can completely hydrolyze these starches to glucose. The reason why 100% hydrolysis is not obtained for starch when passing through the AMG reactor(s) has not been fully elucidated.

When a starch sample passes through a GPC column the various molecular weight fractions of the starch will be separated. Figure 2 shows the chromatograms of the two starches investigated as well as that of glucose. As is clearly evident, both starches contain fractions of high, as well as some intermediate and low molecular weights. Maltose and smaller malto-oligosaccharides will have the same retention times as glucose on this column. An RI detector was used in this instance. The advantage of using this detector is that it is unspecific and will hence also detected components in the sample that are of noncarbohydrate origin. The drawback is that the rectilinear response range for starch, when the enzymatic electrochemical detection system is used, lies an order of magnitude lower than the lowest concentration of starch to be investigated in the RI detector. It is obvious from Figure 2 that the Zulkowsky starch contains components with retention times longer than that of glucose. It is expected that these peaks reveal noncarbohydrate components correlated to the rather high ash content of this starch; see above.

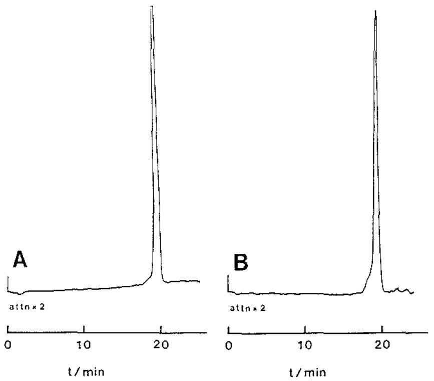

Figure 3. Gel permeation chromatograms of 2.5 mM (A) Lintner starch and (B) Zulkowsky starch hydrolyzed in the AMG reactor.

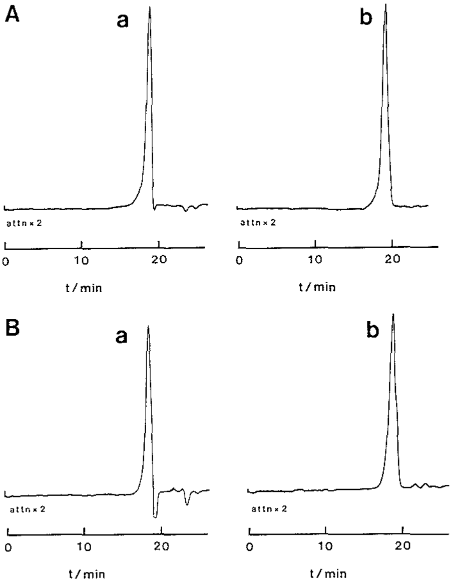

Figure 4. Gel permeation chromatograms of 2.5 mM (A) Lintner starch and (B) Zulkowsky starch hydrolyzed at (a) 20 °C and (b) 60 °C in the Termamyl reactor.

Solutions containing starch were allowed to pass the AMG reactor continuously at a flow rate of 0.5 mL min^{-1}. Samples of the effluent were chromatographed, as above, and analyzed for the molecular weight distribution. Figure 3 shows the resulting chromatograms of the two starches. Compared to the chromatograms in Figure 2, there is a marked difference. The high molecular weight fractions are completely removed and only low molecular weight fractions remain. However, there is a small peak preceding the large one for both starches, revealing that some oligomers still remain unhydrolyzed.

The combination of two hydrolyzing enzymes in native starch analysis is a well-established procedure (*15*). Often soluble Termamyl is added to the starch sample and allowed to react at an elevated temperature. This procedure splits the starch molecule into smaller fragments, thereby making it water soluble according to reaction 1. The procedure also leads to a greatly increased number of nonreducing ends on

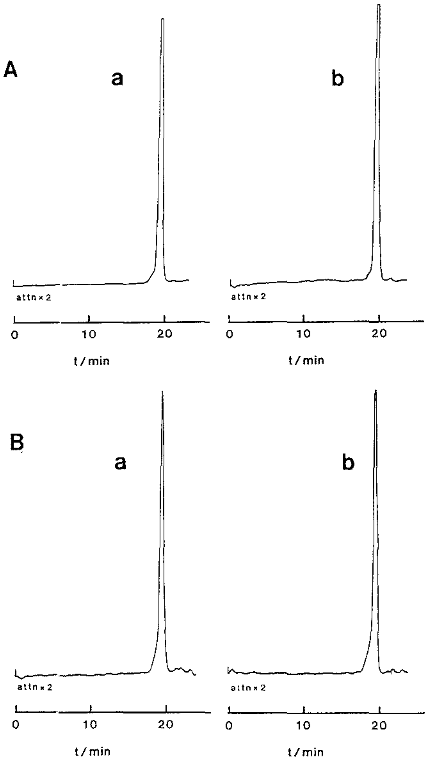

Figure 5. Gel permeation chromatograms of 2.5 mM (A) Lintner starch and (B) Zulkowsky starch hydrolyzed both in the Termamyl reactor ((a) at 20 °C and (b) at 60 °C) and in the AMG reactor.

which AMG can act to totally hydrolyze the remaining fragments to glucose.

In a previous report (*2*) a nonthermostable α-amylase and AMG were coimmobilized on the same CPG support. The combination effect of these two enzymes was advantageous for the hydrolysis of an amylopectin that was only partially hydrolyzed by immobilized AMG alone. As we have the prospect of studying native starch in the near future, Termamyl was chosen in this study, mainly for its reported stability at the elevated temperatures necessary for the rapid gelatinization and solubilization of native starch granules (*11, 15*).

To trace the hydrolytic effect of the α-amylase, starch solutions were passed through the Termamyl reactor at various temperatures. Samples of the effluent were then chromatographed on the GPC column and analyzed. Figure 4 depicts the molecular weight distribution of the two starches after passing through this reactor at 20 and 60 °C. The figure shows that the immobilized α-amylase is active and that the starches are split into smaller fractions. The figure also shows that an increase in temperature results in a more efficient hydrolysis. Experiments at temperatures higher than 60 °C revealed a successive inactivation of the immobilized Termamyl. No such effects were detected with a reactor reloaded with new enzyme glass after continuous operation for 2 weeks at 60 °C. The reloaded reactor was therefore not run at temperatures over 60 °C.

Figure 5 illustrates chromatograms of both starches after passing through the Termamyl reactor (at 60 °C) in series with

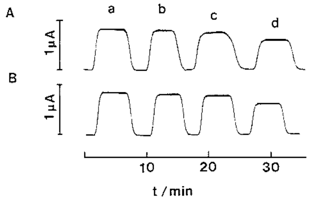

Figure 6. Steady-state FIA response "peaks" (A) of 0.5 mM (a) glucose, (b) maltose, (c) Linter starch, and (d) Zulkowsky starch, and (B) of the same solutions to which soluble AMG was added.

the AMG reactor (at room temperature). A comparison of these chromatograms with those in Figure 3 reveals that the small prepeak has virtually disappeared. It must be pointed out here that the starch concentration in these experiments is at least 5 times higher than the maximum concentration that the FIA system is designed to measure. The oxygen content in the carrier sets the upper limit for the rectilinear response to glucose of the enzymatic-electrochemical detection system; see above.

The performance of the whole FIA system, as depicted in Figure 1, was investigated with two injection volumes. Glucose and starch samples will disperse differently in the FIA system, due to the large difference in their molecular weights and hence in their diffusion coefficients (*16*). The molecular weight distribution of the starch will also add an extra effect to the dispersion of these samples. If an injection loop sufficiently large is used, the center part of the sample plug will not be subjected to dilution. An undiluted portion (steady state) will therefore pass through the detector and the maximum response should be a direct measure of the degree of hydrolyzation of the starch. It was shown that at least a 2.5-mL injection loop was necessary to obtain steady state and an injection loop of 3.3 mL was used in the comparison of the responses to the various substrates. Since the sample throughput with this injection volume was only 5 h^{-1}, for "real" FIA measurements a much smaller injection volume, 160 μL, was chosen. This injection volume will result in a large dilution of the sample plug, as the sample has to pass five sections in the FIA system that will greatly contribute to the dispersion. As the dispersion factor will vary with the substrates, peak height measurements can thus not be used for the evaluation of the conversion efficiency of starch to glucose and also not for the evaluation of the glucose content of starch, even if 100% of the starch has been converted to glucose. At a constant flow rate through the FIA system the response factor of the amperometric detection unit will be constant. Hence, the integrated area of the FIA peaks should be used to compare and evaluate the success of complete hydrolysis of starch and also for calibration.

Figure 6A shows steady-state FIA responses of samples containing glucose, maltose, Lintner starch, or Zulkowsky starch. For comparison Figure 6B shows the responses for the same solutions but with addition of a small amount of dialyzed soluble AMG that had been allowed to act in the sample solutions for 5 h. As can be seen the maximum responses are equal in the two cases, indicating that 100% of the starches can be hydrolyzed to glucose when passing the Termamyl and the AMG reactors. There is one difference, however, namely that the rising and falling slopes of the steady-state FIA "peaks" are somewhat less steep in the absence of added AMG. This indicates a more profound dispersion effect on the boundaries of the sample plugs for untreated starch than for those where the added soluble AMG had hydrolyzed the starch to smaller fragments. Equal responses of these solutions were obtained after 24 h. This indicates that maximum hydrolyzation was obtained already 5 h after the addition of the soluble AMG and also that total hydrolyzation can be obtained after passage through the FIA system without the addition of any soluble enzyme.

Strictly linear calibration curves were obtained for the various substrates when the 160-μL injection loop was used. The lower (twice the S/N ratio) and the upper detection limits for glucose and maltose were 5 μM and 0.5 mM, respectively. Due to the larger dispersion factor for starch, the lower and upper limits of their linear calibration curves are somewhat higher, 10 μM and 0.6 mM, respectively. The ratios of the slopes of the calibration curves (peak area vs concentration) compared with that of glucose were found to be 0.98 (1.00) for maltose, 0.87 (0.87) for Lintner starch, and 0.82 (0.84) for Zulkowsky starch. The values given within the parentheses are the expected values, if 100% of the maximum glucose content in the samples is detected. This means that the responses to all substrates were close to identical, if the samples are corrected for their water and ash contents. The sample throughput was set by the broader FIA peaks for starch and was around 15 h^{-1} with no carryover. The reproducibility of the system was good, with a relative standard deviation for all substrates of less than 0.5% ($n = 20$).

CONCLUSIONS

The investigation of the long-term performance of the AMG and GOx/MUT reactors revealed long lasting stabilities. A slight decrease in the activities of these reactors could be detected only after about 10 months. The Termamyl reactor was stable if run at temperatures not higher than 60 °C in the time range of at least 2 weeks.

A more efficient hydrolysis of starch was obtained when the temperature in the Termamyl reactor was increased from 20 to 60 °C. This indicates that the equilibrium of reaction 1 is not obtained in this reactor. It was therefore concluded that the 500-μL volume of this reactor could not be decreased. All previous papers on starch analysis with immobilized AMG reactors report on large volumes (*1–4*). Equilibrium of reaction 2 for starch is not obtained when the AMG reactor was used alone. It was therefore also concluded that the 740-μL volume of the AMG reactor could not be decreased. However, the combined effects of the two reactors seem to be advantageous for the total hydrolyzation of starch to glucose. The performance of the system with more complex starches than the partially hydrolyzed Lintner and Zulkowsky preparations will be presented in a forthcoming paper.

The enzyme–electrochemical detection system should also be used as a selective detector in combination with the GPC column for the qualitative and quantitative analysis of the various molecular weight fractions of starch (*17*). Today the RI detector is most commonly used but it does not serve this purpose well as it is unselective and the response factors are expected to vary with the molecular weights of the various fragments of starch. A reliable detection system based on the total degradation of the polymers to glucose should give a true picture of the glucose content in each fraction, and a quantification can be realized that is hard to obtain with the RI detector (*17*).

There is, however, a need for an optimization of the hydrolyzing reactors. The large volumes of these, 500 and 740 μL, will act as large dispersing elements of a LC detection system and will add greatly to the band broadening. The pH optimum of soluble Termamyl varies with temperature (*7*). Since we did not want to complicate the FIA system with an extra line, no investigation of the pH effects on the Termamyl reactor was performed. Only one immobilization reagent, glutaraldehyde, was used here and by choosing another (*4*, *18*) a more active reactor will perhaps be obtained.

The pore sizes of the CPG, 2868 Å in the Termamyl reactor and 729 Å in the AMG reactor, were chosen large so that the high molecular weight starch and its hydrolyzed fractions should be able to reach the majority of the immobilized enzymes situated within the CPG structure. The necessity for this is not fully understood. An optimization of these reactors is therefore necessary before their introduction as postcolumn reactors. A series of CPG materials of different pore sizes, 729, 1489, 2139, and 2869 Å, was investigated for the effect and performance of immobilized AMG on the hydrolysis of starch. The various conversion efficiencies obtained for Lintner and Zulkowsky starch on the carriers with larger pore sizes revealed only marginally higher conversion efficiencies.

ACKNOWLEDGMENT

The authors wish to thank Tecator for the loan of the thermostat and the donation of the Termamyl suspension and Allan Sjöstrand, Helsingborg, Sweden, for the gift of the Kathon CG solution.

Registry No. Glucose, 50-99-7; starch, 9005-25-8; α-amylase, 9000-90-2; Termamyl, 9000-85-5; amyloglucosidase, 9032-08-0; mutarotase, 9031-76-9; glucose oxidase, 9001-37-0.

LITERATURE CITED

(1) Emnéus, J.; Appelqvist, R.; Marko-Varga, G.; Gorton, L.; Johansson, G. *Anal. Chim. Acta* **1986**, *180*, 3–8.
(2) Appelqvist, R.; Marko-Varga, G.; Gorton, L.; Johansson, G. *Proceedings of the 2nd International Meeting on Chemical Sensors*; Aucouturier, J.-L., Cauhapé, J.-S., Destriau, M., Hagenmuller, P., Lucat, C., Ménil, F., Portier, J., Salardenne, J., Eds.; Imprimerie Biscaye: Bordeaux, 1986; pp 603–606.
(3) Gorton, L.; Appelqvist, R.; Johansson, G.; Scheller, F.; Kirstein, D. *J. Chem. Technol. Biotechnol.* **1989**, *46*, 327–333.
(4) Larew, L. A.; Mead, D. A., Jr.; Johnson, D. C. *Anal. Chim. Acta* **1988**, *204*, 43–51.
(5) Gorton, L. *Anal. Chim. Acta* **1985**, *178*, 247–253.
(6) Gorton, L.; Svensson, T. *J. Mol. Catal.* **1986**, *38*, 49–60.
(7) Novo Enzyme Information; IB-number B 204f-GB 3000 April 1985, Novo Industri A/S: Bagsvaerd, Denmark, 1977.
(8) Weetal, H. H.; Messing, R. A. In *The Chemistry of Biosurfaces*; Hair, M. L., Ed.; Marcel Dekker: New York, 1972; Vol. 2, Chapter 12.
(9) Johansson, G.; Ögren, L.; Olsson, B. *Anal. Chim. Acta* **1983**, *145*, 71–85.
(10) Appelqvist, R.; Marko-Varga, G.; Gorton, L.; Torstensson, A.; Johansson, G. *Anal. Chim. Acta* **1985**, *169*, 237–247.
(11) Matheson, N. K.; McCleary, B. V. In *The Polysaccharides*; Aspinall, G. O., Ed.; Academic Press: Orlando, FL, 1985; Chapter 1.
(12) Madsen, G. B.; Norman, B. E.; Slott, S. *Starch* **1973**, *25*, 304–308.
(13) Cabral, J. M. S.; Kennedy, J. F.; Novais, J. M. *Enzyme Microb. Technol.* **1982**, *4*, 343–348.
(14) Olsson, B.; Stålbom, B.; Johansson, G. *Anal. Chim. Acta* **1986**, *179*, 203–208.
(15) Holm, J.; Björk, I.; Drews, A.; Asp, N.-G. *Starch* **1986**, *38*, 224–226.
(16) Ruzicka, J.; Hansen, E. H. In *Flow Injection Analysis*, 2nd ed.; Elving, P. J., Ed.; Wiley: New York, 1988; p 100.
(17) Appelqvist, R.; Emnéus, J.; Gorton, L.; Marko-Varga, G.; Johansson, G.; poster presentation at the ANABIOTEC' 88, 2nd International Symposium on Analytical Methods in Biotechnology, Noordwijkerhout, The Netherlands, 29–31 March, 1988.
(18) Crowley, S. C.; Chan, K. C.; Walters, R. R. *J. Chromatogr.* **1986**, *359*, 359–368.

RECEIVED for review April 19, 1989. Accepted October 23, 1989. Financial support from the Swedish Board for Technical Development, STU, from the National Energy Administration, STEV, from "Kungl. och Hvitfeldtska Stipendieinrättningen", and from "Stiftelsen Lars Hiertas Minne" are all gratefully acknowledged.

Simulation of Two-Electron Homogeneous Electrocatalysis for Steady-State Voltammetry at Hemispherical Microelectrodes

Chang Ling Miaw, James F. Rusling,* and Azita Owlia[1]

Department of Chemistry (U-60), University of Connecticut, Storrs, Connecticut 06269-3060

Expanded space grid digital simulation of second-order, two-electron homogeneous electrocatalysis was extended to slow scan voltammetry at hemispherical microelectrodes. Predictions of the simulations are examined for reversible and quasireversible heterogeneous charge transfer of catalyst for a range of homogeneous catalytic rate constants (k_1) and electrode radii. Working curves of catalytic efficiency vs log k_1 were generated assuming reacting species with equal diffusion coefficients. As electrode radii in the $<$10-μm range decrease, progressively larger homogeneous catalytic rates are needed to yield analytically significant amplification of limiting currents. Simulations using hemispherical radii of $(2/\pi)r_d$ can be used to predict catalytic efficiencies for microdisk electrodes with radii r_d. Simulated working curves were used to estimate a log k_1 of 3.88 $\pm$ 0.55 (M^{-1} s^{-1}) for electron transfer from the anion radical of 9,10-diphenylanthracene to 4,4′-dibromobiphenyl from steady-state catalytic efficiencies obtained at carbon microdisk electrodes. This value was in good agreement with 3.90 $\pm$ 0.16 M^{-1} s^{-1} found previously by cyclic voltammetry.

Development of voltammetric microelectrodes with at least one characteristic dimension smaller than 10 μm has greatly extended the scope of electroanalytical studies. Some important analytical advantages of microelectrodes are improved signal to noise ratio (S/N) and greatly decreased ohmic drop of the electrochemical cell compared to larger electrodes (*1*, *2*). Simple, inexpensive two-electrode systems using a voltage ramp generator to apply the input potential and a sensitive amplifier to measure current can be used to obtain steady-state current–potential curves at disk and hemispherical microelectrodes at low scan rates (*3*, *4*). Such simple instrumentation facilitates microsensor applications in which the limiting current of the sigmoid-shaped steady-state voltammogram is proportional to analyte concentration.

Amplification of steady-state current at microelectrodes can be achieved by mediating electron transfer from electrode to analyte by a soluble catalyst. Such homogeneous electrocatalysis lowers overpotentials for reduction of difficult to reduce substrates. This type of chemical amplification of current has been used for many years at conventional-sized electrodes as the basis for sensitive analytical methods (*5*, *6*).

One consequence of the very small size of microelectrodes is that homogeneous catalytic reactions coupled to charge transfer at the electrode must be rather fast to enhance the current compared to those occurring at conventional electrodes of millimeter dimensions (*7*). Previously, approximate electrocatalytic theory was reported for chronoamperometry at microdisk (*7*) and microcylinder electrodes (*8*). Theory was also presented for the steady-state limiting current for pseudo-first-order one-electron catalytic reactions at microdisk

---

[1] Present address: Mobay Corp., Baytown, TX 77520-9730.

0003-2700/90/0362-0268$02.50/0 © 1990 American Chemical Society

electrodes (*9*). Many organic reductions, including cleavage of carbon–halogen bonds of aryl and alkyl halides (*10*), involve two electrons. Electrochemical reductions of organohalide compounds are of analytical importance because of the possibility of detecting such compounds with microelectrodes in the environment. Pathways for mediating such reductions by soluble one-electron catalysts are reasonably well understood (*11–15*). In this paper, we extend a previously developed expanded space grid digital simulation model for second-order, two-electron electrocatalysis to steady-state linear sweep voltammetry at hemispherical microelectrodes. Such second-order simulations are applicable to the important analytical situation where the ratio of substrate to catalyst concentration is small. Predictions of the simulation for second-order conditions are applied to steady-state voltammetric data for the reduction of 4,4′-dibromobiphenyl with 9,10-diphenylanthracene as the mediator.

THEORY

Scheme I illustrates the mechanistic pathway for two-electron reduction of an aryl halide ArX by the soluble one-electron catalyst A. The first step is transfer of an electron from electrode to catalyst (eq 1) with forward and reverse heterogeneous rate constants k_f and k_b. This yields the product B, the reduced form of the catalyst. The rate-determining step (rds) for reductions of halobenzenes, halopyridines, and halobiphenyls with organic catalysts in dry organic solvents is an outer-sphere homogeneous electron transfer from the anion radical B of the catalyst to substrate ArX (*11, 12*). Cleavage of halide ion from aryl halide anion radical $ArX^{\bullet -}$ (eq 3) is fast in these systems. Subsequently, several fast, kinetically invisible steps, represented by eqs 4 and 5, yield the final hydrocarbon product. The essential kinetic features of this pathway also apply to the electrocatalytic reduction of alkyl vicinal dihalides (*14, 15*), although for these aliphatic dihalides eqs 2 and 3 are considered to be concerted. Regeneration of catalyst A in a thin layer of solution close to the electrode by chemical steps in eqs 2 and 4 is responsible for the amplification of the current caused by reduction of A.

The expanding grid digital simulation procedure is essentially the same as described previously for larger electrodes (*12, 16*). Briefly, the width (Δx_i) of the ith space element in the spherical expanded grid increases with distance away from the electrode as shown in eq 6 where Δx_1 is the width of the

$$\Delta x_i = \Delta x_1 \exp[0.5(i - 1)] \qquad i = 1, 2, 3, \ldots n \qquad (6)$$

space element immediately surrounding the electrode. The digital simulation sets up an expanded space grid around the spherical electrode for each small uniform time element. The linear sweep voltammograms are simulated in a stepwise fashion: (i) initial conditions, (ii) surface boundary conditions, (iii) diffusion of reaction participants, and (iv) homogeneous kinetics coupled to heterogeneous charge transfer. In eq 6, $\Delta x_1 = (D\Delta t/0.45)^{1/2}$, where D is the system diffusion coefficient considered to be the same for all diffusing species. Δt was chosen to yield relative errors <0.001 in concentrations, with a typical value of $(8 \times 10^{-7}\ \mathrm{V})/\nu$, where ν is scan rate. The concentration of any species S in the ith space element is computed from

$$C^{S}_{i} = W^{S}_{i} + \Delta(S)_i \qquad (7)$$

where $\Delta(S)_i$ is the change in concentration in the ith space element from homogeneous kinetics and W^{S}_{i} is the concentration anticipated from diffusion alone.

Although the general kinetics of Scheme I can be simulated, in this paper we focus on a common limiting case in which the forward homogeneous electron transfer in eq 2 is the rate-determining step. This case occurs when $k \gg k_2 C^*_A$, where C^*_A is the bulk concentration of A. It should pertain to a large number of analytical situations where catalyst and substrate are present in low concentrations. This is certainly true for alkyl vicinal dihalides (*15*) and many aryl halides, for which k_2 is close to the diffusion limit (*11–13*). The relevant expressions for the $(\Delta S)_i$ are (*12*)

$$\Delta(B)_i = \Delta t[-2k_1 W^{B}_{i} W^{ArX}_{i}] \qquad (7)$$

$$\Delta(ArX)_i = \Delta t[-k_1 W^{B}_{i} W^{ArX}_{i}] \qquad (8)$$

$$\Delta(A)_i = -\Delta(B)_i \qquad (9)$$

Currents were computed at 5-mV intervals as described previously (*12, 14*). These currents were divided by 2 to reflect the electrode geometry of a hemisphere imbedded in an insulating plane. Although results are presented for reductions, they are easily transposed to oxidations by appropriate changes in sign.

Scheme I

$$A + e^- \underset{k_b}{\overset{k_f}{\rightleftharpoons}} B \quad [B = A^{\bullet -}] \quad E^0 \qquad (1)$$

$$ArX + B \underset{k_2}{\overset{k_1}{\rightleftharpoons}} ArX^{\bullet -} + A \qquad (2)$$

$$ArX^{\bullet -} \xrightarrow{k} Ar^{\bullet} + X^- \qquad (3)$$

$$Ar^{\bullet} + B \rightarrow A + Ar^- \qquad (4)$$

$$Ar^- + (H^+) \rightarrow ArH \qquad (5)$$

EXPERIMENTAL SECTION

Microdisk electrodes were made by sealing P55-s grade VSB-32 carbon fibers (Union Carbide) or platinum microwires (Goodfellow Metals) in Corning 7740 glass. The quality of the seal was confirmed by optical microscopy. Microdisks and surrounding glass were polished initially to a smooth planar finish with SiC paper grit No. 600 on a polishing wheel in a stream of cold water. Other details of electrode preparation and apparatus for microelectrode voltammetry were similar to those described previously (*17*). Before each scan carbon microdisks were polished in a stream of water on clean billiard cloth on a polishing wheel for 40 s, ultrasonicated in pure water for 60 s, and then held at 0 V vs SCE for 90 s in the analyte solution. Pretreatment at 800 mV for 40 s, followed by holding of the initial scan potential for 60 s, was also tried but gave poorer precision for the catalytic limiting currents. Nominally hemispherical mercury electrodes were prepared by electroplating mercury onto polished platinum microdisks (at 0 V vs SCE) from 0.5% nitric acid solutions containing 5.7 mM mercurous nitrate and 1 M potassium nitrate, as described previously (*18*). Microelectrode radii (r) were estimated by using eq 10 or 11 with the measured steady-state limiting current (i_l) of 0.8 mM 9,10-diphenylanthracene in 0.1 M tetrabutylammonium iodide in dry *N,N′*-dimethylformamide ($D = 5.74 \times 10^{-6}$ cm^2 s^{-1}). The latter value was estimated with a stationary mercury electrode by conventional cyclic voltammetry (*19*). Sources and purification of chemicals and solvent were described previously (*13*). Voltammetric experiments were thermostated at 25.0 ± 0.2 °C.

Catalytic steady-state voltammetric curves were analyzed by nonlinear regression analysis using the Marquardt algorithm to separate the catalytic component from the background current caused by direct reduction of substrate. Regression procedures were the same as described previously (*17*).

RESULTS AND DISCUSSION

Steady-State Voltammograms. For a charge transfer uncomplicated by chemical reactions, e.g. eq 1 without the following reactions, steady-state current (i) vs potential (E) curves measured at low scan rates at microelectrodes have a sigmoid shape. Limiting currents (i_l) of these i–E curves are independent of scan rate. For a hemispherical electrode of

Table I. Results of Simulations of Steady-State Voltammograms for a Hemispherical Electrode of 6.6-μm Radius[a]

scan rate, mV s^{-1}	k_1, M^{-1} s^{-1}	i_l, nA	$E_{1/2} - E^{\circ\prime}$,[b] mV	i_c/i_d
2	0	1.85	0	0
	10^2	2.22	−2	1.20
	10^5	10.5	8	5.70
5	0	1.87	0	0
	10^2	2.22	−3	1.19
	10^5	10.5	7	5.61
10	0	1.89	0	0
	10^2	2.23	−2	1.18
	10^5	10.5	4	5.56
15	0	1.90	0	0
	10^2	2.23	−3	1.17
	10^5	10.5	5	5.52
20	0	1.91	0	0
	10^2	2.23	−4	1.16
	10^5	10.5	4	5.50

[a] $D = 5.74 \times 10^{-6}$ cm^2 s^{-1}, $k^\circ = 10$ cm s^{-1}, γ = [substrate]/[catalyst] = 4; [catalyst] = 0.8 mM. [b] Simulated currents generated at 5-mV intervals; accuracy in $E_{1/2}$ is about ±2 mV.

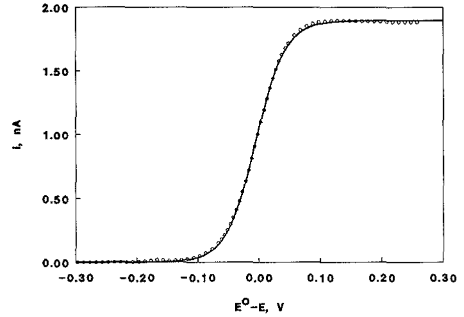

Figure 1. Simulated current–potential curve for reduction of 0.8 mM reactant (k° = 10 cm/s) at a hemispherical microelectrode of radius 6.6 μm for D/A = 1.04. Circles are simulated currents; line is best fit from regression analysis onto eq 12.

radius r_0 the relationship for a one-electron charge transfer is

$$i_l = 2\pi FDC^*r_0 \tag{10}$$

where F is Faraday's constant and C^* is the bulk concentration of A. For microdisk electrodes of radius r_d

$$i_l = 4FDC^*r_d \tag{11}$$

Current–potential curves simulated by the expanded grid program maintained sigmoid steady-state shapes up to about 50 mV s^{-1} for hemispherical electrodes of 8.2-μm radius and up to 100 mV s^{-1} for electrodes of 3-μm radius. Representative simulations for an electrode with radius 6.6 μm show (Table I) that in the absence of electrocatalysis a 3% increase in simulated limiting current is observed for going from 2 to 20 mV s^{-1}. However, when a finite value of k_1 is used, catalytic limiting currents are virtually independent of scan rate.

The sigmoid shape of steady-state voltammograms for reversible charge transfer at hemispherical microelectrodes is given in closed form by *(17, 20)*

$$i = i_l/(1 + \theta) \tag{12}$$

where $\theta = \exp[(E - E^{\circ\prime})F/RT]$, i_l is given by eq 10, R is the universal gas constant, $E^{\circ\prime}$ is the formal potential of the redox couple, and T is the temperature in kelvins. If the simulated i–E data are correct, they should fit eq 12 with the same values of i_l, F/RT, and $E^{\circ\prime}$ as used in the simulated data. When data simulated by the expanded grid program were fit to eq 12 by nonlinear regression analysis using the parameters RT/F, $E^{\circ\prime}$, and i_l, acceptable agreement was found between digitally simulated i–E curves and those computed from the best fit regression parameters (Figure 1). For eight simulated voltammograms using $D = 5.74 \times 10^{-6}$ cm^2 s^{-1}, $3 \leq r \leq 8.2$ μm, and scan rates between 2 and 100 mV s^{-1} an average computed value of $RT/F = 0.0247 \pm 0.0007$ V was found, in good agreement with the theoretical value of 0.0257 V at 298 K. Furthermore, values of $E^{\circ\prime}$ with average error 0.6 mV and limiting current with average error 1.7% were found in these regression analyses. Simulated i_l/C^* values at a given scan rate were constant within 0.1% and gave $D = 5.7 \times 10^{-6}$ cm^2 s^{-1} from eq 10. Dimensionless simulated and analytically computed currents were also in agreement (Table II). Results above show that simulated i–E curves for reversible charge transfer have shapes expected from eq 12 and limiting currents predicted by eq 10 under typical steady-state conditions at hemispherical microelectrodes.

To test simulations against experimental data, simulated steady-state limiting currents for uncomplicated one-electron reductions were compared with limiting currents for the reduction of 9,10-diphenylanthracene (9,10-DPA) on nominally hemispherical mercury electrodes of different radii (Table III). These were prepared by electroplating mercury on Pt microdisks of different radii. Hemispherical radii were estimated from experimental limiting currents via eq 10, and these radii were then used in digital simulation of the i–E curve. Although the shape of such mercury electrodes may not be strictly hemispherical *(21)*, good agreement was found between experimental and simulated limiting currents. The difference

Table II. Comparison of Simulated and Analytical Results for Reversible Charge Transfer at Hemispherical Microelectrode

$E - E^\circ$, V	dimensionless current[a] simultd	dimensionless current[a] anal.[b]
0.10	0.0207	0.0200
0.08	0.0433	0.0426
0.06	0.0893	0.0883
0.04	0.176	0.174
0.02	0.319	0.315
0	0.509	0.500
−0.02	0.699	0.685
−0.04	0.842	0.826
−0.06	0.927	0.912
−0.08	0.971	0.957
−0.10	0.992	0.980
−0.12	1.000	0.991
−0.14	1.003	0.996
−0.16	1.004	0.998
−0.18	1.004	0.999

[a] As $i/2\pi FDC^*r_0$, at 25 °C. [b] i/i_l from eq 12.

Table III. Simulated and Experimental Limiting Diffusion Currents for Reduction of 9,10-Diphenylanthracene[a]

geometry (electrode)	r, μm	C^*, mM	$-E_{1/2}$, V vs SCE	limiting current, nA found	limiting current, nA simultd
hemisphere (Hg)	2.5	0.801	1.85	0.70	0.70
	3.3	0.801	1.89	0.91	0.91
	11.7	0.801	1.82	3.27	3.44
disk (C)	6.8[b]	0.822	1.82[c]	1.22[c]	1.25

[a] Solutions 0.1 M tetrabutylammonium iodide in dry DMF, scan rate 10 mV s^{-1}; $E^{\circ\prime}$ for 9,10-DPA is −1.845 V vs SCE (ref 13). [b] Simulation used hemispherical radius of 4.33 μm to correspond to this disk radius (see text). [c] Average of data from six carbon microdisks with average radius of 6.8 μm.

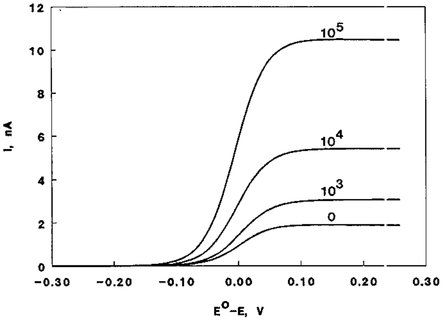

Figure 2. Simulated current–potential curves for reduction of substrate by 0.8 mM catalyst (k° = 10 cm/s) at a hemispherical electrode of radius 6.6 μm for D/A = 1.04, γ = 4, and a series of k_1 values (given on curves).

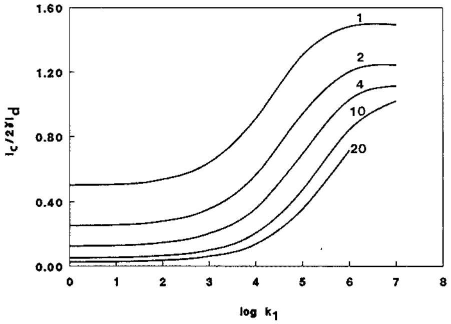

Figure 3. Influence of log k_1 on steady-state catalytic efficiency for D/A = 1.04 and various values of γ (given on curves).

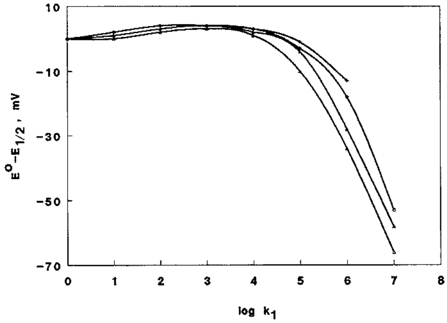

Figure 4. Influence of log k_1 on half-wave potential of catalytic waves for a reversibly reduced catalyst, D/A = 1.04 and γ = (△) 1, (▲) 4, (O) 10, and (+) 20.

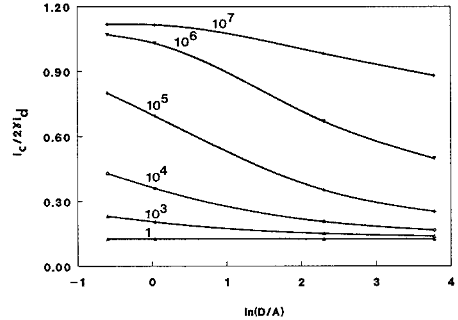

Figure 5. Influence of the ratio of diffusion coefficient to electrode area on catalytic efficiency for reversible charge transfer and various values of k_1 (given on curves).

between simulated and experimental limiting currents degraded from −0.3% on the smallest electrode to +5.2% on the largest (Table III). Nevertheless, limiting current divided by the radius of the electrode, which should be constant according to eqs 10 and 11, was 0.278 nA/μm (experimental) compared to the average simulated value of 0.283 nA/μm.

A hemispherical microelectrode of radius r_0 supports the same diffusion current as a microdisk of radius r_d when (*20*) $\pi r_0 = 2r_d$. Thus, limiting current at a microdisk should be well approximated by using a hemispherical radius of $2r_d/\pi$ for the simulations. In support of this assumption, average limiting currents on microdisk electrodes of average radius 6.8 μm showed excellent correspondence with the hemispherical limiting current for 9,10-DPA simulated with $r_0 = 2(6.8)/\pi$ μm (Table III).

The above results indicate that the simulations provide accurate limiting currents for charge transfer at hemispherical electrodes. Microdisk limiting currents can be simulated by using the radial correspondence discussed above.

Catalytic Efficiencies. Simulations for steady-state conditions showed that as k_1 (cf. eq 2) increases, the limiting current increases and the i–E curves remain sigmoid in shape (Figure 2). The quantity $i_c/2\gamma i_d$, which is independent of scan rate (cf. Table I), can be called the two-electron "steady-state catalytic efficiency", where i_c is the catalytic current with catalyst and substrate present in solution at the concentration ratio γ = [substrate]/[catalyst], and i_d is the limiting diffusion current for catalyst alone. As in other steady-state voltammetric methods (*22*), the measured catalytic efficiency can be used to obtain the rate constant k_1. An additional advantage of using the catalytic efficiency ratio with microelectrodes is that minor relative errors in diffusion and catalytic limiting currents, e.g. as might be caused by inexact model geometry, are minimized in the i_c/i_d ratio.

With the forward homogeneous electron transfer between reduced catalyst and substrate (eq 2) as the rds, the only kinetic constant in Scheme I that influences catalytic efficiency is k_1 (cf. eqs 7–9). Simulations for reversible charge transfer (eq 1) over a range of typical experimental conditions revealed a sigmoid shape to the dependence of steady-state catalytic efficiency on log k_1 (Figure 3). These working curves have shapes similar to those found for rotating disk voltammetry on conventional-sized electrodes (*22*). At $k_1 < 10^{2.5}$ M^{-1} s^{-1} there is little contribution of the catalytic reaction to the limiting current when D/A is close to 1. Catalytic current increases rapidly in the range $10^{3.5} < k_1 < 10^{5.5}$ M^{-1} s^{-1}. This range of rapid increase is shifted downward on the log k_1 axis by decreasing γ. At very large k_1 values the catalytic rate becomes "saturated" and a further increase in k_1 does not influence the catalytic efficiency. The onset of this kinetic saturation shifts to larger k_1 values as γ increases. Half-wave potentials for the catalytic wave are very close to the value of $E^{\circ\prime}$ of the catalyst until k_1 becomes larger than about 10^5 M^{-1} s^{-1} (Figure 4). Further increases in k_1 cause nearly linear shifts in $E_{1/2}$ to more positive potentials. At $k_1 > 10^5$ M^{-1} s^{-1} and γ = 1, $E_{1/2}$ shifts by 28.0 mV per 10-fold increase in k_1.

A series of simulations at different values of k_1, D, and r showed that the ratio D/A (i.e. D/r^2) has a significant influence on catalytic efficiency (Figure 5). However, when D or A was varied such that their ratio remained constant, catalytic efficiency remained constant within about 0.1%. In the range $10^3 < k_1 < 10^7$ M^{-1} s^{-1}, catalytic efficiency decreased as D/A

Table IV. Influence of $k°$ on Simulated Catalytic Voltammograms[a]

	$k° = 10$ cm s^{-1}		$k° = 0.016$ cm s^{-1}	
k_1, M^{-1} s^{-1}	$E_{1/2} - E°$, mV	i_c/i_d	$E_{1/2} - E°'$, mV	i_c/i_d
1	0	1.004	-11	1.004
10	-1	1.036	-12	1.034
10^2	-3	1.180	-16	1.175
10^3	-4	1.626	-22	1.610
10^4	-2	2.874	-34	2.814
10^5	3	5.555	-52	5.382
10^6	28	8.238	-57	8.142

[a] $D/A = 1.04$; γ = [substrate]/[catalyst] = 4; [catalyst] = 0.8 mM.

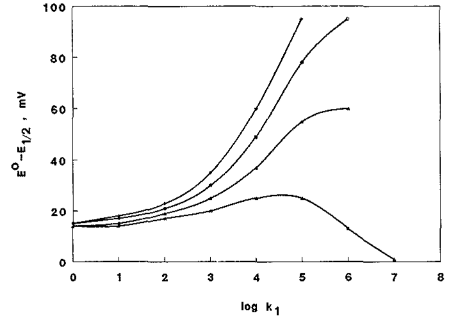

Figure 6. Influence of log k_1 on half-wave potential of catalytic waves for quasireversibly reduced catalyst with $k° = 0.016$ cm s^{-1}, $D/A = 1.04$, and γ = (△) 1, (▲) 4, (○) 10, and (+) 20.

increased. Thus, as r is decreased or D is increased, the catalytic efficiency becomes smaller. For a typical D of 6×10^{-6} cm^2 s^{-1}, Figure 5 predicts that for $10^3 < k_1 < 10^6$ M^{-1} s^{-1} analytical sensitivity is improved by using electrodes of radii in the 10–20-μm range. At larger values of k_1, catalytic efficiency does not drop off as rapidly as r decreases. For estimation of chemical rate constants, good precision for $k_1 > 10^7$ M^{-1} s^{-1} should be possible with electrodes of radius 1 μm or smaller.

As in other steady-state voltammetric methods, the limiting current at microelectrodes should not depend on the standard heterogeneous rate constant for charge transfer ($k°$) at the electrode. Since the simulation has the ability to vary $k°$, we briefly investigated this point. Limiting currents for catalysts alone ($k_1 = 0$) were within 0.8% of each other when $k°$ was changed from 10 to 0.016 cm s^{-1}. Catalytic efficiencies were nearly identical at $k_1 \leq 10^3$ M^{-1} s^{-1} for these two $k°$ values, but the values for $k° = 10$ cm s^{-1} were about 1.2% larger at $k_1 = 10^6$ M^{-1} s^{-1} (Table IV). Although $E_{1/2}$ values shift slightly positive for the highest rate constants when $k° = 10$ cm s^{-1} (Figure 4), a small negative shift in $E_{1/2}$ as k_1 increases is observed at the lower $k°$ for $\gamma = 1$ up to about $k_1 = 10^5$ M^{-1} s^{-1} (Figure 6). However, as k_1 increases above 10^5 M^{-1} s^{-1} at $\gamma = 1$, $E_{1/2}$ begins to shift positive. The negative potential shift predominates and is more pronounced at larger γ for $k° = 0.016$ cm s^{-1} (Figure 6). For a given k_1 at $k° = 0.016$ cm s^{-1}, $E_{1/2}$ shifts negative as γ increases.

Electrocatalytic Debromination of 4,4′-Dibromobiphenyl. 9,10-Diphenylanthracene (9,10-DPA) can be used as an electrocatalyst to reduce 4,4′-dibromobiphenyl (4,4′-DBB) by the pathway in Scheme I (*13*, *23*). These two molecules have sizes similar enough for the equal diffusion coefficient approximation to be used. The rate constant for electron transfer between the 9,10-DPA anion radical and 4,4′-DBB was previously estimated (*23*) from catalytic currents at a conventional hanging drop mercury electrode (HDME); 57 measurements gave a mean log $k_1 = 3.90 \pm 0.16$ M^{-1} s^{-1}.

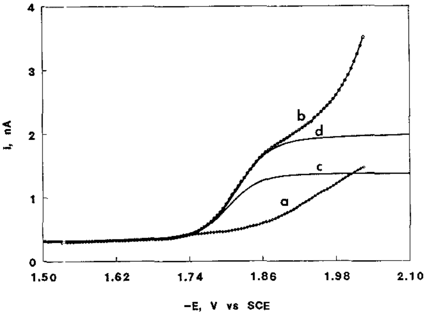

Figure 7. Steady-state voltammograms at 10 mV s^{-1} on a 6-μm carbon microdisk electrode in 0.1 M TBAI in DMF: (a) 1.6 mM 4,4′-DBB alone; (b) 0.8 mM 9,10-DPA and 1.6 mM 4,4′-DBB; circles are experimental data, line is best fit from nonlinear regression onto eq 13; (c) computed current for 0.8 mM 9,10-DPA; (d) computed catalytic current for reduction of 4,4′-DBB by 9,10-DPA anion radical after separation from the total current in curve b by nonlinear regression (see text).

To check simulated catalytic efficiencies with an experimental system, we reinvestigated the reaction of 9,10-DPA anion radical with 4,4′-DBB at carbon microdisk electrodes of 6–9-μm radii in 0.1 M TBAI in DMF. 9,10-DPA in DMF gave fully reversible steady-state voltammograms at the carbon microdisk electrodes. When 4,4′-DBB was added to a solution of 9,10-DPA in DMF, the limiting current increased (Figure 7) as expected for a catalytic reduction following Scheme I. One difficulty in estimating the steady-state catalytic limiting currents in this system is that the rise of current from direct irreversible reduction of 4,4′-DBB begins less than 100 mV negative of the $E_{1/2}$ of 9,10-DPA. Thus, we needed to separate the catalytic limiting current (i_c) from the total measured current, which contained contributions from background and from direct reduction of 4,4′-DBB. This was done as described previously (*24*, *25*) by nonlinear regression analysis of the catalytic i-E data using eq 13:

$$i = i_c/(1 + \theta) + i'\exp[S'(E - E')] + mE + i'' \quad (13)$$

where the first term on the right-hand side describes the sigmoid catalytic i–E curve, the exponential term accounts for contributions from irreversible reduction of 4,4′-DBB, and i' is the current at potential E' (fixed) on the rising portion of the irreversible reduction curve. The final two terms on the right-hand side of eq 13 describe a linear background contribution, where m is the base-line slope and i'' the current at $E = 0$ V. Reliable estimates of m and i'' were obtained by experiment.

Nonlinear regression analysis onto eq 13 of sets of 99 current values equally spaced on the E axis for the electrocatalytic system gave values of $E_{1/2}$ and i_c as regression parameters. Catalytic efficiencies were computed from i_c and separately measured values of i_d. These were used with working curves (cf. Figure 2) simulated for the appropriate experimental conditions to estimate k_1. Eleven sets of experiments under second-order conditions on four different carbon microdisk electrodes (Table V) gave a mean log k_1 of 3.88 ± 0.55 (M^{-1} s^{-1}), in very good agreement with the previously estimated 3.90 ± 0.16 (M^{-1} s^{-1}). A t-test showed no statistically significant difference in these mean values at the 95% confidence level. Poorer precision in the microelectrode results arises from variance in surface preparations of the microdisk electrodes and from errors in extracting the catalytic component from the total current containing the severely overlapped current

Table V. Results of Electrocatalytic Reduction of 4,4′-Dibromobiphenyl by 9,10-Diphenylanthracene at Carbon Microdisk Electrodes in DMF[a]

electrode no.	γ	r, μm	$-E_{1/2}$, V vs SCE	av i_d, nA	i_c/i_d	log k_1/(M^{-1} s^{-1})
1	2	7.23	1.89	1.31 ± 0.07	2.65	4.53
	4		1.87		2.36	4.02
2	2	6.59	1.87	1.18 ± 0.06	1.38	3.32
	2		1.83		1.38	3.32
	4		1.85		2.45	4.05
3	2	8.47	1.89	1.53 ± 0.10	2.51	4.35
	4		1.90		3.67	4.48
	10		1.96		5.88	4.51
4	2	5.96	1.92	1.06 ± 0.02	1.93	3.73
	2		1.87		1.32	3.15
	2		1.81		1.34	3.23
					mean	3.88
					s	±0.55

[a] Electrolyte 0.1 M TBAI, 0.82 mM 9, 10-DPA. $E_{1/2}$ and i_c for catalytic wave found by nonlinear regression of i-E data onto eq 13. Data for each γ value listed was average of three of more scans at 10–30 mV/s; multiple entries of γ values represent replicate runs on different days.

for direct reduction. As discussed previously (*24*), errors in this nonlinear regression procedure begin to increase as the difference between $E^{\circ\prime}$ of the catalyst and $E_{1/2}$ for the irreversible reduction of substrate decreases below about 100 mV. Nevertheless, the rather good agreement obtained for mean k_1 values between the microelectrode and HDME methods demonstrates the applicability of the simulation procedure for two-electron electrocatalysis to disk microelectrodes.

Conclusions. In summary, the expanded space grid simulation of second-order, two-electron homogeneous electrocatalysis developed previously for conventional-sized spherical electrodes can be extended to hemispherical microelectrodes. Results showed that as electrode radius becomes smaller, a larger rate of forward homogeneous electron transfer (eq 2) is needed to yield significant catalytic current. This means that much larger homogeneous rate constants, compared to those on conventional-sized electrodes, are needed for meaningful electrocatalytic amplification of current for analytical methods using microelectrodes. Conversely, very small electrodes should be applicable to estimating rate constants for second-order homogeneous electron transfer approaching the diffusion-controlled limit.

The simulation method itself is general for steady-state homogeneous electrocatalysis at microelectrodes. Cases of unequal diffusion coefficients of catalyst or substrate, a change in rate-determining step, or one-electron reductions can be handled with minor modifications to the program, as shown for larger electrodes (*12, 15*). Results are applicable to disk microelectrodes by using the hemispherical/disk radius conversion discussed in the text. However, attainment of steady-state behavior and the validity of the conversion depend on D/r^2, since steady-state behavior is achieved above a critical value of D/r^2 (*26*). Thus, each new experimental system should be checked by comparing simulated and experimental diffusion currents for the catalyst over the range of experimental conditions to be used.

ACKNOWLEDGMENT

The authors thank Union Carbide for donating the carbon fibers, James Arena for making helpful suggestions in applying the simulation program to microelectrodes, and Alan Brown for preparing the microelectrodes.

LITERATURE CITED

(1) Fleischmann, M.; Pons, S.; Rolinson, D. R.; Schmidt, P. P. *Ultramicroelectrodes*; Datatech Systems: Morganton, NC, 1987.
(2) Wightman, R. M. *Science* **1988**, *240*, 415–420.
(3) Bixler, J. W.; Bond, A. M.; Lay, P. A.; Thormann, W.; Van den Bosch, P.; Fleischmann, M.; Pons, B. S. *Anal. Chim. Acta* **1986**, *187*, 67–77.
(4) Huang, H. J.; He, P.; Faulkner, L. R. *Anal. Chem.* **1986**, *58*, 2889–2890.
(5) Heyrovsky, J.; Kuta, J. *Principles of Polarography*; Academic: New York, 1966.
(6) Brezina, M.; Zuman, P. *Polarography in Medicine, Biochemistry, and Pharmacy*; Interscience: New York, 1958.
(7) Dayton, M. A.; Ewing, A. G.; Wightman, R. M. *Anal. Chem.* **1980**, *52*, 2392–2396.
(8) Aoki, K.; Ishida, M.; Tokuda, K. *J. Electroanal. Chem. Interfacial Electrochem.* **1988**, *245*, 39–50.
(9) Fleischmann, M.; Lasserre, F.; Robinson, J.; Swan, D. *J. Electroanal. Chem. Interfacial Electrochem.* **1984**, *177*, 97–114.
(10) Hawley, D. In *Encyclopedia of Electrochemistry*; (Bard, A. J.; Lund, H., Eds.; Marcel Dekker: New York, 1980; Vol. XIV, pp 1–262.
(11) Andrieux, C. P.; Blocman, C.; Dumas-Bouchiat, J.-M.; Saveant, J. M. *J. Am. Chem. Soc.* **1979**, *101*, 3431–3441.
(12) Arena, J. V.; Rusling, J. F. *J. Phys. Chem.* **1987**, *91*, 3368–3373.
(13) Connors, T. F.; Rusling, J. F.; Owlia, A. *Anal. Chem.* **1985**, *57*, 170–174.
(14) Lexa, D.; Saveant, J. M.; Su, K. B.; Wang, D. L. *J. Am. Chem. Soc.* **1987**, *109*, 6464–6470.
(15) Connors, T. F.; Arena, J. V.; Rusling, J. F. *J. Phys. Chem.* **1988**, *92*, 2810–2816.
(16) Arena, J. V.; Rusling, J. F. *Anal. Chem.* **1986**, *58*, 1481–1488.
(17) Owlia, A.; Rusling, J. F. *Electroanalysis* **1989**, *1*, 141–149.
(18) Wehmeyer, K. R.; Wightman, R. M. *Anal. Chem.* **1985**, *57*, 1989–1993.
(19) Rusling, J. F.; Miaw, C. L., University of Connecticut, unpublished results.
(20) Oldham, K. B.; Zoski, C. G. *J. Electroanal. Chem. Interfacial Electrochem.* **1988**, *256*, 11–19.
(21) Stojek, Z.; Osteryoung, J. *Anal. Chem.* **1989**, *61*, 1305–1308.
(22) Andrieux, C. P.; Dumas-Bouchiat, J. M.; Saveant, J. M. *J. Eleectroanal. Chem. Interfacial Electrochem.* **1980**, *113*, 1–18.
(23) Rusling, J. F.; Miaw, C. L. *Environ. Sci. Technol.* **1989**, *23*, 476–479.
(24) Rusling, J. F.; Connors, T. F. *Anal. Chem.* **1983**, *55*, 776–781.
(25) Shukla, S. S.; Rusling, J. F. *J. Phys. Chem.* **1985**, *89*, 3353–3358.
(26) Aoki, K.; Osteryoung, J. *J. Electroanal. Chem. Interfacial Electrochem.* **1981**, *122*, 19–35.

Received for review July 13, 1989. Accepted November, 1, 1989. This work was supported financially by the Environment Research Institute, College of Engineering, University of Connecticut, the donors of the Petroleum Research Fund, administered by the Americal Chemical Society, and U.S. PHS Grant ES03154, awarded by the National Institute of Environmental Health Sciences.

Determination of Copper at Electrodes Modified with Ligands of Varying Coordination Strength: A Preamble to Speciation Studies

Seong K. Cha and Héctor D. Abruña*

Department of Chemistry, Baker Laboratory, Cornell University, Ithaca, New York 14853-1301

Electrodes modified with seven different ligands (incorporated by ion exchange into a polycationic film of electropolymerized $[Ru(v\text{-}bpy)_3]^{2+}$) (v-bpy, 4-vinyl-4′-methyl-2,2′-bipyridyl)) whose formation constants for copper vary over a very broad range, have been employed in the determination of copper in solution in an effort to ascertain the utility of chemically modified electrodes to carry out speciation studies. The redox response of the surface immobilized copper/ligand complex was used as the analytical signal. In all cases, calibration curves (log of the surface coverage-normalized redox response vs log [Cu]) exhibited an excellent correlation ($r \geq 0.98$) for copper concentrations ranging from 5×10^{-8} to 1×10^{-3} M. More importantly, when the solution concentration of copper is kept constant, we find an excellent correlation between the log of the normalized current (current/surface coverage) for the surface immobilized copper complex (employing the various ligands) and the log of the formation constants, indicating that the relative strength of coordination exhibited in solution is retained for the surface-immobilized ligands. The effects of having present other competing ligands including chloride, bromide, oxalate, ammonia and humic acid on the uptake of copper by the modified electrodes have also been studied. We find that the presence of competing ligands causes a diminution in the analytical signal due to copper incorporation and that the magnitude of this effect is dependent on the relative strength of coordination of the other competing ligands for copper ions as well as on their concentration. The relevance of this work to speciation studies is discussed.

INTRODUCTION

Within the general context of chemically modified electrodes (CME's) (*1–8*), the development of analytical strategies and sensors represent two of the most active areas to which these modified interfaces have been applied. This is due, in part, to the realization by many investigators that there are numberous advantages that accrue from the use of chemically modified electrodes when applied to analytical problems. These include the high specificity that can be achieved by the appropriate choice of modifier in addition to the excellent sensitivity that derives from the fact that many of the analytical applications are based on the preconcentration of the analyte at the surface modified electrode so that all of the advantages of preconcentration methods are applicable. In addition, the methodologies and instrumentation involved are relatively simple and, when coupled to microelectrodes, may allow for analytical studies on very small samples including single cell specimens.

Thus, it is clear that the use of CME in analytical applications offers a wide range of advantages. As mentioned before, such advantages have not gone unnoticed, and a number of analytical applications of chemically modified electrodes have been reported (*9–26*).

We have sought to exploit the advantages of polymer-modified electrodes for the determination of transition-metal ions (*18–23*) and organic functionalities (*24–26*). Our methods are based on the preconcentration of the analyte (metal ion or organic functionality) at the electrode surface by modifying the same with functionalized polymers that carry reagents for the selective and sensitive determination of the species of interest.

For the determination of transition-metal ions we employ bifunctional or multifunctional polymer films containing both electroactive centers as well as coordinating groups. The internal redox center is used to induce precipitation of the polymer on the electrode surface and thus allows for the precise control of the coverage and also serves in the determination of the number of immobilized ligand sites. This latter point is important as it allows an a priori determination of a saturation response. The coordinating group is chosen so as to bind strongly and selectively to the metal ion of interest. In addition, we have also employed carbon paste electrodes where the polymer containing the ligand is mixed with the pasting material. A very attractive feature of this approach is that it allows for the rapid regeneration of the electrode surface.

The analysis is based on the electrochemical determination of the amount of immobilized metal/ligand complex and can be either a metal- or ligand-based redox process, and we have employed both in our studies. This serves as the analytical signal which is then related to the concentration of the ion in solution. We have demonstrated the applicability of this approach to the determination of iron, copper, cobalt, nickel, and calcium (*18–23*).

We have also extended this method to the determination of organic functionalities by exploiting partitioning effects as well as simple chemical transformations that exhibit high selectivity toward a particular functional group (*24–26*).

As part of our continued interest in the analytical application of chemically modified electrodes, we are interested in assessing the utility of such modified interfaces in speciation studies. Speciation studies (that is, the determination of the concentration of a given ion and the identification of the forms in which it is found) are of great importance in the analysis of environmental samples since a wide variety of metal ions are toxic at very low concentration levels and, in addition, their toxicity is often strongly dependent on the particular form in which they are found. Being able to perform such speciation studies, however, is perhaps one of the most demanding things to ask of any analytical technique. Not only are the concentration levels low, but the given ion may be present in numerous forms and one must ensure that the method of analysis not only is sufficiently sensitive but also does not perturb the distribution of species.

At a fundamental level, speciation involves competitive equilibria between the metal ion of interest and ligands present in solution. Since our approach for employing chemically modified electrodes in analytical applications depends on coordination trends, we sought to assess its utility in such

0003-2700/90/0362-0274$02.50/0 © 1990 American Chemical Society

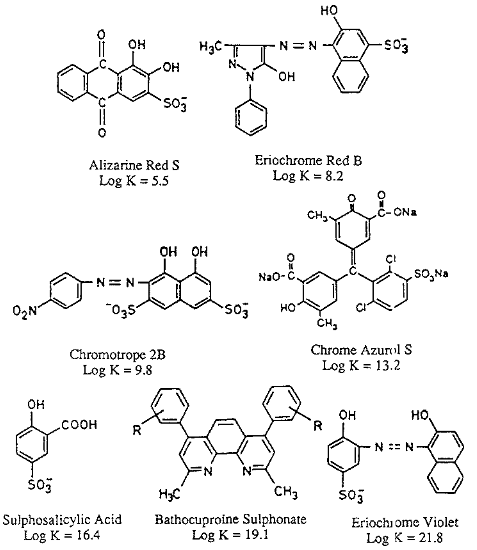

Alizarine Red S Log K = 5.5

Eriochrome Red B Log K = 8.2

Chromotrope 2B Log K = 9.8

Chrome Azurol S Log K = 13.2

Sulphosalicylic Acid Log K = 16.4

Bathocuproine Sulphonate Log K = 19.1

Eriochrome Violet Log K = 21.8

Figure 1. Structure and formation constants for copper for ligands employed in this study.

speciation studies. As an initial step we have investigated the response, for the determination of copper ions in solution, of electrodes modified with seven different ligands whose affinity for copper varies over a very broad range. In addition, we have studied the effects, on the analytical signal, of other competing ligands of varying coordinating strength toward copper and at various concentrations. The relevance of these investigations to speciation studies is discussed.

EXPERIMENTAL SECTION

Reagents. The ligands employed (see Figure 1 for the structures of the ligands and formation constants for copper) and their sources are as follows: 1, Alizarine Red-S (Aldrich); 2, Eriochrome Red-B (Aldrich); 3, Chromotrope 2-B (Aldrich); 4, Chrome Azurol-S (Aldrich); 5, Sulfosalicylic Acid (Aldrich); 6, Buthocuproine Sulfonate (G. F. Smith); 7, Eriochrome Violet (Aldrich). In addition, they were all purified by recrystallization (3 times) from ethanol.

Water was purified by passing through a Millipore Milli-Q system or a Hydro purification train.

Acetonitrile (Burdick and Jackson distilled in glass) was dried over 4-Å molecular sieves. Tetra-*n*-butylammonium perchlorate (TBAP) (G. F. Smith) was recrystallized (3 times) from ethyl acetate and dried under vacuum at 75 °C for 48 h. $[Ru(v\text{-}bpy)_3](PF_6)_2$ (v-bpy, 4-vinyl-4′-methyl-2,2′-bipyridyl) was prepared as previously described (*27*).

All other reagents were of at least reagent grade quality and were used without further purification.

Instrumentation. Platinum disk electrodes (sealed in glass) were used throughout. They were polished prior to use with 1-μm diamond paste (Buehler) and rinsed with water and acetone. Three-compartment electrochemical cells (separated by medium-porosity sintered glass disks) of conventional design were used.

Electrochemical experiments were performed on either an IBM EC225 voltammetric analyzer or a BAS 100 electrochemical analyzer. Data were recorded on a Soltec X-Y recorder. Differential pulse voltammetric experiments were carried out with a 50-mV pulse amplitude and at a sweep rate of 10 mV/s.

All potentials are reported against the sodium-saturated calomel electrode (SSCE) without regard for the liquid junction potential.

Procedures. Electrodes were modified with poly-$[Ru(v\text{-}bpy)_3]^{2+}$ by electroinitiated polymerization (*27*) of the monomer complex (typically at 0.5 mM concentration) from acetonitrile/0.1 M TBAP solution by scanning the potential between 0.0 and −1.60 V for a prescribed amount of time depending on the desired coverage. The exact coverage was determined by measuring the charge under the voltammetric wave for the Ru(III/II) process at about 1.25 V. Typical coverages were in the 2–3 equivalent monolayers range.

Table I. Formal Potentials for Copper Complexes of Selected Ligands

ligand	formal potential[a]
1. Alizarine Red-S	+0.43
2. Eriochrome Red-B	+0.47
3. Chromotrope 2-B	+0.52
4. Chrome Azurol-S	+0.52
5. Sulfosalicylic Acid	+0.57
6. Buthocuproine Sulfonate	+0.56
7. Eriochrome Violet	+0.57

[a] Potentials in volts vs SSCE.

The electrodes modified with a polymeric film of $[Ru(v\text{-}bpy)_3]^{2+}$ were immersed in an aqueous solution of the desired ligand (typically 5–10 mM depending on solubility) for 15 min while stirring. The electrodes were subsequently rinsed with water and placed in an aqueous pH 3.85 acetate buffer solution of Cu(I) (obtained by the addition of hydroxylamine hydrochloride at 5-fold excess) at various concentrations (from 5.38×10^{-8} to 1.07×10^{-3} M) and in the presence (or absence) of other competing ligands for 10 min (with stirring) after which the electrode was rinsed with water and acetone.

The electrochemical response of the copper ligand complex was used as the analytical signal and was determined by differential pulse voltammetry in acetonitrile/0.1 M TBAP. The currents were normalized to the surface coverage, which was determined as described above. All experiments were carried out in at least five replicate determinations and the deviations were typically of the order of 8–10% relative standard deviation.

RESULTS

A. Preliminary Voltammetric Characterization. The redox responses of the copper complexes for all of the ligands were determined in solution and values of the formal potentials are presented in Table I. As can be ascertained, all of the complexes have a redox response that is well removed from that for the poly-$[Ru(v\text{-}bpy)_3]^{2+}$ film so that no interference effects would be anticipated.

Similar responses were obtained for electrodes modified with the various ligands incorporated by ion exchange. Figure 2A shows a cyclic voltammogram for an electrode modified with a thin polymeric film of $[Ru(v\text{-}bpy)_3]^{2+}$ and a very well behaved, reversible response is observed at +1.25 V, and in addition, a very low, flat background is observed from 0.0 to about +1.1 V. By integrating the charge under this voltammetric wave, the polymer coverage for this electrode was determined to be 2.6 equivalent monolayers. Parts B–E of Figures 2 show differential pulse voltammograms for electrodes modified with Chrome Azurol-S (B, E) and Eriochrome Red-B (C, D) after having been contacted with 5.38×10^{-8} (B, C) and 1.04×10^{-4} M (D, E) copper solutions. Well-behaved and quantifiable voltammetric waves were observed. Similar behavior was observed for all the ligands employed in this work.

B. Calibration Curves. By use of the current (or the area under the voltammetric wave) for the surface-immobilized ligand/copper complex (normalized by the surface coverage of polymer) calibration curves (Log i/Γ vs Log [Cu]) for the determination of copper were constructed. Figure 3 shows representative plots employing electrodes modified with (A) Chrome Azurol-S and (B) Eriochrome Red-B, respectively. As can be ascertained, excellent correlations are obtained over the range of copper concentrations from 5×10^{-8} to 1×10^{-3} M. This is illustrative not only of the sensitivity of the method

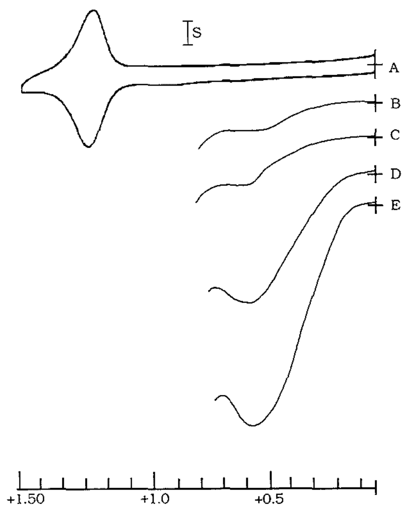

Figure 2. (A) Cyclic voltammogram at 100 mV/s for a platinum electrode modified with a thin polymeric film of $[Ru(v\text{-}bpy)_3]^{2+}$. (B–E) Differential pulse voltammograms for electrodes, modified with a thin polymeric film of $[Ru(v\text{-}bpy)_3]^{2+}$ and with Chrome Azurol-S (B, E) and Eriochrome Red-B (C, D) incoporated by ion exchange, after exposure to copper solutions at 5.38×10^{-8} (B, C) and 1.04×10^{-4} M (D, E). *S* is (A) 20 nA and (B–E) 10 nA.

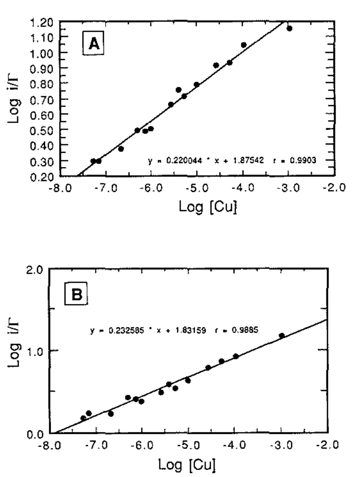

Figure 3. Calibration curves for copper determination with electrodes modified with: (A) Chrome Azurol-S and (B) Eriochrome Red-B.

but also of its wide dynamic range.

At the higher concentrations, there appears to be some evidence of saturation as the observed response begins to level off. This was corroborated by the fact that the current for the immobilized ligand/copper complexes did not increase with further increases in the solution concentration of copper. In addition, the observed currents (at saturation) correlated very well with our estimates for a completely metalated film calculated from the experimentally determined surface coverage of the polymer on the electrode surface and assuming complete neutralization of the charge due to the pendant $[Ru(v\text{-}bpy)_3]^{2+}$ groups by the sulfonate side chains on the

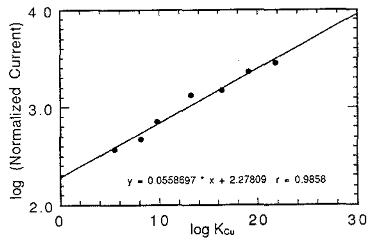

Figure 4. Plot of log of the normalized current vs log of the formation constant for copper for electrodes modified with the various ligands after contacting a solution containing copper at a concentration of 1×10^{-5} M.

ligands. Although saturation behavior was generally observed for all of the ligands employed, the solution copper concentration at which it became manifest varied from ligand to ligand, becoming higher for ligands with lower formation constant.

At the low concentration end, the response appears to level off at a solution copper concentration of about 5×10^{-8} M. This, however, appears to be due not to the limit of detection of the technique but rather to background levels of copper in the reagents employed.

Similar calibration curves were obtained with electrodes modified with each of the ligands and, again, excellent correlations were found for copper concentrations ranging from 5×10^{-8} to 1×10^{-3} M.

We were also interested in determining if, at a fixed solution concentration of copper, the observed response was dependent on the value of the formation constant for copper of each of the various ligands employed. We carried out such a study employing a solution concentration of copper of 1×10^{-5} M. The results are presented in Figure 4 where the log of the normalized current response for the various incorporated ligands is plotted against the log of the formation constant (in solution) for the corresponding ligands. As can be ascertained, an excellent correlation is obtained ($r = 0.98$) indicating that the relative strength of coordination exhibited in solution is also maintained at the surface. However, it should also be noted that the slope of such a line is significantly different from one, pointing to the presence of other effects affecting coordination. This, however, does not alter the previous assertion. Although Cu(I) solutions were employed in the studies described above, similar results (albeit with somewhat lower sensitivity) were obtained with Cu(II) solutions.

C. Effects of Competitive Ligands. As part of our studies aimed at an understanding of the various aspects that can affect the analytical determination, we have studied the effects of competitive binding of other ligands for the copper ions for electrodes modified with the various ligands. These studies will also be helpful in trying to apply the approach described here to speciation studies since at a fundamental level speciation involves competitive equilibria.

In these experiments the modified electrode was exposed to solutions of copper at a fixed concentration of 5×10^{-5} M which in addition contained a competing ligand at various concentrations. In this manner, we have studied the effects of chloride, bromide, oxalate, ammonia, and humic acid as competing ligands. Figure 5 shows representative results obtained when the competing ligands were chloride, bromide, oxalate, and humic acid (in this case since the molecular weight of humic acid is unknown, its concentration is expressed in terms of percent by weight) at electrodes modified with Chrome Azurol-S. There are a number of salient features that are immediately apparent from these plots. First of all, we

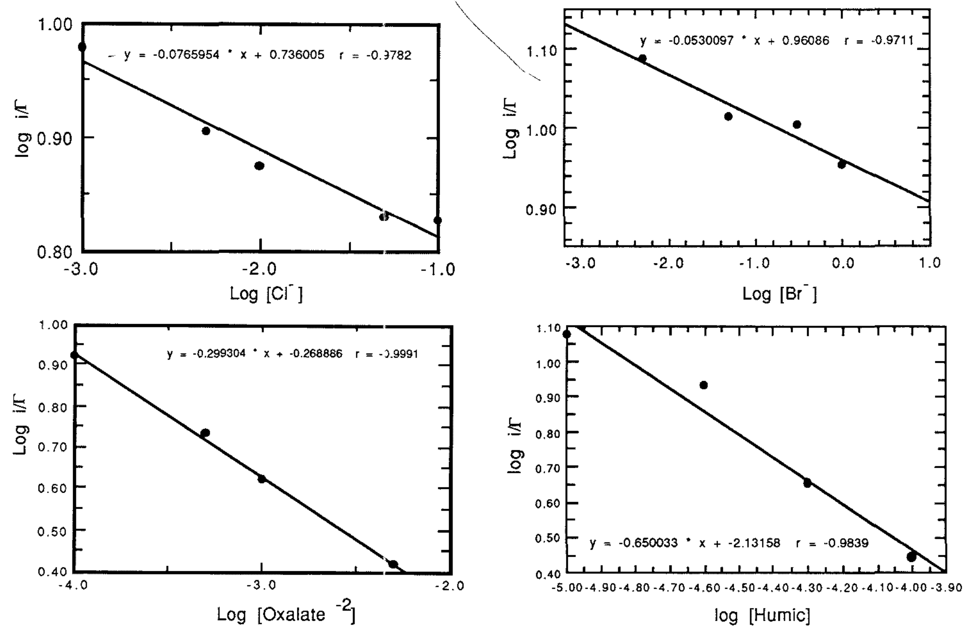

Figure 5. Effects of competing ligands at various concentrations on the determination of copper at a solution concentration of 5×10^{-5} M at electrodes modified with poly-$[\mathrm{Ru(v\text{-}bpy)_3}]^{2+}$ loaded with Chrome Azurol-S.

observe that in all cases there is a diminution in the response for the surface immobilized Chromazurol-S/Cu complex and that the magnitude of this effect is proportional to the solution concentration of the competing ligand (recall that the copper concentration was kept constant at 5×10^{-5} M). The well-behaved nature and excellent correlation ($r \geq 0.97$) of the log i/Γ vs −log [competitive ligand] plots strongly suggests that indeed the observed effects are due to competitive binding between the surface immobilized Chromazurol-S and the ligand in solution. In addition, for the cases where there are reliable values for the formation constant for copper with the various competitive ligands, we find that a plot of log i/Γ vs log K_{Cu} is also linear. Similar results were obtained for electrodes modified with the various other ligands pointing to the generality of this observation.

These are important observations in that they not only support our assertion that competitive binding effects are responsible for the observed diminution in the analytical signal but also, more importantly, establish that the relative strengths of coordination of the various ligands are maintained under the experimental conditions employed. This implies that one can systematically and deliberately control the coordinative properties of an interface (modified electrode in this case) by the choice of the immobilized ligand as well as the presence of other competitive ligands in solution.

DISCUSSION

We believe that the results presented here serve as a preamble to the application of chemically modified electrodes to speciation studies and present here the basic aspects of such an approach.

Conceptually, the approach would be based on the use of a family of ligands whose formation constants for the metal ion of interest vary over a broad range. These materials would be incorporated into the surface of an electrode and would be employed in the determination of the metal ion under study. If, in the immobilized state, the various ligands retain their relative strength of coordination for the metal ion, the measured analytical response (electrochemical in the present context) for the immobilized metal/ligand complex would vary in relation to the magnitude of the formation constant. In addition, if the metal ion in solution is present in various chemical forms (i.e. coordinated to other ligands in the sample such as chloride, oxalate, humic acid, etc.) competitive equilibria, for the metal ion, will exist between the ligands present in solution and the surface immobilized ligand. Again, the larger the value of the formation constant of the surface immobilized ligand for the metal ion of interest, the more effectively it will compete, relative to the other ligands present in solution (competing ligands), for the metal ion. In other words, the response depends on the conditional formation constant for copper under the specified conditions (*28*).

In order to account for such competitive equilibria, the effect of other competing ligands (as a function of their concentration and coordinating strength) on the analytical determination of the ion of interest would be determined for each of the surface immobilized ligands.

Thus, with the electrochemical response of the immobilized metal/ligand complex monitored as a function of the coordinating strength of the surface immobilized ligand and from a knowledge of the concentration of the competing ligands present in solution, one could make an assessment as to the forms (chemical environment) in which the analyte ion is found.

The fact that the proposed analytical approach is based on coordination chemistry allows for a very different and potentially superior approach to speciation studies. In addition, the vast body of literature on coordination chemistry provides a wide range of candidates for study.

In order for this approach to be applicable to speciation studies, we need to first of all establish that the relative strength of coordination (as measured by the formation constant) of the various ligands toward the specific metal ion is retained when the ligands are immobilized on the surface of an electrode. This is a critical point since the analysis will depend on the ability to vary the strength of coordination at the surface so as to distinguish the presence of ions in chemically distinct forms. As shown in Figure 4, this is clearly the case for the family of ligands employed in this study. In addition, the calibration curves for the determination of copper with the various ligands exhibited an excellent correlation over a broad range of copper concentrations, typically from about 3×10^{-8} to 1×10^{-3} M.

The other point that one needs to be concerned with is the effect of other competing ligands for the metal ion of interest. As shown above, the general trends observed are that competing ligands cause a diminution of the signal that is proportional to the concentration of the competing ligand as well as to the formation constant for copper with the corresponding competing ligand.

These two findings are quite significant in that they demonstrate that surface immobilized ligands retain their relative coordination strength for copper and that, similarly, the effects of other competing ligands can be interpreted in terms of concentration and coordinating strength.

From these measurements, along with a measurement of the total copper concentration (e.g. from anodic stripping voltammetry after irradiation of the analysis sample with ultraviolet light to decompose the organic matter present and release the copper ions into solution), one could establish a series of simultaneous equations from which one could, in priniple, extract the fraction of the copper ions present in a given coordination environment.

The main advantage of this procedure is that it relies on a sequence of reagents of increasing and known affinity for the ion of interest and where the effects of other competing ligands are also known. By monitoring the current for the surface immobilized metal/ligand complex as a function of the coordination strength of the immobilized ligand, one could ascertain the fraction of the metal present within a coordination environment of a given strength and from this infer the form in which this fraction is present. Furthermore, since only very small amounts of analyte are required to perform the analysis (due to the high sensitivity of the method), the system will be minimally perturbed. Thus this approach appears to be capable of fulfilling all of the requirements for speciation studies.

CONCLUSIONS

We have shown that electrodes modified (by ion exchange into an electropolymerized thin film of $[Ru(v\text{-}bpy)_3]^{2+}$) with various ligands whose coordination strength for copper varies over a very broad range can be employed in the determination of copper in solution over the range of 5×10^{-8} to 1×10^{-3} M. The relative strength of coordination for copper exhibited by the various ligands for copper in solution is retained when the ligands are immobilized on the surface of an electrode. In addition, the presence of competing ligands causes a diminution in the analytical signal and this effect is dependent on the concentration as well as the coordination strength for copper of the competing ligand. These results point at the feasibility of employing chemically modified electrodes in metal speciation studies.

LITERATURE CITED

(1) Murray, R. W. In *Electroanalytical Chemistry*; Bard, A. J., Ed.; Marcel Dekker: New York, 1984; Vol. 13, p 191.
(2) Murray, R. W. *Annu. Rev. Mater. Sci.* **1984**, *14*, 145.
(3) Murray, R. W. *Acc. Chem. Res.* **1980**, *13*, 135.
(4) Faulkner, L. R. *Chem. Eng. News* **1982**, February 27, 28.
(5) Abruña, H. D. *Coord. Chem. Rev.* **1988**, *86*, 135.
(6) Abruña, H. D. In *Electroresponsive Molecular and Polymeric Systems*; Skotheim, T. A., Ed.; Marcel Dekker: New York, 1988; p 92.
(7) Fujihira, M. In *Topics in Organic Chemistry*; Fry, A. J., Britton, W. R., Eds.; Plenum: New York, 1986; p 255.
(8) Murray, R. W.; Ewing, A. G.; Durst, R. A. *Anal. Chem.* **1987**, *59*, 379A.
(9) Baldwin, R. P.; Christensen, J.-K.; Kryger, L. *Anal. Chem.* **1986**, *58*, 1790.
(10) Prabhu, S. V.; Baldwin, R. P.; Kryger, L. *Anal. Chem.* **1987**, *59*, 1074.
(11) Cox, J. A.; Kulesza, P. J. *J. Electroanal. Chem.* **1983**, *159*, 337.
(12) Gardea-Torresdey, J.; Darnall, D.; Wang, J. *J. Electroanal. Chem.* **1988**, *252*, 197.
(13) Ikariyama, Y.; Heineman, W. R. *Anal. Chem.* **1986**, *58*, 1803.
(14) Cox, J. A.; Das, B. K. *Anal. Chem.* **1985**, *57*, 2739.
(15) Oyama, N.; Anson, F. C. *J. Electrochem. Soc.* **1980**, *127*, 247.
(16) Espenscheid, M. W.; Ghatak-Rog, A. R.; Moore, R. B., III; Penner, R. M.; Szentirmay, M. N.; Martin, C. R. *J. Chem. Soc., Faraday Trans. 1* **1986**, *82*, 1051.
(17) Nagy, G.; Gerhardt, G. A.; Oke, A. F.; Rice, M. E.; Adams, R. N.; Moore, R. B., III; Szentirmay, M. N.; Martin, C. R. *J. Electroanal. Chem.* **1985**, *188*, 85.
(18) Guadalupe, A. R.; Abruña, H .D. *Anal. Chem.* **1985**, *57*, 142.
(19) Wier, L. M.; Guadalupe, A. R.; Abruña, H. D. *Anal. Chem.* **1985**, *57*, 2009.
(20) Guadalupe, A. R.; Wier, L. M.; Abruña, H. D. *Am. Lab.* **1986**, *18* (8), 102.
(21) McCracken, L.; Wier, L.; Abruña, H. D. *Anal. Lett.* **1987**, *20* (10), 1521.
(22) Hurrell, H. C.; Abruña, H. D. *Anal. Chem.* **1988**, *60*, 254.
(23) Kasem, K. K.; Abruña, H. D. *J. Electroanal. Chem.* **1988**, *242*, 87.
(24) Guadalupe, A. R.; Abruña, H. D. *Anal. Lett.* **1986**, *19* (15&16), 1613.
(25) Guadalupe, A. R.; Jhaveri, S.; Liu, K. E.; Abruña, H. D. *Anal. Chem.* **1987** *59*, 2436.
(26) Liu, K. E.; Abruña, H. D., *Anal. Chem.* **1989**, *61*, 2599.
(27) Abruña, H. D.; Denisevich, P.; Umaña, M.; Meyer, T. J.; Murray, R. W. *J. Am. Chem. Soc.* **1981**, *103*, 1.
(28) Laitinen, H. A.; Harris, W. E. *Chemical Analysis*, 2nd. ed.; McGraw-Hill: New York, 1975.

RECEIVED for review August 17, 1989. Accepted November 1, 1989. This work was supported in part by the National Science Foundation. H.D.A. is a recipient of a Presidential Young Investigator Award (1984–1989) and an A.P. Sloan Fellowship (1987–1991). S.K.C. acknowledges support by the Korean Ministry of Education.

Anal. Chem. **1990**, *62*, 279–286

Determination of Linkage Position and Identification of the Reducing End in Linear Oligosaccharides by Negative Ion Fast Atom Bombardment Mass Spectrometry

Domenico Garozzo, Mario Giuffrida, and Giuseppe Impallomeni

Istituto per la Chimica e la Tecnologia dei Materiali Polimerici, Consiglio Nazionale delle Ricerche, Viale A. Doria 6, 95125 Catania, Italy

Alberto Ballistreri and Giorgio Montaudo*

Dipartimento di Scienze Chimiche, Università di Catania, Viale A. Doria 6, 95125 Catania, Italy

Negative ion fast atom bombardment (FAB) mass spectra were found to allow the determination of the linkage position and sugar sequences in a series of (underivatized) disaccharides and of linear oligosaccharides. Discrimination of 1–4, 1–6, 1–3, and 1–2 linkage type and determination of the reducing end and of the monosaccharide sequence is made possible by the analysis of the negative metastable ions produced in linked scans FAB MS. The peculiarity of negative ionization is believed to consist in a *selective* deprotonation of the anomeric hydroxyl (reducing end of the oligosaccharide chain), which is more acidic with respect to the remaining OH groups. Once the negative charge is localized at the oligosaccharide reducing end, the ion fragmentation of this ring occurs rapidly and the mass losses observed are found to be diagnostic of the glycoside linkage type between adjacent sugar units. The overall negative ions fragmentation process outlined above allows the simultaneous identification of the reducing end of the chain, of the monosaccharide units sequence, and of the linkage type between adjacent units.

INTRODUCTION

The structural analysis of biological macromolecules by rapid instrumental methods appears very desirable nowdays and considerable research efforts have been made in the last 2 decades to develop rapid and reliable protocols that may allow the direct determination of the structure of biopolymers with a minimal amount of chemical manipulations.

Among the biological macromolecules, the analysis of polysaccharides still involves laborious chemical procedures (*1–7*).

In fact, the structure elucidation of oligo- and polysaccharides requires the knowledge of several parameters such as sugar sequence, reducing end, linkage type between the monosaccharide units, and anomeric configuration.

The most common method is the permethylation procedure (*1*), where the saccharide is methylated at the free hydroxyl groups, total hydrolysis to monosaccharides is brought about, the carbonyl groups are reduced, and finally the hydroxyl groups liberated are derivatized (*2*). The mixture obtained is usually analyzed by gas chromatography–mass spectrometry (GC–MS) (*3*).

Although a powerful and well-standardized technique, permethylation is time-consuming and fails to be a generally applicable approach (*4*). Therefore it would be desirable to develop alternative and sensitive methods for linkage type analysis in oligo- and polysaccharides.

NMR analysis is very helpful in determining the anomeric and the alcoholic carbons configurations of oligosaccharides and linkage position in disaccharides (*8*). However NMR cannot be easily used to sequence large oligosaccharides available in little quantities.

Table I. List of Compounds Analyzed[a]

no.	name	formula
1	gentiobiose	$\text{Glc1}\xrightarrow{\beta}\text{6Glc}$
2	cellobiose	$\text{Glc1}\xrightarrow{\beta}\text{4Glc}$
3	laminaribiose	$\text{Glc1}\xrightarrow{\beta}\text{3Glc}$
4	soforose	$\text{Glc1}\xrightarrow{\beta}\text{2Glc}$
5	melibiose	$\text{Gal1}\xrightarrow{\alpha}\text{6Glc}$
6	isomaltose	$\text{Glc1}\xrightarrow{\alpha}\text{6Glc}$
7	maltose	$\text{Glc1}\xrightarrow{\alpha}\text{4Glc}$
8	lactose	$\text{Gal1}\xrightarrow{\beta}\text{4Glc}$
9	epilactose	$\text{Gal1}\xrightarrow{\beta}\text{4Man}$
10	nigerose	$\text{Glc1}\xrightarrow{\alpha}\text{3Glc}$
11		$\text{Man1}\xrightarrow{\alpha}\text{3Man}$
12		$\text{GlcNAc1}\xrightarrow{\beta}\text{6Gal}$
13	*N*-acetyllactosamine	$\text{Gal1}\xrightarrow{\beta}\text{4GlcNAc}$
14		$\text{Gal1}\xrightarrow{\beta}\text{3Ara}$
15	β-neocarrabiose	3-*O*-[3,6-anhydro-α-D-galactop]-β-D-galactop
16	maltotriose	$\text{Glc1}\xrightarrow{\alpha}\text{4Glc1}\xrightarrow{\alpha}\text{4Glc}$
17	isomaltotriose	$\text{Glc1}\xrightarrow{\alpha}\text{6Glc1}\xrightarrow{\alpha}\text{6Glc}$
18	maltohexaose	$\text{Glc1}\xrightarrow{\alpha}\text{4Glc1}\xrightarrow{\alpha}\text{4Glc1}\xrightarrow{\alpha}\text{4Glc1}\xrightarrow{\alpha}\text{4Glc1}\xrightarrow{\alpha}\text{4Glc}$
19		$\text{Glc1}\xrightarrow{\alpha}\text{6Glc1}\xrightarrow{\alpha}\text{4Glc1}\xrightarrow{\alpha}\text{4Glc}$

[a] Key: Glc, glucose; Man, mannose; Gal, galactose; Ara, arabinose; GlcNAc, 2-acetamide-2-deoxyglucose.

The use of mass spectrometry for the structural analysis of carbohydrates has increased considerably in the last few years, and it has been shown that desorption techniques such as fast atom bombardment (FAB) (*9, 10*), field desorption (FD) (*11, 12*), and laser desorption (LD) (*13, 14*) allow the detection of molecular ions from underivatized saccharides.

In principle, it should be therefore possible to obtain the structural analysis of the large saccharide ions desorbed in the MS.

Several workers (*15–21*) have recently addressed this problem making important contributions but the results are still tentative, so that the general problem of sequencing underivatized saccharides by MS still appears unsolved.

We have used FAB MS for the structural characterization of some synthetic (*22–25*) and biological (*26–27*) polymers and copolymers and became recently interested in applying FAB MS to the structural analysis of oligo- and polysaccharides.

We present here a method allowing the simultaneous identification of the reducing end of the oligosaccharide chain and of the glycoside linkage type between adjacent units.

The method is illustrated by the results obtained on a series of linear oligosaccharides and of disaccharides listed in Table I.

0003-2700/90/0362-0279$02.50/0 © 1990 American Chemical Society

Our long range goal is to apply this method to the structural delucidation of unknown polysaccharide molecules. In fact, partial hydrolysis or enzymatic attack can be used to reduce the molecular weight of polysaccharides, so that the structure of the macromolecule can be deduced from that of the oligosaccharides produced in the partial degradation.

EXPERIMENTAL SECTION

Materials. All the compounds analyzed were purchased from Sigma Chemical Co., except sophorose, which was purchased from Fluka (Switzerland).

They were of the best purity available and were used without purification.

Mass Spectrometry. A double focusing Kratos MS 50S equipped with the standard FAB source and a DS 90 data system was used to obtain mass spectra. The fast atom bombardment gun (ION TECH) was operated with a 7–8 kV xenon beam. The instrument was scanned from m/z 1000 to m/z 60, with a scan rate of 10 s/decade. Accelerating voltage was 8 kV. Cesium and rubidium iodide (50/50 (w/w)) were used for computer calibration. The resolution was 2000.

Spectra were obtained by using a mixture of triethanolamine (TREA) and tetramethylurea (TMU) (50/50 weight) as matrix (TREA/TMU).

Three microliters of a solution (1 mg/mL) of the oligosaccharide to be analyzed was placed on the copper target of the standard FAB probe and mixed with 1 μL of matrix.

Peak intensity values shown in mass spectra, computed after subtraction of the contribution from the matrix, represent the average of five separate mass spectra.

B/E (daughter ions) and B^2/E (parent ions) linked scans were performed by using a linked scan unit at a scan rate of 20 s/decade and registered on an UV oscillograph.

Metastable decompositions were activated by using helium as collision gas. The pressure in the collision cell was such as to reduce the ion beam to 30% of its usual value.

RESULTS AND DISCUSSION

Principle of the Method. The problem of performing structural analysis by MS is that of finding suitable MS fragments that enable discrimination among alternative structures.

Underivatized saccharides desorb undecomposed, yielding intense molecular ions by positive FAB MS, but they produce little and *unselective* fragmentation even in the collision activated decomposition (CAD) mode.

This is not surprising because protonation of the hydroxyl groups is likely to occur in positive FAB mode. The latter process is not selective since every hydroxyl group in the saccharide molecule enjoys an equal probability of being protonated.

Therefore, a mixture of isomeric pseudomolecular ions is produced, and the observed fragmentation appears as an unselective process.

Negative ion FAB mass spectra were found to yield molecular ions with abundant fragment ions, showing a potential for the determination of structural features in oligosaccharides. In fact, the spectra show appreciable differences as a function of the structure. Discrimination of the glycosidic linkage position and determination of the reducing end are made possible by analysis of the negative FAB mass spectra and of the negative metastable ions detected by linked scans FAB MS.

An example of differentiation is shown in Figure 1, where the only structural difference among the four disaccharides reported is the linkage position existing between the glucose rings (see below for further discussion).

The peculiarity of the negative ionization in the FAB mode is believed to consist in a *selective* deprotonation of the anomeric hydroxyl (reducing end of the oligosaccharide chain).

Using a basic matrix as TREA/TMU, one can expect a selective deprotonation of the anomeric group, more acidic with respect to the alchoholic groups, with formation of a negatively charged ion as described in eq 1.

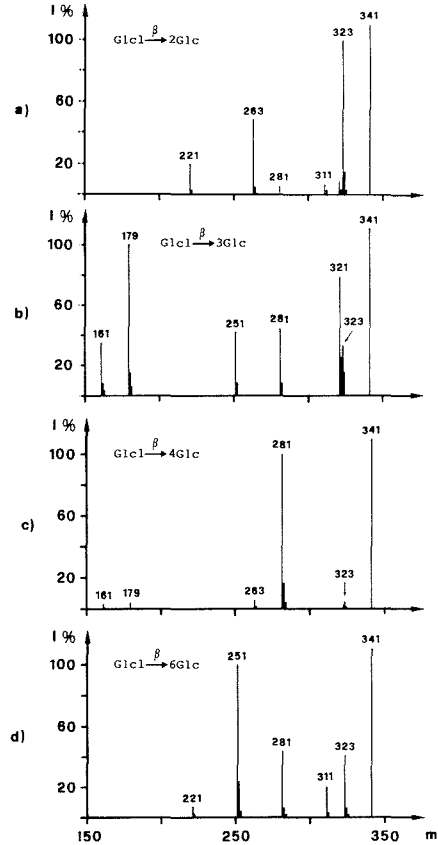

Figure 1. Negative ion B/E linked scans FAB mass spectra of the pseudomolecular ion of (a) sophorose, (b) laminaribiose, (c) cellobiose, and (d) gentiobiose.

Table II. Diagnostic Peaks

linkage position	presence					absence		
1–4		281	263			311		251
1–6	311			251			263	
1–3		281		251		311		
1–2	311	281	263		221			251

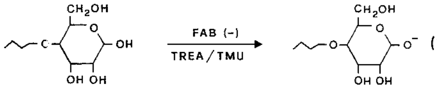

Once the negative charge is localized at the saccharide reducing end, the ion fragmentation of this ring occurs rapidly and the mass losses observed in the daughter ions spectra are found to be *diagnostic* of the glycoside linkage type between adjacent sugar units (see below and Table II).

The fragmentation process of the glucosidic linkages occurs stepwise, going from the reducing end to the nonreducing end. Each stage results in the formation of a saccharide containing one sugar unit less than the progenitor molecular ion and with

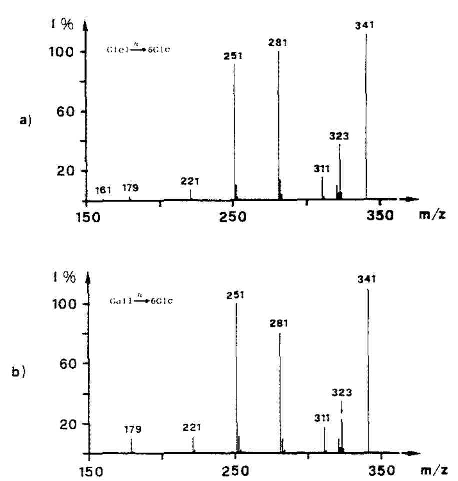

Figure 2. Negative ion B/E linked scans FAB mass spectra of the pseudomolecular ion of (a) isomaltose and (b) melibiose.

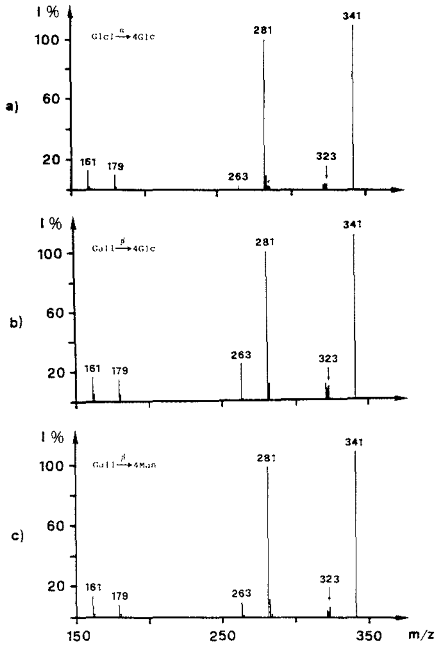

Figure 3. Negative ion B/E linked scans FAB mass spectra of the pseudomolecular ion of (a) maltose, (b) lactose, and (c) epilactose.

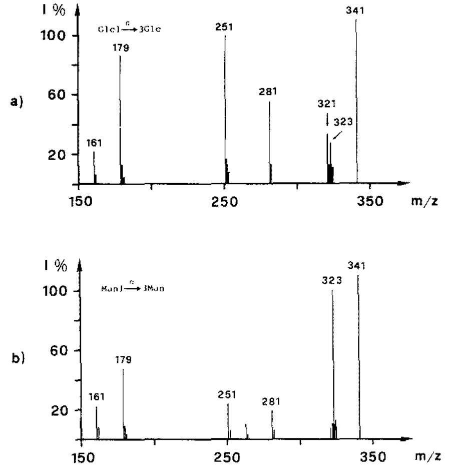

Figure 4. Negative ion B/E linked scans FAB mass spectra of the pseudomolecular ion of (a) nigerose and (b) Man1$\xrightarrow{\alpha}$3Man.

the new anomeric hydroxyl negatively charged, thus reproducing the initial situation at the reducing end.

By recording the daughter ions spectra of the FAB peaks corresponding to these progressively degraded oligosaccharides, it has been possible to observe diagnostic mass losses that characterize the glycoside linkage sequence along the oligosaccharide chain. Sugar sequence is also unequivocally determined from the knowledge of the reducing end (see below).

Model Disaccharides. As mentioned above, the negative ion FAB B/E spectra of the pseudomolecular ions of the four isomeric disaccharides in Figure 1 are different.

In order to check the value of these results, we have examined other disaccharides.

The negative ion FAB B/E linked scans mass spectra of the pseudomolecular ions of two 1–6 linked disaccharides (compounds **5** and **6**, Table I), of three 1–4 linked disaccharides (compounds **7**–**9**, Table I), and of two 1–3 disaccharides (compounds **10** and **11**, Table I), are reported in Figures 2, 3, and 4, respectively.

The three series of spectra show the same ring fragmentation patterns of gentobiose (1–6 linked), cellobiose (1–4 linked), and laminaribiose (1–3 linked) (Figure 1), independent of the monosaccharide structure or of the configuration of the glycosidic carbons.

This result is regarded as strong evidence that the fragmentation observed in negative ion FAB linked scan mass spectra is mainly determined by the linkage position between the hexose rings. The metastable ion transitions observed in the four isomeric disaccharides studied here, are summarized in Schemes I–IV, respectively. The ion structures reported in the schemes are of course tentative.

The schemes deal with fragmentation processes pertaining to the cleavage of the ring bearing the reducing end. The peak at *m/z* 179 (M_2 − 162), corresponding to the loss of a glucose unit, is observed in all four cases in the negative FAB mass spectra (omitted here for brevity).

The negative ion B/E spectra of the 1–6 linked isomers show a series of three peaks at *m/z* 311, 281, and 251, which appear to derive from the pseudomolecular ion by the loss of a multiple of 30 amu (which is most likely related to the CHOH moiety). These transitions have been confirmed by B^2/E linked scans showing that the above peaks have all the molecular ion at *m/z* 341 as parent ion. Instead, the peak at *m/z* 221 in Figure 2b does not originate directly from the molecular ion. A B^2/E scan shows in fact that it originates from a loss of 60 amu from the peak at *m/z* 281 (Scheme I).

It appears furthermore that the 1–4 structure privileges the 60 amu loss, yielding only an intense peak at *m/z* 281 (M_2 − 60) (Figure 2a, Scheme II). Water loss from the peak at *m/z* 281 yields the peak at *m/z* 263, as confirmed by B^2/E scans (Scheme II).

The fragmentation pattern of the 1–3 isomers is very similar to that of 1–6 disaccharides (peaks at *m/z* 281 and 251). However, the systematic absence of the peak at *m/z* 311 allows their discrimination (Scheme III). An intense peak at *m/z*

Scheme I

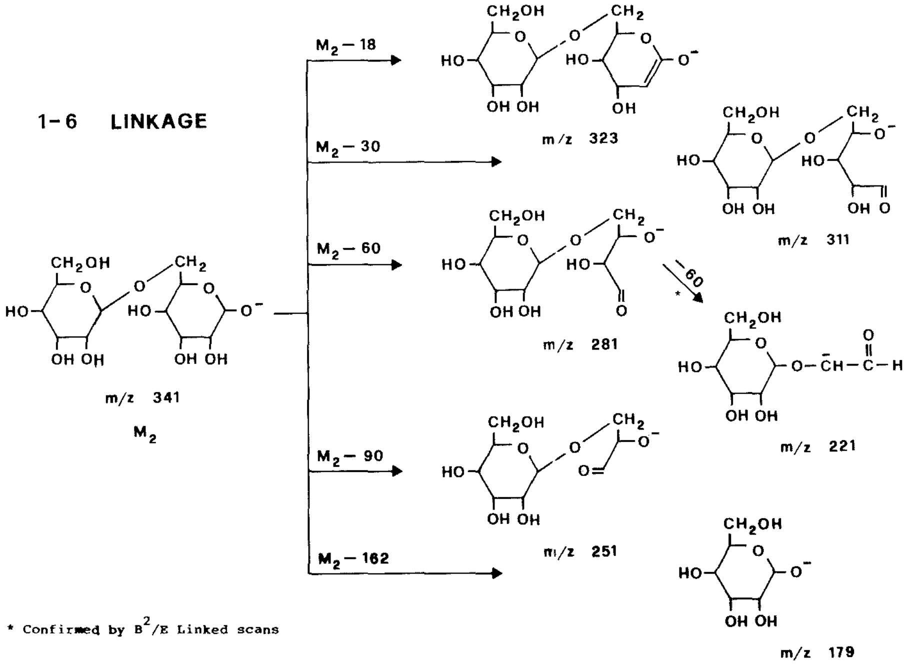
1-6 LINKAGE
m/z 341
M2
M2 − 18
m/z 323
M2 − 30
m/z 311
M2 − 60
m/z 281
60
m/z 221
M2 − 90
m/z 251
M2 − 162
m/z 179

* Confirmed by B^2/E Linked scans

Scheme II

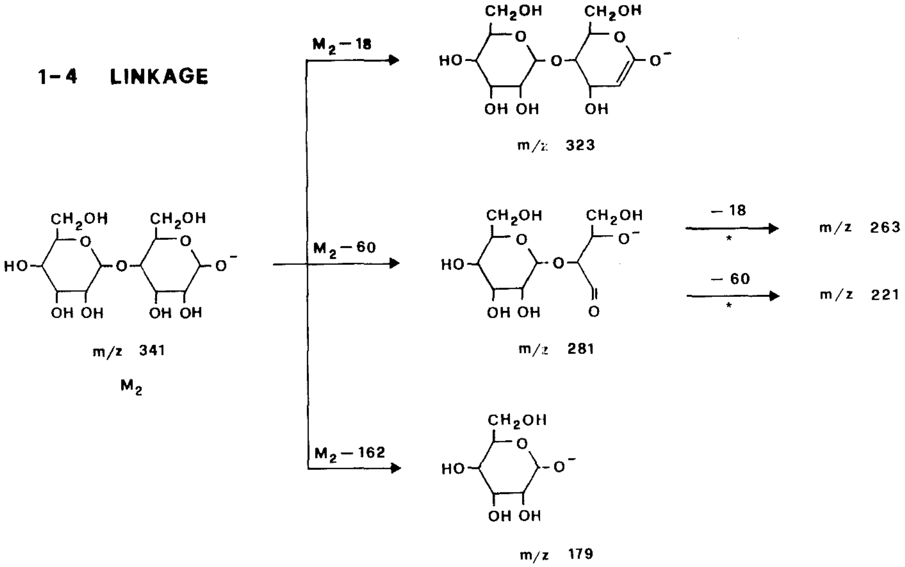
1-4 LINKAGE
m/z 341
M2
M2 − 18
m/z 323
M2 − 60
m/z 281
− 18
m/z 263
− 60
m/z 221
M2 − 162
m/z 179

* Confirmed by B^2/E linked scans

321 is present in two of the 1–3 disaccharides in Figure 5. This peak is also occasionally present in the spectra of other compounds (Figures 2–4). B^2/E scans have shown that it originates from the pseudomolecular ion at m/z 341 by two consecutive losses of 18 and 2 amu.

The presence of peaks at m/z 311 and 251 and the absence of the peaks at m/z 263 appear to be diagnostic of the 1–6 structure. The presence of a peak at m/z 263 accompanied by an intense peak at m/z 281, coupled with the absence of peaks at m/z 311 and 251 is characteristic of the 1–4 structure.

Scheme III

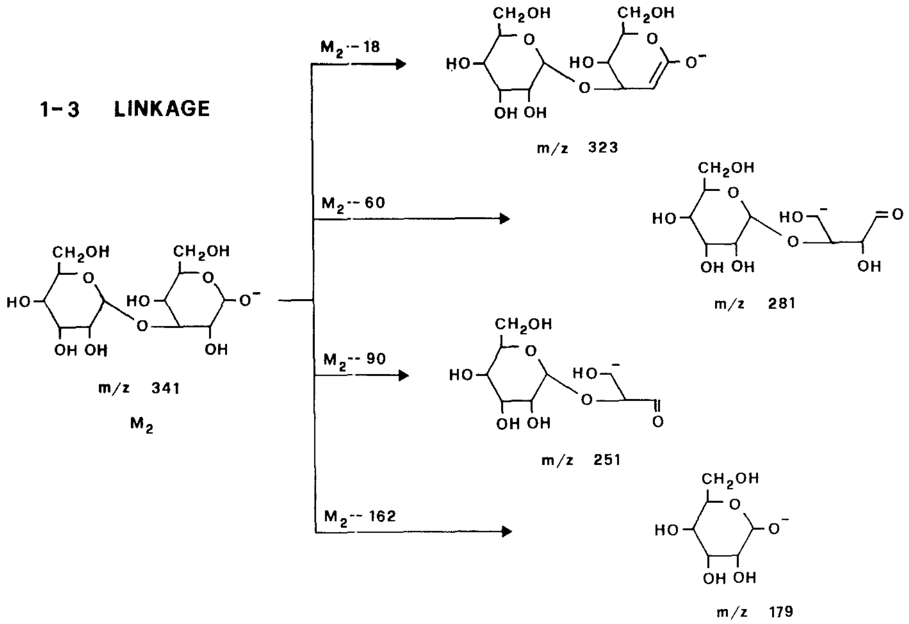
1-3 LINKAGE
CH2OH
HO
OH OH
OH
m/z 341
M2
M2·−18
m/z 323
M2·−60
m/z 281
M2·−90
m/z 251
M2·−162
m/z 179

Scheme IV

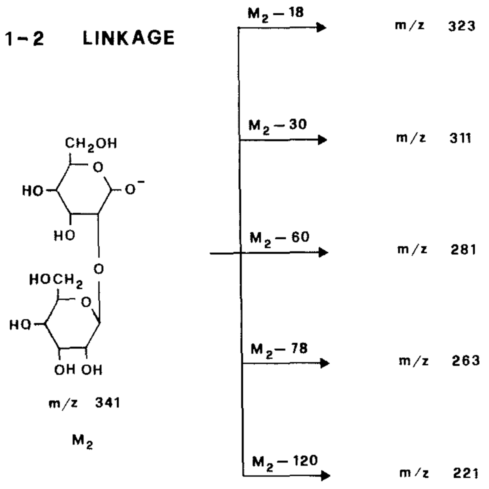
1-2 LINKAGE
CH2OH
HOCH2
HO
OH OH
m/z 341
M2
M2−18
m/z 323
M2−30
m/z 311
M2−60
m/z 281
M2−78
m/z 263
M2−120
m/z 221

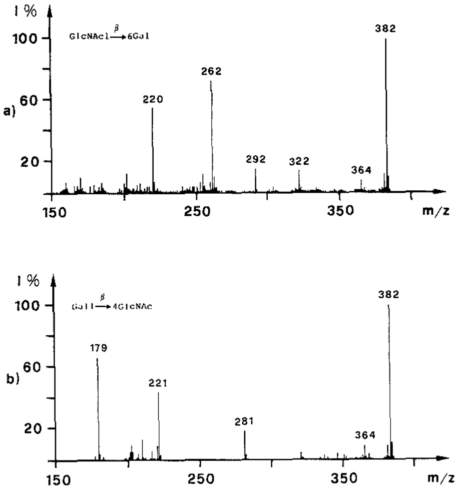

Figure 5. Negative ion FAB mass spectra of (a) GlcNAc1$\xrightarrow{\beta}$6Gal and (b) *N*-acetyllactosamine.

We have summarized in Table II a series of diagnostic peaks for the structures 1–6, 1–4, and 1–3, respectively.

Although only one 1–2 isomer (compound 1, Table I, Figure 1a) has been studied here, its fragmentation pattern (Scheme IV) is highly characteristic. In fact, the presence of peaks at *m/z* 311, 281, 263, and 221 and the absence of the peak at *m/z* 251 allows its discrimination.

Although further 1–2 disaccharides have to be analyzed to confirm these results, we have tentatively included in Table II also a series of peaks diagnostic for the 1–2 glycosidic linkage.

Determination of the Reducing End. The study of the saccharides considered so far has shown that FAB negative ion linked scans mass spectra can be used to differentiate linkage positions in hexose–hexose disaccharides. However, all the monosaccharide units contained in these compounds are stereoisomers and they cannot be discriminated by MS methods.

Sequence information can be obtained by MS when there is a molecular weight difference between the monosaccharide units in the molecule.

The FAB mass spectra of two acetylamino disaccharides (compounds **12** and **13**, Table I) are reported in Figure 5. These sugars are isomeric and their reducing units have different masses.

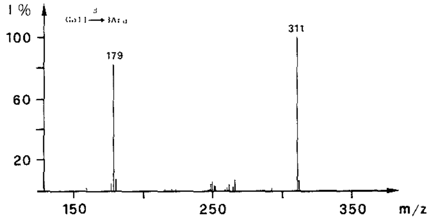

Figure 6. Negative ion FAB mass spectrum of Gal1$\xrightarrow{\beta}$3Ara.

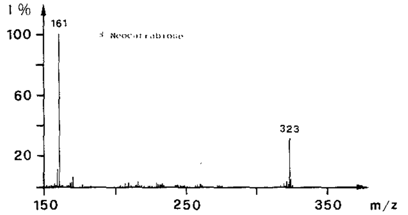

Figure 7. Negative ion FAB mass spectrum of β-neocarrabiose.

The spectra in Figure 5 show intense peaks at m/z 220 (M_2 - 162) and m/z 179 (M_2 - 201), respectively, that reflect the expected mass losses.

This evidence allows the assignments of the saccharides sequencial arrangement and confirms the hypothesis that the formation of the pseudomolecular ion corresponds to a selective deprotonation of the anomeric carbon hydroxyl.

The negative ion FAB mass spectrum of

$$\text{Gal1}\xrightarrow{\beta}\text{3Ara}$$

(compound 14, Table I), reported in Figure 6, shows the pseudomolecular ion at m/z 311, since this compound is an hexose–pentose disaccharide. The peak at m/z 179 in this spectrum corresponds to the loss of the pentose reducing unit.

Noticeably, the peak at m/z 149, which would correspond to hexose unit loss, is not detectable in the spectrum and rules out the alternative isomeric structure with the galactose reducing end unit.

In a further example, the sugar sequence present in β-neocarrabiose (compound **15**, Table I) is established by the appearance of the peak at m/z 161 in the negative ion FAB spectrum reported in Figure 7. This peak corresponds to a 162 amu loss (galactose reducing unit) from the pseudomolecular ion at m/z 323.

Also in this case, the absence of a peak at m/z 179 is highly indicative, since it would correspond to the anhydrogalactose unit loss.

Determination of the reducing end in the above disaccharides is therefore afforded by the study of negative ion FAB mass spectra.

The analysis of the daughter ion spectra should yield information also on the glycosidic linkage position in these compounds, since the ring fragmentation is sensitive to this structural parameter.

In the negative ion B/E spectrum of

$$\text{GlcNHAc1}\xrightarrow{\beta}\text{6Galp}$$

in Figure 8a are present peaks corresponding to losses of 18, 30, 60, 90, 120, and 162 amu and is absent the peak corresponding to loss of 78 amu like in the other 1–6 disaccharides (Table II).

The linked scan B/E mass spectrum of N-acetyllactosamine in Figure 8b shows peaks at m/z 281 and 263 characteristic of the 1–4 glycosidic linkage (Table II).

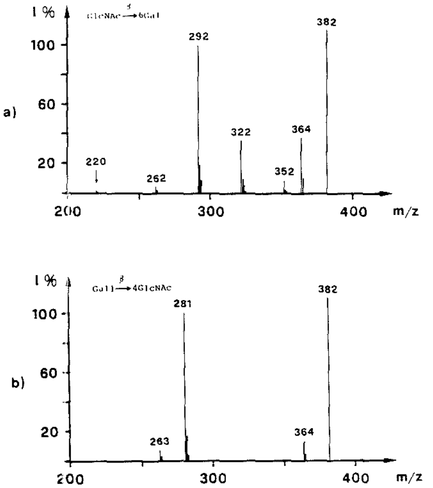

Figure 8. Negative ion B/E linked scans FAB mass spectra of the pseudomolecular ion of (a) GlcNAc1$\xrightarrow{\beta}$6Gal and (b) N-acetyllactosamine.

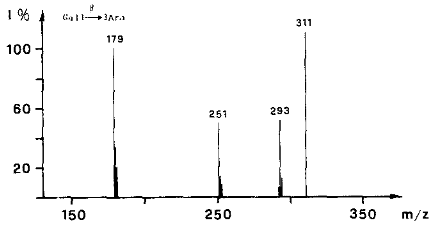

Figure 9. Negative ion B/E linked scans FAB mass spectra of the pseudomolecular ion of Gal1$\xrightarrow{\beta}$3Ara.

The negative ion B/E linked scan mass spectrum of the pseudomolecular ion of

$$\text{Gal1}\xrightarrow{\beta}\text{3Arab}$$

(Figure 9) reveals that the fragmentation pattern of the pentose ring is very similar to that of the 1–3 isomers studies (Scheme III). Particularly relevant appears the absence of the peak corresponding to a 30 amu loss, indicative of a correct assignment to the 1–3 linkage position (Table II). More data on the pentose rings fragmentation patterns should be acquired, however, in order to test further this assignment.

Oligosaccharides. It is now crucial to discuss how the results obtained in the case of disaccharides can be extended to oligosaccharides and how the negative FAB spectra can be used to establish the sequence and linkage position existing in larger saccharide molecules. Success at this stage would open the way to the structural analysis of polysaccharides, since oligosaccharides of significant size may be obtained by partial degradation from the macromolecular saccharides.

The negative ion B/E linked scan FAB mass spectrum of the pseudomolecular ion of maltotriose (compound **16**, Table I) is reported in Figure 10. The primary loss of 60 amu (peak at m/z 443) from the pseudomolecular ion at m/z 503 (M_3) and the peak at m/z 425 (loss of water from the ion at m/z 443), together with the absence of peaks corresponding to losses of 30 and 90 amu clearly reveal the 1–4 linkage of the reducing unit in maltotriose (Scheme II, Table II). The intense peak at m/z 341 (M_2) in Figure 10 is due to the negatively

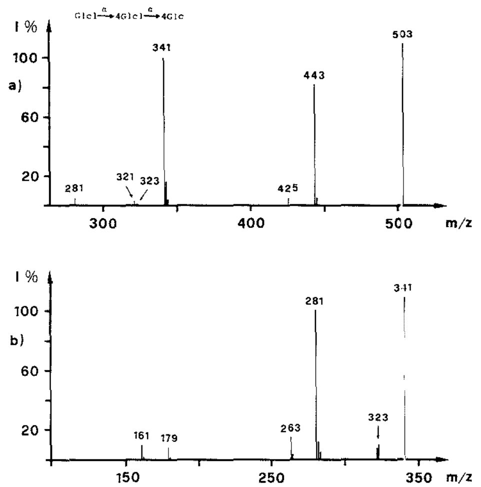

Figure 10. Negative ion B/E linked scans FAB mass spectra of (a) a pseudomolecular ion of maltotriose and (b) peak at m/z 341 of maltotriose.

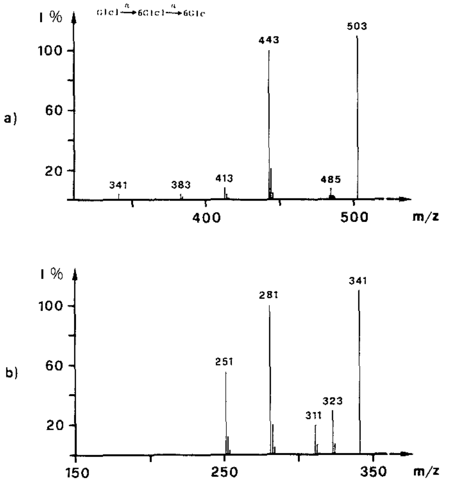

Figure 11. Negative ion B/E linked scans FAB mass spectra of (a) pseudomolecular ion of isomaltotriose and (b) peak at m/z 341 of isomaltotriose.

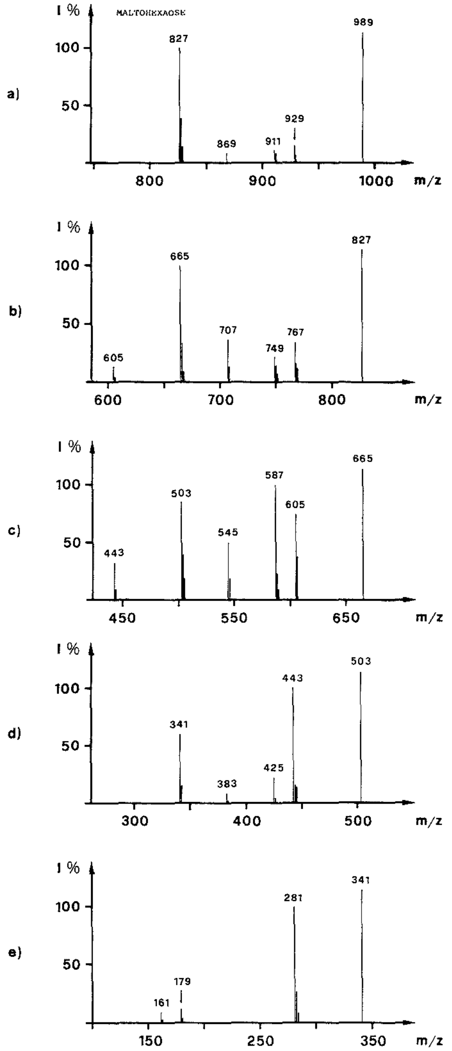

Figure 12. Negative ion B/E linked scans FAB mass spectra of maltoexaose: (a) pseudomolecular ion, (b) peak at m/z 827, (c) peak at m/z 665, (d) peak at m/z 503, (e) peak at m/z 341.

charged disaccharide moiety resulting from the glucose unit loss in maltotriose.

The spectrum in Figure 10a cannot be reliably used in order to get information on the linkage type between the first and second ring in the trisaccharide, since the intensities of the metastable transitions below m/z 341 are too weak.

It is more appropriate, instead, to look at the daughter ions deriving from the peak at m/z 341. The CAD negative ion FAB B/E spectrum of the peak at m/z 341 in maltotriose is reported in Figure 10b. The 1–4 linkage is identified by the presence of the peaks at m/z 281 and 263 and by the absence of peaks at m/z 311 and 251 (Scheme II, Table II).

The negative daughter ion FAB mass spectrum of isomaltotriose (compound 17, Table I) is reported in Figure 11a. The primary losses at m/z 473 ($M_3 - 30$; very weak) and m/z 413 ($M_3 - 90$), together with the absence of the peak at m/z 425 ($M_3 - 78$), are diagnostic of the 1–6 linkage of the reducing unit in isomaltotriose.

The negative ion FAB B/E linked scan mass spectrum of the peak at m/z 341 is reported in Figure 11b. The 1–6 linkage type between the first and second glucose rings in the disaccharide is identified by the presence of the peaks at m/z 311 and 251 together with the absence of the peak at m/z 263 (Scheme I).

This method of linkage type discrimination can be applied also to higher oligomers. The negative daughter ions spectrum of maltohexaose (compound 18, Table I) is reported in Figure 12a.

The losses of 60 and 78 amu from the pseudomolecular ion M_6 at m/z 989 (peaks at m/z 929 and m/z 911, respectively) and the absence of the peaks corresponding to 30 and 90 amu losses (peaks at m/z 959 899, respectively) identify the 1–4

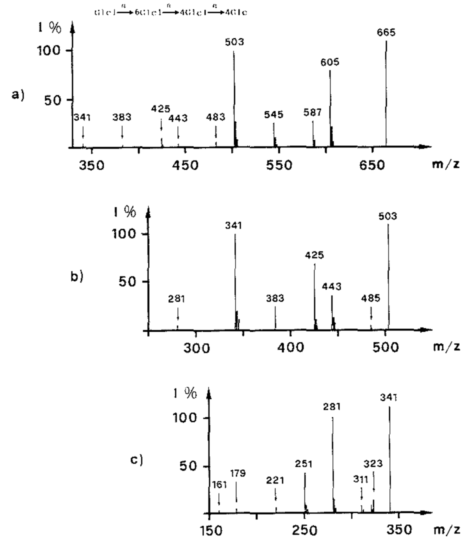

Figure 13. Negative ion B/E linked scans FAB mass spectra of Glc1$\xrightarrow{\alpha}$6Glc1$\xrightarrow{\alpha}$4Glc1$\xrightarrow{\alpha}$4Glc: (a) pseudomolecular ion, (b) peak at *m/z* 503, (c) peak at *m/z* 341.

linkage type between rings 5 and 6 of this oligosaccharide.

B/E spectra in Figures 12b–d show losses identical with those in Figure 11a, identifying therefore the 1–4 linkage type between rings 4–5, 3–4, 3–2, and 2–1, respectively.

Therefore, the 1–4 linkage existing in maltohexaose can be demonstrated for all the ring connections in the oligosaccharide.

The last example that we wish to discuss here is a tetrasaccharide

$$\mathrm{Glc1}\xrightarrow{\alpha}\mathrm{6Glc1}\xrightarrow{\alpha}\mathrm{4Glc1}\xrightarrow{\alpha}\mathrm{4Glc}$$

(compound 19, Table I). The negative daughter ion spectrum of this oligosaccharide is reported in Figure 13a, showing the losses of 60 and 78 amu from the pseudomolecular ion at *m/z* 665 (peaks at *m/z* 605 and *m/z* 587, respectively), and the absence of the peaks corresponding to losses of 30 and 90 amu, diagnostic of the 1–4 linkage between rings 3–4.

The daughter ion spectrum of the peak at *m/z* 503, reported in Figure 13b, shows the same features of the molecular ion at *m/z* 665 in Figure 12c, and therefore also the 1–4 linkage type between rings 2–3 can be ascertained.

Finally, the B/E scan of the peak at *m/z* 341, in Figure 13c, shows the peaks characteristic of the 1–6 linkage (Scheme II).

This result is particularly important because the discrimination of the linkage type establishes the sequence of the glycoside linkages existing in the tetrasaccharide.

Registry No. 1, 554-91-6; 2, 528-50-7; 3, 34980-39-7; 4, 534-46-3; 5, 585-99-9; 6, 499-40-1; 7, 69-79-4; 8, 63-42-3; 9, 50468-56-9; 10, 497-48-3; 11, 34141-02-1; 12, 20212-77-5; 13, 32181-59-2; 14, 6057-48-3; 15, 79297-08-8; 16, 1109-28-0; 17, 3371-50-4; 18, 34620-77-4; 19, 35175-16-7.

LITERATURE CITED

(1) *The Polysaccharides*; Aspinall, G. O., Ed.; Academic: New York, 1982; Vol. 1. 1983; Vol. 2. 1984; Vol. 3.
(2) Bjorndal, H.; Hellerquist, C. G.; Lindberg, B.; Svensson, S. *Angew. Chem., Int. Ed. Engl.* **1970**, *9*, 610.
(3) Bjorndal, H.; Lindberg, B.; Svensson, S. *Carbohydr. Res.* **1967**, *5*, 433.
(4) Bjorndal, H.; Lindberg, B.; Pilotti, A.; Svensson, S. *Carbohydr. Res.* **1970**, *15*, 339.
(5) Hakomori, S. I. *J. Biochem.* **1964**, *55*, 205.
(6) Laine, R. A. *Anal. Biochem.* **1981**, *116*, 383.
(7) Ciucanu, L.; Kerek, F. *Carbohydr. Res.* **1984**, *131*, 209.
(8) *The Polysaccharides*; Aspinall, G. O., Ed.; Academic: New York, 1982; Vol. 1, Chapter 4.
(9) Domon, B.; Costello, C. E. *Biochemistry* **1988**, *27*, 1534.
(10) Dell, A.; Taylor, G. W. *Mass Spectrom. Rev.* **1984**, *3*, 357.
(11) Deutsch, J. *Org. Mass Spectrom.* **1980**, *15*, 240.
(12) Costello, C. E.; Wilson, B. W.; Biemann, K.; Reinhold, V. N. *Cell Surface Glycolipids*; Sweeley, C. C., Ed.; ACS Symp. Ser. 128; **1980**; American Chemical Society: Washington, DC, p 35.
(13) Coates, M. L.; Wilkins, C. L. *Biomed. Mass Spectrom.* **1985**, *12*, 424.
(14) Coates, M. L.; Wilkins, C. L. *Anal. Chem.* **1987**, *22*, 6.
(15) Chen, Y.; Chen, N.; Li, M.; Zhao, F.; Chen, N. *Biomed. Mass Spectrom.* **1987**, *14*, 9.
(16) Kamerling, J. P.; Heerma, W.; Vliengenthart, F. G.; Green, N. B.; Lewis, I. A. S.; Strecker G.; Spik, G. *Biomed. Mass Spectrom.* **1983**, *10*, 420.
(17) Lam, Z.; Comisarow, M. B.; Dutton, G. G. S.; Weil, D. A.; Biarnson, A. *Rapid Commun. Mass Spectrom.* **1987**, *1*, 83.
(18) Prome, J. C.; Aurelle, M.; Prome, D.; Savagnac, D. *Org. Mass Spectrom.* **1987**, *22*, 6.
(19) Laine, R. A.; Pamidimukkala, K. M.; French, A. D.; Hall, R. W.; Abbas, S. A.; Jain, R. K.; Matta, K. L. *J. Am. Chem. Soc.* **1988**, *110*, 6931.
(20) Lam, Z.; Comisarow, M. B.; Dutton, G. G. S. *Anal. Chem.* **1988**, *60*, 2304
(21) Muller, D. R.; Doman, B.; Richter, W. J. In *Advances in Mass Spectrometry 11B*; Longevialle, P., Ed.; Heyden & Son: Chichester, 1989.
(22) Montaudo, G.; Scamporrino, E.; Vitalini, D. *Macromolecules* **1989**, *22*, 623, 627.
(23) Montaudo, G.; Puglisi, C.; Scamporrino, E.; Vitalini, D. *Macromolecules* **1988**, *21*, 1594.
(24) Ballistreri, A.; Garozzo, D.; Giuffrida, M.; Montaudo G. *Anal. Chem.* **1987**, *59*, 2024.
(25) Montaudo, G.; Puglisi, C.; Samperi, F. *Polym. Bull.* **1989**, *21*, 483.
(26) Ballistreri, A.; Garozzo, D.; Giuffrida, M.; Impallomeni, G.; Montaudo, G. *J. Anal. Appl. Pyrolysis* **1989**, *16*, 239.
(27) Ballistreri, A.; Garozzo, D.; Giuffrida, M.; Impallomeni, G.; Montaudo, G. *Macromolecules* **1989**, *22*, 2107.

RECEIVED for review July 21, 1989. Accepted October 18, 1989. Partial financial support from the Italian Ministry of Public Education and from Consiglio Nazionale delle Ricerche (Roma) is gratefully aknowledged.

Anal. Chem. 1990, 62, 287–293

Nitric Oxide Chemical Ionization Mass Spectrometry of Long-Chain Unsaturated Alcohols, Acetates, and Aldehydes

Christian Malosse and Jacques Einhorn*

INRA-CNRS, Laboratoire des Médiateurs Chimiques, Magny-les-Hameaux, 78470 St-Rémy-les-Chevreuse, France

Nitric oxide chemical ionization mass spectrometry (CI-NO$^+$-MS) has proved to be a highly efficient tool for locating the CC double bond in long-chain monounsaturated alcohols, acetates, and aldehydes of type $CH_3(CH_2)_xCH{=}CH(CH_2)_yR$ (R = CH_2OH, CH_2OAc, or CHO). The double bond assignment is mostly provided by the presence of an acylium ion $C_{x+2}H_{2x+3}O^+$ formed from the alkyl side of the molecule. When the double bond is close to the terminal oxygen function ($y \leq 2$), a $C_{y+3}H_{2y+4}NO^+$ ion may also be used as complementary diagnostic ion. In the case of di- or triethylenic compounds, an acylium ion is also formed which characterizes the external (unconjugated) double bond position. From the observed strong influence of the sample pressure on the formation of the acylium ion and results of MS/MS experiments, two mechanisms are proposed to explain the origin of this diagnostic ion. Although some instrument dependence may not be excluded, the method is optimally applicable to moderate sample loads (20–200 ng in our conditions).

INTRODUCTION

Long-chain unsaturated alcohols, acetates, and aldehydes are the most common structures found thus far in insect pheromones (*1*). In several Lepidopteran species of economic importance, these compounds, generally included in multicomponent blends, can play a major role in sexual behavior. In order to assure efficacy and reliability of the synthetic lures used in agriculture or forest pest management, it is thus important to initially determine the pheromone structure and composition with the highest precision (*2*).

In this context, the localization of the double bonds often represents the main difficulty due to the very small amounts of material available (10^{-2} to 10 μg per component). It is usually achieved by chemical derivatization (*3, 4*) or oxidative degradation (*5*) methods followed by gas chromatography–mass spectrometry (GC–MS) analysis. To avoid this time- and material-exhaustive methodology, we have investigated the potentialities of gas-phase ion–molecule reactions for direct determination of the double bond position.

Although electron impact mass spectrometry (EIMS) may be used to differentiate to some extent (*6, 7*) between positionally isomeric alkenes, the in situ chemical derivatization method is the most promising approach for unambiguous assignments. The recent concept of remote charge fragmentation associated with collisionally activated dissociation (CAD) spectra might also be considered (*8–10*), but its use seems limited to the presence of certain terminal functions (mainly acids and acid derivatives) or to certain positions of unsaturation (*11*).

Various reagent gases such as vinyl ethers (*12, 13*), amines (*14, 15*), isobutane (*14*), and the Fe$^+$ cation obtained from $Fe(CO)_5$ (*16*) have been used in the case of usually unfunctionalized monoolefins. CI-NO$^+$-MS may also be used (*14, 17, 18*). In the case of unsubstituted monoolefins, two complementary ions of general formula $C_nH_{2n}NO^+$ and a third one, $C_{n-1}H_{2n}NO^+$, were found by Budzikiewicz and Busker (*14*) to determine the position of unsaturation.

The purpose of this study was to examine the possible application of CI-NO$^+$-MS for double bond location in long-chain alkenes containing a terminal oxygen function, such as acetates (*19*), alcohols, or aldehydes

$$CH_3(CH_2)_xCH{=}CH(CH_2)_yR$$
$$R = CH_2OH,\ CH_2OAc,\ CHO$$

Investigations have also been performed to determine to what extent polyunsaturated compounds and double bond geometry can be analyzed using NO$^+$ as reagent.

EXPERIMENTAL SECTION

The CI-NO$^+$ mass spectra were recorded using Nermag R-10-10C GC-MS equipment (France) with the following conditions: *T*(source), 80 °C; filament current, 200 μA; electron energy, 95 eV; nitric oxide (99.9% from Air Liquide, France) at a 0.2 Torr pressure (or 1.6×10^{-4} Torr in the source housing) giving rise to a $(NO)_2^+/NO^+$ ion ratio $<10^{-3}$. The *Z* or *E* unsaturated alcohols, acetates, and aldehydes were synthesized by standard methods (*20*) in the Laboratoire des Médiateurs Chimiques. Samples (50 ng) were introduced with a Ros injector (unless otherwise specified) via a 25 m × 0.32 mm CPSIL 5CB (Chrompack, The Netherlands) GC capillary column at a temperature depending on the substrate.

The MS–MS spectra were obtained with a triple quadrupole instrument MS/R-30-10 Nermag at Ecole Normale Supérieure and at Université P. et M. Curie, Paris. The source conditions were the same as those indicated above. Laboratory collision energy was 35 eV and argon was used as collision gas in the second quadrupole. Samples were introduced by GC or via direct inlet probe.

Exact mass measurements were performed on a ZAB-2F reverse geometry mass spectrometer.

RESULTS AND DISCUSSION

Reactivity of Monounsaturated Acetates. The CI-NO$^+$-MS spectra obtained from the complete E series of C_{12}-monounsaturated acetates (Figure 1) exhibit ions at *m/z* 256 corresponding to the (M + NO)$^+$ adduct ion and *m/z* 225 (not detected for all isomers) (M – H)$^+$. Ions at *m/z* 214 and 196 are also sometimes present which result from the (M + NO)$^+$ adduct ion by loss of neutral CH_2CO or AcOH, respectively. Two generally abundant ions are observed at *m/z* 165 and 166. The former corresponds to a ((M – H) – AcOH)$^+$ ion, whereas the second one may be formed from the undetected molecular ion M$^{\bullet+}$ (generated by a charge-exchange process) also by loss of an AcOH molecule. More interesting is the presence in the lower mass region of an abundant even- and/or odd-mass ion whose *m/z* value is clearly related to the position of the double bond. The existence of diagnostic ions of two types, i.e. even- or odd-mass ion, indicates a competition between two main processes depending on the position of the double bond relative to the oxygen function:

$y \geqslant 2$. In contrast to the diagnostic ions (even-mass ions containing NO) found in nonoxygenated alkenes (*14*), the diagnostic peak observed in the spectra of most of the positional isomers is due to an *odd*-mass ion. This ion, formed from the alkyl side of the molecule, is of $CH_3(CH_2)_xCO^+$ structure (see Structure and Origin of the Diagnostic Ions section). Remarkably, no complementary ion which would contain (or originate from) the functionalized end of the chain is observed. However, homologous ions may be found, the

© 1990 American Chemical Society

Table I. Main Ion Species from CI-NO^+ Spectra of Monounsaturated Acetates

	$(M + NO)^+$	$M^{\bullet +}$	$(M - H)^+$	$(M - AcOH)^{\bullet +}$	$((M - H) - AcOH)^+$	acylium ion	others
(*E*)-2-undecenyl acetate	242 (1)	212 (1)	211 (2)	152 (56)	151 (7)	141 (<1)	84 (100)
(*Z*)-4-dodecenyl acetate	256 (2)	226 n.d.[a]	225 n.d.	166 (85)	165 (94)	127 (97)	98 (100)
(*Z*)-5-dodecenyl acetate	256 (7)	226 n.d.	225 (<1)	166 (47)	165 (65)	113 (100)	
(*Z*)-8-dodecenyl acetate	256 (7)	226 (<1)	225 (<1)	166 (39)	165 (46)	71 (100)	
(*Z*)-9-dodecenyl acetate	256 (1)	226 (<1)	225 n.d.	166 (4)	165 (14)	57 (100)	
(*Z*)-10-dodecenyl acetate	256 (1)	226 n.d.	225 n.d.	166 (14)	165 (17)	43 (100)	
(*Z*)-5-tetradecenyl acetate	284 (36)	254 n.d.	253 n.d.	194 (82)	193 (100)	141 (78)	
(*E*)-5-tetadecenyl acetate	284 (13)	254 n.d.	253 (4)	194 (53)	193 (70)	141 (100)	
(*Z*)-6-tetradecenyl acetate	284 (18)	254 n.d.	253 (<1)	194 (40)	193 (49)	127 (100)	
(*E*)-6-tetradecenyl acetate	284 (4)	254 n.d.	253 (1)	194 (18)	193 (27)	127 (100)	
(*Z*)-8-tetradecenyl acetate	284 (9)	254 n.d.	253 (1)	194 (38)	193 (36)	99 (100)	
(*E*)-8-tetradecenyl acetate	284 (3)	254 n.d.	253 (2)	194 (49)	193 (51)	99 (100)	
(*Z*)-9-tetradecenyl acetate	284 (14)	254 (<1)	253 (2)	194 (50)	193 (37)	85 (100)	
(*E*)-9-tetradecenyl acetate	284 (6)	254 (<1)	253 (4)	194 (49)	193 (53)	85 (100)	
(*Z*)-11-tetradecenyl acetate	284 (12)	254 n.d.	253 (1)	194 (20)	193 (16)	57 (100)	
(*E*)-11-tetradecenyl acetate	284 (21)	254 (1)	253 (4)	194 (56)	193 (67)	57 (100)	
(*Z*)-7-hexadecenyl acetate	312 (5)	282 (<1)	281 (<1)	222 (56)	221 (39)	141 (100)	
(*Z*)-9-hexadecenyl acetate	312 (5)	282 n.d.	281 (<1)	222 (29)	221 (22)	113 (100)	
(*Z*)-11-hexadecenyl acetate	312 (17)	282 n.d.	281 (<1)	222 (45)	221 (33)	85 (100)	

[a] n.d. = not detected.

Table II. Main Ion Species from CI-NO^+ Spectra of Monounsaturated Alcohols

	$((M - 2H) + NO)^+$	$(M - 2H)^{\bullet +}$	$(M - 3H)^+$	$((M - 2H) - H_2O)^{\bullet +}$	$((M - 3H) - H_2O)^+$	acylium ion	others
(*E*)-2-dodecene-1-ol	212 (3)	182 (14)	181 (100)	164 n.d.	163 n.d.	155 (59)	
(*E*)-3-dodecene-1-ol	212 (4)	182 (8)	181 (19)	164 (42)	163 (5)	141 (48)	84 (61), 70 (41)
(*E*)-5-dodecene-1-ol	212 (2)	182 (11)	181 (33)	164 (23)	163 (11)	113 (60)	
(*E*)-6-dodecene-1-ol	212 (2)	182 (8)	181 (14)	164 (10)	163 (3)	99 (100)	
(*Z*)-6-dodecene-1-ol	212 (1)	182 (3)	181 (4)	164 (7)	163 (2)	99 (100)	
(*E*)-8-dodecene-1-ol	212 n.d.[a]	182 (1)	181 (1)	164 (2)	163 (1)	71 (100)	
(*Z*)-8-dodecene-1-ol	212 n.d.	182 (1)	181 (1)	164 (1)	163 (<1)	71 (100)	
(*E*)-9-dodecene-1-ol	212 n.d.	182 (1)	181 (1)	164 (1)	163 n.d.	57 (100)	
(*Z*)-9-dodecene-1-ol	212 (<1)	182 (1)	181 (<1)	164 (1)	163 n.d.	57 (100)	
(*E*)-5-tetradecene-1-ol	240 (7)	210 (10)	209 (29)	192 (35)	191 (16)	141 (49)	
(*E*)-6-tetradecene-1-ol	240 (1)	210 (5)	209 (20)	192 (42)	191 (12)	127 (78)	
(*E*)-7-tetradecene-1-ol	240 n.d.	210 (4)	209 (14)	192 (27)	191 (4)	113 (100)	
(*Z*)-8-tetadecene-1-ol	240 (2)	210 (9)	209 (13)	192 (28)	191 (3)	99 (100)	
(*Z*)-9-tetradecene-1-ol	240 (2)	210 (5)	209 (5)	192 (10)	191 (2)	85 (100)	
(*E*)-10-tetradecene-1-ol	240 (7)	210 (29)	209 (35)	192 (40)	191 (11)	71 (100)	
(*Z*)-10-tetradecene-1-ol	240 (1)	210 (4)	209 (3)	192 (7)	191 (1)	71 (100)	
(*E*)-11-tetradecene-1-ol	240 (14)	210 (28)	209 (40)	192 (38)	191 (13)	57 (100)	
(*Z*)-11-tetradecene-1-ol	240 (3)	210 (6)	209 (3)	192 (2)	191 (<1)	57 (100)	
(*E*)-8-hexadecene-1-ol	268 (6)	238 (10)	237 (24)	220 (24)	219 (3)	127 (100)	
(*Z*)-9-hexadecene-1-ol	268 (12)	238 (20)	237 (30)	220 (41)	219 (1)	113 (100)	
(*Z*)-11-hexadecene-1-ol	268 (2)	238 (6)	237 (9)	220 (34)	219 (1)	85 (100)	

[a] n.d. = not detected.

lower mass ones being more pronounced for some isomers (from Δ4 to Δ7 in this case). This indicates that some isomerization may occur during the formation of the diagnostic ion.

$y \leqslant 2$. When the double bond is positioned close to the terminal function, an *even*-mass ion presumably containing NO, hence corresponding to a $(C_{y+3}H_{2y+4}NO)^+$ formula (see Structure and Origin of the Diagnostic Ions section), is produced. The mass spectrum of the Δ4 isomer is thus characterized by an abundant ion at m/z 98, but it also exhibits an odd-mass ion of high intensity at m/z 127, corresponding to the process mentioned above. In the CI-NO^+ mass spectra of the two other positional isomers, Δ3 and Δ2, the second process largely predominates. In fact, both spectra exhibit the same ion at m/z 84, due probably to isomerization in the latter case. Besides the odd-mass ions (m/z 141 and m/z 155, respectively) of low relative abundances for these positions of the double bond, examination of the 165/166 ion relative intensity ratio may be used to distinguish between positions 2 and 3 for proper assignment during structural analysis. This ratio which appears >1 for most isomers becomes slightly <1 (Δ3) or much smaller (Δ2) (see Figure 1).

Other examples from C_{11}, C_{12} (*Z* stereochemistry), C_{14}, and C_{16} series have been investigated (Table I). The same two types of diagnostic fragment ions are observed in the CI-NO^+ mass spectra and characterize the double bond position in these compounds.

Reactivity of Monounsaturated Alcohols. The CI-NO^+ mass spectra of the long chain monounsaturated alcohols (Table II) differ from those of the corresponding acetates by the presence of molecular species which are specific of the alcohol function (oxidation processes) (*21*). The $((M + NO) - 2H)^+$, $(M - 2H)^{\bullet +}$, $(M - 3H)^+$ as well as ions $((M - 2H) - H_2O)^{\bullet +}$ and $((M - 3H) - H_2O)^+$ are thus observed. In some cases, $(M - H_2O)^{\bullet +}$ and $((M - H) - H_2O)^+$ are also produced. The location of the CC double bond may be again determined by either an odd-mass and/or an even-mass fragment ion depending on the double bond position.

$y \geqslant 2$. For isomers with a double bond far enough from the terminal oxygen functionality, the formation of the odd-mass diagnostic ion appears as the major (if not the unique) characteristic process. Again, as for the unsaturated acetates,

Table III. Main Ion Species from CI-NO$^+$ Spectra of Monounsaturated Aldehydes

	$(M + NO)^+$	$M^{\bullet+}$	$(M - H)^+$	$(M - H_2O)^{\bullet+}$	$((M - H) - H_2O)^+$	acylium ion
(*E*)-5-dodecenal	212 (6)	182 (6)	181 (19)	164 (100)	163 (19)	113 (54)
(*Z*)-7-tetradecenal	240 (3)	210 (4)	209 (11)	192 (34)	191 (9)	113 (100)
(*Z*)-9-tetradecenal	240 n.d.[a]	210 (1)	209 n.d.	192 (4)	191 n.d.	85 (100)
(*Z*)-11-tetradecenal	240 (6)	210 (13)	209 (5)	192 (20)	191 (4)	57 (100)
(*Z*)-7-hexadecenal	268 (23)	238 (23)	237 (53)	220 (100)	219 (16)	141 (80)
(*E*)-9-hexadecenal	268 (1)	238 (5)	237 (12)	220 (23)	219 (3)	113 (100)
(*Z*)-9-hexadecenal	268 (2)	238 (4)	237 (5)	220 (11)	219 (5)	113 (100)
(*E*)-11-hexadecenal	268 (4)	238 (13)	237 (41)	220 (47)	219 (<1)	85 (100)
(*Z*)-11-hexadecenal	268 (81)	238 (2)	237 (2)	220 (9)	219 (<1)	85 (100)

[a] n.d. = not detected.

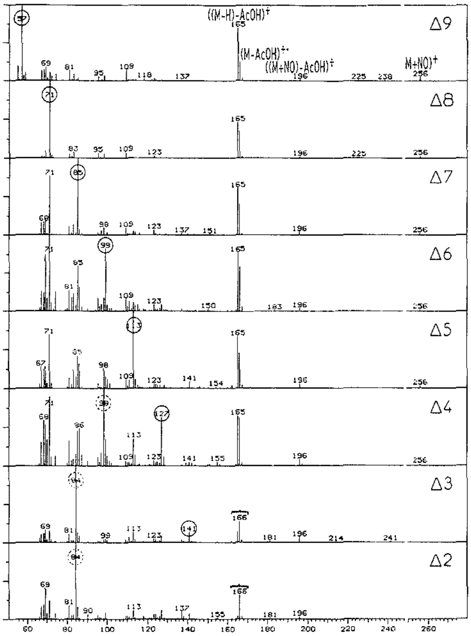

Figure 1. CI-NO$^+$ mass spectra of a series of C_{12}-monounsaturated acetates (*E* geometry) (closed circled number, odd-mass diagnostic ion; open circled number, even-mass diagnostic ion).

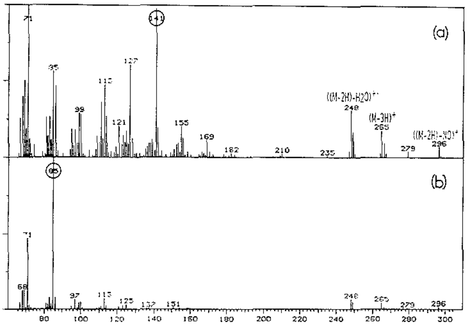

Figure 2. CI-NO$^+$ mass spectra of (*Z*)-9-octadecene-1-ol (a) and (*Z*)-13-octadecene-1-ol (b).

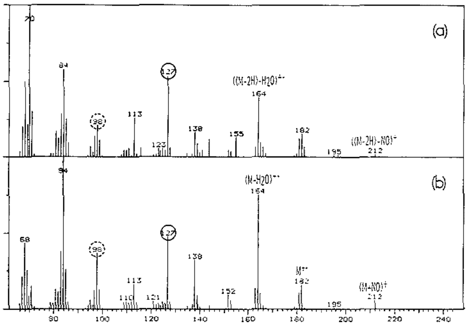

Figure 3. CI-NO$^+$ mass spectra of (*E*)-4-dodecene-1-ol (a) and (*E*)-4-dodecenal (b).

homologous ions, predominantly lower mass ones, are produced. The diagnostic ion is easily recognizable (Figure 2) as either the base peak of this series of ions or as the last one (i.e. highest *m/z* value) when considering only those of high relative abundances. In this case, the higher homologues clearly appear as much less abundant.

$y \leqslant 2$. Investigations carried out for the C_{12} series indicate the occurrence of two types of ions. The Δ4 position is characterized by the odd-mass fragment ion at *m/z* 127 (homologous ions of lower abundances at *m/z* 99 and *m/z* 113). On the other hand, a similar even-mass ion, as found in the Δ4-acetate spectrum, i.e. at m/z 98, is also present together with homologous or related ions at *m/z* 84, 70, and 68. A third series of ions at *m/z* 138 (major one) and *m/z* 152 is also detected (Δ3 and Δ2 isomers). The significance of these ions in relation to the double bond position is not clearly ascertained. However, the ions observed at *m/z* 127 and *m/z* 98 are sufficient to assign the position of the unsaturation. For the Δ3-isomer, the corresponding ions at *m/z* 141 (homologous ions of lower abundances at *m/z* 85, 99, 113, and 127) and *m/z* 84 (homologous ion at *m/z* 70) must be considered as the diagnostic ions. In the spectrum of the Δ2-isomer, the characteristic features are ions *m/z* 155 (odd-mass) and $(M - 3H)^+$ (base peak).

Reactivity of Monounsaturated Aldehydes. The $(M + NO)^+$ adduct ion as well as the $M^{\bullet+}$, $(M - H)^+$, $(M - H_2O)^{\bullet+}$, and $((M - H) - H_2O)^+$ ions are generally observed as molecular species or related fragment ions in the CI-NO$^+$ spectra of the unsaturated aldehydes (Table III). For isomers corresponding to $y \geqslant 2$, the same odd-mass diagnostic ion as that found for acetates and alcohols is generated. When the double bond is closer to the terminal function, the odd-mass fragment ion as well as an even-mass ion of $C_{y+3}H_{2y+4}NO^+$ type are the diagnostic peaks. In the case of (*E*)-4-dodecenal, for instance, these ions appear at *m/z* 127 and *m/z* 98 (homologous ion at *m/z* 84). Interestingly, this spectrum also exhibits ions *m/z* 68 and *m/z* 138 (cf. (*E*)-4-dodecenol) (Figure 3).

Differentiation between *Z* and *E* Isomers. Differentiation between *Z* and *E* isomers is possible by examining ratios of relative abundances of the odd-mass ion and its homologues. When such comparisons are performed after

Table IV. Main Ion Species from CI-NO^+ Spectra of Di- or Triunsaturated Acetates or Alcohols

acetates	$(M + NO)^+$	$M^{\bullet +}$	$(M - H)^+$	$(M - AcOH)^{\bullet +}$	$((M - H) - AcOH)^+$	acylium ion
(*E*,*E*)-7,9-dodecadienyl acetate	254 (5)	224 (63)	223 (2)	164 (100)	163 (2)	57 (26)
(*Z*,*E*)-9,12-tetradecadienyl acetate	282 (100)	252 (49)	251 (50)	192 (73)	191 (6)	43 (60)
(*E*,*Z*)-9,11-hexadecadienyl acetate	310 (1)	280 (5)	279 (2)	220 (4)	219 n.d.	85 (100)
(*Z*,*Z*,*Z*)-5,9,13-hexadecatrienyl acetate	308 (10)	278 (19)	277 (4)	218 (14)	217 (5)	57 (100)
(*E*,*E*,*Z*)-4,6,10-hexadecatrienyl acetate	308 (2)	278 (71)	277 (1)	218 (47)	217 (1)	99 (91)
(*Z*,*E*)-2,13-octadecadienyl acetate	338 (1)	308 n.d.[a]	307 n.d.	248 (16)	247 (5)	85 (100)
(*Z*,*Z*)-3,13-octadecadienyl acetate	338 (2)	308 (1)	307 (<1)	248 (12)	247 (7)	85 (100)

alcohols	$(M + NO)^+$	$M^{\bullet +}$	$(M - H)^+$	$(M - H_2O)^{\bullet +}$	$((M - H) - H_2O)^+$	acylium ion
(*E*,*Z*)-7,9-dodecadiene-1-ol	212 (9)	182 (100)	181 (9)	164 (88)	163 (9)	57 (74)
(*Z*,*E*)-9,12-tetradecadiene-1-ol	240 (26)	210 (61)	209 (38)	192 (27)	191 (4)	43 (27)
(*E*,*Z*)-9,11-hexadecadiene-1-ol	268 n.d.[a]	238 (4)	237 (2)	220 (1)	219 n.d.	85 (100)
(*E*,*Z*)-10,12-hexadecadiene-1-ol	268 (5)	238 (55)	237 (9)	220 (7)	219 (1)	71 (100)
(*E*,*Z*,*Z*)-4,6,10-hexadecatriene-1-ol	266 (<1)	236 (9)	235 (2)	218 (2)	217 (<1)	99 (45)
(*E*,*E*,*Z*)-4,6,10-hexasdecatriene-1-ol	266 (1)	236 (16)	235 (2)	218 (2)	217 (<1)	99 (61)
(*Z*,*Z*)-13,15-octadecadiene-1-ol	296 (5)	266 (65)	265 (10)	248 (7)	247 (<1)	57 (100)
(*Z*,*Z*)-9,12-octadecadiene-1-ol	296 (15)	266 (30)	265 (29)	248 (6)	247 (1)	99 (100)
(*Z*,*Z*,*Z*)-9,12,15-octadecatriene-1-ol	294 (8)	264 (25)	263 (11)	246 (<1)	245 (<1)	57 (34)

[a] n.d. = not detected.

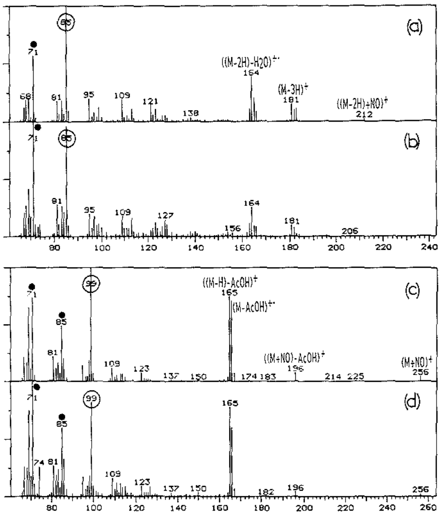

Figure 4. CI-NO^+ mass spectra of (a) (*Z*)- or (b) (*E*)-7-dodecene-1-ol and of (c) (*Z*)- or (d) (*E*)-6-dodecenyl acetate (●, lower homologue of the diagnostic ion).

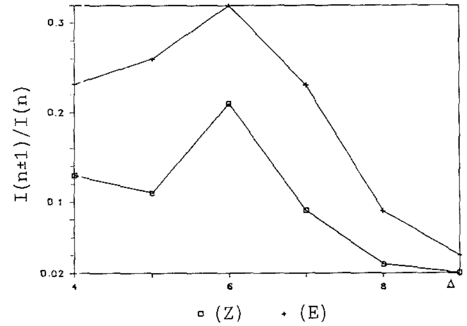

Figure 5. Comparison of the ($n \pm 1$) homologue/diagnostic ion relative abundance ratios in the CI-NO^+ mass spectra obtained from *E* and *Z* isomers of dodecenyl acetate. (The ($n - 1$) homologue is generally considered except if not available ($n + 1$)).

recording isomer series spectra using strictly identical experimental conditions (source temperature, reagent gas pressure, even sample pressure as demonstrated below) the (homologous ion)/(diagnostic-ion) relative intensity ratios appear higher for members of the *E* series than for the corresponding *Z* isomers. The distinction between both series may be done, for instance, on the basis of the ($n - 1$) and/or ($n - 2$) homologous ions (Figures 4 and 5) relative to the diagnostic ion. When the latter ion is of m/z value 71 or lower (i.e. Δ8 and Δ9 in the C_{12} series), the ($n + 1$) and/or ($n + 2$) homologues must be preferentially considered, since the lower mass ones are less accessible or not formed. The noticeable conservation of a stereochemical effect excludes the formation of a common intermediate carbocation in both series. It is evident, however, in spite of these observations, that no prediction of the double bond geometry for any unknown compound should be performed without comparison to both authentic geometrical isomer spectra obtained under exactly the same conditions.

Reactivity of Di- or Triunsaturated Compounds. Several C_{12}–C_{18} linear compounds containing two or three double bonds of various distribution along the chain and a terminal oxygen function have been investigated under CI-NO^+ conditions (Table IV). According to these studies, it appears that a characteristic odd-mass fragment ion is produced from cleavage at the external double bond, providing a method for systematically assigning this position in a polyunsaturated system (Figure 6). The only limitation is, as also noticed for monounsaturated compounds, when the double bond is positioned at the extremity of the chain. No significant diagnostic ion is formed or may be observed (plasma region) in this case. Note also that if the external unsaturation is conjugated, the corresponding odd-mass diagnostic ion is generally produced. However, in some cases (i.e. (*E*,*Z*)-7,9-dodecadienol), the formation of an ($n + 1$) homologous ion of high relative abundance (>50% of the diagnostic peak) may cause some difficulty during assignment of such double bond. Other reagents particularly appropriate for location of conjugated diene systems (*22–24*) should then be used preferentially.

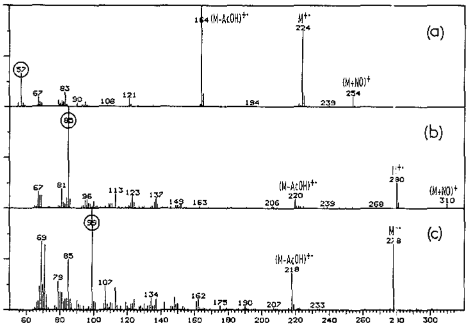

Figure 6. CI-NO$^+$ mass spectra of (*E,Z*)-5,9-dodecadienyl acetate (a), (*Z,Z*)-4,7-hexadecadienyl acetate (b), and (*Z,Z,Z*)-4,6,10-hexadecatrienyl acetate (c).

Scheme I. Origin of the Even-Mass Diagnostic Ion, Possible Pathways According to MS/MS Studies

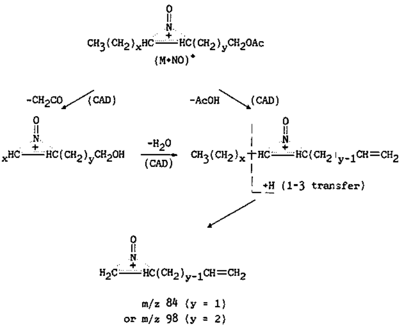

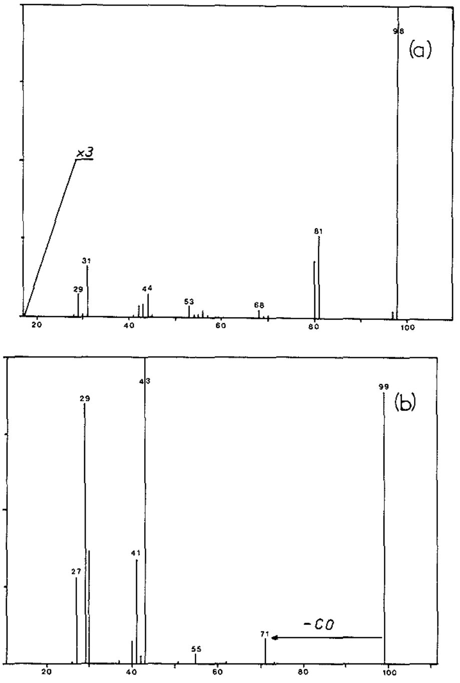

Figure 7. Constant parent ion spectra for ions *m/z* 98 (a) from (*E*)-4-dodecenyl acetate and 99 (b) from (*E*)-6-dodecenyl acetate under CI-NO$^+$ conditions. (The ×3 factor (cf. (a)) applies to all ions except the parent ion.)

As for homoconjugated trienes (i.e. (*Z,Z,Z*)-9,12,15-octadecatriene-1-ol), although acylium ions may be formed from the external double bond, the previously reported diagnostic radical ion fragments (*25*) (i.e., in this case, at *m/z* 108 and 208) appear as much more characteristic.

Structure and Origin of the Diagnostic Ions. Even-Mass Diagnostic Ion. Two ions of this type (i.e. *m/z* 98 and *m/z* 84) have been found that characterize Δ4 and Δ3/or Δ2 isomers, respectively (cf. monounsaturated compounds). The origin of these ions has been studied by using MS/MS experiments.

The constant parent ion spectra determined for ions *m/z* 256 or (M + NO)$^+$, 196 or ((M + NO) − AcOH)$^+$ from (*E*)-4-dodecenyl acetate showed ions *m/z* 196 and 98 as major or highly abundant daughter ions, respectively. On the other hand, the constant daughter ion spectrum examined for *m/z* 98 displayed ion *m/z* 196 as the major precursor ion. Since ion *m/z* 214 corresponding to ((M + NO) − CH_2CO)$^+$ also generated *m/z* 196 (constant neutral spectrum for the loss of 18 amu), the following pathways, involving thermal decomposition from the terminal acetate, might be proposed to rationalize the formation of ion *m/z* 98 (or its homologue *m/z* 84) (Scheme I).

The suggested crude formula ($C_{y+3}H_{2y+4}NO^+$) of the resulting diagnostic ion is in agreement with the constant parent ion spectra for ions *m/z* 98 ((*E*)-4-dodecenyl acetate) (Figure 7a) and *m/z* 84 ((*E*)-3-dodecenyl acetate) which display ions generated by losses of 17 amu (OH$^\bullet$ or likely NH_3) and 18 amu (H_2O). The NO content is particularly apparent from the constant daughter ion spectra for *m/z* 31 (HNO) and *m/z* 45 (CH_3NO) (cf. (*E*)-4-dodecenyl acetate), since both exhibit *m/z* 98 as one of the major precursor ions.

Finally, the constant parent ion spectrum for ion *m/z* 98 ((*E*)-4-dodecenyl acetate) was found to be identical with that obtained for the (M + NO)$^+$ adduct ion formed from 1,4-pentadiene under CI-NO$^+$ conditions, providing further evidence of the proposed structure for the even-mass diagnostic ion.

Odd-Mass Diagnostic Ion. According to accurate mass measurements the odd-mass diagnostic ion is of acylium type (i.e. $C_{x+2}H_{2x+3}O^+$). A small percentage of an alkyl ion was also observed in the low resolution peak (e.g. *m/z* 99 for (*E*)-6-dodecenyl acetate). The acylium/alkyl ion relative intensity ratio increased from 1:1 to 4:1 when NO pressure was raised from 0.8 to 2 × 10^{-4} Torr (source housing). These results agree with other measurements (*26*) in regard to the nature of the diagnostic ion. As to the observed effect of increasing NO pressure on the yield of the acylium ion, it must be noted that an inverse behavior has been reported for increasing source temperature (*26*). These parameters must be taken into account for optimal production of acylium ion as the diagnostic ion as follows: (i) NO pressure set to a sufficiently high value (about 1.5 × 10^{-4} Torr in the source housing of our low resolution instrument); (ii) "cold" source.

Furthermore, we have demonstrated the acylium-type structure by recording the constant parent ion spectrum for *m/z* 99 ((*Z*)-6-dodecenyl acetate). This CAD spectrum (Figure 7b) shows an ion at *m/z* 71 (loss of CO) but none at *m/z* 57 (loss of 42 amu). These data unambiguously characterize (*27*) an acylium ion structure vs an alkyl ion. Moreover, we can conclude that this is $CH_3(CH_2)_4CO^+$ since the above spectrum is found to be identical with the CAD spectrum of ion *m/z* 99 generated from hexanoyl chloride under EI conditions. The acylium structure of the homologous ions *m/z* 71 and *m/z* 85

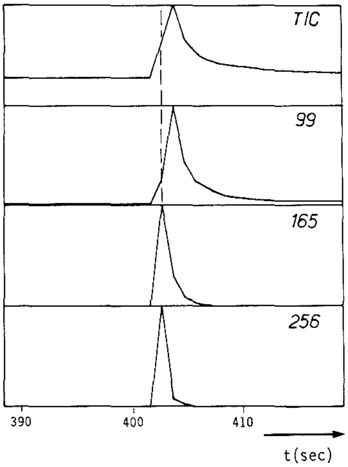

Figure 8. GC-CI-NO$^+$-MS chromatograms (total ion current and specified ions) obtained from (*E*)-7-dodecenyl acetate (GC conditions: 25-m CPSil 5CB, splitless injection, 40–160 °C (40 °C/min), 160–250 °C (10 °C/min)).

(cf. CI-NO$^+$ spectrum of (*Z*)-6-dodecenyl acetate) was also evidenced via similar MS/MS studies.

The absence of ion *m/z* 99 (or homologues from other isomers) in the CAD spectra of ions (M + NO)$^+$, ((M + NO) − AcOH)$^+$, (M − AcOH)$^{\cdot+}$, and ((M − H) − AcOH)$^+$ indicated that the odd-mass fragment ion was generated exclusively in the source. This might occur through an ion–molecule reaction process with NO$^+$ followed by a secondary ion–molecule reaction with neutral radical NO$^\cdot$ of either (i) a highly unstable adduct ion, therefore not detectable by MS or MS/MS; (ii) a stabilized (M + NO)$^+$ adduct ion. Recent experiments conducted with a multiquadrupole triple analyzer (*28*) have led us to exclude the second hypothesis. However, the former suggestion may not be entirely consistent with the two following unusual observations. Firstly when a GC–MS recording is performed, comparison of the reconstructed chromatograms of the diagnostic ion (i.e. *m/z* 99 from (*E*)-7-dodecenyl acetate, Figure 8) to those of ions formed by uni-(or bi-)molecular decompositions from M$^{\cdot+}$ or (M + NO)$^+$ shows a characteristic delay and a broadening for the chromatographic peak of the former. Secondly we have noticed a strong influence of the sample pressure (or injected dose) on the yield of the odd-mass diagnostic ion. At a given NO pressure there is a decrease in the odd-mass ion relative abundance with increasing sample pressure (Figure 9). This phenomenon which also appears using DCI for instance, is independent of the sample introduction mode. In fact, from these observations and other investigations in a more general context (*29*) the hypothesis of a preliminary source surface catalyzed neutral–neutral reaction (*30*) yielding aldehydes (eq 1) can, quite consistently (*31*), also be proposed. The ion–molecule reaction involving the NO$^+$ cation would only occur in a second step (eq 2) for the "detection" of the neutral aldehydes as their acylium (M − H)$^+$ ions (*32*, *33*).

$$CH_3(CH_2)_xCH{=}CH(CH_2)_yR \xrightarrow[\text{[S]}]{NO\cdot} CH_3(CH_2)_xCHO \text{ (major product)} \quad (1)$$

$$R = CH_2OAc,\ CH_2OH,\ \text{or } CHO$$

$$CH_3(CH_2)_xCHO \xrightarrow{NO^+} CH_3(CH_2)_xCO^+ \text{ (acylium diagnostic ion)} \quad (2)$$

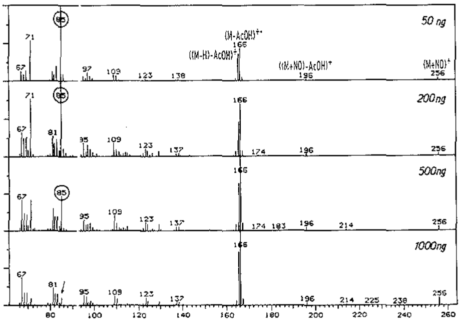

Figure 9. Sample pressure (or injected dose) effect on the CI-NO$^+$ mass spectrum of (*Z*)-7-dodecenyl acetate (25-m CPSil 5CB, 200 °C; *P*(NO) = 1.6 × 10^{-4} Torr).

CONCLUSIONS

The production of a CH$_3$(CH$_2$)$_x$CO$^+$ acylium diagnostic ion is an original feature in these reactions between functionalized alkenes and the NO$^+$/NO$^\cdot$ system. However, the unusual strong effect of the sample pressure that was observed may explain (*29*) at least partially (*26*) some apparent discrepancies in the reactivity of NO$^+$ respectively toward alkenes (*14*) and the polyfunctional compounds herein investigated. For the same reason, excessive amounts of substrate should be avoided, the 20–200 ng (injected via GC) range being preferable for structural determinations.

ACKNOWLEDGMENT

J. C. Tabet, Université P. et M. Curie, Paris, and C. Rolando, Ecole Normale Supérieure, Paris, are gratefully acknowledged for fruitful discussions.

Registry No. NO, 10102-43-9; NO$^+$, 14452-93-8; (*E*)-2-undecenyl acetate, 100288-67-3; (*Z*)-4-dodecenyl acetate, 38363-25-6; (*Z*)-5-dodecenyl acetate, 16676-96-3; (*Z*)-8-dodecenyl acetate, 28079-04-1; (*Z*)-9-dodecenyl acetate, 16974-11-1; (*Z*)-10-dodecenyl acetate, 35148-20-0; (*Z*)-5-tetradecenyl acetate, 35153-13-0; (*E*)-5-tetradecenyl acetate, 34010-13-4; (*Z*)-6-tetradecenyl acetate, 39650-11-8; (*E*)-6-tetradecenyl acetate, 39650-10-7; (*Z*)-8-tetradecenyl acetate, 35835-80-4; (*E*)-8-tetradecenyl acetate, 56218-64-5; (*Z*)-9-tetradecenyl acetate, 16725-53-4; (*E*)-9-tetradecenyl acetate, 23192-82-7; (*Z*)-11-tetradecenyl acetate, 20711-10-8; (*E*)-11-tetradecenyl acetate, 33189-72-9; (*Z*)-7-hexadecenyl acetate, 23192-42-9; (*Z*)-9-hexadecenyl acetate, 34010-20-3; (*Z*)-11-hexadecenyl acetate, 34010-21-4; (*E*)-2-dodecene-1-ol, 69064-37-5; (*E*)-3-dodecene-1-ol, 68900-87-8; (*E*)-5-dodecene-1-ol, 62936-12-3; (*E*)-6-dodecene-1-ol, 52957-14-9; (*Z*)-6-dodecene-1-ol, 40642-39-5; (*E*)-8-dodecene-1-ol, 42513-42-8; (*Z*)-8-dodecene-1-ol, 40642-40-8; (*E*)-9-dodecene-1-ol, 35237-62-8; (*Z*)-9-dodecene-1-ol, 35148-18-6; (*E*)-5-tetradecene-1-ol, 62936-14-5; (*E*)-6-tetradecene-1-ol, 68760-62-3; (*E*)-7-tetradecene-1-ol, 37011-95-3; (*Z*)-8-tetradecene-1-ol, 64470-32-2; (*Z*)-9-tetradecene-1-ol, 35153-15-2; (*E*)-10-tetradecene-1-ol, 64437-35-0; (*Z*)-10-tetradecene-1-ol, 57393-02-9; (*E*)-11-tetradecene-1-ol, 35153-18-5; (*Z*)-11-tetradecene-1-ol, 34010-15-6; (*E*)-8-hexadecene-1-ol, 64470-33-3; (*Z*)-9-hexadecene-1-ol, 10378-01-5; (*Z*)-11-hexadecene-1-ol, 56683-54-6; (*E*)-5-dodecenal, 68820-34-8; (*Z*)-7-tetradecenal, 65128-96-3; (*Z*)-9-tetradecenal, 53939-27-8; (*Z*)-11-tetradecenal, 35237-64-0; (*Z*)-7-hexadecenal, 56797-40-1; (*E*)-9-hexadecenal, 72698-29-4; (*Z*)-9-hexadecenal, 56219-04-6; (*E*)-11-hexadecenal, 57491-33-5; (*Z*)-11-hexadecenal, 53939-28-9; (*E*,*E*)-7,9-dodecadienyl acetate, 54364-63-5; (*Z*,*E*)-9,12-tetradecadienyl acetate, 30507-70-1; (*E*,*Z*)-9,11-hexadecadienyl acetate, 124201-67-8; (*Z*,*Z*,*Z*)-5,9,13-hexadecatrienyl acetate, 78617-60-4; (*E*,*E*,*Z*)-4,6,10-hexadecatrienyl acetate, 101372-99-0; (*Z*,*E*)-2,13-octadecadienyl acetate, 102637-06-9; (*Z*,*Z*)-3,13-octadecadienyl acetate, 53120-27-7; (*E*,*Z*)-7,9-dodecadiene-1-ol, 66471-35-0; (*Z*,*E*)-9,12-tetradecadiene-1-ol, 51937-00-9; (*E*,*Z*)-9,11-hexadecadiene-1-ol, 84643-62-9; (*E*,*Z*)-10,12-hexadecadiene-1-ol, 1002-94-4; (*E*,*Z*,*Z*)-4,6,10-hexadecatriene-1-ol, 101373-00-6; (*E*,*E*,*Z*)-4,6,10-hexadecatriene-1-ol, 101373-01-7; (*Z*,*Z*)-13,15-octadecadiene-1-ol, 124201-68-9; (*Z*,*Z*)-9,12-octadecadiene-1-ol, 506-43-4; (*Z*,*Z*,*Z*)-9,12,15-octadecatriene-1-ol, 506-44-5.

LITERATURE CITED

(1) Inscoe, M. N. In *Insect Suppression with Controlled Release Pheromone Systems*; Kydonieus, A. F., Beroza, M., Eds.; CRC Press: Boca Raton, Fl, 1982; Vol. II, pp 201–295.
(2) Tamaki, Y. In *Comprehensive Insect Physiology Biochemistry and Pharmacology*; Kerkut, G. A., Gilbert, L. I., Eds., Pergamon Press: Oxford, 1985; Vol. 9, pp 145–191.
(3) Bierl-Leonhardt, B. A.; DeVilbiss, E. D.; Plimmer, J. R. *J. Chromatogr. Sci.* **1980**, *18*, 364–367.
(4) Buser, H. R.; Arn, H.; Guerin, P.; Rauscher, S. *Anal. Chem.* **1983**, *55*, 818–822.
(5) Beroza, M.; Bierl, B. A. *Anal. Chem.* **1967**, *39*, 1131–1135.
(6) Leonhardt, B. A.; DeVilbiss, E. D.; Klun, J. A. *Org. Mass Spectrom.* **1983**, *18*, 9–11.
(7) Lanne, B. S.; Appelgren, M.; Bergstrom, G.; Lofstedt, C. *Anal. Chem.* **1985**, *57*, 1621–1625.
(8) Adams, J.; Deterding, L. J.; Gross, M. L. *Spectros. Int J.* **1987**, *5*, 199–228.
(9) Bambagiotti, M.; Coran, S. A.; Giannellini, V.; Vincieri, F. F.; Daolio, S.; Traldi, P. *Org. Mass Spectrom.* **1984**, *19*, 577–580.
(10) Prome, J. C.; Aurelle, H.; Couderc, F.; Savagnac, A. *Rapid Commun. Mass Spectrom.* **1987**, *1*, 50–52.
(11) Takeuchi, G.; Weiss, M.; Harrison, A. G. *Anal. Chem.* **1987**, *59*, 918–921.
(12) Greathead, R. J.; Jennings K. R. *Org. Mass Spectrom.* **1980**, *15*, 431–434.
(13) Chai, R.; Harrison, A. G. *Anal. Chem.* **1981**, *53*, 34–37.
(14) Budzikiewicz, H.; Busker, E. *Tetrahedron* **1980**, *36*, 255–266.
(15) Budzikiewicz, H.; Laufenberg, G.; Brauner, A. *Org. Mass Spectrom.* **1985**, *20*, 65–69.
(16) Peake, D. A.; Gross, M. L. *Anal. Chem.* **1985**, *57*, 115–120.
(17) Hunt, D. F.; Harvey, T. M. *Anal. Chem.* **1975**, *47*, 2136–2141.
(18) Brauner, A.; Budzikiewicz, H.; Francke, W. *Org. Mass Spectrom.* **1985**, *20*, 578–581.
(19) Malosse, C.; Einhorn, J. *Adv. Mass Spectrom.* **1986**, 1369–1370.
(20) Mori, K. In *The Total Synthesis of Natural Products*; Apsimon, J., Ed.; Wiley-Interscience Publishers: New York, 1981; Vol IV, pp 1–183.
(21) Hunt, D. F.; Harvey, T. M.; Brumley, W. C.; Ryan, J. F., III; Russell, J. W. *Anal. Chem.* **1982**, *54*, 492–496.
(22) Einhorn, J.; Virelizier, H.; Gemal, A. L.; Tabet, J. C. *Tetrahedron Lett.* **1985**, *26*, 1445–1448.
(23) Doolittle, R. E.; Tumlinson, J. H.; Proveaux, A. *Anal. Chem.* **1985**, *57*, 1625–1630.
(24) Einhorn, J.; Virelizier, H.; Tabet, J. C. *Spectrosc. Int. J.* **1987**, *5*, 171–182.
(25) Brauner, A.; Budzikiewicz, H.; Boland, W. *Org. Mass Spectrom.* **1982**, *17*, 161–164.
(26) Budzikiewicz, H.; Schneider, B.; Busker, E.; Boland, W.; Francke, W. *Org. Mass Spectrom.* **1987**, *22*, 458–461.
(27) Einhorn, J.; Schey, K.; Cooks, R. G., Purdue University, West Lafayette, IN, unpublished work, 1988.
(28) Einhorn, J.; Rolando, C.; Malosse, C. Presented at the 36th ASMS Conference on Mass Spectrometry and Allied Topics, San Francisco, CA, June 5–10, 1988, pp 27–28.
(29) Einhorn, J.; Malosse, C. *Org. Mass Spectrom.*, in press.
(30) Budzikiewicz, H. *Org. Mass Spectrom.*, **1988**, *23*, 561–565.
(31) Issachar, D.; Yinon, J. *Anal. Chem.* **1980**, *52*, 49–52.
(32) Hunt, D. F.; Ryan, J. F. *J. Chem. Soc., Chem. Commun.* **1972**, 620–621.
(33) Jardine, I.; Fenselau, C. *Org. Mass Spectrom.* **1975**, *10*, 748–751.

RECEIVED for review July 11, 1989. Accepted November 6, 1989.

Amperometric Monitoring of Ozone in Gaseous Media by Gold Electrodes Supported on Ion Exchange Membranes (Solid Polymer Electrolytes)

Gilberto Schiavon* and Gianni Zotti

CNR-IPELP, corso Stati Uniti 4, I-35100 Padova, Italy

Gino Bontempelli*

Institute of Chemistry, University of Udine, viale Ungheria 43, I-33100 Udine, Italy

Giuseppe Farnia and Giancarlo Sandoná

Department of Physical Chemistry, University of Padova, via Loredan 2, I-35131 Padova, Italy

An in situ amperometric sensor suitable for monitoring ozone in gaseous media is described. It consists of a porous gold working electrode (contacting the gaseous sample) supported on one surface of an ion exchange membrane (Nafion 417) which serves as a solid polymer electrolyte. The other side of this membrane faces an internal electrolyte solution (1 M aqueous perchloric acid) containing the counter and reference electrodes. Amperometric measurements are performed at an applied potential of 0.5 V vs SCE, by inserting the sensor in a cell in which ozone–oxygen streams are fed with different controlled rates. A current sensitivity of 38 A M^{-1} cm^{-2} and a response time of 0.5 s are observed. The dynamic range turns out to extend up to 2×10^{-3} M (4.48×10^{-2} atm) with good linearity and a detection limit of 10^{-8} M (2.24×10^{-7} atm) is predicted for $S/N = 3$. These performances are compared with those provided by the corresponding gas-permeation membrane electrodes and by spectrophotometric methods employing suitable reagents. The effect of the flow rate on current responses is also discussed.

INTRODUCTION

The monitoring of ozone is the subject of a growing interest arising from the increased use of this biradical triatomic species for disinfection and purification procedures (*1*). Thus, ozone has been adopted successfully for disinfection of medical tools and of drinking water and wastewaters, as well as in other new fields such as the preservation and storage of foods. Moreover, it is used as an oxidizing agent in the chemical industry for bleaching of oils, waxes, textiles, paper, starch, and sugar.

A large number of methods have been suggested for the determination of ozone involving the use of iodometric techniques after reduction by iodide ions (*2*, *3*) and spectrophotometric measurements either of the direct UV absorption (*4*) or of the absorption in the visible region displayed by the product of the interaction between ozone and acid chrome violet (*1*), bis(terpyridine)iron(II) (*5*, *6*), or indigo (*6*, *7*). Further methods are based on different analytical approaches including chemiluminescence (*8*) or fluorescence (*9*), catalytic

0003-2700/90/0362-0293$02.50/0 © 1990 American Chemical Society

decomposition (*10*), cleavage of an olefinic bond (*11*, *12*), and electrochemical reduction of ozone exploited through either coulometric analyzers (*1*) or amperometric analyzers (*13*–*15*), mostly with a gas-permeable membrane (*16*, *17*) or with an ozone decomposition membrane (*18*).

Effective applications of ozone are largely dependent on the availability of in situ and instantaneous ozone sensors suitable for the control of ozone generation and decay, particularly in gaseous media. Unfortunately, among the methods mentioned above, only membrane electrodes appear to possess the required qualifications, even though their performance is strongly affected by the diffusion of the analyte through the membrane which proves to be a critical step. Thus, a fairly low sensitivity and a quite long response time are peculiar to these electrodes whose response also exhibits a high-temperature dependence resulting from the consequent change of permeability characterizing the membrane. Moreover, only one (*14*) among the reported electroanalytical sensors have been tested so far in gaseous media.

We have recently described (*19*) an electrochemical sensor suitable for monitoring electroactive analytes present in gaseous media or in high-resistive solvents that is based on an alternative approach. It implies the use of a porous working electrode supported on one surface of an ion exchange membrane, the other surface of which is in contact with an electrolyte solution containing the counter and reference electrodes. The porous working electrode is introduced into the analyte sample in which no supporting electrolyte is needed because electroneutrality in the close neighborhood of the electrode surface is maintained by ionic migration through the ion exchange membrane. In such a way, any membrane-permeation step is avoided and the analyte is monitored directly in its natural medium since the membrane separating the sample from the internal electrolyte does not act as a filter for gaseous molecules but it serves to assure the transfer of charged species from the working to counter electrode. A similar approach has also been suggested recently by other authors (*20*, *21*).

In this paper we propose the use of this type of electrode, equipped with an ion exchange membrane as a solid polymer electrolyte (SPE), for the detection of ozone in gaseous media. The expected advantages are an improved performance over membrane electrodes due to a lower detection limit, a shorter response time, and a linear dependence on the ozone concentration of the relevant signal in a wider concentration range.

It is worthwhile to remark, however, that the use of a fairly similar electrode as a gas sensor for carbon monoxide, nitrogen oxides, and alcohol vapors has been suggested previously (*22*–*24*). Also in this sensor, in fact, a porous working electrode (platinum or graphite) supported on one side of a membrane made up with either a solid polymer electrolyte or an aqueous electrolyte adsorbed in a solid matrix is adopted. Nevertheless, in this device also the Pt counter electrode is deposited on the same or on the other side of the membrane, thus causing the relevant redox processes to occur at the metal–membrane interphase. These processes involve reduction (or oxidation) of either water hydrating the membrane or gaseous species contacting spontaneously the counter electrode (oxygen in air) or supplied on purpose (hydrogen). Consequently, interferences arising from reactants and/or products of these redox reactions are expected to affect the response of the working electrode. Thus, for instance, when hydrogen (supplied on purpose or produced by electrochemical reduction of water) is involved in the counter electrode reaction, it can diffuse toward the working electrode, due to the high permeation through Nafion characterizing gaseous species (*25*), thus interfering with any analyte which undergoes oxidation or reduction at potential values higher than 0 V vs NHE. Moreover, such an assembly requires that suitable devices are adopted to maintain the solid electrolyte moist enough to make possible ion transport inside the membrane (*24*).

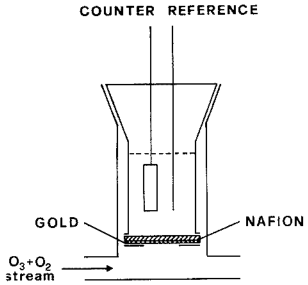

Figure 1. Schematic view of the flow cell.

EXPERIMENTAL SECTION

Chemicals and Instrumentation. All the chemicals used were of reagent grade quality and they were employed without further purification.

Ozone was produced from oxygen using a Fischer Model 502 corona generator whose output was varied from 0 to about 5% by weight in ozone by controlling the voltage applied across the electrical discharge tube and the oxygen flow rate.

Voltammetric and amperometric tests were performed by a three-electrode unit assembled with an Amel 551 potentiostat coupled with an Amel 568 digital logic-function generator. The recording device was a Hewlett-Packard 7080 A measurement plotting system.

UV-absorption spectra for ozone (λ_{max} = 254 nm) were recorded on a Perkin-Elmer Lambda 5 spectrophotometer using a stoppered 1.00 or 10.00 cm path length quartz cuvette.

All the tests were conducted at room temperature.

Electrode Assembly. The ion exchange material used as the solid polymer electrolyte (SPE) was a Nafion 417 cationic perfluorinated membrane 0.425 mm thick, reinforced with Teflon (Aldrich), which was cleaned by boiling in concentrated nitric acid for 1 h and then in Milli-Q reagent grade water for 1 h. The membrane was then cut into disks of 1 cm diameter, and one face was covered by a porous gold or platinum film by following two different procedures described elsewhere (*19*). Gold–Nafion composite electrodes were prepared by metal vapor deposition with a vacuum coating unit Edwards Model E 306 A which was used to produce 0.1 μm thick gold deposits at a deposition rate of 0.5 nm s^{-1}, while platinum films were obtained by the electroless plating method (*26*) by reducing a solution of chloroplatinic acid, contacting one face of the membrane, with an alkaline solution of sodium borohydride diffusing from the other face.

A disk of one of the composite SPE electrodes prepared in this way was clamped, with the porous conductive layer directed downward, at the bottom of a Pyrex cylinder, the end of which was threaded for connection to a drilled Teflon holder sealing the assembly by means of an elastic O-ring resistant to acids and bases. Electrical contact with the porous working electrode was made by placing a gold (or a platinum) ring on the inner circular ring of the drilled holder (at the bottom) on which the border of the conductive film deposited on Nafion was pressed. A gold (or platinum) wire welded to the Au (or Pt) ring permitted electrical connection. Such an assembly allowed ca. 0.4 cm^2 of conductive film to be exposed to external media.

The uncoated side of the membrane faced an internal compartment equipped with a platinum counter electrode and an aqueous silver/silver chloride reference electrode. This internal compartment was obtained by sealing the Pyrex cylinder to the bottom of a standardized hollow glass stopper in order to make possible the use of this electroanalytical sensor as a gas-tight stopper for the standardized glass-flow cell (see Figure 1, V = 20 mL) in which all our experiments were conducted.

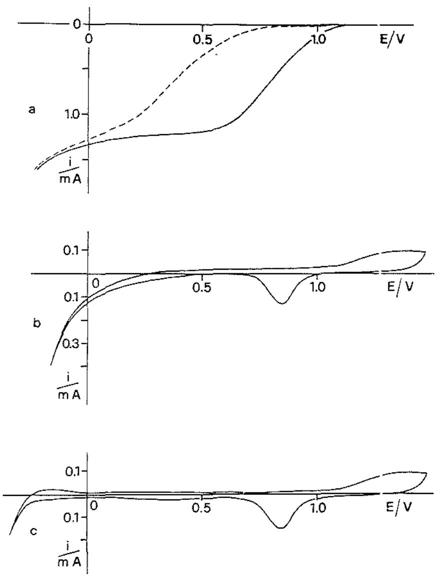

Figure 2. Responses recorded at an Au–Nafion electrode with 1 M perchloric acid as the internal electrolyte: (a) voltammograms for ozone (8 × 10^{-5} M; 1.8 × 10^{-3} atm) in an oxygen stream (full line), same experimental conditions except for the internal electrolyte which is replaced by an acetate buffer at pH = 4 (dashed line); (b) voltammogram for an ozone-free oxygen stream; (c) voltammogram for a nitrogen stream. Scan rate was 0.02 V s^{-1}. Flow rate was 50 mL min^{-1}.

Aqueous perchloric acid solutions (1 M) or other aqueous solutions buffered at suitable pH values were used as electrolytic solutions in the internal compartment (internal electrolyte).

Before use, all coated Nafion disks were conditioned for 1 day with the internal electrolyte to be used, so as to saturate the ion exchange material with the cations of the supporting electrolyte.

The flow cell was fed by an ozone–oxygen stream whose flow rate was kept constant, unless stated otherwise, at 50 mL min^{-1} by a three-way valve attenuating the ozone output. A flowmeter was inserted in the stream to monitor this flow rate.

Although an Ag/AgCl reference electrode was used, all potentials are quoted in the following vs an aqueous SCE.

Determination of Ozone Molar Absorptivity. Since direct ultraviolet detection was adopted as the reference method to evaluate the ozone concentration monitored by SPE electrodes, the molar absorptivity of this species has been preliminarly determined under our experimental conditions. This has been accomplished by employing the iodometric procedure (*2*, *3*) as the standardization method, with titration by sodium thiosulfate and biamperometric detection of the end point.

With this purpose, a stoppered 1.00 cm or 10.00 cm path length quartz cuvette, positioned directly into the light path of the spectrophotometer, was fed with controlled ozone–oxygen streams by a thin Teflon tube connecting the cell with the ozonator, until constant UV absorbances at 254 nm were attained, which depended upon the applied voltage across the electrical discharge tube and the input oxygen flow rate. After each UV measurement, a gas-tight syringe was used to withdraw sequentially a known aliquot of gas (3–8 mL) from the cuvette and an excess amount of potassium iodide solution buffered at pH = 5. The content of the syringe was then shaken and transferred into a cell equipped with the biamperometric apparatus where triiodide ions formed were titrated by standard thiosulfate. In such a way, a series of absorbance–concentration couples of values were obtained in the concentration range 5 × 10^{-5} to 4 × 10^{-4} M, which were plotted to provide a value of 3300 ± 50 M^{-1} cm^{-1} for the ozone molar absorptivity, in good agreement with a recent literature report (*4*).

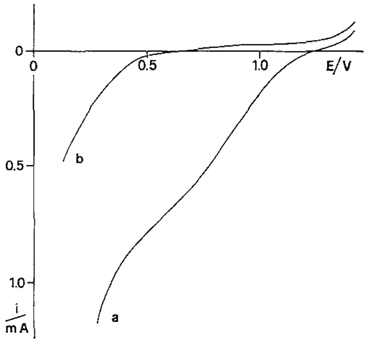

Figure 3. Voltammetric responses recorded at a Pt–Nafion electrode, with 1 M perchloric acid as the internal electrolyte, on ozone (5 × 10^{-5} M; 1.1 × 10^{-3} atm) in oxygen (curve a) and on pure oxygen (curve b). Scan rate was 0.02 V s^{-1}. Flow rate was 50 mL min^{-1}.

RESULTS AND DISCUSSION

Cathodic Behavior of Gaseous Ozone at SPE Electrodes. The full line in Figure 2a reports a typical steady-state voltammogram recorded at 20 mV s^{-1} on an ozone–oxygen stream flowing into the cell in Figure 1 at 50 mL min^{-1}, when a gold-covered Nafion electrode with 1 M aqueous perchloric acid as the internal electrolyte is used. A single well-formed and reproducible but irreversible cathodic wave is observed which resembles closely that found at conventional gold electrodes for the reduction of ozone dissolved in aqueous perchloric acid (*27*), i.e. the internal electrolyte employed on the rear side of the Nafion membrane. The relevant limiting current extends in a quite wide potential range which is limited in the negative direction by the reduction of the oxygen present in the gas stream from the ozonator. This has been proved by comparing the profile of Figure 2a with steady-state voltammograms recorded at the same electrode on an ozone-free oxygen stream under the same experimental conditions (see Figure 2b).

When this electrode is replaced by a platinum–Nafion composite electrode containing once again 1 M perchloric acid as the internal electrolyte, the ozone reduction is found to occur at the same potentials, as shown in Figure 3, curve a. In this case, however, the cathodic wave does not attain a well-defined limiting value, most probably because it extends in a narrower potential range. Comparison of Figure 3, curve b, with the corresponding Figure 2b makes in fact apparent the lower overvoltage which affects the oxygen reduction on platinum, in full agreement with previous findings (*28*).

On the basis of this observation, gold porous films have been selected as the electrode surface since they assure apparently a fairly potential-independent sensitivity for the corresponding amperometric ozone sensor, so that this experimental parameter does not require a careful control.

The effect of the pH of the internal electrolyte on ozone reduction at gold–SPE electrodes has also been examined by using suitable buffers. A pH increase leaves the reduction potential of oxygen practically unaltered (*28*), whereas it causes the cathodic wave for ozone to shift toward less positive potentials. This shift is however larger than that expected on the basis of the following reduction reaction:

$$O_3 + 2H^+ + 2e^- \rightarrow O_2 + H_2O \qquad (1)$$

In particular, for pH values increasing over ca. 2, an abrupt negative shift of the potential for ozone reduction is observed which leads to a cathodic wave extending in a narrower po-

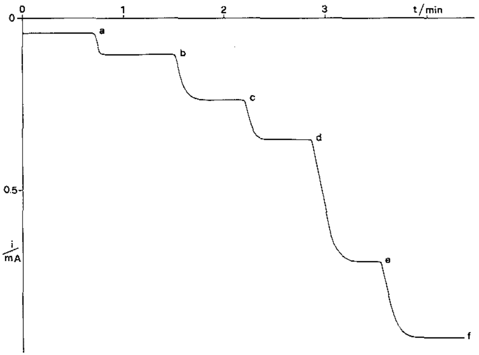

Figure 4. Current-time profile recorded at a gold-Nafion electrode, with 1 M perchloric acid as the internal electrolyte, on ozone-oxygen streams containing ozone in the following concentrations: (a) 3 μM (67 μatm); (b) 7 μM (157 μatm); (c) 15 μM (336 μatm); (d) 24 μM (538 μatm); (e) 47 μM (1053 μatm); (f) 62 μM (1389 μatm). Flow rate was 50 mL min^{-1}. Applied potential was 0.5 V vs SCE.

tential range and exhibiting no real limiting current, as shown in Figure 2a (dashed line). This striking change of the steady-state voltammogram can be conceivably rationalized in terms of the background current for gold electrodes reported in Figure 2c, which shows the well-known anodic-cathodic system relative to the formation and associate reduction of a gold-oxygen layer (*29*). Comparison of this figure with Figure 2a points out that the cathodic process for ozone at pH = 0 starts at a potential at which a clean gold electrode surface is available since the mentioned gold-oxygen layer is removed by reduction. Conversely, at higher pH values, the reduction of such a layer is shifted progressively toward less positive potentials (as checked by us in the absence of ozone), so that ozone reduction is forced to occur on a different electrode surface, i.e. on a gold-oxygen layer which requires apparently a higher overvoltage. Such as explanation agrees quite well with the arguments advanced elsewhere to account for some oddity observed in the voltammetric behavior of ozone in acidic media (*27*).

These results lead us to conclude that the most appropriate internal electrolyte for the gold-SPE electrode is a 1 M aqueous solution of perchloric acid, which also offers the advantage of a lower and more reproducible residual current.

On the basis of voltammograms recorded on ozone under these experimental conditions, an applied potential of 0.5 V vs SCE has been selected for amperometric measurements, in order to maximize the current detection sensitivity of the gold-Nafion sensor and, at the same time, to minimize its dependence on the working potential.

Performances of the Amperometric Sensor. The cell in Figure 1 was also used to test the performance of the gold-covered Nafion electrode as an amperometric sensor for ozone. With this purpose, an oxygen stream containing different ozone concentrations was fed into this cell, typically at 50 mL min^{-1}, and its ozone content was monitored simultaneously by amperometric and spectrophotometric measurements. This was accomplished by connecting the cell, with a short Teflon tube, in series with a quartz cuvette positioned directly into the light path of the spectrophotometer. The ozone concentration in the cell could be thus determined everytime by exploiting the ozone molar absorptivity estimated as described in the Experimental Section. In such a way, amperometric currents measured at gold-SPE electrodes could be correlated with ozone concentrations.

A typical current-time response obtained at an applied potential of 0.5 V is reported in Figure 4. It shows that each increase in the ozone output from the ozonator causes a rapid rise in the current which attains in a short time a constant value satisfactorily stable with time. This constant value is found to be reproducible within about ±2% and depends linearly on ozone concentration in a quite wide range, as shown in Figure 5. From this figure a sensitivity of about 38 A M^{-1} cm^{-2}, with a correlation coefficient of 0.998, is inferred in a dynamic range which extends up to about 5×10^{-4} M (24 mg L^{-1}; 1.12×10^{-2} atm). It is worthwhile to emphasize that this dynamic range is estimated in the absence of any positive-feedback iR compensation. As a matter of fact, the high currents flowing at the electrode surface for ozone concentrations higher than 5×10^{-4} M make the relevant iR drops no longer negligible. Consequently, the actual potential at the sensor electrode, with respect to the apparent one, is shifted toward more positive values where current sensitivity decreases appreciably (see Figure 2a), thus causing the relevant current-concentration points to deviate downward from linearity in the plot of Figure 5. A careful iR drop compensation is hard to achieve with these composite electrodes in that the potential oscillations caused by a positive feedback overshooting the correct value lead to partial deactivation of the gold film. However, we have proved that a partial compensation of the effective iR drop, by imposing a positive feedback equivalent to a slightly underestimated resistance (30 Ω) allows the dynamic range to be extended up to about 2×10^{-3} M (ca. 100 mg L^{-1}; 4.48×10^{-2} atm).

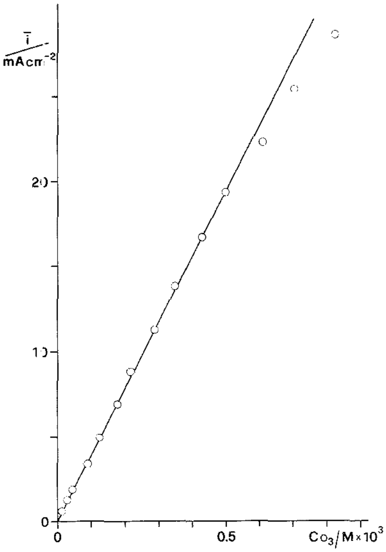

Figure 5. Steady-state current density recorded at a gold-Nafion electrode for ozone reduction as a function of its concentration in an oxygen stream. Flow rate was 50 mL min^{-1}. Applied potential was 0.5 V vs SCE.

The residual current density at the working potential is about 1 μA cm^{-2} with a standard deviation of 0.12 μA cm^{-2}. This last figure allows the estimation of a detection limit of ca. 10^{-8} M (0.5 μg L^{-1}; 2.24×10^{-7} atm) for $S/N = 3$.

The response time cannot be inferred correctly from current-time profiles reported in Figure 4, since the time required to attain a steady-state current is due mainly to the inertia opposed by the flowing system to achieve equilibrium conditions after each increase of the ozone concentration. Consequently, this characterizing parameter has been evaluated by suitable experiments. A 95% response is observed in 0.5

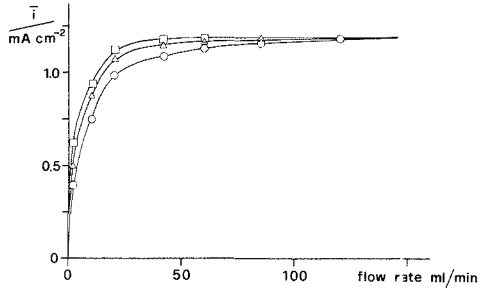

Figure 6. Steady-state current density recorded at a gold–Nafion electrode for ozone reduction as a function of the ozone–oxygen flow rate. Ozone concentration was 3×10^{-5} M (6.7×10^{-4} atm). Applied potential was 0.5 V vs SCE. Volume of the flow cell was (○) 20 mL, (△) 5mL, and (□) 2 mL.

s when the electrode is transferred rapidly from air to the cell in Figure 1 fed with a gas stream containing approximately 2×10^{-4} M (ca. 10 mg L^{-1}; 4.48×10^{-3} atm) of ozone. This response time remains practically the same also when the electrode is transferred from air to gas streams with higher or lower ozone contents.

Finally, it must be remarked that different gold–Nafion electrodes, prepared by adopting exactly the same constructive details, lead to very similar amperometric responses when tested on the same ozone–oxygen stream, thus pointing out that quite reproducible electrode surfaces are obtained by the coating procedure followed by us.

Effect of the Flow Rate. The effect of the flow rate on the current response provided by the amperometric sensor is illustrated in Figure 6, which shows that the electrode sensitivity increases at first with the flow rate until it becomes practically constant for flow rates higher than about 80 mL min^{-1}. The same trend is also observed when the sensor is tested in flow cells with the same shape as that in Figure 1 but with a reduced size, even if the current reaches the same limiting value at lower flow rates, as shown by upper lines in Figure 6.

The attainment of this limiting current value at fairly low flow rates can be accounted for by the convective motions caused by the ozone–oxygen stream, which keeps the ozone concentration uniform at its bulk value only outside a stagnant layer near the electrode surface within which mass transfer occurs only by diffusion. Therefore, steady-state conditions are attained even with rather low streams since in our case this stagnant layer is conceivably relatively thick, as it is determined by two main factors both arising from the particular sensor assembly adopted by us. Firstly, the protruding border of the Teflon holder, sealing the sensor, shields partially the electrode surface. Secondly, ozone molecules from the gaseous stream must diffuse across the thin porous gold film before reaching the gold/Nafion interphase where they undergo reduction. Consequently, a diffusion-permeation gold layer exists whose thickness is of course independent of the flow rate. The presence of this second effect has been proved by using composite electrodes with different thickness of the gold deposit. As this thickness increases from 0.05 to 0.5 μm the recorded current decreases almost linearly from 1.25 to 1.0 mA cm^{-2} with an ozone–oxygen stream flowing at 80 mL min^{-1}, under the same experimental conditions as in Figure 6. Therefore, it must be remarked that the sensitivity of our sensor can be varied slightly by choosing suitably the thickness of the gold film.

It is worth noting, however, that the scarce dependence of the current response on the flow rate found for flow rates higher than ca. 50 mL min^{-1} represents a favorable outcome in that ozone determinations can be performed without controlling carefully the rate of the gaseous stream supplied to the sensor.

CONCLUSIONS

The results obtained in this investigation point out that electrodes supported on ion exchange membranes are good alternatives to conventional membrane electrodes for the electroanalytical detection of species present in gaseous phase. In the latter sensors, the polymeric membrane serves in fact as a gas-permeable interphase between the sample and the indicator electrode, while Nafion in SPE electrodes acts as an "ion-permeable" membrane separating an electrolytic solution from the working electrode which contacts directly the sample, so that any gas-permeation step is avoided and it is just this circumstance which makes SPE electrodes particularly profitable. Thus, in the particular case here considered, these porous electrodes supported on ion exchange membranes turn out to be characterized by a high sensitivity (38 A M^{-1} cm^{-2}) and a low response time (0.5 s), which are markedly better than those reported for the corresponding membrane electrodes (ca. 10 μA M^{-1} cm^{-2} and 18 s (*16*) or ca. 18 μA M^{-1} and 7 s (*17*)). Also the lower detection limit (10^{-8} M instead of 1.3×10^{-6} M (*16*, *17*)) and the wider dynamic range (10^{-8} to 2×10^{-3} M with respect to 1.3×10^{-6} to 4×10^{-5} M (*16*, *17*)), as well as the very scarce effect of the temperature expected on the current response, must be considered among the advantageous features deriving from the absence of a gas-permeation step which make SPE electrodes preferable to conventional membrane electrodes.

In this connection, it must be noted that the performance of the electroanalytical sensor suggested by us is advantageous even when compared with those provided by spectrophotometric methods for ozone employing suitable reagents. Thus, one of the best of these spectrophotometric approaches, i.e. the indigo blue method, is characterized by a slightly higher detection limit (ca. 2×10^{-8} M; 4.48×10^{-7} atm) (*30*) and a narrower dynamic range (extending up to about 6×10^{-4} M) (*30*).

Moreover, the long-term stability of these gold-covered Nafion electrodes in ozone–oxygen streams is satisfactory in that no appreciable change of their current response is observed even after 2 months of continuous use.

The whole of these features makes this type of electrode not only suitable for applications to the control of ozonation processes based on in situ measurements of residual ozone but also particularly attractive for the monitoring of any other electroactive species present in gaseous phase, as well as in highly resistive solutions, provided that the working potential is appropriately chosen.

The only drawback affecting amperometric measurements performed at SPE electrodes seems to be their selectivity which may be insufficient in some cases, due almost exclusively to the value of the working potential. Thus, in the particular case of ozone monitoring, we have found that also the reduction of two possible interfering species like chlorine and nitrogen dioxide occurs at the applied potential, in agreement with the high positive reduction potentials characterizing these oxidizing agents. Chlorine, however, should be a real interfering species only in measurements devoted to environmental control, to which purpose the sensor here proposed is not applicable because of its insufficient detection limit. In fact, ozone contents in the environmental atmosphere higher than ca. 4×10^{-9} M (ca. 9×10^{-8} atm) are not admitted in many countries by legal provisions. Conversely, nitrogen dioxide would be in principle an interfering species also in control of ozonation processes as it is a side product in ozone corona generators, but its concentration is so low (a 1% maximum total content of nitrogen oxides is expected when these generators are fed with air (*31*)) that its effect on ozone measurements can be neglected.

For these reasons, the sensor here described appears to be well suited for ozone monitoring in general applications of this reagent, such as chemical syntheses or disinfection and preservation procedures.

ACKNOWLEDGMENT

We thank S. Sitran of CNR-IPELP (Padova) for skillful experimental assistance.

Registry No. Nafion 417, 77323-49-0; ozone, 10028-15-6; gold, 7440-57-5.

LITERATURE CITED

(1) *Handbook of Ozone Technology and Application*; Rice, R. G., Netzer, A., Eds.; Ann Arbor Science: Ann Arbor, MI, 1982; Vol. 1; Butterworth Publishers: Boston, MA, 1984; Vol. 2.
(2) *NIOSH Manual of Analytical Methods*, 2nd ed.; National Institute for Occupational Safety and Health: Cincinnati, OH, 1977; Vol. 1, Method No. P&CAM 153.
(3) American Public Health Association; *Standard Methods for the Examination of Water and Waste Water*, 16th ed.; American Public Health Association: Washington, DC, 1985.
(4) Bahnemann, D.; Hart, E. J. *J. Phys. Chem.* **1982**, *86*, 252-255.
(5) Tomiyasu, H.; Gordon, G. *Anal. Chem.* **1984**, *56*, 752-754.
(6) Straka, M. R.; Gordon, G.; Pacey, G. E. *Anal. Chem.* **1984**, *56*, 1799-1803.
(7) Straka, M. R.; Pacey, G. E.; Gordon, G. *Anal. Chem.* **1984**, *56*, 1973-1975.
(8) Regner, W. H. *J. Geophys. Res.* **1960**, *65*, 3975-3977.
(9) Watanabe, H.; Nakodoi, T. *J. Air Pollut. Control Assoc.* **1966**, *16*, 614-617.
(10) Olmer, F. J. *Adv. Chem. Ser.* **1959**, *No. 21*, 87-92.
(11) Hauser, T. A.; Bradley, D. W. *Anal. Chem.* **1966**, *38*, 1529-1532.
(12) Sachdev, S. L.; Lodge, J. P., Jr.; West, P. W. *Anal. Chim. Acta* **1972**, *58*, 141-147.
(13) Fabjan, C.; Bauer, P. *Z. Anal. Chem.* **1976**, *280*, 121-126.
(14) Suzuki, S.; Nayashima, K. *Anal. Chim. Acta* **1982**, *144*, 261-266.
(15) Santacesaria, E.; Danise, P.; Gelosa, D. *J. Electroanal. Chem.* **1983**, *153*, 175-183.
(16) Stanley, J. H.; Johnson, J. D. *Anal. Chem.* **1979**, *51*, 2144-2147.
(17) Smart, R. B.; Dormond-Herrera, R.; Mancy, K. H. *Anal. Chem.* **1979**, *51*, 2315-2319.
(18) Toshiba Corp. Japan Pat. 57 37 024. *Chem. Abstr.* **1982**, *98*, 118806.
(19) Schiavon, G.; Zotti, G.; Bontempelli, G. *Anal. Chim. Acta* **1989**, *221*, 27-41.
(20) Kaaret T. W.; Evans, D. H. *Anal. Chem.* **1988**, *60*, 657-662.
(21) De Wulf, D. W.; Bard, A. J. *J. Electrochem. Soc.* **1988**, *135*, 1977-1985.
(22) LaConti, A. B. U.S. Patent 40 25 412. *Chem. Abstr.* **1977**, *87*, 86843h.
(23) LaConti, A. B.; Nolan, M. E.; Kosek, J. A.; Sedlak, J. M. In *Chemical Hazards in the Workplace*, Choudary, G., Ed.; ACS Symposium Series 149, American Chemical Society: Washington, DC, 1981; pp 551-573.
(24) Dempsey, R. M.; LaConti, A. B.; Nolan, M. E. U.S. Patent 42 27 984. *Chem Abstr.* **1981**, *94*, 113915m.
(25) Sakai, T.; Takenaka, H.; Torikai, E. *J. Electrochem. Soc.* **1986**, *133*, 88-92
(26) Aramata, A.; Nakajima, H.; Fujikawa, K.; Kita, H. *Electrochim. Acta* **1983**, *28*, 777-780.
(27) Johnson, D. C.; Napp, D. T.; Bruckenstein, S. *Anal. Chem.* **1968**, *40*, 482-488.
(28) Hoare, J. P. In *Encyclopedia of Electrochemistry of the Elements*; Bard, A. J., Ed.; Marcel Dekker: New York, 1974; Vol. 2, p 319.
(29) Adams, R. N. *Electrochemistry at Solid Electrodes*; Marcel Dekker, New York, 1969; p 194.
(30) Lachowichz, E.; Rozanska, B. *Chem. Anal.* (*Warsaw*) **1987**, *32*, 433-450.
(31) Masschelein, W. J. In *Ozonization Manual for Water and Wastewater Treatment*; Masschelein, W. J. Ed.; J. Wiley: New York, 1982; p 10.

RECEIVED for review March 24, 1989. Accepted October 23, 1989. The financial aid of the Italian National Research Council (C.N.R.) and of the Ministry of Public Education is gratefully acknowledged.

Comparison of Photoacoustic Spectroscopy, Conventional Absorption Spectroscopy, and Potentiometry as Probes of Lanthanide Speciation

Richard A. Torres,* Cynthia E. A. Palmer, Patricia A. Baisden, Richard E. Russo,[1] and Robert J. Silva

Lawrence Livermore National Laboratory, P.O. Box 808, L-234, Livermore, California 94551

We measured the stability constants of praseodymium acetate and oxydiacetate complexes by laser-induced photoacoustic spectroscopy, conventional UV-visible absorption spectroscopy, and pH titration. For the spectroscopic studies, changes in the free Pr absorption peaks at 468 and 481 nm were monitored at varying ligand concentrations. The total Pr concentration was 1×10^{-4} M in solutions used for the photoacoustic studies and 0.02 M for conventional spectroscopy. For the pH titrations, we used solutions whose Pr concentrations varied from 5×10^{-3} to 5×10^{-2} M, with total ligand-to-metal ratios ranging from 1 to 10. A comparison of the results obtained by the three techniques demonstrates that photoacoustic spectroscopy can give the same information about metal-ligand speciation as more conventional methods. It is particularly suited to those situations where the other techniques are insensitive because of limited metal concentrations.

INTRODUCTION

Modeling the solution behavior of metal ions requires information about the thermodynamics of metal complexation reactions, that is, the magnitude and temperature dependence of stability constants, β_{pqr}, for a reaction between a metal (M), ligand (L), and/or proton (H)

$$pM + qH + rL = M_pH_qL_r \qquad (1)$$

$$\beta_{pqr} = [M_pH_qL_r]/[M]^p[H]^q[L]^r$$

This fundamental knowledge is important, for example, in understanding metal separations schemes (chromatography and solvent extraction), and the sequestering/transport of trace metals under environmental conditions. The most commonly used methods of measuring stability constants are potentiometry and UV-visible spectroscopy (*1*). The sensitivity of the two techniques depends on several factors; however, they all relate in some fashion to the total concentrations of the reactants. The sensitivity of the potentiometric technique depends on the minimum concentration change that

---

[1] Present address: Lawrence Berkeley Laboratory, MS-90-2024, Berkeley, CA 94720.

0003-2700/90/0362-0298$02.50/0 © 1990 American Chemical Society

can be reliably measured by the electrode system. Reactants with large stability constants require less concentrated solutions than those with smaller stability constants. For absorption spectroscopy, the product of the concentration and the extinction coefficient is the pertinent figure of merit. Analytes with large molar extinction coefficients require less concentrated solutions than those with smaller coefficients. A complicating factor for metal–ligand speciation studies is that frequently the relevant equilibria change as the total metal concentration changes. For example, mononuclear complexes might form at low metal concentrations and polynuclear complexes at higher metal concentrations. Therefore, it is often desirable to measure stability constants at metal concentrations too low for potentiometry or conventional absorption spectroscopy.

Spectroscopy based on photothermal effects is potentially more sensitive than conventional absorption spectroscopy by as much as 3 orders of magnitude (*2–7*). Conventional absorption spectroscopy measures the change in the amount of light reaching a detector when the sample is introduced into the light path. As the absorbance of the solution decreases, sensitivity is lost because of the difficulty in accurately measuring the small change compared to the relatively large total light intensity reaching the detector. However, photothermal detection schemes detect the nonradiative relaxation of the excited state directly. The nonradiative relaxation transfers the energy of the excited state to the solvent as heat. Photoacoustic spectroscopy (PAS) detects the pressure wave produced after absorption of an excitation pulse. As the wavelength of the excitation source is scanned over an absorption band, the number of atoms that are excited changes, producing a photoacoustic spectrum analogous to a conventional absorption band.

We have built a photoacoustic spectrometer that uses pulsed-laser excitation to study aqueous actinide complexation. However, in order to verify that our PAS system performs well enough to measure stability constants, we wished to compare results from potentiometric and spectroscopic techniques for internal consistency without the experimental difficulties inherent in using highly radioactive actinides. Since the intensities and widths of the forbidden f–f transitions of trivalent lanthanides are comparable to the corresponding actinide transitions, they provide convenient analogues for the spectroscopic technique. We chose the praseodymium–oxydiacetate system as a reasonable test. Stability constants for three successive praseodymium–oxydiacetate complexes have been measured previously by potentiometry (*8*), and the 481-nm absorption peak has been shown to systematically shift as much as 3.5 nm to longer wavelength as complexation occurs (*9*). Since the relatively large shift is probably correlated with the large stability of the oxydiacetate complexes (log $\beta_{101} > 5$), we also examined the praseodymium–acetate system as a test involving weaker complexes (log $\beta_{101} \sim 2$) (*10*).

The works described in refs 3–7 amply document the application of photothermal spectroscopy to quantitate trace concentrations of metals, as well as its utility for identifying their different oxidation states based on their characteristic absorption bands. However, they only qualitatively indicate its potential use for measuring metal–ligand complexation constants by noting that changes in the characteristic absorption bands occur in the presence of ligands. We know of only one study in which stability constants were measured by absorption spectroscopy using photothermal detection. In this study thermal lensing spectroscopy was used to measure the first and second hydrolysis constants of uranium(IV) in solutions of $\sim 1 \times 10^{-5}$ M total uranium by monitoring a single wavelength (*11*). Our work is the first in which an entire absorption band is monitored by photothermal detection to extract the stability constants. Constraining the speciation model to fit the entire absorption spectrum can only improve the reliability of the stability constants.

EXPERIMENTAL SECTION

Solutions and Reagents. We prepared a stock solution of Pr by dissolving the oxide, Pr_6O_{11} (99.9% min, Alfa Products), in a minimum of perchloric acid, boiling the solution to remove as much excess acid as possible, and diluting with water to the final volume. We measured the Pr content by colorimetric EDTA titration with xylenol orange indicator, and the free acidity by direct titration with base using a glass electrode.

Anhydrous sodium perchlorate (G. F. Smith), glacial acetic acid, perchloric acid, and sodium hydroxide were all of reagent grade quality. We took no special precautions to exclude atmospheric carbon dioxide during the preparation of stock solutions of sodium hydroxide. Sodium hydroxide solutions were standardized by titrating weighed amounts of potassium acid phthalate. Oxydiacetic acid (98% min, Aldrich) was used without additional purification. We measured its purity as 99.1% of theoretical by means of acid–base titration, and we included this factor for the concentrations of its solutions.

All measurements were made with a total ionic strength of $I = 1.00$ M using sodium perchlorate as the supporting electrolyte. For the preparation of a working solution, we calculated the amount of sodium perchlorate necessary by including the contributions from free Pr, free acid, and the ionized ligands. No allowance was made for changes due to metal–ligand complexation.

Potentiometry. Our apparatus for potentiometric titrations consisted of a glass-piston autoburet, a digital pH meter, a double-walled titration cell (to allow temperature control by circulating thermostated water), a low sodium response glass electrode, and a calomel reference electrode (all from Radiometer). The reference electrode was filled with saturated sodium chloride (instead of potassium chloride) to avoid the precipitation of $KClO_4$ at the reference junction. All potentiometric titrations were performed at 25.00 ± 0.02 °C under a nitrogen atmosphere. The incremental titrant addition and data acquisition (titrant volume vs electrode potential) were controlled by an IBM-PC using a Data Translation A/D-I/O board (Model DT-2801A). To measure the stability constants, appropriate aliquots from four constant ionic strength working solutions (acid, metal, ligand, or blank) were titrated with sodium hydroxide titrant at the same ionic strength.

We calibrated the electrode response directly in terms of the log of the hydrogen ion concentration ($pCH = -\log [H^+]$) by titrating perchloric acid (*12*). Calibration data over the ranges of pCH 1–4 and 9–12 were fit to the exponential form of the Nernst equation, modified to allow for a sodium ion interference

$$E = E_0 + RT/F \ln ([H^+] + k[Na^+]) \qquad (2)$$

where the selectivity coefficient, k, accounts for the relative sensitivities toward the two ions (*13*). For our particular case, it was sufficient to consider the sodium concentration as identically 1 M throughout the titration. It was necessary to include the term for sodium response of the electrode only for the highest base concentrations; all calibration curves were linear at least as high as pCH 11.5. We used $pK_w = 13.79$ at 25 °C and $I = 1.0$ M for the calibration and stability constant calculations (*14*).

Conventional Spectroscopy. We recorded conventional UV–visible absorption spectra over the wavelength range 400–550 nm with a Varian 2300 spectrophotometer operating in the double-beam mode. An IBM-PC equipped with an IEEE-488 interface (National Instruments, Model GPIB-PC2A) controlled the data acquisition. The instrumental parameters relating to spectral resolution were 0.2 nm nominal spectral bandwidth, 1.0 s nominal detector response time, and 0.2 nm/s scan rate. The reference cell contained 1.0 M $NaClO_4$. We recorded the spectra at 25.0 ± 0.1 °C using a thermostated cell holder. The solutions were 2×10^{-2} M Pr and 0.0–0.4 M acetate at pH ~ 4.5 or 0.00–0.08 M oxydiacetate at pH ~ 4.

Photoacoustic Spectroscopy. A Nd:YAG laser (Spectra-Physics, Model DCR-3) pulsed at 20 Hz pumps a tunable dye laser (Spectra-Physics, Model PDL-2), which excites the sample. We used the laser dye LD466 (Exciton) to provide light of suitable wavelengths for exciting the Pr absorption bands at 468 and 481 nm. A photodiode (United Detector Technology, Model PIN-

Table I. Praseodymium Stability Constants Measured by Potentiometry at I = 1.0 M ($NaClO_4$) and T = 25.0 °C for Ligand (L) (a) Acetate, and (b) Oxydiacetate[a]

total Pr, M	total (L/Pr)	log β_{101}	log β_{102}	log β_{103}
(a) 0.026	0.98	1.888 ± 0.008		
0.014	1.99	1.902 ± 0.013	2.87 ± 0.12	
0.044	2.47	1.883 ± 0.011	2.953 ± 0.045	
0.024	5.02	1.899 ± 0.013	3.037 ± 0.055	
0.019	10.0	1.881 ± 0.010	2.886 ± 0.062	
average		1.890 ± 0.005	2.942 ± 0.038	
(b) 0.0059	1.05	5.727 ± 0.005	9.567 ± 0.011	
0.0055	2.09	5.606 ± 0.014	9.642 ± 0.011	12.183 ± 0.022
0.0053	3.15	5.774 ± 0.029	9.806 ± 0.025	12.494 ± 0.027
0.0094	5.27	5.706 ± 0.097	9.695 ± 0.087	12.367 ± 0.090
average		5.707 ± 0.034	9.686 ± 0.052	12.366 ± 0.086

[a] Errors for the individual titrations are (1σ) errors from the least-squares fits.

10DFP) that has a flat spectral response (±7%) from 450 to 950 nm monitors the intensity of each dye-laser pulse. Solutions are placed in a 1 cm square UV-quartz cell. The cell is bonded to a quartz cylinder (1 cm diameter × 1 cm) with UV-cured epoxy, which is bonded in turn to a cylindrical piezoelectric transducer (Vernitron PZT-5A, 1.5 cm diameter × 6 mm) with reflective silver epoxy. We placed the PZT inside an anodized aluminum box (~1 in. square) to shield it as much as possible from electrical noise. The entire cell-detector assembly attaches to a precision X-Y-Z translator that is rigidly fixed to the laser table. Locating pins on the bottom of the cell-detector assembly allow it to be removed from and reattached to the X-Y-Z translator without altering the geometry with respect to the laser beam.

The detector signal is amplified and shaped with a charge-sensitive pre-amp (ORTEC, Model 142C) and a differentiating amplifier (ORTEC, Model 570) with a 1-μs shaping time. A gated integrator (Stanford Research, Model SR250) samples the amplitude of the photoacoustic pulse ~20 μs after the laser trigger with a gate width of ~1 μs. A second gated integrator measures the photodiode signal from each laser pulse in order to correct for both the pulse-to-pulse power variations at a fixed wavelength as well as the variations in laser power with wavelength that arise from the dye gain.

The acquisition of a spectrum involves stepping the dye-laser monochromator to the desired starting wavelength, averaging the signal from enough laser pulses to give sufficient signal-to-noise ratio (S/N), stepping to the next wavelength, and repeating the process until the stopping wavelength is reached. An IBM-PC controls the monochromator through an IEEE-488 interface (National Instruments, Model GPIB-PC2A); it measures the voltages from the gated integrators on a pulse-by-pulse basis with an A/D-I/O board (Data Translation, Model DT-2801A). All the data for this study were acquired in a single-beam arrangement with off-line background subtraction.

The PAS spectra over the wavelength range 450–495 nm were acquired after adjusting the incident laser power to 1.5 mJ/pulse at the LD466 dye gain maximum (~473 nm). The acetate spectra were obtained by averaging 40 pulses/wavelength at a spectral resolution of 0.2 nm; the oxydiacetate spectra were obtained by averaging 50 pulses/wavelength at a spectral resolution of 0.25 nm. We measured the photoacoustic spectra at ambient temperature (~24 °C). The solutions were 1 × 10^{-4} M Pr and 0.0–0.2 M acetate at pH ~ 4.5 or 0.00–0.08 M oxydiacetate at pH ~ 4.

CALCULATIONS

Our codes for refining the stability constants from potentiometric data use a compiled BASIC version of the Marquardt algorithm for nonlinear least-squares fitting, weighted by the uncertainties in the experimental data (*15*). In general, we minimize

$$Q = \sum (Y_i^{\mathrm{exp}} - Y_i^{\mathrm{calc}})^2 / w_i \qquad (3)$$

where Y^{exp} is the total concentration of a component determined from the experimental mass balance, Y^{calc} is the total concentration calculated from the stability constants being fit, and w is the appropriate weighting factor. For measuring the ligand protonation constants and metal–ligand stability constants, we fit the total acid and total ligand concentrations, respectively. The programs were written to model the formation of only mononuclear metal/proton complexes of a single ligand in the absence of any hydrolyzed species. The weighting factors are of the form

$$w_i = \sigma^2_{Y_i^{\mathrm{exp}}} + \sigma^2_{Y_i^{\mathrm{calc}}} + \sigma^2_{Y_i^{\mathrm{exp}} Y_i^{\mathrm{calc}}} \qquad (4)$$

The programs calculate the weights by using analytical derivatives of Y^{exp} and Y^{calc} with respect to the important experimental variables of titrant volume, measured pCH, and the values of any fixed stability constants. Thus in the measurement of the ligand protonation constants, titration points near the end point are weighted less heavily than earlier points because of the dependence of the total experimental acidity (Y^{exp}) on the titrant volume. For the measurement of metal–ligand stability constants, later points are also weighted less heavily than earlier ones because of the dependence of the calculated total ligand concentration (Y^{calc}) on the uncertainty in the protonation constants.

We used a modification of the program SQUAD (*16*) for the refinement of stability constants from our spectroscopic data. SQUAD optimizes the stability constants and extinction coefficients of the assumed model to minimize the squared difference between the measured absorbance and the sum of the absorbances of each species in solution. We did not allow SQUAD to optimize the ligand protonation constants; we fixed the protonation constants to the values we measured by potentiometry, which agree within 0.01 log unit of the values recommended in a critical review of the literature (*14*).

RESULTS AND DISCUSSION

Potentiometry. To measure the protonation constants, we titrated acidic solutions of ligand at concentrations similar to those used in experiments which included praseodymium. From the weighted averages of the results from each titration, we find log β_{011} = 4.585 ± 0.011 for acetate, and log β_{011} = 3.752 ± 0.004, log β_{021} = 6.499 ± 0.006 for oxydiacetate. The (1σ) errors from the least-squares fits for any single titration were ~0.003 and ~0.006 log units for β_{011} and β_{021}, respectively.

Table I summarizes the metal–ligand stability constants we measured by potentiometry for the two ligands at various ligand/metal ratios. A convenient way of comparing titrations performed at these different conditions is to calculate the average number of ligands bound per metal, n_L, which for mononuclear complexes depends only on the free ligand concentration at any point in the titration (*1*)

$$n_L = \sum n\beta_{10n}[L]^n / (1 + \sum \beta_{10n}[L]^n) \qquad (5)$$

Table II. Stability Constants Measured by Conventional and Photoacoustic Spectroscopy of Two Pr Absorption Bands at I = 1.0 M ($NaClO_4$) and T = 25.0 °C for Ligand (L) (a) Acetate and (b) Oxydiacetate[a]

		481 nm	468 nm	481 + 468 nm
(a) UV-vis	log β_{101}	1.676 ± 0.024	1.535 ± 0.048	1.621 ± 0.028
	log β_{102}	2.383 ± 0.068	1.59 ± 0.76	2.30 ± 0.10
PAS	log β_{101}	1.636 ± 0.053		
	log β_{102}	2.61 ± 0.16		
(b) UV-vis	log β_{101}	5.445 ± 0.082	5.26 ± 0.28	5.443 ± 0.076
	log β_{102}	9.30 ± 0.11	8.98 ± 0.42	9.30 ± 0.10
	log β_{103}	11.90 ± 0.11	11.61 ± 0.41	11.90 ± 0.10
PAS	log β_{101}	5.16 ± 0.16	5.21 ± 0.24	5.22 ± 0.12
	log β_{102}	9.16 ± 0.15	9.15 ± 0.27	9.21 ± 0.12
	log β_{103}	11.81 ± 0.16	11.79 ± 0.28	11.86 ± 0.12

[a] Errors for the individual titrations are (1σ) errors from the least-squares fits.

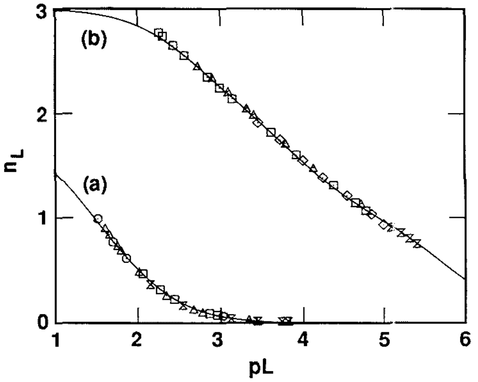

Figure 1. Comparison of the Pr speciation measured experimentally (points) by potentiometry to the speciation calculated from the stability constants (curves) expressed as n_L, the average number of ligands bound per metal ion, for (a) acetate and (b) oxydiacetate. Total ligand/metal ratios are 1 (hourglass), 2 (diamond), 3 (triangle), 5 (square), and 10 (circle).

Figure 1 shows the comparison between the experimental n_L (data points) and that calculated from the averages of the stability constants from all the titrations. Our data for oxydiacetate are consistent with the formation of three consecutive complexes, in agreement with the previous study (*8*). The stability constants are such that large percentages of each complex are reached, and there is little question as to the number of complexes formed. However, our data for acetate indicate the formation of only two complexes. Previous potentiometric studies have postulated up to four complexes at metal concentrations and ligand/metal ratios that are quite similar to those used in this study (*17*).

Spectroscopy. Ordinary UV-visible spectra indicative of the changes which occur as complexation increases are shown in Figure 2. Both the 468- and 481-nm absorption bands progressively shift to longer wavelengths as complexation increases. Table II summarizes the stability constants we measured when the 468- and 481-nm bands were analyzed individually, and when the data from both bands were analyzed simultaneously. From our analysis it is clear that the 481-nm peak is more sensitive to the effects of complexation than the 468-nm peak, since the standard deviations of the stability constants determined from the 468-nm peak are significantly higher than the errors determined from the 481-nm peak.

Inspection of the residuals between the calculated and experimental absorbances when the wrong model is fit to both peaks simultaneously also demonstrates the sensitivity of the different bands to the particular speciation model. Figure 3 compares such residual plots (for the spectra shown in Figure 2) assuming one or two acetate complexes (a) and two or three oxydiacetate complexes (b). When the models with too few complexes are used to fit the data, the magnitudes of the residuals in the 481-nm band are much larger than the corresponding residuals in the 468-nm band. This also indicates that the 468-nm peak is less sensitive to effects of complexation than the 481-nm peak. In fact for acetate, although analyzing the 468-nm peak alone tells us that more than one

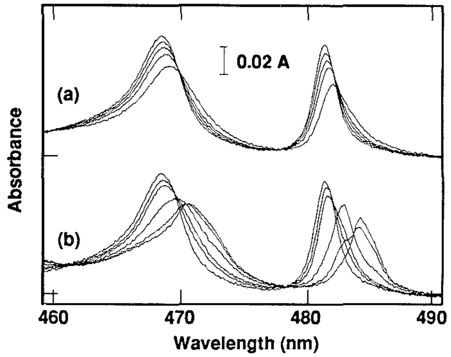

Figure 2. UV-visible absorption spectra of 0.02 M Pr showing the shift to longer wavelength with increasing ligand concentration: (a) pH ~ 4.5, total acetate 0.0, 0.015, 0.039, 0.079, and 0.30 M; (b) pH ~ 4, total oxydiacetate 0.0, 0.012, 0.020, 0.040, 0.060, 0.079 M.

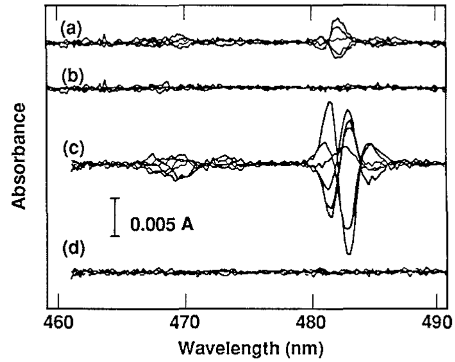

Figure 3. Absorbance residuals for the spectra shown in Figure 2: for acetate, (a) fit with one complex, (b) fit with two complexes; for oxydiacetate, (c) fit with two complexes, (d) fit with three complexes.

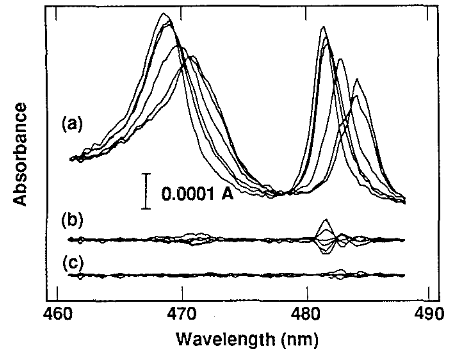

Figure 4. Photoacoustic spectra of 1 × 10^{-4} M Pr at pH ~ 4 showing the shift to longer wavelength with increasing ligand concentration. (a) total oxydiacetate, 0.0, 7.8 × 10^{-5}, 1.2 × 10^{-4}, 7.9 × 10^{-4}, 7.9 × 10^{-3}, and 2.0 × 10^{-2} M. The residuals for fitting the spectra in (a) with two and three complexes are shown in (b) and (c), respectively.

Table III. Praseodymium Stability Constants Measured at I = 1.0 M ($NaClO_4$) and T = 25.0 °C for Ligand (L) (a) Acetate and (b) Oxydiacetate

	log β_{101}	log β_{102}	log β_{103}
(a) potentiometry	1.890 ± 0.005	2.942 ± 0.038	
UV–vis	1.676 ± 0.024	2.383 ± 0.068	
PAS	1.636 ± 0.053	2.61 ± 0.16	
ref 17	1.813 ± 0.013	2.813 ± 0.040	3.279 + 0.069
(b) potentiometry	5.707 ± 0.034	9.686 ± 0.052	12.366 ± 0.086
UV–vis	5.445 ± 0.082	9.30 ± 0.11	11.90 ± 0.11
PAS	5.16 ± 0.16	9.16 ± 0.15	11.81 ± 0.16
ref 8	5.334 ± 0.010	9.225 ± 0.010	11.625 ± 0.021

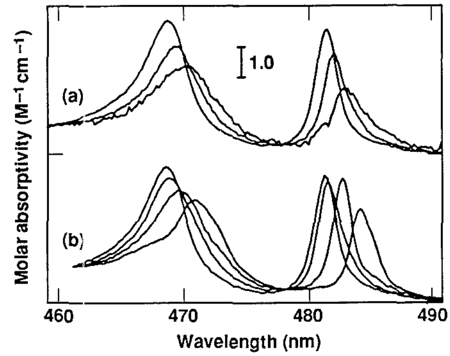

Figure 5. Absorption spectra of free Pr and the individual Pr–ligand species showing the shift to longer wavelength with increasing complexation for (a) acetate and (b) oxydiacetate.

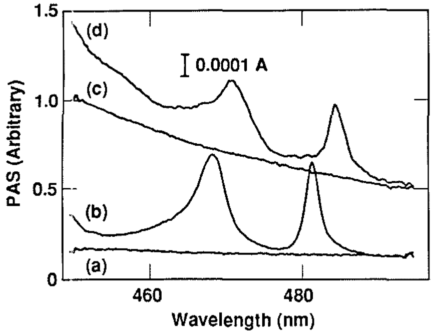

Figure 6. Photoacoustic spectra at pH ~ 4 and I = 1.00 M $NaClO_4$: (a) blank, (b) 1 × 10^{-4} M Pr, (c) 0.079 M oxydiacetate, (d) 1 × 10^{-4} M Pr + 0.079 M oxydiacetate.

complex is necessary to fit the data, we cannot extract an accurate value for the second constant from this peak. The sensitivity of the 481-nm peak is so much greater that the values measured by fitting both bands simultaneously always converge on the values determined from fitting the 481-nm peak alone (Table II).

Praseodymium also has an absorption band at 444 nm which shifts to longer wavelength as complexation increases. However, our attempts to extract stability constants from the changes in this peak were unsuccessful for both ligands. One reason for this apparent failure might be that the 444-nm peak, like the 468-nm peak for the case of acetate complexation, is too insensitive at the S/N conditions of our experiments.

Photoacoustic spectra for the praseodymium–oxydiacetate system are shown in Figure 4, along with the residuals from fitting the spectra with two and three complexes. Although the absolute concentrations of metal–ligand species for these spectra are ~200 times smaller than those whose spectra are shown in Figure 2, the same features are readily observable. Like the case for conventional absorption spectra, the residuals from fitting the photoacoustic spectra also show that the 481-nm peak is more sensitive to the effects of complexation than the 468-nm band.

Table III directly summarizes the values we measured for the stability constants by all three techniques, along with the literature values from refs 8 and 17, which were determined by potentiometry. For the spectroscopic techniques, we report the values determined from the more sensitive 481-nm band. The values of the stability constants measured by the two spectroscopic techniques agree within the uncertainties determined from the fits, even though the metal concentrations differed by a factor of ~200. This is strong evidence that praseodymium forms only mononuclear complexes over the range of metal concentrations studied. However, the stability constants measured by potentiometry appear slightly larger than those determined by the two spectroscopic techniques. We understand how this might occur when different models are fit, such as for acetate; fitting a third complex would probably lower the first and second stability constants compared to a fit to only two complexes. However, this cannot explain the apparent discrepancy for the oxydiacetate stability constants, since our model agrees with the number of complexes found by previous workers.

Figure 5 shows the absorption spectra calculated for the free Pr and the individual Pr–ligand species from fitting the conventional absorption data. In general, the extinction coefficients of the various Pr complexes derived from the two spectroscopic techniques agree within 5% across the entire absorbance band. This agreement is acceptable, since the spectral response of the photodiode used to correct for the change in laser power with wavelength can vary by ±7%. However, the extinction coefficients calculated by the two techniques did not agree as well for the second acetate complex. While the extinction coefficients near the second complex's absorbance maximum (480–486 nm) agree to within 5%, the photoacoustic data show progressively larger extinction coefficients (factors of 2–3) at the wings of the absorption band. This is probably a result of the larger uncertainties associated with measuring such a small stability constant. The uncertainty in the extinction coefficients of the second acetate complex are ~3–4 times larger than those of the free Pr or the first acetate complex, as the noise in the calculated spectrum of the second acetate complex indicates.

We should point out some observations pertinent to studying solution equilibria by the photoacoustic technique. As is true for any measurement technique where the sensitivity has been increased, the importance of experimental control over solution blanks also is increased. This is illustrated in Figure 6. The wavelength region of our study is almost ideal, since the water background is relatively low and flat. Also, there is almost no difference between the spectrum of water and the 1.0 M $NaClO_4$ used as the supporting electrolyte or for acetate at the highest concentration we used. However, oxydiacetic acid absorbs appreciably in this spectral region, and the absorption increases at shorter wavelengths. An oxydiacetate concentration of 0.08 M is the highest that we were able to use and still make an accurate background correction. At this concentration, the oxydiacetate contributes as much to the total photoacoustic signal at 484 nm as the Pr, and at 471 nm contributes more than the Pr. This did not limit our measurement of three successive stability constants for this particular system, since the total formation curve was adequately covered by this range of ligand concentrations. However, the situation with other ligand systems might be less amenable.

CONCLUSIONS

We have demonstrated that photoacoustic spectroscopy can provide basic information about metal–ligand speciation, such as the number and strength of complexes, at metal concentrations where the usual techniques of UV-visible absorption spectroscopy or potentiometry are insensitive. We verified this by comparing the praseodymium–acetate and –oxydiacetate stability constants measured by photoacoustic spectroscopy with the values measured by ordinary UV–visible spectroscopy and potentiometry at higher metal concentration. Stability constants measured by the two spectroscopic techniques agree within the experimental errors of the measurements. The number of complexes formed with each ligand are also consistent with potentiometric measurements, although it appears that the magnitudes of the stability constants determined from potentiometry are slightly larger than those measured by the two spectroscopic techniques.

LITERATURE CITED

(1) Rossotti, F. J. C.; Rossotti, H. S. *The Determination of Stability Constants*; McGraw-Hill: New York, 1961.
(2) Tam, A. C. *Rev. Mod. Phys.* **1986**, *58*, 381–431.
(3) Kitamori, T.; Suzuki, K.; Sawada, T.; Gohshi, Y.; Motojima, K. *Anal. Chem.* **1986**, *58*, 2275–2278.
(4) Klenze, R.; Kim, J. I. *Radiochim. Acta* **1988**, *44*/45, 77–85.
(5) Beitz, J. V.; Bowers, D. L.; Doxtader, M. M.; Maroni, V. A.; Reed, D. T. *Radiochim. Acta* **1988**, *44/45*, 87–93.
(6) Pollard, P. M.; Liezers, M.; McMillan, J. W.; Philips, G.; Thomason, H. P.; Ewart, F. T. *Radiochim. Acta* **1988**, *44/45*, 95–101.
(7) Moulin, C.; Delorme, N.; Berthoud, T.; Mauchien, P. *Radiochim. Acta* **1988**, *44/45*, 103–106.
(8) Grenthe, I.; Tobiasson, I. *Acta Chem. Scand.* **1963**, *17*, 2101–2112.
(9) Davidenko, N. K.; Goryushko, A. G.; Yatsimirskii, K. B. *Russ. J. Inorg. Chem.* **1973**, *18*, 943–947.
(10) Martell, A. E.; Smith, R. M. *Critical* Stability Constants, *Vol. 3: Other Organic Ligands*; Plenum Press: New York, 1977.
(11) Grenthe, I.; Bidoglio, G.; Omenetto, N. *Inorg. Chem.* **1989**, *28*, 71–74.
(12) Martell, A. E.; Motekaitis, R. J. *The Determination and Use of Stability Constants*; VCH: New York, 1988; Chapter 4.
(13) Serjeant, E. P. *Potentiometry and Potentiometric Titrations*; Wiley-Interscience: New York, 1984; p 237.
(14) Martell, A. E.; Smith, R. M. *Critical Stability Constants*, *Vol. 5*: *First Supplement*; Plenum Press: New York, 1982.
(15) Bevington, P. R. *Data Reduction and Error Analysis for the Physical Sciences*; McGraw-Hill: New York, 1969; Chapter 11.
(16) Leggett, D. J. *Computational Methods for the Determination of Formation Constants*; Leggett, D. J., Ed.; Plenum Press: New York, 1985; Chapter 6.
(17) Sonesson, A. *Acta Chem. Scand.* **1958**, *12*, 1937–1954.

RECEIVED for review August 28, 1989. Accepted November 13, 1989. This work was performed under the auspices of the U.S. Department of Energy by Lawrence Livermore National Laboratory under Contract No. W-7405-Eng-48. Neither the United States Government nor the University of California nor any of their employees, makes any warranty, express or implied, or assumes any legal liability or responsibility for the accuracy, completeness, or usefulness of any information, apparatus, product, or process disclosed, or represents that its use would not infringe privately owned rights. Reference herein to any specific commercial products, process, or service by trade name, trademark, manufacturer, or otherwise, does not necessarily constitute or imply its endorsement, recommendation, or favoring by the United States Government or the University of California.

Anal. Chem. 1990, 62, 304–308

Kinetics of the Reaction between Aromatic Aldehydes and *o*-Dianisidine

Mayda Lopez-Nieves,[1] **Peter D. Wentzell,**[2] **and S. R. Crouch***

Department of Chemistry, Michigan State University, East Lansing, Michigan 48824

Kinetics studies were performed to investigate the mechanism of Schiff base formation in the reaction between aromatic aldehydes and *o*-dianisidine. The studies were conducted at 40 °C with ethanol as solvent and acetic acid and stannic chloride as catalysts. The evidence supports a three-path mechanism. Two paths are catalyzed by acetic acid and the other by stannic chloride. In the acetic acid catalyzed pathways, it is proposed that the first step involves the reaction of the aldehyde with a solvated proton (i.e., specific acid catalysis). Depending on the acidity of the medium, free or monoprotonated *o*-dianisidine attacks the carbonyl carbon to form a carbinolamine intermediate which then dehydrates to form the product. In the stannic chloride catalyzed path, it is proposed that the aldehyde is first complexed to stannic chloride. The complexed aldehyde is then attacked by a 2:1 *o*-dianisidine–stannic chloride complex to form a carbinolamine which continues to react to form the product. The rate law derived from the proposed mechanism is in agreement with the experimental data and observations. Analytical implications of the kinetics studies are discussed.

INTRODUCTION

There is currently a good deal of interest in the automated determination of aromatic aldehydes. It is important to determine trace levels of aldehydes in the air (*1*), in water (*2*), in foods (*3*), and in many other samples (*4*).

The most widely used instrumental methods for determining aromatic aldehydes involve UV–visible absorption spectrophotometry (*4–6*) and molecular fluorescence spectrometry (*7*). Unfortunately, many of these methods are subject to interferences, especially from ketones. Furthermore, many of the procedures are difficult to automate because they require somewhat extreme conditions, such as mixing with concentrated acids, high temperatures, or long reaction times (*4, 7*).

One potential reaction that has not been widely studied is the Schiff base formation reaction of *o*-dianisidine with aromatic aldehydes. This reaction was originally used as a spot test by Feigl (*8*) and has been reported by Wasicky and Frehden (*9*) to be sensitive and selective for aromatic aldehydes. However, the reaction has not been extensively applied, probably because of the reported instability of the colored product (*10*) and the positive, although lower, response of some ketones (*11*).

Because of the potential analytical applications of the *o*-dianisidine reaction with aldehydes, we have undertaken a kinetics and mechanistic study. Addition reactions of primary amines to carbonyl groups (in water as solvent) have been studied extensively (*12–15*). In water as solvent, the addition of amines to aldehydes is proposed to occur by forming a carbinolamine intermediate which subsequently dehydrates to form an imine. The initial attack of the amine at the carbonyl carbon has been reported to occur via specific or general acid catalysis depending on the basicity of the amine and the strength of the acid catalyst (*14, 15*). The kinetics studies reported here of the reaction of *o*-dianisidine with a representative aldehyde, 2,4-dichlorobenzaldehyde, in ethanolic media are interpreted in terms of a mechanism that is similar to those previously reported for aqueous reactions. Analytical implications of the results are discussed.

PRELIMINARY CONSIDERATIONS

The reaction of aromatic aldehydes with *o*-dianisidine can be described by the simplified equilibrium shown below

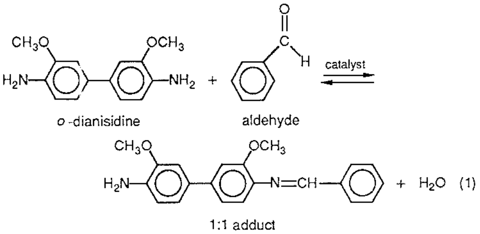

Preliminary tests indicated that ethanol was an excellent solvent because the equilibrium lies to the right and most aldehydes are soluble in ethanol. Stannic chloride and acetic acid were employed as catalysts. When they were used simultaneously, there was an interaction that led to a higher and more rapid response than obtained with either catalyst alone. A small amount of product decomposition was observed at high stannic chloride concentrations. For the kinetics studies, concentrations were chosen so as to obtain reasonable rates with minimal product decomposition.

For solutions containing acetic acid, the solvated proton concentration, $EtOH_2^+$ here abbreviated as simply H^+, was calculated from eq 2 which assumes that the dissociation of acetic acid in ethanol ($K_a = 5.92 \times 10^{-11}$ at 25 °C) is very small

$$[H^+] = (K_a C_{HOAC})^{1/2} \qquad (2)$$

where C_{HOAC} is the analytical concentration of acetic acid.

Preliminary experiments were also performed to ascertain the conditions under which the 1:1 adduct shown in eq 1 was formed preferentially over a 2:1 aldehyde to *o*-dianisidine adduct. A 10-fold molar excess of *o*-dianisidine to aldehyde was found necessary to ensure formation of only the 1:1 adduct. Hence, in the kinetics studies, the molar ratio of *o*-dianisidine to aldehyde was never lower than 10.

EXPERIMENTAL SECTION

Reagents. Commercial absolute ethanol was dried with 3-Å molecular sieves (Davison Chemical, Baltimore, MD). After being decanted, it was filtered through a 0.40 μm pore filter (Millipore Corp., Bedford, MA).

---

* Author to whom correspondence should be addressed.

[1] Present address: University of Puerto Rico, Aguadilla Regional College, P.O. Box 160, Ramey Station, Aguadilla, PR 00604.

[2] Present address: Department of Chemistry, Dalhousie University, Halifax, NS, Canada B3H 4J3.

0003-2700/90/0362-0304$02.50/0 © 1990 American Chemical Society

The *o*-dianisidine was recrystallized 4 to 5 times from ethanol by using 50–200 mesh activated coconut charcoal as a decolorizing agent (Fisher Scientific, Springfield, NJ). The final product was vacuum dried and stored in a desiccator in the dark. The net yield was approximately 38% of white to off-white crystals. These are stable for more than 6 months if all solvent is removed. Solutions of *o*-dianisidine must be prepared fresh daily.

The 2,4-dichlorobenzaldehyde was of commercial origin. It was recrystallized from ethanol and then vacuum dried. NMR spectra and melting points were used to check identity and purity.

Procedure. For the kinetics studies, the method of initial rates was employed in order to avoid complications from product decomposition at high catalyst concentrations. Absorbance (380 nm) versus time data were acquired with an IBM compatible personal computer (Bentley Model T, Round Rock, TX) interfaced to a thermostated, modular single-beam spectrophotometer (CGA McPherson, Acton, MA). Triplicate runs were made at each concentration. After data acquisition, initial rates were calculated by dividing the initial slope of the absorbance versus time plot by the molar absorptivity of the product (for the 1:1 adduct of *o*-dianisidine and 2,4-dichlorobenzaldehyde $\epsilon = 1.34 \times 10^4$ L mol^{-1} cm^{-1}). Preliminary reaction orders were determined from slopes of log (initial rate) versus log (concentration) plots. The concentration of *o*-dianisidine was fixed at 6.31×10^{-3} M and that of 2,4-dichlorobenzaldehyde at 6.00×10^{-5} M, unless otherwise noted (e.g., when determining the order with respect to either of these reagents). Because of the difficulty in estimating ionic strength in ethanolic solutions, the influence of ionic strength was not investigated.

For the kinetics experiments, the desired volume of *o*-dianisidine was first added into a 1.0 cm path length quartz cuvette with a micropipet. The aldehyde solution was then added and the solution mixed manually. The cuvette was placed in the spectrophotometer and allowed to equilibrate thermally for 5.0 min. The catalyst solution (0.50 mL) was then added with a syringe.

Reaction temperature was maintained at 40.0 ± 0.2 °C by circulating water from a constant-temperature bath around the spectrophotometer cuvette. All solutions were maintained at 40 °C for at least 15 min prior to use.

RESULTS

Characterization of the Product. The molar ratio method of Yoe and Jones (*16*) suggested that both a 1:1 aldehyde–*o*-dianisidine adduct and a 2:1 product could be formed. These studies indicated that the 1:1 adduct forms exclusively at low molar ratios of aldehyde–*o*-dianisidine (<0.10). This was confirmed by comparing NMR spectra of reaction mixtures at these molar ratios to those obtained of the isolated 1:1 adduct, the isolated 2:1 adduct, and mixtures of these adducts. Mass spectral studies of reaction mixtures at low molar ratios of aldehyde to *o*-dianisidine detected only the molecular ion of the 1:1 adduct. The molecular ion of the 2:1 adduct was detected only when it was purposely added to the mixture. Additional details may be found in ref 17.

Dependence on Aldehyde Concentration. The concentration of the aldehyde was varied from 6.31×10^{-6} to 3.98×10^{-4} M. The calculated orders from the log–log plots of initial rate versus the aldehyde concentration were 0.93 ± 0.06 when catalyzed by 3.98×10^{-4} M stannic chloride, 0.87 ± 0.03 when catalyzed by 1.00 M acetic acid, and 0.86 ± 0.05 for a mixture of both catalysts (2.51×10^{-4} M stannic chloride and 0.562 M acetic acid).

Dependence on Stannic Chloride Concentration. The concentration of stannic chloride was varied from 1.00×10^{-6} to 2.51×10^{-3} M. At concentrations below 1.59×10^{-5} M in stannic chloride, the reaction rate becomes immeasurably slow. At these low concentrations of stannic chloride, when 1.00×10^{-2} M acetic acid is also present, the reaction that occurs is due to the acetic acid only (Figure 1). The effect of the stannic chloride at these very low concentrations of acetic acid is to cause decomposition of either the product or an intermediate formed by the acetic acid catalyzed reaction. At concentrations above 1.59×10^{-5} M, the order with respect to stannic chloride was found to be 1.8 ± 0.6 in the presence and in the absence of acetic acid. At concentrations of stannic chloride above 2.50×10^{-3} M, the log–log plots show negative slopes. This parallels the occurrence of a decomposition side reaction as the concentration of stannic chloride is increased.

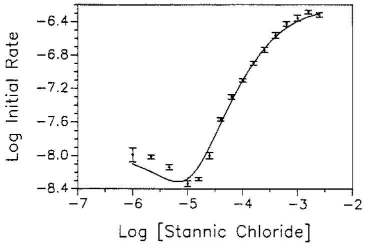

Figure 1. log initial rate vs log stannic chloride concentration in the presence of 0.0100 M acetic acid. The *o*-dianisidine concentration was 6.31×10^{-3} M, while the 2,4-dichlorobenzaldehyde concentration was 6.00×10^{-5} M. The error bars represent the experimental points ± one standard deviation (calculated from three determinations). The solid line represents the predictions of the best fitting rate law.

Dependence on *o*-Dianisidine Concentration. The concentration of *o*-dianisidine was varied from 6.31×10^{-4} to 0.0126 M. The lower limit of the concentration range was set by our desire to maintain the *o*-dianisidine to aldehyde molar ratio greater than 10. The solubility of *o*-dianisidine in ethanol limited stock solutions to a maximum concentration of 0.0300 M.

At concentrations of *o*-dianisidine lower than 3.16×10^{-3} M, the slopes of the log–log plot were found to be 0.73 ± 0.1 and 0.86 ± 0.06 at acetic acid concentrations of 0.0178 and 0.562 M respectively. Both orders decreased to lower values as the *o*-dianisidine concentration was increased. The order with respect to *o*-dianisidine was found to be 1.7 ± 0.2 in the presence of 3.98×10^{-4} M stannic chloride and 1.3 ± 0.3 when a mixture of the catalysts (6.31×10^{-4} M stannic chloride and 0.100 M acetic acid) was employed. Again, both orders decreased to lower values as the *o*-dianisidine concentration increased.

Dependence on Acid Concentration. The dependence of the initial rate on the solvated H$^+$ concentration is affected by the concentration of *o*-dianisidine. As the concentration of *o*-dianisidine was increased from 6.39×10^{-4} to 0.0240 M, a gradual break in the initial rate profile of the log–log plots began to appear which suggests a change in order with respect to H$^+$ as the concentration of *o*-dianisidine increases. This break can be seen for an *o*-dianisidine concentration of 0.0240 M in Figure 2. In Figure 2 the order is 1.1 ± 0.2 at concentrations of acetic acid between 1.00×10^{-2} M and 5.62×10^{-2} M and 2.0 ± 0.3 at concentrations between 1.78×10^{-1} M and 1.78 M. At 6.39×10^{-4} M *o*-dianisidine, a linear log–log plot was obtained in which a mixed order of 1.46 ± 0.05 is observed.

Experimental Rate Law. The general purpose curve fitting program KINFIT (*18*) was used to test a variety of potential rate laws. Global fits of all the experimental points to the rate laws were performed in which each data point was weighted according to its variance. To guide the search for the best experimental rate law, the known mechanisms for Schiff base formation in water were used along with modifications to the limiting rate laws obtained from the preliminary reaction-order experiments (log–log plots). In the mechanisms shown below letters are used to represent the species involved as follows: A, 2,4-dichlorobenzaldehyde; B, *o*-dianisidine; H$^+$, solvated proton; S, stannic chloride. About 450 rate laws were tested. The rate law shown in eq 3 gave the best fit.

$$\text{initial rate} = [A]\left[\text{Par}(1)[B][H^+]^2 + \frac{\text{Par}(2)[B][H^+]}{1 + \text{Par}(3)[B] + \text{Par}(7)[S]} + \frac{\text{Par}(4)[S]^2[B]^2}{\text{Par}(8) + \text{Par}(5)[S]^2[B] + [S][B]^2}\right] \quad (3)$$

In this equation, Par(1) to Par(7) are parameters that represent products or ratios of rate and/or equilibrium constants. The statistical figures of merit of the experimental rate law as calculated by the KINFIT program are listed in Table I.

DISCUSSION

Only a few mechanisms can be written that produce the empirical rate law. The mechanism proposed below is the most chemically plausible. In the proposed mechanism, there are three distinct paths. Two of the paths are catalyzed by acetic acid, the other by stannic chloride.

Acetic Acid Path at Low Acid Concentrations. At low acetic acid concentration the second term in brackets in eq 3 is expected to dominate when the concentration of *o*-dianisidine is large relative to that of the acid. A possible mechanism is as follows:

step 1

$$A + H^+ \underset{k_{-1}}{\overset{k_1}{\rightleftharpoons}} A^+H$$

step 2

$$A^+H + B \underset{k_{-2}}{\overset{k_2}{\rightleftharpoons}} AHB^+$$

postequilibrium

$$AHB^+ \rightleftharpoons \text{product} + H_2O + H^+ \qquad \text{fast}$$

side reaction

$$A^+H + S \xrightarrow{k_d} \text{decomposition}$$

At low concentrations of acetic acid, step 1 is relatively slow. The steady-state approximation was used to find an expression for the concentration of the intermediate A^+H. The reverse of step 2 was neglected because initial rates are used. Since all of the steps following step 2 are rapid, the initial rate of product formation is given by the rate of step 2. Equation 4 is obtained after substituting for the concentration of intermediate A^+H in the rate expression. This is equivalent to the middle term in the experimental rate law.

$$\text{initial rate} = \frac{k_1k_2[A][H^+][B]}{k_{-1} + k_2[B] + k_d[S]} \quad (4)$$

where

$$\text{Par}(2) = k_1k_2/k_{-1},\ \text{Par}(3) = k_2/k_{-1},\ \text{and}\ \text{Par}(7) = k_d/k_{-1}.$$

Acetic Acid Path at High Acetic Acid Concentrations. As the acetic acid concentration increases, the first term in brackets in eq 3 becomes increasingly important. Because the concentration of acid is high, step 1 in the above mechanism is rapid. Consequently, there is a fast and large production of the intermediate A^+H in a preequilibrium step. At this high concentration of acetic acid most of the *o*-dianisidine should also be protonated. Therefore, a plausible mechanism is that the A^+H intermediate is attacked by protonated *o*-dianisidine rather than by neutral *o*-dianisidine giving rise to a different path for product formation. In this new path the protonated species A^+H and B^+H originate in equilibria prior to the rate-determining step as illustrated below.

Table I. Figures of Merit of the Experimental Rate Law

parameter	value	std dev	mul corr coef
1	0.344	0.018	0.72
2	0.604	0.074	0.95
3	24.1	4.8	0.95
4	22.5	1.3	0.97
5	14.7	1.4	0.95
6	2.14×10^{-9}	2.5×10^{-10}	0.83
7	9.76×10^5	3.1×10^5	0.55

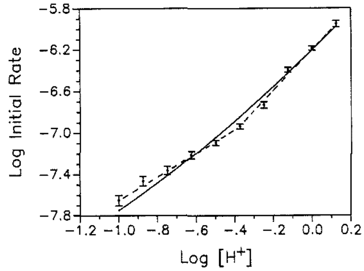

Figure 2. Log initial rate vs log hydrogen ion concentration at 0.0240 M *o*-dianisidine and 6.00 × 10^{-5} M 2,4-dichlorobenzaldehyde. The error bars represent the experimental points ± one standard deviation (calculated from three determinations). The solid line represents the predictions of the best fitting rate law.

preequilibria:

$$A + H^+ \rightleftharpoons A^+H \quad K_{AH} = \frac{[A^+H]}{[A][H^+]}$$

$$B + H^+ \rightleftharpoons B^+H \quad K_{BH} = \frac{[B^+H]}{[B][H^+]}$$

rate-determining step:

$$A^+H + B^+H \underset{k^{-1''}}{\overset{k_1''}{\rightleftharpoons}} AHB^+ + H^+$$

postequilibrium:

$$AHB^+ \rightleftharpoons \text{product} + H_2O + H^+ \qquad \text{fast}$$

After the concentrations of A^+H and B^+H in the rate expression are substituted for in terms of the concentration of the initial reactants, eq 5 is obtained (the reverse step with rate constant k_{-1} was neglected). This agrees with the first term in the experimental rate law with Par(1) being $k_1''K_{AH}K_{BH}$.

$$\text{initial rate} = k_1''K_{AH}K_{BH}[A][B][H^+]^2 \quad (5)$$

In a separate set of experiments it was confirmed by pH titrations that only free and monoprotonated *o*-dianisidine exist under the conditions used in the kinetics experiments with acetic acid as the catalyst.

Two parallel paths have been proposed when acetic acid is the catalyst. The total rate in the presence of acetic acid is given by the sum of the two rate expressions given previously (first two terms of eq 3). A gradual shift from one reaction path to the other should be observed as the concentration of free *o*-dianisidine varies with changes in the acetic acid concentration. This explains the change in order with respect to H^+ (Figure 2).

The kinetics of the reaction using HCl as the acid were also investigated. It was confirmed by pH titrations that HCl easily protonates both amino groups of *o*-dianisidine. Hence, the mechanism is expected to be more complex with HCl than with acetic acid. Unfortunately, the kinetics results were not reproducible with HCl and no meaningful rate law was obtained.

Stannic Chloride Catalyzed Path. The stannic chloride catalyzed path is characterized by the third term in the experimental rate law (eq 3). It is known that stannic chloride rapidly forms stable coordination complexes (*19–22*) upon mixing with ethanol, acetic acid, amines, and carbonyl compounds. The usual stoichiometry of these compounds is L_2SnCl_4, but the presence of 1:1 complexes has also been demonstrated in solution (*22*). The kinetics experiments using stannic chloride as catalyst suggest the presence of both 1:2 and 2:1 stannic chloride–*o*-dianisidine complexes. Expressions for the concentration of these species in terms of the starting reagents were derived assuming equilibrium reactions leading to their formation. One plausible mechanism is

preequilibria:

$$\mathrm{S} + \mathrm{B} \rightleftarrows \mathrm{SB} \quad K_{1\mathrm{SB}} = \frac{[\mathrm{SB}]}{[\mathrm{S}][\mathrm{B}]}$$

$$\mathrm{SB} + \mathrm{B} \rightleftarrows \mathrm{SB}_2 \quad K_{2\mathrm{SB}} = \frac{[\mathrm{SB}_2]}{[\mathrm{SB}][\mathrm{B}]}$$

step 1 $$\mathrm{A} + \mathrm{S} \underset{k_{-1}'}{\overset{k_1'}{\rightleftarrows}} \mathrm{AS}$$

step 2 $$\mathrm{AS} + \mathrm{SB}_2 \underset{k_{-2}'}{\overset{k_2'}{\rightleftarrows}} \mathrm{ASB} + \mathrm{SB}$$

postequilibria:

$$\mathrm{ASB} \rightleftarrows \mathrm{AB} + \mathrm{S} \quad \text{fast}$$

$$\mathrm{AB} + \mathrm{H}^+ \rightleftarrows \text{product} + \mathrm{H_2O} + \mathrm{H}^+ \quad \text{fast}$$

side reactions:

$$\mathrm{SB} + \mathrm{S} \rightleftarrows \mathrm{S_2B} \quad K_{3\mathrm{SB}} = \frac{[\mathrm{S_2B}]}{[\mathrm{SB}][\mathrm{S}]}$$

$$\mathrm{AS} + \mathrm{S_2B} \xrightarrow{k_d'} \text{decomposition}$$

Application of the steady-state approximation to the AS intermediate results in

$$\text{initial rate} = \frac{k_2'k_1'K_{1\mathrm{SB}}K_{2\mathrm{SB}}[\mathrm{A}][\mathrm{S}]^2[\mathrm{B}]^2}{k_{-1}' + k_d'K_{1\mathrm{SB}}K_{3\mathrm{SB}}[\mathrm{S}]^2[\mathrm{B}] + k_2'K_{1\mathrm{SB}}K_{2\mathrm{SB}}[\mathrm{S}][\mathrm{B}]^2} \quad (6)$$

This rate expression is identical with the stannic chloride catalyzed term in the experimental rate law, where

$$\mathrm{Par}(4) = k_1',\ \mathrm{Par}(5) = \frac{k_d'K_{3\mathrm{SB}}}{k_2'K_{2\mathrm{SB}}},\ \text{and}$$

$$\mathrm{Par}(6) = \frac{k_{-1}'}{k_2'K_{1\mathrm{SB}}K_{2\mathrm{SB}}}$$

The proposed mechanism is consistent with the observation that an increase in the stannic chloride concentration increases the decomposition side reaction, by presumably increasing the production of S_2B. On the other hand, it was observed that an increase in the *o*-dianisidine concentration decreased the decomposition side reaction. Larger concentrations of *o*-dianisidine should favor the equilibrium leading to the formation of SB_2 at the expense of the formation of S_2B. The formation of S_2B may occur initially, upon mixing of the reagents, and during the course of the reaction as SB and S are released in step 2 and in the first postequilibria step, respectively.

Aminostannanes of the form >Sn–N< cannot generally be prepared by direct aminolysis of stannic chloride (*23*). Therefore, the following possible formulas for the active species are proposed: $S_2B = SnCl_4$·*o*-dianisidine·$SnCl_4$, and $SB_2 = SnCl_4$·(*o*-dianisidine)$_2$.

The net stoichiometric equation derived from this mechanism is

$$\mathrm{A} + 2\mathrm{S} + 2\mathrm{B} \rightarrow \text{product} + \mathrm{H_2O} + \mathrm{S} + \mathrm{SB} \quad (7)$$

The stoichiometric equation points to the necessity of having excess *o*-dianisidine to enhance the formation of the SB_2 species over that of the S_2B species. As inferred from the stoichiometric equation, the minimum concentration of *o*-dianisidine should be set to not less than 2 times the concentration of the stannic chloride plus the concentration of the aldehyde present, $[\mathrm{B}]_{\min} = 2[\mathrm{S}] + [\mathrm{A}]$, to avoid the formation of the S_2B species.

In the stannic chloride catalyzed path, hydrogen ions are needed for the postequilibria to occur. In the absence of acetic acid and at short reaction times, the required hydrogen ions probably come from the solvolysis reaction of stannic chloride in ethanol (*20, 22*), as shown in eq 8. The presence of hydrogen ions in the absence of acetic acid suggests the possibility of the reaction proceeding simultaneously via a mechanism analogous to the one proposed for low acetic acid concentrations.

$$\mathrm{SnCl_4} + 2\mathrm{CH_3CH_2OH} \rightarrow \mathrm{SnCl_3OCH_2CH_3{\cdot}HOCH_2CH_3} + \mathrm{HCl} \quad (8)$$

In general, the proposed mechanisms for all three paths are very similar. The first step involves the reaction of the aldehyde with the catalyst, either H^+ or stannic chloride, followed by the formation of the protonated carbinolamine and a subsequent dehydration to form the product. The fact that *o*-dianisidine only protonates one of its two amino groups explains why, in ethanol, an increase in rate is still observed with increasing high acetic acid concentrations while in water; the carbinolamine formation is proposed to be hindered due to the protonation of the amine (*12*). These results are not contradictory. Water is a better donor and acceptor of protons than ethanol. Consequently, high concentrations of acids are not needed for the reaction to occur in water. The small basicity of *o*-dianisidine, and the smaller dissociation constant of the ethanol relative to water, are two reasons for the requirement of an initial protonation of the aldehyde prior to the amine attack.

ANALYTICAL IMPLICATIONS

Reagent Concentrations. The *o*-dianisidine concentration should be made as high as its solubility permits. High *o*-dianisidine concentrations not only increase the rate of the reaction but also shift the equilibrium toward products. Hence, a higher response is obtained for the same amount of aldehyde, which increases the sensitivity. A high *o*-dianisidine concentration is also helpful in decreasing the amount of decomposition observed at high concentrations of stannic chloride. As predicted by the stoichiometric equation, the *o*-dianisidine concentration should be set to not less than 2 times that of the stannic chloride plus that of the aldehyde to favor formation of the SB_2 complex in preference over the S_2B complex. At the same time, the concentration of the *o*-dianisidine relative to that of the aldehyde should never be less than 10, to favor the formation of the 1:1 aldehyde to *o*-dianisidine adduct in preference to the 2:1 adduct.

Of the two catalysts studied, stannic chloride is a better catalyst than acetic acid. With stannic chloride, the reaction reaches equilibrium in a shorter reaction time, even though its concentration is 3 orders of magnitude less than that required with acetic acid.

Experimental Conditions. The first choice of experimental conditions is to decide which temperature to use. Although the effect of temperature was not rigorously studied in these kinetics experiments, it was observed that increasing the temperature increased the rate at which the reaction occurred. Therefore, temperatures above room temperature are recommended when implementing this reaction as an analytical procedure. Temperatures in the 30–50 °C range should be tested during optimization experiments.

A second concern deals with the possible interference of water in the method. All three proposed mechanisms form water as a byproduct. It has been documented in the literature, and observed during these studies, that the presence of water shifts the equilibrium towards reactants. Precautions that can be taken to remove the water interference include drying the ethanol, as in our case with molecular sieves, or using the standard addition method when analyzing samples containing water.

Registry No. SnCl$_4$, 7646-78-8; 2,4-dichlorobenzaldehyde, 874-42-0; *o*-dianisidine, 119-90-4; acetic acid, 64-19-7.

LITERATURE CITED

(1) Grosjean, D. *Environ. Sci. Technol.* **1982**, *16*, 254–262.
(2) Noordsij, A.; Puyker, L. M.; Van Der Gaag, M. A. *Sci. Total Environ.* **1985**, *47*, 273–292.
(3) Nagy, S.; Randall, V. *J. Agric. Food Chem.* **1973**, *21*, 272–275.
(4) Sawicki, E.; Sawicki, C. R. *Aldehydes Photometric Analysis*; Academic Press: London, 1975–1978; Vols. 1–5.
(5) Siggia, S.; Hanna, J. G. *Quantitative Organic Analysis via Functional Groups*, 4th ed.; Wiley-Interscience: New York, 1979; pp 95–160.
(6) Siggia, S. *Instrumental Methods of Organic Functional Group Analysis*; Wiley-Interscience: New York, 1972; pp 75–102.
(7) Nakamura, M.; Toda, M.; Saito, H.; Ohkura, Y. *Anal. Chim. Acta* **1982**, *134*, 39.
(8) Feigl, F. *Qualitative Analysis by Spot Test*, 3rd ed.; Elsevier Publishing Co.: New York, 1946; pp 340–344.
(9) Wasicky, R.; Frehden, O. *Mikrochim. Acta* **1937**, *1*, 55–63.
(10) Wearn, R. B.; Murray, W. M., Jr.; Ramsey, M. P.; Chandler, N. *Anal. Chem.* **1948**, *20*, 922–924.
(11) Cerdá, V.; Mongay, C. *Analusis* **1976**, *4* (2), 94–97.
(12) Jencks, W. P. In *Progress in Physical Organic Chemistry*; Cohen, S. G., Streitwieser, A., Jr., Taft, R. W., Eds.; Wiley-Interscience: New York, 1964; Vol. 2.
(13) Sayer, J. M.; Pinsky, B.; Schonbrunn, A.; Washtien, W. *J. Am. Chem. Soc.* **1974**, *96*, 7998–8009.
(14) Rosenberg, S.; Silver, S. M.; Sayer, J. M.; Jencks, W. P. *J. Am. Chem. Soc.* **1974**, *96*, 7986–7998.
(15) Sayer, J. M.; Edman, C. *J. Am. Chem. Soc.* **1979**, *101*, 3010–3016.
(16) Yoe, J. H.; Jones, A. L. *Ind. Eng. Chem. Anal. Ed.* **1944**, *16*, 111.
(17) Lopez-Nieves, M., Ph.D. Dissertation, Michigan State University, East Lansing, MI, 1989.
(18) Dye, J. L.; Nicely, V. A. *J. Chem. Educ.* **1971**, *48*, 443–448.
(19) Bradley, D. C.; Caldwell, E. V.; Wardlaw, W. *Chem. Soc. J.* **1957**, 3039–3042.
(20) Guenzet, J.; Camps, M.; Toumi, A. *C.R. Acad. Sci.* **1972**, *274* (12), 1211–1214.
(21) Laubengayer, A. W.; Smith, Wm. C. *J. Am. Chem. Soc.* **1954**, *76*, 5985–5989.
(22) Beattie, I. R. *Q. Rev. Chem. Soc.* **1963**, *17*, 382–405.
(23) Jones, K.; Lappert, M. F. *Organomet. Chem. Rev.* **1966**, *1*, 67–92.

RECEIVED for review July 26, 1989. Accepted November 8, 1989. The authors gratefully acknowledge the financial support of the National Science Foundation through NSF Grant No. CHE 8705069.

CORRESPONDENCE

Comparison of Diffuse Reflectance and Diffuse Transmittance Spectrometry for Infrared Microsampling

Sir: For over 10 years, techniques for the application of Fourier transform infrared (FT-IR) spectrometry to the detection and identification of substances separated by high-performance liquid chromatography (HPLC) by mobile phase elimination have been studied. Depending on the nature of the substrate, the infrared measurement can be made by diffuse reflectance (*1–7*), transmittance (*8–11*), reflection-absorption (*12, 13*) or diffuse transmittance (11) spectrometry; see Figure 1. Each technique has certain disadvantages. For deposition on a smooth substrate such as a salt window or metallic strip, the sample spreads over an area of at least 1 mm^2 unless aspiration techniques are used (*7, 11*). Even then, spreading can occur if high gaseous flow rates are involved if the solvent has not completely evaporated before the liquid droplets reach the substrate surface. Complete elimination of the solvent has necessitated either that the effluent be subjected to high temperatures, with the concomitant risk of thermal degradation (*12, 13*), or that sophisticated, and hence expensive, approaches such as monodisperse aerosol generation (*14*) are required. The use of diffusely reflecting substrates with a high effective surface area increases the rate of solvent evaporation at the substrate, thereby minimizing lateral spreading of the solute, apparently favoring the application of diffuse reflectance (DR) infrared spectrometry from HPLC/FT-IR measurements. From measurements made in this laboratory, however, it was found that the intensity of absorption bands in diffuse reflectance HPLC/FT-IR spectra is greatest if the eluting analyte was deposited near the top surface of the diffusely reflecting medium, since the intensity of the beam decays rapidly as a function of depth. Although effective measurements can be made when low boiling normal-phase HPLC solvents are used, we have found that for solvents with a boiling point greater than 80 °C, evaporation is often so slow that significant quantities of each analyte are carried to the lower portion of the powdered medium and the analytical signal is greatly reduced in intensity. Since all mobile phases used for reverse-phase HPLC have reasonably high boiling points and the most commonly used solvent, water, is the least amenable to rapid evaporation because of its unique thermodynamic properties, it became clear that an alternative technique would have to be found.

Diffuse transmittance (DT) spectrometry has certain advantages over diffuse reflectance, and preliminary HPLC/FT-IR results using this technique are very promising (*11, 15*). Although it was obvious to us that diffuse transmittance could be effective since the entire sample depth is interrogated by the infrared beam, little is known about DT from a practical standpoint in terms of either sensitivity or variation of band intensity with concentration or path length. In the conventional application of the Beer–Lambert equation, it is usually assumed that the absorptivity of any band remains constant, and the path length and concentration may be varied. For

0003-2700/90/0362-0308$02.50/0 © 1990 American Chemical Society

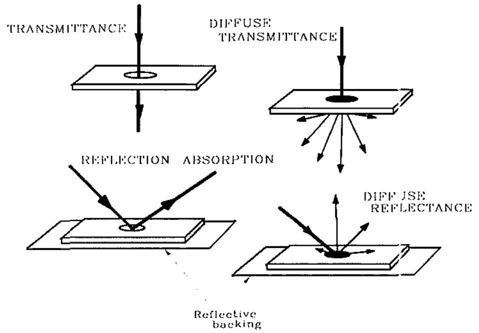

Figure 1. Sampling techniques used for HPLC/FT-IR measurements with mobile phase elimination.

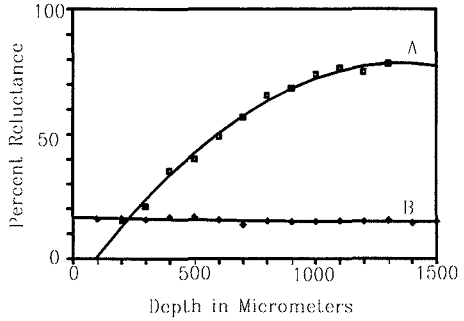

Figure 2. Comparison of reluctance as a function of depth for diffuse reflectance (◆) and diffuse transmittance (■) spectrometry.

a uniform sample composed of an infrared-absorbing organic analyte on a nonabsorbing powdered substrate, the integrated product of path length and concentration gives rise to the measured absorption. Therefore, for transmittance measurements, regardless of how the sample is distributed with respect to depth, it might be thought that the absorption caused by a given quantity of analyte should be constant. However the extent to which the beam is scattered may lead to an increase in the effective path length in the manner discussed by Kortüm (*16*). In addition, the signal-to-noise ratio (SNR) of the analyte spectrum will vary with the thickness of the substrate because of scattering of light away from the detector by the diffuse medium.

Typical quantities of each component of a sample injected into a liquid chromatograph for which FT-IR techniques are applicable are in the low microgram to nanogram range. Subnanogram quantities would not be expected to give an appreciable signal in HPLC/FT-IR measurements, while greater quantities will overload the column. With respect to the Beer–Lambert law, maximization of the path length and concentration terms produces the largest absorption. Thus to maximize the signal due to any component in an HPLC/FT-IR measurement, the eluite must be deposited in as small an area as possible to increase the path length. Through the use of flow focusing techniques coupled with a sprayer for deposition, we have demonstrated the feasibility of making such depositions as a spot of less than 250 μm in diameter (*11*, *15*), suggesting that a microscope would be the optimal sampling accessory with which to obtain diffuse reflectance and diffuse transmitance spectra of such samples. Even though the relative merits of diffuse reflectance and diffuse transmittance as sampling techniques for HPLC/FT-IR measurements have been demonstrated (*11*, *15*), it is probable that the operational parameters for neither technique were fully optimized. In this note, we report the first study designed to study band intensities in DR and DT measurements of the same samples.

Diffuse reflectance spectra of analytes at low concentration in a nonabsorbing matrix usually obey the Kubelka–Munk equation, which is a limiting equation for which the sample has to be at "infinite depth". Eight years ago the dependence of the absorption of a model analyte (carbazole dispersed in KCl) on sample depth for diffuse reflectance measurements was described (*17*). It was shown that a reasonable estimate of the sample thickness in order that the infinite depth criterion be fulfilled was between 1.5 and 3.0 mm. To maintain an adequate SNR for diffuse transmittance spectrometry, the thickness of the substrate in an HPLC/FT-IR measurement should therefore be less than 1 mm. Kortüm (*16*) has derived several equations relating diffuse reflectance with path length and concentration for samples of finite thickness. These more complicated theoretical forms of the Kubelka–Munk equation can be used to predict the reflectance and transmittance of thin powdered samples of less than infinite depth. The application of these equations requires an accurate knowledge of the scattering coefficient, and their validity in predicting band intensities in DR and DT measurements will be reported by us in the near future.

The present purely experimental study was conducted by using samples prepared in a stepped strip, with the thickness of each step increasing in increments of 100 μm from 200 to 1500 μm. This range of depths was selected to cover the range from finite to almost infinite depth commonly believed to be applicable for infrared DR spectrometry (*17*). A 1-mm diameter hole was drilled through the strip at each thickness. Mixtures of phenanthrenequinone (PAQ) of varying concentrations in KCl were prepared. Each mixture was loaded into the sampling strip, which was backed with a removable microscope slide. A small metal rod was used to pack the samples into the holes such that the samples were self-supporting when the slide was removed. Both sides of the sample were leveled with the edge of a razor blade. The sample holder was then inserted into the stage of an IR-Plan microscope (Spectra-Tech, Stamford, CT) and centered in the field-of-view. To minimize edge effects, the aperture was reduced to 100 μm. The single-beam spectrum of the contents of each sample cup was then measured in both the reflectance and transmittance mode on the microscope by using a Perkin-Elmer Model 1800 FT-IR spectrometer. Each spectrum was then ratioed against the corresponding spectrum of pure KCl of the same thickness. The spectra measured from these experiments were base-line corrected, converted to reluctance, i.e. $(1 - R)$ or $(1 - T)$, and absorbance, i.e. $\log (1/R)$ or $\log (1/T)$, and fit with both linear and quadratic equations.

A comparison of the reluctances obtained at various depths by diffuse transmittance and diffuse reflectance is shown in Figure 2. It can be seen that the reluctance of a 200 μm thick sample of 100 ppm PAQ in KCl measured by diffuse reflectance spectrometry is no smaller than that of the 1500-μm sample, within our error limits. The average diameter of the KCl particles is about 5 μm. Photons penetrating to a depth of 200 μm and returning to the top surface of the sample will be transmitted through at least 80 particles if there is no scattering, and more than this if scattering is significant. On the basis of the results of a study of near-infrared diffuse reflectance from this laboratory (*18*), it is probable that the beam interrogates only about 60 particles. Although the result shown in Figure 2 is obviously in disagreement with earlier data from our laboratory (*17*), a careful examination of Figure 15 in the previous report shows that the band intensity for the thinnest sample investigated was more than 90% of the

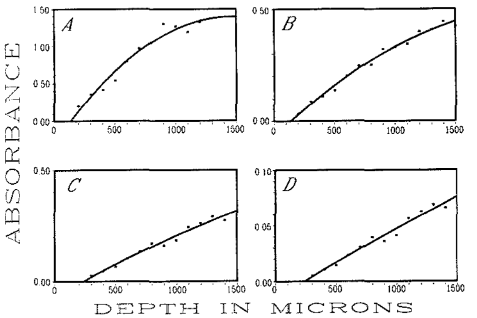

Figure 3. Variation of absorbance (log 1/*T*) for a strong band (at 1678 cm^{-1}) and a weaker band (at 768 cm^{-1}) in diffuse transmittance spectra of PAQ at high (0.1 wt %) and low (0.01 wt %) concentration in KCl: (A) C = 0.1 wt % PAQ, a = 1.7 × 10^4 cm^{-1}; (B) C = 0.1 wt %, a = 5.4 × 10^3 cm^{-1}; (C) C = 0.01 wt %, a = 1.7 × 10^4 cm^{-1}; (D) C = 0.01 wt %, a = 5.4 × 10^3 cm^{-1}.

intensity of the same band measured at "infinite depth". It is possible that the variation of packing density for the samples prepared in our previous study caused a sufficient change in the scattering coefficient to account for the difference between the results of the previous investigation and the data shown in Figure 2.

Measurements of the energy penetrating the sample from transmittance measurements indicate that less than 1% of the incident energy reaches the detector once the sample thickness exceeds 1000 μm. Therefore, it is likely for diffusely reflecting samples, radiation penetrating 500 μm below the surface of the sample cannot return to the surface with sufficient intensity to give a significant signal at the detector. While it could be naively assumed from the data shown in Figure 2 that no radiation penetrating beyond 200 μm below the sample surface is detected in a diffuse reflectance measurement, the diffuse transmittance spectra indicate that some light penetrates to a depth of at least 1 mm. Thus a small fraction of the radiation that penetrates 200 μm below the surface must be back-scattered and emerge from the sample as part of the diffuse reflection signal. The absorptance of this component of the signal at the detector is at least twice as great as that of radiation penetrating only to 100 μm, but it comprises a very small percentage of the total signal. Thus, while one would expect to see a dependence of band intensity on the thickness of the sample for diffuse reflectance spectra, clearly it would not be expected to be strong.

The absorptance of a certain band measured by diffuse transmittance becomes much greater than the absorptance of the same band measured by diffuse reflectance as the layer thickness increases beyond 200 or 300 μm. Four plots of absorbance as a function of sample depth are shown in Figure 3 for a strong (absorptivity = 1.7 × 10^4 cm^{-1}) and relatively weak (absorptivity = 5.4 × 10^3 cm^{-1}) band in samples of PAQ at high (0.1 wt %) and low 0.01% wt %) concentration in KCl. While absorbance as defined by Beer's law does not accurately describe the theoretical dependence of diffuse transmittance spectra as a function of sample thickness derived by Kortüm (*16*), there is no simple function which does. It can be seen that fitting the data to a second-order polynomial predicts absorbance values less than zero for samples of very short path length. Self-supporting samples could not be prepared with a thickness less than 200 μm. We believe the plot almost certainly passes through the origin. This effect is probably caused by an increase in the scattering coefficient of very thin samples; this effect has been discussed in another report from this laboratory (*19*). When the analytical band is small, linear plots do result. If the product of absorptivity and concentration is large, marked deviations from linearity result. The plots in Figure 3 demonstrate qualitatively how changing either band absorptivity or concentration can affect the linearity of "Beer's law" plots for scattering samples.

Because of the increased band intensity when powdered samples of uniform composition are characterized by diffuse transmittance rather than by diffuse reflectance, as shown in Figure 2, diffuse transmittance infrared spectrometry has been found to be a useful technique for the identification of small quantities of solutes eluting from a microbore liquid chromatograph when the analyte penetrates well below the surface of the powdered substrate. Quantities of PAQ as low as 5 ng have yielded identifiable infrared specta using this technique (*11*). Diffuse reflectance appears to remain the superior technique when the sample can be deposited in the top layer of the substrate as it is, for example, when eluites from supercritical fluid chromatographs are collected (*20*), since the mobile phase is gaseous on emerging from the pressure/flow restrictor. The optimum sampling technique for any chromatography/FT-IR interface involving mobile phase elimination will therefore depend strongly on the volatility of the mobile phase, with diffuse transmittance being favored when less volatile mobile phases are employed.

LITERATURE CITED

(1) Kuehl, D.; Griffiths, P. R. *J. Chromatogr. Sci.* **1979**, *17*, 471–476.
(2) Kuehl, D.; Griffiths, P. R. *Anal. Chem.* **1980**, *52*, 1394–1399.
(3) Conroy, C. M.; Duff, P. J.; Griffiths, P. R.; Azarraga, L. V. *Anal. Chem.* **1984**, *56*, 2636–2642.
(4) Conroy, C. M.; Griffiths, P. R.; Jinno, K. *Anal. Chem.* **1985**, *57*, 822–825.
(5) Griffiths, P. R.; Conroy, C. M. *Adv. Chromatogr.* **1986**, *25*, 105–138.
(6) Kalasinsky, K. S.; Smith, J. A. S.; Kalasinsky, V. F. *Anal. Chem.* **1985**, *57*, 1969–1974.
(7) Kalasinsky, V. F.; Whitehead, K. G.; Kenton, R. C.; Smith, J. A. S.; Kalasinsky, K. S. *J. Chromatogr. Sci.* **1987**, *25* (7), 273–208.
(8) Jinno, K.; Fujimoto, C.; Ishii, D. *J. Chromatogr.* **1982**, *239*, 625–632.
(9) Jinno, K.; Fujimoto, C. *HRC CC, J. High Resolut. Chromatogr. Chromatogr. Commun.* **1981**, *4*, 532–533.
(10) Jinno, K.; Fujimoto, C. *Appl. Spectrosc.* **1982**, *36*, 67–69.
(11) Fraser, D. J. J.; Norton, K. L.; Griffiths, P. R. In *Infrared Microspectrometry: Theory and Applications*; Messerschmidt, R. G., Harthcock, M. A., Eds.; Marcel Dekker: New York, 1988; pp 197–210.
(12) Gagel, J. J.; Biemann, K. *Anal. Chem.* **1986**, *58*, 2184–2189.
(13) Gagel, J. J.; Biemann, K. *Anal. Chem.* **1987**, *59*, 1266–1272.
(14) Robertson, R. M.; de Haseth, J. A.; Browner, R. F. *Mikrochim. Acta (Wien)* **1988**, *II*, 199–202.
(15) Fraser, D. J. J.; Norton, K. L.; Griffiths, P. R. Paper presented at 193rd National American Chemical Society Meeting, Denver, CO, April, 1987.
(16) Kortüm, G. *Reflectance Spectroscopy*; Springer-Verlag: New York, 1969.
(17) Griffiths, P. R.; Fuller, M. P. In *Advances in Infrared and Raman Spectroscopy*; Clark, R. J. H., Hester, R. E., Eds.; Heyden Publishing Co.: London, 1982; Vol. 9, pp 63–1299.
(18) Olinger, J. M.; Griffiths, P. R. *Anal. Chem.* **1988**, *60*, 2427–2435.
(19) Fraser, D. J. J.; Griffiths, P. R. *Appl. Spectrosc.*, in press.
(20) Shafer, K. H.; Griffiths, P. R. *Anal. Chem.* **1986**, *58*, 58–64.

* Author to whom correspondence should be addressed.

[1] Present address: Department of Chemistry, University of Idaho, Moscow, ID 83843.

David J. J. Fraser
Kelly L. Norton[1]
Peter R. Griffiths*,[1]

Department of Chemistry
University of California
Riverside, California 92521-0403

RECEIVED for review June 26, 1989. Accepted November 6, 1989. This work was supported in part by Grant No. R-81441-0 from the U.S. Environmental Protection Agency and in part by a grant from the University of California Toxic Substances Research Program.

Anal. Chem. **1990**, *62*, 311–313

Differentiation of Leucine and Isoleucine Residues in Peptides by Consecutive Reaction Mass Spectrometry

Sir: Fast atom bombardment (FAB) and tandem mass spectrometry (MS/MS) have emerged as potent techniques for peptide sequencing (*1–3*), but there are some remaining problems. One such problem is the differentiation of two isomeric amino acid residues, leucine and isoleucine, in peptides (*1*). If the peptide in question contains only a single leucine or isoleucine residue, they can be differentiated by using MS/MS spectra of the m/z 86 immonium ions corresponding to the leucine or isoleucine residue, that is, $CH_3CH(CH_3)CH_2CH{=}NH_2^+$ or $CH_3CH_2CH(CH_3)CH{=}NH_2^+$, present in the FAB spectrum of the peptide (*4*). However, this approach is not useful for peptides containing both leucine and isoleucine residues because, in the FAB spectra of such peptides, the ion at m/z 86 is usually a mixture of isomeric immonium ions formed from both residues.

Another approach based on FAB and tandem mass spectrometry was proposed by Biemann's group (*5, 6*). They used $(A_n - 42)^+$ and $(A_m - 28)^+$ ions (d-series ions) in the daughter ion spectrum of protonated molecular ions (MH^+) of a peptide where A_n and A_m ions are sequence-specific daughter ions in which leucine or isoleucine is now C-terminal. Although this approach is applicable to the peptide containing both residues, its usefulness is limited only to the cases where A-series daughter and the diagnostic d-series ions are sufficiently strong to be recognized.

The use of w-series daughter ions (side chain cleaved C-terminal ions) was also proposed (*6–9*). This approach is useful for the differentiation of the isomers in the peptide containing both residues as well. However, in analogy with d-series ions, w-series ions are not always observed (*7*).

In this paper, we present a new strategy that is widely applicable for the assignment of leucine and isoleucine in peptide molecules. The new strategy is based on consecutive reaction mass spectrometry, MS^n (*10–14*), and consists of three steps. First, the peptides (or proteins) are digested with an endopeptidase, thermolysin. This enzyme can hydrolyze the peptide bond containing the N atom of leucine or isoleucine residues. Thus, some of the peptides in the resulting digest have leucine or isoleucine as their N-terminal residues. Second, the proteolytic digest is analyzed by FAB MS and MS/MS, and the peptides having leucine or isoleucine as the N-terminal residues are assigned from the peptides in the digest. Finally, leucine and isoleucine residues in each fragment peptide are identified on the basis of the MS^3 (MS/MS/MS) spectra of each MH^+ of the leucine/isoleucine terminal peptides. The usefulness of the strategy has been demonstrated in the case of the peptide human calcitonin.

EXPERIMENTAL SECTION

Materials. Human calcitonin, leucylalanine, and thermolysin were purchased from Sigma Chemical Co. (St. Louis, MO). Isoleucylphenylalanine was obtained from Research Organics, Inc. (Cleveland, OH). The peptides and enzymes were used without further purification.

Preparation of Samples for Mass Spectrometric Analysis. Human calcitonin was digested with thermolysin in the usual way except for the use of a volatile buffer solution, i.e., 0.1 M *N*-ethylmorpholine/acetic acid (*3*). The digest (3–10 nmol) in the buffer solution (1–3 μL) was mixed with 1 μL of thioglycerol followed by glycerol (1 μL), and the mixture was applied to a stainless steel FAB target and used for analysis.

Measurement of Spectra. All FAB MS, MS/MS, and MS/MS/MS spectra were obtained with a JEOL JMS-HX100 tandem mass spectrometer (EBE geometry) equipped with an additional analog circuit, "MS/MS/MS interface", which allows manual operation of E1 and B, keeping a constant B/E1 ratio. The operating parameters for the measurements were as follows: fast atom beam, Xe (6 kV); accelerating voltage, 5 kV; voltage on the conversion dynode of the postacceleration detector, −20 kV. The MS/MS spectra were obtained by the use of E2 scanning.

The procedure described by Cooks, Gross, and co-workers (*10*) was used for the MS/MS/MS acquisition. Collision gas was introduced into the first gas cell in the first field-free region (FFR) to give approximately 70% beam attenuation of the parent ion (M_p^+) and into the second gas cell located at the third FFR to give approximately 90% beam attenuation of the daughter ion (M_d^+). The resultant daughter ions of Md$^+$ (graddaughter ions of M_p^+: Mg$^+$) were analyzed by E2 scanning. To improve the signal to noise ratio of the spectra, 10–100 E2 scans (5 s/scan) were accumulated on the data system (JEOL JMS-DA5000). The total data acquisition times varied from 1 to 10 min and were dependent on the abundance of the granddaughter ions.

RESULTS AND DISCUSSION

Human calcitonin is a peptide containing 32 amino acid residues, including two leucine and one isoleucine. Figure 1 shows the FAB mass spectrum of the thermolytic digest of the peptide. At a minimum, MH^+ ions of 12 peptides can be recognized in the spectrum. Structures were assigned to the digest peptides as shown in the figure on the basis of the MS/MS experiments.

There are four leucine/isoleucine terminal peptides, namely peptides containing residues 4-8, 9-11, 27-28, and 27-32, in the assigned fragments. The protonated molecular ions of these four peptides, i.e., m/z 554, 290, 189, and 512, are seen in the FAB mass spectrum (Figure 1). The mass of m/z 189 also corresponds to residues 9-10 (Leu-Gly), but the substrate specificity of the enzyme (*15*) suggests that the ion is the MH^+ of the peptide containing residues 27-28 (Ile-Gly). Collisional activation of these four ions gave abundant N-terminal immonium ions, m/z 86. Hence, we tried to use daughter ion spectra of the immonium ions, granddaughter ion spectra (MS/MS/MS spectra) of each leucine/isoleucine terminal peptide, for the differentiation of those residues. Namely, MH^+ of each fragment peptide was used as M_p^+, the m/z 86 immonium ion formed from M_p^+ in the first FFR was used as M_d^+, and the third FFR daughters of M_d^+, M_g^+, were analyzed by using E2.

First, we looked at the MS/MS/MS spectra of simple dipeptides containing leucine and isoleucine. Figure 2 shows the MS/MS/MS spectra, the daughter ion spectra of the immonium ions at m/z 86 (Md^+) formed in the first FFR from the MH^+ of leucylalanine and isoleucylphenylalanine (M_p^+, ionized by FAB). Both of the spectra have the same features as that of the daughter ion spectra of m/z 86 immonium ions formed from leucine and isoleucine in an ion source (*4*). Higher mass peaks (m/z 56, 69) are relatively abundant for m/z 86 from isoleucylphenylalanine (Figure 2b), whereas m/z 43 and 44 are predominant in the spectrum of the immonium ion from leucylalanine (Figure 2a). Consequently, the MS/MS/MS spectra can also be used as fingerprints of the ions in a manner similar to the case of MS/MS spectra (*2, 16, 17*). Recently, Tomer and co-workers reported that the spectra obtained by MS^4 (MS/MS/MS/MS) experiments on the m/z 86 ions from Leu-Gly-Gly, Gly-Gly-Leu, and Gly-Gly-Ile were comparable with the MS/MS spectra of m/z 86 from leucine and isoleucine (*14*). Although their method clearly has the potential to differentiate between the isomeric amino acid residues in peptides, the reported sensitivity of the experiments (acquisition time for an MS/MS/MS/MS spectrum

0003-2700/90/0362-0311$02.50/0 © 1990 American Chemical Society

H-Cys-Gly-Asn-Leu-Ser-Thr-Cys-Met-Leu-Gly-Thr-Tyr-Thr-Gln-Asp-Phe-
Asn-Lys-Phe-His-Thr-Phe-Pro-Gln-Thr-Ala-Ile-Gly-Val-Gly-Ala-Pro-NH_2

1 - 3	H-Cys-Gly-Asn-OH	MH^+ = 293
4 - 8	H-Leu-Ser-Thr-Cys-Met-OH	MH^+ = 554
9 - 11	H-Leu-Gly-Thr-OH	MH^+ = 290
12 - 15	H-Tyr-Thr-Gln-Asp-OH	MH^+ = 526
16 - 18	H-Phe-Asn-Lys-OH	MH^+ = 408
19 - 25	H-Phe-His-Thr-Phe-Pro-Gln-Thr-OH	MH^+ = 877
26 - 28	H-Ala-Ile-Gly-OH	MH^+ = 260
29 - 32	H-Val-Gly-Ala-Pro-NH_2	MH^+ = 342
22 - 25	H-Phe-Pro-Gln-Thr-OH	MH^+ = 492
26 - 32	H-Ala-Ile-Gly-Val-Gly-Ala-Pro-NH_2	MH^+ = 583
27 - 28	H-Ile-Gly-OH	MH^+ = 189
27 - 32	H-Ile-Gly-Val-Gly-Ala-Pro-NH_2	MH^+ = 512

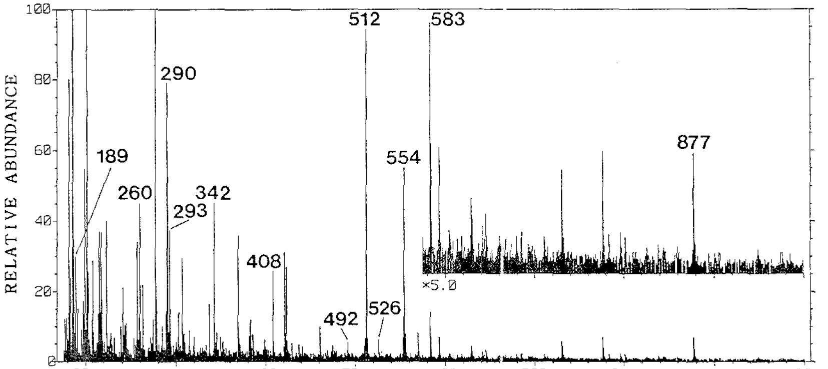

Figure 1. FAB mass spectrum of the thermolytic digest of human calcitonin. Amino acid sequences of the native peptide and the digest peptides are given at the top. Each digest peptide is marked with arrows in the native sequence. The disulfide bond between Cys-1 and Cys-7 was reduced by thioglycerol prior to the mass spectrometric analysis.

of a small peptide was 1.5–3 h) seems to be insufficient for routine analysis.

Next, MS/MS/MS experiments were carried out on the MH^+ of the fragment peptides of human calcitonin, i.e., m/z 554 (residues 4-8), m/z 290 (9-14), m/z 189 (27-28), and m/z 512 (27-32), respectively. The granddaughters of m/z 554 and 290, the daughters of m/z 86 (M_d^+) formed in the first FFR, are shown in Figure 3a,b. These spectra agreed well with the spectrum of the granddaughters of leucylalanine shown in Figure 2a. Hence, these spectra clearly show that the fourth and ninth residues of human calcitonin are leucine.

On the other hand, the collisional activation of m/z 86 (M_d^+) formed from m/z 189 (M_p^+) gave more abundant higher mass peaks (Figure 3c) comparable to those in the spectrum obtained from the isoleucylphenylalanine (Figure 2b). The MS/MS/MS spectrum of m/z 512 (m/z 86 from m/z 512 was used as M_d^+) also was similar to Figure 2b. These findings show that isoleucine is the 27th residue. Moreover, the assumption on the hydrolyzed peptide bonds was proved to be correct.

In conclusion, leucine and isoleucine residues in peptides can unambiguously be differentiated by use of MS/MS/MS methodology involving proteolysis without any chromatographic separation procedure. Recently, Welinder reported that the thermolysin specificity was restricted to leucine/isoleucine and phenylalanine, in a special experimental condition (*18*). This may be helpful in simplifying the digest mixture and the procedure for the assignment of leucine/isoleucine terminal peptides.

A limitation of the present methodology is the difficulty in analyzing sequential leucine/isoleucine residues. If there are two sequential leucine/isoleucine residues in a peptide chain, the enzyme most likely hydrolyzes the peptide bond either at the N-terminal side of the two residues or between

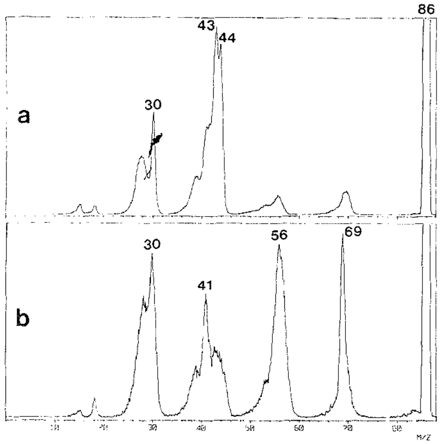

Figure 2. MS/MS/MS spectra of MH$^+$ of the dipeptides leucylalanine (a) and isoleucylphenylalanine (b). The *m/z* 86 ions produced from MH$^+$ in the first FFR were used as M$_d$$^+$.

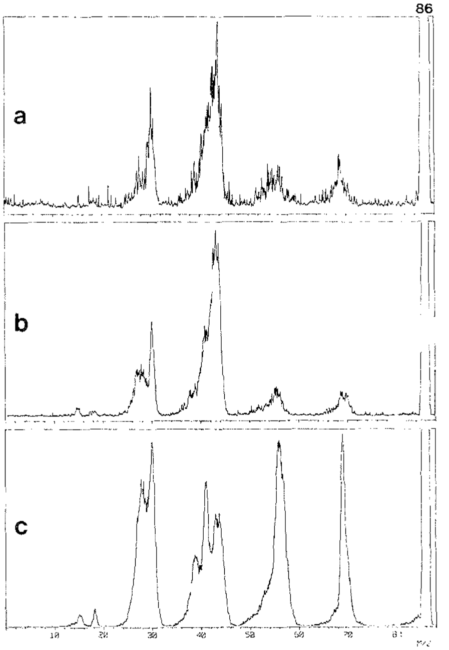

Figure 3. MS/MS/MS spectra of MH$^+$ of the thermolytic peptides of human calcitonin. The *m/z* 86 ions produced from (a) *m/z* 554, (b) *m/z* 290, and (c) *m/z* 189 in the first FFR were used as M$_d$$^+$.

them. In either case, a fragment peptide containing two leucine/isoleucine residues will be formed. The results of the preliminary study using small peptides showed that the major contribution to the *m/z* 86 daughter ion was from the N-terminal leucine/isoleucine residue even if there was another leucine/isoleucine residue in the peptide. For example, the MS/MS/MS spectra of leucylisoleucine and isoleucylleucine (*m/z* 86 ions from MH$^+$ of each peptide were used as M$_d$$^+$) were indistinguishable from those of leucylalanine and isoleucylphenylalanine, respectively. Hence, the N-terminal leucine/isoleucine residues of the peptides containing two (or more) leucine/isoleucine residues may be identified by the use of MS/MS/MS spectra whereas the other(s) cannot be. If, fortunately, a peptide digest contains both the peptide attributable to the cleavage of the N-terminal side of the two sequential leucine/isoleucine residues and that attributable to the cleavage between them, either of the residues can be identified.

The MS/MS/MS spectra also were usable for the isomer differentiation of the peptides containing a single leucine/isoleucine residue in the chain or at the C-terminal, but the signal intensity of *m/z* 86 daughter ions and the granddaughter ions arising from MH$^+$ of such peptides was much lower than that of leucine/isoleucine N-terminal peptides.

The amount of the sample required for the acquisition of MS/MS/MS spectra (3–10 nmol) was larger than those for the MS/MS spectra (*6–9*). However, the present methodology may be applicable to the peptides to which the MS/MS methodology (*5–9*) could not be applied, since all of the leucine/isoleucine N-terminal small peptides that have been tested (peptides mentioned above and those in a thermolytic digest of hen egg lysozyme) gave the *m/z* 86 N-terminal immonium daughter ions with the intensity sufficient for the acquisition of MS/MS/MS spectra. Accordingly, the present methodology will be useful as a complement to the MS/MS methodology.

LITERATURE CITED

(1) Biemann, Klaus; Martin, Stephen A. *Mass Spectrom. Rev.* **1987**, *6*, 1–75 and references cited therein.
(2) Nakamura, Takemichi; Nagaki, Hidemi; Kinoshita, Takeshi. *Mass Spectrosc.* (*Tokyo*) **1986**, *34*, 307–319.
(3) Nakamura, Takemichi; Nagaki, Hidemi; Kinoshita, Takeshi; Tamaoki, Hidetsune. *Proceedings of 2nd Japan-China Joint Symposium on Mass Spectrometry*, Osaka, Japan; Bando Press: Osaka, 1987; pp 85–88.
(4) Aubagnac, I. L.; Amarani, B. El; Devienne, F. M.; Conbarieu, R. *Org. Mass Spectrom.* **1985**, *20*, 428–429.
(5) Martin, Stephen A.; Biemann, Klaus. *Collected Abstracts*; 34th Annual Conference on Mass Spectrometry and Allied Topics; American Society for Mass Spectrometry: East Lansing, MI, 1986; pp 854–855.
(6) Johnson, Richard S.; Martin, Stephen A.; Biemann, Klaus. *Int. J. Mass Spectrom. Ion Processes* **1988**, *86*, 137–154.
(7) Johnson, Richard S.; Martin, Stephen A.; Biemann, Klaus; Stults, John T.; Watson, J. Throck. *Anal. Chem.* **1987**, *59*, 2621–2625.
(8) Stults, John T.; Watson, J. Throck. *Biomed. Environ. Mass Spectrom.* **1987**, *14*, 583–586.
(9) Biemann, Klaus. *Biomed. Environ. Mass Spectrom.* **1988**, *16*, 99–111.
(10) Burinsky, David J.; Cooks, R. Graham; Chess, Edward K.; Gross, Michael L. *Anal. Chem.* **1982**, *54*, 295–299.
(11) Gross, Michael L.; McCrery, David; Crow, Frank; Tomer, Kenneth B. *Tetrahedron Lett.* **1982**, *23*, 5381–5384.
(12) Gueveremont, R.; Wright, J. L. C. *Rapid Commun. Mass Spectrom.* **1987**, *1*, 12–13.
(13) Zaretskii, Z. V. I.; Curtis, J. M.; Brenton, A. G.; Beynon, J. H.; Djerassi, Carl. *Org. Mass Spectrom.* **1988**, *23*, 453–459.
(14) Tomer, Kenneth B.; Guenat, Christian R.; Deterding, Leesa J. *Anal. Chem.* **1988**, *60*, 2232–2236.
(15) Matsubara, H.; Sasaki, R.; Singer, A.; Jukes, T. H. *Arch. Biochem. Biophys.* **1966**, *115*, 324–331.
(16) Levsen, K.; Wipf, H.-K.; McLafferty, F. W. *Org. Mass Spectrom.* **1974**, *8*, 117–128.
(17) Nakamura, Takemichi; Nagaki, Hidemi; Kinoshita, Takeshi. *Bull. Chem. Soc. Jpn.* **1985**, *58*, 2798–2800.
(18) Welinder, Karen G. *Anal. Biochem.* **1988**, *174*, 54–64.

Takemichi Nakamura*
Hidemi Nagaki
Yasuko Ohki
Takeshi Kinoshita

Analytical and Metabolic Research Laboratories
Sankyo Co., Ltd.
2-58, Hiromachi 1-Chome, Shinagawa-ku
Tokyo 140, Japan

RECEIVED for review July 10, 1989. Accepted November 2, 1989. Presented in part at the 16th International Symposium on the Chemistry of Natural Products, Kyoto, Japan, May 29–June 3, 1988; Abstracts, p 162.

Continuous On-Line Monitoring of Biomolecules Based on Automated Homogeneous Enzyme-Linked Competitive Binding Assays

Sir: Previous efforts in continuous biosensing have centered mainly around the development of analytical sensors for ions and gases of either optical or electrochemical nature (*1–5*). In the case of biomolecules, considerable work has been directed toward developing highly selective biocatalytic-based sensors (*6, 7*). These devices have good selectivity and adequate response times and can be modified for use in on-line measurements. However, their detection limits are usually restricted to concentrations higher than 10^{-5} M. Furthermore, the fabrication of these sensors is limited to those analytes for which highly selective biocatalytic reagents exist. For many important biomolecules, no appropriate biocatalysts are known. Thus, this approach does not offer a "generic" solution to continuous biomolecule monitoring.

Immunosensors complement enzyme electrodes for continuous monitoring of molecules that do not take part in enzymatic reactions. These sensors use competitive binding principles and are based on immobilizing the binding reagent on the surface of an electrochemical, piezoelectric, or optical detector (*1, 5, 6, 8–11*). Because antibodies and naturally occurring binding proteins have rather high affinities for their target molecules (i.e., binding constants in the range 10^{6}–10^{15} M^{-1}), reversibility of such sensing arrangements is usually rather slow (dissociation rate constants are small) (*5, 11*). Indeed, in order to gain reliable results for sequential analysis of samples, it is necessary to regenerate the binding reagent each time, or use disposable-type devices for each determination. The former is normally accomplished with an acid wash. Exceptions to this situation include the optical sensors for glucose (*12*) and phenytoin (*13*), the potentiometric ionophore modulation immunoassay sensor for dinitrophenol (*14, 15*), and the chemoreceptor-based sensor for glutamate (*16*). However, in these cases a lectin or an antibody with relatively low affinity (fast dissociation rate constants) was used as the binder to sense rather high concentrations of analyte (1 μM–1 mM). Thus, alternate analytical techniques capable of real continuous measurements of molecules at low levels are still higher desirable.

In order to develop biosensing arrangements with adequate sensitivity, it seems necessary to employ some type of chemical amplification step in the detection scheme (*17*). To this end, several immunoassay techniques have been adapted for use in flow injection (*18, 19*) and air-segmented analysis (*20–22*). Although these approaches employed continuous flow instrumentation (e.g., the Technicon AutoAnalyzer II (*21*)), they have only been applied for the analysis of discrete samples.

Moreover, the groups of Wilson (*23, 24*), Meyerhoff (*25*), Hara (*26*), and Mattiasson (*27*) have reported the use of flow-through bioreactors with immobilized antibodies or lectins and principles of heterogeneous enzyme immunoassays for the determination of immunoreagents. However, none of these systems have continuous on-line monitoring capabilities.

A new method is described here by which the concentration of biologically important molecules can be monitored continuously. Two well-characterized homogeneous enzyme-linked competitive binding assays for the vitamins folate (*28*) and biotin (*29*) serve as model systems for these investigations. In the proposed system, continuous reagent streams of an enzyme–ligand conjugate, an appropriate ligand binding protein, and the sample (ligand) are mixed in a sequential mode, and the final mixture is then merged with a substrate stream to generate the analytical signal (i.e., product of the enzymatic reaction). The extent of product formation detected downstream is directly proportional to the concentration of analyte (e.g., folate or biotin) present in the sample. To our knowledge, this represents the first attempt to adapt homogeneous enzyme-linked binding assays for the purpose of continuous on-line monitoring.

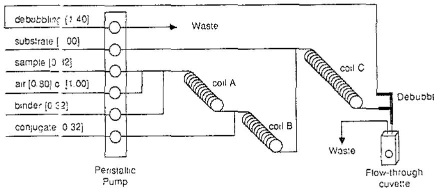

Figure 1. Schematic diagram of the flow manifold used in the automated determination of biomolecules.

Table I. Instrumental Parameters

parameter	folate	biotin
coil A	3.0 min	2.0 min
coil B	3.0 min	1.8 min
coil C	10.0 min	2.1 min
conjugate	7.2×10^{-9} M	7.6×10^{-9} M
binder	see Table II	4.2 μg/mL[b]
β-NAD[a]	see Table II	1.01 mg/mL
glucose-6-phosphate[a]	5.1 mg/mL	5.3 mg/mL

[a] Concentration in substrate mixture. [b] Corresponds to 6.4×10^{-8} M avidin.

EXPERIMENTAL SECTION

Reagents. Difco nutrient broth was obtained from Fisher Scientific (Cincinnati, OH). Avidin was from Calbiochem (La Jolla, CA). Glucose-6-phosphate dehydrogenase (G6PDH) from *Leuconostoc mesenteroides*, as well as all the other chemicals used were purchased from Sigma (St. Louis, MO) and were of the highest purity available. The assay buffer solution was 0.0500 M Tris-HCl, 0.100 M NaCl, 0.010% (w/v) sodium azide, pH 7.8. Tris–gelatin buffer (0.10% gelatin in assay buffer) was used to dilute the avidin, the folate binding protein, the enzyme, and the conjugates. All folate and biotin standards were prepared by dissolving appropriate amounts of these compounds in Tris–gelatin buffer. For the biotin spiking experiments, a solution of biotin (4.00×10^{-4} M) in Tris–gelatin buffer was prepared and the rest of the standards were made from this stock solution by diluting with a nutrient broth solution (80% (w/v)) in distilled–deionized water.

Apparatus. Figure 1 shows the schematic diagram of the air-segmented flow system used in these studies. A sample stream is merged with a reagent stream containing the ligand-specific binder (flow rates are in parentheses). After a brief incubation period (reaction coil A), a reagent stream containing the enzyme-ligand conjugate is added. Following incubation in coil B, a reagent stream containing the substrates for the enzyme merges and after passing through coil C, the activity of the enzyme is detected by monitoring the change in optical absorbance of the stream at 340 nm. This change in absorbance is directly related to the concentration of ligand (biotin or folate) in the sample. For the biotin system, a Perkin-Elmer Lambda 4B spectrophotometer equipped with a temperature-controlled cuvette holder (thermostated at 25 °C throughout the experiments) was used as the detector and a Technicon peristaltic pump (Model I) was utilized to feed the sample. In the case of the folate system, the

0003-2700/90/0362-0314$02.50/0 © 1990 American Chemical Society

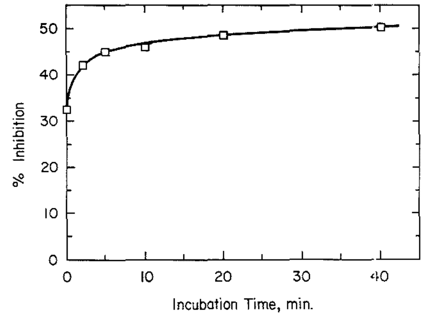

Figure 2. Association curve for a 1:200 dilution of the G6PDH–folate conjugate with 0.75 g/mL β-lactoglobulin using a batch-mode protocol. The incubation time was varied from zero (minimum time to mix the reagents and measure the enzymatic activity) to 40 min.

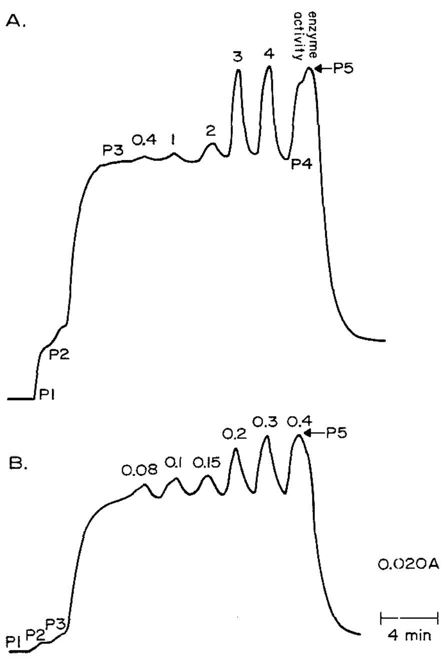

Figure 3. Typical tracings for the discrete sample analysis of folate using a continuous enzyme-linked assay system. The increase in signal at P1 is due to background absorbance by the substrates and at P2 to background absorbance by the substrates and β-lactoglobulin. The signal at P3 (base-line signal) is due to conjugate converting NAD to NADH in the presence of the binder. The increase in signal at point P4 is a result of assay buffer being pumped through the β-lactoglobulin stream (100% enzyme activity). The reduction of absorbance after point P5 is a consequence of assay buffer being passed through both the conjugate and β-lactoglobulin reagent streams (zero enzyme activity). Concentrations of folate are in μM units: (A) 7.74 mg/mL NAD, 110 mg/mL β-lactoglobulin; (B) 1.93 mg/mL NAD, 28 mg/mL β-lactoglobulin.

detector was a Linear Model UV-106 interfaced with a Fisher Recordall Series 5000 strip-chart recorder. All the flow-rated tubing was purchased from Fisher Scientific. The residence time of the sample stream in the three reaction coils is given in Table I. This table also summarizes the concentrations of the reagents used in the automated determination of the two vitamins.

Table II. Optimization of Reagents for the Folate Monitoring System

β-NAD,[a] mg/mL	β-lactoglobulin, mg/mL	absorbance range,[b] absorbance units	cost per hour[c] (U.S. $)
7.74	110	0.026	37.2
3.87	110	0.025	30.8
1.93	110	0.024	27.6
0.97	110	0.021	26.0
1.93	28	0.019	11.0
0.97	56	0.016	14.9
0.97	28	0.017	9.4
0.97	14	0.014	6.7

[a] Concentration in substrate mixture. In all cases the concentration of glucose-6-phosphate in the substrate mixture was 5.1 mg/mL. [b] Refers to difference between the signal in the presence of a high concentration of folate and that of base line. [c] Based on 1989 prices from Sigma Chemical Co.

Preparation and Characterization of G6PDH–Folate and G6PDH–Biotin Conjugates. A fresh G6PDH–folate conjugate was prepared by using a 1:800 initial mole ratio of folic acid to enzyme (*28*). On the average, this conjugate had 20 folate molecules bound to the enzyme (determined spectrophotometrically (*28*)). In order to further characterize the conjugate, an association time study between the conjugate and the binder β-lactoglobulin was performed in a batch mode. Specifically, a volume of 100 μL of a solution containing 1 g of β-lactoglobulin (1 mg of β-lactoglobulin binds 7.9×10^{-12} mol of folate) in 5 mL of assay buffer was incubated for variable periods of time with 100 μL of a 1:200 dilution of the G6PDH–folate conjugate. After this incubation, 100 μL of β-NAD (0.060 M in assay buffer), 100 μL of glucose-6-phosphate (0.10 M in assay buffer), and 700 μL of assay buffer were added and the enzymatic activity was measured by following the rate of appearance of NADH at 340 nm. For this purpose, a SYVA S-III spectrophotometer (with the temperature-controlled cuvette thermostated at 30 °C) interfaced with a SYVA CP-5000 Plus clinical processor was used (*28*). The G6PDH–biotin conjugate BC-1 has been characterized elsewhere (*29*). On the average, three avidin molecules could be bound simultaneously to biotins on this conjugate (*30*).

Discrete Sample Analysis. A stable base line was established by pumping assay buffer or nutrient broth through the sample stream while conjugate, binder, and substrate were passed through their corresponding reagent streams. At this point, the first folate or biotin standard was fed for 1 or 3 min, respectively. After this time, assay buffer in the case of folate or nutrient broth in the case of biotin was passed through the sample stream (1 min for the folate and 3 min for the biotin system) in order to return the signal to base line. Then, the next standard was pumped and the washing procedure was repeated after each standard.

Continuous On-Line Monitoring. This protocol differs from the previous one in that there were no washing steps involved, and therefore, there was no return of the signal to base line after the addition of each standard. Nutrient broth, binder (avidin), conjugate, and the substrate mixture were pumped through the system at the same time, and when a stable base line was established, the standards were added.

Recovery Studies. The continuous on-line monitoring apparatus was used to follow the change in the concentration of a solution of biotin in nutrient broth (1.50×10^{-7} M). After a base line was established, the concentration of biotin was altered by spiking with known amounts of the vitamin or by diluting the mixture with a biotin-free nutrient broth solution. The concentration of biotin in the beaker was correlated to the one found experimentally.

RESULTS AND DISCUSSION

Among the many competitive binding methods developed thus far, homogeneous enzyme–immunoassay techniques appear to be the most suitable for adaptation to continuous monitoring arrangements. The technique was pioneered by Rubenstein et al. (*31*) and makes use of an enzyme–ligand conjugate and appropriate antiligand binders. In the presence of the binder, the activity of the enzyme conjugate is inhibited. When free ligand molecules (analyte) are present, they interact with the binding protein, and the activity of the enzyme is regained in an amount dependent on the concentration of analyte.

Recently, we have demonstrated that naturally occurring binding proteins can be used in place of antibodies for the development of homogeneous enzyme-linked competitive binding assays (*28*, *29*). Conjugates of glucose-6-phosphate dehydrogenase with folate and biotin were employed in conjunction with folate binding protein and avidin (a natural binding protein for biotin) to devise fast, simple, and rather sensitive assay methods for folate and biotin, respectively. This previous work also pointed out certain potential advantages to the use of binding proteins rather than antibodies in such competitive binding arrangements. Indeed, the dose–response curves for folate and biotin were much steeper than the ones typically observed in antibody-based systems. This enhanced steepness was attributed to favorable binding constants between the binder and the unlabeled ligand relative to that between the enzyme–conjugate and the binder (*28*). Further, it was shown that inexpensive impure preparations of folate binding protein could be used as the reagent in the folate assay (e.g., β-lactoglobulin) without seriously diminishing the detection capabilities of the method.

The time-dependent inhibition of a G6PDH–folate conjugate by excess β-lactoglobulin is shown in Figure 2. While this conjugate can be inhibited up to 50% after incubation with the β-lactoglobulin for a total of 40 min, at least 42% inhibition was observed after mixing the two reagents for 2 min. Therefore, only a short delay time (equal to 3 min) is necessary in the continuous monitoring arrangement (Table I). This short time assures that the final enzyme activity measurements reflect the real-time concentration of analyte in the sample. In the case of the biotin conjugate, the precent inhibition observed after 2 min of incubation is even higher (*29*). This high inhibition has been attributed to the relatively deep binding pocket of avidin as well as to the strong interaction between biotin and avidin (*29*, *32*).

Figure 3 shows the response obtained when various folate standards prepared in gel buffer were passed through the automated continuous monitoring system. Assay buffer was pumped through the sample stream after each standard to return the signal to base line. The use of 7.74 mg/mL NAD in the substrate mixture and 110 mg/mL β-lactoglobulin resulted in curve A. In curve B, the concentration of β-lactoglobulin was reduced to 28 mg/mL. This resulted in an improvement in the detection limits of the system. Lowering the concentration of the binder has also been used to improve the detection limits of a batch-mode competitive binding assay for folate (*28*). It should be noted that in the manifold of Figure 1, folate is mixed first with the binder in coil A before addition of the enzyme conjugate. Therefore, this technique can be classified as a sequential binding homogeneous enzyme–immunoassay (*33*).

As illustrated in Figure 3, the response of the continuous system is very sensitive to small changes in the levels of analyte. Similar effects have been reported previously for the batch assay for folate (*28*). This unique behavior makes the system ideally suited for continuous monitoring in process control situations, where the goal is to maintain a constant level of some media component. Thus, by control of the reagent concentrations used, the detector could be fine-tuned to register large changes only over the concentration range where one wishes to maintain the analyte molecules.

The major concern in using soluble bioreagents on a continuous basis is the high cost associated with such use. For this reason, the continuous flow manifold was designed to minimize consumption of reagents. This was accomplished by using slow reagent flow rates and optimized reagent concentrations. A parametric study was performed in which the concentrations of NAD and β-lactoglobulin were varied and the absorbance signal was recorded (Table II). In general, the larger the difference between the absorbance signal recorded in the presence of a high folate concentration and that of the background (i.e., base line) the more precise the determination. However, as shown in Table II there is a trade-off between signal and cost of operation. Specifically, it was found that the concentration of NAD affected both the signal and the background by approximately the same proportion. On the other hand, β-lactoglobulin affected the background while the signal, in the presence of high folate concentrations, remained virtually unchanged. Since in the case of the folate system both NAD and β-lactoglobulin add substantially to the cost of operation, it is necessary to reduce their concentration as much as possible. It was determined that the use of 1.93 mg/mL NAD and 28 mg/mL β-lactogloublin provided both an acceptable absorbance range and operational cost. Indeed, curve B in Figure 3 was recorded using these reagent concentrations.

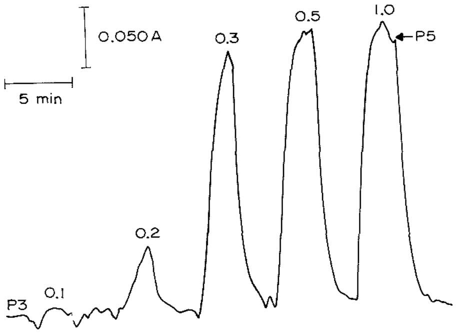

Figure 4. Typical tracing for the discrete sample analysis of biotin. Parameters are as shown in Table I. Points P3 and P5 are as described in Figure 3. Concentrations of biotin are in μM units.

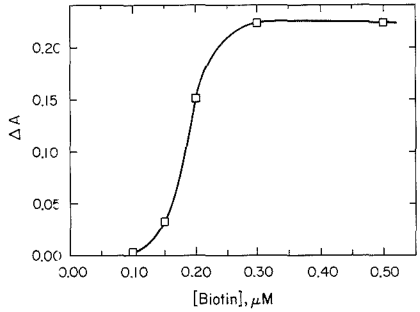

Figure 5. Dose–response curve obtained by passing biotin standards (prepared in nutrient broth) sequentially through the continuous on-line monitoring system. Δ*A* corresponds to the difference between the steady-state absorbance signal and that of base line.

In the case of the avidin–biotin system, the binder is relatively inexpensive and, therefore, the concentration of NAD is primarily what determines the cost of operation. Consequently, for the continuous monitoring of biotin the concentration of NAD was 1.01 mg/mL. The rest of the instrumental parameters are given in Table I. Under these conditions the operation of the system costs only $4.20 per hour (based on a 1989 price of $160.00 per 100 mg of avidin; Calbiochem).

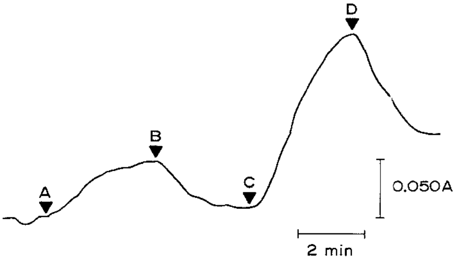

Figure 6. Continuous on-line monitoring of biotin in nutrient broth. Initially, the concentration of biotin in the sample reservoir was 1.50 $\times 10^{-7}$ M. At denoted points, a change in the concentration of biotin in the sample reservoir occurred by addition of extra biotin or dilution of the solution sampled: (A) 1.66 $\times 10^{-7}$ M; (B) 1.33 $\times 10^{-7}$ M; (C) 2.04 $\times 10^{-7}$ M; (D) 1.65 $\times 10^{-7}$ M.

Table III. Continuous On-Line Monitoring of Biotin

[biotin], M		
found	expected	% error
1.67×10^{-7}	1.66×10^{-7}	0.6
1.49×10^{-7}	1.33×10^{-7}	12
2.17×10^{-7}	2.04×10^{-7}	6.4
1.69×10^{-7}	1.65×10^{-7}	2.4

As demonstrated previously (*29*), the avidin–biotin system behaves somewhat differently than the folate system. Indeed, avidin inhibits biotinylated G6PDH up to 100% which indicates that if such a conjugate is used in the continuous on-line monitoring of biotin, the background absorbance should be low. For a given conjugate concentration, the lower the background absorbance, the higher the useful absorbance range and, consequently, the better the accuracy and precision of the determination. Moreover, the higher absorbance range implies that lower concentrations of avidin may be used which should result in better detection limits.

The response of the automated system to different concentrations of biotin is shown in Figure 4. These results were obtained by using the discrete analysis protocol and biotin standards prepared in nutrient broth. Vitamin-free nutrient broth was passed through the sample stream between each standard in order to wash the system. The absorbance at base line, which corresponds to the activity of the enzyme conjugate in the presence of avidin, was 0.006 absorbance unit above that recorded when nutrient broth was passed through the sample and conjugate streams (the rest of the reagents were pumped as indicated in Figure 1). In comparison, the signal recorded in the presence of a high biotin concentration was 0.186 absorbance unit above the base line. This corresponds to 97% inhibition of the enzymatic activity, which is consistent with the high inhibition of biotinylated G6PDH observed previously (*29*). As with the folate determination, the biotin system is also sensitive to very small changes in the levels of biotin. Indeed, a concentration of 1 $\times 10^{-7}$ M biotin causes no change in the signal but when the concentration of biotin is increased to 3 $\times 10^{-7}$ M, almost full enzymatic activity is observed. Although such sensitivity is not common in enzyme-immunoassays, it is not atypical when binding proteins are being used as the selective binders (*28*, *29*, *32*).

The systems described here can also be applied for continuous on-line monitoring of analytes in samples. To demonstrate this concept, biotin standards prepared in nutrient broth were passed sequentially through the sample stream (i.e., there was no washing between standards) and the difference between the steady-state signal and that of base line was recorded. Figure 5 is a dose–response curve obtained under these conditions. After these results were obtained, the sample stream was connected to a beaker containing a biotin solution in nutrient broth. The concentration of biotin in this solution was then altered by addition of either a more concentrated biotin solution (to increase the concentration of the vitamin) or biotin-free nutrient broth (to dilute the solution). The levels of biotin in the beaker were monitored continuously and the signal registered by the spectrophotometer is shown in Figure 6. By use of the dose–response curve of Figure 5, the concentrations recorded by this system were compared to those expected (Table III). The relative error ranges from 0 to 12% with an average of 5.4%. These data also suggest the absence of matrix effects.

Although the above experiments where performed to prove the applicability of the described system to the continuous monitoring of fermentation media, it should be noted that in this application, the background absorbance could change due to the growth of microorganisms. This additional complexity could be circumvented by measuring the optical absorbance of the reagent–sample stream at two points along the flow path; first at the point immediately after the substrates are added and subsequently at a fixed point downstream. The difference in the absorbance between the two detectors would be a measure of the enzymatic activity in the flow system.

Finally, it should be mentioned that one of the parameters that controls the magnitude of the signal recorded by this system is the length of the substrate coil. Longer coils will give rise to higher signals and should improve the precision of the analysis. However, for continuous monitoring applications this would increase the difference between the time when a change in concentration occurs and when it is recorded.

In conclusion, a novel biosensing arrangement is described that is capable of continuously monitoring biomolecules in complex samples. This system is based on the use of homogeneous enzyme-linked competitive binding principles in conjunction with optimized continuous flow methodologies. Given the "generic" analytical nature of the enzyme-linked assay systems, it is likely that this approach could be readily adapted for the detection of biomolecules other than folate and biotin by using different enzyme conjugates and binders (including more traditional antibody-based systems). Finally, with the advent of monoclonal antibodies, in which an unlimited supply of appropriate binder can be manufactured by hybridoma cells, the cost of operation should be reduced substantially.

Registry No. G6PDH, 9001-40-5; folic acid, 59-30-3; biotin, 58-85-5.

LITERATURE CITED

(1) Rechnitz, G. A. *Chem. Eng. News* **1988**, *66* (36), 24–36.
(2) Czaban, J. D. *Anal. Chem.* **1985**, *57*, 345A–356A.
(3) Wolfbeis, O. S. *Fresenius' Z. Anal. Chem.* **1986**, *325*, 387–392.
(4) Seitz, W. R. *Anal. Chem.* **1984**, *56*, 16A–34A.
(5) Seitz, W. R. *J. Clin. Lab. Anal.* **1987**, *1*, 313–316.
(6) Arnold, M. A.; Meyerhoff, M. E. *CRC Crit. Rev. Anal. Chem.* **1988**, *20*, 149–196.
(7) Guilbault, G. C. *Ion-Sel. Electrode Rev.* **1982**, *4*, 187–231.
(8) Ikariyama, Y.; Furuki, M.; Aizawa, M. *Anal. Chem.* **1985**, *57*, 496–500.
(9) Muramatsu, H.; Kajiwaru, K.; Tamiyai, E.; Karube, I. *Anal. Chim. Acta* **1986**, *188*, 257–261.
(10) Tromberg, B. T.; Sepaniak, M. J.; Vo-Dihn, T.; Griffin, G. D. *Anal. Chem.* **1987**, *59*, 1226–1230.
(11) Ives, J. T.; Lin, J. N.; Andrade, J. D. *Am. Biotechnol. Lab.* **1989**, *7* (3), 10–14.
(12) Schultz, J. S.; Mansouri, S. *Methods Enzymol.* **1988**, *137*, 349–366.
(13) Anderson, F. P.; Miller, W. G. *Clin. Chem.* **1988**, *34*, 1417–1421.
(14) Bush, D. L.; Rechnitz, G. A. *Anal. Lett.* **1987**, *20*, 1781–1790.
(15) Bush, D. L.; Rechnitz, G. A. *Anal. Lett.* **1988**, *21*, 1947–1967.
(16) Belli, S. L.; Rechnitz, G. A. *Fresenius' Z. Anal. Chem.* **1988**, *331*, 439–447.

(17) Monroe, D. *Anal. Chem.* **1984**, *56*, 920A–931A.
(18) Kelly, T. A.; Christian, G. D. *Talanta* **1982**, *29*, 1109–1112.
(19) Worsfold, P. J.; Hughes, A.; Mowthorpe, D. J. *Analyst* **1985**, *110*, 1303–1305.
(20) Ismail, A. A. A.; West, P. M.; Goldie, D. J. *Clin. Chem.* **1978**, *24*, 571–579.
(21) Nolan, J. P.; DiBenedetto, G.; Tarsa, N. J. *Clin. Chem.* **1981**, *27*, 738–741.
(22) Bernard, A. M.; Lauwerys, R. R. *Clin. Chem.* **1983**, *29*, 1007–1011.
(23) De Alwis, W. U.; Wilson, G. S. *Anal. Chem.* **1985**, *57*, 2754–2756.
(24) De Alwis, W. U.; Wilson, G. S. *Anal. Chem.* **1987**, *59*, 2786–2789.
(25) Lee, I. H.; Meyerhoff, M. E. *Mikrochim. Acta* **1988**, *III*, 207–221.
(26) Hara, T.; Toriyama, M.; Imaki, M. *Bull. Chem. Soc. Jpn.* **1985**, *58*, 1299–1303.
(27) Mattiasson, B.; Berdén, P.; Ling, T. G. I. *Anal. Biochem.* **1989**, *181*, 379–382.
(28) Bachas, L. G.; Meyerhoff, M. E. *Anal. Chem.* **1986**, *58*, 956–961.
(29) Daunert, S.; Bachas, L. G.; Meyerhoff, M. E. *Anal. Chim. Acta* **1988**, *208*, 43–52.
(30) Daunert, S.; Payne, B. R.; Bachas, L. G. *Anal. Chem.* **1989**, *61*, 2160–2164.
(31) Rubenstein, K. F.; Schneider, R. S.; Ullman, E. F. *Biochem. Biophys. Res. Commun.* **1972**, *37*, 846–851.
(32) Kjellström, T. L.; Bachas, L. G. *Anal. Chem.* **1989**, *61*, 1728–1732.
(33) Zettner, A.; Duly, P. E. *Clin. Chem.* **1974**, *20*, 5–14.

Sylvia Daunert
Leonidas G. Bachas*

Department of Chemistry
University of Kentucky
Lexington, Kentucky 40506-0055

Genevieve S. Ashcom
Mark E. Meyerhoff

Department of Chemistry
The University of Michigan
Ann Arbor, Michigan 48109-1055

RECEIVED for review July 20, 1989. Accepted November 2, 1989. This research was supported by grants from the National Institutes of Health (Grant No. R29-GM40510) (L.G.B.) and the National Science Foundation (CHE-8813952) (M.E.M.). G.S.A. acknowledges support by the Program in Scholarly Research for Urban/Minority High School Students of the University of Michigan.

TECHNICAL NOTES

Polishable and Robust Biological Electrode Surfaces

Joseph Wang* **and Kurian Varughese**

Department of Chemistry, New Mexico State University, Las Cruces, New Mexico 88003

Tremendous research efforts are being devoted to the surface immobilization of appropriate biological entities (*1*, *2*). Electrochemical probes have been exploited for biosensing more extensively than other devices (*3*). Depending on the specific biocomponent, a variety of surface immobilization procedures have been explored in the fabrication of electrochemical biosensors. Most commonly, the biological element is placed on top of the electrode surface, where it is being held physically (behind membranes) or chemically (via intermediate linkage). Alternatively, biocomponents can be incorporated directly into a carbon paste matrix to produce rapidly responding, inexpensive, and miniature sensing devices. The cumbersome renewal procedures and/or the poor mechanical and chemical stability of such biosurfaces often limit their practical bioanalytical utility.

The motivation of the work described in this note was to develop biologically modified electrodes that would be mechanically robust, polishable, durable, and inexpensive. For example, to enhance the day-to-day practicality of electrochemical biosensors, it is highly desirable to renew their surfaces by simple polishing procedures, common with conventional (solid) electrodes. One promising concept is that of bulk modified electrodes (*4–7*). In this new class of chemically modified electrodes, the modifier is incorporated into the bulk of a robust carbon/polymer matrix. The bulk of the electrode thus serves as a "reservoir" of the modifier in a manner analogous to modified carbon paste electrodes (*8–10*). (The latter, however, are soft, nonpolishable, and not stable in most organic solvents.) The successful incorporation of various chemical modifiers (electrocatalysts, preconcentrating agents) into composite electrodes containing carbon black (*4*, *5*), graphite epoxy (*6*), or carbon fiber (*7*) have been reported recently. A similar avenue for the fabrication of reusable biologically modified electrodes and the challenges involved in the use of biological entities for this task are explored in the following sections.

EXPERIMENTAL SECTION

Apparatus. The 10-mL electrochemical cell (Model VC-2, Bioanalytical Systems) was joined to the working electrode, reference electrode (Ag/AgCl, Mode RE-1, Bioanalytical Systems), and platinum wire auxiliary electrode through holes in its Teflon cover. The three electrodes were connected to a Princeton Applied Research Model 174A polarographic analyzer, the output of which was displayed on a Houston Omniscribe strip-chart recorder. The flow injection was described elsewhere (*8*).

Electrode Preparation. Biologically modified graphite–epoxy electrodes were prepared by adding the desired quantity of the biocomponent (7.5–25% (w/w)) to the 1:1 resin/accelerator mixture of a commercial epoxy-bonded graphite (Grade RX, Dylon, Cleveland, OH); a through mixing proceeded for 10 min. The enzyme/cofactor electrode were prepared in a similar manner, by adding the glucose oxidase/1,1′-dimethylferrocene mixture to the resin/accelerator mixture. A portion of the electrode material was packed into the end of a 5-mm-i.d. glass tube. The electrode was then cured at room temperature for 15–20 h. The surface was polished with silicon carbide papers (150 and 320 grit) for a time period of 5 s each and then with 0.05-μm alumina slurry for 30 s. Residual polishing material was removed from the surface after each step by thoroughly rinsing with doubly distilled water. Such polishing procedure was repeated before each experiment. Between experiments, the bioelectrodes were stored at 4 °C.

Reagents. All solutions were prepared with doubly distilled water. Supporting electrolytes were 0.05 M phosphate buffer (pH 7.4) and 0.1 M acetate buffer (pH 5.0). Dopamine, catechol, glucose, β-nicotinamide adenine dinucleotide (NAD^+) (Sigma), ascorbic acid, potassium ferrocyanide, copper nitrate (Baker), 1,1′-dimethylferrocene (Aldrich), ethanol (U.S. Industrial Chemicals), and methanol (Fisher) were used without further purification. The dry active yeast granules ("Red Star", Universal Food, Milwaukee, WI) and the brown alga *Eisenia bicyclis* (Westbrae Natural Food, Berkeley, CA) were ground with a mortar and pestle. Tyrosinase (EC 1.10.3.1), horseradish peroxidase (EC 1.11.1.7), and glucose oxidase (EC 1.1.3.4) were obtained from Sigma.

0003-2700/90/0362-0318$02.50/0 © 1990 American Chemical Society

Table I. Summary of Experimental Conditions

biocomponent	% in graphite epoxy	working solution	operating potential, V
tyrosinase[a,b]	7.5[a] 20[b]	0.05 M phosphate buffer (pH 7.4)	−0.2
horseradish peroxidase[a]	25	0.05 M phosphate buffer (pH 7.4), containing 10 mM $K_4Fe(CN)_6$	−0.2
dry yeast[a]	20	0.05 M phosphate buffer (pH 7.4) containing 1 mM NAD^+ and 1 mM $F_3Fe(CN)_6$	+0.6
Eisenia bicyclis[a]	20	0.1 M acetate buffer (pH 5.0)	scan from +0.6 to −0.7
glucose oxidase[a,c]	20	0.5 M phosphate buffer (pH 7.4)	+0.5

[a] Batch experiments with 400 rpm stirring. [b] Flow injection analysis with 20-μL samples flowing at 1.0 mL/min. [c] Also containing 26% 1,1-dimethylferrocene.

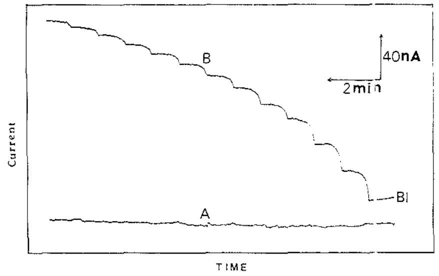

Figure 1. Current-time recording upon increasing the ethanol concentration in 5 × 10^{-4} M steps: unmodified (A) and yeast-modified (B) graphite-epoxy electrodes. Batch experiment with a 400 rpm solution stirring and +0.6 V operating potential. Other conditions are given in Table I.

Procedure. Amperometric detection was performed by applying the desired potential and allowing the background current to decay to a steady-state value. Solution stirring (400 rpm) or flow (1.0 mL/min) were used in batch and flow injection experiments. The preconcentration/medium-exchange/voltammetric scheme for algae-containing electrodes was described elsewhere (*9*). Specific details of the experimental conditions are summarized in Table I.

RESULTS AND DISCUSSION

The major challenge in fabricating reusable and robust bioelectrodes based on the bulk modification concept is the heating requirement of the curing/polymerization process. While this has no effect upon the incorporation of most chemical modifiers (*4*–*7*), the high temperature may have a deleterious effect on the activity of biological entities. Unlike carbon black or carbon-fiber composite electrodes (*4*, *5*, *7*), the graphite–epoxy fabrication strategy (*6*) offers the advantage that the curing process can take place at room temperature. Although this requires longer (12–20 h) curing times (vs high-temperature curing), it is essential when biocomponents are concerned. The electrodes are very rigid upon formation. They render their bioactivity upon polishing for immediate reuse and appear to be smooth to the naked eye. The incorporation of four different biological entities (of relevance to bioanalysis) into the graphite epoxy material is used in the following sections to illustrate the concept of polishable and robust biosurfaces.

Figure 1 demonstrates the response of conventional (A) and yeast-containing (B) graphite–epoxy electrodes, to successive standard additions of ethanol, each addition effecting a 5 × 10^{-4} M increase in concentration. In the absence of an enzymatic reaction, the former is not responding to additions of ethanol. In contrast, the yeast electrode (with its alcohol dehydrogenase activity) responds rapidly to the change in ethanol concentration, producing the steady-state current response within 28 s. The fast response is attributed to the intimate contact of the biocatalytic and graphite sites. The yeast actually becomes an integral part of the rigid sensing element, in a manner analogous to nonpolishable carbon paste bioelectrodes (*8*).

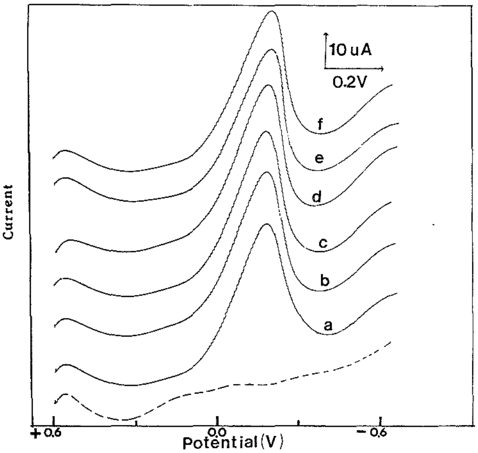

Figure 2. Differential pulse voltammograms for 1 × 10^{-3} M copper obtained at the *Eisenia*/graphite–epoxy electrode using the preconcentration/medium-exchange/voltammetric approach. Five minutes accumulation in a stirred copper solution, followed by rinsing and placing the electrode in a blank (electrolyte) solution to record the voltammogram. Scan rate was 10 mV/s. The electrode was polished prior to each cycle. The dotted line represents the response in the absence of copper. Other conditions are given in Table I.

Algae represent another class of microorganisms that can be incorporated in a stable and active manner into robust graphite–epoxy surfaces. The bioaccumulation of metal ions by alga-modified electrodes has been exploited for designing new sensing devices (*9*). Figure 2 demonstrates the ability to polish an alga-modified electrode to reproducibly renew its surface. It shows a series of six successive copper measurements, each recorded with a freshly polished *Eisenia*-containing surface. The effective collection of the metal by the surface-bound alga is indicated from the well-defined voltammograms obtained after transfer of the electrode to the blank solution. The shape of the voltammogram and overall signal-to-background characteristics are similar to those obtained at nonpolishable alga surfaces (*9*). Both faradaic and background currents are unaffected by polishing. This series yielded a mean peak current of 38.4 μA, with a range of 38.0–39.2 μA and a relative standard deviation of 1.6%. Such precision indicates that the electrode preparation results in homogeneous dispersion of the biological modifier within the graphite epoxy matrix and that the polishing step does not adversely affect the bioaccumulation process.

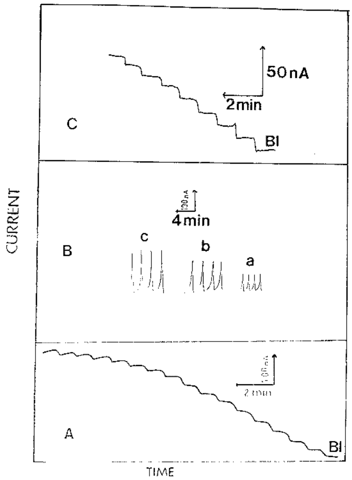

Figure 3. Amperometric measurements of catechol (A, B) and glucose (C) at enzyme/graphite–epoxy electrodes: (A) current–time recording upon increasing the catechol concentration in 1 × 10^{-5} M steps; (B) flow-injection detection of catechol solutions of increasing concentration from 2.5 × 10^{-5} to 7.5 × 10^{-5} M (a–c); flow rate, 1.0 mL/min; (C) current–time recording upon increasing the glucose concentration in 5 × 10^{-4} M steps; solutions, 50:50 (v/v) methanol–phosphate buffer (pH 7.4) (A) and 0.05 M phosphate buffer (pH 7.4) (B, C). Other conditions are given in Table I.

Isolated enzymes were subsequently tested as biological modifiers, to examine whether the room-temperature curing process has a detrimental effect on their bioactivity. Figure 3 A,B shows the batch and flow amperometric response for catechol at the tyrosinase-modified electrode. For both operations, the rigid enzyme electrode responds very rapidly to the change in the substrate concentration. The reductive detection of the enzymatically produced quinone species, with its favorable signal-to-noise characteristics, allows convenient measurements of micromolar concentrations. Besides high sensitivity and speed, the graphite–epoxy enzyme electrode may be used in organic solutions. For example, a 50:50 (v/v) methanol–phosphate-buffer solution was employed in part A of Figure 3. Tyrosinase is known for its ability to catalyze reactions in nonaqueous media (*11*). Unlike mixed-enzyme/carbon-paste electrodes, where the oil binder may dissolve upon exposure to organic solutions, the graphite–epoxy biosurface is stable and robust. The high sensitivity and speed of the flow injection data, coupled with the ability to operate in organic media hold prospect for detection in liquid chromatography.

Figure 3C illustrates the ability to coimmobilize an enzyme and its cofactor in the graphite–epoxy matrix. The glucose oxidase/dimethylferrocene/graphite–epoxy electrode responds rapidly to successive additions of 5 × 10^{-4} M glucose. Horseradish peroxidase represents another enzyme that was incorporated in an active and stable form within the graphite–epoxy matrix. A series of ten concentration increments of 1 × 10^{-4} M hydrogen peroxide yielded a fast amperometric response (18 s for attainment of steady state) and a linear concentration dependence (conditions as in Table I; not shown).

The ability to renew by polishing fresh enzyme electrodes was tested for ten calibration plots for dopamine (50–500 μM) obtained at ten individual tyrosinase surfaces (conditions as in Figure 3A). For all surfaces, linearity prevailed up to 3.5 × 10^{-4} M. The mean sensitivity value (slope of linear portion) found was 9.2 nA/μM, with relative standard deviation of 10%. Similar surface-to-surface reproducibility experiments at the horseradish peroxidase or glucose oxidase/dimethylferrocene containing electrodes, involving additions of hydrogen peroxide or glucose, yielded relative standard deviations of 12% and 14%, respectively. Indeed, single tyrosinase, glucose oxidase, and horseradish peroxidase electrodes were able to be used for periods of several weeks, performing several hundred measurements with no noticeable loss of stability. Hence, the needs to re-create (by immobilization) the enzyme layer each time are eliminated. While the above data indicate no significant loss of bioactivity during the electrode preparation and routine operation, future studies will explore the utility of thermostable enzymes (isolated from thermophilic bacteria or artificial ones) in connection with the bulk modification approach.

In conclusion, the experiments described above indicate that carbon composites can be used to prepare robust bioelectrodes for bioanalytical applications. Such electrodes mimic the behavior of their corresponding carbon paste counterparts (*8–10*), but possess the advantage that they may be polished (to renew the surface reproducibly) and can operate in organic media. Speed of response, simple modification scheme, versatility, miniaturization, and controlled bulk composition represent other advantages of graphite–epoxy bioelectrodes. Interferences (from coexisting electroactive or surface-active substances) are similar to those encountered at modified carbon-paste probes. Even though the concept is presented in terms of four model biocomponents, it could be extended to the incorporation of numerous biological modifiers. The simultaneous incorporation of a second enzyme (for sequence or competitive operations) or of chemical moieties (e.g. electrocatalyst) should further enhance the power of these composite biosurfaces.

Registry No. Peroxidase, 9003-99-0; glucose oxidase, 9001-37-0; tyrosinase, 9002-10-2; hydrogen peroxide, 7722-84-1; ethanol, 64-17-5; copper, 7440-50-8; graphite, 7782-42-5; catechol, 120-80-9; glucose, 50-99-7.

LITERATURE CITED

(1) Rechnitz, G. A. *Chem. Eng. News* **1988**, Sept 5, 24.
(2) Arnold, A. M.; Meyerhoff, M. E. *CRC Crit. Rev. Anal. Chem.* **1988**, *20* (3), 149.
(3) Kobos, R. K. *TrAC, Trends Anal. Chem.* **1987**, *6*, 1987.
(4) Shaw, B.; Creasy, K. E. *Anal. Chem.* **1988**, *60*, 1241.
(5) Park, J.; Shaw, B. *Anal. Chem.* **1989**, *61*, 848.
(6) Wang, J.; Golden, T.; Varughese, K.; El-Rayes, I. *Anal. Chem.* **1989**, *61*, 508.
(7) Creasy, K. E.; Shaw, B. R. *Anal. Chem.* **1989**, *61*, 1460.
(8) Wang, J.; Lin, M. S. *Anal. Chem.* **1988**, *60*, 1545.
(9) Gardea-Torresdey, J.; Darnall, D.; Wang, J. *Anal. Chem.* **1988**, *60*, 72.
(10) Santos, L. M.; Baldwin, R. P. *Anal. Chem.* **1986**, *58*, 848.
(11) Hall, G. F.; Best, D.; Turner, A. R. F. *Anal. Chim. Acta* **1988**, *213*, 113.

RECEIVED for review July 17, 1989. Accepted November 1, 1989. This work was supported by the National Institutes of Health (Grant No. GM 30913-06).

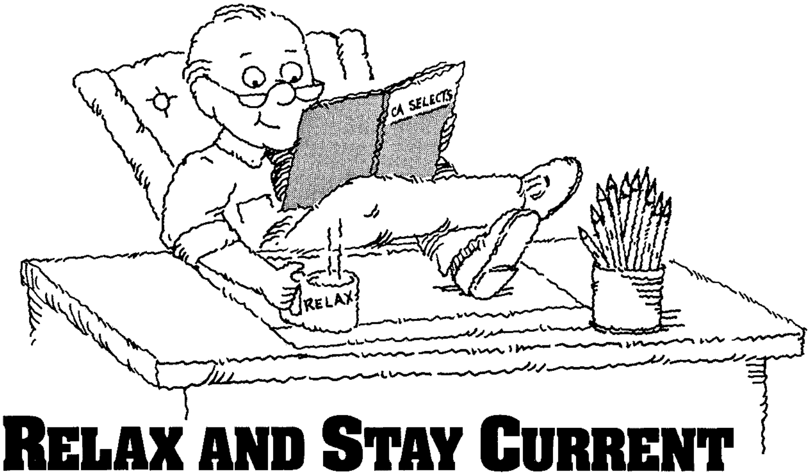

RELAX AND STAY CURRENT WITH CHEMICAL LITERATURE

CA SELECTS is a series of current awareness publications that are produced from the Chemical Abstracts (CA) database. *You can relax,* knowing that a profile will be run every other week to search all relevant current literature covered by CA for your area of interest. From our computer to you, a review of chemical literature in just 10–12 pages (on the average).

All this for just $170.00—$6.54 an issue, about 5 cents per abstract! Find out if CA SELECTS covers your research interests by sending for your FREE copy of all 215 topic descriptions.

Mail coupon to:
Chemical Abstracts Service
Marketing Dept. 31390
2540 Olentangy River Road
P.O. Box 3012
Columbus, Ohio 43210, U.S.A.

Or call us at: (614) 447-3731;
or 1-800-848-6538 (ask for Customer Service).

CA SELECTS Catalog Coupon

YES! Please send me the descriptions of all 215 topics.

Name ______________________

Job Title ______________________

Organization ______________________

Address ______________________

____

City ______________________

State/Zip ______________________

Country ______________________

Phone Number ______________________

Chemical Abstracts Service is a division of the American Chemical Society.

Bring your microsample CHNS analyses into the 1990's with the LECO® CHNS series of elemental determinators

The LECO® CHNS series of carbon, hydrogen, nitrogen and sulfur determinators can make your current microsample CHNS methods obsolete. The nominal 4 minute analysis time along with the outstanding precision make the CHNS series ideal for the analysis of pharmaceutical, chemical and other hetrogeneous organic materials.

The CHNS series includes the CHN-900, which is designed for carbon, hydrogen and nitrogen determination only, and the CHN-932 which adds sulfur determination capabilities to the analysis. Both systems feature built-in 16-bit microprocessors coupled to icon-driven, touch screen software making the systems one of the easiest to operate available. A standard 19-sample or optional 49-sample autoloader further reduces operator interface by allowing a number of samples to be analyzed automatically.

The CHNS series is more than just another laboratory instrument, the self-contained database with built-in archival, statistical and sort routines allows use as a lab management system. Compare the LECO® CHNS series to other systems and you will see it is the instrument for you in the 1990's and beyond.

For more information about these new systems, call or write today!

LECO®

LECO® Corporation
3000 Lakeview Avenue
St. Joseph, MI 49085-2396 U.S.A.
Phone: (616) 983-5531
Facsimile: (616) 983-3850

LECO
CHN-900
OKIDATA
LECO-450

CIRCLE 94 ON READER SERVICE CARD